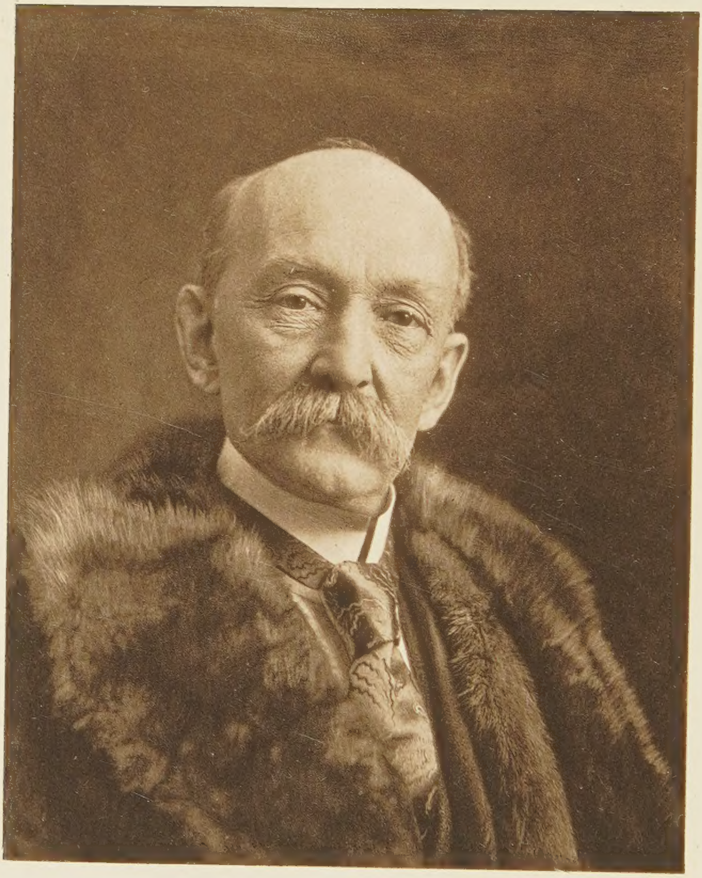

CONTRIBUTIONS

FROM THE

JEFFERSON PHYSICAL LABORATORY

AND FROM

COLLEAGUES AND FORMER STUDENTS

DEDICATED TO

PROFESSOR JOHN TROWBRIDGE, S.D.

FOR THE YEAR

1910

Vol. VIII

CAMBRIDGE, MASS., U.S.A.

UNIVERSITY OF ARIZONA
530.4
H33
LIBRARY

To JOHN TROWBRIDGE

who projected a great physical laboratory for Harvard University and found the means to build and equip it, who by his foresight, invention, and care has kept this laboratory among the foremost in opportunities for scientific achievement, and by his magnanimity has made it a place proverbial for good feeling, this volume is gratefully and affectionately dedicated by those who have profited by his labors and enjoyed his friendship.

Digitized by the Internet Archive
in 2023 with funding from
Kahle/Austin Foundation

https://archive.org/details/contributionsfro0003unse_l1l5

CONTENTS

1. The Physiological Tolerance of Alternating-Current Strengths up to Frequencies of 100,000 Cycles per Second.
A. E. Kennelly and E. F. W. Alexanderson.
Electrical World, July 21, 1910.

2. Tables of Demagnetizing Factors for Iron Rods.
C. L. B. Shuddemagen.
Physical Review, Vol. XXXI, No. 2, 1910.

3. The Magnitude of an Error which sometimes affects the Results of Magnetic Tests upon Iron and Steel Rings.
B. O. Peirce.
Proc. Am. Acad. XLVI, No. 3.

4. Note on Kirchhoff's Law.
G. C. Evans.
Proc. Am. Acad. XLVI, No. 4.

5. On Four-Dimensional Vector Analysis, and its Application in Electrical Theory.
G. N. Lewis.
Proc. Am. Acad. XLVI, No. 7.

6. The Resistivity of Hardened Cast Iron as a Measure of its Temper and of its Fitness for Use in Permanent Magnets.
B. O. Peirce.
Proc. Am. Acad. XLVI, No. 8.

7. The Magnetic Permeabilities at Low Excitations of Two Kinds of very Pure Soft Iron.
B. O. Peirce.
Proc. Am. Acad. XLVI, No. 9.

8. The Propagation of Long Electric Waves along Wires.
E. P. Adams.
Proc. Am. Phil. Soc. Vol. XLIX, 1910.

9. Theory of Coupled Circuits, under the Action of an Impressed Electromotive Force, with Applications to Radiotelegraphy. G. W. Pierce.
Proc. Am. Acad. XLVI, No. 13.

10. The Action of Mercury on Steel at High Pressures. P. W. Bridgman.
Proc. Am. Acad. XLVI, No. 14.

11. Vector-Diagrams of Oscillating-Current Circuits. A. E. Kennelly.
Proc. Am. Acad. XLVI, No. 17.

12. The General Circulation of the Mean and High-Level Calcium Vapor in the Solar Atmosphere. C. E. St. John.
Contributions from the Mount Wilson Solar Observatory, No. 48.

13. Volume Ionization Produced by Light of Extremely Short Wave-Length. F. Palmer, Jr.
Physical Review, Vol. XXXII, No. 1, 1911.

14. The Hall Effect and Some Allied Effects in Alloys. A. W. Smith.
Physical Review, Vol. XXXII, No. 2, 1911.

15. The Spectra of Some Gases in the Schumann Region. T. Lyman.
Astrophysical Journal, XXXIII, No. 2, 1911.

16. On the Heat Generated by Radio-Active Substances. W. Duane.
American Journal of Science, Vol. XXXI, April, 1911.

17. A Method for Determining Heat of Evaporation as Applied to Water. T. W. Richards and J. H. Mathews.
Proc. Am. Acad. XLVI, No. 19.

18. The Effects of Sudden Changes in the Inductances of Electric Circuits as Illustrative of the Absence of Magnetic Lag and of the Von Waltenhofen Phenomenon in Finely Divided Cores. Certain Mechanical Analogies of the Electrical Problems. B. O. Peirce.
Proc. Am. Acad. XLVI, No. 20.

19. The Internal Resistance of the Lead Accumulator.
H. W. Morse and L. W. Sargent.
Proc. Am. Acad. XLVI, No. 21.

20. Notes on the Electrical Conductivity of Argentic Sulphide.
H. V. Hayes.
Proc. Am. Acad. XLVI, No. 22.

21. On the Electromagnetic and the Thermomagnetic Transverse and Longitudinal Effects in Soft Iron.
E. H. Hall and L. L. Campbell.
Proc. Am. Acad. XLVI, No. 23.

22. An Investigation of the Errors in Cooling Curves and Methods for Avoiding these Errors; also a New Form of Crucible.
H. C. Hayes.
Proc. Am. Acad. XLVII, No. 1.

23. Cisoidal Oscillations. G. A. Campbell.
Proc. Am. Institute of Elec. Engineers, Vol. XXX, No. 4, April, 1911.

24. Spark Length, Potential and Frequency of Oscillation: the "Lag Effect" in Electric Discharge. J. C. Hubbard.
Physical Review, Vol. XXXII, No. 6, 1911.

25. Determination of the Altitude of Aeroplanes.
R. W. Willson.
Proc. Am. Acad. XLVII, No. 2.

26. Sense of Loudness. W. C. Sabine.
Privately printed.

The Physiological Tolerance of Alternating-Current Strengths Up to Frequencies of 100,000 Cycles per Second.

By A. E. Kennelly and E. F. W. Alexanderson.

Reprinted from ELECTRICAL WORLD July 21, 1910

THE PHYSIOLOGICAL TOLERANCE OF ALTERNATING-CURRENT STRENGTHS UP TO FREQUENCIES OF 100,000 CYCLES PER SECOND.

By A. E. Kennelly and E. F. W. Alexanderson.

It was announced many years ago by Tesla,[1] Elihu Thomson[2] and D'Arsonval,[3] that alternating currents of high frequency produced little sensation when passed through the human body, compared with alternating currents of low frequency and equal strength. This relative insensibility to high-frequency currents was attributed by D'Arsonval to the inability of the sensory nerves to respond to high-frequency stimuli. It is known that an alternating current of sufficient strength to light up an ordinary ½-amp incandescent lamp, included in circuit with the body of an observer, can be easily tolerated at very high frequencies, although only a small fraction of that current strength could be supported without distress at ordinary industrial frequencies up to 150 cycles per second.

Beyond the above facts, but little appears to be known, from the physical standpoint, concerning the influence of frequency on the physiological sensibility of the human body to the passage of alternating currents.

In making observations of alternating-current toleration, it has been difficult to determine the frequency or frequencies employed, owing to the nature of the generating apparatus. This apparatus has in nearly every case consisted of a condenser, discharging through an inductive circuit including the body of the observer. Very recently, however, it has been found practicable to construct, for industrial purposes, alternators giving frequencies up to 100,000 cycles per second. The frequency of these machines is readily measured and controlled. The machines can deliver a steady terminal potential-difference and current, both of which can be easily measured with hot-wire instruments.

The writers have made a series of measurements on different individuals to determine their relative sensibility to alternating-current strengths at different frequencies up to 100,000 cycles per second, using one of the above-mentioned high-frequency alternators for this purpose.

---

[1] N. Tesla, "Experiments with alternate currents of very high frequency and their application to methods of artificial illumination." *Trans.* Am. Inst. El. Engrs., May 20, 1891, Vol. 8, pp. 267-319.

[2] Elihu Thomson, "Physiological Effects of Alternating Currents of High Frequency." *"Elec. World,"* N. Y., Vol. 17, No. 11, March 14, 1891, p. 214.

[3] D'Arsonval, *L'Ind. Electrique,* March 25, 1893.

Application of the Current.

In all of the measurements, the current was passed through the arms and across the chest, by inserting the hands of the subject, up to the wrist (ulnar condyle), in jars of saline solution containing electrodes connected with the alternator. The alternating current, entering the body through the skin of the hands, distributes itself through the liquid electrolytes within the arms, and must diffuse through the chest and trunk of the body. It is well known that when a high-frequency current passes through a cylinder, wire, or prism of good conducting material, such as copper, and particularly a good electrical conducting material with strong magnetic properties, like iron, it penetrates only to a small depth within the conductor, or is confined to a thin surface layer; this effect is commonly called the "skin effect." The skin effect is, however, easily demonstrated arithmetically to be very small with conductors of such relatively low conductivity as saline solutions, so that unless our quantitative data and formulas for the skin effect are very largely wrong, it is certain that the skin effect in the human body is practically negligible, and that up to the highest frequency here considered, the current diffuses throughout the cross-sections of the body in substantially the same manner as a continuous current.

High-Frequency Alternator.

The high-frequency alternator was a 2-kw machine with a stator double armature and an inductor rotor, as built by the General Electric Company for wireless telegraph and telephone work. The machine was similar to that described in a paper by one of the writers, last year,[4] before the American Institute of Electrical Engineers. It was designed to give either 110 volts or 220 volts on open circuit, with multiple or series connections respectively, and to deliver the full output of 2 kw with the aid of a series or shunt condenser. The voltage and current that can be selected for full output may be varied widely, depending upon the capacity and connection of the condenser, under the limitation that the current should not exceed 40 amp in multiple connection. In the experiments here described, a resistance and condenser load (R, C, Fig. 1) was used to raise the voltage above the normal no-load voltage. The maximum voltage used in the tolerance test was 360 volts, with a corresponding current of 0.8 amp taken through the body. The machine was driven by a direct-current electric motor at the full speed of 20,000 r.p.m., through gearing of velocity increasing ratio 10:1. By reducing the speed of the driving motor, the frequency of the alternator was adjustably reduced. The wave form of the e.m.f. generated by the alternator is approximately sinusoidal.

---

[4] E. F. W. Alexanderson, "Alternator for One Hundred Thousand Cycles," *Proceedings* Am. Inst. El. Engrs., June 6, 1909, pp. 655-668.

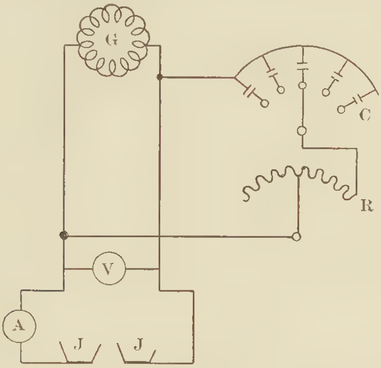

Fig. 1—Electrical Connections Employed in Tolerance Tests.

Electrical Connections.

The electrical connections employed are indicated in the accompanying diagram Fig. 1. *G* is the high-frequency alternator, *C* is the variable condenser and *R* the variable resistance used in a shunt circuit in order to increase and regulate the voltage. *V* is a hot-wire voltmeter, *A* a hot-wire milliammeter, *JJ* metallic jars containing water with approximately 3 per cent of common salt. In the ordinary method of conducting the test, the generator voltage was reduced to a comparatively low value by lowering the excitation of the machine. The subject then inserted his hands in the jars *JJ*. The voltage was then slowly and steadily raised until the subject considered that any further increase would give him distress. The readings of current and voltage at the instruments *A* and *V* were then noted and the voltage again reduced. The speed of the driving motor would then be altered so as to obtain another frequency, and the measurement repeated. A series of such measurements would thus be obtained on the same subject at, say, five frequencies between 15,000 and 100,000 cycles per second, within an interval of about 20 minutes. The limiting current strength which the subject could take through his arms and body, without marked discomfort or distress, at any given frequency, may be designated as the *tolerance current* for that subject and frequency.

Observations.

The observations are collected in the table on page 6. Column I gives the initials of each subject's name. Column II

TABLE OF OBSERVATIONS.

I Initials of Subject	II Frequency Cycles per Sec n	III P.D. Volts	IV Tolerance Current Ampere I	V Inferred Resistance Ohms	VI Tolerance Cyclic Quantity I/n Coulombs per Cycle ÷ 1,000,000	VII REMARKS
D. M.	100,000	250	0.5	500	5	Sensation of heat only.
	75,000	160	0.32	500	4.3	" " " "
	50,000	110	0.18	612	3.6	Slight muscular contractions.
	30,000	50	0.09	557	3.0	" " "
	16,000	27	0.044	614	2.8	" " "
	11,000	17	0.028	614	2.5	" " "
A. E. K.	100,000	200	0.33	600	3.3	Tingling and warmth in wrists.
	50,000	100	0.17	590	3.4	Slight muscular contractions.
	30,000	35	0.07	500	2.3	" " "
P.R.	100,000	360	0.8	450	8.0	Check test on a different date.
	50,000	125	0.2	625	4.0	
	30,000	95	0.15	633	5.0	Muscular contractions in arms.
	16,000	32	0.05	640	3.1	" " " wrists and arms.
	11,000	20	0.03	667	2.7	" " " " " "
P. M.	100,000	240	0.45	534	4.5	
	80,000	150	0.26	577	3.3	
	60,000	105	0.18	584	3.0	
	40,000	70	0.12	583	3.0	
	25,000	40	0.065	616	2.6	
	16,000	25	0.040	625	2.5	
	11,000	16	0.025	625	2.3	
C. M S.	100,000	200	0.48	417	4.8	
	80,000	150	0.38	395	4.8	
	60,000	80	0.21	381	3.5	
	40,000	50	0.13	384	3.3	
	25,000	35	0.085	412	3.4	
	16,000	22	0.05	440	3.1	
	11,000	12	0.027	440	2.5	
J. T.	62.5	7	0.0055	1272	88	Muscular contractions in wrists and arms.
C. A. W.	62.5	7.1	0.0035	2020	56	" " " " " "
P. H. C.	62.5	8.4	0.0105	800	168	" " " " " "
A. E. K.	62.5	5.1	0.0041	1240	66	" " " " " "
C. P.	62.5	6.6	0.0053	1240	85	" " " " " "

the frequency in cycles per second. Column III specifies the potential-difference at jar electrodes as measured by voltmeter *V*. The tolerance current is recorded in column IV, and the inferred resistance of the subject from the potential-

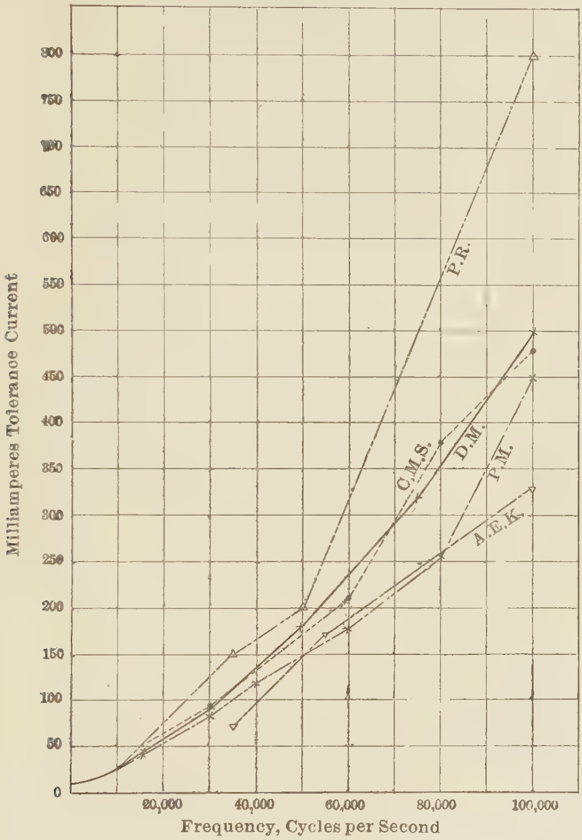

Fig. 2—Curves of Tolerance Current Strengths at Different Frequencies in the Cases of Five Different Subjects.

difference and current, including the resistance in jar solutions, is given in column V. Column VI gives the ratio of the tolerance current to the frequency. This ratio may be called the *tolerance cyclic quantity*. It is a quantity expressed in coulombs per cycle. The actual figures within the column give the result in virtual, or root-mean-square, microcoulombs per cycle. With a sinusoidal current wave, the maximum quantity of electricity passed through the body in each half-cycle will be this virtual quantity multiplied by $\sqrt{2} \div \pi$.

It will be seen that the tolerance current increases from 0.03 amp at 11,000 cycles per second to about 0.45 amp, or even 0.8 amp, at 100,000 cycles per second. This means that the tolerance cyclic quantity increases from about 2.5 microcoulombs per cycle at 11,000 cycles per second to about 4.5 microcoulombs at 100,000 cycles per second.

The last five observations were made near the ordinary lighting frequency of 60 cycles per second. It will be seen that the tolerance e.m.f. varied between 5.1 volts and 8.4 volts with different subjects and the tolerance current between 4 milliamperes and 10 milliamperes. The tolerance cyclic quantity varied between 56 microcoulombs and 168 microcoulombs per cycle.

It was the unanimous testimony of all the subjects experiencing the high-frequency current that at or near 100,000 cycles per second there was a sensation of tingling and heat in the wrists, when the tolerance current was approached, but no muscular contractions were produced, either in the hands or arms. When the frequency was reduced to about 50,000 cycles per second, muscular contractions commenced in the muscles of the forearm. As the frequency was reduced below 50,000 cycles per second, the muscular contractions became more evident.

The tolerance currents for the high-frequency range 11,000 to 100,000 cycles per second, and are given in the accompanying curve sheet, Fig. 2.

Conclusions.

It is evident from the tables and curves that there is a very marked increase in the tolerance current strength as the frequency is increased from 11,000 to 100,000 cycles per second. A man can tolerate only about 30 milliamperes at 11,000 cycles per second, but can tolerate nearly half an ampere at 100,000 cycles per second.

Between 60 and 11,000 cycles per second there is not a very great change in tolerance current, namely, from about 5 milliamperes to about 30 milliamperes.

To a first approximation, between 11,000 and 100,000 cycles per second, the tolerance current strength increases with the frequency, although it is not certain that the increase follows a straight line law. Some of the subjects seem to follow nearly a straight line law of tolerance with frequency. Others seem to show a parabolic law, or a tolerance increasing faster than the frequency. Thus the mean tolerance cyclic quantity was 2.5 microcoulombs per cycle at 11,000 cycles per second and 5.3

microcoulombs per cycle at 100,000 cycles per second, or, roughly, twice as much at the upper as at the lower limit. It is difficult to say what the precise law is, from the observations thus far made. The tolerance current cannot be measured with great precision. It is a physiological estimate subject to variation, not only in different individuals, but also in the same individual at different times.

Since the mean tolerance cyclic quantity was nearly 100 microcoulombs per cycle at 60 cycles per second and seemed to diminish below 2.5 microcoulombs per cycle at 11,000 cycles per second, a minimum is to be expected somewhere between these limits, i. e., at some frequency between 60 and 11,000 cycles per second, a maximum sensibility to current should be looked for, in the sense of a minimum tolerance cyclic quantity I/n.

The reason for the increase of tolerance current with frequencies above 11,000 cycles per second is to be looked for in the condition of reduced nervous sensibility at high frequencies, as suggested by D'Arsonval. That is, it cannot apparently be accounted for physically; so that the explanation may be expected to be physiological.

[Reprinted from the PHYSICAL REVIEW, Vol. XXXI., No. 2, August, 1910.]

TABLES OF DEMAGNETIZING FACTORS FOR IRON RODS.

BY C. L. B. SHUDDEMAGEN.

WHEN an iron rod is subjected to a magnetic field H_0 in a long solenoid it becomes magnetized, and its own magnetism gives rise to a magnetic field H_m which is everywhere superposed upon the original field H_0 due to a current in the solenoid itself, which latter is uniform within the solenoid, at least near the middle part of its length. The vector addition of these two fields gives the resultant magnetizing field H, which controls the actual intensity of magnetization I at every point of the iron rod. The following formulas now define the "susceptibility" k, the "magnetic induction" B, and the "permeability" μ:

$$I = kH,$$

$$B = 4\pi I + H = (4\pi k + 1)H = \mu H.$$

The field H_m is in all parts of the iron rod except near its ends, directed so as to weaken the field H_0 parallel to the axis of the rod. It is therefore usually spoken of as a "demagnetizing field," since when acting alone it always tends to demagnetize the rod. Near the middle of the iron rod H_m is directed oppositely to H_0 so that the resultant field there is

$$H = H_0 - H_m.$$

Now if the iron rod be magnetized continuously from neutrality to any state in which the intensity of magnetization in the middle part of the rod is I, then H_m will depend on I, and we can write

$$H_m = NI,$$

where N is some function of I to make the equation true. It was formerly thought that N was constant and depended only on the ratio of the length to the diameter of the cylindrical iron rod, or $m = L/D$. Investigations by Benedicks[1] and by the writer[2] showed, however, that N is only approximately constant in the interval from $I = 100$ to $I = 800$. Beyond this it decreases rapidly to a minimum value as the magnetization approaches saturation. Moreover, the N varies also for different absolute values of D, the diameter of the iron rod, being somewhat less for thick rods than for the thin ones, when L/D remains constant.

---

[1] Wied. Ann., 6, 726–760, 1901.

[2] Proc. Amer. Acad., 43, 185–256, 1907.

In the experiments of the writer the iron rods magnetized varied from 0.3175 cm. to 1.905 cm. in diameter. Two magnetizing solenoids were used, for which

No. 1, length = 207.7 cm.; $H_0 = 20.5 \times$ (no. of amperes).
No. 2, length = 485.3 cm.; $H_0 = 27.064 \times$ (no. of amperes).

The magnetic induction in the middle part of the iron rod was found by wrapping a secondary coil around it, connecting it in series with a Thomson galvanometer and a known resistance, and observing the ballistic throw when the current, and the field H_0, were either suddenly increased (method of steps) or completely reversed (method of reversals). The galvanometer was calibrated ballistically by discharging a known quantity of electricity through it from a condenser.

Magnetization curves of B *vs.* H_0 were thus obtained for many iron rods. Long rods were used to get the first curves, and they were then progressively cut down in length in order to obtain rods for which m $(=L/D)$ was smaller. Thus for a constant diameter a series of magnetization curves for various m's were obtained. From these curves a close approximation to the "normal curve," or magnetization curve or an infinitely long rod, for which there would be no demagnetizing field, can be obtained. Having found this "normal curve" it is easy to find the demagnetizing field H_m $(=NI)$ for any value of the magnetic induction B observed in a rod with a given ratio m. It is simply the horizontal distance between the normal curve and the one for m, measured on a level with the B considered, in the scale-units used for H_0. This H_m is the amount by which the curve for m must be "back-sheared" to the left, in order to give a point on the normal magnetization curve, from which the true permeability of the iron must be calculated.

This demagnetizing field H_m may be expessed in two ways:

$$H = H_0 - H_m = H_0 - NI,$$

$$H = H_0 - KB;$$

and the latter is evidently the easier to use if one of the ballistic methods of measuring the magnetic induction B is used; while if I is measured by a magnetometric method, the first equation is preferable.

For convenience in correcting the original field H_0 because of the demagnetizing field H_m the writer has, from the results of his experiments, constructed the two tables of "demagnetizing factors," N and K, for various ratios of m, or L/D and, for various diameters, D, of cylindrical iron rods of the common Bessemer steel.

It will be noticed that the demagnetizing effect is somewhat greater in the case when the method of steps, or slow increase of magnetic field H_0, is used, than when H_0 is suddenly reversed. It seems as if the N and K were practically constants for any iron rod whose diameter is 0.6 cm. or over, provided L/D is the same. However, as the diameter of the rod is made smaller, keeping L/D constant, the demagnetizing effect seems to increase continuously.

Suppose n secondary turns are wound around the middle part of a cylindrical iron rod of length L cm. and diameter D cm. Let this rod be placed inside a still longer magnetizing solenoid, and parallel to its axis. The two ends of the secondary coil are to be twisted together and led out from one opening of the solenoid to the terminals of a ballistic galvanometer; usually various known extra resistances must also be included in this circuit in order to regulate the ballistic throw. Then the charge Q which passes through the galvanometer, resulting in a throw of t cm., when the total number of magnetic lines through the secondary coil is suddenly changed by ΔN, will be

$$Q = n \cdot \Delta N/R = kt,$$

where R is the total "apparent resistance" of the circuit, and k is the constant for ballistic throws. The change in the magnetic induction B will be

$$\Delta B = \frac{\Delta N}{A},$$

$$A = \pi(D/2)^2 = \text{cross-section of the rod.}$$

Values for N.

m	Method of Steps.		Method of Reversals.		
	$D = 0.32$ cm. (1/8 in.).	$D = 0.6–2$ cm. (1/4–3/4 in.).	$D = 0.32$ cm. 1/8 in.).	$D = 0.4$ cm. (5/32 in.).	$D = 0.6–2$ cm. (1/4–3/4 in.).
10	.220	.204	.215	.210	.200
15	.117	.106	.113	.1095	.104
20	.074	.0672	.0720	.0690	.0655
25	.0515	.0467	.0503	.0480	.0455
30	.0382	.0344	.0372	.0356	.0335
35	.0295	.0264	.0279	.0273	.0258
40	.0234	.0211	.0228	.0217	.0206
45	.0191	.0172	.0186	.0177	.0167
50	.0160	.0144	.0154	.01475	.0139
60	.0115	.0104	.0112	.0107	.0101
70	.0087	.00795	.0085	.00816	.0077
80	.0069	.00625	.0067	.00645	.0061
90	.0056	.00507	.0054	.00521	.00495
100	.0046	.00420	.00445	.00432	.00410
125	.0031	.00280	.00297	.00282	.00273
150	.00222	.00204	.00214	.00209	.00198
175	.00166	.00154	.00161	.00158	.00150
200	.00130	.00120	.00125	.00122	.00117

Values for K.

m	Method of Steps.		Method of Reversals.		
	$D = 0.32$ cm. (1/8 in.).	$D = .6–2.0$ cm. (1/4–3/4 in.).	$D = 0.32$ cm. (1/8 in.).	$D = 0.4$ cm. (5/32 in.).	$D = 0.6–2.0$ cm. (1/4–3/4 in.).
10	.0175	.0162	.0171	.0167	.0159
15	.0093	.0084	.0090	.0087	.0083
20	.0059	.00535	.0057	.0055	.0052
25	.0041	.00372	.0040	.00382	.00362
30	.00304	.00274	.00296	.00283	.00267
35	.00235	.00210	.00222	.00217	.00205
40	.00186	.00168	.00181	.00173	.00164
45	.00152	.00137	.00148	.00141	.00133
50	.00127	.00115	.00122	.00117	.00110
60	.00091	.00083	.00089	.00086	.00080
70	.00069	.00063	.00067	.00065	.000613
80	.00055	.00050	.00053	.00051	.000485
90	.000445	.000404	.00043	.000415	.000394
100	.000366	.000334	.000354	.000344	.000326
125	.000247	.000223	.000236	.000224	.000217
150	.000177	.000162	.000170	.000166	.000158
175	.000132	.000122	.000128	.000126	.000119
200	.000103	.000096	.000100	.000097	.000093

If a Thomson ballistic galvanometer is used, then the "apparent resistance" will be the actual ohmic resistance; but if the galvanometer is a D'Arsonval, then the "apparent resistance" is usually much more, because of the counter E.M.F. induced in the galvanometer coil when it is set moving in its strong magnetic field. In the first case, the Thomson galvanometer may be calibrated ballistically by sending a known charge Q_0 from a condenser over the galvanometer circuit. Then if t_0 is the throw observed, we have $Q_0 = kt_0$; and, finally, the change in B when the throw t cm. was obtained, will be

$$\Delta B = \frac{Rkt}{nA} = \frac{RQ_0t}{nAt_0}.$$

If R is expressed in ohms, and Q in microcoulombs, then the right-hand members of this equation must be multiplied by 100 in order that ΔB may be expressed in maxwells per sq. cm.

In case a D'Arsonval galvanometer is used, it becomes advisable to calibrate its throws by means of known changes of magnetic flux through a secondary coil, including also in the galvanometer circuit the various extra resistances which are used in the work. It is usually most convenient to find B by reversing the current in the solenoid, thus reversing the B and H_0, and then in the formula above $\Delta B = 2B$.

Having calculated a series of values of B and the corresponding values of H_0 from the equation $H_0 = GI$, where I = number of amperes of current flowing through the solenoid, and G = the "constant" of the solenoid, the true magnetizing field is found by multiplying the B by the value of K for the m, or L/D, of the rod and subtracting this from H_0, in accordance with the formula $H = H_0 - KB$.

If m for the test-iron rod has a value different from those given in the table, the K for it may be found fairly accurately by interpolation on the curve of Km^2 *vs.* m, constructed from the data in the tables.

Proceedings of the American Academy of Arts and Sciences.

Vol. XLVI. No. 3. — September, 1910.

CONTRIBUTIONS FROM THE JEFFERSON PHYSICAL LABORATORY, HARVARD UNIVERSITY.

THE MAGNITUDE OF AN ERROR WHICH SOMETIMES AFFECTS THE RESULTS OF MAGNETIC TESTS UPON IRON AND STEEL RINGS.

By B. Osgood Peirce.

CONTRIBUTIONS FROM THE JEFFERSON PHYSICAL LABORATORY, HARVARD UNIVERSITY.

THE MAGNITUDE OF AN ERROR WHICH SOMETIMES AFFECTS THE RESULTS OF MAGNETIC TESTS UPON IRON AND STEEL RINGS.

By B. Osgood Peirce.

Presented May 11, 1910. Received May 20, 1910.

The theory of the magnetic properties of a homogeneous ring of iron or steel uniformly wound about by turns of insulated wire through which a steady current of electricity can be made to pass, was first investigated by Kirchhoff, who showed that the intensity of the magnetic field in the metal which thus forms the core of a ring solenoid, must be inversely proportional to the distance from the axis of revolution of the ring. He computed the mean value of the field in a ring of rectangular cross section,[1] and pointed out the advantages which rings offer for measurements of the magnetic permeabilities of the metals of which they are made. The next year, Stoletow, working under the advice of Kirchhoff, took up the subject practically in the Physical Laboratory of the University of Heidelberg and in 1872 published the results of a long series of experiments upon a ring forged from a wrought iron rod. In 1873 appeared an account of the important work of Rowland, begun three years before, on rings (toroids) of circular cross section, made of various kinds of iron and steel, and since that time countless measurements of permeability have been made by many observers[2] upon iron and steel rings; and when these rings have been turned out of masses of solid metal, and not forged up and welded from bars, the results have usually been satisfactory. The value of the mean intensity of the magnetic force within the mass of a ring of circular cross section was given without proof by Bauer in 1880; a proof was printed by Lehmann in 1893, and an interesting diagram based on the formulas of Kirchhoff and Bauer, and showing the ratio of the mean magnetizing force to the value of the force at the mean radius for rings and toroids of different relative dimensions, was given by Morton[3] in the Bulletin of the Bureau of Standards for February, 1909.

---

[1] Gustav Kirchhoff, Pogg. Ann. Ergzbd. **5**, 1 (1870). Gesammelte Abhandlungen, 223; A. Stoletow, Pogg. Ann. **146**, 442 (1872); H. Rowland, Phil. Mag. **46**, 140 (1873); **48**, 321 (1874); C. Bauer, Wied. Ann. **11**, 349 (1880).

[2] J. A. Ewing, Magnetic Induction in Iron and other metals; G. vom Hofe, Wied. Ann. **37**, 482 (1889); H. Lehmann, Wied. Ann. **48**, 406 (1893); A. von Ettingshausen, Wied. Ann. **8**, 554 (1879); H. du Bois, Magnetische Kreise, 110 *et seq.* Berlin, 1894; L. Boltzmann, Anz. d. Wiener Akademie, 203 (1878); J. Sauter, Wied. Ann. **62**, 85 (1897); L. Mues, Inaug. Diss. Greifswald (1893); I. Schuetz, Journal f. Mathematik, **113**, 161 (1894); Carl Neumann, Ueber Ring Potentiale, Halle (1864).

In determining the permeability of an iron ring it is usual to demagnetize the metal as thoroughly as possible at the outset, and then, either by the "Method of Ascending Reversals" or the "Step-by-step Method" to determine for each of a number of values of the magnetomotive force, the whole flux of magnetic induction through the ring. The ratio (B') of this flux to the area of the cross section of the ring is then plotted against the mean value of the magnetic force in the metal to get an HB diagram for the given magnetic journey of the iron. It is clear, however, as the earliest workers in this field saw, that the process here described is only approximately exact, for the induction often has very different values at the points of the ring nearest the axis of revolution and at those farthest away from it. Indeed, in a ring of soft iron of the dimensions of the specimens employed in a well-known form of commercial testing apparatus used in Europe, the value of B at points on the inner edge of the ring when the average value of the force in the metal is unity, may be as high as 2,000, while the value at points at the outer surface is only 700. In this case there is a considerable difference between the average value (B') of the flux in the metal and the real value (B'') of B at points of the ring where H has the average value. For relatively slender rings and fairly high excitations the discrepancy is not so great, and various attempts have been made to estimate its amount beforehand for materials of different kinds. It sometimes happens, however, that one has at command only a small piece of the iron to be tested, and it becomes necessary to make the measurements upon a relatively stout ring not much larger than a finger ring, as Dr. A. Campbell of the National

---

[3] J. A. Moellinger, Elect. Zs., **22**, 379 (1901); B. Soschinski, Elect. Zs., **24**, 292 (1903); J. W. Esterline, Proc. Am. Soc. for Testing Materials, **3**, 288 (1903); R. Richter, Elect. *Zs.*, **24**, 710 (1903); R. Edler, Mitt. Techn. Gewerbe-Museums, Vienna, **16**, 67 (1906); M. G. Lloyd, Bulletin of the Bureau of Standards, Feb. (1909).

Physical Laboratory, Teddington, Middlesex, England, has so successfully done. If in such a case great accuracy is required, the work has to be carried out with considerable care and some attention has to be paid to the fact that there is a real, if usually small, difference between the value of B corresponding to the mean H, and the mean value of B.

I have had occasion of late to determine the permeability of a small ring of extremely pure soft iron, and have found it helpful to compute by the aid of accurate HB diagrams, previously made for two or three different kinds of iron and steel in the form of long rods, what the discrepancy $(B' - B'')$ would be for these materials at different excitations, if they were made into rings of the dimensions of the one I was compelled to use. This paper gives some results which seem instructive, for a very soft kind of Norway wrought iron and for a specimen of Bessemer steel fairly typical of what one meets with in practice.

The straight rods used were magnetized and demagnetized in a uniform solenoid about five meters long, consisting of 20904 turns of well-insulated wire wound on a stout, solid-drawn brass tube through which a stream of tap water could be kept running about the rod to prevent any sensible rise of temperature. The axis of the solenoid was horizontal and perpendicular to the meridian. The flux of induction in the rods was measured by means of a test coil of fine wire wound on the rod at its centre. This coil was protected by rubber tape and its leads were insulated from the water by rubber tubes of fine bore slipped over them. The ballistic galvanometer employed had a period so long[4] that no detectable error was introduced into the readings by the fact that a measurable time was needed to make the magnetic changes incident to a reversal of current in the solenoid. The rods were demagnetized by means of a long series of currents in the solenoid, alternating in direction and gradually decreasing in intensity; and the fact that this process was successful showed that the rods were practically homogeneous throughout. The rods were so long that the corrections for the ends, as given by du Bois or by Shuddemagen,[5] were very small.

Tables I and II give the results of determinations[6] of corresponding values of H and B made by the method of ascending reversals by Mr. John Coulson and myself. A number of diagrams were obtained for each rod to make sure that the rather elaborate apparatus for demagnetizing the specimens was effective and that the metal was practically homogeneous throughout, and although the larger values of B are given in the tables rather more exactly than the observations warrant, the slow-moving ballistic galvanometers employed permitted of very accurate measurements of the flux changes in the testing coil.

---

[4] Peirce, These Proceedings, **44**, 283 (1909).

[5] C. L. B. Shuddemagen, These Proceedings, **43**, 183 (1907).

[6] Peirce, American Journal of Science, **27**, 273 (1909).

After a good HB diagram, accurately drawn on a large scale, has been obtained for a given kind of iron or steel, it is possible to find out how nearly the mean value of the magnetic induction in a given ring made of this material would differ from the real induction corresponding to the mean value of the field in the metal, for any given excitation. Suppose, for example, that the ring is to be a toroid and that the radius of the circular cross section is to be a, while the centre of the section is distant c cms. from the axis, OY, of revolution of the ring. Suppose that the excitation is to be such as to make the value of H, at points distant c from OY, H_c, then the value of H at a point P (Figure 1) is $H_c \cdot c/(\mathrm{OP})$. Let the numerical value of this quantity be computed for say $n + 1$ points evenly dividing the space WV, and let the numerical values of B corresponding to these values of H be read with the help of a lens from the HB diagram. Let P represent one of the points of

TABLE I.

Annealed Norway Iron Rod 1.25 cms. in Diameter, magnetized in a Uniform Solenoid about five Meters long. Results obtained by the Method of Reversals.

H.	*B.*	*H.*	*B.*	*H.*	*B.*
0	0	4.0	11280	16.	15700
0.2	90	4.5	11980	18.	15900
0.4	260	5.0	12560	20.	16040
0.5	395	5.5	13000	25.	16320
0.6	570	6.0	13400	30.	16520
0.8	1125	6.5	13700	35.	16740
1.0	2150	7.0	13900	40.	16920
1.2	3160	7.5	14100	45.	17100
1.4	4140	8.0	14300	50.	17220
1.5	4600	8.5	14490	60.	17450
1.6	5200	9.0	14660	70.	17630
1.8	5825	9.5	14800	80.	17820
2.0	6600	10.	14940	90.	18020
2.5	8240	11.	15100	100.	18210
3.0	9480	12.	15360	105.	18300
3.5	10460	14.	15540		

division, let y represent the product of the value of B corresponding to the value of H at P, and the width, ST, of the ring at P, and let a curve be drawn with the y's as ordinates and the OP's as abscissas. The ratio of the area under this curve, — obtained by the help of a good Amsler's planimeter, — to πa^2, gives the mean value (B') of the magnetic induction in the ring. The average value of the field (H) is $\frac{2\,cH_c}{a^2}(c - \sqrt{c^2 - a^2})$ and the value (B'') of the induction corresponding to this value of H can be found from the HB diagram.

TABLE II.

Rod of Bessemer Steel 1.25 *cm. in Diameter, magnetized in a Uniform Solenoid about five Meters long. Results obtained by the Method of Reversals.*

H.	*B.*	*H.*	*B.*	*H.*	*B.*
0	0	4.5	4830	40.	15200
0.2	40	5.0	5700	50.	15720
0.4	90	5.5	6410	60.	16120
0.5	115	6.0	7060	70.	16460
0.6	145	6.5	7650	80.	16750
0.8	210	7.0	8130	90.	17000
1.0	280	7.5	8600	100.	17220
1.2	354	8.0	9040	120.	17640
1.4	426	8.5	9420	160.	18240
1.5	465	9.0	9760	200.	18800
1.6	505	9.5	10070	240.	19200
1.8	610	10.0	10390	270.	19620
2.0	730	10.5	10650	300.	19800
2.5	1180	11.	10890	350.	20240
3.0	1935	15.	12400	400.	20660
3.5	2800	20.	13360		
4.0	3760	30.	14480		

An illustration may help to make the details of the process more intelligible. Consider a toroid of the Norway iron, the circular cross section of which has a radius of one centimeter and the mean radius (c) of which is 7 centimeters. If the excitation is to be such that the value of the magnetic field at C is unity, the values of H at points distant 6, 6.1, 6.2, 6.4, 6.6, 6.8, 7.0, 7.2, 7.4, 7.6, 7.8, 8 cms. respectively from the axis of revolution of the ring, are 1.167, 1.147, 1.129, 1.094, 1.061, 1.030, 1.000, 0.972, 0.946, 0.921, 0.897, 0.875, and the values of B which correspond to these as determined from the HB diagram for the iron, are 2995, 2895, 2810, 2635, 2460, 2310, 2150, 2005, 1870, 1745, 1620, 1505. If 2895 be multiplied by the thickness of the ring at a distance of 6.1 cms. from the axis (OY), 2810 by the thickness at a distance of 6.2 cms. from OY, etc., a curve of the form KNQ shown in Figure 1 will be obtained. This curve was actually laid down on a large scale by the help of a needle point on a sheet of good coördinate paper, and the area under it was determined to be 6816, though the last significant figure is not determined. This divided by πa^2 gives 2170 as the mean value (B') of B in the ring. The mean value of H in the ring is 1.0052 and the value (B'') of B which corresponds to this is 2176. Although these results have been obtained with great care, they cannot of course be assumed to be quite correct; but it appears to be true that the error in this case is not very large.

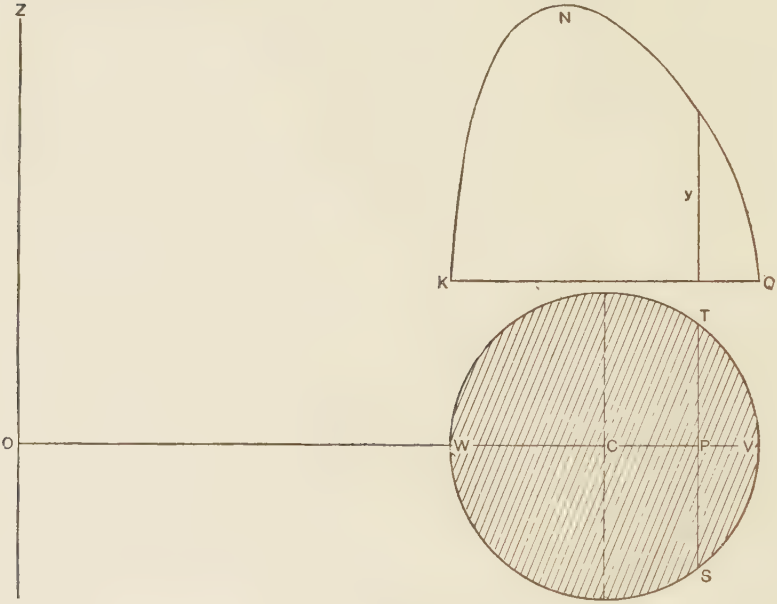

FIGURE 1.

The corresponding process in the case of a ring with rectangular cross section is much simpler and the results are more trustworthy, for the ring has a uniform thickness and the curve which bounds the nearly trapezoidal area to be measured often has so slight a curvature that the application of some form of Simpson's Rule may be made to yield a result much more accurate than a planimeter can be expected to furnish.

In the case of such a ring, as appears from the last two columns of Tables III, IV, and V, B' is usually a trifle larger than B'', for very small values of the mean H in the iron, but is equal to it for a single somewhat larger value. Then, with increasing values of H, B' is a trifle smaller than B''; but the ratio B'/B'' soon approaches unity from the under side, and, for high excitations, is sensibly equal to one. It is evident, however, that the form of B'/B'' as a function of the average value of H in the ring must depend upon the dimensions of the latter as well as upon the magnetic properties of the material of which the ring is made.

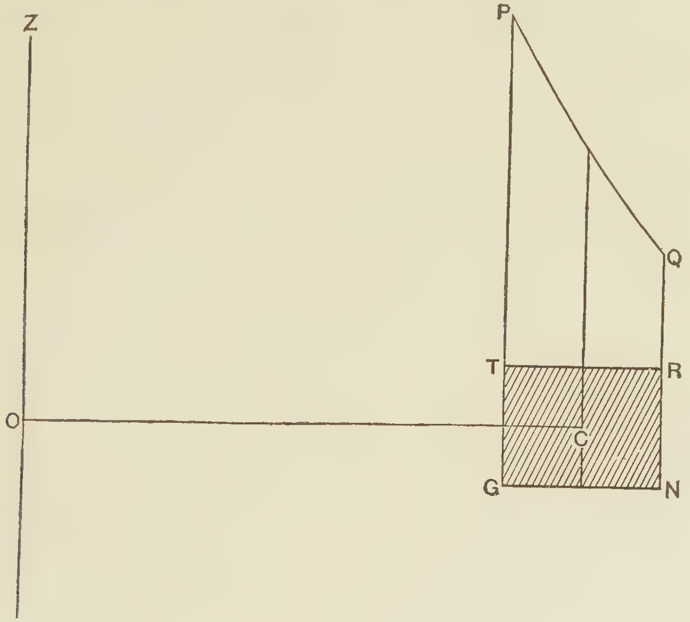

FIGURE 2.

If a ring of rectangular cross section, of the same inner and outer diameters as the toroid just described, be made of the Norway iron, and if the excitation be made such that the average value of the magnetic field in the metal at the centre (C) of the cross section is unity, the values of H and B already found may be used to draw the curve PQ, Figure 2. The area under this curve as computed by Simpson's

TABLE III.

Ring of the Pure Annealed Norway Iron. (Rectangular Cross Section. Inner Radius, 2 a; Outer Radius, 3a.)

H_0.	H_m.	H_1.	B_0.	B_m.	B_1.	H'.	B'.	B''.
0.5	0.4	0.33	400	280	190	0.405	267	255
1.0	0.8	0.67	2150	1140	710	0.811	1235	1195
1.5	1.2	1.00	4600	3155	2150	1.216	3435	3230
2.0	1.6	1.33	6600	5020	3835	1.622	5090	5130
3.0	2.4	2.00	9480	7950	6600	2.433	7970	8040
4.0	3.2	2.67	11280	9870	8660	3.244	9910	9950
6.0	4.8	4.00	13400	12350	11280	4.866	12340	12410
8.0	6.4	5.33	14300	13630	12880	6.488	13610	13680
10.0	8.0	6.67	14940	14300	13760	8.110	14310	14330

H_0 and B_0 are the values of the magnetic force and of the induction at the inner surface of the ring; H_1, B_1 and H_m, B_m the values of the same quantities at the outer surface of the ring and at the mean radius, respectively. H' is the mean value of the magnetic field in the steel. B' is the mean value of the induction in the ring as obtained by mechanical integration from a diagram of ascending reversals for the steel, and B'' is the value of the induction corresponding to H' as shown by the same diagram. The table shows the error made by using, B'/H' instead of the exact value B''/H' for the permeability corresponding to H'.

TABLE IV.

Thinner Ring of the Annealed Norway Iron. (Rectangular Cross Section. Inner Radius, 4 a; Outer Radius, 5 a.)

H_0.	H_m.	H_1.	B_0/B_2.	B.	H'.	B'.	B''.
0.62	0.555	0.50	1.59	405	0.558	502	490
0.94	0.833	0.75	1.90	1275	0.837	1325	1310
1.25	1.111	1.00	1.58	2702	1.116	2728	2740
2.50	2.222	2.00	1.25	7365	2.231	7386	7404
3.75	3.333	3.00	1.15	10130	3.347	10140	10150
6.25	5.555	5.00	1.08	13060	5.578	13070	13080
10.00	8.888	8.00	1.04	14600	8.924	14610	14620

TABLE V.

Ring of the Bessemer Steel. (Rectangular Cross Section. Inner Radius, 2 a; Outer Radius, 3 a.)

H_0	H_m.	H_1.	B_0.	B_m.	B_1.	B_0/B_1.	H'.	B'.	B''.
1.0	0.8	0.67	280	201	170	1.65	0.811	209	205
2.0	1.6	1.33	725	502	385	1.88	1.622	521	510
3.0	2.4	2.00	1920	1060	725	2.65	2.433	1150	1100
4.0	3.2	2.67	3760	2260	1360	2.77	3.244	2365	2330
6.0	4.8	4.00	7060	5350	3760	1.88	4.866	5370	5470
8.0	6.4	5.33	9030	7530	6190	1.46	6.488	7550	7630
10.	8.0	6.67	10490	9030	7800	1.35	8.110	9060	9130
20.	16.	13.33	13360	12660	11830	1.06	16.219	12630	12710

Rule appears to be 2185, and the value of B corresponding to the average value 1.0069 of H is also 2185, so for these dimensions and for this particular excitation, the error represented by $B' - B''$ seems non existent.

For an excitation great enough to make the value of H at the mean radius 2, a process similar to that just described shows that B' would be 6630 and B'', 6650; but if H_c were made 5, the value of B' would be 12560 and B'', 12590. The difference in this instance is less than one quarter of one per cent of either quantity and lies within the limits of error of most magnetic measurements made upon ring specimens. For work that must be very accurate, rings much thinner than this one — in which the ratio of the outer radius to the inner radius is 4/3 — are usually employed, and the error is then practically negligible for almost all excitations.

If magnetic measurements are to be made upon rings of the dimensions sometimes used in practical permeameters, the errors arising from the difference between B' and B'' become relatively important as appears from Tables III and V, where the results for two practical cases are given. A comparison of Tables III and IV will show how fast the error decreases when the ring is made thinner.

My thanks are due to the Trustees of the Bache Fund of the National Academy of Sciences for the loan of apparatus.

The Jefferson Physical Laboratory,
Cambridge, Mass.

Proceedings of the American Academy of Arts and Sciences.

Vol. XLVI. No. 4. — September, 1910.

CONTRIBUTIONS FROM THE JEFFERSON PHYSICAL LABORATORY, HARVARD UNIVERSITY.

NOTE ON KIRCHHOFF'S LAW.

By Griffith C. Evans.

Investigations on Light and Heat made or published, wholly or in part, with Appropriation from the Rumford Fund.

CONTRIBUTIONS FROM THE JEFFERSON PHYSICAL LABORATORY, HARVARD UNIVERSITY.

NOTE ON KIRCHHOFF'S LAW.

By Griffith C. Evans.

Presented by George W. Pierce. Received May 27, 1910.

Kirchhoff's Law in its simple statement says that the energy radiated at a given temperature divided by the absorption coefficient for that temperature is the same for all bodies of the same shape and size, that is, equal to the energy radiated by a perfectly absorbing body of the same shape and size at that temperature. The relation is easily shown to hold for total radiation, and depends merely on the First and Second Laws of Thermodynamics. But for separate wave lengths, a reduction of the law to a firm thermodynamic basis, though often attempted,[1] seems not to have been completely obtained. Unwarrantable assumptions, sometimes tacit, seem unavoidably to have been introduced.

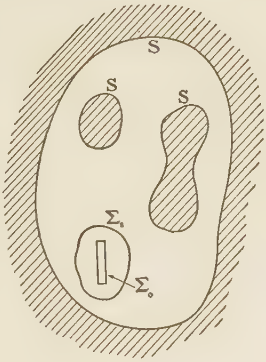

Figure 1.

The present paper, in order to show the nature of the assumptions that must be introduced, attempts to set up a system of assumptions from which the law will rigidly follow.

Pursuing in the main a method of proof due to E. Pringsheim,[2] we take now a body S, in which there is a cavity (see Figure 1). This body need not be all in one piece nor need the cavity be filled homogeneously with one medium. Suppose, however, that there is in the cavity a simple closed surface Σ_1, enclosing another closed surface Σ_0 and not touching it at any point. The space between Σ_0 and Σ_1 is supposed filled with a medium that is fixed rigidly with Σ_1 wherever in the cavity Σ_1 may be. Σ_0 is fixed rigidly in this medium. We shall regard Σ_0 as a slab whose dimensions are small in regard to the other dimensions of the cavity, and whose thickness is small in comparison to its width and height. This surface Σ_0 we consider filled with various substances; we may have it so that the two faces consist of different materials. Let us denote the two surfaces by σ_1 and σ_2, each of area σ.

---

[1] For such considerations see H. Kayser: Handb. der Spectroscopie, II, 13 ff.

[2] E. Pringsheim: Einfache Herleitung des Kirchhoffschen Gesetzes, Verh. deutsche Phys. Ges. **3**, 81. Also Kayser: Spectroscopie, p. 37.

For a criticism of this proof see M. P. Rudski: Zeitschr. f. Wiss. Photog. **3**, 217, 1905. A reply by Pringsheim, ibid. p. 281.

We have two quantities of energy to consider in regard to Σ_0, that which passes out of Σ_0, and that that passes in. The amounts of energy that in unit time pass out of Σ_0 at wave lengths between $\lambda = a$ and $\lambda = b$ through the two faces σ_1 and σ_2 we can denote respectively by

$$\sigma \int_a^b E_{\sigma_1}(\lambda)\, d\lambda + H_{21}\Big]_a^b \tag{1}$$

and

$$\sigma \int_a^b E_{\sigma_2}(\lambda)\, d\lambda + H_{12}\Big]_a^b \tag{2}$$

where $E_{\sigma_1}(\lambda)$ and $E_{\sigma_2}(\lambda)$ are functions of the substance of the element of surface, of its temperature, and of the nature of the medium in which it is immersed, but not of the temperature or position of other bodies in its neighborhood. $H_{21}\Big]_a^b$ and $H_{12}\Big]_a^b$ are two functions that depend on the surrounding conditions and approach zero as Σ_0 is removed from the influence of other radiating bodies; they represent the amounts of energy at wave lengths between $\lambda = a$ and $\lambda = b$, transmitted through Σ_0 from σ_2 to σ_1 and from σ_1 to σ_2 respectively. We shall denote the total amounts of energy transmitted by H_{21} and H_{12}. These assumptions that we have made in regard to $E_{\sigma_1}(\lambda)$ and $E_{\sigma_2}(\lambda)$ constitute essentially Prevost's Law of Exchange.

The amounts of energy at wave lengths between $\lambda = a$ and $\lambda = b$ that in unit time reach Σ_0 at the two faces σ_1 and σ_2 from outside, we can denote respectively by

$$\sigma \int_a^b e_{\sigma_1}(\lambda)\, d\lambda \tag{3}$$

and

$$\sigma \int_a^b e_{\sigma_2}(\lambda)\, d\lambda, \tag{4}$$

and the total amounts of energy that in unit time enter Σ_0 through the two faces σ_1 and σ_2 respectively by

$$\sigma \int_0^\infty A_1(\lambda)\, e_{\sigma_1}(\lambda)\, d\lambda + H_{12} \tag{5}$$

and

$$\sigma \int_0^\infty A_2(\lambda)\, e_{\sigma_2}(\lambda)\, d\lambda + H_{21}. \tag{6}$$

$A_1(\lambda)$ and $A_2(\lambda)$ are called absorption coefficients and denote functions that depend on the nature and temperature of σ_1 and σ_2, and possibly on the temperature of the body S. The existence of such functions is assumed. In the physical case the functions E, e, and A seem to be continuous in λ. And accordingly although it is not strictly necessary for the development of the proof, we shall make this assumption. We assume also that the functions E, e, and A are positive or zero at every λ, and that the functions A are $\leqq 1$.

Before seeking to obtain relations among the several kinds of energies, it is well to consider more in detail the nature of the functions $e_{\sigma_1}(\lambda)$ and $e_{\sigma_2}(\lambda)$. Let us denote by $\sigma \int_0^\infty e_1(\lambda)\, d\lambda$ the amount of energy that would reach σ' — the section of Σ_0 half way between σ_1 and σ_2 — from the σ_1 side, and $\sigma \int_0^\infty e_2(\lambda)\, d\lambda$ the amount of energy that would reach σ' from the σ_2 side, if Σ_0 were filled merely with the same medium that occupies the space between Σ_0 and Σ_1.

Let

$$e_{\sigma_1}(\lambda) = e_1(\lambda) + \delta_{\sigma_1}(\lambda) \tag{7}$$

$$e_{\sigma_2}(\lambda) = e_2(\lambda) + \delta_{\sigma_2}(\lambda). \tag{8}$$

Now as we change the slab Σ_0 in size, the functions $\delta_{\sigma_1}(\lambda)$ and $\delta_{\sigma_2}(\lambda)$ will change. If the body Σ_0 is small, the energy that reaches it will depend little on its own influence,[3] and $\delta_{\sigma_1}(\lambda)$ and $\delta_{\sigma_2}(\lambda)$ will be small. We make the assumption that as Σ_0 approaches zero, keeping the same relative proportions, both σ_1 and σ_2 approach zero, and approach zero in such a way that

$$\Delta_{\sigma_1} = \int_0^\infty |\, \delta_{\sigma_1}(\lambda)\, |\, d\lambda$$

and (9)

$$\Delta_{\sigma_2} = \int_0^\infty |\, \delta_{\sigma_2}(\lambda)\, |\, d\lambda$$

both approach zero.

---

[3] See, however, p. 103.

Let us now put our apparatus in operation. At the start we put everything that has a temperature (ether, of course, has not) at one temperature T, and throughout succeeding time maintain S at temperature T. The body Σ_0 will thereafter, according to the Second Law of Thermodynamics, remain at temperature T. According to the First Law of Thermodynamics the amounts of energy absorbed and emitted by Σ_0 are equal. We have then the equation

$$\sigma\int_0^{\infty} E_{\sigma_1}(\lambda)\,d\lambda + H_{21} + \sigma\int_0^{\infty} E_{\sigma_2}(\lambda)\,d\lambda + H_{12} = \tag{10}$$
$$\sigma\int_0^{\infty} A_1(\lambda)\,e_{\sigma_1}(\lambda)\,d\lambda + H_{12} + \sigma\int_0^{\infty} A_2(\lambda)\,e_{\sigma_2}(\lambda)\,d\lambda + H_{21}$$

or

$$\int_0^{\infty} E_{\sigma_1}(\lambda)\,d\lambda + \int_0^{\infty} E_{\sigma_2}(\lambda)\,d\lambda =$$
$$\int_0^{\infty} A_1(\lambda)\,e_{\sigma_1}(\lambda)\,d\lambda + \int_0^{\infty} A_2(\lambda)\,e_{\sigma_2}(\lambda)\,d\lambda. \tag{11}$$

We can at this point deduce that

$$\int_0^{\infty} E_{\sigma_1}(\lambda)\,d\lambda + \int_0^{\infty} E_{\sigma_2}(\lambda)\,d\lambda =$$
$$\int_0^{\infty} A_1(\lambda)\,e_1(\lambda)\,d\lambda + \int_0^{\infty} A_2(\lambda)\,e_2(\lambda)\,d\lambda. \tag{12}$$

For if this equation did not hold, but if, on the other hand, the left hand member were equal to the right hand member plus a quantity ϵ, we could by taking Σ_0 small enough secure a contradiction from equation (11), and the assumption that Δ_{σ_1} and Δ_{σ_2} approach 0 as Σ_0 decreases indefinitely.

If we replace S by any other solid body fulfilling the conditions we get an equation

$$\int^{\infty} E_{\sigma_1}(\lambda)\,d\lambda + \int_0^{\infty} E_{\sigma_2}(\lambda)\,d\lambda =$$
$$\int_0^{\infty} A_1(\lambda)\,e_1'(\lambda)\,d\lambda + \int_0^{\infty} A_2(\lambda)\,e_2'(\lambda)\,d\lambda. \tag{13}$$

The question now arises as to what is the relation among the e's, — $e_1(\lambda)$, $e_2(\lambda)$, $e_1'(\lambda)$, $e_2'(\lambda)$. If the functions $A_1(\lambda)$ and $A_2(\lambda)$ were perfectly arbitrary it could easily be shown that all the functions $e(\lambda)$ are identical; but we have no right to make such an assumption.[4]

---

[4] See page 104. This is in fact the assumption in the proof of E. Pringsheim.

The principal difficulty of the proof lies precisely in this step. The purpose is to make as modest a requirement as possible for the function $A(\lambda)$. We shall assume that there exist, or can be constructed, physical bodies such that the resulting assemblage of absorption coefficients is what we may call densely distributed between some two absorption coefficients that are distinct for every value of λ. We define densely distributed as follows :

Let $A'(\lambda)$ and $A''(\lambda)$ be two functions positive or zero and continuous for all positive values of λ. Let $f(\lambda)$ be any function finite and continuous for all positive values of λ, such that

$$A'(\lambda) \geqq f(\lambda) \geqq A''(\lambda), \qquad \lambda > 0,$$

or

$$A'(\lambda) \leqq f(\lambda) \leqq A''(\lambda), \qquad \lambda > 0,$$

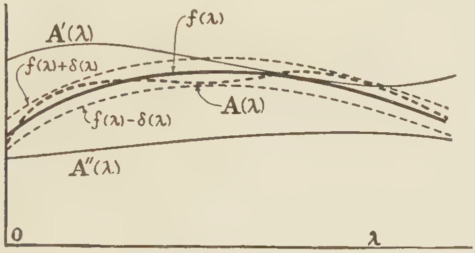

Figure 2.

and let δ be any quantity > 0. We say then that the functions $A(\lambda)$ are densely distributed between $A'(\lambda)$ and $A''(\lambda)$ provided that no matter what $f(\lambda)$ and δ are taken, there is an $A(\lambda)$ such that

$$|f(\lambda) - A(\lambda)| \leqq \delta, \quad 0 < \lambda.$$

We shall assume that $A_1(\lambda)$ and $A_2(\lambda)$ are independently densely distributed between two functions $A_1'(\lambda)$ and $A_1''(\lambda)$, and two functions $A_2'(\lambda)$ and $A_2''(\lambda)$ respectively, where

$$A_1''(\lambda) > A_1'(\lambda), \quad 0 < \lambda,$$

and

$$A_2''(\lambda) > A_2'(\lambda), \quad 0 < \lambda.$$

Suppose now that $e_1'(\lambda) \neq e_1(\lambda)$ at some value

$$\lambda = \lambda_0, \quad 0 < \lambda_0.$$

It will then be unequal to $e_1(\lambda)$ throughout a small neighborhood $\lambda_1 \leqq \lambda \leqq \lambda_2$, — let us say that $e_1'(\lambda) - e_1(\lambda) > \epsilon > 0$ throughout the interval.

Now if we subtract (12) from (13) we have

$$\int_0^\infty A_1(\lambda)\,[e_1'(\lambda) - e_1(\lambda)]\,d\lambda + \int_0^\infty A_2(\lambda)\,[e_2'(\lambda) - e_2(\lambda)]\,d\lambda = 0. \quad (14)$$

In particular we have

$$\int_0^\infty A_1'(\lambda)\,[e_1'(\lambda) - e_1(\lambda)]\,d\lambda + \int_0^\infty A_2'(\lambda)\,[e_2'(\lambda) - e_2(\lambda)]\,d\lambda = 0,$$

whence

$$\int_0^\infty [A_1(\lambda) - A_1'(\lambda)]\,[e_1'(\lambda) - e_1(\lambda)]\,d\lambda + \int_0^\infty [A_2(\lambda) - A_2'(\lambda)]\,[e_2'(\lambda) - e_2(\lambda)]\,d\lambda = 0. \quad (15)$$

On account of the freedom of choice for $A_1(\lambda)$ and $A_2(\lambda)$ we can now get a contradiction out of (15). For we can choose $A^1(\lambda)$ in reference to $A_1'(\lambda)$ and $A_2(\lambda)$ in reference to $A_2'(\lambda)$ in such a way that the only significant part of the integrals in (15) will be

$$\int_{\lambda_1}^{\lambda_2} [A_1(\lambda) - A_1'(\lambda)]\,[e_1'(\lambda) - e_1(\lambda)]\,d\lambda,$$

which can be made unequal to zero. But this contradicts (15). Hence $e_1'(\lambda_0) = e_1(\lambda_0)$ and $e_1'(\lambda) \equiv e_1(\lambda)$.

And not only for every body S but also for every position of Σ_0 in the cavity is $e_1'(\lambda) \equiv e_1(\lambda)$. For different positions of Σ_0 can be regarded as the same position of Σ_0 with different S. Hence in particular $e_1(\lambda) = e_2(\lambda)$. We have then the theorem that the character of the radiation impinging on either face of any element of surface σ anywhere in the cavity S is a function merely of the temperature of the cavity and the nature of the medium in which the element of surface is immersed.

If we denote the function $e_1(\lambda) = e_2(\lambda)$ by $e(\lambda)$, we may call $e(\lambda)$ perfectly black radiation. It is approximately the radiation emitted through a hole of unit area in the bounding surface of a large cavity whose interior walls are kept at the uniform temperature T.

We can now easily prove Kirchhoff's Law. Suppose that in the cavity S we have any body K, enclosed by a surface S, just outside the surface of K. A surface S_1' is assumed outside S_1; between K and S_1' there is an arbitrary medium. K itself may be solid, liquid or gaseous, though if K is liquid or gaseous the medium in which it is enclosed must be solid. We have then, at the temperature T,

$$\iint_{(S_1)} E(\lambda)\,dS_1 + \iint_{(S_1)} [1-A(\lambda)]\,e(\lambda)\,dS_1 = \iint_{(S_1)} e(\lambda)\,dS_1 \tag{17}$$

since the amount of radiation of wave length λ reaching any element of surface dS, *from either side* is $e(\lambda)$.

Hence

$$\iint_{(S_1)} E(\lambda)\,dS_1 = \iint_{(S_1)} A(\lambda)\,e(\lambda)\,dS_1, \tag{18}$$

which is an expression of Kirchhoff's Law. The expression looks more natural if we denote by $\bar{A}(\lambda)$

$$\bar{A}(\lambda) = \frac{\iint_{(S_1)} A(\lambda)\,e(\lambda)\,dS_1}{\iint_{(S_1)} e(\lambda)\,dS_1};$$

we then have

$$\iint_{(S_1)} E(\lambda)\,dS_1 = \bar{A}(\lambda) \iint_{(S_1)} e(\lambda)\,dS_1. \tag{19}$$

If the $E(\lambda)$ is a function of the element of surface only, we can by taking a spherical K of the material under investigation deduce from symmetry that

$$E(\lambda) = A(\lambda)\,e(\lambda).$$

Discussion of the Assumptions.

On page 99 certain assumptions are made in regard to the functions $\delta_{\sigma_1}(\lambda)$ and $\delta_{\sigma_2}(\lambda)$,— namely, that as the body Σ_0 decreases in size, $\delta_{\sigma_1}(\lambda)$ and $\delta_{\sigma_2}(\lambda)$ approach zero as a limit in such a way that

$$\Delta_{\sigma_1} = \int_0^\infty |\,\delta_{\sigma_1}(\lambda)\,|\,d\lambda$$

and

$$\Delta_{\sigma_2} = \int_0^\infty |\,\delta_{\sigma_2}(\lambda)\,|\,d\lambda$$

both approach zero. This amounts in effect to assuming that

$\sigma(\Delta_{\sigma_1} + \Delta_{\sigma_2})$, the difference in the radiation reaching the surface Σ_0 when there is and when there is not a different material in Σ_0 from the medium between Σ_0 and Σ_1, is an infinitesimal of the second order. This supposition seems more reasonable than it really is.

For let us suppose, if it is possible, that the body *S* is composed of a material which emits and absorbs only a partial spectrum, i.e. there are wave lengths for which *S* emits and absorbs no energy. With no body Σ_0 and ether for the medium throughout, the radiation $e(\lambda)$ reaching any element of surface within the cavity will not contain energy of these wave lengths which the body *S* does not emit. But if we insert a body Σ_0, however small, which has a complete spectrum, the energy of the forbidden wave lengths will build up until it reaches such intensity that the amount absorbed by the small body Σ_0 will be equal to the amount emitted by it. Since both of these quantities will therefore be infinitesimals of the first order, $\delta_1(\lambda)$ and $\delta_2(\lambda)$ will not approach zero at all as Σ_0 decreases in size.

We cannot therefore regard the invariance of the function $e(\lambda)$ as itself a statement of the non-existence of bodies of partial spectra.[5] For that invariance depends upon the assumption that Δ_{σ_1} and Δ_{σ_2} approach zero as Σ_0 becomes smaller and smaller, and hence gives no contradiction when *S* is a body of partial spectrum.

However, bodies of partial spectra, if they exist, must satisfy Kirchhoff's Law. For the analysis of pages 101 and 102 applies. And a body that has a partial emission spectrum must have an absorption spectrum extending over precisely the same region of wave lengths; and vice versa.

The second assumption of importance is the supposition that there can be constructed a dense distribution of absorption coefficients between some two distinct functions of λ. This assumption does not by any means demand the existence of an arbitrary absorption coefficient. Indeed the requirements of the proof can be met by a denumerable system[6]. And yet we cannot be certain of the possibility of physically constructing even this denumerable set.

---

[5] See, however, in this connection W. Wien, Annalen d. Physik, **52**, 163, 1894.

[6] That is, a system of the same order of infinity as the natural numbers, or the rational fractions.

If $A'(\lambda)$ and $A''\lambda)$ (see p. 8) have the same limit at ∞, a denumerable set sufficient for the demands of the proof can be set up by requiring that $f(\lambda)$ be continuous with continuously turning tangent (except at a finite number of points), and by replacing, in the definition of density, the two curves $f(\lambda) \pm \delta(\lambda)$ by two curves distant δ from the curve $f(\lambda)$.

Although the present proof depends, indeed, on this assumption of the physical existence of ideal elements, the proof is not completely invalidated by the lack of such a system. There is in this instance the considerable advantage that the existence of even a finite physical system approximately fulfilling the conditions of the postulated ideal system carries with it the approximate fulfilment of the thesis. Kirchhoff's Law is approximately satisfied in any case.

It is worth while noting that, although establishing a particular property of any particular substance, namely that its emission and absorption coefficient must stand in a certain fixed relation, the proof, on account of its nature, holds only in so far as the particular substance is a member of a physical system that contains as a subset the dense system postulated.[7] The properties of the individual are determined by the environment.

Finally there is a third assumption that needs some attention. For on page 103, in deducing equation (17), which holds for any particular value of λ, it is assumed that the wave length of energy is unchanged by reflection. And Kirchhoff's Law will therefore hold for any bodies whose surfaces are such that they do not change wave length by reflection.

In certain cases this assumption about the nature of the body itself is equivalent to a condition on the environment. For if the body under consideration be a member of a dense system of absorption coefficients, the above assumption may be replaced by postulating that a single member of that system be known to obey Kirchhoff's Law. And from this postulate the other, that wave length be unchanged by reflection, may be deduced. The two, though they do not look alike, are in a sense mathematically equivalent.

Conclusion.

The fruitfulness of Kirchhoff's Law depends upon the degree to which the absorption coefficient is invariant in regard to different conditions of the body or its surroundings, i.e., for instance in regard to (1) different temperatures of the absorbing body, and (2) different intensities of radiation reaching the surface from outside [corresponding to different temperatures of the body *S*]. For in general the absorption coefficient has to be measured under one set of conditions when it is desired to apply the results to another set.

---

[7] Some proofs err in assuming the existence of bodies of partial spectra or in attempting to construct them; e. g.: Kirchhoff (1859) and Drude (1900).

In regard to other proofs it may be noted that those of B. Stewart and Prevostaye are not logically complete, and that Kirchhoff's second proof, besides being involved, is not strictly thermodynamic and assumes the existence of bodies with questionable properties.

For detailed references see Kayser's Spectroscopie II, pages 7–31.

Hence it may seem that Kirchhoff's Law holds very well for one set of bodies and very poorly for another set, if the absorption coefficient is regarded as a constant. The preceding analysis shows, however, that carefully stated, the law holds as well for one substance as another, as well for gases and liquids as for solids.

In closing I should like to acknowledge my indebtedness to Professor G. W. Pierce of Harvard University for helpful criticism.

Jefferson Physical Laboratory,
Harvard University,
Cambridge, Mass.

Proceedings of the American Academy of Arts and Sciences.

Vol. XLVI. No. 7. — October, 1910.

CONTRIBUTIONS FROM THE RESEARCH LABORATORY OF
PHYSICAL CHEMISTRY OF THE MASSACHUSETTS
INSTITUTE OF TECHNOLOGY. — No. 58.

ON FOUR-DIMENSIONAL VECTOR ANALYSIS, AND ITS APPLICATION IN ELECTRICAL THEORY.

By Gilbert N. Lewis.

CONTRIBUTION FROM RESEARCH LABORATORY OF PHYSICAL CHEMISTRY OF THE MASSACHUSETTS INSTITUTE OF TECHNOLOGY.—No. 58.

ON FOUR-DIMENSIONAL VECTOR ANALYSIS, AND ITS APPLICATION IN ELECTRICAL THEORY.

By Gilbert N. Lewis.

Received June 28, 1910.

The great generalization of Einstein, known as the principle of relativity, and its interpretation by Minkowski, have opened a new domain of natural science. The apparent artificiality and paradox of some of the consequences of the relativity theory disappear completely when with Minkowski we regard the science of kinematics as identical with the geometry of four-dimensional space.

Minkowski[1] and, following him, Abraham[2] have made an important beginning in the use of four-dimensional vector analysis. In general, however, Minkowski used for his more important deductions, not the vectorial method, but the matrix calculus of Cayley. This was undoubtedly due to the restricted and specialized character of our present vector analysis, for the vector method, permitting as it does a ready survey, and often a visualization of the results to which it leads, has shown its superiority over all other methods in several branches of physics, and there can be no doubt that it is also peculiarly well adapted to the solution of the new problems introduced by Minkowski.

I shall attempt to show in this paper what simple changes must be made in our present system of vector analysis to make it immediately adaptable to a space of higher dimensions. Only such changes will be made as are imperatively demanded by the nature of the problem, and these few changes will, I believe, recommend themselves, not only because of the increased generality of the resulting analysis, but because they restore many features of the original, and much neglected, system of Grassmann.[3]

---

[1] Göttingen, Nachricht., 1908, p. 53.

[2] Rendiconti di Palermo, **30**, 1 (1910).

[3] References to Grassmann will be to the edition of 1894, Teubner, Leipzig.

In the second section several of the most useful formulae of four-dimensional vector analysis will be presented, and the last section will be devoted to some applications of these formulae in electromagnetic theory and the theory of relativity.

The Vector Analysis of Three Dimensions.

The simplest type of quantity which is distinguished from others of its class by magnitude and direction is the familiar line-vector, a one-dimensional quantity which we shall call a vector of the first order, or in brief, a 1-vector.

Just as two parallel line-vectors of the same length are regarded as equal, so two parallel plane surfaces of the same area are also considered equal. A plane area[4] constitutes a vector of the second order, or a 2-vector.

In general in a space of n dimensions we may distinguish 0-vectors or scalars; 1-vectors, 2-vectors, 3-vectors, etc., up to the n-vectors, which, like the 0-vectors, have no direction and may therefore be called pseudo-scalars.

In three-dimensional space the only true vectors which exist are 1-vectors and 2-vectors. Moreover, every 2-vector determines uniquely the 1-vector normal to it. In common vector analysis the 2-vector is regarded as equivalent to and replaceable by its normal 1-vector of the same magnitude, and therefore this analysis deals solely with 1-vectors. This simplification has certain obvious advantages which, however, are for the most part superficial. In some cases moreover it leads to difficulties.[5] In any case it must be abandoned when we pass to space of higher dimensions, where a 2-vector no longer uniquely determines a 1-vector.

Our first departure, then, from common vector analysis will consist in distinguishing between vectors of different orders. A 1-vector will be represented by a small letter in heavy type (e. g., **a**, **s**). A 2-vector will be represented by a capital letter in heavy type (e. g., **A**, **S**).

---

[4] For simplicity we may deal only with the straight vectors (straight line, plane surface, etc.) since any curve terminating in two points may be regarded as equivalent to the straight line terminating in the same points, and a curved surface terminating in a *plane* closed curve, as equivalent to the plane area having the same boundary. Such a vector as a curved surface bounded by a closed curve which does not lie in a plane we shall not consider here.

[5] See, for example, the discussion of scalars and pseudo-scalars in Abraham-Föppl, Theorie der Elektrizität, p. 22–23. We shall have frequent occasion to cite this standard work, which contains an admirable presentation of the current system of vector analysis, as well as of electrical theory. References are to the edition of 1904 (Teubner, Leipzig).

Let us consider a coördinate system of three perpendicular axes, x_1, x_2, x_3, and represent by $\mathbf{k}_1$, $\mathbf{k}_2$, $\mathbf{k}_3$, the three unit vectors in these three directions. If the lengths of the components of a 1-vector **a** on the three axes are a_1, a_2, a_3, then

$$\mathbf{a} = a_1\mathbf{k}_1 + a_2\mathbf{k}_2 + a_3\mathbf{k}_3. \qquad (1)$$

In general the addition and subtraction of 1-vectors follow the law.[6]

$$\mathbf{a} \pm \mathbf{b} = (a_1 \pm b_1)\,\mathbf{k}_1 + (a_2 \pm b_2)\,\mathbf{k}_2 + (a_3 \pm b_3)\,\mathbf{k}_3. \qquad (2)$$

Similarly we may project a surface vector, or 2-vector, upon the three coördinate planes determined by x_1, x_2; x_1, x_3; x_2, x_3. The unit 2-vectors in these planes we will denote by $\mathbf{k}_{12}$, $\mathbf{k}_{13}$, $\mathbf{k}_{23}$,[7] and the areas of the projections of a 2-vector **A** by A_{12}, A_{13}, A_{23}. Then,

$$A = A_{12}\mathbf{k}_{12} + A_{13}\mathbf{k}_{13} + A_{23}\mathbf{k}_{23} \qquad (3)$$

$$A \pm B = (A_{12} \pm B_{12})\,k_{12} + (A_{13} \pm B_{13})\,k_{13} + (A_{23} \pm B_{23})\,k_{23}. \qquad (4)$$

Further we may adopt the convention,

$$\mathbf{k}_{12} = -\,\mathbf{k}_{21}\,;\ \mathbf{k}_{13} = -\,\mathbf{k}_{31}\,;\ \mathbf{k}_{23} = -\,\mathbf{k}_{32} \qquad (5)$$

which requires the further convention,

$$A_{12} = -\,A_{21}\,;\ A_{13} = -\,A_{31}\,;\ A_{23} = -\,A_{32}. \qquad (6)$$

Just as $\mathbf{k}_1$ represents a vector of unit length, $\mathbf{k}_{12}$ one of unit area, $\mathbf{k}_{123}$ will represent unit volume. It is the unit 3-vector or, in three-dimensional space, the unit pseudo-scalar. We shall adopt the convention

$$\mathbf{k}_{123} = \mathbf{k}_{312} = \mathbf{k}_{231} = -\,\mathbf{k}_{132} = -\,\mathbf{k}_{213} = -\,\mathbf{k}_{321}. \qquad (7)$$

Equations (5) and (7) may be expressed in the following general rule which we shall also adopt in space of higher dimensions: Interchanging any two adjacent subscripts of a unit vector changes the sign of the vector.

---

[6] The addition both of 1-vectors and 2-vectors is best defined geometrically. (See Grassmann, Ausdehnungslehre von 1844, p. 78.) The introduction of coördinate axes brings a foreign element into pure vector analysis, but on the other hand it will permit us to translate the vector equations more readily into Cartesian equations.

[7] In this case we depart from our rule that 2-vectors shall be represented by capital letters. On account of the subscripts there will be no confusion.

Multiplying any vector by a scalar, multiplies its magnitude by that scalar. Multiplication of a vector by a scalar follows the laws of association, commutation and distribution.

$$m\mathbf{a} = ma_1\mathbf{k}_1 + ma_2\mathbf{k}_2 + ma_3\mathbf{k}_3 \tag{8}$$

In multiplying one vector by another two kinds of product are to be distinguished, which, following Grassmann, we shall call the inner and outer products,[8] and define as follows.

The inner product follows the distributive and commutative laws. It is in general a vector and its order is the difference between the orders of the factors. (Thus the inner product of two 1-vectors is a 0-vector, or scalar, the inner product of a 1-vector and a 2-vector is a 1-vector.)

The outer product follows the distributive and associative laws. It is a vector of which the order is the sum of the orders of the factors. (Thus the outer product of two 1-vectors is a 2-vector, that of a 1-vector and a 2-vector is a 3-vector, which in three-dimensional space is a pseudo-scalar.)

The inner product of two vectors will be indicated merely by their juxtaposition, for example, **ab** ; **AB** ; **aA**.

The outer product will be indicated by a cross[9] placed between two vectors, for example, $\mathbf{a}\times\mathbf{b}$; $\mathbf{A}\times\mathbf{B}$; $\mathbf{a}\times\mathbf{A}$.

Since both kinds of products follow the distributive law they may be completely defined by the rules governing the multiplication of the simple unit vectors. The rules for inner multiplication are as follows,

$$\left.\begin{array}{rl}
\mathbf{k}_1\mathbf{k}_1 = 1\,; & \mathbf{k}_1\mathbf{k}_2 = \mathbf{k}_2\mathbf{k}_1 = 0 \\
\mathbf{k}_{12}\mathbf{k}_{12} = 1\,; & \mathbf{k}_{12}\mathbf{k}_{13} = \mathbf{k}_{13}\mathbf{k}_{12} = 0 \\
\mathbf{k}_{123}\mathbf{k}_{123} = 1\,; & \\
\mathbf{k}_2\mathbf{k}_{12} = \mathbf{k}_{12}\mathbf{k}_2 = \mathbf{k}_1\,; & \mathbf{k}_1\mathbf{k}_{23} = \mathbf{k}_{23}\mathbf{k}_1 = 0 \\
\mathbf{k}_3\mathbf{k}_{123} = \mathbf{k}_{123}\mathbf{k}_3 = \mathbf{k}_{12}\,; & \\
\mathbf{k}_{23}\mathbf{k}_{123} = \mathbf{k}_{123}\mathbf{k}_{23} = \mathbf{k}_1\,; &
\end{array}\right\}. \tag{9}$$

These statements may be generalized, and the following rules will hold also for unit vectors mutually perpendicular, in space of any dimensions :

---

[8] The terms scalar product and vector product would obviously be misnomers in the present system.

[9] This symbol for the outer product is used by Gibbs and his followers (see Gibbs, Collected Papers; Wilson-Gibbs, Vector Analysis: Coffin, Vector Analysis), and has several advantages over the more awkward square brackets [a, b] frequently used to express the outer product. The brackets were used by Grassmann, but had a far more general significance than the product defined above. (Ausdehnungslehre von 1862, p. 28.)

If each factor has a subscript which the other has not, the inner product is zero.

The inner product of two identical unit vectors is equal to unity.

In the remaining case, one factor having a higher order than the other, the subscripts of the former should be transposed until those subscripts occurring at the right are the same and in the same sequence as in the factor of lower order. These common subscripts are then cancelled and a unit vector with the remaining subscripts, in the sequence in which they stand, forms the inner product. Thus for example,

$$\mathbf{k}_{13}\mathbf{k}_{123} = -\,\mathbf{k}_{13}\mathbf{k}_{213} = -\,\mathbf{k}_{2}.$$

From these rules we obtain immediately the equations,

$$\mathbf{ab} = a_1b_1 + a_2b_2 + a_3b_3. \tag{10}$$

$$\mathbf{aa} = \mathbf{a}^2 = a_1{}^2 + a_2{}^2 + a_3{}^2. \tag{11}$$

$$\mathbf{AB} = A_1B_1 + A_2B_2 + A_3B_3. \tag{12}$$

These products are scalars. On the other hand the product **aA** is a 1-vector lying in the plane **A** and perpendicular to the projection of **a** upon **A**, namely,

$$\mathbf{aA} = \mathbf{Aa} = (A_{12}a_2 + A_{13}a_3)\,\mathbf{k}_1 + (A_{21}a_1 + A_{23}a_3)\,\mathbf{k}_2 + (A_{31}a_1 + A_{32}a_2)\,\mathbf{k}_3. \tag{13}$$

Finally, the product of a pseudo-scalar and a 1-vector is the perpendicular 2-vector, that of a pseudo-scalar and a 2-vector is the perpendicular 1-vector, the product in each case having a magnitude equal to the product of the magnitudes of the factors.

The rules for outer multiplication may likewise be stated by stating the rules for the unit vectors.

$$\begin{gathered}\mathbf{k}_1\times\mathbf{k}_2 = \mathbf{k}_{12}\,;\ \mathbf{k}_1\times\mathbf{k}_{23} = \mathbf{k}_{12}\times\mathbf{k}_3 = \mathbf{k}_{123},\\ \mathbf{k}_1\times\mathbf{k}_1 = 0\,;\ \mathbf{k}_1\times\mathbf{k}_{12} = 0\,;\ \mathbf{k}_{12}\times\mathbf{k}_{12} = 0\,;\ \mathbf{k}_{12}\times\mathbf{k}_{13} = 0\,;\\ \mathbf{k}_1\times\mathbf{k}_{123} = 0\,;\ \mathbf{k}_{12}\times\mathbf{k}_{123} = 0\,;\ \mathbf{k}_{123}\times\mathbf{k}_{123} = 0.\end{gathered} \tag{14}$$

These statements may be generalized and the following rules will hold also for unit, mutually perpendicular, vectors in space of any dimensions :

If two unit vectors possess any subscript in common, their outer product is zero.

In all other cases the outer product is a unit vector having all the subscripts of both factors, in the sequence in which they occur in the factors.

From these rules[10] we obtain the equations,

$$\mathbf{a}\times\mathbf{a} = 0. \tag{15}$$

$$\mathbf{a}\times\mathbf{b} = -\,\mathbf{b}\times\mathbf{a} = (a_1b_2 - a_2b_1)\,\mathbf{k}_{12} + (a_1b_3 - a_3b_1)\,\mathbf{k}_{13} + (a_2b_3 - a_3b_2)\,\mathbf{k}_{23}. \tag{16}$$

$$\mathbf{a}\times\mathbf{A} = \mathbf{A}\times\mathbf{a} = (a_1A_{23} + a_2A_{31} + a_3A_{12})\,\mathbf{k}_{123}. \tag{17}$$

When the 2-vector in (17) is expressed as a product of two 1-vectors, $\mathbf{b}\times\mathbf{c}$, that equation becomes

$$\mathbf{a}\times(\mathbf{b}\times\mathbf{c}) = (\mathbf{a}\times\mathbf{b})\times\mathbf{c} = \mathbf{a}\times\mathbf{b}\times\mathbf{c} = \begin{vmatrix} a_1 & a_2 & a_3 \\ b_1 & b_2 & b_3 \\ c_1 & c_2 & c_3 \end{vmatrix}\,\mathbf{k}_{123}. \tag{18}$$

$$\text{and } \mathbf{a}\times(\mathbf{a}\times\mathbf{b}) = 0. \tag{18a}$$

We thus see that $\mathbf{a}\times\mathbf{b}$ represents the parallelogram determined by $\mathbf{a}$ and $\mathbf{b}$, and $\mathbf{a}\times\mathbf{b}\times\mathbf{c}$ the parallelopiped determined by $\mathbf{a}$, $\mathbf{b}$ and $\mathbf{c}$.

It is important at this point to rewrite equation (13) using $\mathbf{b}\times\mathbf{c}$ in place of $\mathbf{A}$; expanding and rearranging the terms gives

$$\mathbf{a}\,(\mathbf{b}\times\mathbf{c}) = \mathbf{a}\mathbf{b}\times\mathbf{c}\,^{11} = (\mathbf{a}\mathbf{c})\,\mathbf{b} - (\mathbf{a}\mathbf{b})\,\mathbf{c}. \tag{19}$$

These equations (18) and (19) deserve especial attention, for they show the only essential difference between our system and the common system of vector analysis. The two systems give the same result for the outer multiplication of two 1-vectors and for the inner product of two 1-vectors or two 2-vectors. But the meanings of the outer and inner products of $\mathbf{a}$ and $\mathbf{b}\times\mathbf{c}$ are just reversed in the two systems.

Finally we find from our rules for unit vectors the outer product of two 2-vectors,

$$\mathbf{A}\times\mathbf{B} = 0. \tag{20}$$

By our general principle the outer product must in this case have the order 2 + 2, and a 4-vector cannot exist in three-dimensional space.[12]

---

[10] The rules here given are somewhat redundant. For example, the distributive law, and $\mathbf{a}\times\mathbf{a} = 0$, alone suffice to prove $\mathbf{a}\times\mathbf{b} = -\,\mathbf{b}\times\mathbf{a}$, for

$$(a + b) \times (a + b) = 0 = \mathbf{a}\times\mathbf{a} + \mathbf{b}\times\mathbf{b} + \mathbf{a}\times\mathbf{b} + \mathbf{b}\times\mathbf{a} = \mathbf{a}\times\mathbf{b} + \mathbf{b}\times\mathbf{a}.$$

See Grassmann, Ausdehnungslehre von 1844, p. 87.

[11] The parentheses may be removed simply because $(\mathbf{a}\mathbf{b}) \times \mathbf{c}$ has no meaning.

[12] In ordinary vector analysis a meaning is given to the outer product of $(\mathbf{a}\times\mathbf{b})$ and $(\mathbf{c}\times\mathbf{d})$. It represents a vector determined by the line of intersection of the surface $\mathbf{a}\times\mathbf{b}$ and $\mathbf{c}\times\mathbf{d}$. We have seen that in n-dimensional space an n-vector has some properties of a scalar or vector of the order n–n. So we may modify our rules of multiplication so that the product of a p-vector and a

The inner product of $(\mathbf{a}\times\mathbf{b})$ and $(\mathbf{c}\times\mathbf{d})$ may be obtained from the preceding equations, and is the same as in ordinary vector analysis,

$$(\mathbf{a}\times\mathbf{b})\,(\mathbf{c}\times\mathbf{d}) = (\mathbf{ac})\,(\mathbf{bd}) - (\mathbf{bc})\,(\mathbf{ad}). \tag{21}$$

The differential operator ∇ ("del") we may define in the usual way,[13] namely,

$$\nabla = \mathbf{k}_1 \frac{\partial}{\partial x_1} + \mathbf{k}_2 \frac{\partial}{\partial x_2} + \mathbf{k}_3 \frac{\partial}{\partial x_3}. \tag{22}$$

Since the scalar operator $\frac{\partial}{\partial x}$, when applied to a single variable, can be treated as an algebraic quantity, the operator ∇ may be treated formally as a 1-vector, and we may derive a number of important equations by substituting ∇ for $\mathbf{a}$ or $\mathbf{b}$ in the preceding equations. Thus from (8) we obtain from the scalar ϕ the function known as gradient of ϕ

$$\nabla\phi = \mathbf{k}_1 \frac{\partial\phi}{\partial x_1} + \mathbf{k}_2 \frac{\partial\phi}{\partial x_2} + \mathbf{k}_3 \frac{\partial\phi}{\partial x_3}. \tag{23}$$

Combined with a 1-vector by inner and outer multiplication we obtain by equations (10) and (16), the functions known as the divergence and curl, respectively.

$$\nabla\mathbf{a} = \frac{\partial a_1}{\partial x_1} + \frac{\partial a_2}{\partial x_2} + \frac{\partial a_3}{\partial x_3}. \tag{24}$$

$$\nabla\times\mathbf{a} = \left(\frac{\partial a_2}{\partial x_1} - \frac{\partial a_1}{\partial x_2}\right)\mathbf{k}_{12} + \left(\frac{\partial a_3}{\partial x_1} - \frac{\partial a_1}{\partial x_3}\right)\mathbf{k}_{13} + \left(\frac{\partial a_3}{\partial x_2} - \frac{\partial a_2}{\partial x_3}\right)\mathbf{k}_{23}. \tag{25}$$

Evidently $\nabla\phi$ is a 1-vector, $\nabla\mathbf{a}$ a scalar, and $\nabla\times\mathbf{a}$ a 2-vector.

By equations (13) and (17) we may write expressions for $\nabla\mathbf{A}$ (a 1-vector), and $\nabla\times\mathbf{A}$ (a 3-vector, or pseudo scalar).

---

q-vector, when $p + q > n$, is a vector of the order $p + q - n$. Such a product, which Grassmann calls "regressive," is formed according to a new set of rules and may best be regarded as a new type of product entirely distinct from the regular or "progressive" outer product. It is possible in the system here described to avoid the introduction of this new kind of product. Thus

$$((\mathbf{a}\times\mathbf{b})\,\mathbf{k}_{123}) \times (\,(\mathbf{c}\times\mathbf{d}\,\mathbf{k}_{123}) \;=\; \mathbf{e}\mathbf{k}_{123}),$$

where $\mathbf{e}$ is the 1-vector obtained in the ordinary vector analysis as the outer product of $(\mathbf{a}\times\mathbf{b})$ and $(\mathbf{c}\times\mathbf{d})$.

[13] Like other vector quantities and operators ∇ may be simply defined without reference to coördinates. See, for example, Wilson, Bull. Amer. Math. Soc. (2) **16**, 415 (1910).

$$\nabla \mathbf{A} = \left(\frac{\partial A_{12}}{\partial x_2} + \frac{\partial A_{13}}{\partial x_3}\right)\mathbf{k}_1 + \left(\frac{\partial A_{21}}{\partial x_1} + \frac{\partial A_{23}}{\partial x_3}\right)\mathbf{k}_2 + \left(\frac{\partial A_{31}}{\partial x_1} + \frac{\partial A_{32}}{\partial x_2}\right)\mathbf{k}_3. \tag{26}$$

$$\nabla \times \mathbf{A} = \left(\frac{\partial A_{23}}{\partial x_1} + \frac{\partial A_{31}}{\partial x_2} + \frac{\partial A_{12}}{\partial x_3}\right)\mathbf{k}_{123}. \tag{27}$$

When the quantity operated upon by ∇ contains two or more variables it may be expanded in terms of its components and these scalar quantities may then be differentiated in the ordinary way. We thus obtain such equations as the following:

$$\nabla\,(\phi\mathbf{a}) = \phi\,(\nabla\mathbf{a}) + \mathbf{a}\,(\nabla\phi), \tag{28}$$

$$\nabla\times(\phi\mathbf{a}) = \phi\,(\nabla\times\mathbf{a}) + (\nabla\phi)\times\mathbf{a}, \tag{29}$$

$$\nabla\times(\mathbf{a}\times\mathbf{b}) = \mathbf{b}\times(\nabla\times\mathbf{a}) - \mathbf{a}\times(\nabla\times\mathbf{b}). \tag{30}$$

By the above rules new operators may be formed from ∇ such as $\mathbf{a}\nabla$, $\mathbf{A}\nabla$, and $\nabla\,\nabla$ or ∇^2 which may be applied to any scalar or vector. The last is the well-known Laplacian operator and may obviously be expanded by equation (11),

$$\nabla^2 = \frac{\partial^2}{\partial x_1^2} + \frac{\partial^2}{\partial x_2^2} + \frac{\partial^2}{\partial x_3^2}. \tag{31}$$

Other operations involving ∇ twice are $\nabla(\nabla\mathbf{a})$ and $\nabla(\nabla\times\mathbf{a})$ or $\nabla\,\nabla\times\mathbf{a}$.

These quantities are connected by an important equation which we obtain by expanding according to (13), (23) and (10), namely

$$\nabla\,\nabla\times\mathbf{a} = \nabla\,(\nabla\mathbf{a}) - \nabla^2\mathbf{a}. \tag{32}$$

Finally we have from (18a) and (15) the important identities,

$$\nabla\times(\nabla\times\mathbf{a}) = 0. \tag{33}$$

$$\nabla\times(\nabla\phi) = 0. \tag{34}$$

Equations (32), (33) and (34) are evidently equivalent to the familiar equations:[14]

$$\begin{aligned} &\text{curl}^2\,\mathbf{a} = \text{grad}\,(\text{div}\,\mathbf{a}) - \nabla^2\mathbf{a},\\ &\text{div curl}\,\mathbf{a} = 0.\\ &\text{curl grad}\,\phi = 0. \end{aligned}$$

---

[14] Abraham-Föppl, 1, equations 95, 94, 91 a.

Here as elsewhere our equations differ from those in common use whenever the product of a 1-vector and a 2-vector is concerned.

The Vector Analysis of Four Dimensions.

The revised system of three-dimensional vector analysis has been elaborated somewhat fully in the preceding section, since the methods there adopted may be used without any modification in developing the vector analysis of space of higher dimensions.

Let us consider a four-dimensional space in which any two points uniquely determine a straight line, any three points not in a line uniquely determine a plane, and any four points not in a plane uniquely determine a straight or Euclidean 3-space. This may be called a Euclidean four-dimensional space.

In such a space let us construct four mutually perpendicular coördinate axes, x_1, x_2, x_3, x_4. The 1-vectors of unit length in these four directions we may call $\mathbf{k}_1$, $\mathbf{k}_2$, $\mathbf{k}_3$, $\mathbf{k}_4$. Each pair of axes determines a plane, thus forming six coördinate planes. The 2-vectors of unit area parallel to these planes we may call $\mathbf{k}_{12}$, $\mathbf{k}_{13}$, $\mathbf{k}_{14}$, $\mathbf{k}_{23}$, $\mathbf{k}_{24}$, $\mathbf{k}_{34}$. These six planes are mutually perpendicular. Moreover the plane $\mathbf{k}_{12}$ is *completely* perpendicular to the plane $\mathbf{k}_{34}$, in the sense that every line in $\mathbf{k}_{12}$ is perpendicular to every line in $\mathbf{k}_{34}$. The same is true of the pairs $\mathbf{k}_{23}$, $\mathbf{k}_{14}$, and $\mathbf{k}_{13}$, $\mathbf{k}_{24}$.

Each set of three axes determines a straight 3-space and the four coördinate 3-spaces thus determined may be represented by the unit 3-vectors $\mathbf{k}_{123}$, $\mathbf{k}_{124}$, $\mathbf{k}_{134}$, $\mathbf{k}_{234}$. Finally all four axes together determine the unit 4-vector or pseudo-scalar, $\mathbf{k}_{1234}$.

A 1-vector may be represented as the sum of its projections on the four axes,

$$\mathbf{a} = a_1\mathbf{k}_1 + a_2\mathbf{k}_2 + a_3\mathbf{k}_3 + a_4\mathbf{k}_4. \tag{35}$$

A 2-vector may be represented as the sum of its projections on the six coördinate planes.

$$\mathbf{A} = A_{12}\mathbf{k}_{12} + A_{13}\mathbf{k}_{13} + A_{14}\mathbf{k}_{14} + A_{23}\mathbf{k}_{23} + A_{24}\mathbf{k}_{24} + A_{34}\mathbf{k}_{34}. \tag{36}$$

A 3-vector may likewise be represented as the sum of its four projections on the coördinate 3-spaces.[15]

The addition and subtraction of vectors follow the same rules as in the case of three dimensions (equations 2 and 4). Moreover both forms of multiplication are completely defined by the distributive law, and by the rules already given for the transposition of subscripts, and for inner and outer multiplication among the unit vectors. We may therefore write at once a large number of equations, of which some of the more important are the following,

---

[15] We shall not use the 3-vectors often enough in this paper to justify the introduction of a special symbol for them.

$$\mathbf{A}\times\mathbf{B} = \mathbf{B}\times\mathbf{A} = (A_{12}B_{34} + A_{13}B_{24} + A_{14}B_{23} + A_{23}B_{14} + A_{24}B_{13} + A_{34}B_{12})\mathbf{k}_{1234}. \quad (37)$$

$$\mathbf{a}\times\mathbf{A} = \mathbf{A}\times\mathbf{a} = (a_1A_{23} + a_2A_{31} + a_3A_{12})\mathbf{k}_{123} + (a_1A_{24} + a_2A_{41} + a_4A_{12})\mathbf{k}_{124} + (a_1A_{34} + a_3A_{41} + a_4A_{13})\mathbf{k}_{134} + (a_2A_{34} + a_3A_{42} + a_4A_{23})\mathbf{k}_{234}. \quad (38)$$

$$\mathbf{a}\times\mathbf{b} = (a_1b_2 - a_2b_1)\mathbf{k}_{12} + (a_1b_3 - a_3b_1)\mathbf{k}_{13} + \ldots \quad (39)$$

$$\mathbf{a}\times\mathbf{a} = 0. \quad (40)$$

Here also $\mathbf{a}\times\mathbf{b}$ evidently represents the parallelogram determined by $\mathbf{a}$ and $\mathbf{b}$, so $\mathbf{a}\times\mathbf{b}\times\mathbf{c}$ will represent a parallelopiped, and $\mathbf{a}\times\mathbf{b}\times\mathbf{c}\times\mathbf{d}$ a parallel four-dimensional figure. It is very important to observe that all of our four-dimensional vector equations may be given simple geometrical definitions, and retain complete validity whatever set of coördinate axes be arbitrarily chosen.

Some of the more important inner products are the following :

$$\mathbf{ab} = \mathbf{ba} = a_1b_1 + a_2b_2 + a_3b_3 + a_4b_4. \quad (41)$$

$$\mathbf{AB} = \mathbf{BA} = A_{12}B_{12} + A_{13}B_{13} + A_{14}B_{14} + A_{23}B_{23} + A_{24}B_{24} + A_{34}B_{34}. \quad (42)$$

$$\mathbf{aA} = \mathbf{Aa} = (A_{12}a_2 + A_{13}a_3 + A_{14}a_4)\mathbf{k}_1 + (A_{21}a_1 + A_{23}a_3 + A_{24}a_4)\mathbf{k}_2 + \ldots \quad (43)$$

$$(\mathbf{a}\times\mathbf{b})\,(\mathbf{c}\times\mathbf{d}) = (\mathbf{ac})\,(\mathbf{bd}) - (\mathbf{bc})\,(\mathbf{ad}). \quad (44)$$

$$\mathbf{a}\,(\mathbf{b}\times\mathbf{c}) = (\mathbf{ac})\,\mathbf{b} - (\mathbf{ab})\,\mathbf{c}. \quad (45)$$

This is a 1-vector lying in the plane $\mathbf{b}\times\mathbf{c}$ and perpendicular to the projection of $\mathbf{a}$ thereon. So $\mathbf{a}\,(\mathbf{b}\times\mathbf{c}\times\mathbf{d})$ is a 2-vector lying in the 3-space $\mathbf{b}\times\mathbf{c}\times\mathbf{d}$ and perpendicular to the projection of $\mathbf{a}$ on that 3-space ; $(\mathbf{a}\times\mathbf{b})\,(\mathbf{c}\times\mathbf{d}\times\mathbf{e})$ is a 1-vector in the 3-space $\mathbf{c}\times\mathbf{d}\times\mathbf{e}$ and perpendicular to the projection of $\mathbf{a}\times\mathbf{b}$ thereon.

The inner product of any vector with unit pseudo-scalar, $\mathbf{k}_{1234}$, is another vector of the same magnitude which may be called its *complement.* The complement of a scalar is a pseudo-scalar, and vice versa. The complement of a 1-vector is a 3-vector normal to it, and vice versa.

The complement of a 2-vector is the completely perpendicular 2-vector. In the vector analysis at present in use it is customary to identify a vector with its complement, and this is also done by Abraham[16] in the paper in which he makes use of four-dimensional vector analysis. In our present analysis there is no advantage to be gained by this step, which may cause much confusion.

As in the case of three dimensions we may define a differential operator, having the form of a 1-vector, as follows :

$$\Diamond = \mathbf{k}_1 \frac{\partial}{\partial x_1} + \mathbf{k}_2 \frac{\partial}{\partial x_2} + \mathbf{k}_3 \frac{\partial}{\partial x_3} + \mathbf{k}_4 \frac{\partial}{\partial x_4}. \tag{46}$$

This operator[17] $\Diamond$ (read "quad") may be treated like a simple vector under the same conditions as in the case of ∇. We thus obtain a number of important equations such as the following.

$$\Diamond \phi = \mathbf{k}_1 \frac{\partial \phi}{\partial x_1} + \mathbf{k}_2 \frac{\partial \phi}{\partial x_2} + \mathbf{k}_3 \frac{\partial \phi}{\partial x_3} + \mathbf{k}_4 \frac{\partial \phi}{\partial x_4}. \tag{47}$$

$$\Diamond \mathbf{a} = \frac{\partial a_1}{\partial x_1} + \frac{\partial a_2}{\partial x_2} + \frac{\partial a_3}{\partial x_3} + \frac{\partial a_4}{\partial x_4}. \tag{48}$$

$$\Diamond \times \mathbf{a} = \left(\frac{\partial a_2}{\partial x_1} - \frac{\partial a_1}{\partial x_2}\right) \mathbf{k}_{12} + \left(\frac{\partial a_3}{\partial x_1} - \frac{\partial a_1}{\partial x_3}\right) \mathbf{k}_{13} + \dots \tag{49}$$

These three expressions correspond to gradient, divergence and curl in three-dimensional analysis. We may also apply $\Diamond$ to vectors of higher orders, for example, by (43) and (38),

$$\Diamond \mathbf{A} = \left(\frac{\partial A_{12}}{\partial x_2} + \frac{\partial A_{13}}{\partial x_3} + \frac{\partial A_{14}}{\partial x_4}\right) \mathbf{k}_1 + \left(\frac{\partial A_{21}}{\partial x_1} + \frac{\partial A_{23}}{\partial x_3} + \frac{\partial A_{24}}{\partial x_4}\right) \mathbf{k}_2 + \dots \tag{50}$$

$$\Diamond \times \mathbf{A} = \left(\frac{\partial A_{23}}{\partial x_1} + \frac{\partial A_{31}}{\partial x_2} + \frac{\partial A_{12}}{\partial x_3}\right) \mathbf{k}_{123} + \dots \tag{51}$$

We may form other operators like, $\mathbf{A}\Diamond$, a 1-vector operator, and the scalar operators $\mathbf{a}\,\Diamond$, and $\Diamond^2$. The last is the very important operator which Lorentz in a special case calls the d'Alembertian operator,

$$\Diamond^2 = \frac{\partial^2}{\partial x_1^{\,2}} + \frac{\partial^2}{\partial x_2^{\,2}} + \frac{\partial^2}{\partial x_3^{\,2}} + \frac{\partial^2}{\partial x_4^{\,2}}. \tag{52}$$

---

[16] Abraham (loc. cit.).

[17] The operator $\Diamond$ has the same scalar components as the operator *lor* used by Minkowski.

Any of these operators may be applied to a scalar or to a vector of any order.

Two other important operations are connected with $\Diamond^2$ by the formula analogous to (32):

$$\Diamond(\Diamond\times\mathbf{a}) = \Diamond\Diamond\times\mathbf{a} = \Diamond(\Diamond\,\mathbf{a}) - \Diamond^2\mathbf{a}. \tag{53}$$

And we have here also two important identities

$$\Diamond\times(\Diamond\times\mathbf{a}) = 0, \tag{54}$$

$$\Diamond\times(\Diamond\phi) = 0. \tag{55}$$

In the same way that we obtained equations (28), (29), (30), we find

$$\Diamond(\phi\mathbf{a}) = \phi(\Diamond\mathbf{a}) + \mathbf{a}\,(\Diamond\phi), \tag{56}$$

$$\Diamond\times(\phi\mathbf{a}) = \phi\,(\Diamond\times\mathbf{a}) + (\Diamond\phi)\times\mathbf{a}, \tag{57}$$

$$\Diamond\times(\mathbf{a}\times\mathbf{b}) = \mathbf{b}\times(\Diamond\times\mathbf{a}) - \mathbf{a}\times(\Diamond\times\mathbf{b}). \tag{58}$$

These equations will suffice to illustrate how readily the generalized vector analysis of the preceding section may be applied in a space of any dimensions.

SOME APPLICATIONS OF FOUR-DIMENSIONAL VECTOR ANALYSIS IN THE THEORY OF ELECTRICITY.

The principle of relativity as interpreted by Minkowski can be summed up in the statement[18] that a Euclidean four-dimensional space is determined by the coördinates, x, y, z, and ict, where i is the unit of imaginaries, $\sqrt{-1}$; and c is the velocity of light. The whole science of kinematics is merely the geometry of this four-dimensional space. As Minkowski himself has shown, there is no domain in which this new conception is more fruitful than in the science of electricity and magnetism.

Let us consider a system composed of electric charges moving in free space. The density of charge at any point we may call $\frac{\varrho}{c}$ in electromagnetic units, and if we call the velocity of the charge $\mathbf{v}$, then $\frac{\varrho}{c}\mathbf{v}$ represents the current density at a point. This 1-vector $\frac{\varrho}{c}\mathbf{v}$ lies wholly in the 3-space x, y, z.

---

[18] This statement is subject to certain restrictions that we will not discuss.

Following Minkowski we may define a 1-vector, $\mathbf{q}$, in the space x, y, z, ict (or x_1, x_2, x_3, x_4) of which the projection on the 3-space is $\frac{\varrho}{c}\mathbf{v}$ and the scalar component along the x_4 (or ict) axis is $i\varrho$, by the equation,

$$\mathbf{q} = \frac{\varrho}{c}\mathbf{v} + i\varrho\mathbf{k}_4, \tag{59}$$

or

$$\mathbf{q} = \frac{\varrho}{c}v_1\mathbf{k}_1 + \frac{\varrho}{c}v_2\mathbf{k}_2 + \frac{\varrho}{c}v_3\mathbf{k}_3 + i\varrho\mathbf{k}_4. \tag{60}$$

Furthermore, from the electrical force $\mathbf{e}$, and the magnetic force $\mathbf{h}$, we shall find it convenient to define two new 2-vectors, $\mathbf{E}$ and $\mathbf{H}$, by the equations,[19]

$$\mathbf{E} = - i\mathbf{e}\times\mathbf{k}_4, \tag{61}$$

and

$$\mathbf{H} = \mathbf{h}\mathbf{k}_{123}. \tag{62}$$

$\mathbf{H}$ is the 2-vector complementary to $\mathbf{h}$ in the 3-space x, y, z. From these definitions we have

$$H_{12} = h_3\,;\ H_{23} = h_1\,;\ H_{31} = h_2, \tag{63}$$

$$E_{14} = - ie_1\,;\ E_{24} = - ie_2\,;\ E_{34} = - ie_3. \tag{64}$$

From $\mathbf{H}$ and $\mathbf{e}$ we may define[20] the vector potential $\mathbf{a}$ and the scalar potential ϕ by the familiar equations,

$$\mathbf{H} = \nabla\times\mathbf{a}, \tag{65}$$

$$-\mathbf{e} = \nabla\phi + \frac{1}{c}\frac{\partial\mathbf{a}}{\partial t}. \tag{66}$$

Finally we shall define a new 1-vector m by the equation,

$$\mathbf{m} = \mathbf{a} + i\phi\mathbf{k}_4, \tag{67}$$

or

$$\mathbf{m} = a_1\mathbf{k}_1 + a_2\mathbf{k}_2 + a_3\mathbf{k}_3 + i\phi\mathbf{k}_4. \tag{68}$$

Thus m is a vector of which the projection on the 3-space x, y, z is the vector potential, and of which the scalar component in the ict direction is the scalar potential multiplied by $\sqrt{-1}$.

---

[19] Compare in this connection the discussion of $\mathbf{e}$ as a "polar" vector, $\mathbf{h}$ as an "axial" vector, in Abraham-Föppl (1, p. 243).

[20] This definition is evidently not complete, since $\mathbf{a}$ and ϕ are derived from $\mathbf{H}$ and $\mathbf{e}$ by a process of integration. We shall return to this point.

We shall call $\mathbf{m}$ the *fundamental electromagnetic 1-vector*, and show that the four important field equations of Maxwell and Lorentz, as well as other well-known equations, are all contained in the strikingly simple formula,

$$\Diamond\Diamond\times\mathbf{m} = \mathbf{q}. \tag{69}$$

In addition to this equation which states the experimental facts, we have from (54) the important identity

$$\Diamond\times\Diamond\times\mathbf{m} = 0. \tag{70}$$

The quantity $\Diamond\times\mathbf{m}$, which might be called the four-dimensional curl of $\mathbf{m}$, is the fundamental electromagnetic 2-vector.[21] We will give it the symbol $\mathbf{M}$,

$$\Diamond\times\mathbf{m} = \mathbf{M}. \tag{71}$$

Expanding $\Diamond\times\mathbf{m}$ by equation (49) gives

$$\begin{aligned}\mathbf{M} = {} & \mathbf{k}_{12}\left(\frac{\partial a_2}{\partial x_1} - \frac{\partial a_1}{\partial x_2}\right) + \mathbf{k}_{13}\left(\frac{\partial a_3}{\partial x_1} - \frac{\partial a_1}{\partial x_3}\right) + \mathbf{k}_{23}\left(\frac{\partial a_3}{\partial x_2} - \frac{\partial a_2}{\partial x_3}\right) \\ & + \mathbf{k}_{14}\left(\frac{\partial i\phi}{\partial x_1} - \frac{\partial a_1}{\partial x_4}\right) + \mathbf{k}_{24}\left(\frac{\partial i\phi}{\partial x_2} - \frac{\partial a_2}{\partial x_4}\right) + \mathbf{k}_{34}\left(\frac{\partial i\phi}{\partial x_3} - \frac{\partial a_3}{\partial x_4}\right).\end{aligned} \tag{72}$$

The first three terms are evidently equal to the curl of $\mathbf{a}$; the last three may be put in the form

$$\left(i\mathbf{k}_1\frac{\partial\phi}{\partial x_1} + i\mathbf{k}_2\frac{\partial\phi}{\partial x_2} + i\mathbf{k}_3\frac{\partial\phi}{\partial x_3} - \frac{\partial a}{\partial x_4}\right)\times\mathbf{k}_4;$$

and further collecting terms, and writing ict for x_4, gives

$$i\left(\nabla\phi + \frac{1}{c}\frac{\partial\mathbf{a}}{\partial t}\right)\times\mathbf{k}_4.$$

Hence,

$$\mathbf{M} = \nabla\times\mathbf{a} + i\left(\nabla\phi + \frac{1}{c}\frac{\partial\mathbf{a}}{\partial t}\right)\times\mathbf{k}_4, \tag{73}$$

and thus by equations (61), (65) and (66)

$$\mathbf{M} = \mathbf{H} + \mathbf{E}. \tag{74}$$

This equation gives a better idea of the physical significance of the 2-vector $\Diamond\times\mathbf{m}$, or $\mathbf{M}$. $\mathbf{H}$ is a 2-vector lying wholly in the x, y, z 3-space. $\mathbf{E}$ is a 2-vector perpendicular to the x, y, z 3-space in a plane determined by the 1-vectors $\mathbf{e}$ and $\mathbf{k}_4$. We may therefore write,

---

[21] This is the equivalent of the f or F of Minkowski.

$$\mathbf{M} = M_{12}\mathbf{k}_{12} + M_{13}\mathbf{k}_{13} + M_{23}\mathbf{k}_{23} + M_{14}\mathbf{k}_{14} + M_{24}\mathbf{k}_{24} + M_{34}\mathbf{k}_{34},$$

$$= H_{12}\mathbf{k}_{12} + H_{13}\mathbf{k}_{13} + H_{23}\mathbf{k}_{23} + E_{14}\mathbf{k}_{14} + E_{24}\mathbf{k}_{24} + E_{34}\mathbf{k}_{34}. \tag{75}$$

By our fundamental equation (69) we have

$$\diamond\mathbf{M} = \mathbf{q}.$$

Expanding this equation by (50) with the aid of (75) gives four equations

$$\begin{aligned}
\left(\frac{\partial H_{12}}{\partial x_2} + \frac{\partial H_{13}}{\partial x_3} + \frac{\partial E_{14}}{\partial x_4}\right)\mathbf{k}_1 &= \frac{\rho}{c}\, v_1\mathbf{k}_1,\\
\left(\frac{\partial H_{21}}{\partial x_1} + \frac{\partial H_{23}}{\partial x_3} + \frac{\partial E_{24}}{\partial x_4}\right)\mathbf{k}_2 &= \frac{\rho}{c}\, v_2\mathbf{k}_2,\\
\left(\frac{\partial H_{31}}{\partial x_1} + \frac{\partial H_{32}}{\partial x_2} + \frac{\partial E_{34}}{\partial x_4}\right)\mathbf{k}_3 &= \frac{\rho}{c}\, v_3\mathbf{k}_3,\\
\left(\frac{\partial E_{41}}{\partial x_1} + \frac{\partial E_{42}}{\partial x_2} + \frac{\partial E_{43}}{\partial x_3}\right)\mathbf{k}_4 &= \rho\, i\mathbf{k}_4.
\end{aligned} \tag{76}$$

Collecting the first three equations into one, with the aid of (25), (63) and (64), and writing *ict* for x_4 gives

$$\nabla\times\mathbf{h} - \frac{1}{c}\frac{\partial\mathbf{e}}{\partial t} = \frac{\rho}{c}\,\mathbf{v}, \tag{77}$$

and the last equation by (24) and (64) changing E_{41} to $-E_{14}$, etc., gives

$$\nabla\,\mathbf{e} = \rho. \tag{78}$$

By a similar expansion of equation (70)

$$\diamond\times\mathbf{M} = 0,$$

we find with the aid of (49)

$$\nabla\times\mathbf{e} + \frac{1}{c}\frac{\partial\mathbf{h}}{\partial t} = 0, \tag{79}$$

and

$$\nabla\,\mathbf{h} = 0. \tag{80}$$

Equations 77–80, in the more familiar notation, are the well-known equations,

$$\text{curl}\ \mathbf{h} - \frac{1}{c}\frac{\partial\mathbf{e}}{\partial t} = \frac{\rho}{c}\,\mathbf{v}, \tag{α}$$

$$\text{div}\ \mathbf{e} = \rho, \tag{β}$$

$$\text{curl}\ \mathbf{e} + \frac{1}{c}\frac{\partial\mathbf{h}}{\partial t} = 0, \tag{γ}$$

$$\text{div}\ \mathbf{h} = 0. \tag{δ}$$

Let us return to the discussion of the complete definition of the vector **m**. All that we have hitherto said of this vector is comprised in the statement,

$$\Diamond \times \mathbf{m} = \mathbf{E} + \mathbf{H}.$$

It is evident that this equation does not completely define **m**, for in general if **m′** is a vector satisfying the equation

$$\Diamond \times \mathbf{m}' = \mathbf{E} + \mathbf{H},$$

we may superpose upon the field of the vector **m′** the field of another vector **m″** for which

$$\Diamond \times \mathbf{m}'' = 0.$$

Then if $\mathbf{m} = \mathbf{m}' + \mathbf{m}''$, we also have

$$\Diamond \times \mathbf{m} = \mathbf{E} + \mathbf{H}.$$

Suppose now[22] that **m″** be so chosen that at every point in the field

$$\Diamond \mathbf{m}'' = - \Diamond \mathbf{m}'.$$

Then **m** satisfies the two equations,

$$\begin{aligned} \Diamond \times \mathbf{m} &= \mathbf{E} + \mathbf{H}, \\ \Diamond \mathbf{m} &= 0. \end{aligned} \tag{81}$$

We may, therefore, without in any way modifying what has preceded, complete the definition of **m** by the equation (81). This equation combined with (67) gives the well-known expression,

$$\nabla \mathbf{a} + \frac{\partial i\phi}{\partial x_4} = 0, \tag{82}$$

or

$$\operatorname{div} \mathbf{a} + \frac{1}{c}\frac{\partial \phi}{\partial t} = 0.$$[23]

Now by equations (53) and (69),

$$\Diamond \times \mathbf{m} = \Diamond\, (\Diamond \mathbf{m}) - \Diamond^2 \mathbf{m} = \mathbf{q},$$

or by (81)

$$\Diamond^2 \mathbf{m} = - \mathbf{q}. \tag{83}$$

---

[22] This is not offered as a rigorous proof, for we have assumed that a field can be chosen with pre-determined values of $\Diamond \mathbf{m}''$ and $\Diamond \times \mathbf{m}''$.

[23] Abraham-Föppl, II, equation (30).

This is another simple form of our fundamental equation. Substituting for **m** by (67) gives the important equations[24]

$$\nabla^2 \mathbf{a} - \frac{1}{c^2}\frac{\partial^2 \mathbf{a}}{\partial t^2} = -\frac{\rho}{c}\mathbf{v}, \tag{84}$$

$$\nabla^2 \phi - \frac{1}{c}\frac{\partial^2 \phi}{\partial t^2} = -\rho. \tag{85}$$

Let us emphasize once more that all the equations of this section are mere definitions, or purely mathematical deductions, with the sole exception of the one equation which embodies the experimental facts, namely,

$$\Diamond\Diamond\times\mathbf{m} = \mathbf{q}.$$

In conclusion let us consider what is meant by the rotation of the axes in this four-dimensional space. The theory of relativity, as here employed, is equivalent to the statement that our four-dimensional vector equations are invariant in any orthogonal transformation of the axes x, y, z, ict.

The axis ict is characterized by the equation $\frac{\partial x}{\partial t} = \frac{\partial y}{\partial t} = \frac{\partial z}{\partial t} = 0$ and may be regarded as the four-dimensional locus ("Weltlinie") of a point at rest. A straight line, making a small angle with this axis in the plane passing through x and ict, is the locus of a point in uniform motion along the x axis. Taking this line as a new axis (ict') and in place of x, a new axis x', perpendicular to y, z, and ict', we have a new coördinate system in which our fundamental equation (69) retains complete validity. In other words, as Einstein pointed out, the equations of the electromagnetic field remain true, whatever point is arbitrarily chosen as a point of rest.

---

[24] Abraham-Föppl, II, Equations (30 a) and (30 b).

Proceedings of the American Academy of Arts and Sciences.

Vol. XLVI. No. 8. — October, 1910.

CONTRIBUTIONS FROM THE JEFFERSON PHYSICAL LABORATORY, HARVARD UNIVERSITY.

THE RESISTIVITY OF HARDENED CAST IRON AS A MEASURE OF ITS TEMPER AND OF ITS FITNESS FOR USE IN PERMANENT MAGNETS.

By B. Osgood Peirce.

With a Plate.

CONTRIBUTIONS FROM THE JEFFERSON PHYSICAL
LABORATORY, HARVARD UNIVERSITY.

THE RESISTIVITY OF HARDENED CAST IRON AS A MEASURE OF ITS TEMPER AND OF ITS FITNESS FOR USE IN PERMANENT MAGNETS.

By B. Osgood Peirce.

Presented May 11, 1910. Received August 26, 1910.

It has long been known that the specific electrical resistance of a piece of soft tool steel is materially less than that of the same piece after it has been hardened, and that the relaxing of the temper of any piece of steel or iron makes the specific resistance less; but the first systematic study of this phenomenon was made by Messrs. Barus and Strouhal whose work is summarized in Bulletin 14 of the U. S. Geological Survey.[1]

In one experiment which these gentlemen made upon rods of "English Silver" steel, 0.15 cm in diameter and all originally glass-hard, different pieces were tempered by heating them to different fairly high temperatures, as indicated by the oxide tints on their surfaces, and were then cooled. When the specimens thus treated were tested it appeared that the harder the temper, the higher was the specific resistance (s) referred to the centimeter cube, and the lower the temperature coefficient (a) of the specific resistance. In the case of a certain glass-hard rod, s, in microhms, was 45 and a was 0.0016; while in a thoroughly annealed rod of the same lot, s was 16 and a about 0.0040. From these

---

[1] Wiedemann, Lehre von der Elektricität, Vol. I, p. 502; Benoit, Comptes Rendus. **76**, 342 (1873); Matthiessen and Vogt, Pogg. Ann., **122**, 10 (1864); Auerbach, Wied. Ann., **5** (1878); Wied. Ann., **8**, 479 (1879); Callendar, Phil. Trans. 1887; Strouhal and Barus, Wied. Ann., **11**, 976 (1880); Barus, Phil. Mag., **8**, 341 (1879); Chernoff, Vortrag gehalten in der Russischen Technischen Gesellschaft, 1868; Jarolimek, Dingler's Journal, **221**, 436 (1876); Jarolimek and Ackermann, Zeitschrift für das Chemische Grossgewerbe, 1880; Percy-Wedding, Eisenhüttenkunde, II, p. 130, 1864; Karsten, Karsten und von Dechen's Archiv, **25**, 223 (1853); Barus and Strouhal, Bulletin of the United States Geological Survey, No. 14; Caron, Comptes Rendus, **56**, 43 (1863); Barus, Physical Review, **30**, 348 (1910).

TABLE I.

s.	a.	s.	a.
10	0.0050	30	0.0024
12	46	32	22
14	42	34	21
16	39	36	20
18	36	38	19
20	34	40	18
22	32	42	17
24	29	46	16
26	27	50	15
28	26	60	14

and similar experiments, Barus and Strouhal made out a table connecting s and a which they subsequently found to fit other kinds of steel pretty well. Some of their results are given in Table I.

If corresponding values of s and a be used as coördinates, a fairly smooth curve results, and the mean values of 79 for s and 0.0013 for a which Barus and Strouhal got for three pieces of cast iron which they tested, yield a point which seems to lie closely enough upon the prolongation of this curve. It appears also that the values of s and a which Matthiessen, Vogt, and Benoit obtained for different kinds of wrought iron agree numerically with the values for steel; and some persons have thought that it is possible to determine the position of any piece of iron or steel in the scale of mechanical hardness, without any knowledge of the percentage of combined carbon, by finding s alone.

For bar magnets or for simple bent magnets, fine tool steel, or better, some of the kinds of special magnet steel, serve very well, but if a permanent magnet is required of such a shape that the steel has to be heated red hot a number of times during the process of forging and before it is made glass-hard, irregular temper thus introduced into the material often shows itself in the presence of irregular magnetization when the magnet is finally charged, and this sometimes makes the magnet worthless. For this and other reasons, some makers of electrical instruments are now using chilled cast iron for such magnets, and these have usually proved to be satisfactory. They are cheap, they can be made quite as strong as tool steel magnets of the same dimensions, they are very permanent after they have once been aged, and the temperature coefficients of their magnetism are almost always much smaller than those of forged steel magnets. Cast iron for permanent magnets must, however, be really hard, and, unfortunately, mechanical tests of the hardness of this metal are often deceptive; it seems desirable, therefore, to inquire whether the electric resistivity of a piece of chilled cast iron is a criterion of its temper.

This paper gives briefly a few of the results of a large number of observations made originally with the object of testing the relative efficiencies of different methods of hardening cast iron for magnets, in use in the Jefferson Laboratory. The details of this work have mainly a local interest and are not enumerated here, but some general facts may be useful to persons who have to make such magnets for themselves.

Each of the test pieces was a rod about 30 cms. long and a little less than 0.6 cm. in diameter. These were all milled down from stouter pieces about 1.5 cms. in diameter which were usually cast in sets of a dozen from a grid pattern to insure that they should be of the same kind of iron. Different specimens from the same grid, however, often showed different resistivities before they were annealed and occasionally one or two pieces from a grid would differ sensibly from the other pieces after all had been softened with great care. These differences are to be expected, as Karsten showed long ago, for the outer layers of a mass of chilled cast iron sometimes contain a greater proportion of combined carbon than the inner layers in which most of the carbon may be free, and an unequal chilling of a grid in the mould would naturally make the material slightly different in different parts. It is easy in practice to avoid abnormal specimens. All the test pieces were prepared, annealed, and hardened by Mr. George W. Thompson, the mechanician of the Jefferson Laboratory, whose experience in treating cast iron extends over many years.

The measurements of the specific resistances of the rods (usually three for each specimen) were mostly made with the help of a standard Kelvin Double Bridge, but in a few cases the test piece was connected in series with a standard manganin resistance bar and a constant storage battery, and the small potential drop across a measured length of the rod was compared with the corresponding drop across the standard. Three commutators were used with this apparatus so that the effects of disturbing electromotive forces at the contacts might be avoided. The ultimate standard was Wolff No. 2718 furnished with the certificate of the Reichsanstalt.

In the determinations of the temperature coefficients of resistivity two large tanks of water were used. One of these was approximately at room temperature. The water in the other, which was kept in constant motion by a set of four propellers run by a small motor, was heated to a constant definitely determined temperature by means of a Simplex Electric Heater attached to a 110 volt circuit and dominated through a relay by a delicate thermostat. The annealing effects of very hot water upon hard cast iron had to be avoided, but the water in the second tank was usually made uncomfortably warm for the hand.

In making cast iron magnets, it is very necessary that the iron just before it is chilled shall be much hotter than it is safe to heat ordinary tool steel in making it hard. Dr. Campbell, of the National Physical Laboratory, Teddington, Middlesex, England, finds that a temperature of 1000° C. has been sufficient for the iron he has used, but some specimens of American iron seem to work best at a slightly higher temperature, just below the melting point. If a massive piece of cast iron weighing, say, fifty pounds be heated thus hot and then chilled in a proper bath, the material, as magnetic tests can be made to show, becomes hard throughout, whereas it is practically impossible to make a similar piece of tool steel glass-hard inside. The experiments of Chernoff upon a certain kind of steel, made more than forty years ago, showed that if the temperature from which the steel was chilled was made higher and higher, from, say, 400° C., the hardening effect was almost inappreciable until a cherry red was reached, when suddenly the chilled specimen was found to be glass-hard. It is not very surprising, therefore, that cast iron shows very little temper when chilled from a temperature of 800° C. or 900° C., but may easily be made glass-hard if its temperature just before the chilling is high enough, say 1050° C. for some kinds.

The rods were heated for the hardening, under a compressor blast, in a special gas furnace made for the purpose by Messrs. J. Connors and J. Coulson, and most of them were placed inside an iron tube to protect them from direct exposure to the flames. In annealing the rods they were packed in iron filings inside an iron tube closed at the ends by screw caps and heated thoroughly to a white heat for possibly 30 minutes before the tube was packed in ashes for many hours. Although the work was done with the greatest care, it soon appeared that it is usually impossible, at least by this particular annealing process, to bring a piece of cast iron once made glass-hard back to as low a resistivity as it originally had, and if the piece be repeatedly hardened and annealed, its resistivity in the relaxed state increases every time the cycle is passed through. The diameter of the piece also increases perceptibly much as the cast iron bars of a fire box grate grow longer with hard use. Two or three examples will show the complicated nature of the phenomena involved.

Two test pieces from the Broadway Iron Works, Cambridgeport, were annealed as they came from the foundry and then had resistivities 102.5 and 102.7 and a diameter of 0.574 cm. After both had been hardened, the resistivities at about 20° C. were 122.5 and 122.0, and after they had been again through the annealing furnace their resistivities were 108.7 and 107.1. The fourth time they were relaxed the specific resistances were 112.6 and 112.6, and their average diameters about 0.578 and 0.576. When they were finally hardened again, the resistivities were 136.7 and 137.8 and both diameters were 0.581. It did not seem worth while to carry the process farther.

TABLE II.

CAST IRON ROD FOUR TIMES HARDENED AND ANNEALED.

H.	*B.*	*H.*	*B.*
1.13	57	7.70	964
1.40	79	9.15	1521
2.03	120	13.2	2910
3.31	222	20.6	4585
4.40	326	32.7	6030
5.75	518	42.4	6430
6.54	681		

Another rod, presumably of a very different kind of iron, began with a diameter of 0.574 and after four annealings had a mean diameter of 0.578. Its resistivity in the relaxed state rose in four steps from 93.9 to 102.5; the first time it was hardened its resistivity was 112.0, the last time 116.5.

In the three cases here mentioned the specimens would cut common window glass easily the first time they were hardened; they were mechanically too soft to scratch the same glass when, having been repeatedly hardened and relaxed, they were finally hardened so that they had a higher resistivity than at first.

Another rod from the same foundry had a resistivity of 102.0 when it was first annealed, and a resistivity of 119.8 when it was hardened for the first time. After an hour in steam at 100° this fell to 118.0, and after five hours farther steaming to 116.6. The second time it was annealed the rod had a resistivity of 106.5, and the third time of 107.2.

The temperature coefficient of the resistivity of the first rod spoken of above was 0.00102 when the rod was soft; the third rod had a temperature coefficient of 0.00094.

Cast iron which has been several times hardened and annealed is finally in its annealed state not so permeable as once-annealed soft cast iron is. Table II gives the results of tests upon a rod of resistivity 98.3 which has been four times heated white hot and chilled and then annealed.

If the process of heating and chilling a number of cast-iron rods be carried out many times in succession without proper annealing after each chilling, there does not seem to be a progressive increase in the resistivity; the results are anomalous.

Several kinds of chilling baths were used for hardening the cast iron, among them ice cold water, cold brine, sulphuric acid and water, an acid bath (X) the constitution of which is a trade secret, but which, I understand, has been much used in commercial work; mineral oil, and paraffine.

It has long been known that in the hardening of tool steel from a dull red heat, it is much more important that the fall of the temperature of the piece down to say 300° C. shall be quickly brought about than that the rest of the journey to room temperatures shall be rapid. It is not difficult to cool quickly a slender rod, but a large piece of hot metal suddenly immersed in a water bath is immediately surrounded by a layer of steam and, unless the water be very vigorously stirred as in die hardening, the metal may remain red hot for a comparatively long time. Many attempts have been made by varying the chemical nature of the bath to lessen the effect of the steam cloak, and some persons have used a bath of easily fusible metal for the first part of the chilling process (as is now the practice for some of the new high power steels), and have completed the cooling in a water bath, the temperature of which within wide limits seems to be unimportant.

In the light of the behavior of steel, it seemed unlikely that in the hardening of cast iron from a temperature much higher than can be used with ordinary tool steel, there would be much advantage in making the hardening baths especially cold, and experience justified this assumption. Sometimes the hardening bath was chilled with ice, but usually it was used at room temperatures or even lukewarm.

For rods of the dimensions of the test pieces I used, water, brine, sulphuric acid and water, and the X mixture seemed almost equally effective in making the cast iron glass-hard, whether resistivity or magnetic permeability of the hardened piece was used as the criterion.

For massive pieces of iron the N mixture, which certainly is very good, is said to work more uniformly than a water bath. Several specimens which were chilled in iced water and iced brine developed minute cracks which showed in irregularities when the rods were magnetized, but these, which were tested before the construction of the special gas furnace, may not have been uniformly heated. The oil bath was nearly as good, so far as increasing the resistivity of the specimen, as the water bath, but the hardened pieces did not seem so hard mechanically. The melted paraffine wax, at as low a temperature as would keep the wax liquid, also increased the resistivity of a specimen chilled in it, provided it had not been hardened before, quite as much as the water bath, but a piece thus hardened would not scratch glass.

Most of the pieces of American cast iron which I have tested had, when soft, resistivities referred to the centimeter cube, which at 0° C. would lie between 73 microhms and 104 microhms. These pieces when hardened for the first time had resistivities which at the same temperature lay between 80 and 126. Nine pieces of American cast iron tested when soft by Barus and Strouhal had on the average a resistivity at 20° C. of about 79.1 microhms with a temperature coefficient of 0.00120. Four grids, typical of the softer kinds of iron which I have used, gave on the average when soft at the same temperature the results which appear in Table III.

TABLE III.

Grid.	s.	*a*.
I	76.5	0.00104
II	86.1	0.00106
III	89.9	0.00099
IV	94.2	0.00084

To show the effect of hardening upon the temperature coefficient of the resistivity, I may instance six specimens with three different coefficients when hard. (See Table IV.)

When a number of steel bars of the same length and cut from the same long rod are hardened and are then magnetized in the same solenoid and aged, it frequently happens, as is well known, that the ultimate magnetic moments of the bars differ somewhat widely from one another; and the same thing is true of magnets made from cast-iron rods cut from the same grid. In Table V are given the magnetic

TABLE IV.

Rod.	s'.	a'.	s''.	a''.
1	94	0.00086	114	0.00070
2	97	0.00085	117	0.00070
3	79	0.00105	103	0.00086
4	75	0.00108	102	0.00086
5	88	0.00103	113	0.00091
6	86	0.00106	117	0.00091

s' and s'' are the resistivities at 20° C. in the soft and in the glass-hard states, respectively; a' and a'' are the temperature coefficients.

moments (M) and the temperature coefficients of the moments (k) of eight typical bar magnets which have been tested with great care by Mr. John Coulson.

TABLE V.

Grid.	Rod.	M.	k.	Chilling bath.	s.
A	1	1550	0.00022	Water	110
A	2	1580	22	Water	104
B	3	1720	24	Water	94
B	4	1740	26	Water	94
B	5	1560	26	H_2SO_4 and water	96
C	6	1410	27	H_2SO_4 and water	109
C	7	1500	27	H_2SO_4 and water	106
C	8	1600	27	"X" mixture	106

Mr. Coulson tested at the same time three magnets of the same dimensions as these but made of glass-hard Stubs tool steel. They had on the average a moment of about 1690 and a temperature coefficient of about 0.00095, which is more than three times as large as the corresponding value for cast iron.

After the moments of the eight cast-iron magnets had been determined, the rods were thoroughly demagnetized inside a solenoid through which a long series of currents, gradually decreasing in intensity and alternating in direction, could be sent. Then each was placed inside another solenoid and an HB diagram was found for it by the method of ascending reversals with the aid of a small test coil about its centre and a ballistic galvanometer of period sufficiently long for the purpose. Each rod was about 50.9 of its own diameters long and, according to the formula of Dr. Shuddemagen for the end corrections of rods of these dimensions, the actual magnetic intensity (H) inside the metal at the centre is equal to $H' - 0.00107\ B$, where H' is the force inside the solenoid when the rod is removed. It is possible, therefore, to determine very approximately the relative values of H and B from the observed values of H' and B, and the computation has been made by Mr. Coulson for these rods. The results of this work show that though the moments of the magnets differed so much among themselves, the permeabilities of the pieces of metal for excitations up to $H = 50$, at least, are much the same. Magnet B4, for instance, had a moment

TABLE VI.

H.	B.	H.	B.
10	310	70	4250
20	720	80	4950
30	1290	90	5550
40	2100	100	5950
50	2870	120	6480
60	4100		

TABLE VII.

Rod.	H_{1000}.	B_{120}.
A 1	26.3	6020
A 2	25.9	6200
B 3	26.5	6480
B 4	25.9	6480
B 5	25.2	6180
C 6	25.9	5960
C 7	26.1	6045
C 8	25.8	6150

much larger than the moment of C6, but the value of H corresponding to an induction of 1000 was in each case about 25.9.

For the rod B4 the relation between H and B is indicated approximately at all events by the numbers given in Table VI.

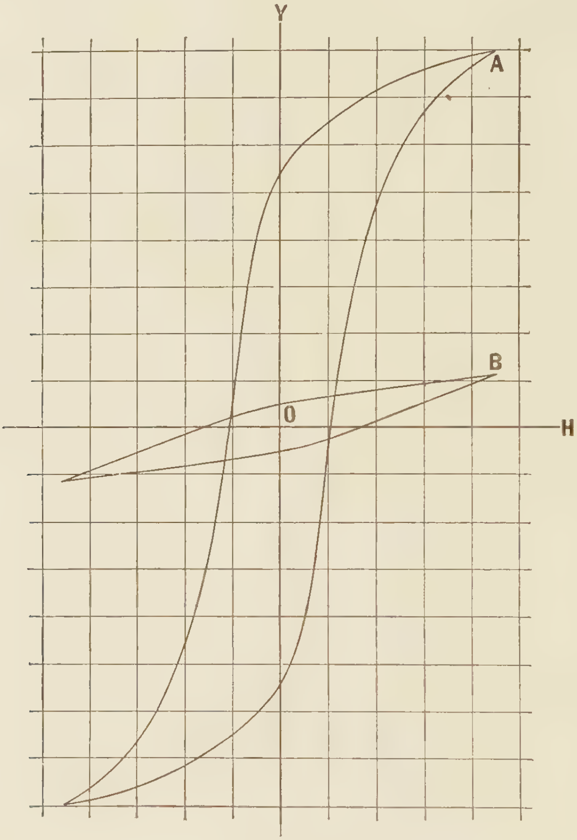

FIGURE 1.

Table VII gives under H_{1000} the value of the excitation corresponding to $B = 1000$, and under B_{120} the value of the induction corresponding to $H = 120$ for all the rods.

The specimens used were cast at different times in order that they might fairly represent the best mixtures used by the foundries from which they came, and in view of this fact the near agreement of the measurements recorded in this table is very striking. The differences are not greater than one might expect to find in a number of rods of fine polished drill rod from the same lot. For the present discussion it is of interest to notice that the permeabilities of the hard rods seem not to be connected in any obvious way with the resistivities. For any single specimen of cast iron, however, it is well known that hardening usually decreases the permeability especially at comparatively low excitations, and Figure 1 shows a rough kind of hysteresis diagram which I obtained some years ago for a cast-iron frame of several kilograms weight. Curve A corresponds to the soft state and B to the hardened state of the same piece of iron. At high excitations the difference is not so striking but is very real.

TABLE VIII.

H.	*B.* (Rod hard.)	*B.* (Rod soft.)
100	6800	9650
200	8850	11160
300	10310	12460
400	11420	13550
500	12130	14400
600	12660	14980
10000	25650	28250
11000	26600	29300
12000	27500	30400
13000	28450	31300
14000	29400	32050
15000	30350	33600

Table VIII gives approximately the results of some measurements made two or three years ago upon cylinders and isthmuses of a certain kind of cast iron from the Broadway Iron Foundry. It must be clearly understood, however, that this applies only to iron which has once been through the annealing and subsequent hardening. A repetition of the process makes the hardened iron mechanically softer. As we have seen, a piece of cast iron properly hardened for the first time makes as strong a permanent magnet as a piece of Stubs Drill Rod does, but if the cast iron be several times hardened it becomes incapable of retaining the charge given it in the solenoid and the resulting magnet is perhaps only half as strong as the steel magnet.

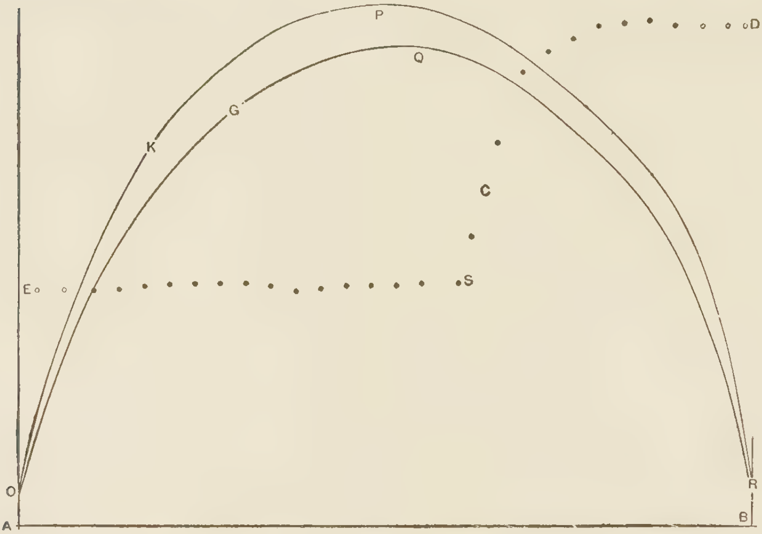

Figure 2.

The same phenomenon appears in the case of tool steel, though it is not very easy to harden a piece of tool steel glass-hard a number of times in succession without working it under the hammer to avoid the appearance of minute cracks in the metal.

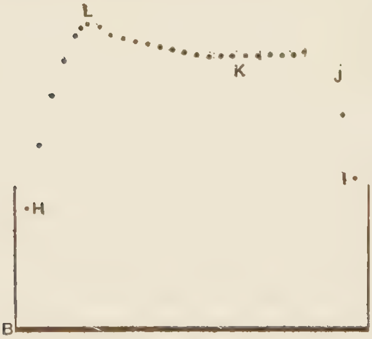

Figure 3.

For many years small magnets made of cast iron as it comes from the founder have been used in toys and in small "magnetos," but such magnets are not nearly permanent and are not so strong at the outset as similar magnets made of properly chilled iron. A certain annealed rod which I tested had when magnetized to saturation a moment of 605 on a certain scale, but a few minutes in boiling water reduced this to 455; when the rod had been hardened and again magnetized, its moment on the same scale as before was 831 and boiling reduced this to 740. The same magnetized castings are tested year after year in the Jefferson Laboratory, and so far as my experience goes, a properly hardened and aged magnet made of cast iron is quite permanent if it is exposed to such fields as that of the earth, and mechanical shocks do not injure them in any way, if the metal is not broken or abraded.

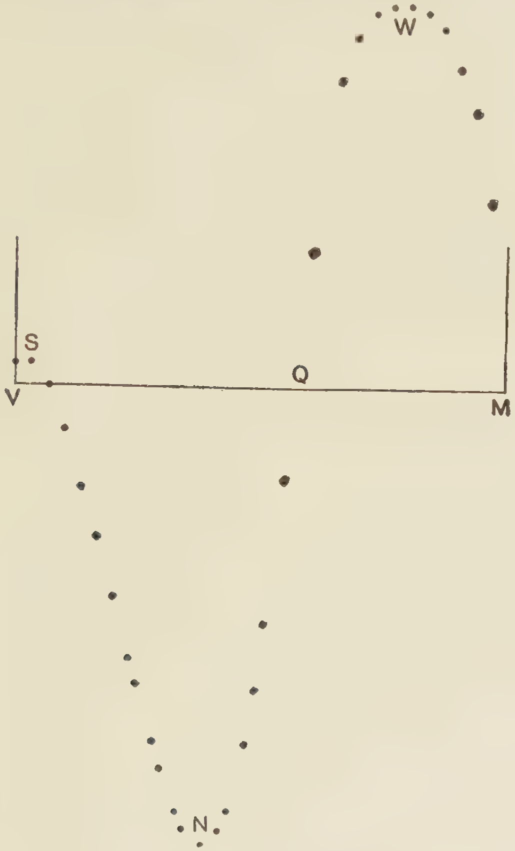

FIGURE 4.

Although a knowledge of the resistivity of a piece of cast iron tells very little about its temper unless one knows also its resistivity in the annealed state, yet the resistivity of different portions of the same piece is a trustworthy measure of the uniformity of temper. Tried by this test, many a piece of steel which has been hardened with care proves to be far from homogeneous.

Occasionally great differences of resistivity may be found in a magnetized steel rod which yields a fairly uniform iron-filing diagram.

The curve OKPR of Figure 2 shows the induction flux (B) at different points of the axis of a rod of Crescent Polished Drill Rod 29 cm. long and 0.5 cm. diameter just after it had been magnetized to saturation in a solenoid. Curve OGQR shows the same quantity after the rod had been exposed to steam for some time. AB is the common base of these curves. The distribution is in each case nearly uniform, and the iron-filing curve seems entirely so, but the resistivity of the metal is far from uniform, as the dotted diagram ESCD shows. This was obtained by measuring the resistances of a large number of very short lengths of the rod and determining from the results values for the resistance per centimeter at about thirty points on the axis. Of course a small portion at each end could not be treated in this way, and the fact is indicated by the open dots. One end of this bar was in the soft state in which this excellent steel comes in the market; the other end had been heated red hot and chilled, so that its resistivity was quite double that of the soft end. This magnet was not so strong as a hardened magnet of this steel should be, but was otherwise normal enough.

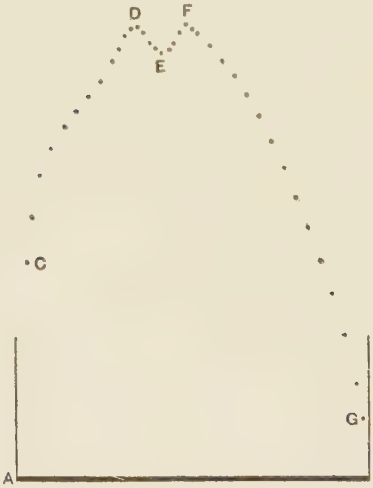

FIGURE 5.

Sometimes the iron-filing diagram belonging to a bar magnet seems very irregular when the distribution of magnetism in the metal is not very abnormal. Figure A shows a filing diagram belonging to a piece of Crescent steel of the same dimensions as that just described, while Figure 3 shows the values of B at different points in the axis. The "centre of gravity" of the magnetism is in this case not far distant from the middle of the bar. This same bar was remagnetized by rubbing a point near its centre upon one pole of a large motor, and then gave a filing diagram represented by Figure B. Here there are real consequent poles, and the distribution of the induction flux in the bar is shown by Figure 4. After this rod had been demagnetized as well as possible in a solenoid by the use of a series of currents alternating in direction and gradually decreasing in intensity, and then had been magnetized again to saturation in a solenoid as before, Diagram A came back again.

Another unequally hardened steel rod of the same kind gave the filing diagram shown in Figure C, and in this case the distribution of magnetism was that indicated in Figure 5.

Figure 6 shows in the curve HYU, of which the horizontal line through E is the base, the resistivity of a rod of cast iron of the dimensions of the specimens used in this investigation. For this particular piece the resistivity at one end corresponded to the annealed state and at the other end to glass-hardness. After this rod had been magnetized in a solenoid, the distribution of magnetism in it was that represented by the dotted curve GZX. This rod when magnetized irregularly on the motor gave the diagram LCK, but when the rod was demagnetized and again magnetized in the solenoid, the distribution GZX returned. It is interesting to notice that in the cases shown in Figures 4 and 6, the motor gave a smooth distribution of B while the solenoid gave an irregular one. When real consequent poles are pres-

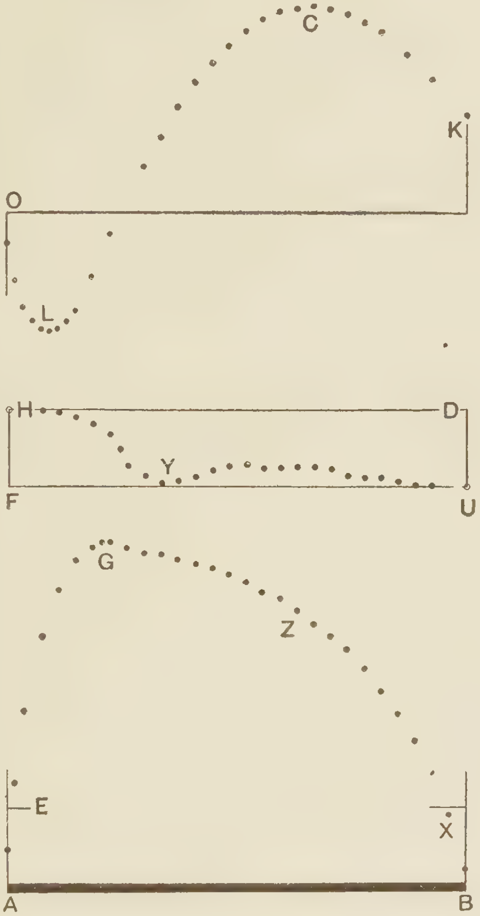

FIGURE 6.

ent, the value of B is at its greatest smaller than in the case of the solenoid magnetization.

Figure 7 shows in the curve PADQ the distribution of magnetism in an unequally hardened cast-iron rod when the magnetization took place in a long solenoid. Curve PDBQ shows on an exaggerated scale the distribution when the rod was magnetized between the poles of a large electromagnet. The greatest value of B was in this latter case about two thirds the corresponding value when the solenoid was used. In all the instances I have met, the solenoid gave the greatest value of B and any other distribution gave an appreciably smaller value. Table IX gives the resistivity at points distant n cm. from the end of the rod which corresponds to G in Figure 7. It is evident that one end of the rod is glass-hard and the other very soft.

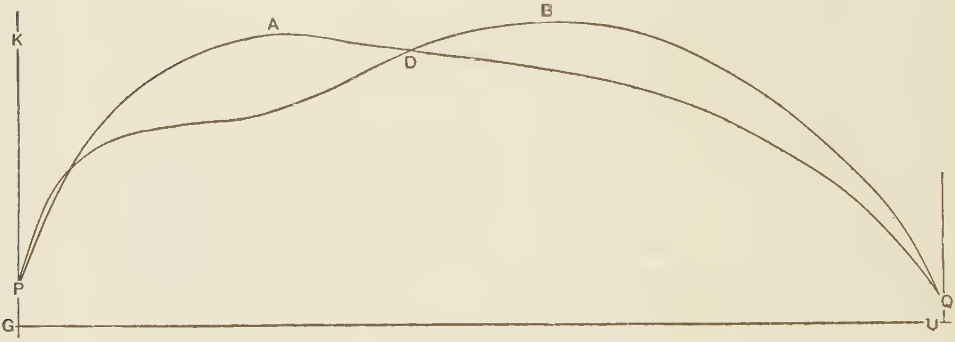

FIGURE 7.

The most common form of irregularity in a cast-iron bar magnet seems to consist, if one may judge from a filing diagram, in a simple displacement of the magnetic centre from the geometric centre towards one end of the axis. This usually corresponds to a comparatively slight difference of resistivity along the bar. This case may be illustrated by a rod (K) which had once been hardened irregularly and then had been rehardened as uniformly as possible. In all such cases it is extremely difficult to get rid of the effects of careless hardening, though the irregularity may come up in a slightly different form. The next table (X) gives the resistivity of the metal, and, on an arbitrary scale, the value of B at a point distant n cm. from one end of this bar, which was 29 cm. long.

Table XI gives the resistivities and the relative values of B on the axis of a cast-iron magnet (Q) made of a rod hard in the middle and soft at the ends.

TABLE IX.

n.	*s.*	*n.*	*s.*
3	0.000121	16	0.000097
4	122	17	94
5	121	18	94
6	121	19	92
7	120	20	92
8	117	21	92
9	115	22	93
10	111	23	94
11	104	24	94
12	097	25	94
13	097	26	93
14	097	27	93
15	097		

TABLE X.

n.	*s.*	*B.*	*n.*	*s.*	*B.*
0		60	15	127	551
1		227	16	126	560
2		317	17	126	568
3	121	368	18	127	572
4	118	405	19	129	578
5	119	430	20	129	580
6	118	448	21	129	578
7	120	460	22	129	573
8	121	470	23	129	565
9	121	480	24	126	535
10	122	493	25	125	505
11	123	509	26	124	453
12	123	520	27		374
13	126	532	28		260
14	126	541	29		72

TABLE XI.

n.	*s.*	*B.*	*n.*	*s.*	*B.*
0		40	15	155	412
1		140	16	150	429
2		207	17	147	445
3	117	261	18	141	458
4	119	305	19	128	448
5	117	339	20	119	433
6	118	371	21	118	417
7	120	394	22	117	399
8	121	416	23	116	359
9	132	434	24	115	330
10	149	440	25	113	292
11	153	428	26		257
12	153	417	27		198
13	156	409	28		135
14	158	407	29		37

If the material used in these experiments may be considered typical of the so-called "pure cast iron" from good foundries, it appears, then, that an annealed casting may have at room temperatures a resistivity, referred to the centimeter cube, as low as 0.000073 or as high as 0.000104; that it is always possible to make the specimen glass-hard throughout by heating it to a temperature a little below the melting point and chilling it in a suitable bath; and that the process, as Barus and Strouhal showed, is always accompanied by an increase in resistivity. This increase is sometimes only about ten per cent of the original value, though it is oftener nearly twenty-five per cent and may rise somewhat higher. Only one kind of iron that I used resisted successfully a noticeable relaxation of temper in the hardened pieces by prolonged boiling in water. Of two pieces of iron from the same pouring, which have equal resistivities when first annealed, that one has the higher resistivity, after both have been hardened, which has the lower magnetic permeability. Tests of mechanical hardness are difficult to make upon cast iron and often disagree with the resistivity test. A repetition of the annealing and hardening process increases somewhat the size of a specimen and increases the resistivity for both the annealed and the chilled states, but in the hardened state the iron is never so hard mechanically as at the first hardening, and the bar loses in great measure its magnetic retentiveness, as do most kinds of tool steel which have been through the same experience. Many kinds of chilling liquids serve to make cast iron glass-hard, but for massive pieces cold water seems not to give such uniform results as the acid bath used by some professional hardeners. The temperature coefficient (a) of the resistivity of every one of my specimens was decreased by the hardening, though this does not seem to have been the case for the special cast iron used by Barus and Strouhal, which had a larger coefficient (120) than any I used. The coefficient a is not always smallest in that one of a number of specimens of cast iron which has the largest resistivity.

Castings from different sources often show when glass-hard a very close agreement in magnetic permeability, though their resistivities and the temperature coefficients of the resistivities may differ widely. The temperature coefficient of the magnetic moment of a cast-iron bar magnet is usually not more than one third as large as that of a similar magnet made of tool steel.

A uniformly hardened cast-iron or steel rod may have been irregularly magnetized, but if it be thoroughly demagnetized and then carefully remagnetized in a solenoid, its magnetism will become regular. Only irregular hardening seems to lead to persistently irregular magnetization in the case of a bar magnet, though the use nowadays of electromagnetic crane lifters sometimes magnetizes iron and steel rods in a manner which is difficult to deal with in the laboratory. Even an irregularly hardened slender rod may usually be demagnetized well enough for all practical purposes in a solenoid which carries currents alternating in direction and gradually decreasing in intensity, but large thick pieces are very tenacious of charges once given to them. The shield of a certain Rubens Panzer galvanometer in use in the Jefferson Laboratory was twice heated white hot and was kept hot for some time in a vain attempt to get rid of a slight magnetization. The resistivity of different portions of a casting gives trustworthy information about the uniformity of the hardening. Occasionally, as in a case cited above, an irregularly hardened piece of tool steel may be magnetized nearly normally, but usually irregular hardening leads to an irregular distribution of the magnetism which shows itself in an abnormal iron-filing diagram. An unusual filing diagram does not however, as some instances given show, always indicate that the distribution of the magnetic induction in the bar is very irregular.

My thanks are due to the Trustees of the Bache Fund of the National Academy of Sciences who have kindly lent me some of the apparatus used in making the observations described in this paper.

The Jefferson Laboratory,
Harvard College,
Cambridge

PEIRCE.—THE RESISTIVITY OF HARDENED CAST IRON.

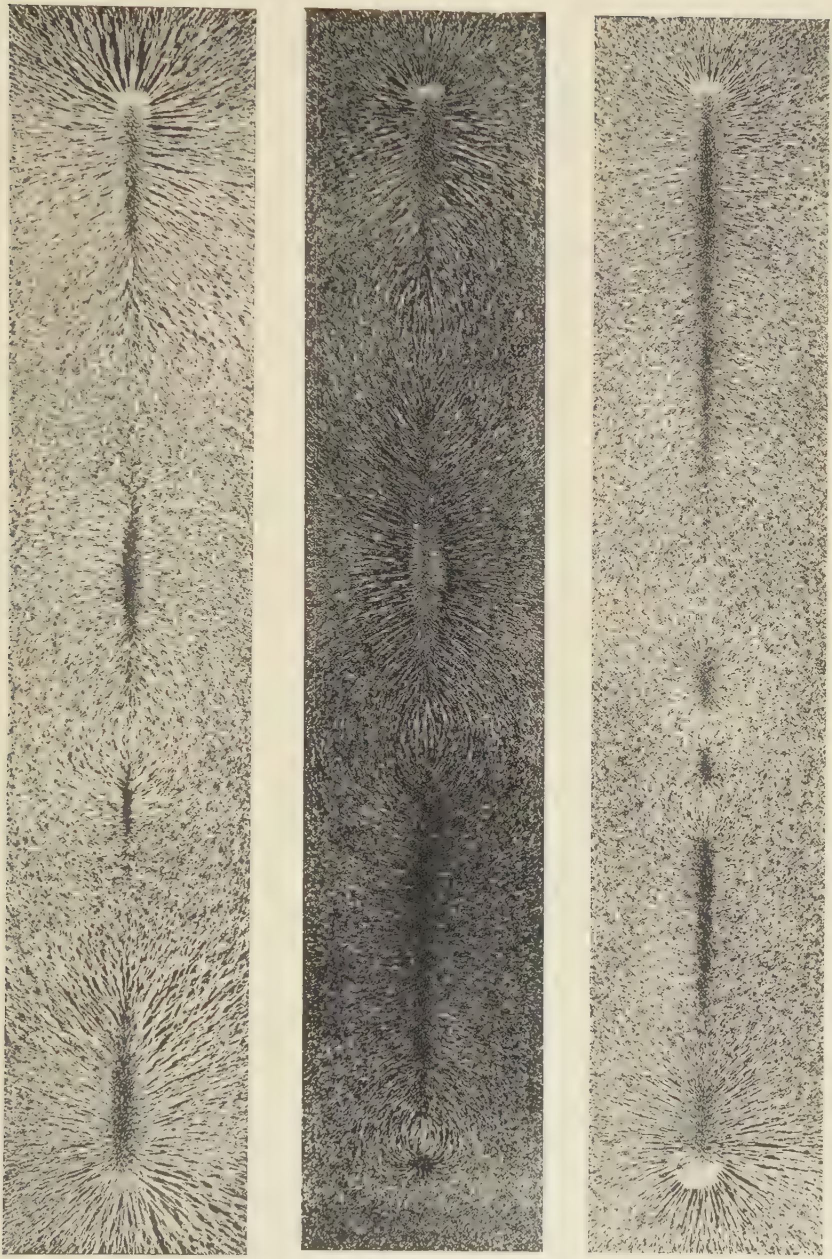

A B C

THE PROPAGATION OF LONG ELECTRIC WAVES ALONG WIRES.

By E. P. ADAMS.

(*Read December 2, 1910.*)

In the usual deduction of the equations of propagation of electric waves along wires the notion of the electric constants per unit length is introduced. While there is no difficulty involved in this as far as resistance and leakage are concerned, the legitimacy of the extension of this notion to self-induction and capacity is not obvious. In order to determine the exact meaning to be attached to these terms it is convenient to consider a line in which the electric properties are localized in a finite number of coils, condensers and leaks, joined by ideal conductors of no resistance, self-induction and capacity. For the special case of long electric waves the solution can readily be obtained by means of the calculus of finite differences. On passing to the limit, by letting the number of coils, etc., increase indefinitely while their electric constants decrease indefinitely, the equations of propagation and their solution for a uniform line are at once obtained. There appears to be a considerable advantage in the use of this method in respect to its simplicity, particularly where the terminal conditions are at all complicated. Two problems are worked out in this paper; the first that of the free vibrations of a line earthed at both ends, and the second that of the forced vibrations when a periodic impressed electromotive force is applied to the circuit.

Consider a line of length l, in which are inserted at equal intervals n coils each of resistance R' and self-induction L. At points between each pair of coils one plate of a condenser of capacity S is connected, the other plate being earthed; and at the same points leaks to earth, each of conductance K', are introduced. The current in the kth coil is C_k, and the potential at a point between the

Reprinted from Proceedings American Philosophical Society, Vol. xlix., 1910.

coils k and $k+1$ is V_k. For the first problem we then have $V_0 = V_n = 0$. Let L_1 be the coefficient of mutual induction between any coil and one of its nearest neighbors; L_2 the coefficient of mutual induction between the same coil and its next nearest neighbor but one, and so on. Similarly, let S_1 be the electric induction coefficient between any condenser and one of its nearest neighbors; S_2 the induction coefficient between two alternate condensers, etc. We can then write for the kth coil:

$$\begin{aligned} V_{k-1} - V_k = \frac{d}{dt}\Big(L C_k + L_1 C_{k-1} + L_1 C_{k+1} \\ + L_2 C_{k-2} + L_2 C_{k+2} + \cdots\Big) + R' C_k \end{aligned} \tag{1}$$

and for the kth condenser:

$$\begin{aligned} C_k - C_{k+1} = \frac{d}{dt}\Big(S V_k + S_1 V_{k-1} + S_1 V_{k+1} \\ + S_2 V_{k-2} + S_2 V_{k+2} + \cdots\Big) + K' V_k \end{aligned} \tag{2}$$

Now in the case of long electric waves the currents in any coil and its near neighbors will be very nearly the same. The terms in the series in (1) containing currents in distant coils become relatively unimportant on account of the diminution of their coefficients. In this special case it will therefore be legitimate to replace the series by a single term and we can therefore write:

$$V_{k+1} - V_k = L' \frac{d}{dt} C_k + R' C_k, \tag{3}$$

in which L' may be termed the effective coefficient of self-induction of any one of the coils. When we pass to the limit by increasing indefinitely the number of coils, etc., and at the same time decreasing indefinitely all the electric constants, the limiting value which the product of L' by the number of coils in a unit length approaches will be the self-induction per unit length of the uniform line. Equation (2) modified in an analogous manner reduces to:

$$C_k - C_{k+1} = S' \frac{d}{dt} V_k + K' V_k \tag{4}$$

Subtracting the equation for the coil $k+1$ from (3) and substituting from (4), we get:

$$V_{k-1}-(2+h)V_k+V_{k+1}=0, \tag{5}$$

where

$$h=R'K'-L'S'p^2+ip(L'K'+R'S'), \tag{6}$$

in which it is assumed that the potentials and currents all vary as e^{ipt}. (5) is a linear difference equation of the second order. By the usual method we put

$$V_k=A_k\alpha^k e^{ipt},$$

and find:

$$\alpha=\frac{2+h}{2}\pm\tfrac{1}{2}\sqrt{4h+h^2}\cdot \tag{7}$$

Let these two values be α and β, the former with the positive sign of the radical. In general α and β are different, and so we get the two distinct solutions required by an equation of the second order. But for $h=0$ or $h=-4$ α and β have the same values. The complete solution of (5) is therefore:

$$\begin{aligned}V_k=(A_1+B_1k)e^{ip_1t}+(A_2+B_2k)e^{ip_2t}+(A_3+B_3k)(-1)e^{ip_3t}\\+(A_4+B_4k)(-1)^k e^{ip_4t}+\sum(A_p\alpha^k+B_p\beta^k)e^{ipt}.\end{aligned}$$

Since $V_0=V_n=0$, whatever t, $A_1=A_2=A_3=A_4=B_1=B_2=B_3=B_4=0$; $A_p+B_p=0$ and

$$\alpha^n-\beta^n=0. \tag{8}$$

Let now

$$h=-4\sin^2\theta, \tag{9}$$

(7) reduces to

$$\alpha,\beta=\cos 2\theta\pm i\sin 2\theta, \tag{10}$$

and (8) gives

$$\theta=\frac{m\pi}{2n}, \tag{11}$$

where m is any integer. $m=0$ and $m=n$ are excluded because these give $h=0$ and $h=-4$, which are already disposed of. If we take $m=n+1$, $n+2$, etc., we get the same series of values obtained from $m=1$ to $m=n-1$. We thus get:

$$V_k = \sum_{m=1}^{m=n-1} A_m \sin \frac{km\pi}{n} e^{ip_m t}. \tag{12}$$

A_m and p_m are complex quantities. Writing $p_m = p_m' + ip_m''$, we get from (6), (9) and (10):

$$p_m' = \sqrt{\frac{4 \sin^2 \frac{m\pi}{2n}}{L'S'} - \frac{(L'K' - R'S')^2}{4L'^2S'^2}}, \tag{13}$$

$$p_m'' = \frac{L'K' + R'S'}{2\,L'S'} = p''. \tag{14}$$

p_m'' is thus independent of m. The real part of (12) may now be written

$$V_k = e^{-p''t} \sum_1^{n-1} A_m \cos (p_m't - \phi_m) \sin \frac{km\pi}{n}, \tag{15}$$

where A_m and ϕ_m are new arbitrary real constants.

The currents in the several coils may be obtained from (3) combined with (12). Taking the real part we find

$$C_k = e^{-p''t} \sum_1^{n-} B_m \cos (p_m't - \psi_m) \cos (2k - 1) \frac{m\pi}{n} \tag{16}$$

where B_m and ψ_m are known in terms of A_m and ϕ_m in (15).

The last four equations give the complete solution of the problem. The constants A_m and ϕ_m may be determined by Fourier's method when the initial conditions are known.

Now let n increase indefinitely while R', L', S' and K' all decrease indefinitely. Let $L = \text{limit}\ L'n/l$, and similarly for the others. Let δx be the distance between two coils, so that $n\delta x = l$. Measuring x from the end of the line corresponding to $k=0$, we have $k = nx/l$ and we get in the limit:

$$V = e^{-p''t} \sum_1^{\infty} A_m \cos (p_m't - \phi_m) \sin \frac{m\pi x}{l}, \tag{17}$$

$$C = e^{-p''t} \sum_1^{\infty} B_m \cos (p'_m t - \psi_m) \cos \frac{m\pi x}{l}, \tag{18}$$

$$p_m' = \sqrt{\frac{m^2\pi^2}{l^2LS} - \left(\frac{LK - RS}{2LS}\right)^2}, \tag{19}$$

$$p'' = \frac{LK + RS}{2LS}, \tag{20}$$

which are the well-known solutions for the free vibrations of a uniform line for long waves.

The differential equation of which (17) is the solution is obtained by passing to the limit in the difference equation (5). We thus get

$$\frac{\partial^2 V}{\partial x^2} = LS\frac{\partial^2 V}{\partial t^2} + (LK + RS)\frac{\partial V}{\partial t} + RKV.$$

Equations (3) and (4) on passing to the limit give:

$$-\frac{\partial V}{\partial x} = L\frac{\partial C}{\partial t} + RC,$$

$$-\frac{\partial C}{\partial x} = S\frac{\partial V}{\partial t} + KV.$$

For the second problem, that of a periodic impressed electromotive force applied to one end of a line, the other end being earthed, we have to solve equation (5) subject to the conditions:

$$\begin{aligned} k &= 0, \quad V_k = Ee^{i\nu t}, \\ k &= n, \quad V_k = 0. \end{aligned} \tag{21}$$

The resulting solution may of course be applied to a closed circuit with the periodic force $Ee^{i\nu t}$ introduced in it at any point. After the free vibrations have been damped out, the solution will be

$$V_k = (A\alpha^k + B\beta^k)Ee^{i\nu t},$$

where A and B are arbitrary constants and α and β are given by (10). Determining A and B by means of (21) we get

$$V_k = \frac{\sin 2(n-k)\theta}{\sin 2n\theta} Ee^{i\nu t}. \tag{22}$$

θ is a complex angle defined by (6) and (9) if ν is written for p

in (6). Putting $\theta = \theta' + i\theta''$, we get as the real part of (22)

$$V_k = \frac{E}{2\,(\cosh 4n\theta'' - \cos 4n\theta')}\{e^{2(2n-k)\theta''}\cos(\nu t + 2k\theta')$$
$$+ e^{-2(2n-k)\theta''}\cos(\nu t - 2k\theta') - e^{2k\theta''}\cos(\nu t + 4n\theta' \tag{23}$$
$$- 2k\theta') - e^{-2k\theta''}\cos(\nu t - 4n\theta' + 2k\theta')\},$$

which together with

$$4(\sin^2\theta'\cosh^2\theta'' - \cos^2\theta'\sinh^2\theta'') = \nu^2 L'S' - R'K' \tag{24}$$
$$-4\sin 2\theta'\sinh 2\theta'' = \nu(L'K' + R'S') \tag{25}$$

gives the complete solution.

Now on passing to the limit as before, we can replace $\sin\theta$ by θ, $L' = L\delta x$, etc., and we find

$$2\theta' = -Q\delta x,$$
$$2\theta'' = P\delta x,$$

where

$$P,\ Q = \frac{1}{\sqrt{2}}\{(\nu^2L^2 + R^2)(\nu^2S^2 + K^2) \pm (RK - \nu^2LS)\}^{\frac{1}{2}},$$

We thus have

$$4n\theta'' = 2Pl, \quad 4n\theta' = -2Ql,$$
$$2k\theta'' = Px, \quad 2k\theta' = -Qx;$$

(23) thus reduces to

$$V = Ee^{-Px}\cos(\nu t - Qx) + \frac{Ee^{-Pl}}{2(\cosh 2Pl - \cos 2Ql)^{\frac{1}{2}}}$$
$$\times\{e^{Px}\cos(\nu t + Qx + \phi) - e^{-Px}\cos(\nu t - Qx + \phi)\},$$

where

$$\tan\phi = \frac{\sin 2Ql}{e^{-2Pl} - \cos 2Ql},$$

which is the solution for this case as given by Heaviside,[1] except that leakage is here considered and the real impressed force is $E\cos\nu t$ instead of $E\sin\nu t$.

[1] "Electrical Papers," Vol. 2, p. 62.

PRINCETON UNIVERSITY.

Proceedings of the American Academy of Arts and Sciences.

Vol. XLVI. No. 9. — October, 1910.

CONTRIBUTIONS FROM THE JEFFERSON PHYSICAL
LABORATORY, HARVARD UNIVERSITY.

THE MAGNETIC PERMEABILITIES AT LOW EXCITATIONS OF TWO KINDS OF VERY PURE SOFT IRON.

By B. Osgood Peirce.

CONTRIBUTIONS FROM THE JEFFERSON PHYSICAL LABORATORY, HARVARD UNIVERSITY.

THE MAGNETIC PERMEABILITIES AT LOW EXCITATIONS OF TWO KINDS OF VERY PURE SOFT IRON.

By B. Osgood Peirce.

Presented May 11, 1910. Received August 26, 1910.

More than a year ago, I had occasion to study the magnetic properties under very high excitations of a piece of Norway iron[1] (P), which proved when analyzed to be extraordinarily pure. The tests made in the Chemical Laboratory of Harvard University by Mr. E. R. Riegel, for nickel, cobalt, tungsten, and even manganese, as well as for the metals of Groups IV and V, were all negative. There was less than 0.03 per cent of carbon, less than 0.047 per cent of phosphorus, less than 0.03 per cent of silicon, and less than 0.003 per cent of sulphur. A slender rod of this remarkable iron, of which we had originally a round bar five centimeters in diameter and thirty-four centimeters long, had, when annealed, an extremely high permeability under excitations above 200, but, because of the local reluctance at the joints, it did not prove easy to determine the permeability of this rod in a yoke at low excitations. The metal showed to the eye a fibrous structure with striae parallel to the length of the bar, as if minute quantities of scale had been included in the bar in the rolling; and it seemed likely that the specific reluctance to magnetization across the grain of the iron, would be greater than to magnetization parallel to the grain. Under these circumstances it was probable that the permeability of a ring, so cut from the metal that its axis should be parallel to the grain, would appear low. It happened, however, that I had two such rings, but that there was not enough of the iron left to make rings with axes perpendicular to the grain, and I was forced to get what information I could from them, though it soon became evident that for excitations above five gausses the permeability fell below what commercial Norway iron should show.

---

[1] American Journal of Science, 28, July, 1909.

This paper gives the results of some tests made at low excitations, which are interesting because of the great susceptibility which the rings showed in fields less than two gausses, and compares the magnetic behavior of this metal with that of a ring of the so-called "American Ingot Iron," which I obtained through the kindness of Dr. P. W. Bridgman. This well-known iron, which was made by the American Rolling Mill Company of Middletown, Ohio, seems to be perfectly homogeneous, and, according to the makers, contains less than 0.03 per cent of impurities all told.

All the rings were very accurately made by Mr. G. W. Thompson, the mechanician of the Jefferson Laboratory. The external diameters of the Norway iron rings were 5.000 cm. and 4.996 cm. respectively; their thicknesses were 0.250 cm. and 0.254 cm., and their breadths were 1.2204 cm. and 1.210 cm. The measurements were made with the help of Zeiss Comparator No. 3196 and a set of auxiliary gauges. After each ring had been measured, a coil of very fine double-silk-covered copper wire was wound on the metal in a single layer and then baked in shellac. Over this was wound, usually in two layers, the exciting coil of well-insulated wire nearly one millimeter in diameter. The ballistic galvanometers were of the moving coil type, and had periods amply long enough[2] for the work. The fine coil on the ring was always in simple circuit with the galvanometer and the secondary coil of a standard of self inductance tested by the Bureau of Standards.

The maximum value of the permeability (5480) which I obtained for the first ring tested seemed so high that at first I suspected that there was some error in the determination, so I changed the galvanometer, and then took off the coils and wound on new ones with different numbers of turns; but when the result was unchanged and the second ring gave values for the ordinates of the HB diagram which were practically indistinguishable from those obtained from the first ring, there seemed to be no doubt that the work had been accurately done. The two rings lay side by side in the original bar, and both must have had nearly the same discontinuities. Table I, founded upon several hundred separate determinations, gives values of the permeability of the metal obtained from 35 different excitations of the first ring and 25 of the second. A ring of very pure annealed iron from the Armstrong Works at Elswick gave in the hands of Wilson the same maximum value of the permeability as the rings just mentioned; but apart from the reports of some tests upon thin pieces of electrolytically deposited iron,

---

[2] Peirce, These Proceedings, **44**, 1909 (283).

I have found no other records of permeabilities so high as this.[3] For excitations above six gausses, however, the rings were distinctly less permeable than good iron should be, and this anomalous behavior is perhaps due to discontinuities across the lines of magnetization.

TABLE I.

Annealed Ring of Norway Iron (P), Axis parallel to the Axis of the Original Bar. Measurements made by the Method of Ascending Reversals.

H.	B.	B/H.	I.	H.	B.	B/H.	I.
0.05	22	440	1.7	1.70	9040	5320	719
0.10	54	540	4.3	1.80	9340	5190	743
0.15	92	613	7.3	1.90	9640	5070	767
0.20	145	725	11.3	2.00	9870	4935	785
0.25	205	820	16	2.20	10300	4680	820
0.30	280	933	22	2.40	10690	4450	851
0.35	390	1114	31	2.60	11010	4230	876
0.40	495	1238	39	2.80	11310	4040	900
0.45	620	1377	49	3.00	11560	3850	920
0.50	790	1580	63	3.50	12010	3430	956
0.55	990	1800	79	4.00	12310	3080	980
0.60	1260	2100	100	4.50	12550	2790	991
0.65	1585	2440	126	5.00	12760	2550	1016
0.70	1980	2830	158	6.00	13060	2180	1039
0.75	2405	3205	191	7.00	13300	1900	1058
0.80	2850	3560	227	8.00	13510	1690	1075
0.85	3310	3890	263	9.00	13700	1520	1090
0.90	3780	4200	301	10.00	13870	1387	1103
0.95	4255	4480	339	20.00	14950	748	1188
1.00	4730	4730	376	30.00	15520	517	1233
1.10	5620	5110	499	40.00	15850	396	1258
1.20	6380	5320	508	50.00	16080	322	1276
1.30	7070	5440	563	60.00	16300	271	1292
1.40	7670	5480	610	70.00	16510	236	1308
1.50	8200	5470	653	80.00	16700	209	1322
1.60	8640	5400	687				

---

[3] Stoletow, Ann. d. Physik, **146**, 1872 (439); Riecke, Ann. d. Physik, **149**, 1873; Rowland, Phil. Mag., **46**, 1873 (140); Roessler, Inaugural Diss., Zürich, 1892; Holz, Ann. d. Physik, **8**, 1876 (353); Ewing, Magnetic Induction in Iron and Other Metals; Bauer, Ann. d. Physik, **11**, 1880 (349); G. vom Hofe, Ann. d. Physik, **37**, 1889 (482); Lehmann, Ann. d. Physik, **48**, 1893 (406); Benedicks, Ann. d. Physik, **6**, 1901; Lydall and Pocklington, Proc. Roy. Soc., **52**, 1892;

A well annealed isthmus of this iron cut lengthwise of the bar gave for *I*, under excitations as high as 18000 gausses, a final value of 1795, and an unannealed rod tested in a yoke gave 1730. These remarkable values point to a much higher permeability at medium excitations than the rings just mentioned show.

TABLE II.

Ring of Annealed "American Ingot Iron." Measurements made by the Method of Ascending Reversals.

H.	*B.*	*B/H.*	*I.*	*H.*	*B.*	*B/H.*	*I.*
0.1	35	175	2 8	4 0	11900	2975	947
0.3	106	530	8.4	4.5	12450	2777	991
0.2	198	660	15.7	5.0	12850	2570	1022
0 4	324	810	25	5.5	13200	2400	1050
0.5	482	964	38	6.0	13500	2250	1074
0.6	688	1147	55	6.5	13780	2120	1096
0.7	990	1414	79	7.0	13960	1994	1111
0.8	1325	1656	105	7 5	14180	1891	1128
0.9	1720	1911	137	8.0	14350	1794	1142
1.0	2320	2320	185	8.5	14480	1763	1152
1.5	5150	3433	410	9.0	14600	1622	1162
2.0	7340	3670	584	9.5	14720	1550	1171
2.5	9050	3620	720	10.0	14830	1483	1180
3.0	10220	3406	813	20.0	15850	792	1261
3.5	11150	3186	887				

Table IV shows corresponding values of *H* and *B* for a ring of annealed "American Ingot Iron" cut out by Mr. Thompson from a large plate of the metal. The outside diameter of the ring was 5.012 cm., its thickness was 0.283 cm., and its breadth about 2.116 cm. There were 112 turns in the testing coil and 74 turns in the exciting coil.

Table III gives for comparison the results of the determinations of the permeabilities of a number of different specimens of soft iron by different observers. Some of the numbers which I have obtained graphically from the published figures are only approximately correct.

Columns 7 and 9 give the records of observations made upon two small rings of very pure iron given by Colonel Dyer of the Elswick works to

---

Wilson, Proc. Roy. Soc., **62**, 1898; du Bois, Ann. d. Physik, **51**, 1894 (537); Taylor Jones, Ann. d. Physik, **54**, 1895 (641); Phil. Mag., **39**, 1895 (254); Stefan, Wiener Berichte, **81**, 1880 (89); Ewing, Roy. Soc. Trans.

TABLE III.

H.	B.											
	Norway Iron (P) Rings, 1 and 2.	Long Rod of Norway Iron. (R.)	American Ingot Iron.	Hopkinson's Annealed Wrought Iron. (Average.)	Lehmann's Swedish Iron Ring.	Rössler's Iron Ellipsoid.	Wilson's Ring of Pure Iron (No. 2).	Ewing's Soft Iron Wire.	Lydall and Pocklington's Ring of Pure Iron (No. 1).	Hopkinson's Ring.	Rowland's Norway Iron Ring.	Norway Iron (Q).
0.2	145	90	106	110	140	68	300	26	46	80	100	115
0.4	495	260	324	340	450	165	800	55	128	170	380	340
0.6	1260	570	688	740	1180	282	1400	100	467	330	1100	780
0.8	2850	1125	1325	1280	2050	410	2050	160	1020	550	2500	1750
1.0	4730	2150	2320	2400	3020	560	3400	230	2150	950	4500	3050
1.5	8200	4600	5150	4700	4700	1550	8000	500	6020	3650	6950	5450
2.0	9870	6600	7340	5900	6050	4350	10700	900	7720	5400	8650	7200
2.5	10850	8240	9050	6800	7200	6950	12000	2500	8920	6780	9900	8200
3.0	11560	9480	10220	7600	8300	8700	12800	5800	9850	7800	10800	9150
3.5	12010	10460	11150	8350	9150	9800	13400	8400	10600	8800	11450	10050
4.0	12310	11280	11900	9000	9700	10600	13800	10350	11300	9600	12020	10800
4.5	12550	11980	12450	9500	10150	11240	14150	11650	11850	10250	12500	11400
5.0	12760	12560	12850	9950	10650	11800	14360	12480	12350	10750	12070	11900
6.0	13060	13400	13500	10700	11400	13700	14700	13500	13200	11500	13700	12800
7.0	13300	13900	13960	11300	12050	13400	14950	14100	13900	12100	14100	13400
8.0	13510	14300	14350	11800	12550	13780	15100	14350	14400	12550	14400	13850
9.0	13700	14660	14600	12180	12900	13960	15250	14750	14800	12950	14680	14200
10.0	13870	14940	14830	12500	13280	14050	15320	14950	15050	13350	14950	14400

Sir Frederick Abel, who presented them to Dr. John Hopkinson. The tests upon the first ring by Messrs. Pocklington and Lydall seem to show that they did not anneal the iron; the remarkable measurements of Wilson upon the second ring were made after the iron had been softened. Norway Iron (R) was a long annealed rod about half an inch in diameter. This was tested in a solenoid. An analysis of Hopkinson's ring made by the Whitworths, showed manganese 0.143 per cent, phosphorus 0.271 per cent, sulphur 0.012 per cent, carbon 0.01 per cent and "slag" 0.436 per cent. The Elswick iron contained 0.1 per cent of manganese and 0.013 per cent of sulphur but no phosphorus and hardly a trace of carbon or other impurity. Norway Iron (Q) was an annealed ring cut from a bar of "pure iron" obtained in the Boston market.

My thanks are due to Professor John Trowbridge, who furnished me with the pure iron described above, and to the Trustees of the Bache Fund of the National Academy of Sciences who loaned me some of the apparatus used in the work.

THE JEFFERSON LABORATORY,
CAMBRIDGE, MASS.

Proceedings of the American Academy of Arts and Sciences.

Vol. XLVI. No. 13. — January, 1911.

CONTRIBUTIONS FROM THE JEFFERSON PHYSICAL
LABORATORY, HARVARD UNIVERSITY.

THEORY OF COUPLED CIRCUITS, UNDER THE ACTION OF AN IMPRESSED ELECTROMOTIVE FORCE, WITH APPLICATIONS TO RADIOTELEGRAPHY.

By George W. Pierce.

CONTRIBUTIONS FROM THE JEFFERSON PHYSICAL
LABORATORY, HARVARD UNIVERSITY.

THEORY OF COUPLED CIRCUITS, UNDER THE ACTION OF AN IMPRESSED ELECTROMOTIVE FORCE, WITH APPLICATIONS TO RADIOTELEGRAPHY.

By George W. Pierce.

Presented October 12, 1910. Received October 20, 1910.

I. Introduction.

Persistent, or sustained, electric oscillations have recently come into extensive use in wireless telegraphy. With these oscillations, which are produced continuously while the transmitting key is depressed, tens of thousands of waves arrive at the receiving station during even the production of a single dot of the Morse code. This permits the establishment of a practically steady state at the receiving station, so that by the use of these persistent oscillations the mathematical treatment of the problem of the resonance conditions at the receiving station reduces to a problem of forced vibration.

The exact solution for the radiotelegraphic circuits, however, still presents considerable difficulty on account of the effect of the distributed capacity of the antennae. An approximation to a solution of the practical problem can be obtained by supposing that the antenna of the receiving station of the practical case can be replaced by a localized capacity so that the circuits become those represented in Figure 1. While this simplified system is a considerable departure from the actual practical circuits, calculations made from the simplified circuits seem nevertheless to be of importance, because the resonance in the simplified system is sharper than in the actual circuits, and the simplified computations thus afford a means of assigning certain theoretical limits to practical attainments.

It is the purpose of the present communication to give a solution of the equations representing the flow of electricity in a system of circuits of the form of Figure 1, under the action of a sinusoidal impressed electromotive force at *e*, and to make from this solution deductions in regard to the wireless telegraphic receiving station. It will not be necessary to neglect the resistances of the system, and, in fact, the influence of the resistances upon the resonance relations and upon the resultant current is the most interesting part of the investigation. The results of the mathematical treatment are illustrated by numerical examples.

II. An Experiment on Received Current.

In pursuing the mathematical development I have received aid from an examination of some experimental data previously published, and I take the liberty of presenting one set of these experimental results [1] as an introduction to the theoretical investigation. These experimental data were obtained five years ago with a spark-discharge method of excitation instead of with a persistent source of waves, so that the experimental case is to be regarded in this connection merely as an aid to a concrete statement of the problem under consideration.

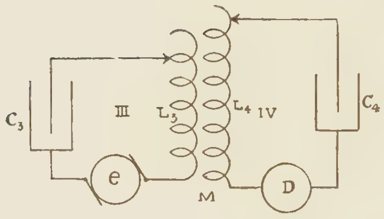

Figure 1. Diagram of coupled circuits with impressed e. m. f.

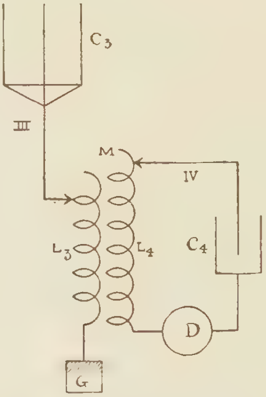

Figure 2. Electro-magnetically coupled wireless telegraph receiving station.

The experiments were made with a receiving station of the electro-magnetically connected type, like that shown in Figure 2. With electric waves of fixed period arriving from a distant sending station the receiving station of Figure 2 was attuned by adjustment of the condenser C_4 which is in the side-circuit. Readings of the received current in the side-circuit were made by the use of a low-resistance high-frequency dynamometer *D*. The inductances L_3 and L_4 and their mutual inductance were kept constant. Since, however, a single variation at the receiving circuit — namely, the variation of the condenser C_4 — is not sufficient to disclose the resonance conditions at the receiving station, the length of the receiving antenna was also given various values. The results are plotted in the curves of Figure 3, and were obtained as follows:

---

[1] G. W. Pierce, Physical Review, **20**, 220, 1905.

With a given length (23.8 meters) of the four-wire receiving antenna the capacity C_4 was set at a particular value and the deflection of the dynamometer *D* was read. The capacity C_4 was then set at another value and the deflection of the dynamometer was read. Thus keeping the length of antenna at 23.8 meters, I took the readings of the dynamometer for a whole series of values of C_4. The results are shown in Curve 1 of Figure 3, in which the deflections of the dynamometer (current square) are plotted against values of "receiving capacity" C_4 (in arbitrary units). We shall call this kind of a curve a "resonance curve." When this resonance curve (Curve 1) was completed, the antenna was shortened to 20.8 meters and a second resonance curve, Curve 2, Figure 3, was taken. Again shortening the antenna successively to 17.8, 15.8, 14.8, 13.8, and 12.8 meters, I obtained the curves 3, 4, 5, 6, and 7 respectively of Figure 3.

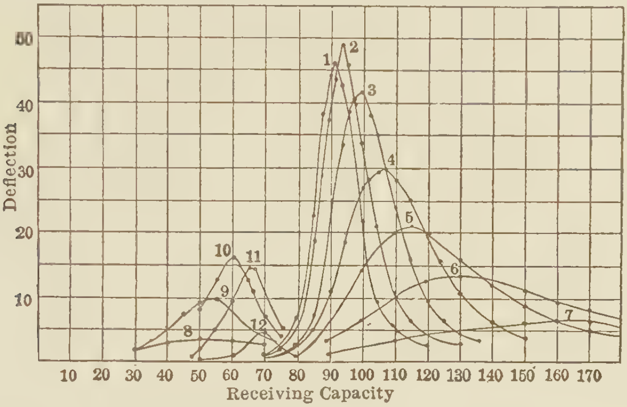

FIGURE 3. Family of experimental curves obtained with various heights of antenna (each height giving one of the curves), and various values of receiving capacity C_4.

From this it is seen that for each particular capacity of the antenna, varied by varying the length, there is a characteristic capacity C_4 that gives a maximum of current. We shall call the condenser capacity that gives a maximum of current the "resonant C_4" for a given C_3. In seeking an expression for the condition for resonance, it is to be noticed that, as C_3 has been diminished, the value of the "receiving capacity" C_4 required for resonance has been increased (compare Curves 1 to 7). On passing to a smaller length of antenna, in the neighborhood of 11.8 meters, the value of C_4 for resonance became very great and the amount of current received became inappreciably small. With this length of antenna, 11.8 meters, the condition of the receiving circuit was at its worst, for upon further decreasing the length of antenna to 10.5 meters resonance reappeared in the form of Curve 8. The resonance relation had undergone a discontinuity and the capacity C_4 for resonance had jumped back toward the origin. Now, decreasing the length of the antenna further to 10, 9, 8, and 7 meters successively, I obtained the resonance curves 9, 10, 11, and 12 respectively[2] of Figure 3.

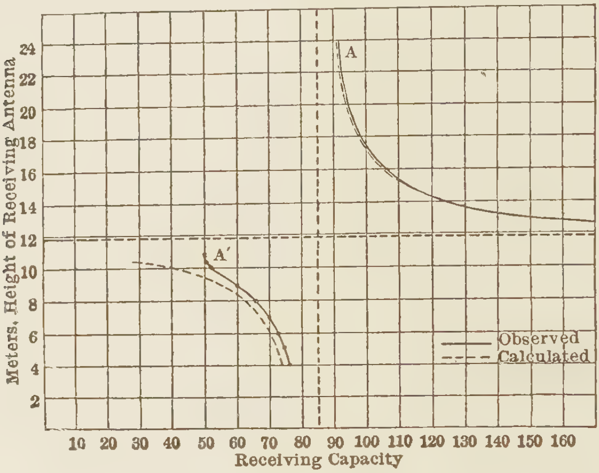

FIGURE 4. Relation of height of Antenna to C_4 for resonance.

---

[2] Curves 9 to 12 are plotted magnified about five times in comparison with Curves 1 to 8. In examining these curves it should be borne in mind that the decrease of length or height of the receiving antenna carries with it a double effect; namely, (1) a decrease of *reach* of the antenna into the field of force, and (2) a shift of the resonance relations of the receiving station with respect to the incident waves. We are at present concerned only with the second of these effects.

The relation between the height of antenna, H, and the capacity C_4 required for resonance was found to be approximately represented by the empirical equation:

$$(H - 11.8)(C_4 - 84.6) = 88, \tag{1}$$

which is the equation of an equilateral hyperbola with axes at $H = 11.8$ and $C_4 = 84.6$. The nature of the agreement between the observed and the calculated values is shown in Figure 4. Evidently the relation expressed in equation (1), though an interesting approximation, is not exact.

III. Theoretical Treatment.

Let us now turn from the experiment to the theory of the oscillation. The problem undertaken is the investigation of the relative current in the detector circuit (Circuit IV of Figure 1) for various adjustments of the constants of Circuit III and Circuit IV. In the theoretical treatment this carries with it (1) a determination of the adjustments that must be made to obtain resonance, (2) a determination of the adjustment for best resonance, (3) a determination of the effect of the resistances on the resonance relations and on the amount of current receivable, (4) a discussion of the resistance that a detector must have for greatest sensitiveness, (5) a computation of the amount of disturbing current that will be obtained from an undesired source of waves, and (6) a quantitative judgment as to the sharpest selectivity that can be attained by circuits of the form of Figure 2.

As stated in the Introduction, in treating these general questions it has been found necessary to depart from strict observance of the actual practical wireless-telegraphic conditions and to assume the capacity of the antenna, which is a distributed capacity in practical wireless telegraphy, to be replaceable by a localized capacity C_3. This modification of the problem will not completely destroy the validity of the discussion, because the simplified problem enables us to derive certain important conclusions in regard to the problem with the less simple conditions.

Referring to the localized-capacity circuits of Figure 1, and supposing an electromotive force $E \cos \omega t$ at e, the differential equations of the current in the two circuits are

$$L_3 \frac{\partial x}{\partial t} + M \frac{\partial y}{\partial t} + R_3 x + \frac{1}{C_3} \int x dt = E \cos \omega t, \tag{2}$$

$$L_4 \frac{\partial y}{\partial t} + M \frac{\partial x}{\partial t} + R_4 y + \frac{1}{C_4} \int y dt = 0, \tag{3}$$

in which x and y are the values of the current in the Circuits III and IV respectively. Eliminating x between these equations we have

$$(4)\quad (L_3L_4-M^2)\frac{\partial^4 y}{\partial t^4}+(R_4L_3+R_3L_4)\frac{\partial^3 y}{\partial t^3}+\left(\frac{L_3}{C_4}+\frac{L_4}{C_3}+R_3R_4\right)\frac{\partial^2 y}{\partial t^2}$$
$$+\left(\frac{R_3}{C_4}+\frac{R_4}{C_3}\right)\frac{\partial y}{\partial t}+\frac{y}{C_3C_4}=-EM\omega^3\sin\omega t.$$

If for brevity we call the left-hand member of equation (4) $f(y)$, the complete solution of (4) is any particular solution of (4) plus the general solution of

$$(5)\qquad f(y)=0.$$

Now the general solution of (5) involves exponentials with negative exponents as multipliers, and becomes zero after a few oscillations, so that all we need for the current y in case a large number of oscillations are performed, as with a persistent source of waves, is the "steady-state" solution for equation (4).

In order to get the steady-state solution of (4) let us write, in the place of (4), the equation

$$(6)\quad (L_3L_4-M^2)\frac{\partial^4 y}{\partial t^4}+(R_3L_4+R_4L_3)\frac{\partial^3 y}{\partial t^3}+\left(\frac{L_3}{C_4}+\frac{L_4}{C_3}+R_3R_4\right)\frac{\partial^2 y}{\partial t^2}$$
$$+\left(\frac{R_3}{C_4}+\frac{R_4}{C_3}\right)\frac{\partial y}{\partial t}+\frac{y}{C_3C_4}=-EM\omega^3e^{i\omega t},$$

which is (4) with $\sin\omega t$ replaced by an appropriate exponential with imaginary exponent.

Our required solution for (4) can then be obtained from a solution of (6) by getting y from (6), rationalizing the result, taking the imaginary part and dividing by i.

Now a particular solution of (6) is seen to be of the form of

$$(7)\qquad y=Ye^{i\omega t},$$

in which Y is to be determined by substitution of (7) in equation (6).

Making this substitution we obtain

$$(8)\qquad AY\omega^4-BiY\omega^3-CY\omega^2+DiY\omega+FY=-EM\omega^3,$$

where A, B, C, D, and F are the coefficients of equation (6). Whence

$$(9)\qquad Y=\frac{-EM\omega^3}{(A\omega^4-C\omega^2+F)-(B\omega^3-D\omega)i},$$

or writing the real part of the denominator as P, the imaginary as Qi,

$$(10) \qquad Y = \frac{-EM\omega^3}{P - Qi};$$

whence from equation (7),

$$(11) \qquad y = \frac{-EM\omega^3 e^{i\omega t}}{P - Qi},$$

$$= \frac{-EM\omega^3 (\cos \omega t + i \sin \omega t)}{P - Qi}.$$

Rationalizing equation (11), taking only the imaginary part and dividing by i, we have

$$y = \frac{-EM\omega^3 (P \sin \omega t + Q \cos \omega t)}{P^2 + Q^2},$$

$$(12) \qquad = \frac{-EM\omega^3 \sin\left(\omega t + \tan^{-1}\frac{Q}{P}\right)}{\sqrt{P^2 + Q^2}}.$$

Replacing P and Q in the denominator by their values in terms of the constants of the circuits, we have

$$(13) \quad y = \frac{-EM\omega^3 \sin\left(\omega t + \tan^{-1}\frac{Q}{P}\right)}{\sqrt{\left\{(L_3L_4 - M^2)\omega^4 - \left(\frac{L_3}{C_4} + \frac{L_4}{C_3} + R_3R_4\right)\omega^2 + \frac{1}{C_3C_4}\right\}^2 + \left\{(R_4L_3 + R_3L_4)\omega^3 - \left(\frac{R_4}{C_3} + \frac{R_3}{C_4}\right)\omega\right\}^2}}$$

Equation (13) is a well-known solution of equation (4), and gives the value of the current y in Circuit IV after the effect of the free-period initial disturbance has subsided. It is seen that the current y in Circuit IV is sinusoidal, with the frequency of the e.m.f. impressed on Circuit III. We shall concern ourselves only with the absolute value of the amplitude Y of this current.

Dividing numerator and denominator of equation (13) by ω^2 and factoring, we obtain

$$(14) \quad Y = \frac{EM\omega}{\sqrt{\left\{\left(L_3\omega - \frac{1}{C_3\omega}\right)\left(L_4\omega - \frac{1}{C_4\omega}\right) - M^2\omega^2 - R_3R_4\right\}^2 + \left\{R_4\left(L_3\omega - \frac{1}{C_3\omega}\right) + R_3\left(L_4\omega - \frac{1}{C_4\omega}\right)^2\right\}}}$$

Now let

$$(15) \qquad U = L_3\omega - \frac{1}{C_3\omega}, \qquad V = L_4\omega - \frac{1}{C_4\omega}.$$

Then equation (14) may be written

$$(16) \qquad Y = \frac{EM\omega}{\sqrt{(UV - M^2\omega^2 - R_3R_4)^2 + (R_4U + R_3V)^2}}.$$

This is another form of the expression for the current in Circuit IV, after the effect of the free-period initial disturbance has subsided. From equation (16) it can be seen that L_3 and C_3 enter in the equation only in the form U; L_4 and C_4 enter only in the form V.

In seeking the dependence of Y on the constants of the circuits let us now follow mathematically the steps taken in the experiment above described.

First, we shall take a fixed value of U and determine what value of V makes Y a maximum. This value of V that makes Y a maximum we shall call the "resonant value of V." The resonant value of V is obtained by making

$$(17) \qquad \frac{\partial Y}{\partial V} = 0.$$

This gives

$$(18) \qquad (UV - M^2\omega^2 - R_3R_4)\,U + (R_4U + R_3V)\,R_3 = 0$$

or

$$(19) \qquad V = \frac{M^2\omega^2U}{U^2 + R_3^2}.$$

Equation (19) gives the value of V for resonance with any particular given value of U. This relation will be further examined in a later section.

By the use of equation (19), when we have a given fixed value of U we can calculate the value of V for resonance. The current in Circuit IV for this resonant value of V may be obtained by substituting the value of V given by equation (19) into the equation for Y (equation (16)). If we designate this resonant value of Y by Y_{max}, we have

$$Y_{max} = \frac{EM\omega}{\sqrt{\left(\frac{M^2\omega^2U^2}{U^2 + R_3^2} - M^2\omega^2 - R_3R_4\right)^2 + \left(R_4U + \frac{R_3M^2\omega^2U}{U + R_3^2}\right)^2}}$$

$$= \frac{EM\omega}{\sqrt{\left(\frac{R_3^2M^2\omega^2}{U^2 + R_3^2} + R_3R_4\right)^2 + \left(\frac{R_3M^2\omega^2U}{U^2 + R_3^2} + R_4U\right)^2}}$$

Factoring the denominator of this expression, we have

$$(20) \qquad Y_{max} = \frac{EM\omega}{\left(\frac{R_3M^2\omega^2}{U^2 + R_3^2} + R_4\right)\sqrt{R_3^2 + U^2}}.$$

For any given value of U and the necessary other constants of the circuits, equation (19) enables us to compute the resonant adjustment of Circuit IV, and equation (20) gives the amplitude of the received current at the resonant adjustment. We have thus found the best V and the best Y *for a given* U. It is proposed next to find what would be the best value to give to U, while also keeping V at its best value, and thus to determine the best possible Y, which we shall call $Y_{max\,max}$.

To obtain the best U we must apply to equation (20) the condition

$$\frac{\partial Y_{max}}{\partial U} = 0.$$

This gives

$$-\frac{R_3 M^2\omega^2 \cdot 2U}{(U^2+R_3^2)^2}\sqrt{R_3^2+U^2} + \left(\frac{R_3M^2\omega^2}{U^2+R_3^2} + R_4\right)\frac{U}{\sqrt{R_3^2+U^2}} = 0,$$

or

$$(20\,\text{a}) \qquad -R_3M^2\omega^2U + R_4U^3 + R_3^2R_4U = 0.$$

Whence, omitting for the present the case of $U = 0$, which is treated on page 302, we have, after dividing by U and transposing,

$$(21) \qquad U_{opt} = \pm\sqrt{\frac{R_3}{R_4}(M^2\omega^2 - R_3R_4)},$$

in which the subscript "opt" is introduced to designate the optimum value. At the same time V must satisfy equation (19) which combined with equation (21) gives

$$(22) \qquad V_{opt} = \pm\sqrt{\frac{R_4}{R_3}(M^2\omega^2 - R_3R_4)}.$$

According to the conditions imposed by equation (19) U_{opt} and V_{opt} must either both be positive or both be negative. They cannot have opposite signs.

Equations (21) and (22) show what values to give U and V in order to obtain the largest possible current (which we shall call $Y_{max\,max}$) in Circuit IV. The value of the current, under these conditions, is found by substituting the optimum value of U, namely U_{opt} of equation (21), into the equation for Y_{max} (equation 20). When this is done, we have, after simplification,

$$(23) \qquad Y_{max\,max} = \frac{E}{2\sqrt{R_3R_4}}.$$

Equation (23) gives the max max current in Circuit IV provided equations (21) and (22) express the optimum resonance relation. Instead of (21) an alternative possible solution of equation (20_a) is

$$U_{opt} = 0.$$

Under this condition, according to equation (19)

$$V_{opt} = 0, \text{ also.}$$

This would give by equation (20)

$$(Y_{max\ max})_0 = \frac{EM\omega}{M^2\omega^2 + R_3R_4}. \tag{23 a}$$

The question arises under what conditions $(Y_{max\ max})_0$ of equation (23 a) is greater than $Y_{max\ max}$ of equation (23). The answer is seen to be that

$$(Y_{max\ max})_0 > Y_{max\ max}$$

when

$$\frac{EM\omega}{M^2\omega^2 + R_3R_4} > \frac{E}{2\sqrt{R_3R_4}};$$

that is, when

$$M\omega + \frac{R_3R_4}{M\omega} < 2\sqrt{R_3R_4}.$$

Squaring,

$$M^2\omega^2 + 2\,R_3R_4 + \frac{R_3{}^2R_4{}^2}{M^2\omega^2} < 4\,R_3R_4,$$

i. e.,

$$M^2\omega^2 - 2\,R_3R_4 + \frac{R_3R_4}{M^2\omega^2} < 0.$$

Extracting square root,

$$M\omega - \frac{R_3R_4}{M\omega} < 0,$$

$$M^2\omega^2 - R_3R_4 < 0. \tag{23 b}$$

In this case, the conditions (21) and (22) would give imaginary value of U_{opt} and V_{opt}.

Whence we conclude, that we are to use equations (21), (22) and (23) as solutions of the resonance problems, whenever $M^2\omega^2 > R_3R_3$. In other cases the alternative values

$$U_{opt} = 0, \qquad V_{opt} = 0, \quad \text{and} \quad (Y_{max\ max})_0 = \frac{EM\omega}{M^2\omega^2 + R_3R_4}$$

are to be used.

IV. Numerical Examination of the General Resonance Relation.

The equations above derived we shall now submit to numerical examination. Let us first examine the general resonance relation as expressed in equation (19). Replacing U and V in equation (19) by their values (15), we have the general resonance relation in the following form:

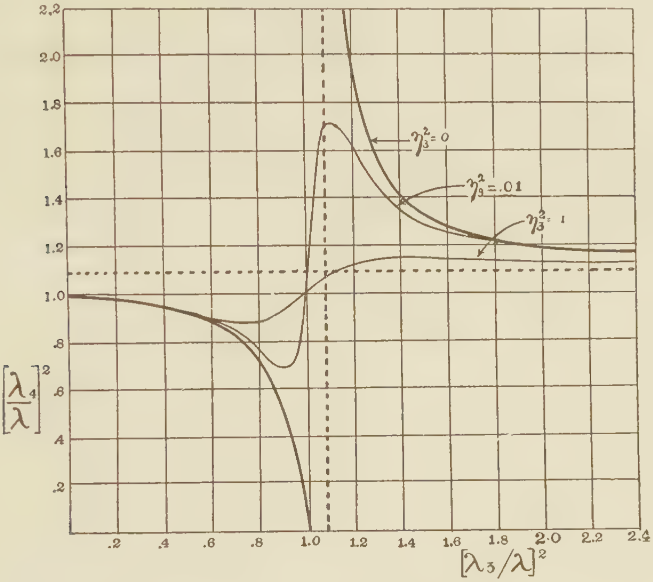

Figure 5. Theoretical relation of λ_4 to λ_3 for resonance. The different curves are for different values of damping in Circuit III. Given $\tau = .29$.

(24)
$$L_4\omega - \frac{1}{C_4\omega} = \frac{M^2\omega^2\left(L_3\omega - \frac{1}{C_3\omega}\right)}{\left(L_3\omega - \frac{1}{C_3\omega}\right)^2 + R_3^2},$$

or

(25)
$$1 - \left(\frac{\omega_4}{\omega}\right)^2 = \frac{\tau^2\left\{1 - \left(\frac{\omega_3}{\omega}\right)^2\right\}}{\left\{1 - \left(\frac{\omega_3}{\omega}\right)^2\right\}^2 + \eta_3^2},$$

in which

$$(26)\qquad \begin{cases} \omega_4{}^2 = \dfrac{1}{L_4C_4}, \\ \omega_3{}^2 = \dfrac{1}{L_3C_3}, \\ \tau^2 = \dfrac{M^2}{L_3L_4}, \\ \eta_3 = \dfrac{R_3}{L_3\omega}, \\ \eta_4 = \dfrac{R_4}{L_4\omega}. \end{cases}$$

TABLE I.

SHOWING RESONANT VALUES OF $(\omega/\omega_4)^2$ CORRESPONDING TO VARIOUS VALUES OF $(\omega/\omega_3)^2$. THE COEFFICIENT OF COUPLING, τ, IS ASSUMED TO BE .29.

$(\omega/\omega_3)^2$.	$(\omega/\omega_4)^2$ for.			$(\omega/\omega_3)^2$.	$(\omega/\omega_4)^2$ for.		
	$\eta_3{}^2 = 0.$	$\eta_3{}^2 = .01.$	$\eta_3{}^2 = .1.$		$\eta_3{}^2 = 0.$	$\eta_3{}^2 = .01.$	$\eta_3{}^2 = .1.$
2.50	1.16	1.17	1.12	.95	.373	.75	.96
2.00	1.20	1.19	1.13	.90	.54	.70	.93
1.66	1.27	1.25	1.15	.82	.70	.75	.89
1.43	1.39	1.33	1.15	.77	.78	.80	.88
1.25	1.72	1.51	1.13	.71	.82	.83	.88
1.17	2.27	....	....	.67	.85	.86	.89
1.11	6.25	1.72	1.08	.50	.93	.93	.93
1.05	−1.47	1.50	1.04	.30	.96	.96	.96
1.00	0.00	0.00	0.00	.25	.97	.97	.97

Some numerical calculations are given in Table I and plotted in Figure 5. Assuming $\tau = .29$, three different values of $\eta_3{}^2$ have been employed in calculating Table I, by the aid of equation (25) namely, $\eta_3{}^2 = 0$, .01, and .1, respectively.

Table I and Figure 5 give the resonant values of $\left(\dfrac{\omega}{\omega_4}\right)^2$ corresponding to different values of $\left(\frac{\omega}{\omega_3}\right)^2$. In examining the table and the figure it should be remembered that

$$(27)\quad \begin{cases} \left(\dfrac{\omega}{\omega_4}\right)^2 = \left(\dfrac{\lambda_4}{\lambda}\right)^2 = L_4 C_4 \omega^2, \\ \left(\dfrac{\omega}{\omega_3}\right)^2 = \left(\dfrac{\lambda_3}{\lambda}\right)^2 = L_3 C_3 \omega^2, \end{cases}$$

in which ω and λ are respectively the angular velocity and the wave length of the incident waves; λ_3 and λ_4 are the wave lengths corresponding to the natural period of Circuits III and IV respectively when standing alone. The abscissas of the curves of Figure 5 are values of $\left(\frac{\lambda_3}{\lambda}\right)^2$, or $\left(\frac{\omega}{\omega_3}\right)^2$, which equals $L_3 C_3 \omega^2$; the ordinates are values of $\left(\frac{\lambda_4}{\lambda}\right)^2$, or $\left(\frac{\omega}{\omega_4}\right)^2$, which equals $L_4 C_4 \omega^2$. For fixed values of L_3, L_4, and ω the abscissas and ordinates are, therefore, proportional to C_3 and C_4 respectively.

V. THE GENERAL RESONANCE RELATION (*continued*). SPECIAL CASE WHERE $\eta_3^2 = 0$.

An examination of equation (25) shows that when $\eta_3^2 = 0$ the curve of $\left(\frac{\lambda_3}{\lambda}\right)^2$ vs. $\left(\frac{\lambda_3}{\lambda}\right)^2$ for resonance is an equilateral hyperbola, with horizontal asymptote at $\left(\frac{\lambda_4}{\lambda}\right)^2 = \frac{1}{1-\tau^2}$, and vertical asymptote at $\left(\frac{\lambda_3}{\lambda}\right)^2 = \frac{1}{1-\tau^2}$. This curve with its asymptotes is also plotted in Figure 5. In the part of the curves plotted in Figure 5, even when η_3^2 is not equal to zero the curve does not appreciably depart from the equilateral hyperbola provided $\eta_3^2 \overset{=}{<} .001$. The corresponding curve in C_4 vs. C_3 for $\eta_3^2 = 0$, or $\eta_3^2 \overset{=}{<} .001$, has its asymptotes at $C_3 = \frac{1}{(1-\tau^2) L_3 \omega^2}$ and $C_4 = \frac{1}{(1 = \tau^2) L_4 \omega^2}$, and the equation giving the resonance relation of C_4 to C_3 in this case, obtained by a transformation of equation (25), is

$$(28)\quad \left(C_3 - \frac{1}{(1-\tau^2) L_3 \omega^2}\right)\left(C_4 - \frac{1}{(1-\tau^2) L_4 \omega^2}\right) = \frac{\tau^2}{(1-\tau^2)^2 L_3 L_4 \omega^4}.$$

This is the equation to which the empirical equation (1) corresponds, provided the height of antenna H is proportional to the capacity of the antenna C_3, assumed localized. The condition that C_3 should be localized, and particularly the conditions that the incident waves should be undamped, persistent and single-valued, were not fulfilled in the illustrative experiment cited above, and therefore it does not seem important to enter into a detailed comparison of equation (28) with equation (1). This has been partially done in the previous account of the experiment.[3]

The manner in which the resonance relation is affected by the resistance of Circuit III, corresponding to the antenna circuit, is shown in the curves marked $\eta_3{}^2 = .01$ and $\eta_3{}^2 = .1$ of Figure 5. The resistance R_4 of Circuit IV, corresponding to the detector circuit, is without effect in determining the form of these curves, which represent the general resonance relation. On the other hand, R_4 does have an effect in determining at which point of the curve of resonance relation the resonance is best, and R_4 is also significant in determining the sharpness of resonance. Some computations on this subject are given below.

VI. On the Optimum Resonance Relation.

Let us next examine the conditions for best resonance. We are still concerned merely with the steady-state vibration of the coupled circuits of Figure 1, under the action of the impressed sinusoidal electromotive force. The conditions for best resonance provided $M^2\omega^2 > R_3R_4$ are given in the equations (21) and (22), which after substitution from (15) become respectively

$$\left(L_3\omega - \frac{1}{C_3\omega}\right)_{opt} = \pm\sqrt{\frac{R_3}{R_4}(M^2\omega^2 - R_3R_4)}, \tag{29}$$

and

$$\left(L_4\omega - \frac{1}{C_4\omega}\right)_{opt} = \pm\sqrt{\frac{R_4}{R_3}(M^2\omega^2 - R_3R_4)}. \tag{30}$$

Dividing both sides of equation (29) by $L_3\omega$ and employing the notation of equation (26) we have

$$1 - \left(\frac{\omega_3}{\omega}\right)^2_{opt} = \pm\,\eta_3\sqrt{\frac{\tau^2}{\eta_3\eta_4} - 1}. \tag{31}$$

---

[3] G. W. Pierce, Physical Review, **20**, 220, 1905.

In like manner equation (30) becomes

$$1 - \left(\frac{\omega_4}{\omega}\right)^2_{opt} = \pm\, \eta_4 \sqrt{\frac{\tau^2}{\eta_3\eta_4} - 1}. \tag{32}$$

Replacing the ratio of angular velocities by the reciprocal ratio of wave lengths, in accordance with equations (27), we may transform equations (31) and (32) into the following equations:

$$\left(\frac{\lambda_3}{\lambda}\right)^2_{opt} = \frac{1}{1 \pm \eta_3 \sqrt{\frac{\tau^2}{\eta_3\eta_4} - 1}}, \tag{33}$$

and

$$\left(\frac{\lambda_4}{\lambda}\right)^2_{opt} = \frac{1}{1 \pm \eta_4 \sqrt{\frac{\tau^2}{\eta_3\eta_4} - 1}}. \tag{34}$$

It should be borne in mind that in order to get properly corresponding resonant values of λ_3 and λ_4, one must use either the plus sign in both of the equations or else the minus sign in both the equations. If one employs the plus sign in one of the equations and the minus sign in the other equation, the values of λ_3 and λ_4 so obtained are not appropriate simultaneous adjustments for best resonance. This is seen by an examination of equation (19).

By an examination of the discussion on p. 302 it will be seen that the optimum condition in the form of equations (33) and (34) can be attained only provided

$$\frac{\tau^2}{\eta_3\eta_4} > 1. \tag{35}$$

In order to facilitate the computation of λ_3 and λ_4 for various values of τ, η_3, η_4 and λ, equations (33) and (34) may be put in the form

$$\left(\frac{\lambda_3}{\lambda}\right)_{opt} = \frac{1}{\sqrt{1 \pm \phi_3}}, \quad \text{where } \phi_3 = \eta_3 \sqrt{\frac{\tau^2}{\eta_3\eta_4} - 1}, \tag{36}$$

and

$$\left(\frac{\lambda_4}{\lambda}\right)_{opt} = \frac{1}{\sqrt{1 \pm \phi_4}}, \quad \text{where } \phi_4 = \eta_4 \sqrt{\frac{\tau^2}{\eta_3\eta_4} - 1}. \tag{37}$$

The following table (Table II) gives the values of $\left(\frac{\lambda_3}{\lambda}\right)_{opt}$ for various values of ϕ_3.

TABLE II.

VALUES OF $\left(\frac{\lambda_3}{\lambda}\right)_{opt.}$ CORRESPONDING TO DIFFERENT VALUES OF ϕ_3. COMPUTED FROM EQUATIONS (36) AND (37).

ϕ_3.	$\left(\frac{\lambda_3}{\lambda}\right)_{opt.}$		ϕ_3.	$\left(\frac{\lambda_3}{\lambda}\right)_{opt.}$	
	using + sign.	using — sign.		using + sign.	using — sign.
.0	1.000	1.000	1.4	.646	Imaginary
.1	.953	1.054	1.5	.632	"
.2	.913	1.118	1.6	.620	"
.3	.877	1.196	1.7	.608	"
.4	.845	1.292	1.8	.597	"
.5	.817	1.414	1.9	.587	"
.6	.791	1.581	2.0	.577	"
.7	.767	1.825	2.1	.568	"
.8	.746	2.236	2.2	.559	"
.9	.725	3.162	2.3	.550	"
1.0	.707	∞	2.4	.542	"
1.1	.690	Imaginary	2.5	.535	"
1.2	.675	"	2.6	.527	"
1.3	.660	"			

These results are plotted in the curves of Figure 6, with $\left(\frac{\lambda_3}{\lambda}\right)_{opt}$ as ordinates and ϕ_3 as abscissas. The same curves give the values of $\left(\frac{\lambda_1}{\lambda}\right)_{opt}$ as ordinates provided the abscissas are read as values of ϕ_4. If the lower branch of the curve is used in obtaining the values of $\left(\frac{\lambda_3}{\lambda}\right)_{opt}$, the same branch must be employed in finding the corresponding values of $\left(\frac{\lambda_1}{\lambda}\right)_{opt}$. In like manner the top branch of the curve may be employed in both cases, provided the value of ϕ_3 or ϕ_4 is less than unity. For values equal to unity the wave length for the top branch of the curve is infinite, and for greater values the wave lengths of the top branch become imaginary. In this case the optimum wave-length adjustment becomes single-values and must be read from the lower branch of the curve.

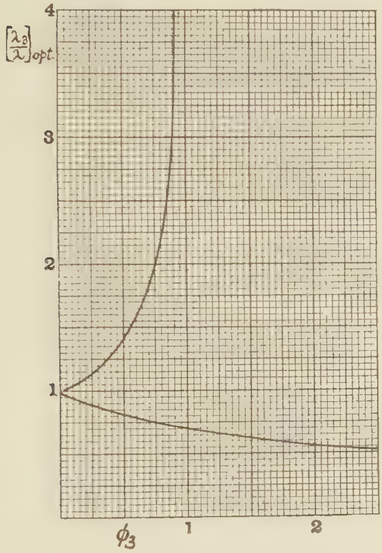

FIGURE 6. Auxiliary curve to assist in calculation of the optimum resonance adjustment. $\phi_3 = \eta_3 \sqrt{\frac{\tau^2}{\eta_3\eta_4} - 1}$. This curve also gives optimum value of λ_4 if ϕ_3 is replaced by $\phi_4 = \eta_4 \sqrt{\frac{\tau^2}{\eta_3\eta_4} - 1}$.

As an example of the manner of using the auxiliary curve (Figure 6) in the actual calculation of the optimum values of λ_3 and λ_4, let us take a special case. Suppose $\tau = .30$, $\eta_3 = .1$, let us give various values to η_4, and compute the corresponding optimum wave-length adjustments of the Circuits III and IV. A tabulation of the computation follows as Table III.

In compiling this table the values of ϕ_3 and ϕ_4 corresponding to the different values of η_4 were calculated by equations (36) and (37). The corresponding wave-length ratios were then taken from the curve of Figure 6.

The results contained in Table III are plotted in Figure 7. In a similar way the resonance relations for various values of τ and of η_3 may also be obtained, but the single example here computed and plotted serves to show the manner in which the coefficient of coupling and the damping factors contribute to determine the optimum resonance adjustment of the two circuits. The important facts to be noted are the following:

1. With given values of the coefficient of coupling and the damping factors of the two circuits the adjustment for best resonance is in general double valued. One may in general get best resonance either by setting both circuits to a wave length appropriately longer than that of the incident waves, or by setting both circuits to a wave length appropriately shorter than the incident waves.

TABLE III.

COMPUTATION OF OPTIMUM RESONANCE VALUES IN A SPECIAL CASE, IN WHICH
$\tau = .30$
$\eta_3 = .1$
η_4 IS GIVEN VARIOUS VALUES

η_4	ϕ_3	ϕ_4	$\left(\frac{\lambda_3}{\lambda}\right)_{opt.}$	$\left(\frac{\lambda_4}{\lambda}\right)_{opt.}$	$\left(\frac{\lambda_3}{\lambda}\right)_{opt.}$	$\left(\frac{\lambda_4}{\lambda}\right)_{opt.}$
.01	.943	.094	.720	.955	4.07	1.053
.02	.662	.133	.777	.940	1.73	1.070
.03	.539	.162	.806	.930	1.47	1.090
.04	.464	.186	.827	.917	1.37	1.110
.05	.412	.206	.840	.910	1.30	1.123
.06	.374	.224	.850	.905	1.26	1.135
.07	.345	.242	.862	.900	1.23	1.148
.08	.319	.255	.870	.895	1.205	1.152
.09	.300	.270	.875	.890	1.196	1.168
.1	.282	.282	.882	.882	1.180	1.180
.2	.187	.374	.917	.853	1.110	1.262
.3	.141	.423	.935	.837	1.078	1.310
.4	.112	.448	.950	.832	1.060	1.345
.5	.089	.445	.960	.830	1.048	1.340
.6	.071	.426	.970	.837	1.036	1.320
.7	.054	.378	.975	.852	1.032	1.262
.8	.035	.280	.980	.885	1.010	1.175
.9	.000	.000	1.000	1.000	1.000	1.000

Either pair of values under the brace is to be employed simultaneously for best resonance.

2. The adjustment for best resonance is materially influenced by the resistances of the two circuits. If, for example, with fixed incident

waves one tunes a wireless telegraph system of the coupled type to resonance with the use of a given detector, and then changes to a detector of different resistance, it is necessary to shift the wave length of both of the circuits in order to bring the system back to its best adjustment. This is a familiar experience, and serves to explain the

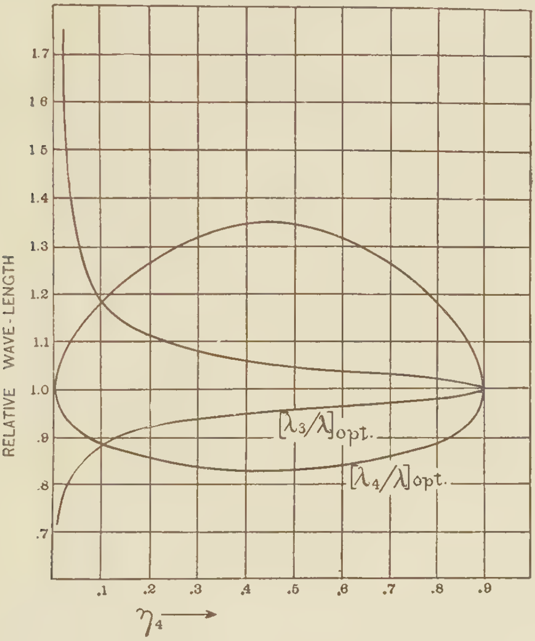

Figure 7. Relation of optimum wave-length adjustment to damping in Circuit IV, for a given value of η_3 and τ. ($\eta_3 = .1$, $\tau = .30$).

fact that with a vacuum detector of the type of Fleming's valve or Deforest's Audion or Hewitt's Mercury-arc detector one may attune the receiving station without change of its capacity or inductance merely by bringing a magnet up near the gaseous path of the detector. This merely changes the resistance of the circuit, and when the change is made in the proper direction and to the proper extent the system is thereby brought into resonance. The same thing may be effected in some cases by changing the strength of the local heating or ionizing current employed with detectors of this type.

3. The shifting of the resonance relation with change of resistance of the circuit has an influence on the sharpness of resonance when one

employs any of the ordinary detectors, because the resistance of the detectors is a function of the received current. This is a complex phenomenon and will enter into the consideration of sharpness of resonance, which is discussed below.

VII. On the Sharpness of Resonance and on the Possibility of Preventing Interference.

By reference to the previous pages it is seen that in order to obtain the best resonance, which gives a maximum of current in Circuit IV, it is necessary to adjust the period of both Circuit III and Circuit IV. We have given an expression for the value of the maximum current (that at best resonance) in equation (23), and we have also obtained a general expression for the current in Circuit IV (equation (16)), so that it is now possible to plot the current as best resonance is approached, and to form an estimate of the sharpness of resonance, whenever the constants of the circuits are known. This may conveniently be done in either of two ways, — which I shall classify as Case I and Case II, as follows:

Case I. Let us assume that the Circuit III is put at its best value (equation (21)), and let us compute the current in Circuit IV as the wave length of Circuit IV is varied. This corresponds to fixing the antenna circuit and tuning with the detector circuit.

Case II. Assume Circuit IV to be set at its best value (equation (22)) and compute the current in Circuit IV as the wave length of Circuit III is varied. This corresponds to fixing the constants of the detector circuit and tuning with the antenna circuit.

In either case we must know certain constants of the circuits, and I shall carry through the computation for both cases with several sets of constants. First it is necessary to transform the equations into suitable forms for making the computations.

Development of Equations for computing Case I. — The general expression for the amplitude of current in Circuit IV is given in equation (16); namely,

$$(16) \qquad Y = \frac{EM\omega}{\sqrt{(UV - M^2\omega^2 - R_3R_4)^2 + (R_4U + R_3V)^2}}.$$

Let us combine with this the condition that U shall have its optimum value, equation (22),

$$(22) \qquad U_{opt} = \pm \sqrt{\frac{R_3}{R_4}}(M^2\omega^2 - R_3R_4),$$

where $M^2\omega^2 > R_3R_4$, and let us suppose that V has, in general, not its optimum value, but a value k times its optimum value ; that is,

$$V = k \cdot V_{opt}, \tag{38}$$

in which k is a variable parameter, which may be positive, negative, whole, or fractional.

Equation (16) then becomes

$$Y_{(U_{opt})} = \frac{EM\omega}{\sqrt{(k \cdot U_{opt} V_{opt} - M^2\omega^2 - R_3R_4)^2 + (R_4 U_{opt} + R_3 \cdot k \cdot V_{opt})^2}}. \tag{39}$$

Replacing U_{opt} and V_{opt} by their values (equations (21) and (22)) we have after simplification

$$Y_{(U_{opt})} = \frac{E}{\sqrt{(k-1)^2 (M^2\omega^2 - R_3R_4) + 4\, R_3R_4}}. \tag{40}$$

Now dividing the square of equation (40) by the square of equation (23) we have

$$\left(\frac{Y_{(U_{opt})}}{Y_{max\ max}}\right)^2 = \frac{1}{\frac{(k-1)^2}{4}\left(\frac{M^2\omega^2}{R_3R_4} - 1\right) + 1} \tag{41}$$

$$= \frac{1}{\frac{(k-1)^2}{4}\left(\frac{\tau^2}{\eta_3\eta_4} - 1\right) + 1}.$$

This equation gives the current in terms of the parameter k provided $\tau^2 > \eta_3\eta_4$. Let us now obtain the wave lengths in terms of the same parameter. The values of V and V_{opt} from equations (15) and (22) substituted in (38) give

$$L_4\omega - \frac{1}{C_4\omega} = \pm\, k \sqrt{\frac{R_4}{R_3}(M^2\omega^2 - R_3R_4)}. \tag{42}$$

Dividing (42) by $L_4\omega$ gives

$$1 - \left(\frac{\omega_4}{\omega}\right)^2 = \pm\, k \sqrt{\frac{R_4}{R_8}(M^2\omega^2 - R_3R_4)} \tag{43}$$

$$= \pm\, k\eta_4 \sqrt{\frac{\tau^2}{\eta_3\eta_4} - 1}.$$

Whence

$$(44)\qquad \left(\frac{\lambda_4}{\lambda}\right)^2 = \frac{1}{1 \pm k\eta_4\sqrt{\dfrac{\tau^2}{\eta_3\eta_4} - 1}}$$

$$= \frac{1}{1 \pm k\phi_4}, \quad \text{where} \quad \phi_4 = \eta_4\sqrt{\frac{\tau^2}{\eta_3\eta_4} - 1}.$$

This equation (44) gives the relation of the wave lengths to the parameter k, and is applicable only provided U has its optimum value and $\tau^2 > \eta_3\eta_4$. The condition that V have its optimum value is conveniently expressed in the form of equation (36) above. Equations (44) and (36) must both be used with the same sign in order to be simultaneously correct.

In case $\tau^2 \gtreqless \eta_3\eta_4$, equations (44) and (41) cannot be employed. In this case U_{opt} and V_{opt} are both zero (see page 302), and a special investigation is necessary. This proves to be simple. Let us take equation (16), make $U = U_{opt} = 0$, and we have

$$(45)\qquad Y_{(U_{opt})} = \frac{EM\omega}{\sqrt{(M^2\omega^2 + R_3R_4)^2 + R_3{}^2V^2}}.$$

Expressing this result in terms of $Y_{max\,max}$ by dividing equation (45) by equation (23), we have

$$(46)\qquad \left(\frac{Y_{(U_{opt})}}{Y_{max\,max}}\right) = \frac{M^2\omega^2 \cdot 4\,R_3R_4}{(M^2\,\omega^2 + R_3R_4)^2 + R_3{}^2\left(L_4\omega - \dfrac{1}{C_4\omega}\right)^2}$$

$$= \frac{M^2\omega^2 \,/\, R_3R_4}{\dfrac{1}{4}\left(\dfrac{M^2\omega^2}{R_3R_4} + 1\right)^2 + \dfrac{1}{4}\dfrac{L_4{}^2\omega^2}{R_4{}^2}\left\{1 - \left(\dfrac{\omega_4}{\omega}\right)^2\right\}^2}$$

$$= \frac{\tau^2 \,/\, \eta_3\eta_4}{\dfrac{1}{4}\left(\dfrac{\tau^2}{\eta_3\eta_4} + 1\right)^2 + \dfrac{1}{4\,\eta_4{}^2}\left\{1 - \left(\dfrac{\lambda}{\lambda_4}\right)^2\right\}^2}.$$

Equation (46) is to be employed in place of (41) whenever

$$\tau^2 \,/\, \eta_3\eta_4 \leqq 1.$$

An interesting case arises when $\tau^2 \,/\, \eta_3\eta_4 = 1$. Equation (46) then simplifies to

$$(47)\qquad \left(\frac{Y_{(U_{opt})}}{Y_{max\,max}}\right)^2 = 1 + \frac{1}{\dfrac{1}{4\,\eta_4{}^2}\left\{1 - \left(\dfrac{\lambda}{\lambda_4}\right)^2\right\}^2}.$$

Equation (47) holds only when $\tau^2 = \eta_4\eta_4$; that is, $M^2\omega^2 = R_4R_4$. In this case also $U_{opt} = V_{opt} = 0$.

Computation and Discussion of Case I. In the above paragraphs the equations have been derived for the current developed in Circuit

TABLE IV.

$$\text{Given } \tau = .30 \qquad \tau^2 = .09$$

$$\eta_3 = .01 \qquad \frac{\tau^2}{\eta_3\,\eta_4} = 900$$

$$\eta_4 = .01$$

$$\left(\frac{Y(U_{opt})}{Y_{max\,max}}\right)^2 = \frac{1}{\frac{(k-1)^2}{4}\left(\frac{\tau^2}{\eta_3\eta_4} - 1\right) + 1} = \frac{1}{225(k-1)^2 + 1}$$

$$\left(\frac{\lambda_4}{\lambda}\right) = \frac{1}{1 \pm k\eta_4\sqrt{\frac{\tau^2}{\eta_3\eta_4} - 1}} = \frac{1}{1 \pm .3\,k}.$$

$k.$	λ_4/λ		$\left[\frac{Y}{Y_{mm}}\right]^2$	$k.$	λ_4/λ		$\left[\frac{Y}{Y_{mm}}\right]^2$
	With plus sign.	With minus sign.			With plus sign.	With minus sign.	
1.8	.806	1.490	.007	.95	.882	1.183	.640
1.7	.814	1.428	.009	.9	.887	1.170	.307
1.6	.822	1.387	.012	.8	.898	1.147	.100
1.5	.831	1.348	.018	.7	.909	1.125	.047
1.4	.839	1.313	.027	.6	.921	1.104	.027
1.3	.848	1.280	.047	.5	.933	1.084	.018
1.2	.857	1.250	.100	.4	.945	1.066	.012
1.1	.868	1.222	.307	.3	.958	1.048	.009
1.05	.872	1.208	.640	.2	.971	1.030	.007
1.0	.877	1.196	1.000				

IV for any adjustment of this circuit, while Circuit III is kept at its optimum value. This corresponds to keeping the antenna circuit of a wireless telegraph station set at its best value for given conditions and tuning the system by variation of Circuit IV. Assuming any given constants of the two circuits and any given wave length of incident waves, we can now make computations which will give the shape and form of the resonance curve. In making the calculations if $M^2\omega^2 > R_3R_4$ we can take convenient values of the parameter k and calculate the wave-length adjustment corresponding to the given values of k (equation 44) and also the relative current for the same values of k (equation 41). The results will give relative current corresponding to various wave-length adjustments.

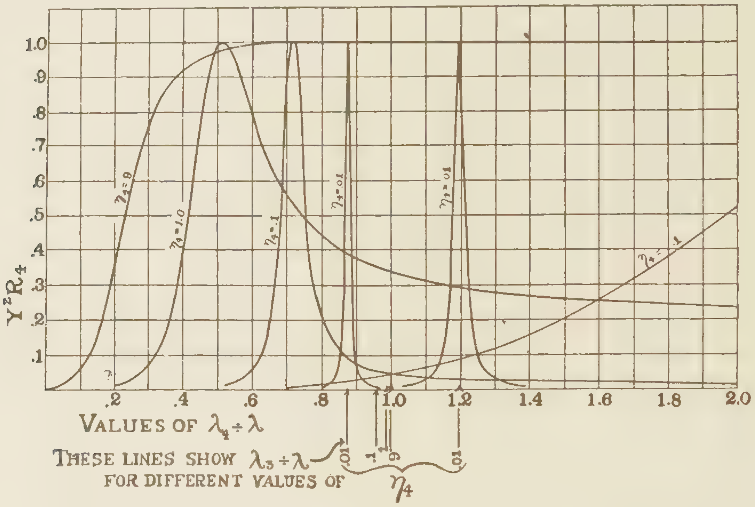

FIGURE 8. Resonance curves giving theoretical relation of current-square times resistance of Circuit IV to wave-length adjustment in the neighborhood of the optimum adjustment of Circuit IV when Circuit III is at optimum — for $\eta_3 = .01$, $\tau = .30$.

Case I with $\eta_4 = .01$, $\eta_3 = .01$, $\tau = .30$. — A sample set of computed results assuming $\tau = .30$, $\eta_3 = .01$ and $\eta_4 = .01$ is given in Table IV.

These results are plotted as the two curves marked "$\eta_4 = .01$" of Figure 8. The abscissas are values of the wave-length adjustment relative to the wave length of the incident waves (λ_4/λ). The ordinates are values of $\left(\dfrac{Y}{Y_{max\,max}}\right)^2$ but since $Y_{max\,max} = \dfrac{E}{2\sqrt{R_3R_4}}$, and since all the curves of the figure are plotted with constant R_3 (i.e., constant η_3), constant E, and constant M, it is perhaps more instructive to regard the ordinates of Figure 8 as relative values of Y^2R_4, and they are so designated in the figure. Referring again to the figure, these two curves marked "$\eta_4 = .01$" are obtained as resonance curves of square of current in Circuit IV plotted against wave-length adjustment of Circuit IV, and are obtained by setting Circuit III at its best value and leaving it at that value during the tuning. The appropriate best-value settings of the wave length of Circuit III are indicated by the positions of the two lines marked "$\eta_4 = .01$" at the lower margin of the figure. The short-wave adjustment of λ_3 (at $\lambda_3/\lambda = .877$) is required for the short-wave resonance curve (with its maximum at $\lambda_4/\lambda = .877$), and the long-wave adjustment of λ_3 (at $\lambda_3/\lambda = 1.196$) is required for the long-wave resonance curve (with maximum at $\lambda_4/\lambda = 1.196$). It is seen that in this particular case, with $\eta_3 = \eta_4 = .01$, the resonant adjustment of Circuit III and that of Circuit IV have the same wave-length $\lambda_3 = \lambda_4$; and because of the smallness of the damping factors η_3 and η_4, the two curves are sharp.

Case I (continued). Assuming again $\tau = .30$, $\eta_3 = .01$, *but with* $\eta_4 = .1$. — Suppose now that we give to Circuit IV a higher resistance so that $\eta_4 = .1$. This may be done by using a higher resistance detector in Circuit IV. This will cut down the maximum value of the current in Circuit IV, but will leave the square of the current times the resistance (namely, Y^2R_4) the same as before, so that the curve in terms of Y^2R_4 will have the same maximum amplitude for $\eta_4 = .1$ as for $\eta_4 = .01$. Complete computations from equations (44) and (41) show that the curve will have the form and position given in Figure 8 and marked "$\eta_4 = .1$." The corresponding appropriate adjustment of Circuit III is given by the line marked "$\eta_4 = .1$" of the lower margin. The curve going out to the right, also marked "$\eta_4 = .1$" in Figure 8, is a part of another possible resonance curve in this case. This second resonance curve culminates beyond the limit of the figure with its maximum at $\lambda_4/\lambda = 4.18$, and requires the adjustment of λ_3/λ at 1.05.

The results of the computations in this case show in an interesting manner the necessity of tuning both circuits to get resonance, and show how markedly the adjustment of Circuit IV may be affected by the adjustment of Circuit III; since with the constants here assumed, the change of Circuit III from $\lambda_3/\lambda = .96$ to $\lambda_3/\lambda = 1.05$ necessitates the shifting of λ_4/λ from .716 to 4.18. The resonance in the former case is sharp, and that in the latter case is very dull.

Case I (continued). Assuming again $\tau = .30$, $\eta_3 = .01$, *while* η_4 *is made* $= 1$. We obtain the resonance curve marked $\eta_4 = 1.0$ (Figure 8) with appropriate adjustment of λ_3/λ_4 at .986. In this case the second resonance value in the region of long waves is imaginary.

Case I (continued). $\tau = .30$, $\eta_3 = .01$, *while* $\eta_4 = 9$. — This is the special case requiring the use of equation (47) and gives the curve marked "$\eta_4 = 9$," requiring λ_3/λ to be 1.0. This curve is almost flat on top and for this condition tuning with Circuit IV is impossible. There is left here, as with all the curves of this figure, the alternative of leaving Circuit IV fixed at its best value and tuning with Circuit III. This is Case II, which we presently come to consider. It is proposed first, however, to present a new set of curves under Case I with a larger damping factor (η_3) in Circuit III, corresponding to the antenna circuit.

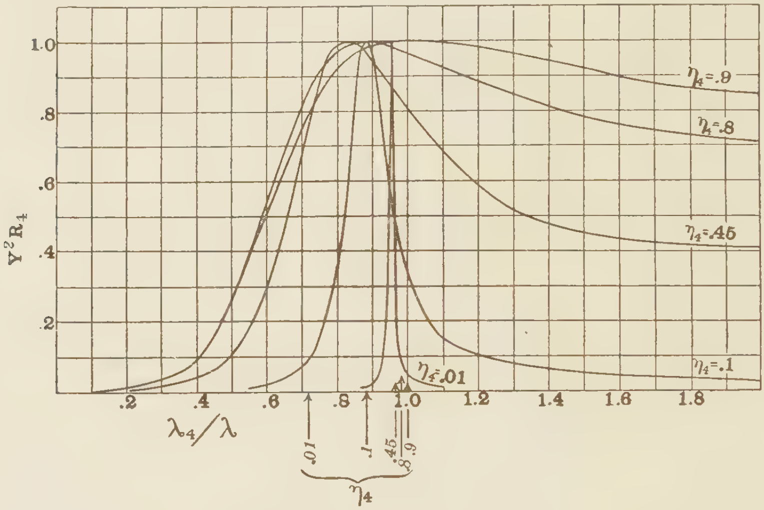

FIGURE 9. Curves similar to Figure 8, but with $\eta_3 = .1$, $\tau = .30$.

Case I (continued). Assuming $\tau = .30$, $\eta_3 = .1$, *and* η_4 *various.* — The curves for these conditions are plotted in Figure 9 for only the short-wave adjustment. The corresponding long-wave adjustments are presented in Figure 10.

The Equations and Computation of Case II. — It is now proposed to set Circuit IV at its best value, with any given constants of circuits, and to tune with Circuit III. The equations giving the current in Circuit IV for various values of wave length of Circuit III, are obtained from (41) and (44) by a simple interchange of subscripts, — giving

$$(48) \qquad \left(\frac{Y(V_{opt})}{Y_{max\ max}}\right)^2 = \frac{1}{\frac{(k-1)^2}{4}\left(\frac{\tau^2}{\eta_3\eta_4} - 1\right) + 1},$$

where k is determined by the equation

$$\left(\frac{\lambda_3}{\lambda}\right)^2 = \frac{1}{1 \pm k\eta_3\sqrt{\frac{\tau^2}{\eta_3\eta_4} - 1}}. \tag{49}$$

By a comparison of (48) and (49) with equations (41) and (44) it will be seen that the method of Case II will give sharper resonance than that of Case I whenever $\eta_3 < \eta_4$. With the high resistance detectors in ordinary use in wireless telegraphy, η_3 is generally much less than η_4, and the sharp tuning is best attained by the method of Case II; that is, by fixing the condenser circuit (Circuit IV) by successive approximations to a setting somewhere near its best value for the given incident waves, and then making the final adjustment by changing Circuit III.

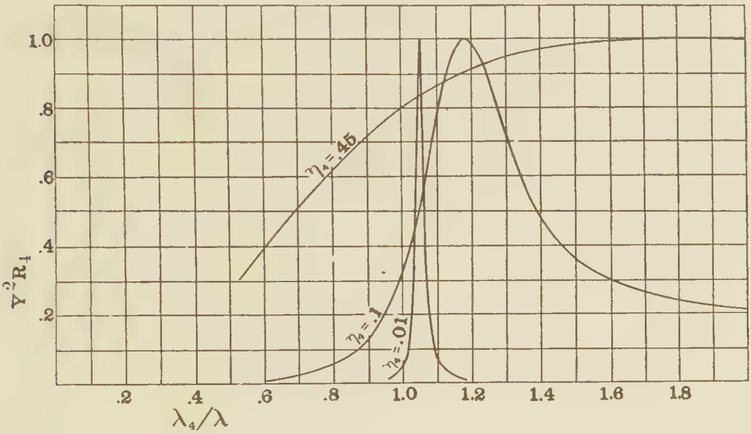

FIGURE 10. Long-wave adjustments corresponding to the short-wave adjustments of Figure 9.

Three numerical examples are given in the curves of Figure 11. For all these curves τ is assumed to be .30, and η_4 is taken as 1.0. The values of η_3 are marked on the respective curves.

Application to Actual Wireless Telegraphic Cases. — Now the corresponding actual wireless-telegraph resonance curves taken with coupled circuits, one of which has distributed capacity, will be less sharp than the corresponding curves here computed and drawn, so that as soon as we know the damping constants and the coefficient of coupling of the wireless-telegraph circuits we can select from the curves here computed a set of curves that will be more selective than the wireless-telegraph curves, and we can in this way fix a limit to the sharpness of resonance that can be attained in practice. Some computations of this character on the extent to which interference can be prevented under certain conditions, assumed as practical, have been published elsewhere.[4]

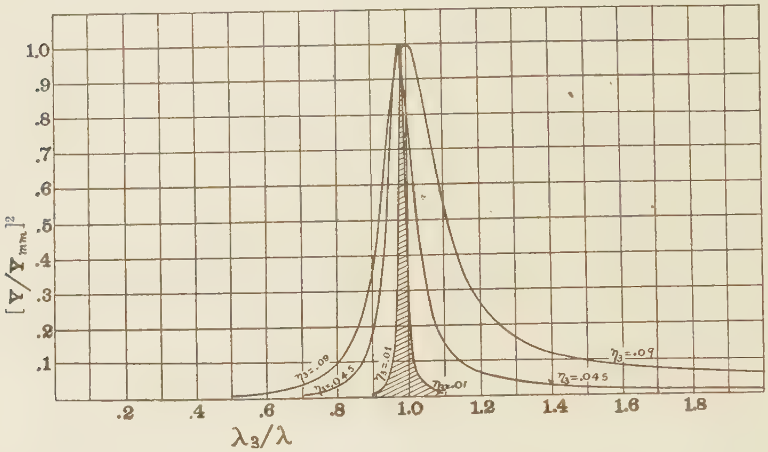

FIGURE 11. Resonance curves obtained by tuning with Circuit III while Circuit IV is at best value. $\tau=.30$, $\eta_4=1$.

VIII. THE MAXIMUM CURRENT, AND DETECTOR RESISTANCE.

Equation (23) is an expression for the maximum current that can be obtained in Circuit IV, when the inductances and capacities of Circuits III and IV are given their best values.

An interesting fact that can be obtained from an examination of equation (23) is that the square of the current multiplied by R_4 gives a quantity independent of R_4. This means that the heat developed in Circuit IV is independent of R_4; that is to say, the same amount of heat is developed in Circuit IV, at best resonance, whether a high-resistance or a low-resistance detector is employed. This means that, if the detector is an instrument for measuring heat, a low-resistance detector would be as sensitive as a high-resistance detector if it were not for the fact that the lower the resistance of the detector the less the proportion of the total heat that is developed in the detector itself, because of the larger development of heat in the rest of the Circuit IV. Since the resonance is sharper with the low-resistance circuit, the resistance of a thermal detector, provided its indications are proportional merely to the heat developed in it, ought to be as low as is consistent with the localization of a large part of the energy in the detector; that is, for example, in order to get 9/10 of the maximum effect, the resistance of the detector, if its indications are proportional merely to the heat developed in it, ought to be nine times the high-frequency resistance of the rest of Circuit IV.

---

[4] Pierce, Principles of Wireless Telegraphy, McGraw-Hill Book Company, New York, 1910.

Similar considerations apply to a detector of the electrodynamometer type. If the deflections of the electrodynamometer are proportional to $n^2 Y^2$, where n is the number of turns of wire in the coil, and if the size of the channel of windings is fixed so that the resistance R of the detector is $\frac{\rho l}{S}$, l and S being the length and cross section of the wire in the coil, then we have

$$l = 2\,\pi r \cdot n,$$

in which r is the mean radius of the windings; and approximately

$$S = \frac{A}{n},$$

A being the area of the channel.

Therefore,
$$R = \frac{\rho\, 2\,\pi r n^2}{A},$$

or
$$R \sim n^2.$$

Whence if the deflection,
$$D \sim n^2 Y^2,$$
$$D \sim R\ Y^2.$$

In this, R is the resistance of the detector alone. Now according to equation (23) the quantity of $R_4 Y^2$ is not changed by changing R_4. Hence if the resistance R is made nine times the resistance of the rest of Circuit IV, the deflection of the high-frequency dynamometer will be 9/10 as large as would be obtained with a detector of very high resistance, and the resonance with the low resistance detector will be much sharper than with the detector of very high resistance.

However, it must be borne in mind that this conclusion holds only between different detectors of the same type, and presupposes that the factor by which $R\,Y^2$ is to be multiplied to get the deflection or other indication is independent of R. In the case of the dynamometer or hot-wire ammeter the factor of convertibility of the energy of rapid alternations into deflection is probably fairly constant but is small; whereas, with certain other types of detectors, notably the electrolytic and the crystal rectifiers the convertability of the energy of rapid alternations into direct current energy is not constant, and appears to be relatively large only provided the resistance of the detector is large. This has constrained wireless telegraphic practice to high-resistance detectors, with the consequent deficiency in sharpness of resonance. The analysis given in the present paper shows that there is no inherent necessity in using these high-resistance detectors provided only detectors of lower resistance can be found with a large efficiency in converting electric energy of rapid alternations into energy of direct current or slowly-varying periodic current.

Jefferson Physical Laboratory, Harvard
University, Cambridge, Mass.
October, 1910.

Proceedings of the American Academy of Arts and Sciences.

Vol. XLVI. No. 14. — January, 1911.

CONTRIBUTIONS FROM THE JEFFERSON PHYSICAL LABORATORY, HARVARD UNIVERSITY.

THE ACTION OF MERCURY ON STEEL AT HIGH PRESSURES.

By P. W Bridgman.

With a Plate.

THE ACTION OF MERCURY ON STEEL AT HIGH PRESSURES.

By P. W. Bridgman.

Presented by John Trowbridge, November 9, 1910. Received October 28, 1910.

Under ordinary circumstances steel and mercury are inert with respect to each other, as is shown by the possibility of carrying mercury for indefinite periods of time in steel flasks. But there seems to be a widely spread notion that under higher pressures there may be some action not operative at lower pressures. This possibility is usually ascribed to the extraordinary mobility of the mercury molecule. For instance, every one who has had experience in making joints for pressures of a few atmospheres knows that mercury will easily find its way through holes impervious to water or less viscous fluids. It has therefore been thought probable that under higher pressures the easily moving mercury molecule might be forced through the very pores of the solid metal itself, and that in consequence it might be impossible to hold mercury at all in metal receptacles at high pressures. This view has received its highest confirmation from some often cited experiments of Amagat. Amagat[1] has described how in one case mercury was forced by a pressure of 3000 atmospheres in a fine spray through 8 cm. of cast steel, in which no flaw could be afterward detected with the microscope. Amagat explained this effect in the way suggested above by assuming that the mercury was forced by the high pressure through the very intermolecular pores of the solid steel. It is worthy of notice that it was found possible to avoid this difficulty merely by making another apparatus with thicker steel parts. There is also work by Cailletet and Collardeau[2] on the vapor pressure of mercury at high temperatures that seems to demand in explanation that the mercury was forced through solid steel by comparatively low pressures at sufficiently high temperatures.

---

[1] Amagat, Ann. de Chim. et Phys. (6), **29**, 87–88 (1893); also Compt. Rend. March 2, 1885.

[2] Cailletet, Colardeau and Riviere, Compt. Rend. **130**, 1585–1591 (1900).

In measurements undertaken by the author of various physical constants at high pressures, this question of the action of mercury and steel became of vital importance. For instance, the methods adopted to measure compressibility assumed that there was no penetration of the mercury into the steel containing vessel, as do also the methods used more recently in determining the variation with pressure of the freezing temperature of mercury and its change of volume on freezing. The preliminary work at low pressures made it seem probable that at least over the pressure range used by Amagat the effect described by him does not really exist in the grades of steel used by him, and that the observed effect was due more likely to flaws in the steel. At the same time it was found that at higher pressures there is undoubtedly an effect important enough to demand the redesigning of the apparatus for the measurement of the change of volume on freezing. It is the purpose of this paper to describe the various experiments made to prove the undoubted existence of the effect, and to offer a qualitative explanation. The effect was run across only incidentally, and it was examined only so much as was necessary for the work in hand. No endeavor has been made to make the experimental investigation or the explanation complete, as this would lead too far afield.

The effect was first found during an attempt to measure the change of volume of mercury on freezing by a method similar in many respects to that of Tammann.[3] It was found that cylinders of hardened chrome nickel steel would support very much less internal pressure when this pressure was transmitted by mercury than when the transmitting fluid was some other liquid such as water. The pressure might be less in the ratio of three or four to one; thus cylinders which stood without breaking 24000 atmospheres when the pressure was transmitted to the interior by a mixture of water and glycerine broke on the next application of pressure at 5–8000 atmos. if the transmitting fluid were mercury. These few preliminary experiments under varying conditions made the existence of an effect seem probable, but pointed to nothing conclusively. It might well be that there was a flaw running the entire length of the steel bar from which all these pieces were cut, into which the mercury forced its way in consequence of its greater mobility, in preference to the water, or it might be that there was here a fatigue effect, the steel breaking more readily on the second application of pressure with the mercury because of the exceedingly high pressure to which it had been previously exposed by the water. This explanation, however, was opposed by all previous experience with this steel. In any event, the effect of the mercury was entirely different from that found by Amagat, as there was never any tendency for the mercury to squirt through the steel, but there was always sudden rupture, the cylinder cracking down one side in a plane containing the axis. To show conclusively that a cylinder of hardened nickel steel will really not stand so much pressure when the transmitting liquid is mercury as when it is some other liquid such as water, the following experiment was undertaken. A bar of this special steel (Krupp Special Chrome Nickel Steel E. F. 60.0) was cut into twelve pieces each $8\frac{1}{2}''$ long and $2''$ diameter. (See Figure 1.) The pieces were numbered and their orientation in the original bar carefully noted. They were then each pierced with a $\frac{1}{2}''$ hole reamed to size, turned on the outside true with the hole, and hardened by heating to a bright cherry red and quenching in a heavy tempering oil. Every other cylinder (Nos. 1, 3, 5, 7, 9, 11) was filled with mercury and tested by applying pressure to the mercury by means of a piston actuated by a hydraulic press. The test conditions of these different cylinders were varied somewhat by changing the rapidity with which pressure was applied; in other respects the conditions were the same. The other cylinders were tested in a similar way, except that the fluid transmitting the pressure was not mercury; being in four of the six cases water and glycerine, in the others ether and carbon disulphide respectively. The pressure in the test cylinders was determined from the pressure of the fluid actuating the hydraulic ram, multiplying in the ratio of the areas of the two pistons. An unknown error is introduced here by the friction of the packing, but in other experiments with similar cylinders in which the pressure inside the small cylinders was measured directly it was found that the error so introduced was nearly constant and easy to correct for. The correction so found was used in the results to be given. In any event, the correction is less than the irregularities introduced by other causes.

---

[3] Tammann, Kristallisieren und Schmelzen (1903), p. 204.

FIGURE 1. Form of the test cylinders broken with mercury.

The accompanying table (see Table I) shows the results found with the six cylinders containing mercury. The pressure was increased more slowly for the higher numbered cylinders; with the four first the pressure was increased uniformly at the rate indicated, while with the two others it was increased in discontinuous steps as shown. In making the tests, pressure was first pushed to 1500 atmos. and kept there for several minutes to make sure that there was no leak and everything was in working order. The time given in the duration column is exclusive of the time occupied by the preliminary application of 1500. It is evident that the data admit of no quantitative comparison as the great discrepancy between tests 1 and 3 made under as nearly as possible the same conditions shows. However, these two tests were made with a high rate of increase of pressure. Those made with a slower rate show much more consistent results. In general it appears that the slower the rate of increase of pressure the lower the bursting pressure, which apparently has as its lower limit about 3000 atmos. The data are not inconsistent with the view that there is a critical pressure which will produce rupture if applied for an infinite time; pressures above this produce rupture in constantly less times.

TABLE I.

No. of Cylinder.	Breaking Pressure $\frac{\text{Kgm}}{\text{cm}^2}$.	Rate of Increase of Pressure.	Total Euration.	Location of Crack.	Remarks.
1	10250	1250 kgm. in 30 sec.	$3\frac{1}{2}$ min.	−123°	Pressure on 1, 3,5, 7, was increased uniformly
3	4750	" " "	$1\frac{1}{3}$ "	+107°	
5	3250	1250 kgm. in 60 sec.	$1\frac{2}{5}$ "	+ 64°	Broke on second trial
7	3375	625 kgm. in 60 sec.	$4\frac{1}{4}$ "	+ 11°	Leaked on first at 2750
9	4000	1500 for $3\frac{1}{2}$ min. 2750 for 10 min.; breaks at 4000 after $\frac{1}{2}$ min.	14 "	− 25°	Pressure on 9 and 11 increased discontinuously
11	3000	At 2750 for 46 min. Breaks at 3000 after 5 min.	51 "	−106°	

The location of the crack is an important consideration. The crack in each cylinder is in an axial plane, extending the entire length of the cylinder. It was located by measuring the angular distance from a fiducial line marked the length of the bar from which the pieces were cut. The diagram (see Figure 2) showing the location of the crack in the several cylinders makes clear that the rupture does not take place along a flaw in an axial plane extending originally throughout the entire bar. Furthermore, since the manner of fracture of each cylinder demands that the flaw be in an axial plane if the fracture is due to a flaw, and since it seems improbable that a flaw throughout the length of one cylinder should not extend into the neighboring cylinders, the conclusion seems justified that the rupture is not due to a flaw.

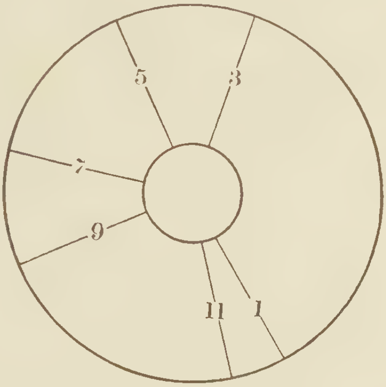

Figure 2. Orientation of the crack with respect to the original bar in the six cylinders broken with mercury.

Now compare with this the tests for the other set of six cylinders from the same bar. (See Table II.)

The difference between these two sets of tests is sufficiently striking. Not one of the cylinders filled with a fluid other than mercury was broken during the tests, although in several cases the test was terminated by an irrelevant accident. The

TABLE II.

No. of cylinder.	Maximum Pressure $\frac{\text{Kgm}}{\text{cm}^2}$	Manner of applying Pressure.	Remarks.	Fluid.
2	23500	Rate of increase not noted	Packing plug blows out	Glycerine and water
4	19000	From 1500 to 15000 at rate of 1250 in 30 sec. Held at 15000 for 2½ min., 17500 for 3 min.	Packing plug blows out	Glycerine and water
6	15200	From 1500 to 11000 uniformly in 4½ min. Held here for 3 min., then at 13500 for 1 min.	Terminated by leak	Glycerine and water
8	24000	15 min. in reaching max. Held here for 6 min.	Leak after 6 min.	Glycerine and water
10	20250	Held at 16500 for 2 min.; at 20250 for 45 sec.	Plug blows out	Ether
12	24000	1 hour in reaching max. at uniform rate. Held her for 8 min.	No leak	CS_2

maximum pressure reached by three of the cylinders without breaking was 24000 atmos., over 8 times the lowest breaking pressure of the cylinders filled with mercury, and nearly 2½ times the maximum breaking pressure. Greater pressure than 24000 atmos. was not applied because the limit of the press was reached. Of course the stress produced in a cylinder by internal fluid pressure depends only on the pressure in the fluid and not on the nature of the fluid. It must be, then, that the mercury takes some special part in producing rupture quite apart from the stress produced by it.

The magnitude of the fluid pressures mentioned here requires brief comment, because without a word of explanation it may seem so large as to cast discredit on the accuracy of all the data. In the first place, a steel of the kind described above with the indicated heat treatment is the only steel known to the author that will stand the pressures used. The best grades of carbon tool steels will not stand much more than 18000 atmos. As to the measurement of the pressure, similar apparatus has been used up to 13000 atmos. and the pressure measured directly with an absolute gauge with an accuracy of $\frac{1}{10}$ per cent. Absolute measurements have not been made above this, and it is possible that the friction of the packing may become unexpectedly large, although no evidence of this has been found. However, it makes no difference what the friction above 13000 is; the fact stands incontestable, for the breakage produced by mercury is in a region open to easy direct measurement, while the other cylinders have stood a pressure certainly several-fold greater.

All these results so far were obtained with hardened chrome nickel steel. Search was now made for the same effect in other steels. A cylinder of nickel steel of similar dimensions to the above, but left soft, was tried. This was filled with mercury. Pressure was kept at 8000 for 3 hours, then pushed gradually to 15000, where the increasing non-elastic stretch became so great as to let the mercury past the packing. The behavior here was exactly like that of a similar cylinder filled with water and stretched beyond the elastic limit: the elastic limit in the two cases was the same, as also the manner of yield and the shape into which the cylinder was deformed. Apparently, then, mercury exerts no selective action on the soft nickel steel. A similar cylinder of bessemer steel filled with mercury was left exposed to 3500 atmos. for 14 hours, and subsequently the pressure was increased until the mercury blew past the packing, exactly as for similar cylinders filled with water. It should be noted that non-elastic yield occurs for bessemer steel at pressures much lower than 3500, perhaps as low as 2000 atmos. The explanation finally adopted attaches some significance to the value of the elastic limit. The two cylinders above were tested at pressures beyond this limit. To test whether a soft cylinder would be broken by a pressure under the elastic limit if the pressure were sufficiently prolonged, a cylinder of soft nickel steel filled with mercury was exposed for three weeks to 4000 atmos. without rupture. At the end of three weeks, pressure was increased and rupture took place at 12000 atmos. The break was remarkable, as the cylinder showed no preliminary stretch as all soft steels do, but snapped like a piece of hardened tool steel. This may have been due to fatigue from the prolonged application of pressure, or it may be that weakening by the action of mercury had started at the lower pressure and that the cylinder would have finally broken at 4000, had the application been sufficiently prolonged.

An attempt was made to make a series similar to that on the nickel steel on cylinders cut from a bar of tool steel containing 1.25 per cent carbon. Several of these cylinders cracked in hardening so that a complete set of observations could not be made. The few successful tests made with the hardened tool steel cylinders, however, confirm the conclusions reached with the hardened nickel steel. Thus one cylinder with no hardening flaw burst at 4000 atmos. when filled with mercury, and a similar cylinder, which had a hardening flaw in it, broke at 6500 on the second application of pressure when filled with water.

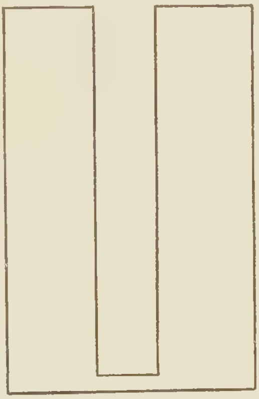

FIGURE 3. Another form of test cylinder for water or mercury, made of hardened nickel steel.

Another series of tests was now tried which gave the clue to the final explanation. Pressure was applied to cylinders of the form shown (see Figure 3), in which the end opposite the piston is left solid, and may be of varying thickness. In the first tests this bottom was left only $\frac{1}{8}''$ thick. The cylinders were made of the same nickel steel as above, hardened in oil. One, filled with mercury, ruptured by blowing out of the bottom at a pressure of 2400 atmos. The bottom blew out of a second in which the transmitting fluid was water, at a pressure of 12700 atmos. The manner of rupture was very different in the two cases. When water was used, the bottom was blown out in the form of a clean punching, slightly less in diameter than the hole and slightly bulged as one would expect. (See Figure 4.) On the other hand, the piece blown out by the mercury was in the form of a conical cap twice the diameter of the hole, as indicated in Figure 5. The structure of the ruptured metal from A to B was very coarse and granular, remarkably like the structure of brass made rotten by mercury. Between the grains of the steel were minute drops of mercury, and the fractured surface was partially wetted by mercury when plunged beneath a mercury surface. The only clean break was around the edge of the cap (BC), where the rupture took the form of a clean shear as for the piece broken with water.

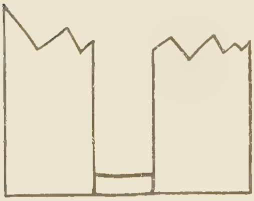
FIGURE 4. Form of the break of the cylinder of Figure 3 when the fluid exerting the pressure is water.

The corresponding tests with tool steel cylinders were hard to carry out because of loss of the cylinders on hardening. However, two successful tests were made. The bottom of one cylinder, when filled with mercury, blew off at 2700 atmos., while a similar cylinder filled with water did not fail until 5200 atmos. The manner of failure was different from that of the nickel steel, the detached piece being in the form of a frustum of a cone, as shown in Figure 6. The form of this cap was the same for both water and mercury, the only difference being that the one fractured with mercury showed unmistakable amalgamation over a limited region (AB). This, together with the curious fracture of the nickel steel piece, suggested the amalgamation of steel by pressure as a possible explanation.

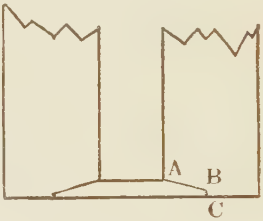

FIGURE 5. Form of the break of the cylinder of Figure 3 when the fluid exerting the pressure is mercury.

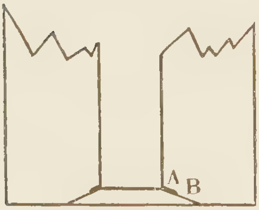

FIGURE 6. Form of the break in a cylinder like that of Figure 3 of hardened tool steel when the fluid exerting the pressure is mercury.

Experiment was also made on two cylinders of tool steel similar to the above, except that the bottom was $\frac{1}{2}''$ thick instead of $\frac{1}{8}''$. The cylinder filled with water stretched non-elastically and leaked at a pressure of 8000 atmos., while that filled with mercury failed at 4000 by the blowing out of mercury along a crack. This break was more like that described by Amagat than any other in the course of these experiments, but even here the break was distinctly visible, while Amagat states that he could find no trace of the crack with a microscope. (See Figure 7.)

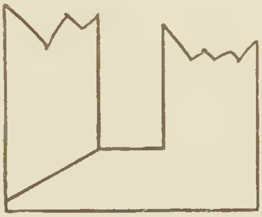

Figure 7. Form of the fracture in a cylinder of soft tool steel when the fluid exerting the pressure is mercury.

In all these tests of the soft steel cylinders the punched out pieces were found more or less amalgamated around the sheared edges. In particular, when the cylinder of soft tool steel last mentioned was cut so that the fissure was exposed, it showed beautiful amalgamation over the entire surface of the rupture. This led to a short investigation of the possibility of amalgamating iron or steel. It has been known for some time that mercury is capable of dissolving a small quantity of iron, and that conversely an iron surface may be amalgamated by mercury.[4] This amalgamation is a matter of some difficulty, which may be made to take place by certain chemical or electrical reactions, but under ordinary conditions does not occur at all. It does not seem to have been noticed that under proper conditions the amalgamation of iron is a matter of the greatest ease, the difficulty under ordinary conditions being due apparently to a thin protecting layer of oxide. The following experiment showed strikingly how great the affinity between clean iron and mercury is. A piece of iron was broken underneath a mercury surface so that the freshly ruptured surface came directly in contact with the mercury. The diagram illustrates the form of experiment. (See Figure 8.) The test piece, in the shape of a thin hollow cylinder, is covered with mercury in an iron receptacle, and broken by forcing a wedge into the hole. In every case the broken surface is brightly and completely amalgamated, the mercury wetting it exactly as water wets a surface to which it adheres. The same result was obtained with hard and soft nickel steel, hard and soft tool steel, bessemer steel

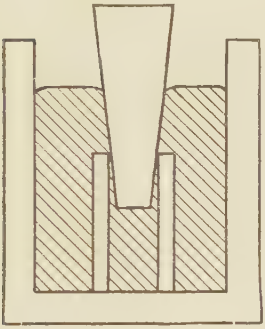

Figure 8. Apparatus for fracturing steel under the surface of mercury.

---

[4] See, for example, Richards, Wilson, and Garrod-Thomas, Pub. Carnegie Inst. Wash., No. 118, 54, 1909; also Richards and Garrod-Thomas, ZS. Phys. Chem., **72**, 181 (1910).

both in its natural state and quenched from a red heat, and with cast iron.[5] The same effect is shown by the same grades of steel when broken off by twisting under a mercury surface, showing that the amalgamation does not depend on the nature of the rupturing stress. This effect was shown in a striking way by one of the hardened tool steel cylinders. (See Plate.) This cylinder broke on the first application of pressure at 1500 atmos. Examination showed a small hardening crack at A from which the crack spread into the sound metal. The mercury, escaping under pressure through the freshly opened crack, produced nearly complete amalgamation of the entire section of the cylinder, as the photograph shows.

But on the other hand, all attempts failed to amalgamate the freshly broken surface if it had once come in contact with the air. A test piece like the above was supported directly over a mercury surface so that the fragments fell immediately into the mercury when rupture occurred. No trace of amalgamation was obtained here, as was also no trace with several modified forms of the experiment in which immersion was not so immediate.

Experiments were now made to find whether the amalgamation so produced might be made to work its way through the mass of the metal. Fragments of the above amalgamated test pieces were sealed into a bulb containing mercury so designed that the pieces should be kept below the surface of the mercury. The air was boiled out, the bulb sealed, and the whole kept at a temperature of 180° C. for three hours in an oil bath. The pieces were then examined for amalgamation by breaking them across. The hardened nickel steel piece showed amalgamation throughout its entire mass, the bessemer showed isolated splotches of amalgamation, while none of the others showed any effect. Similar amalgamated bits from the broken test pieces were now submerged in mercury, which was subjected to a pressure of 6500 atmos. at room temperature for six hours. All of the specimens, except the soft tool steel, now showed amalgamation throughout the interior. The hardened nickel steel piece was amalgamated completely, while the amalgamation of the others was not so perfect, being confined to patches near the surface.

Further, pressure by itself is not capable of producing amalgamation on a steel surface or in the mass of the metal unless the amalgamation has been started on the surface by some other means. This was shown by subjecting rods of the three kinds of steel (hard and soft nickel steel, hard and soft tool steel, soft and quenched bessemer) to a pressure of about 6500 atmos. for twelve hours or more under mercury. These rods were scoured bright with fine emery paper immediately before being plunged into the mercury. The fracture after pressure treatment showed not the slightest trace of amalgamation. Reference may be made to some earlier experiments in which no gain of weight could be detected in steel pieces subjected to hydrostatic pressure in mercury. The possibility of amalgamation by pressure was also tried in another form. A hollow cylinder of hardened nickel steel was submerged in mercury, and pressure applied to the outside. The only difference between this and the case of the solid rod is that in the former the stress throughout the metal is not uniform, as it is in the latter. It was thought conceivable that mercury might be forced through metal in which the stress was not the same in every direction, while it might show no tendency to work its way through a mass in which the stress was already hydrostatic. The experiment, however, showed no amalgamation in this case either.

---

[5] Aluminum may also be amalgamated by rupturing under the surface of mercury. Aluminum so treated, when exposed to the air, shows the characteristic tree-like growth of the oxide. The same effect is also shown in nickel and cobalt. It should be remarked that the amalgamated iron surface shows no tendency to oxidize in the air, but keeps its silver luster untarnished at least for months.

This test for amalgamation by examining the nature of the fracture showed itself so easy to apply and so unmistakable in its indications that it was now applied to the examination of the cylinders which had formed the subject of the first tests. The possibility of the amalgamation of the cylinders as an explanation had at first been discarded because the inner wall of the cylinder, where it was to be most expected, showed no indications of any amalgamation and because attempts to detect the presence of mercury throughout the mass of the metal by microscopic analysis of the polished and etched cross section had given no result. Professor Sanveur had been kind enough to examine four test pieces cut from different cylinders, three of which were ruptured with mercury and one with water. He found martensitic structure in the three former pieces, and only a very fine granular structure in the other. There was no visible trace of mercury in the pores, nor anything to suggest amalgamation. The differences of structure might be due merely to the slight differences in heat treatment occasioned by the separate hardening of the cylinders. More careful regulation of the conditions would be necessary to settle this point.

The fracture test was applied by cutting a scarf about $\frac{1}{4}''$ deep all around the cylinder with a thin emery wheel, and then breaking the cylinder at this scarf with a hammer. All the cylinders broken with the mercury showed the same characteristics. (See Figure 9.) The crack was in a radial plane; surrounding this crack on either side was a band within which the coarser structure and the silver luster showed that the steel had been amalgamated. Besides this band of amalgamation flanking the crack, which was present in every cylinder, there were other irregular splotches of amalgamation growing either from the central hole or from the flanking band. No cases were found of isolated islands of amalgamation in the midst of untouched metal. The diagram gives an idea of typical forms of this amalgamation, although so many varieties were seldom found in one specimen. In one specimen the amalgamation had grown in the form of a nearly complete ring with no contact with the interior except through the infected region about the crack, in the manner shown in the drawing. The tool steel cylinders showed the same effect, except that the amalgamated band about the crack was not so broad as for the nickel steel, and the other patches of amalgamation were less numerous. The peculiar fracture indicating amalgamation was found in none of the cylinders which were broken in the absence of mercury. Several such cylinders were examined, some of hard or soft tool steel, and some of nickel steel, broken with water after the repeated action of the maximum pressure of 24000 atmos.

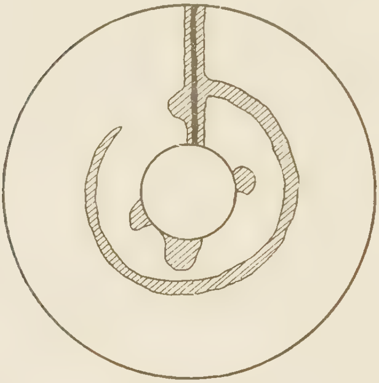

FIGURE 9. The form of the amalgamated region in cylinders like those of Figure 1 when broken with mercury.

Such are the experimental facts which must be explained. It seems evident that the premature breaking of the cylinders filled with mercury was due to the weakening of the steel produced by amalgamation. The fact of amalgamation seems sufficiently proved by the study of the fracture. That amalgamated steel would be weaker than the untouched steel seems obvious enough without the necessity of special experiment to prove it. The fact was proved incidentally several times, however, when parts of the steel packing appliances which had been used with the mercury cylinders were used over again with the cylinders filled with water. The packing plugs in these circumstances always broke at a pressure very much less than the normal breaking pressure and with a fracture showing bright amalgamation. In explanation of the amalgamation of these cylinders we have in the first place the strong natural affinity between iron and mercury. This is prevented from coming into play under ordinary circumstances by a thin layer of dirt on the surface. But it seems reasonable to suppose that amalgamation will start in the mass of the metal if the mercury can be once forced into the pores, since under these circumstances the iron and mercury coming into contact with each other would be clean and the natural chemical affinity come into play. The argument consists in showing that in those cases where amalgamation took place the conditions were such as to favor the introduction of mercury into the pores of the steel, even if the surface were not amalgamated. Then after amalgamation is once started in the mass of the metal it is assisted in the rapidity of its growth from the amalgamated region by the action of hydrostatic pressure.

This discussion demands a slight consideration of the nature of the strain in a hollow cylinder exposed to internal fluid pressure. The stresses in the metal of the cylinder consist of a pressure (negative) across planes perpendicular to the radii, and a tension (positive) across radial planes. These stresses are greatest arithmetically at the interior surface, but the algebraic sum is constant throughout the mass of the cylinder. This has as a consequence that the volume strain in the cylinder is a dilation and is everywhere constant, so that the pores are opened up by the action of the stress and the entrance of mercury facilitated. This holds while the strain remains elastic. But when the internal pressure exceeds a certain value so that at the inner surface the algebraic difference between the radial pressure and the circumferential tension exceeds a critical value depending on the elastic limit, the strain becomes inelastic, the tension changes over to a pressure so that both principle stresses become compressions, the volume strain changes from a dilatation to a compression, and the pores close up. So that with a steel of low elastic limit the type of stress may change, giving a volume compression, at a lower value of the fluid pressure and therefore at a smaller preliminary volume dilatation than in a steel of higher elastic limit. This view as to the nature of the stress in a thick cylinder stressed beyond the elastic limit is supported by many other experiments on the bursting of thick cylinders. An account of these experiments will be published in another paper.

The difference found in the rupture points between soft and hardened steel is to be ascribed to two causes. One is the greater intrinsic ease of driving amalgamation through a mass of hardened steel by hydrostatic pressure. This was proved by the experiments on the broken amalgamated test pieces. It may be due in part to chemical difference between the hard and soft steel, but is almost certainly also due in part to the greater porosity of the hardened steel. It is well known that steel decreases in density on hardening. The other cause is the higher elastic limit of the hardened steel and the consequent wider opening of the pores before non-elastic closing sets in. For facility of comparison the elastic limits of the cylinders of the various grades of steel are given (see Table III), on the usual assumption that the elastic limit is determined by the maximum stretch at the interior. This assumption is probably not very near the truth, so the results can be expected to show only qualitative agreement. This table does not apply to the cylinders in which the bottoms were blown out, as here the stress is of a different nature and the above values of the elastic limit do not hold. It appears from the table that only those cylinders were broken in which the stress was below the elastic limit. That the cylinders of bessemer and soft nickel steel were not broken may be explained by supposing that the pressure required to open the pores wide enough to force the mercury in is higher than the elastic limit.

TABLE III.

Kind of Steel.	Assumed Elastic Limit in Tension $\frac{\text{lbs}}{\text{in}^2}$.	Internal Pressure required to reach Elastic Limit. Atmos.	Minimum Bursting Pressure with Mercury. Atmos.
Bessemer . . .	40000	2000	Same as with water
Soft tool steel .	75000	4000	Same as with water
Hard tool steel .	150000	8000	4000
Soft nickel steel	90000	4800	Same as with water
Hard nickel steel	225000	12000	3000

It remains to explain the form of the amalgamated region found in the hardened nickel steel cylinders; i. e., bands on either side of the crack. It seems certain that slight inequalities in the structure of the steel will greatly affect the ease of amalgamation. This seems proved by the splotches of amalgamation found throughout the broken test pieces amalgamated by hydrostatic pressure and throughout the broken cylinders. Conceive, then, of a hollow cylinder filled with mercury subjected to pressure. The pressure expands the pores of the metal, and in consequence of the high mobility of the mercury molecule the mercury is forced into these pores through the layer of dirt lining the hole. At certain places where the metal is more susceptible the amalgamation spreads more rapidly than it does at others. But now the metal is weakened at each of these infected places, and the type of strain is modified as it would be by the presence of a flaw. The strain will be redistributed, the brunt of the strain coming at the point farthest removed from the center, where consequently the pores of metal will be still further distended. That is, at this point the amalgamation will proceed most rapidly. It is evident that the continuation of this process will produce a band of amalgamation travelling out along the radius. When the amalgamation reaches the outside, or approaches sufficiently close, the metal gives way, the crack appearing through the midst of the weakest region, that is, through the center of the amalgamated band. It is evident that when the process of amalgamation has once started in this way, it will proceed more and more rapidly as the resisting thickness of sound metal becomes less, thus accounting for the smallness of the other amalgamated regions. One cylinder was found, however, in which an amalgamated patch had worked its way nearly half way to the outside diametrically opposite the crack.

Failure to produce amalgamation in the rods subjected to hydrostatic pressure is to be explained by the fact that neither can the amalgamation begin at the surface, because of the thin layer of dirt, nor can the mercury force its way into the steel to begin amalgamation there because the interstices in the metal are closed up by the hydrostatic pressure. The same argument of course applies still more to the hollow cylinder submerged in mercury and subjected to pressure on the outside.

The experiments with the cylinders in which the bottoms were blown off are to be explained in the same way. The amalgamation grows most rapidly in the direction in which the distension is greatest, which in this case is diagonally from the corner of the hole. As the amalgamation proceeds it carries the hydrostatic pressure with it. When the region over which this pressure acts has extended so far that the sound metal left can no longer support the stress, it gives way as usual by a clean shear. The fact that mercury was forced through the bottom of a cylinder of soft tool steel (Figure 7), while soft tool steel cylinders of the form of Figure 1 were unbroken by the action of pressure, is probably to be explained by the different strain types in the two cases. In the case of Figure 7 distension in a direction diagonally from the corner of the hole is great enough to allow amalgamation before the pores are closed up by viscous yield. The point has not been worked out in greater detail, however. The disconcerting experiments in which a clean punching was blown out of the bottom of a soft cylinder with the sides of the punching amalgamated, are to be explained by the fact previously noted that a freshly fractured surface is amalgamated by mere contact with mercury. Breaking across of the punchings showed no evidence of amalgamation in the mass of the punching, so that all the amalgamation must have taken place after rupture. A similar experiment on the hardened nickel steel punching mentioned above showed more or less complete honeycombing of the metal with mercury.

This is as far as the explanation has been carried. Enough has been done to show that there is here a genuine effect, so that pressure can not be transmitted directly by mercury in hardened steel cylinders, and that the effect is due to amalgamation. One-sided pressure is necessary to start this amalgamation, so that when steel is entirely surrounded by mercury there is no danger of amalgamation or of penetration of the mercury into the pores. This fact was made use of in modifying the design of the apparatus spoken of in the first part of the paper.

Summary.

The fact has been established that cylinders of hardened steel will burst at very much lower than the natural bursting pressure when the fluid exerting the pressure is mercury. Soft steel cylinders show the effect hardly at all, the yield point being reached before the pressure can be raised high enough to produce the effect. The fact that this rupture is due to the amalgamation of the steel is established by the examination of the fracture of such cylinders. The unexpectedly great affinity between steel and mercury was established by the complete amalgamation of surfaces broken under mercury, and the enormous effect of the slightest contact with the air was shown. When this amalgamation is once started, the rapidity with which it spreads through the metal is greatly increased by the action of hydrostatic pressure. The spread of mercury through the mass of the steel and the subsequent destruction of the hollow cylinders is produced by two causes, both of which must act together. One is the natural chemical affinity between mercury and steel, shown by the ready amalgamation of freshly broken surfaces. But the amalgamation is never started by the action of pressure alone. In all those cases in which we have had amalgamation, we have had in addition to the chemical affinity a strain of such a nature as to distend the pores of the metal. This allows the entrance of mercury into the pores so that amalgamation may begin, and also facilitates its further growth, which is most rapid in the

direction in which the pores are most distended. It was shown in detail that in all cases in which rupture occurs the strain is of such a type as to distend the metal, and that on the other hand in all those cases in which amalgamation is not produced by pressure, the strain is such as to compress the metal, closing up the pores.

This work was done in the course of an experiment on the thermal properties of mercury and water under high pressure, the expenses of which were partially defrayed by a liberal appropriation from the Rumford Fund of the American Academy of Arts and Sciences.

Jefferson Physical Laboratory, Harvard
University, Cambridge, Mass.
October, 1910.

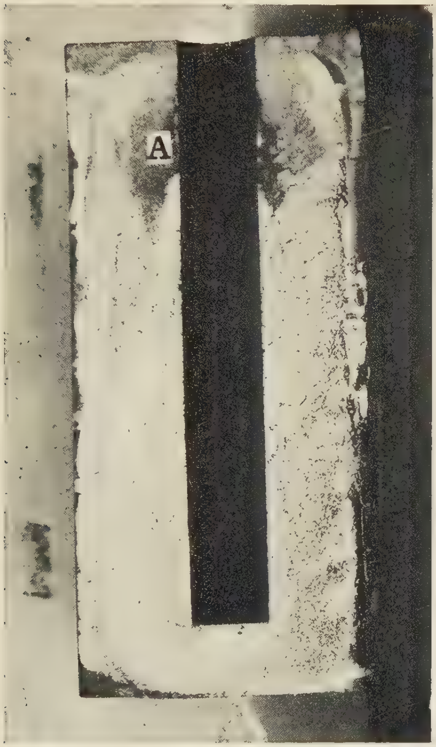
A

Proceedings of the American Academy of Arts and Sciences.

Vol. XLVI. No. 17. — January, 1911.

VECTOR-DIAGRAMS OF OSCILLATING-CURRENT CIRCUITS.

By A. E. Kennelly.

VECTOR-DIAGRAMS OF OSCILLATING-CURRENT CIRCUITS.

By A. E. Kennelly.

Presented November 9, 1910. Received November 25, 1910.

Although, as the appended bibliography indicates, the analysis of oscillating-current circuit phenomena has received much attention, and has attained a considerable degree of development, yet the methods of vector-diagrams do not seem to have been applied to it. It is believed that these vector-diagram methods offer marked advantages to the student, and particularly to students of electrical engineering who have already become familiar with the use of vector-diagrams in connection with alternating-current circuits.

Definition.

An oscillating-current circuit may be defined as a circuit which, in undergoing a change of energy, carries a current that oscillates periodically about an ultimate value. In such a circuit not only the electric current, but also the emf. quantity, power, and energy oscillate freely. For brevity, the term oscillating current may be designated by the letters *o. c.* In practice, an o. c. circuit comprises a condenser as an essential element, the energy oscillating, or tending to oscillate, between the electric and magnetic types, at a frequency determined solely by the constants of the circuit. The oscillations decay in amplitude, energy being expelled irrecoverably from the circuit, during the process, by a regular sequence of dwindling impulses. These impulses may be either of the joulean or *hertzian* type, or of both combined.

Simple Resistanceless Oscillating-Current Circuits.

The simplest type of o. c. circuit comprises a condenser AB, Figure 1, of capacity or permittance c farads, inserted in a circuit of negligible resistance, containing a total inductance of l henrys. Let n be the free-oscillation frequency of the circuit, in cycles per second, and let $\omega = 2\pi n$ be the free-oscillation angular velocity of the circuit, in radians per second. Then the reactance jX_l of the inductance DE at this frequency will be

$$jX_l = jl\omega \qquad \text{ohms} \quad (1)$$

where $j = \sqrt{-1}$, the quadrantal operator.

The reactance $-jX_c$ of the condenser at the same frequency will be

$$-jX_c = -j\frac{1}{c\omega} = -j\frac{s}{\omega} \qquad \text{ohms} \qquad (2)$$

where $s = 1/c$ is the elastance of the condenser in darafs.[1]

Discharging and Charging Oscillations. — An oscillatory circuit may be excited into activity either when energy is added to it, or when energy is withdrawn from it. In the former case *charging oscillations,* and in the latter case *discharging oscillations* are produced. Thus the circuit may be initially devoid of electric or magnetic energy, and a certain constant potential difference of U_0 volts, as from a storage battery, may be inserted in the circuit between the terminals TT, Figure 1. The condenser will then be charged by an oscillatory process, or series of charging oscillations.

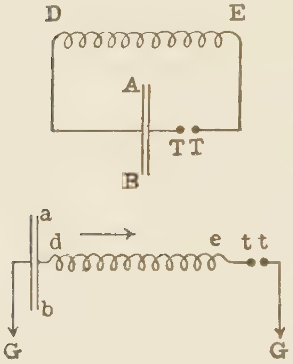

FIGURE 1. Diagram of connections of simple oscillating-current circuit, and schematic representation of the same.

Again, the condenser may be initially charged to a potential difference of U_0 volts, and allowed to discharge by short-circuiting the terminals TT. Discharging oscillations will then be produced. Or, the condenser may be initially without charge, but the inductance DE (Figure 1) may be charged by allowing a steady current of I_0 amperes to pass through it from some external source. If then the gap TT be closed, and the source of charging current is suddenly withdrawn sparklessly, discharging oscillations will be produced in the circuit.

Discharging oscillations may even be considered as taking place in an active initially energised circuit, in the limiting case where the circuit is assumed to be resistanceless; so that energy ceases to be dissipated during the discharge.

In any of the above cases, the circuit selects the frequency of free oscillation such that the reactance of the circuit remains zero. This is the law of all oscillating-current circuits, whether they contain small or large resistance, up to the aperiodic limit. Consequently :

---

[1] Prof. V. Karapetoff seems to have been the first writer to have had the courage to print the useful term *daraf* as a unit of elastance the reciprocal of a *farad.* "The Electric Circuit," Ithaca, N. Y. 1910, p. 72. See also "Electrical Papers," O. Heaviside, 1892, Vol. 2, p. 125.

$$jX_l - jX_c = 0 \qquad \text{ohms} \quad (3)$$

$$jl\omega = j\frac{1}{c\omega} = j\frac{s}{\omega} \qquad \text{ohms} \quad (4)$$

whence

$$\omega = \frac{1}{\sqrt{lc}} = \sqrt{\frac{s}{l}}. \qquad \text{radians/sec.} \quad (5)$$

When condensers are connected in parallel, their permittances are more readily dealt with; and when connected in series, their elastances.

Discharging Oscillations of a Simple Resistanceless Oscillating-Current Circuit. — The oscillatory system of Figure 1 may be given its initial stock of energy either electrically or magnetically; that is, either by giving an initial electric charge of Q_0 coulombs to the condenser, or by exciting a total initial linked magnetic flux $\Phi_0 = I_0 l$ ampere-henrys in the coil, where I_0 is the initial exciting current-strength, supposed to be suddenly withdrawn from the coil without loss of energy in sparking. With respect to amplitude, the discharging oscillations of the coil will be the same as those of the condenser, provided that :

$$\Phi_0 = Q_0 z_0 \qquad \text{volt-seconds} \quad (6)$$

where $z_0 = \sqrt{\frac{l}{c}} = \sqrt{ls}$ is the surge impedance of the system. With respect to phase, however, the discharging oscillations of the excited coil will be in quadrature with those of the excited condenser. In cases where both the condenser and the coil are initially excited, and are allowed to discharge simultaneously, each may be considered independently, and the two sets of oscillations may then be summed.

General Rotating Vector-Diagram of Simple Resistanceless Oscillating-Current Discharging Circuit. — In Figure 2, let $O\overline{U}_0'$ represent to volt-scale the initial p. d. applied to the condenser of Figure 1, and producing therein an initial electric charge Q_0. Then $O\overline{U}_0$ will be the equal and opposite p. d. of U_0 volts, tending to discharge the condenser. The direction of the discharging p. d. OU_0 may be taken as the direction of reference or voltage phase-standard, and XOX as the axis of reference. The vector $O\overline{I}_0$ then represents the discharging current established by the discharging p. d. $O\overline{U}_0$. The vector system $O\overline{U}_0$, $O\overline{I}_0$, $O\overline{E}_0$ is to be pivoted about the point O, and, starting at time

$t = 0$ from the position shown, to rotate positively in the plane $\overline{U}_0\overline{I}_0\overline{E}_0$ with the angular velocity ω, as determined by formula (5). At any time t seconds after the release of the discharge, the orthogonal projections on XOX of the three vectors $O\overline{U}_0$, $O\overline{I}_0$, and $O\overline{E}_0$ will represent the corresponding instantaneous values of the discharging p. d. at condenser terminals, the current strength, and the emf. of self-induction in the coil. The vector discharging current therefore rotates in quadrature between the two opposed and equal electromotive forces of discharge and of self-induction, developing with them reactive power and cyclic energy; but with no dissipated energy, under the assumption of negligible resistance.

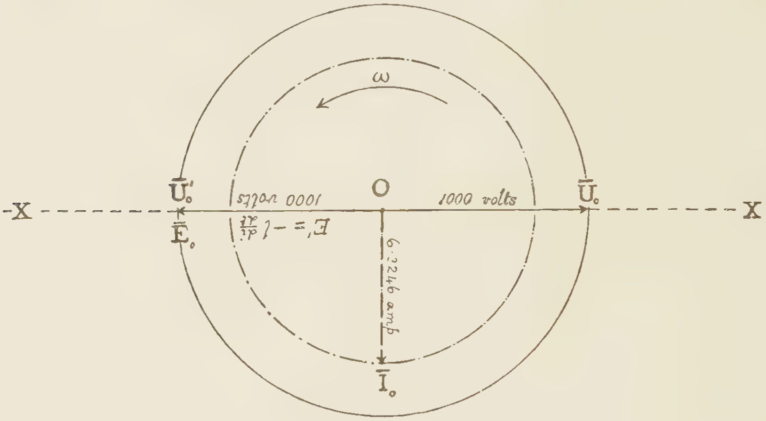

FIGURE 2. Rotative vector-diagram of simple resistanceless oscillating-current circuit.

Figure 3 presents a series of stationary vectors; ω, Y, I, P, W. The vector ω is drawn in the $-j$ direction, and with a length $\omega = 1/\sqrt{cl} = \sqrt{s/l}$ radians-per-second, according to formula (5). If we take, as an example, a condenser of $c = 4$ microfarads ($s = 0.25$ megadarat), charged to an initial p. d. of $U_0 = 1000$ volts, and discharged through a resistanceless inductance of $l = 0.1$ henry, we find $\omega = 1581.14$ radians per second, corresponding to a frequency of $n = 251.646$ cycles per second, and a complete period of $T = 0.003{,}974$ second.

Starting from the initial position of Figure 2, the subsequent position of any vector in the system, after the lapse of t seconds, is determined by multiplying the vector by

$$\epsilon^{-(-j\omega t)} = \epsilon^{j\omega t} = \epsilon^{j\frac{t}{\sqrt{cl}}} = \epsilon^{j1581.14t}. \qquad \text{numeric } \angle \quad (7)$$

The admittance of the oscillating-current circuit is given by the Y vector, Figure 3, which is drawn in the $-j$ direction to a scale of mhos, and a length of $c\omega$ mhos. In the case considered $Y = -j0.006{,}324{,}6$ mho.

The initial vector oscillating current is given by the I vector, Figure 3, which is drawn in the $-j$ direction to a scale of amperes, and a length of $\bar{U}_0 Y$, as the amplitude, or maximum cyclic value, of the p. d. at condenser terminals. Or, expressed in terms of the quantity of electricity in the condenser, $\bar{I}_0 = \bar{Q}_0\omega$, where $\bar{Q}_0$ is the initial condenser charge in coulombs, and the vector amplitude or maximum cyclic quantity. $\bar{Q}_0$ is also $Q\sqrt{2}$, where Q is the root-mean-square of the oscillating condenser charge, in coulombs. In the case considered, $\bar{I}_0$ is $-j$ 6.3246 amperes, and $I = 4.472{,}14$ r. m. s. amperes. This shows that in Figure 2 the current vector $O\bar{I}_0 = 6.3246$ max. cyclic amperes, lies 90° in phase behind the discharging p. d. OU_0.

The oscillatory power in the circuit is given by the P vector, Figure 3. Since the current is in quadrature with the emfs. in a resistanceless circuit, the power will be wholly reactive or non-dissipative. The P_m vector is drawn in the $-j$ direction, to a scale of watts, and to a length of $P_m = \frac{\bar{U}_0\bar{I}_0}{2} = UI$ units on this scale. In the case considered $P_m = -j3162.3$ watts. This is the maximum cyclic value, or amplitude, of the power of the condenser. The power is positive when the condenser is doing work, or discharging, and is negative when the condenser is receiving energy from the magnetic field of the coil, or is charging.

The oscillatory energy in the circuit is given by the W vector. This vector is drawn in the $= -j$ direction, to a scale of joules, and to a length of $W_m = P/2\omega$ units on that scale. In the case considered, $W_m = -j1$ joule. This is the maximum cyclic value, or amplitude, of the energy delivered by the condenser into the magnetic field of the coil at each oscillation.

The time variation of the various oscillating quantities is represented in Figure 5, for one complete cycle of the current and p. d. The sinusoid u, u, u, of 1000 volts amplitude, is the graph of the condenser p. d., commencing at $U_0 = 1000$ volts. The sinusoid e is the emf. of self-induction in the coil, and is always equal and opposite to the p. d. of the condenser. The sinusoid ii, of 6.3246 amperes amplitude, is the graph of the discharging current, and is 90° in phase behind the discharging p.d. The sinusoid p, of double frequency, and of amplitude

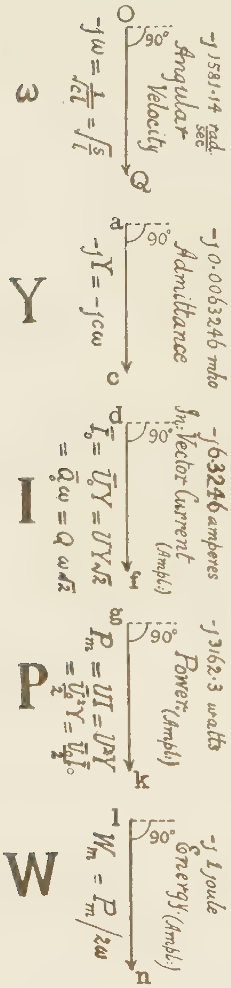
ω
O
Q
90°
-j 1581.14 rad/sec
Angular Velocity
$-j\omega = \frac{1}{\sqrt{cl}} = \sqrt{\frac{s}{l}}$
Y
a
c
-j 0.0063246 mho
Admittance
$-jY = -jc\omega$
I
d
f
-j 6.3246 amperes
In: Vector Current (Ampl.)
$\bar{I}_0 = \bar{U}_0 Y = UY\sqrt{2}$
$= \bar{Q}_0\omega = Q\omega\sqrt{2}$
P
g
k
-j 3162.3 watts
Power (Ampl.)
$P_m = UI = U^2Y$
$= \frac{\bar{U}_0^2}{2}Y = \frac{\bar{U}_0\bar{I}_0}{2}$
W
l
n
-j 1 joule
Energy (Ampl.)
$W_m = P_m/2\omega$

FIGURE 3. Stationary vector-diagrams of angular velocity, admittance, r. m. s., current strength, maximum cyclic power, and maximum cyclic energy in a simple resistanceless oscillating-current circuit to phase of p. d. as standard.

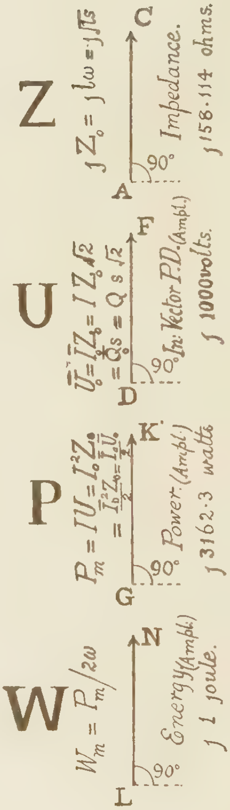

FIGURE 4. Stationary vector-diagrams of impedance, r. m. s., potential difference, maximum cyclic power, and maximum cyclic energy in a simple resistanceless oscillatory-current circuit to phase of current as standard.

3.1623 kilowatts, is the power developed in the condenser. It starts from zero, in the positive direction, at the moment of release. The opposite sinusoid p_l, of double frequency, and also of amplitude 3.1623 kw., is the power developed in the inductance. The condenser and coil are reciprocally and successively generator and recipient in respect to power.

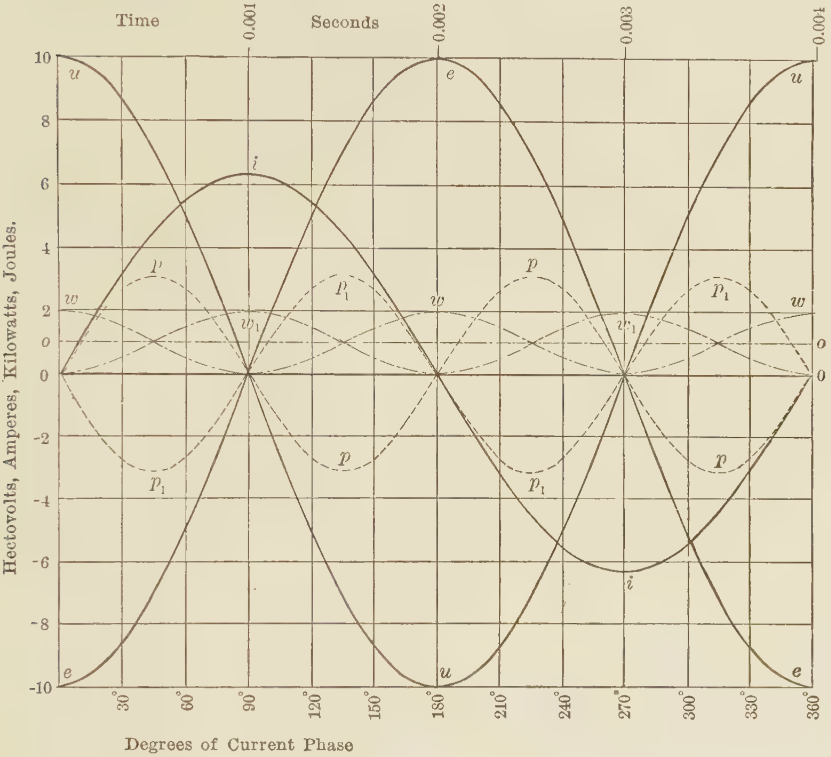

FIGURE 5. Analysis of p. d., current, power, and energy in a simple resistanceless discharging circuit.

The sinusoid w_l, of double frequency, is the graph of the energy expended by the condenser and stored in the coil. It has an amplitude of 1 joule above and below the line *oo* as axis. The total energy in the coil, therefore, reckoned from zero, is

$$2\ W_m = \frac{UI}{\omega} = \frac{\bar{U}_0 \bar{I}_0}{2\ \omega} = \frac{1}{2}\, l I_0^2. \qquad \text{joules} \quad (8)$$

The opposite sinusoid w_c, also of double frequency, and 1 joule amplitude, is the graph of energy in the condenser. It is evident that at every instant

$$w_c + w_l = W_0 \qquad \text{joules (9)}$$

where W_0 is the initial energy $U_0{}^2c/2$ of the system, or 2 joules in the case considered.

All of the vectors in Figure 3 are stationary, and in the series $\underline{I}$, P, and W, are all drawn to the phase of the discharging p. d. $\bar{U}_0$ as standard. This means that the vector current i is 90° behind that of u (Figure 5), the condenser power p is quadrature power, or purely reactive power, and the delivered energy W_m is also quadrature or reactive energy.

With respect to current-phase as standard, we have the series of vectors in Figure 4, commencing with Z_0 the impedance of the circuit, which is drawn in the $+j$ direction to a scale of ohms and a length of $l\omega$ on this scale. In the case considered, $Z_0 = j158.114$ ohms. Z_0 is thus a purely reactive impedance, or reactance.

The vector $\bar{U}_0$, Figure 4, represents the amplitude or initial value of the p. d. at condenser terminals. It is drawn in the $+j$ direction, or is 90° ahead of the current, and to a scale of volts, to a length of $\bar{I}_0 Z_0 = IZ_0\sqrt{2}$ on that scale, where I is the r.m. s. value of the vector $\bar{I}_0$. In the case considered, $\bar{I}_0 = 6.3246$ amplitude amperes and $I = 4.472$ r. m. s. amperes. In terms of the electric quantity, however, it may also be expressed as $\bar{Q}_0 s = Qs\sqrt{2}$ volts. In the case considered, this vector amplitude p. d. $\bar{U}_0$ is 1000 volts, with an effective or r. m. s. value of $U = 707.1$ volts.

The vector P_m in Figure 4 represents the amplitude, or maximum cyclic value, of the oscillatory power of the condenser. It is drawn in the $+j$ direction, being leading quadrature power with respect to current phase, to watt scale, and to a length of $\frac{\bar{I}_0 \bar{U}_0}{2} = IU$ units on that scale. In the case considered, $P_m = j\,3162.3$ watts.

The vector W_m in Figure 4 represents the amplitude or maximum cyclic value of the oscillatory energy expended by the condenser. It differs only from the vector W_m of Figure 3, by being drawn in the $+j$ instead of in the $-j$ direction. This is because the energy and power are leading quadrature quantities with reference to the current, but lagging quadrature quantities with respect to the discharging p. d.

The stationary vector-diagrams of Figures 3 and 4 may be considered as graphically corresponding to the following vector equations:

With respect to the potential difference as standard of phase,

$$\bar{I}_0 = \bar{U}_0 Y \lvert\overline{90^\circ} = \bar{Q}_0 \omega \lvert\overline{90^\circ}, \qquad \text{maximum cyclic amperes}$$

$$P_m = \frac{U_0 \bar{I}_0}{2} \lvert\overline{90^\circ} = UI \lvert\overline{90^\circ} = \frac{\bar{U}_0^{\,2} Y}{2} \lvert\overline{90^\circ} = U^2 Y \lvert\overline{90^\circ}, \qquad \text{max. cyclic watts}$$

$$W_m = \frac{P_m}{2\,\omega} \lvert\overline{90^\circ} = \frac{U_0^{\,2} Y}{4\,\omega} \lvert\overline{90^\circ} = \frac{UI}{2\,\omega} \lvert\overline{90^\circ}. \qquad \text{maximum cyclic joules}$$

With respect to the current as standard of phase :

$$\bar{U}_0 = \bar{I}_0 Z_0 \lvert\underline{90^\circ} = \bar{Q}_0 s \lvert\underline{90^\circ}, \qquad \text{maximum cyclic volts} \quad (10)$$

$$P_m = \frac{\bar{I}_0 U_0}{2} \underline{90^\circ} = \frac{\bar{I}_0^{\,2} Z_0}{2} \lvert\underline{90^\circ} = IU \lvert\underline{90^\circ} = I^2 Z_0 \lvert\underline{90^\circ}, \quad \text{max. cyc. watts} \quad (11)$$

$$W_m = \frac{P_m}{2\,\omega} \lvert\underline{90^\circ} = \frac{\bar{I}_0^{\,2} Z_0}{4\omega} \lvert\underline{90^\circ} = \frac{IU}{2\omega} \lvert\underline{90^\circ}. \quad \text{maximum cyclic joules} \quad (12)$$

The vector-diagrams *I*, *P*, and *W*, of Figure 3, as well as *U*, *P*, and *W*, of Figure 4, may also be treated as rotative vector-diagrams, for deducing instantaneous values of their respective quantities projectively. Thus in the case of *I*, Figure 3., we may rotate the vector I_0 about the point *d*, in the positive direction, with angular velocity ω, commencing at time $t = 0$, from the position shown. The instantaneous orthogonal projections of the vector on the dotted line, or "real" axis, will then give the corresponding instantaneous o. c. strengths.

In the case of the *P* vector, Figure 3, the vector *gk* may be rotated about the point *g* with positively directed angular velocity $2\,\omega$, commencing from the position shown in Figure 3, at time $t = 0$. Instantaneous orthogonal projections on the dotted line, or "real" axis, will then give the corresponding instantaneous oscillating-current power, as indicated by the double-frequency sinusoid *p* in Figure 5. This is the power of the condenser. The same rotating power-vector may also be used to project the power of the inductance, if displaced in phase by 180°, that is, if it starts from rest in the diametrically opposite position to that shown in Figure 3.

In the case of the *W* vector, Figure 3, the vector *ln* may be rotated in the positive direction about the point *l* with angular velocity 2ω. If the vector starts, at time $t = 0$, from the position indicated in Figure 3, projections must be taken on the line *ln*, or axis of imaginaries. Instantaneous projections of the vector on this axis will then mark off instantaneous values of the energy in the condenser ($u^2c/2$ joules).

If the rotating vector be displaced 180° in phase, its projections will mark off instantaneous values of energy, ($i^2l/2$ joules) in the inductance. For reasons that will be evident on considering oscillating-current circuits containing resistance, it is preferable to describe a circle upon a diameter *LSC*, Figure 6, with the radius $ln = W_m$, Figure 3, and rotate this circle in the positive direction, with the angular velocity $2\,\omega$, at the same time rolling it along the axis *OY*, drawn through the point *L*. The orthogonal projection of the center *S* upon *OY* will mark time, as indicated in Figure 6 both to a scale of seconds, and to degrees of energy phase. The projection of the point *C* in the circle on the *OX* axis, commencing at *c*, will mark off a distance *Oc* corresponding to the instantaneous energy $u^2c/2$ joules in the condenser. Similarly, the projection of the opposite point *L* in the circle on the *OX* axis, commencing at *l*, will mark off a distance *Ol* corresponding, on the same scale, to the instantaneous energy $i^2l/2$ joules in the inductance.

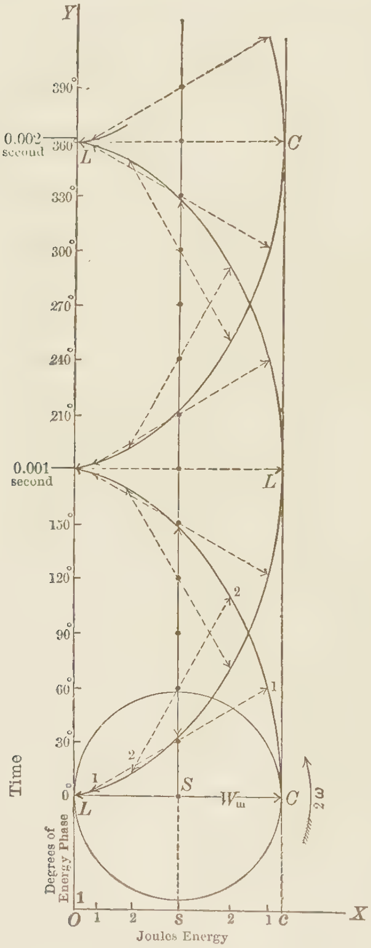

FIGURE 6. Rotating and rolling vector-diagram of the condenser energy, the inductance energy, and the semi-system energy in a resistanceless oscillating-current circuit.

If we connect the points *L* and *C* by a straight line, and take the middle point, it will coincide, in the resistanceless case here considered, with the center *S* of the rolling circle. Consequently, the projection of the point *S* on the *OX* axis at *s*, will mark off a length *Os*, equal to half the sum of the instantaneous energy in the condenser and in the inductance, i. e., equal to half the instantaneous energy remaining in the system. We may call this quantity *Os*, for brevity, the semi-system-energy. Since there can be no dissipation of energy from such a circuit devoid of joulean and hertzian resistance, the semi-system-energy *Os* does not vary with time as the circle rolls along the OY axis. CCC and LLL are cycloids differing 180° in phase.

Inductance-Discharging Oscillations in a Simple Resistanceless Oscillating-Current Circuit. — We have thus far considered condenser-discharging oscillations. If, however, the inductance be charged with current and magnetic energy from a separate source, and this source is suddenly and sparklessly removed, while the condenser circuit Figure 1 is closed at $T\,T$, the inductance will set up a series of discharging oscillations. If we assume that the initial steady current strength I_0, at the moment of release, is equal to the maximum cyclic value of the current in the case already considered, then the oscillations of the inductance-discharging system will differ only in phase from the oscillations of the condenser-discharging system already discussed. Thus, if the current in the inductance were 6.3246 amperes at the instant of release, and the condenser were initially without charge, the oscillations of the system would be those of Figure 5, except that the time would start from the instant denoted by 90° in that diagram. If the initial direction of the current in the coil were reversed, the starting point in time would be at 270° in Figure 5. Consequently, with condenser-discharging oscillations, we start in Figure 5 with $t = 0$, either from the phase of 0° or of 180°, according to the direction of the p. d. impressed upon the condenser; while with inductance-discharging oscillations, we start with $t = 0$, either from the phase of 90° or of 270°, according to the direction of the current impressed upon the coil. The sequence of all the phenomena will then remain in each case as presented in Figure 5.

Not only Figures 2 and 5, but also Figures 3 and 4 apply equally to inductance and condenser-discharging oscillations. The diagrams of Figure 4 apply more directly, however, to inductance discharges, and those of Figure 3 to condenser discharges, because in the former the initial current is the independent common variable; while in the latter initial p. d. is the independent common variable. Thus, if in Figure 1 the inductance was initially charged with a current of 10 amperes, and an energy of 5 joules, the maximum cyclic current $\bar{I}_0$ would be 10 amperes, the r. m. s. or virtual current, I, 7.071 amperes. The maximum cyclic oscillating p. d. $\bar{U}_0$, in the absence of resistance, would be 1581.14 volts, the r. m. s., or virtual, p. d. U, would be 1118.0 volts, the maximum cyclic power P_m would be 7905.9 watts, and the maximum cyclic condenser or inductance energy $7905.7/3162.3 = 2.5$ joules. The semi-system-energy would also be 2.5 joules.

Charging Oscillations in a Simple Resistanceless Oscillating-Current Circuit. — If with the system of Figure 1 initially unchanged, we suddenly impress upon the circuit, assumed resistanceless, between the terminals TT, a constant potential difference U_0, also assumed resistanceless, as from a storage battery of large cells, then both the condenser and the inductance will be subjected to charging oscillations. In this case, if the impressed p. d. U_0 is the same as that already assumed for the initial p. d. of the discharging condenser, the conditions represented in Figure 5 will apply to the charging oscillations, except in regard to phase, and to the meaning of the zero line OO. The sign of the oscillations will be reversed, or the phase displaced 180°, from those corresponding to a p. d. of the direction *Ou*, Figure 5. That is, an impressed p. d. having the + direction will set up from the start the same system of oscillations as those from the discharge of a condenser impressing a + direction of p. d. on the circuit. The zero line OO of Figure 5, in regard to p. d. and to condenser energy, instead of representing zero p. d. and zero condenser energy, will also have to be interpreted respectively in the charging case, as the constant value of impressed p. d., and the mean energy of the condenser under the impressed p. d. That is, the horizontal line through − 10 will be the zero line of p. d. if the impressed p. d. is 1000 volts tending to make the condenser p. d. positive.

SIMPLE OSCILLATING-CURRENT CIRCUITS CONTAINING RESISTANCE.

When such a circuit as that shown in Figure 1 is allowed to discharge through a known total resistance r ohms, including both joulean and hertzian resistances (all types that involve dissipation of power in proportion to the square of the current), the first step is to find the resistanceless angular velocity ω of Figure 3, that is to determine the angular velocity of discharge on the basis of no resistance ($r = o$). Let this value of resistanceless angular velocity be denoted by ω_0. We then proceed to determine the angular velocity ω in the presence of the actual resistance r.

Let

$$\rho = r/2 \qquad \text{ohms} \quad (13)$$

be the semi-resistance of the circuit, and

$$\tau = l/\rho \qquad \text{seconds} \quad (14)$$

will then be a time-constant, which may, for convenience, be called the *oscillation time-constant* of the circuit, as distinguished from the ordinary time-constant l/r when the circuit is non-oscillatory and the condenser is short-circuited. The oscillation time-constant is thus double the ordinary time-constant. If, as in Figure 7, we take $r = 200$ ohms in the same circuit as has been considered in Figures 3, 4 and 5, $\tau = 0.001$ second.

The time-constant reciprocal of the oscillating-current circuit is

$$\perp = \frac{1}{\tau} = \frac{\rho}{l} \cdot \quad \text{seconds}^{-1} \qquad (15)$$

In the ω-diagram of Figure 7, draw $OP = \perp$, to a suitable scale of reciprocal-seconds, in the direction of reference, or along the real axis in the positive direction. From P draw a line PQ in the $-j$ direction, or perpendicular to OP. With center O, and radius OQ equal, on the adopted scale, to the value of the resistanceless angular velocity

$$\omega_0 = \sqrt{s/l},$$

obtained as in Figure 3, intersect the line PQ in Q. Then the intercept PQ will measure, to scale, the angular velocity ω of the oscillation in the circuit with the resistance r present.

Or analytically,

$$\omega = \sqrt{\omega_0^{\,2} - \perp^2} = \omega_0 \sin \phi \quad \text{radians per sec.} \qquad (16)$$

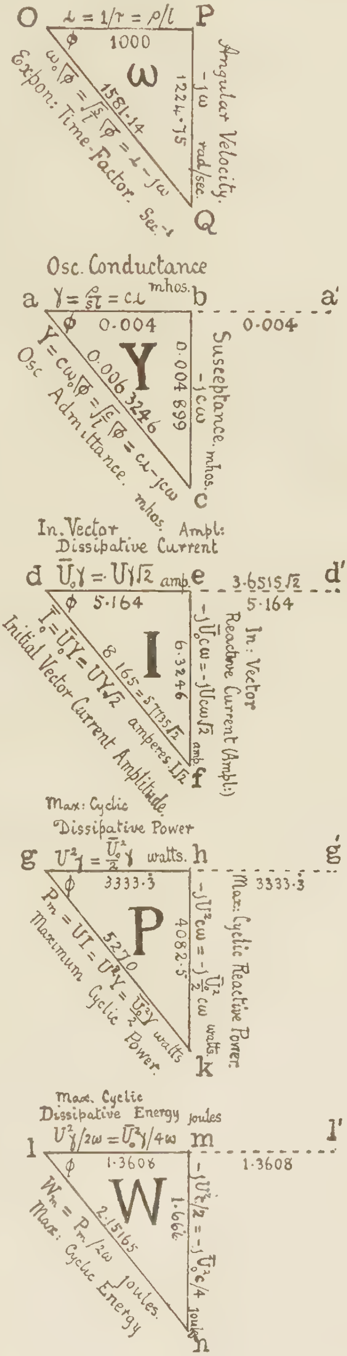

O
$\perp = 1/\tau = \rho/l$
P
ϕ
1000
ω
1224·75
$-j\omega$ rad/sec.
Angular Velocity.
1581·14
$\omega_0 \backslash\!\underline{\phi} = \sqrt{\frac{s}{l}} \backslash\!\underline{\phi} = \perp - j\omega$
Expon: Time-Factor. Sec.$^{-1}$
Q
Osc. Conductance
a
$\gamma = \frac{\rho}{sl} = c\perp$ mhos.
b
a′
0·004
ϕ
0·004
Y
0·004 899
$-jc\omega$
Susceptance. mhos.
0·006 3246
$Y = c\omega_0 \backslash\!\underline{\phi} = \sqrt{\frac{s}{l}} \backslash\!\underline{\phi} = c\perp - jc\omega$
Osc Admittance. mhos.
c
In. Vector Ampl: Dissipative Current
d
$\bar{U}_0\gamma = U\gamma\sqrt{2}$ amp.
e
3·6515$\sqrt{2}$
d′
5·164
ϕ
5·164
I
6·3246
$-j\bar{U}_0 c\omega = -jUc\omega\sqrt{2}$ amp.
In: Vector Reactive Current (Ampl:)
8·165 = 5·7735$\sqrt{2}$ amperes. $\sqrt{2}$
$\bar{I}_0 = \bar{U}_0 Y = UY\sqrt{2}$
Initial Vector Current Amplitude.
f
Max: Cyclic Dissipative Power
g
$U^2\gamma = \frac{\bar{U}_0^2}{2}\gamma$ watts.
h
g′
3333·3̇
ϕ
3333·3̇
P
4082·5
$-jU^2c\omega = -j\frac{\bar{U}_0^2}{2}c\omega$ watts.
Max: Cyclic Reactive Power.
5270
$P_m = UI = U^2Y = \frac{\bar{U}_0^2}{2}Y$ watts
Maximum Cyclic Power.
k
Max. Cyclic Dissipative Energy joules
$U^2\gamma/2\omega = \bar{U}_0^2\gamma/4\omega$
l
m
l′
1·3608
ϕ
1·3608
W
1·666
$-jU^2c/2 = -j\bar{U}_0^2c/4$ joules
2·15165
$W_m = P_m/2\omega$ Joules.
Max: Cyclic Energy
n

FIGURE 7. Stationary vector-diagrams of angular velocity, admittance, vector current strength, maximum cyclic power, and energy in a simple o. c. circuit containing resistance. Phase of p. d., standard.

and T, the period of current and p. d. is $2\,\pi/\omega$. seconds (17)
In the case considered $\omega = 1224.75$ radians per second, and $T = 0.00513$ second.

The matter may be viewed in another direction by considering that with the resistanceless circuit of Figure 3, the vector condition of the p. d. in the circuit, at any instant t seconds after release is

$$u = \bar{U}_0 \epsilon^{-t(-j\omega_0)} = \bar{U}_0 \epsilon^{j\omega_0 t} \qquad \text{volts} \quad (18)$$

where $-j\,\omega_0$ of Figure 3 is the factor of the time in the exponential variable $\epsilon^{j\omega_0 t}$. The effect of introducing a resistance r into the circuit is to alter (18) to

$$u = \bar{U}_0 \epsilon^{-t(\omega_0 \overline{|\phi})} = \bar{U}_0 \epsilon^{-t(\perp - j\omega)} = \bar{U}_0 \epsilon^{-\perp t + j\omega t}. \qquad \text{volts} \quad (19)$$

That is, the exponential time-factor $-j\omega_0$ of the resistanceless case (Figure 3) is deflected from the $-j$ direction to a direction making an angle $\overline{\backslash\phi}$ with the direction of reference; such that

$$\overline{\backslash\phi} = \cos^{-1}(\perp/\omega_0). \qquad \text{radians or degrees} \quad (20)$$

In the case considered, $\phi = 50°.46'.06'' = 0.8861$ radian.

The rotative vector-diagram of the resistant circuit is shown in Figure 8. OU_0, measured to scale along the axis of projection $-XOX$, is the initial p. d. between condenser terminals at release. $O\bar{U}_0$ is the initial position of the vector p. d. whose projection is OU_0. In a certain sense, $O\bar{U}_0$ is a fictitious vector; because it has a value OU_0 cosec $\phi = 1291$ volts, which is greater than the initial p. d. at the moment of release; but, owing to the effect of damping, this seeming inconsistency gives rise to no error in the result. $O\bar{E}_0$ is the vector emf. of self-induction in its initial position. Midway between $O\bar{U}_0$ and $O\bar{E}_0$ lies the vector current $\bar{I}_0$, whose projection on XOX is initially zero. The cophase component Od (5.164 amperes), of the current along $O\bar{U}_0$, is the dissipative component taking power from the discharging p. d. while the component in quadrature thereto, $d\bar{I}_0$ is the reactive component, taking reactive power from $O\bar{U}_0$. The "drop" of vector $\bar{I}_0 r$ volts in the circuit would thus be a vector in line with $\bar{I}_0$ and terminating at the point r. This would also be the resultant of the two vectors $O\bar{E}_0$ and $O\bar{U}_0$. If we take a vector $-Ir$ drop $= OR$, or Or reversed, we have three vectors $O\bar{E}_0$, $O\bar{U}_0$, and OR whose vector sum is zero. This triple set of vectors is to be rotated about the center O, with the uniform angular velocity ω, obtained from Figure 7. But instead of rotating in simple circles, as in the resistanceless case of Figure 2, the three vectors of Figure 8 rotate in equiangular spirals, the angle of each spiral being ϕ as defined in equation 20. That is,

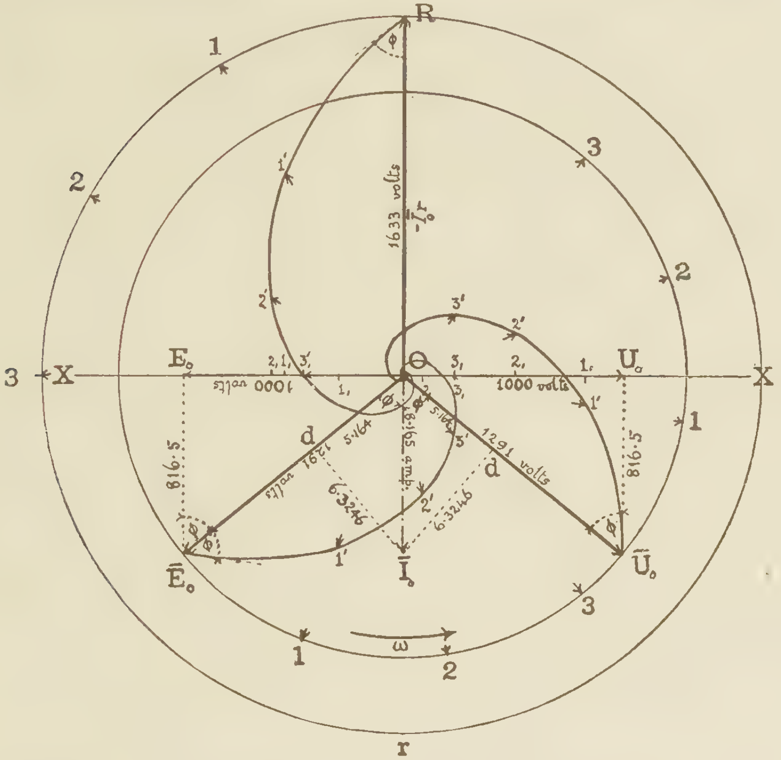

Figure 8. Rotative vector-diagram of an oscillating-current circuit containing resistance. Instant of release of condenser charge.

the tangent to the spiral at any point makes with the radius vector the constant angle ϕ. The vectors rotating with the uniform angular velocity ω of formula (16), describe equiangular spirals because energy is dissipated from the system in the resistance r, and each vector shrinks with time at the uniform exponential rate $\epsilon^{-\alpha t}$; or falls to $1/\epsilon$th of its value in a time τ equal to the oscillatory time-constant. Since, however, all three vectors shrink at the same exponential rate, and since their vector sum in Figure 8 is initially zero, their vector sum will always be zero, and the sums of their projections on the $-XX$ axis will also always be zero. That is, at all times

$$u - l\frac{di}{dt} - ir = 0. \qquad \text{volts} \quad (21)$$

It is noteworthy that in Figure 8, both the discharging p. d. $O\bar{U}_0$ and the emf. of self-induction make an angle ϕ with the current $O\bar{I}_0$, the former leading and the latter lagging. Each of these emfs. therefore develops power on the current. This is a general condition of the o. c. circuit, different from that of the a. c. circuit, in which the emf. of self-induction exerts no dissipative power on the current, being in quadrature therewith.

We may, however, dispense with the equiangular spirals of Figure 8 by assuming that all the vectors rotate in circles with uniform angular velocity ω, provided we apply to their instantaneously projected values on XOX, the proper damping factor $\epsilon^{-\alpha t}$ for the instant considered.

The positions of the three vector emfs. and also their projections on $-XX$, are indicated in Figure 8 for three successive instants angularly separated by 30°, or 0.000,427,5 second.

Returning to the stationary vectors of Figure 7, if we multiply the ω-diagram by the condenser-capacity c, we obtain the oscillatory admittance diagram Y to a scale of mhos. The oscillatory admittance is numerically the same as in the resistanceless case of Figure 3, (0.006,324,6 mho), but makes a negative angle ϕ with the reference axis, instead of 90°. The oscillatory conductance is the real component, and the oscillatory susceptance the $-j$ component, of the oscillatory admittance.

Multiplying the Y diagram by $\bar{U}_0$, the vector amplitude of the initial discharging p. d., we obtain the current or $\bar{I}$ diagram, $d\,e\,f$, of Figure 7. The initial vector oscillatory current $\bar{I}_0$ is 8.165 amperes, corresponding to a r. m. s. initial oscillatory current I of 5.7735 amperes. The reactive component $e\,f$ is the same as in the resistanceless case. The dissipative component $d\,e$ is the component in phase with the discharging p. d. $O\bar{U}_0$ Figure 8. A like component is also in phase with the self-inductive emf. OE; so that the total equivalent component of dissipation current would be $d\,d'$ Figure 7, or 10.328 amperes maximum cyclic initial value.

Multiplying the I diagram, Figure 7, by $\frac{\bar{U}_0}{2}$, we obtain the stationary-vector power-diagram P, or the watts triangle $g\ h\ k$, which may be drawn to any suitable scale of watts. This gives the maximum cyclic power P_m, of which the component $h\ k$ is the maximum cyclic reactive power, or the maximum cyclic power in the inductance; while the real component $g\ h$ is the maximum cyclic power expended in resistance by the discharging p. d. $O\bar{U}_0$, Figure 8. But a like dissipation of power occurs under the influence of the emf. of self-induction $O\bar{E}_0$, so that the total undamped maximum cyclic dissipative power in the circuit is gg', Figure 7, of 6666.6 watts.

Finally, if we divide the P diagram by $2\ \omega$, or twice the resistant angular velocity, we obtain the W diagram of Figure 7, or the triangle $l\ m\ n$, which may be drawn to a suitable scale of joules. The stationary vector $l\ n$ is the undamped maximum cyclic energy W in the oscillatory circuit as measured, at condenser terminals, or 2.151,65 joules in the case considered. The $-j$ component, or $1.6\dot{6}$ joules, is the undamped maximum cyclic energy in the reactance, and the real component $l\ m = 1.3608$ is the undamped maximum cyclic energy dissipated by the discharging p. d. $O\bar{U}_0$, Figure 8, on the oscillatory current. But a like amount of energy will be dissipated by the self-inductive emf. OE. Consequently, the total undamped maximum cyclic dissipative energy in the circuit will be $l\ l'$, Figure 7, or 2.7216 joules.

The condition of either the vector p. d. $O\bar{U}_0$ (Figure 7), the vector self-inductive emf. $O\bar{E}_0$, or the vector current $O\bar{I}_0$ after t seconds, is obtained by applying the exponential $(\epsilon^{-(\iota - j\omega)\,t})$, as in (19). This exponential may be expressed as $\epsilon^{-\iota t} .\ \epsilon^{j\omega t}$, the first of which is a damping-factor, and the second a rotating factor. The diagrams of Figure 7 apply only to the effects of the rotating factor, as though no damping existed. That is, they represent undamped oscillating quantities, or quantities which would be projected on $-XOX$ by the rotation of the vectors $O\bar{U}_0$, $O\bar{E}_0$, OR, in pure circles, instead of in spirals. The damping-factor $\epsilon^{-\iota t}$ to be applied, is represented in Figure 9, which is drawn on semi-logarithm paper, i.e., on paper ruled to a logarithmic scale of ordinates, but to a uniform scale of abscissas. The ordinates give the damping-factor, and the abscissas the time from release, to a scale of degrees, and also of seconds. The straight line OA represents the damping-factor for voltage and currents. The straight line OB represents the damping-factor for powers and energies. The time in which the voltage and current fall to $1/\epsilon$th of their initial value is τ, the oscillatory time-constant, or 0.001 second in the case considered. The number of radians through which the vectors of Figure 8 must rotate in order to shrink to $1/\epsilon$th of their initial values, i. e., the time-angle for a damping-factor of $\epsilon^{-1} = 0.367,88$, is $l\omega/\rho = \tan\phi$, or, in the case considered, 1.22475 radians $= 70.2°$.

Figure 10 shows the undamped time-values of the various quantities considered, or the values before applying the damping-factor. The sinusoid $\bar{u}$, of 1291 volts amplitude, corresponds, to the projection of $O\bar{U}_0$, Figure 8, on the XOX axis. Similarly, the sinusoid $\bar{e}$, of 1291 volts amplitude, corresponds to the projection of $O\bar{E}_0$, Figure 8, on the same axis. The heavy sinusoid $\bar{i}$, of 8.165 amperes amplitude, gives the undamped current, starting positively from zero at O. The emfs.

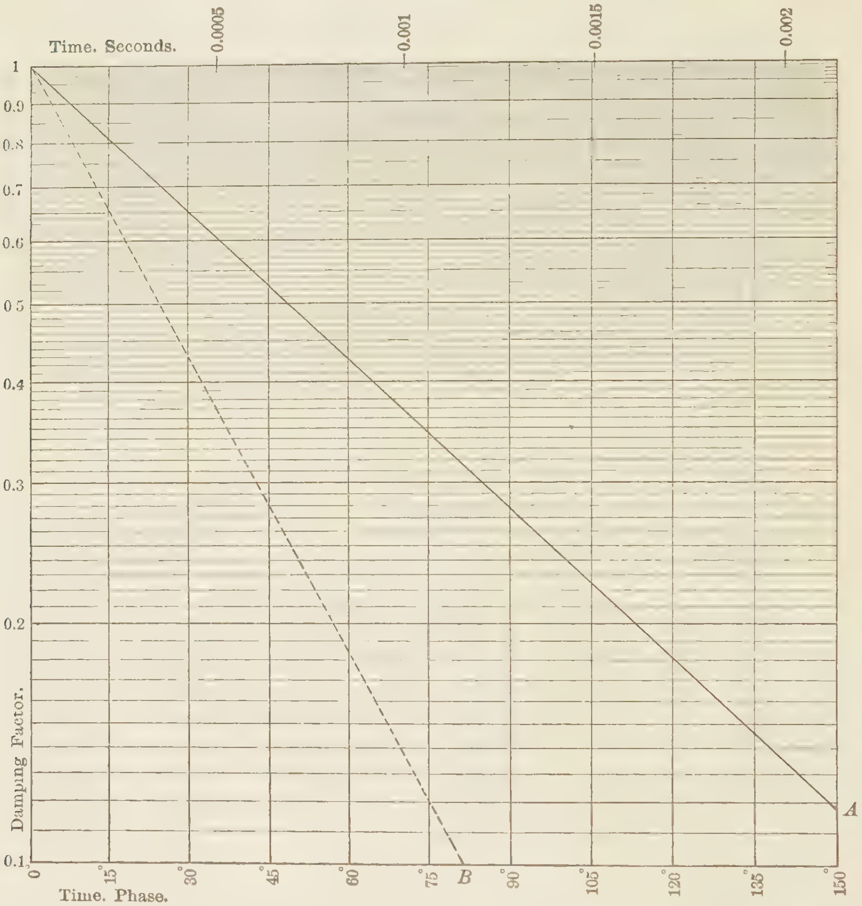

FIGURE 9. Damping-factors at different time-intervals after release.

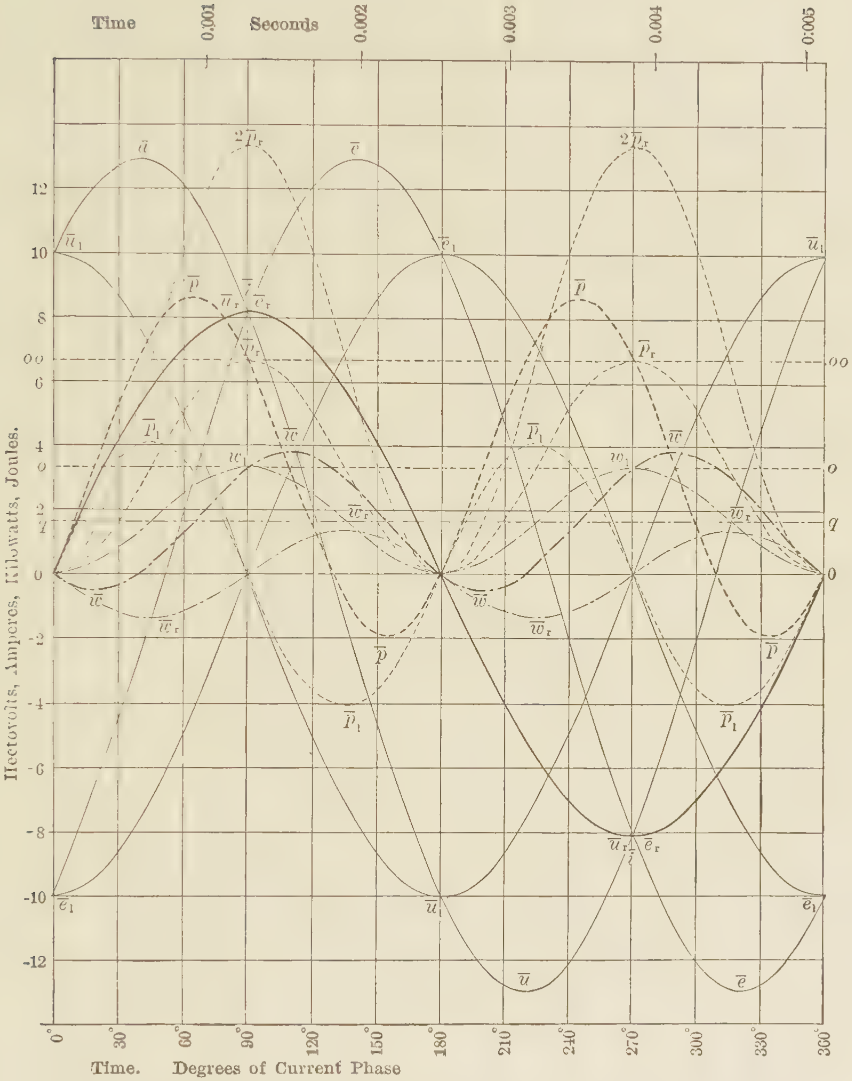

FIGURE 10. Curves of potential difference, current, power and energy in simple oscillating-current circuit containing resistance, leaving damping out of account.

$\bar{u}$ and $\bar{e}$, being out of phase with the current, are divided each into two components $\bar{u}_r$ $\bar{u}_l$ and $\bar{e}_r$ $\bar{e}_l$, the former being in phase with the current, the latter in quadrature therewith. The maximum cyclic values of $\bar{u}_r$ and $\bar{e}_r$ will be 816.5 volts each as at U, Figure 12, and the maximum cyclic values of $\bar{u}_l$ and $\bar{e}_l = 1000$ volts each. The undamped power of the cophase components $\bar{i}$ and $\bar{u}_r$ is the double-frequency $\bar{p}_r$ of 3333.3 watts amplitude about the zero line oo, itself elevated 3333.3 watts. The power of $\bar{i}$ and $\bar{e}_r$ will be an identical sinusoid. The total power of cophase components is thus the sinusoid $2\,\bar{p}_r$ of 6666.6 watts amplitude, about the zero line oo, oo, itself elevated 6666.6 watts. The reactive power expended by the quadrature voltage component of $\bar{u}_l$ upon the current i, is the double-frequency sinusoid $\bar{p}_l$ of 4082.5 watts as at P, Figure 12. This power is in the magnetic field of the reactance. The total power exerted by $\bar{u}$ upon $\bar{i}$ is the heavy double-frequency sinusoid $\bar{p}$, of 5270 watts amplitude, about the zero line oo elevated 3333.3 watts.

The undamped energy of reactance magnetic flux is the double frequency sinusoid w_l, of $1.6\dot{6}$ joules amplitude, about the zero line qq, elevated 1.66 joules. The undamped energy of dissipation in resistance due to $\bar{u}_r$ and $\bar{i}$, is the double-frequency sinusoid w_r of 1.3608 joules. An identical sinusoid would represent the energy of dissipation due to $\bar{e}_r$ and $\bar{i}$; so that the total unattenuated energy of dissipation would be a double-frequency sinusoid of 2.7216 joules amplitude, as at W, Figure 12. The total undamped energy of $\bar{u}$ acting on $\bar{i}$ is the heavy double-frequency sinusoid $\bar{w}$, of 2.151,65 joules amplitude, about the zero line qq.

If we apply the attenuation-factors of Figure 9 to the ordinates of Figure 10, that is, multiplying the currents and voltages by $-{}^{\alpha t}$, while multiplying the powers and energies by $\epsilon - {}^{2\alpha t}$, we obtain the curves of Figure 11 (with the exceptions of w and w_r). This diagram represents the actual succession of events in the oscillating-current circuit. The p. d. at terminals falls along u. The emf. of self-induction pursues the opposite curve e. The current follows the heavy line i, reaching a maximum of 3.04 amperes near to 45° of its phase, or 0.00064 second after release. The components of voltage in phase with the current — u_r and e_r — both coincide with its curve. The quadrature components of voltage are u_l and e_l. The total component of voltage in phase with the current follows the curve marked $2\,u_r$. The power curve p reaches a maximum of 2200 watts at about 60° of its phase. This power rapidly subsides, and only crosses the zero line in feeble measure. The total dissipative power is shown by the curve $2\,p_r$.

The energy in the inductance follows the curve w_l. This corresponds to $\overline{w}_l$, in Figure 10, after applying the factor $\epsilon^{-2\Delta t}$. The total energy dissipated in the resistance, and the total energy expended by the condenser, follow respectively the curves w_r and w, which do not correspond with the cyclic curves $\overline{w}_r$ and $\overline{w}$ of Figure 10, being energy summations instead of instantaneous values. Consequently, the curves of $\overline{w}_r$, and $\overline{w}$ in Figure 10 must be interpreted otherwise than by the application of an attenuation-factor.

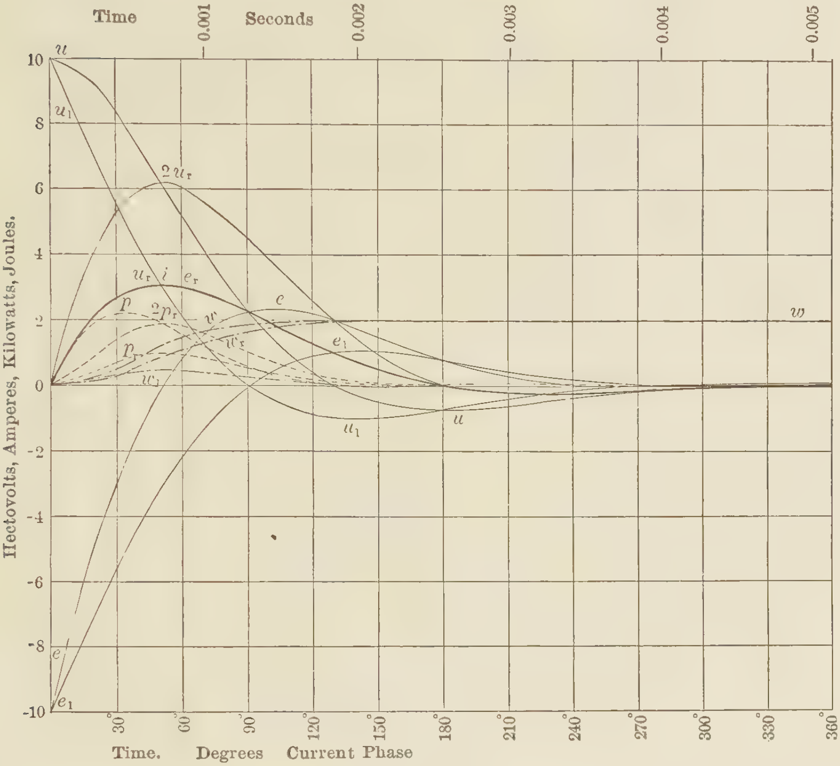

FIGURE 11. Curves of potential difference, current, power and energy in simple oscillating-current circuit containing resistance after applying damping-factors to the ordinates of Figure 10.

With respect to the phase of the oscillating-current as standard, we have the series of stationary vector-diagrams of Figure 12. The oscillatory impedance of the circuit is $Z = \rho + jl\omega$ ohms, or $Z_0 \underline{/\phi}$; where Z_0 is the impedance in the resistanceless condition of Figure 4. The total resistance r of the circuit is represented by AA'. The initial vector potential difference has an amplitude $\bar{U}_0 = \bar{I}_0 Z_0$ volts. The total initial drop of potential resistance is indicated by DD'. The undamped maximum cyclic power is indicated at P, and the undamped cyclic energy at W. The P and W diagrams to standard current phase are inverted with respect to those of standard p. d. phase, because the undamped power lags behind the p. d. but leads the undamped current.

The diagrams in Figures 7 and 12 of the oscillating-current circuit correspond to similar diagrams in connection with the alternating-current circuit.[2] The U, I, P, and W diagrams are stationary vector-diagrams, but they may be converted into rotating vector-diagrams. Thus I may be made a rotating vector-diagram by mounting it on the point d as center, and giving a positive angular velocity ω to the triangle, starting with df in the $-j$ direction. The projection of df on the real axis, after applying the damping-factor ϵ^{-ut}, will

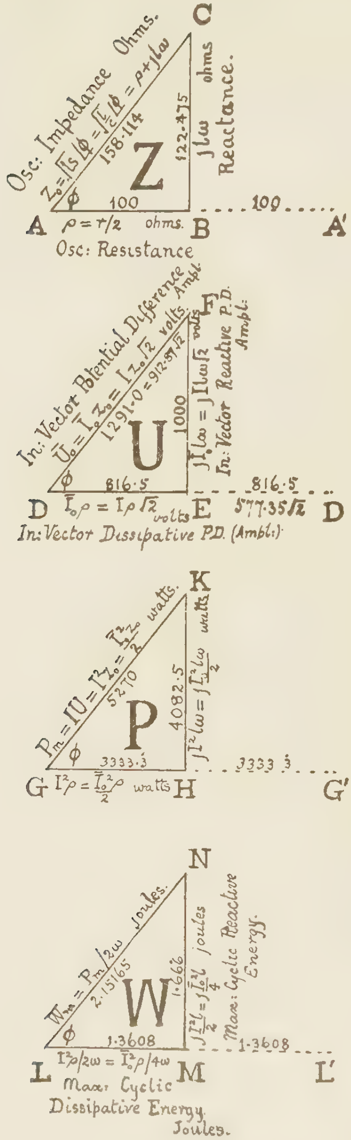
C
Osc: Impedance Ohms.
$Z_0 = \sqrt{15}\,\underline{/\phi} = \sqrt{\frac{L}{C}}\,\underline{/\phi} = \rho + jl\omega$
158.114
Z
122.475
$jl\omega$ ohms
Reactance.
ϕ
100
A
$\rho = r/2$ ohms.
B
100
A'
Osc: Resistance
F
In: Vector Potential Difference Ampl.
$\bar{U}_0 = \bar{I}_0 Z_0 = \bar{I}_0 Z_0 \sqrt{2}$ volts.
1291.0 = 912.87√2
1000
$j\bar{I}_0 l\omega = jIl\omega\sqrt{2}$ volts
In: Vector Reactive P.D. Ampl.
U
ϕ
816.5
D
$\bar{I}_0\rho = I\rho\sqrt{2}$ volts
E
816.5
577.35√2
D
In: Vector Dissipative P.D. (Ampl.)
K
$P_m = \bar{I}\bar{U} = \bar{I}_0^2 Z_0 = \frac{\bar{I}_0^2 Z_0}{2}$ watts.
5270
P
4082.5
$jI^2 l\omega = j\frac{\bar{I}_0^2 l\omega}{2}$ watts
ϕ
3333.3
G
$I^2\rho = \frac{\bar{I}_0^2}{2}\rho$ watts
H
3333.3
G'
N
$W_m = P_m/2\omega$ joules.
2.15165
W
1.662
$j\frac{I^2 l}{2} = j\frac{\bar{I}_0^2 l}{4}$ joules
Max: Cyclic Reactive Energy.
ϕ
1.3608
L
$I^2\rho/2\omega = \bar{I}_0^2\rho/4\omega$
M
1.3608
L'
Max: Cyclic Dissipative Energy. Joules.

FIGURE 12. Stationary vector-diagrams of impedance, vector potential difference, maximum cyclic power and energy in a simple o. c. circuit containing resistance. Phase of current, standard.

---

[2] "Vector Power in Alternating-Current Circuits" by A. E. Kennelly. Trans. American Inst. Elect. Engrs. June, 1910. Vol. 29.

give the actual current at any instant. This is equivalent to rotating df in an equiangular spiral of angle ϕ in the manner of Figure 8.

Similar treatment will convert U into a rotating vector-triangle, except that DF should start from the position $O\bar{U}_0$ of Figure 8.

The P diagram, in either Figure 7 or Figure 12, can be made into a rotating vector-diagram, by rotating the triangle with angular velocity 2ω about the vertex k or K respectively. Thus, taking the power triangle ghk of Figure 7, we mount it on an axis at k, Figure 13, and draw kr equal and parallel to hg. The three-vector system, kh, kg, and kr is then allowed to rotate with the angular velocity 2ω, in the case considered 2449.5 rad/sec, starting from the position shown, when the p. d. vector $O\bar{U}_0$, Figure 8, starts with angular velocity ω from the position KH, or parallel to OY. The orthogonal projections on $-XOX$ of the three vectors kh, kg, and kr, then define at any instant the undamped reactive, total, and dissipative power, under the action of $O\bar{U}_0$ on the oscillatory current. The total undamped power $\bar{p} = 5270$ watts thus lags $\frac{\pi}{2} + \phi$ behind the p. d. vector in terms of power phase, or $\frac{\pi}{4} + \frac{\phi}{2}$ in terms of p. d. phase (70° .23′). The total undamped power is measured on the OX axis from the point O and oscillates between the limits $O\bar{p} = 8603.3$ and $O{-}\bar{p} = -1936.6$ watts, as shown in Figure 10.

The undamped dissipative power $\bar{p}_r$ oscillates between the limits $O\bar{p}_r = 6666.6$ watts and zero. The total undamped dissipative power is $2\,\bar{p}_r = 13{,}333.3$ watts, owing to the separate actions of $O\bar{U}_0$ and $O\bar{E}_0$, Figure 8.

The undamped reactive power $\bar{p}_l$ is reckoned from o as zero, and oscillates between ±4082.5 watts.

The damping-factor $\epsilon^{-2\alpha t}$ must be applied to $\bar{p}$ and $\bar{p}_r$ as measured from O, and to $\bar{p}_l$ as measured from o, along the OX axis.

If we employ the phase of the oscillating current as standard, and as taken in Figure 10, we mount the power triangle GHK of Figure 12 on an axis at K, and rotate it, as before, at angular velocity 2ω, starting from the position GHK shown in Figure 13 when the current vector $O\bar{I}_0$ of Figure 8 is passing through the position KHo with angular velocity ω. The total power $\bar{p}$ will then lag $\frac{\pi}{2} - \phi$ behind the current vector, in terms of power-phase, or $\frac{\pi}{4} - \frac{\phi}{2}$, in terms of current phase

(19° 37′) as indicated in Figure 10. The $\bar{p}_r$ vector Kr then follows, 90° of power phase or 45° of current phase, behind the current at release. The vector KH, or undamped reactive power vector, Figure 13, starts in phase with the current.

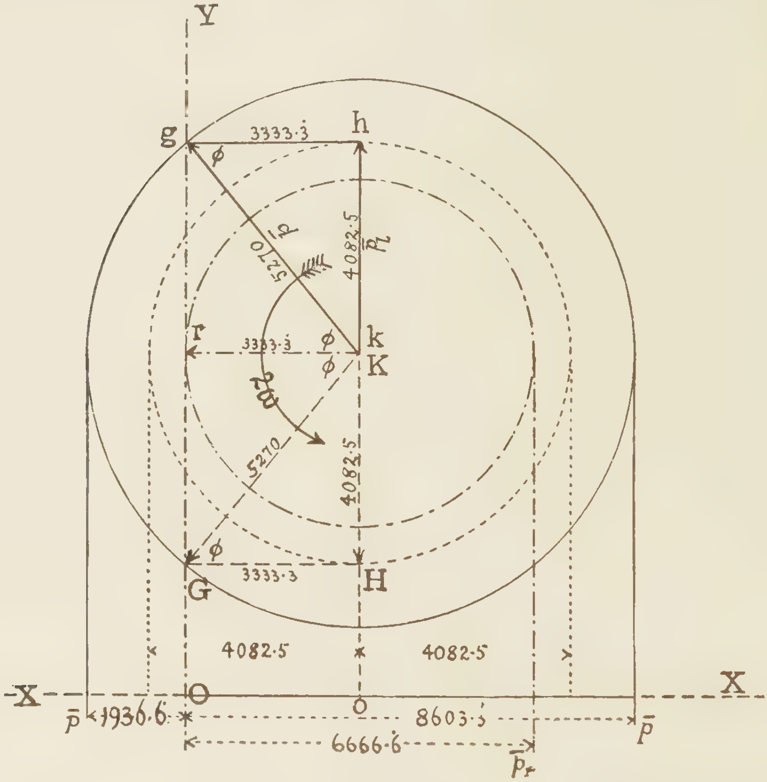

FIGURE 13. Rotative vector power diagram for p. d. standard phase and for current standard phase.

The stationary vector-diagrams of Figure 7 may be understood as involving the following phase relations, with respect to the phase of the undamped vector p. d. $O\bar{U}_0$, Figure 8.

$$\bar{I}_0 = \bar{U}_0 Y \overline{|\phi} = UY\sqrt{2}\,\overline{|\phi} = \bar{U}_0 c\omega_0 \overline{|\phi} \qquad \text{max. cyclic amperes} \qquad (22)$$

$$P_m = UI \overline{|\phi} = \frac{U_0 I_0 Y}{2} \overline{|\phi} = \frac{U_0^2}{2} Y \overline{|\phi} \qquad \text{max. cyclic watts} \qquad (23)$$

That is, the undamped current lags ϕ° of p. d. phase behind the discharging undamped p. d. The undamped power reaches its positive

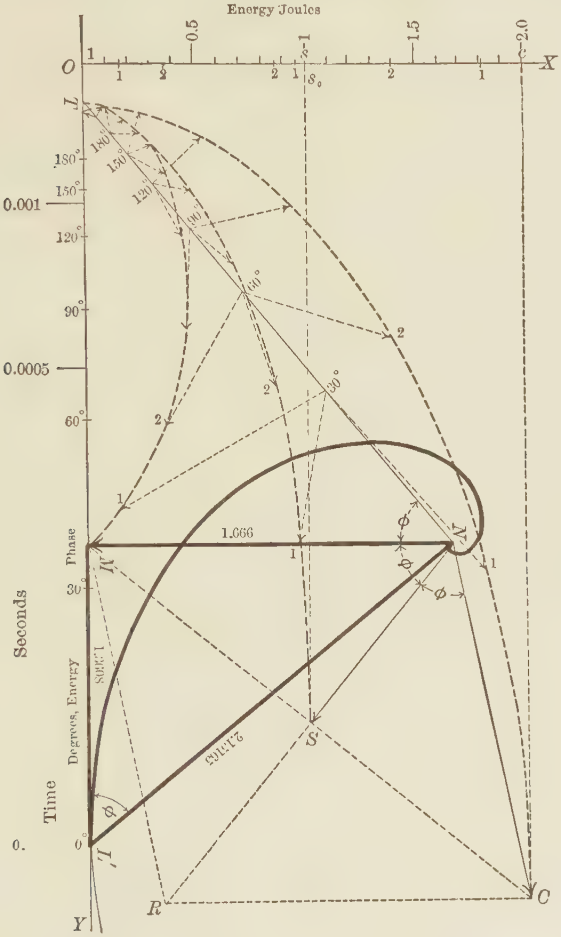

Figure 14. Rotating and rolling vector-diagram of the condenser energy, the inductance energy, the semi-system energy and the semi-dissipated energy in an oscillating-current circuit.

maximum ϕ° of its phase behind the discharging undamped p. d. Similarly in Figure 12, we may write the relations

$$\bar{U}_0 = \bar{I}_0 Z \,\underline{/\phi} = IZ\sqrt{2}\,\underline{/\phi} = \bar{I}_0 l\omega_0 \,\underline{/\phi} \qquad \text{max. cyclic volts} \quad (24)$$

$$P_m = IU\,\underline{/\phi} = \frac{\bar{I}_0^2 Z}{2}\,/\underline{\phi} = \frac{I_0 \dot{U}_0 Z}{2}\,\underline{/\phi}. \qquad \text{max. cyclic watts} \quad (25)$$

Or the discharging p. d. is $\phi°$ of current phase ahead of the current and the undamped power reaches its maximum $\phi°$ of its phase ahead of the current, all being considered as undamped.

In order to derive a rotative energy vector-diagram, we take the triangle *lmn* of Figure 7, or $L'MN$ of Figure 12 and lay $L'M$ along the OY axis as shown in Figure 14. With the point N as pole, the equiangular spiral NL' is drawn, of angle ϕ. This will be tangent to the OY axis at L'. We then draw a vector $NC = NM$ and making with NM an angle of 2ϕ. The mid-point S of the straight line NC is then connected to N by the vector NS. We may call NC the condenser-energy vector, NM the reactive-energy vector, and NS the semi-system-energy vector; i. e., the vector of the half sum of the energy in the condenser and reactance. We now rotate the three vectors and the spiral, with angular velocity 2ω, while permitting the spiral to roll along the axis OY. The successive turns of the spiral are to be capable of rolling on this axis, as by displacing them infinitesimally out of the plane of the paper, like the wards of a conical band spring. The vectors NC, NS, and NM are also to shrink as they rotate by application of the damping-factor $\epsilon^{-2\perp t}$. Then the projections of C, M, and S, on the OX axis, will define the instantaneous energy in the condenser, reactance and semi-system respectively. The path of the pole N will be the straight line NT, pursued with damped velocity. The paths C and M will be exponential cycloids, that of S an exponential trochoid. The positions of C, S, and M are traced in Figure 14 for several energy phase intervals of 30°, or 0.000,213,8 second, the first two of which are marked 1, 2, on each curve. It will be seen that taking the energy scale along OX conformably with that of LMN, the condenser energy starts at 2 joules, and after 60° or 0.000,427,6 second, it falls to 1.3811 joules. The reactive energy *ol* commences at zero and after 60° power and energy phase it rises to 0.3544 joule. The semi-system energy *Os* starts at 1 joule, and after 60° falls to 0.8678 joule. The displacement $s_0 s$ is therefore half the dissipated energy $= 0.1322$ joule. The total dissipated energy at this instant is thus $2\,s_0 s = 0.2645$ joule. All three vectors finally terminate and shrink into the point T. The distance $TL' = NL'/\cos\phi$, and NT is perpendicular to NL'.

The fundamental differential equation for quantity q is satisfied by

$$q = A\epsilon^{-(\perp + j\omega)t} + B\epsilon^{-(\perp - j\omega)t}, \qquad \text{coulombs} \quad (26)$$

where A and B are integration constants, while $\perp$ and ω follow from the construction of the triangle OPQ, Figure 7.

Choosing the constants consistently with the discharge of the condenser initially charged to potential U_0 volts, the potential at time t is

$$u = U_0 \operatorname{cosec} \phi \, \epsilon^{-\perp t} \sin(\omega t + \phi) \qquad \text{volts} \quad (27)$$

$$= \bar{U}_0 \epsilon^{-\perp t} \sin(\omega t + \phi), \qquad \text{volts} \quad (28)$$

from which q follows by the relation $q = u/s = uc$ coulombs. $\bar{U}_0$ is the initial value of the vector discharging p. d. as obtained from Figures 8 and 12.

The instantaneous current is

$$i = Q_0 \omega \operatorname{cosec}^2 \phi \, \epsilon^{-\perp t} \sin \omega t \qquad \text{amperes} \quad (29)$$

$$= U_0 c \omega_0 \operatorname{cosec} \phi \, \epsilon^{-\perp t} \sin \omega t \qquad \text{amperes} \quad (30)$$

$$= \frac{\bar{U}_0}{z_0} \epsilon^{-\perp t} \sin \omega t = \bar{I}_0 \epsilon^{-\perp t} \sin \omega t, \qquad \text{amperes} \quad (31)$$

where $$\bar{I}_0 = \bar{U}_0 / l\omega = \bar{U}_0 / z_0 = \bar{U}_0 c \omega_0. \qquad \text{amperes} \quad (32)$$

The emf. of self-induction in the circuit at any instant is

$$e = U_0 \operatorname{cosec} \phi \, \epsilon^{-\perp t} \sin(\omega t - \phi) \qquad \text{volts} \quad (33)$$

$$= \bar{U}_0 \epsilon^{-\perp t} \sin(\omega t - \phi). \qquad \text{volts} \quad (34)$$

The instantaneous power of the condenser in the circuit is

$$p = ui = \bar{U}_0 \bar{I}_0 \epsilon^{-2\perp t} \sin \omega t \cdot \sin(\omega t + \phi) \qquad \text{watts} \quad (35)$$

$$= \frac{\bar{U}_0 \bar{I}_0}{2} \epsilon^{-2\perp t} [\cos \phi - \cos(2\,\omega t + \phi)] \qquad \text{watts} \quad (36)$$

$$= UI \epsilon^{-2\perp t} [\cos \phi - \cos(2\,\omega t + \phi)]. \qquad \text{watts} \quad (37)$$

The instantaneous power of the reactance in the circuit is

$$p' = ei = \bar{U}_0 \bar{I}_0 \epsilon^{-2\perp t} \sin \omega t \cdot \sin(\omega t - \phi) \qquad \text{watts} \quad (38)$$

$$= \frac{\bar{U}_0 \bar{I}_0}{2} \epsilon^{-2\perp t} [\cos \phi - \cos(2\,\omega t - \phi)] \qquad \text{watts} \quad (39)$$

$$= UI \epsilon^{-2\perp t} [\cos \phi - \cos(2\,\omega t - \phi)]. \qquad \text{watts} \quad (40)$$

The total dissipation power of the condenser and reactance is after t seconds,

$$2p_r = p + p' = \bar{U}_0^2 \gamma \epsilon^{-2\perp t}(1 - \cos 2\omega t), \qquad \text{watts} \quad (41)$$

$$= \bar{I}_0^2 \rho \epsilon^{-2\perp t}(1 - \cos 2\,\omega t), \qquad \text{watts} \quad (41a)$$

where $\gamma = c\perp$, the oscillation conductance of the circuit. The energy in the condenser t seconds after release, if $W_l = mn$, Figure 7, $= MN$, Figure 12, is

$$w_c = \frac{\bar{U}_0^2}{4} c \epsilon^{-2\perp t}[1 - \cos(2\,\omega t + 2\,\phi)] \qquad \text{joules} \quad (42)$$

$$= W_l \epsilon^{-2\perp t}[1 - \cos(2\,\omega t + 2\phi)]. \qquad \text{joules} \quad (43)$$

The energy in the reactance t seconds after release is

$$w_l = \frac{\bar{U}_0^2}{4} c \epsilon^{-2\perp t}(1 - \cos 2\,\omega t) \qquad \text{joules} \quad (44)$$

$$= W_l \epsilon^{-2\perp t}(1 - \cos 2\,\omega t). \qquad \text{joules} \quad (45)$$

The total energy of the system t seconds after release is

$$w = w_c + w_l = \frac{\bar{U}_0^2}{2} c \epsilon^{-2\perp t}[1 - \cos(2\,\omega t + \phi)\cos\phi] \quad \text{joules} \quad (46)$$

$$= 2\,W_l \epsilon^{-2\perp t}[1 - \cos(2\,\omega t + \phi)\cos\phi]. \quad \text{joules} \quad (47)$$

The semi-system energy w_s at time t is therefore

$$w_s = W_l \epsilon^{-2\perp t}[1 - \cos(2\,\omega t + \phi)\cos\phi]. \quad \text{joules} \quad (48)$$

The initial energy of the system is

$$W_0 = \frac{U_0^2 c}{2}\sin^2\phi = 2\,W_l \sin^2\phi = 2\,W_m \sin^8\phi = \frac{U_0^2 c}{2}. \quad \text{joules} \quad (49)$$

The total loss by dissipation is at any instant

$$w_d = W_0 - w$$

$$= \frac{U_0^2 c}{2}\{\sin^2\phi - [1 - \cos(2\,\omega t + \phi)\cos\phi]\,\epsilon^{-2\perp t}\}. \quad \text{joules} \quad (50)$$

This is the total expenditure of energy in I^2r up to time t. At any complete energy cycle, when $\cos(2\omega t + \phi) = \cos\phi$, and $t = m\frac{T}{2}$,

$$w_d = \frac{\bar{U}_0^{\,2}c}{2}\left[\sin^2\phi\left(1 - \epsilon^{-2\perp m\frac{T}{2}}\right)\right] = W_0\left(1 - \epsilon^{-\perp mT}\right). \quad \text{joules} \quad (51)$$

The energy dissipated in the first energy cycle, when $t = T/2$,

$$w_1 = W_0\left(1 - \epsilon^{-\perp T}\right). \qquad \text{joules} \quad (52)$$

The dissipation in successive energy cycles 1st, 2d, 3rd, 4th, etc., is

$$w_1, \quad w_1\epsilon^{-\perp T}, \quad w_1\epsilon^{-2\perp T}, \quad w_1\epsilon^{-3\perp T}, \quad \text{etc.} \qquad \text{joules} \quad (53)$$

The total ultimate energy dissipated is

$$W_0 = w_1\left(1 + \epsilon^{-\perp T} + \epsilon^{-2\perp T} + \ldots\right) \qquad \text{joules} \quad (54)$$

$$= \frac{w_1}{1 - \epsilon^{-\perp T}} \qquad \text{joules} \quad (55)$$

With the values in the case considered of $\bar{U}_0 = 1291$, $U_0 = 1000$, $c = 4 \times 10^{-6}$, $\omega = 1224.75$, $\phi = 50^\circ\ 46'$, $\perp = 1000$, $T = 0.00513$, $W_0 = 2$, we have, for the attenuation factor of one power period or semi-period of p. d., $\epsilon^{-\perp T} = 0.005{,}987$. The energy dissipated by I^2r in the first energy cycle is thus $2 \times 0.994{,}01 = 1.988{,}02$ joules. The second cycle dissipates $0.005{,}987 \times 1.988{,}02 = 0.0119$ joule. Each successive cycle dissipates 0.5987 per cent of the amount dissipated in the last preceding cycle. It is thus evident that in a damped oscillatory discharge, a relatively large fraction of the energy is rejected from the system in the first half-cycle of voltage or current, i. e., the first complete energy cycle.

Logarithmic Decrement.

If v be any vector oscillating-quantity of the type

$$v = V_0\epsilon^{-\perp t}\sin(\omega t + \phi), \qquad \text{Ph. Q.} \quad (56)$$

such as a voltage, current, or force.

Then the rotating vector of this quantity $V_0\epsilon^{-\perp t}\epsilon^{j\omega t}$, in passing from one assigned position to another, in a time t_1 seconds, decreases from the first to the second value by the exponential, or damping factor, $\epsilon^{-\perp t_1}$. The exponent, $\perp t_1$, of the damping may be defined as the Naperian logarithm of the decrement during the interval, or simply as the log-decrement in the interval. If the log-decrement be denoted by δ, then

$$\delta = \perp t_1. \qquad \text{numeric} \quad (57)$$

If the rotating vector moves through one radian at the actual angular velocity ω, the time t_1 occupied in the passage will be $1/\omega$ seconds; so that

$$\delta_1 = \frac{\perp}{\omega} = \cot\phi. \qquad \text{numeric} \quad (58)$$

If the rotating vector moves through a half-cycle, semi-revolution, or π radians, the time occupied in the passage will be $t_1 = \pi/\omega$ seconds; so that

$$\delta_\pi = \pi\frac{\perp}{\omega} = \frac{\perp}{2\,n} = \pi\cot\phi, \qquad {}^3\text{numeric} \quad (59)$$

which is the log-decrement of any two successive elongations of the vector's projection in opposite directions on the axis of reference XX. If the vector moves through a whole cycle, revolution, or $2\,\pi$ radians, the time occupied will be $t_1 = 2\,\pi/\omega$ seconds, and

$$\delta_{2\pi} = 2\,\pi\frac{\perp}{\omega} = \frac{\perp}{n} = \frac{T}{\tau} = 2\,\pi\cot\phi, \qquad \text{numeric} \quad (60)$$

which is the log-decrement of any two successive elongations of the vector's projection in one and the same direction on the reference axis. Consequently, from any pair of successive maxima of the oscillating quantity v, the log-decrement is obtainable, and from this the angle ϕ of the equiangular spiral and of the stationary vectors for the quantity is obtainable. In the case considered, $\delta_1 = 0.8165$, $\delta_\pi = 2.5651$, and $\delta_{2\pi} = 5.1302$.

Root of Mean Square of Oscillating-Current Quantities.

If v be any vector oscillating quantity of the type $V_0\epsilon^{-\perp t}\sin\omega t$, such as an oscillating-voltage, current, or force; then if the damping coefficient $\perp$ is taken as zero, the square root of the mean square of the quantity during any integral number of cycles is $V = V_0/\sqrt{2}$, as in ordinary alternating-current theory. If, for instance, the initial voltage is 1000, and there were no damping, the r. m. s. voltage of the o. c.

---

[3] The condition expressed in (59) was first pointed out by Prof. Clerk-Maxwell, in a somewhat different manner. See Bibliography.

circuit as shown by an ideally perfect voltmeter would be 707.1 volts. The question is what would such an instrument show in the presence of a known damping? The reading of the instrument would evidently fall as the damping continued, and, in most practical cases, would fall very rapidly; so that the inquiry must be limited to a certain definite instant during the charge or discharge; or at least to a certain definite interval of time within the process. At any instant we have

$$v^2 = V_0^{\,2}\epsilon^{-2\perp t}\sin^2\omega t. \qquad (\text{Ph. Q.})^2 \quad (61)$$

The time integral of this square from time $t = 0$ to $t = \infty$ is

$$\int_0^\infty v^2 dt = \frac{V_0^{\,2}}{4\perp}\left(\frac{\omega^2}{\perp^2+\omega^2}\right) = \frac{V_0^{\,2}}{4\perp}(1-\cos^2\phi). \quad (\text{Ph. Q.})^2 \text{ secs.} \quad (62)$$

But after the lapse of a time t_1 seconds, including m complete periods of the oscillating quantity, its value will have become

$$v_{mT} = V_0\epsilon^{-\perp mT}\sin\omega t = V_0\epsilon^{-\perp t_1}\sin\omega t, \qquad \text{Ph. Q.} \quad (63)$$

where T is the period of the oscillation, and m is any positive integer; so that

$$\int_0^{t_1} v^2 dt = \frac{V_0^{\,2}}{4\perp}(1-\cos^2\phi)(1-\epsilon^{-2\perp t_1}). \qquad (\text{Ph. Q.})^2 \text{ secs.} \quad (64)$$

The mean of this square during the interval is

$$\frac{1}{t_1}\int_0^{t_1} v^2 dt = \frac{V_0^{\,2}}{4\perp t_1}(1-\cos^2\phi)(1-\epsilon^{-2\perp t_1}), \qquad (\text{Ph. Q})^2 \quad (65)$$

and the root of this mean square during the interval is

$$V = \sqrt{\frac{1}{t_1}\int_0^{t_1} v^2 dt} = \frac{V_0}{\sqrt{2}}\left(\sin\phi\sqrt{\frac{1-\epsilon^{-2\perp t_1}}{2\perp t_1}}\right)$$

$$= \frac{V_0\epsilon^{-\perp\frac{t_1}{2}}}{\sqrt{2}}\left(\sin\phi\sqrt{\frac{\sinh\perp t_1}{\perp t_1}}\right). \qquad \text{Ph. Q.} \quad (66)$$

But $V_0/\sqrt{2}$ is the r. m. s. value of the undamped oscillating quantity, and $V_0\epsilon^{-\perp\frac{t_1}{2}}/\sqrt{2}$ would be the r. m. s. value of the oscillating quantity at the mid-interval if it were to continue thereat throughout undamped. Consequently the r. m. s. value of an oscillating quantity $V_0\epsilon^{-\perp t}\sin\omega t$ during any number of complete periods, is either the r. m. s. value of its initial undamped vector multiplied by

$$\left(\sin\phi\sqrt{\frac{1-\epsilon^{-2\perp t_1}}{2\perp t_1}}\right)$$

or the r. m. s. value of its mid-interval damped vector, multiplied by $\sin\phi\sqrt{\dfrac{\sinh\perp t_1}{\perp t_1}}$. After $\perp t_1$ passes the numeric 2, the first of these rapidly converges to $\dfrac{\sin\phi}{\sqrt{2\perp t_1}}$, so that when the oscillatory damping is rapid, the r. m. s. value of the oscillatory quantity varies inversely as the square root of the interval during which the summation is effected. If the summation be confined to a single period, starting with radius vector V_0, $m = 1$ and

$$V=\sqrt{\frac{1}{T}\int_0^T v^2dt}=\frac{V_0}{\sqrt{2}}\left(\sin\phi\sqrt{\frac{1-\epsilon^{-2\perp T}}{2\perp T}}\right)$$

$$=\frac{V_0\epsilon^{-\perp\frac{T}{2}}}{\sqrt{2}}\left(\sin\phi\sqrt{\frac{\sinh\perp T}{\perp T}}\right). \qquad \text{Ph. Q.} \quad (67)$$

In the case considered, the current is $i = 8.165\ 2^{-1000t}\sin 1224.75t$. If we take the first complete period of $T = 0.00513$ second, with

$$\sin\phi = 0.7746;\ \text{and}\left(\sin\phi\sqrt{\frac{1-\epsilon^{-2\perp T}}{2\perp T}}\right) = 0.7746\sqrt{\frac{1}{10.26}} = 0.242;$$

so that the r. m. s. value of the current during the first complete damped oscillation would be 1.396 amperes.

If the oscillating quantity is a cosinusoid of the type

$$v = V_0\epsilon^{-\perp t}\cos\omega t. \qquad \text{Ph. Q.} \quad (68)$$

The integral to infinite time of its square:

$$\int_0^\infty v^2dt = \frac{V_0^{\ 2}}{4\perp}(1+\cos^2\phi). \qquad (\text{Ph. Q.})^2 \quad (69)$$

So that by the same reasoning as before

$$V=\sqrt{\frac{1}{t_1}\int_0^{t_1} v^2 dt}=\frac{V_0}{\sqrt{2}}\sqrt{\frac{(1+\cos^2\phi)\,(1-\epsilon^{-2\text{℩}t_1})}{2\text{℩}t_1}}$$

$$=\frac{V_0}{\sqrt{2}}\epsilon^{-\text{℩}\frac{t_1}{2}}\sqrt{(1+\cos^2\phi)\left(\frac{\sinh\text{℩}t_1}{\text{℩}t_1}\right)},\quad \text{Ph. Q.} \qquad (70)$$

which differs from the preceding corresponding expression (66) in the substitution of $\sqrt{1+\cos^2\phi}$ for $\sqrt{1-\cos^2\phi}$. By the combination of formulas (66) and (70) the r. m. s. values of oscillating quantities containing a sum of sine and cosine terms can be evaluated.

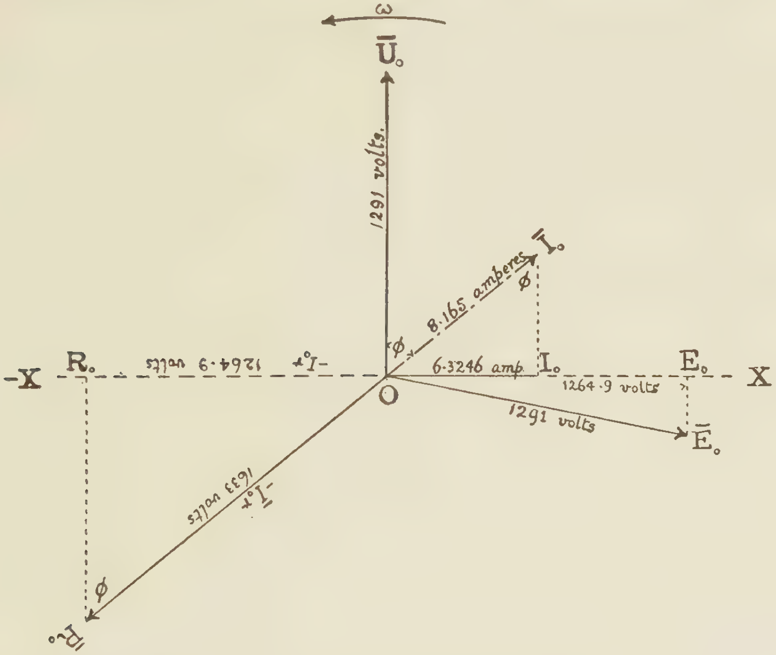

FIGURE 15. Rotative vector-diagram of an oscillating-current circuit containing resistance. Instant of release of reactance charge.

Discharging Oscillations from Reactance. — If with the condenser (Figure 1) uncharged, and resistance r in the circuit, we charge the reactance with magnetic energy, by passing through it a steady current of I_0 amperes, we may then allow the reactance to discharge through the condenser and resistance. We first find ω_0 the angular velocity of discharge for $r = 0$ and then determine ω by the stationary vector-diagram of Figure 7, taking the full resistance r into account.

Upon the axis $-XOX$ of reference, Figure 15, lay off the initial value OI_0 of the current in the reactance, at the instant of release, assumed in this case to be 6.3246 amperes. The initial energy in the reactance will be $lI_0^2/2 = 2$ joules. Lay off an angle $XO\bar{I}_0 = 90_0 - \phi$, and a vector initial current $\bar{I}_0 = I_0 \operatorname{cosec} \phi = 8.165$ amperes. All of the diagrams in Figures 7 and 12 now apply. The U diagram gives us the initial position of the condenser p. d. vector $O\bar{U}_0, = 1291$ volts. The projection of this on $-XOX$ is $OU_0 = 0$, corresponding to the uncharged condition of the condenser. $O\bar{E}_0$ is the initial position of the vector inductive emf. in the reactance, and the initial self-inductance emf. in the circuit is $OE_0 = 1264.9$ volts propelling the discharging current. The initial Ir drop in the circuit coincides in phase with $\bar{I}_0$, and taken negatively, extends to $O\bar{R}_0 = 1633$ volts. The projection of this on $-XOX$ gives an initial Ir emf. in the circuit of 1264.9 volts just equilibrating the emf. of self-induction. The entire vector system is to be considered as starting to rotate at angular velocity ω. If the diagram is to include the effects of damping, then each vector must rotate in an equiangular spiral of angle ϕ as indicated in Figure 8. But if we apply independent damping factors, the vectors in Figure 15 may rotate in circles as undamped quantities.

It will be seen that Figure 15 corresponds to Figure 8 except that it is advanced $\pi - \phi$ in phase. Thus a given energy charge discharged from the condenser, in this case 2 joules, with an initially uncharged reactance, will give rise to precisely the same rotative vector-diagram as the same energy discharged from the reactance, except in regard to the phase of the diagram. The rotative diagrams of U, I, P, and W will also be the same in either case; except that in the rotating and rolling vector-diagram Figure 14, NM and NC interchange in significance, NM being the reactance-energy vector in one case and the condenser-energy vector in the other.

Simultaneous Discharging Oscillations from Condenser and Reactance. — It is possible for a circuit like that of Figure 1, containing resistance, inductance, and capacity in simple series, to be released with an electric charge in the condenser, and an independent magnetic charge in the coil. The discharge which follows is then in part a condenser discharge, and in part a reactance discharge. If we know the initial charges, we can obtain the vector-diagram of the discharge by determining the ω-diagram of the system (Figure 7) and then making two separate rotative vector-diagrams, one, like Figure 8, for the discharging condenser and the other, like Figure 15, for the discharging reactance. These two vector-diagrams are now to be combined vectorially, into a new resultant vector-diagram, which will represent the behavior of the mixed discharge. Since each of the component diagrams obeys the geometry of Figures 7 and 12, the resultant diagram will also obey it. The rotative vector-diagrams U, I, P, and W will also follow, but the W diagram of Figure 13 will be ambiguous, except in regard to the dissipated energy.

It is evident, moreover, that since the energy of a simple resistance-reactance-condensance oscillator exchanges harmonically from the electric to the magnetic form, after correcting for dissipation, any initial state of assigned separate electric and magnetic energies must correspond to some phase of a discharge from a certain single stock of energy, electric or magnetic.

Charging Oscillations of Circuit Containing Resistance. — If in the circuit of Figure 1, assumed to possess resistance, and with no initial charge, we insert a constant charging p. d. between the terminals t, t, in such a direction as will cause a subsequent discharge to flow in the positive sense of the arrow $d\ e$; then both the charging emf. and the initial direction of the charging current must be reckoned negative, or in the sense e, d. The charging vector-diagram will then be the same as that of Figure 8, with a phase difference of 180^0, or read upside down. The stationary vector-diagrams of Figures 7 and 12 apply as before, as well as the rotative vector-diagrams of Figures 13 and 14. In the last-named, however, the condenser energy Oc must be counted from c to O, or in the reversed direction, since the energy in the condenser is initially nil and increases to its final full value.

We may consider that Figure 8 is the vector-diagram of a charging condenser system in which the constant impressed emf. between the terminals $t\ t$ (Figure 1) is positive, or in the direction of the arrow $d\ e$. If as before $c = 4 \times 10^{-6}$ farad ; $r = 200$ ohms ; $l = 0.1$ henry and $E = 1000$ volts, we first find $\omega_0 = 1581.14$ radians per second as in Figure 3, then the angle ϕ, and $\omega = 1581.14 \overline{\backslash 50^\circ 46'}$, as in Figure 7.

We then lay off $OU_0 = E = 1000$ volts in Figure 8 and $O\bar{U}_0 = OU$. cosec $\phi \overline{\backslash \frac{\pi}{2} - \phi} = 1291 \overline{\backslash 39^\circ 14'}$ volts. This is the vector charging p. d. The vector current follows from Figure 7 as 8.165 amperes, and the vector emf. of self-induction symmetrical with OU_0 in regard to the current. The graphs of Figures 10 and 11 then apply as before, except that in Figure 11 the p. d. must be read from the top line as zero, since the potential of the condenser at d, Figure 1, commences at zero and falls to a final value of — 1000 volts. The other graphs in Figure 11 remain unaltered.

The charging oscillations of a simple circuit containing resistance differ only from the discharging oscillations with the same resistance, in regard to phase direction, and to the absolute numerical values of the condenser potential u, condenser charge q, and condenser energy W_0.

Condensers and Reactances in Series.

If we have a circuit (Figure 16), containing a plurality of condensers, or of reactances, or of both, in simple series, containing also resistances, and subject to charging or discharging oscillations, we may compute the behavior of the system as follows :

Let $r' =$ sum of the individual joulean resistances. (ohms).
$r'' =$ sum of the individual hertzian resistances. (ohms).
$r = r' + r'' =$ the sum of all the individual resistances. (ohms).
$s = s_1 + s_2 + s_3$ etc., the sum of the individual elastances. (darafs).
$l = l_1 + l_2 + l_3$ etc., the sum of the individual inductances. (henrys).

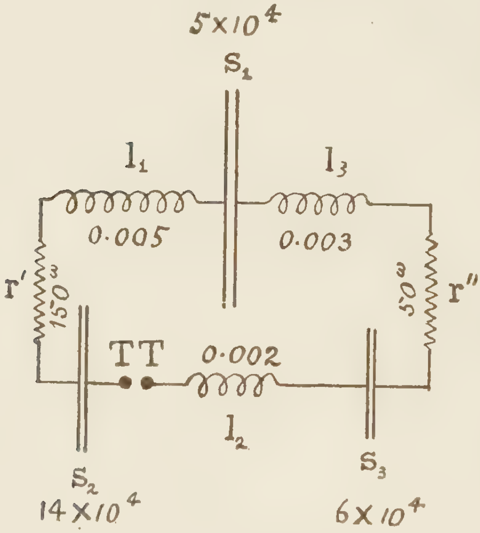

Figure 16. Simple series oscillation circuit of composite elements. Inductances in dekahenrys.

Then if we have only charging oscillations to consider, under the action of a constant impressed emf. E', inserted between terminal TT, we may replace the multiple element system by the equivalent single element system of Figure 1 with resistance r, elastance s, and inductance l.

Discharging Oscillations of Condenser in Simple Series Circuit of Multiple Elements. — Let one of the condensers, say s_1, Figure 16, be initially charged with a quantity Q_1 coulombs to an initial potential $U_0 = Q_1 s_1$ volts, the rest of the system being without charge. Then, after release, the discharge of condenser s_1 will charge the other condenser oppositely, in such a manner as to check the oscillation. The oscillations will take place about a condition of voltage equilibrium, such that the emf. of the discharging condenser is equal and opposite to the sum of the emfs. in the other condensers. If the quantity necessary to flow through the circuit in order to attain the condition of emf. equilibrium is q_e coulombs, then

$$(Q_0 - q_e)\, s_1 = q_e\, (s_2 + s_3), \qquad \text{volts} \quad (71)$$

or

$$q_e = Q_0 \frac{s_1}{s_1 + s_2 + s_3} = Q_0 \frac{s_1}{s}. \qquad \text{coulombs} \quad (72)$$

This is the oscillatory part of the charge in s_1. The remainder would reside permanently in the condensers, if there were no dielectric leakage.

Since the passage of q_e coulombs attains the point of equilibrium about which oscillation takes place, the first swing, neglecting damping, carries 2 q_e coulombs through the circuit.

Of the initial stock of energy $W_0 = Q_0^2 s_1/2$ joules, the portion subject to oscillation is, neglecting damping,

$$W_0 \frac{s_1}{s_1 + s_2 + s_3} = W_0 \frac{s_1}{s}, \qquad \text{joules} \quad (73)$$

This portion is alternately electric and magnetic energy. The remainder persists in the electric form, disregarding leakage.

If the impressed voltage E', instead of being applied initially to the component condenser s_1, were applied initially to the equivalent resultant condenser s of Figure 1, whose elastance is the sum of the component elastances, the charge taken by s would be

$$q_0 = Q_0 \frac{s_1}{s}, \qquad \text{coulombs} \quad (74)$$

and the energy of the charge would be

$$w_0 = W_0 \frac{s_1}{s}. \qquad \text{joules} \quad (75)$$

But we have seen that these are precisely the amounts of oscillation-charge and oscillation-energy available in the case of the charged component condenser. Hence we obtain the following rule for the treatment of composite simple series circuits with component condenser discharges : — Form the equivalent single-element series circuit (Figure 1). Impress the same initial emf. on the single condenser as would be impressed on the component condenser. The discharging oscillations of the single-element system will then be identical with those that would occur in the composite system. After the oscillations have subsided, there will be in the composite system a residual electric energy to take into account, which does not appear in the equivalent single-element system.

Thus in the case of Figure 16, let $s_1 = 5 \times 10^4$, $s_2 = 14 \times 10^4$, $s_3 = 6 \times 10^4$ darafs, $l_1 = 0.05$, $l_2 = 0.02$, $l_3 = 0.03$ henry; $r' = 150$ ohms, $r'' = 50$ ohms, and let an initial charge of 0.02 coulomb be given to s_1 by an impressed emf. of 1000 volts, the other elements being without charge. The initial electric energy of the system $W_0 = 10$ joules. To find the oscillation of the system, we form the equivalent single-element system (Figure 1) with $s = 25 \times 10^4$ darafs, $l = 0.1$ henry, $r = 200$ ohms, and impress 1000 volts initially on the condenser s. This will take a charge of 0.004 coulomb, and an electric energy of 2 joules. These are the oscillation-charge and oscillation-energy of the composite system considered. The oscillations of the system are the same as those indicated in Figures 7 to 15. After the oscillations have subsided, there will be a residual energy of 8 joules in the system, neglecting dielectric leakage, 0.016 coulomb at 800 volts in s_1, -0.004 coulomb at -560 volts, in s_2, and -0.004 coulomb at -240 volts in s_3.

NON-OSCILLATORY CONDENSER DISCHARGES.

Although the non-oscillatory discharge of a condenser lies outside of the title of this paper, an outline of the case may be admitted, not only in order to complete the discussion, but also to present therein certain important analogies to the oscillating-current discharge.

If in Figure 12, the semi-circuit resistance ρ is increased until it is equal to z_0, the resistanceless impedance, both the reactance $jl\omega$, the angle ϕ, and the angular velocity ω disappear ; so that the discharge becomes non-oscillatory and aperiodic. If ρ is increased beyond this aperiodic value, the discharge continues to be non-oscillatory, but becomes what may be called *ultraperiodic*. We may first consider the ultraperiodic case.

In Figure 17 let op be the exponential time-factor of an ultraperiodic circuit. About op as diameter, construct the semicircle oqp. With center o, and radius $oq = \omega_0$, the resistanceless angular velocity, intersect the semicircle in q. Then the chord pq is the non-oscillatory or hyperbolic angular velocity Ω of the currents in the circuit.[4] In the case of a circuit resistance $r = 500$ ohms, the hyperbolic angular velocity will be $\Omega = 1936.492$ hyperbolic radians per second, as shown at OPQ, Figure 17.

Analytically, $$\Omega = \sqrt{\iota^2 - \omega_0^{\,2}} \qquad \text{hyp. radians/sec.} \qquad (76)$$

and the hyperbolic period T of the current and p. d. is $2\,\pi/\Omega$ seconds.

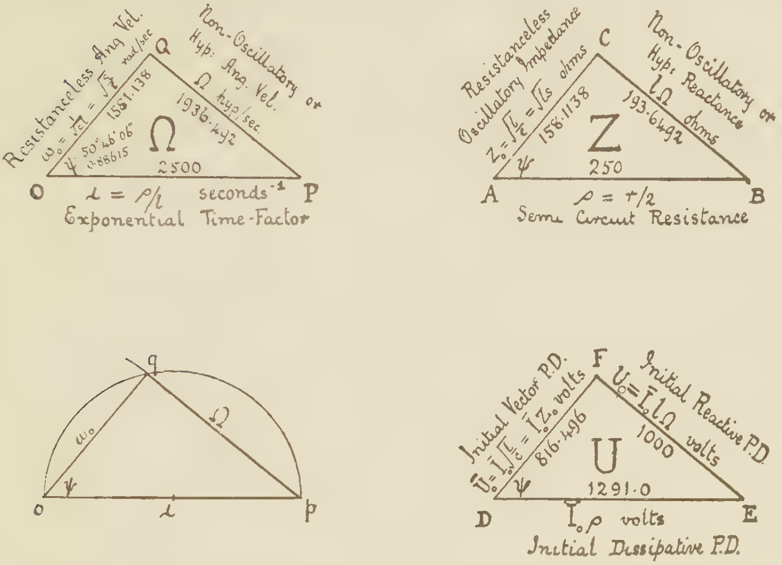

FIGURE 17. Stationary vector-diagrams of hyperbolic angular velocity, impedance, and discharging potential difference in a simple non-oscillating condenser circuit with ultraperiodic resistance.

Similarly, the Z-triangle of Figure 17 has a base $AB = \rho = r/2 = 250$ ohms, and a side AC equal to the resistanceless oscillatory impedance $\sqrt{ls} = 158.1138$ ohms, as in Figures 4 and 12. The remaining side CB opposite to the angle ψ and perpendicular to AC, represents the non-oscillatory or hyperbolic reactance 193.6492 ohms. Operating upon the Z triangle by multiplication with 5.164 amperes, the initial vector-current, we obtain the U triangle DEF, Figure 17.

---

[4] For the first publication of the conception of hyperbolic angular velocity of discharges in ultraperiodic circuits, we are indebted to Dr. Alexander Macfarlane. See appended Bibliography.

Figure 18 shows the rotative vector-diagram of voltage and current for the ultraperiodic case considered, and corresponding to Figure 8, the rotative vector-diagram for the oscillating-current case. Lay down the p. d. triangle DEF of Figure 17 at $\bar{I}_0 U_0 O$, Figure 18, to voltage scale as shown. On OI_0 as semi-axis, construct the rectangular hyperbola $H\bar{E}_0\bar{I}_0\bar{U}_0H'$, whose asymptotes OA and OA' make angles of 45° with $O\bar{I}_0$. From U_0, draw a parallel to $O\bar{I}_0$, intersecting the hyperbola at U_0. Join $O\bar{U}_0$. Then the angle $\bar{I}_0 O \bar{U}_0 = \psi$ will be the gudermannian of the hyperbolic sector $\bar{I}_0 O U_0$; or the hyperbolic sector angle $\bar{I}_0 O \bar{U}_0$ the anti-gudermannian of ψ. From the opposite corresponding point E_0 of the hyperbola, draw the straight line $O\bar{E}_0$. Then OU_0 represents the initial vector discharging p. d. in the circuit considered, $O\bar{E}_0$ the initial vector emf. of self-induction, and $O\bar{I}_0$ the initial vector discharging current, corresponding respectively to the vectors of the same denomination in Figure 8. These three vectors, starting at the positions shown, at the moment when the condenser of 4 microfarads, after being charged at 1000 volts p. d., is released through $l = 0.1$ henry and $r = 500$ ohms, run along the hyperbola $H\bar{I}_0H'$, in the positive direction, with uniform hyperbolic angular velocity $\Omega = 1936.492$ hyps. per second. That is, the sectorial areas described by each vector in each second of time are constant and equal to 1936.492 hyperbolic radians, taking the length of the semi-axis OI_0 as unity. Consequently, at any instant, the sectorial areas $\bar{E}_0 O \bar{I}_0$ and $I_0 O \bar{U}_0$ remain equal to that shown, this area being the hyperbolic angle of either, and equal to 1.03172 hyps. $= gd.^{-1}\ 50°.\ 46'.\ 06''$. As the three vectors $O\bar{E}_0$, OI_0 and $O\bar{U}_0$ rotate with this uniform angular velocity in contact with the hyperbola, they continually approach the asymptote OA', without ever actually reaching it.

The resultant, or vector sum of $O\bar{U}_0$ and $O\bar{E}_0$ is $Or = 2582$ volts, and is equal to the initial vector product of the discharging current $O\bar{I}_0$ and the resistance r of the circuit. This vector also rotates with uniform hyp. angular velocity Ω, over the rectangular hyperbola $h\ r\ h'$, in the direction rh, corresponding to Or, Figure 8. As in Figure 8, the negative of vector Or, or $-\ \bar{I}_0\ r$, should be drawn in the direction $\bar{I}_0\ O$; but is omitted from the diagram for economy of space. It may be demonstrated that this negative extension of Or, rotating positively over a rectangular hyperbola, the image of $h\ r\ h'$, will always be in vector equilibrium with $O\bar{E}_0$ and $O\bar{U}_0$, so that the geometrical sum of these three vectors at any instant will be zero, just as in the case of Figure 8.

The orthogonal projections of $O\bar{E}_0$, $-Or$, and $O\bar{U}_0$ give the instantaneous values of the discharging p. d., the Ir drop, and the emf.

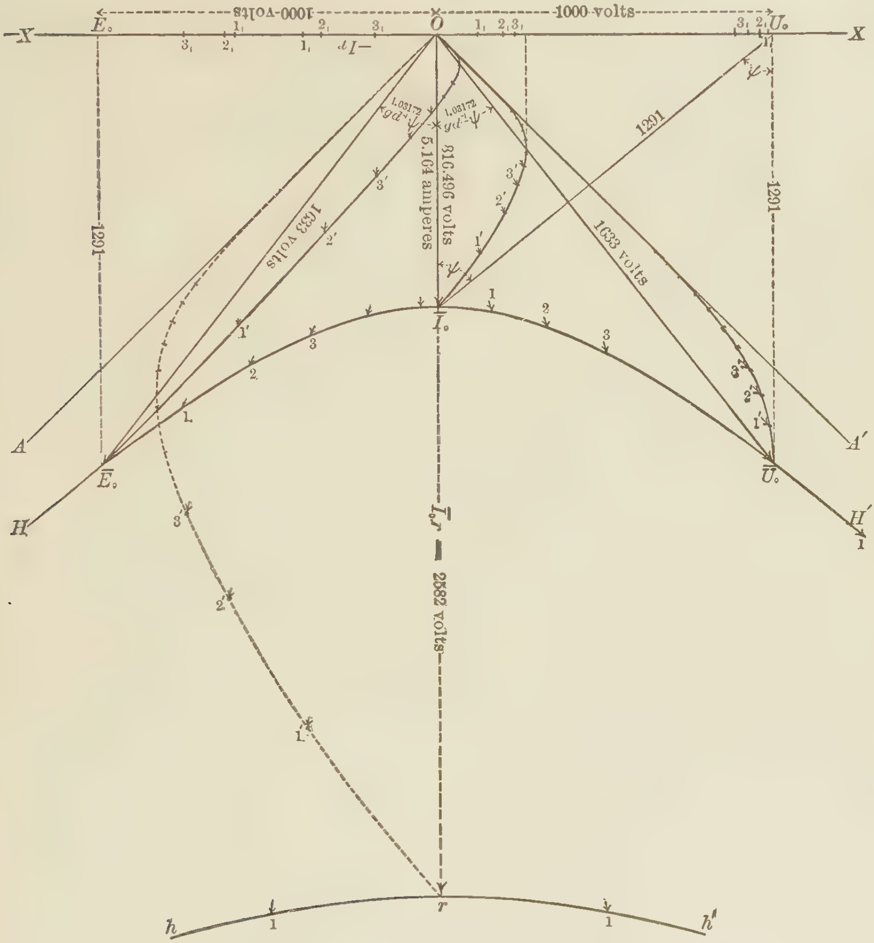

FIGURE 18. Rotative vector-diagram of a non-oscillating current ultra-periodic circuit containing resistance. Instant of release of condenser charge.

of self-induction respectively, after applying the damping factor $\epsilon^{-\alpha t}$. That is, we may take the instantaneous XX projections of these undamped vectors, and then apply the damping factor for the instant considered; or, we may shrink the vectors by the application of the damping factor before taking projections, as in Figure 8. In the case considered, the damping coefficient $\perp = 2500$, as in Figure 17; so that applying the damping factor ϵ^{-2500t}, we obtain the curved lines of Figure 18. The dotted line $o3'2'1'r$ is drawn as though with negative rotation of Or, to simulate the projective effect of a negative vector $- I_0 r$.

The points 1, 2, and 3 on the hyperbolas, indicate the positions of the various vectors after the lapse of 1, 2 and 3 ten-thousandths of a second respectively, after release. The corresponding points $1'$, $2'$, $3'$ on the curved lines, give the termini of the same vector as reduced by damping, and the projections of the latter, 1, 2, 3, on the XX axis, give the corresponding instantaneous values in the circuit of the discharging p. d. u, the ir drop, the current, and the emf. of self-induction, in the same manner as in Figure 8. It will be observed that while the undamped vectors all increase in length without limit, the actually projected values under the dominating influence of the damping factor, diminish in time without limit. In particular, the current i reaches a maximum when the vector $O\bar{I}_0$ has swept over 1.0317 hyp. radians, in a time $1.0317/1936.492 = 0.000,532,8$ second. At the same instant, the self-inductive emf. vector $O\bar{E}_0$ will have reached the transverse axis $O\bar{I}_0$, and its projection on XX will momentarily vanish. Consequently, there will be no emf. of self-induction in the circuit at this instant; because the current is stationary for that instant, being about to diminish. After this instant, the self-inductive emf. changes sign, and propels the current along with the discharging p. d.

It will be noticed that as in the oscillatory-current case, both the discharging voltage and the voltage of self-induction exert dissipative activity upon the discharging current.

It may also be noticed that although the orthogonally-projecting rotating-crank vector-diagrams used in this paper are convenient and useful devices for representing the actions in o. c. circuits, the polar-coordinate vector-diagram, sometimes called the "time" diagram, is not so well adapted for this purpose. The undamped vector quantities in the periodic case may indeed be represented by circles on the polar-coordinate diagram; but the corresponding damped quantities are represented by spirals that are not so easily interpreted as equiangular spirals. Moreover, in the ultraperiodic case, the hyperbolic analogue is missing in the polar-coordinate diagram; so that apparently there is no analogy presented in polar-coordinate representation between the periodic and ultraperiodic cases. It would seem, therefore, that the orthogonally projected "crank-diagram" or "clock-diagram" has wider applications, in these respects, than the polar-coordinate vector-diagram.

Analytically, we have the following relations : —

The fundamental differential equation for quantity q is satisfied by

$$q = A\epsilon^{-(℩-\Omega)\,t} + B\epsilon^{-(℩+\Omega)t} \qquad \text{coulombs} \quad (77)$$

where A and B are integration constants, while $℩$ and Ω follow from the construction of the triangle OPQ of Figure 17. Choosing the constants consistently with the discharge of a condenser initially charged to potential U_0 volts, the discharging p. d. after t seconds is

$$u = U_0 \cot\psi\,\epsilon^{-℩t} \sinh(\Omega t + gd^{-1}\psi) \qquad \text{volts} \quad (78)$$

$$= \bar{U}_0\epsilon^{-℩t} \sinh(\Omega t + gd^{-1}\psi) \qquad \text{volts} \quad (79)$$

form which q follows by the relation $q = u/s = uc$ coulombs. $\bar{U}_0$ is the initial vector value of the discharging p. d. by Figures 17 and 18.

The instantaneous current i is

$$i = \bar{I}_0\epsilon^{-℩t} \sinh \Omega t \qquad \text{amperes} \quad (80)$$

where

$$\bar{I}_0 = U_0/l\Omega = \bar{U}_0/z_0. \qquad \text{amperes} \quad (81)$$

The current i will therefore be a maximum when

$$\tanh \Omega t = \Omega\tau = \sin\psi, \qquad \text{numeric} \quad (82)$$

or

$$\Omega t = gd^{-1}\psi. \qquad \text{hyp. radians} \quad (83)$$

The emf. of self-induction in the circuit at any instant is

$$e = U_0 \cot\psi\,\epsilon^{-℩t} \sinh(\Omega t - gd^{-1}\psi) \qquad \text{volts} \quad (84)$$

$$= \bar{U}_0\epsilon^{-℩t} \sinh(\Omega t - gd^{-1}\psi). \qquad \text{volts} \quad (85)$$

The apparent resistance of the circuit u/i is

$$Z = \rho + l\Omega \coth \Omega t. \qquad \text{ohms} \quad (86)$$

That is, the apparent resistance of the circuit, judging from the discharging p. d. and the discharging current, commences at ∞ and tends rapidly to the limit $(\rho + l\Omega)$ ohms.

The instantaneous power of the condenser in the circuit is

$$p = U_0\bar{I}_0 \cot\psi\,\epsilon^{-2℩t} \sinh \Omega t \cdot \sinh(\Omega t + gd^{-1}\psi) \qquad \text{watts} \quad (87)$$

$$= \bar{U}_0\bar{I}_0\epsilon^{-2℩t} \sinh \Omega t \cdot \sinh(\Omega t + gd^{-1}\psi). \qquad \text{watts} \quad (88)$$

A complete series of stationary vector-diagrams might be presented following those of Figure 17, and corresponding to those of Figures 7 and 12; but in view of the relative simplicity of formulas (78) to (88), such vector-diagrams have more theoretical than practical interest.

APERIODIC CASE.

When ρ, the semi-resistance of the circuit, is just equal to the surge impedance $z_0 = \sqrt{ls}$ of the same; then the circuit is aperiodic, and there is neither a circular angular velocity ω, nor a hyperbolic angular velocity Ω. The aperiodic case may also be represented by a special rotating vector-diagram as has been suggested by Macfarlane; but it is easier, for practical purposes, to treat it as a limiting case of the ultra-periodic circuit. We have by (78)

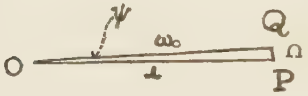

FIGURE 19. Aperiodic case as limiting condition of ultra-periodic circuit, when $\omega_0 = \perp$. Ω stationary vector-diagram.

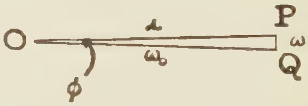

FIGURE 20. Aperiodic case as limiting condition of o. c. circuit, when $\perp = \omega_0$. ω stationary vector-diagram.

$$u = \bar{U}_0 \cot\psi \, \epsilon^{-\perp t} \sinh(\Omega t + gd^{-1}\psi). \qquad \text{volts} \quad (89)$$

Now let Ω become very small, as in Figure 19. Consequently, ψ becomes very small; so that $\cot\psi$ may be replaced by $1/\psi$, and $\sinh(\Omega t + gd^{-1}\psi)$ by $(\Omega t + gd^{-1}\psi)$.

Hence $$u_{\psi=0} = \frac{U_0}{\psi} \epsilon^{-\perp t} (\Omega t + gd^{-1}\psi). \qquad \text{volts} \quad (90)$$

But $\Omega = \perp\psi$ and $gd^{-1}\psi = \psi$ when ψ approaches zero; thus

$$u_{\psi=0} = \frac{U_0}{\psi} \epsilon^{-\perp t} (\perp\psi t + \psi) = U_0 \epsilon^{-\perp t} (\perp t + 1), \quad \text{volts} \quad (91)$$

and $$q_{\psi=0} = Q_0 \epsilon^{-\perp t} (\perp t + 1), \qquad \text{coulombs} \quad (92)$$

$$i_{\psi=0} = -\frac{dq}{dt} = Q_0 \perp^2 t \epsilon^{-\perp t}. \qquad \text{amperes} \quad (93)$$

This is a maximum when $t = \tau$; when

$$i_m = Q_0 \text{℩} \epsilon^{-1} = \frac{Q_0}{\tau} \epsilon^{-1}. \qquad \text{amperes} \quad (94)$$

The power in the circuit is

$$p = U_0 Q_0 \text{℩}^2 t \epsilon^{-2\text{℩} t} (\text{℩} t + 1). \qquad \text{watts} \quad (95)$$

We may also derive (91) from the limiting case of the oscillatory discharge. Taking (27), we have

$$u = U_0 \operatorname{cosec} \phi \, \epsilon^{-\text{℩} t} \sin (\omega t + \phi), \qquad \text{volts} \quad (96)$$

and if ω becomes very small, as in Figure 20, the angle ϕ becomes very small; so that $\operatorname{cosec} \phi$ may be replaced by $1/\phi$ and $\sin (\omega t + \phi)$ by $(\omega t + \phi)$. Hence

$$u_{\phi=0} = \frac{U_0}{\phi} \epsilon^{-\text{℩} t} (\omega t + \phi). \qquad \text{volts} \quad (97)$$

But $\omega = \text{℩}\phi$ when ϕ approaches zero; thus,

$$u_{\phi=0} = \frac{U_0}{\phi} \epsilon^{-\text{℩} t} (\text{℩} \phi t + \phi) = U_0 \epsilon^{-\text{℩} t} (\text{℩} t + 1), \quad \text{volts} \quad (98)$$

as in (91). So that the aperiodic case may be computed either as the limiting oscillatory case with $\omega = 0$, or as the limiting ultraperiodic case with $\Omega = 0$.

Summary of Conclusions.

The orthogonal-projection or rotating-crank vector-diagram of the ordinary a. c. circuit applies also, by extension, to the o. c. circuit.

With the aid of the stationary vector-diagrams, the principal features of any given o. c. case may be simply and speedily deduced.

By making the above stationary vector-diagrams rotative, and subsequently applying the proper damping-factor, the process of oscillation in any given o. c. circuit may be readily visualised.

By interpreting the above diagrams and formulas hyperbolically, the corresponding properties of the ultraperiodic case may be readily computed and visualised. That is, the rotating-crank vector-diagram of the ordinary a. c. circuit applies also, by extension, to the non-oscillatory ultraperiodic condenser circuit.

The properties of the condenser circuit, whether oscillatory or ultraperiodic, are intimately connected with a certain angle, $cos^{-1}\ (\rho/z)$ or $cosh^{-1}\ (\rho/z)$, connected with the circuit constants.

The polar-coordinate type of vector-diagram is not so conveniently adapted to the o. c. circuit as the crank-projection diagram.

The aperiodic case may be treated as the limiting case either of the oscillatory, or of the ultraperiodic, circuit.

List of Symbols Employed.

$A.\ B.$	Constants of integration (coulombs).
a. c.	abbreviation for alternating current.
c, c_1, c_2, c_3	Permittance of a condenser, or of each of several condensers (farads).
γ	Oscillation conductance of an o. c. circuit (mhos).
$\delta_1,\ \delta_\pi,\ \delta_{2\pi}$	Logarithmic decrement of an oscillating quantity $\left(\log_\epsilon \frac{V_0}{v}\right)$ during the angular interval of 1 radian, π radians (semi-period), and 2 π radians (complete period), of the radius vector (numeric).
ϵ	$= 2.71828\ .\ .\ .$
$\bar{E}_0$	Initial vector amplitude of emf. of self-induction (volts $\angle$).
E_0	Initial emf. of self-induction in circuit (volts).
E'	Charging emf. impressed upon a condenser (volts).
$e, \bar{e}$	Instantaneous value of emf. of self-induction in an o. c. circuit, and the undamped value of same (volts).
$\bar{e}_r, e_r$	Undamped and damped instantaneous values of self-induction emf. in phase with the current (volts).
I_0	Initial current strength in a circuit (amperes).
$\bar{I}_0$	Initial vector amplitude oscillating current (amperes $\angle$).
I	$= \bar{I}_0/\sqrt{2}$, the r. m. s. value of initial vector current amplitude (amperes).
$\bar{i}, i$	Undamped and damped instantaneous currents (amperes).
j	$= \sqrt{-1}$, quadrantal operator.
$l, l_1, l_2, l_3,$	Inductance of an o. c. circuit, and of particular parts thereof (henrys).
m	any positive integer (numeric).
n	Frequency of oscillation of a circuit (cycles per second).
o. c.	abbreviation for oscillating-current.
π	$= 3.14159\ .\ .\ .$ (numeric)
$Ph.\ Q.$	Any oscillatory physical quantity pertaining to an o. c. circuit.

P_m. $\bar{p}$, p	Undamped maximum cyclic power developed by condenser, undamped instantaneous value of same, and damped instantaneous value of same (watts).
$\bar{p}_l$, p_l	Undamped and damped instantaneous values of power in inductance (watts).
p_r, p_r	Undamped and damped instantaneous values of power developed by condenser in the resistance of an o. c. circuit (watts).
$p' = ei$	Instantaneous power of the emf. of self-induction (watts).
$2\bar{p}_r$, $2p_r$	Total undamped, and total damped, intantaneous values of power developed in the resistance of an o. c. circuit by condenser and inductance combined (watts).
Q_0. q_0	Initial charge in a condenser (coulombs).
$\bar{Q}_0$	Initial vector amplitude of electric charge in condenser (coulombs ∠).
Q	$= \bar{Q}_0/\sqrt{2}$, the r. m. s. value of the initial vector amplitude (coulombs).
Q_1	Initial charge of one among several condensers in series (coulombs).
q	Instantaneous charge in condenser (coulombs).
q_e	Quantity required to flow through an o. c. circuit in order to establish p. d. equilibrium (coulombs).
r'	Joulean resistance in an o. c. circuit (ohms).
r''	Hertzian resistance in an o. c. circuit (ohms).
$r = r' + r''$	Total resistance in an o. c. circuit (ohms).
r. m. s.	Square root of mean square of an oscillatory quantity.
ρ	$= r/2$, Semi total of resistance in an o. c. circuit (ohms).
Φ_0	Total initial magnetic flux linked with a discharging circuit counting all of the turns in the same (volt-seconds).
ϕ	Phase angle in an o. c. circuit, and angle of a spiral (radians or degrees).
ψ	Phase angle in an ultraperiodic circuit (radians or degrees).
$gd^{-1}\psi$	Antigudermannian of a circular angle, or the hyperbolic angle of which ψ is the gudermannian (hyp. radians).
s, s_1, s_2, s_3,	$= 1/c$, elastance of a condenser, or of each of several condensers (darafs).
t	Elapsed time from the release of an o. c. system (seconds).
t_1	Time interval (seconds).
T	Period of an o. c. circuit (seconds).
τ	$= l/\rho$, Oscillation time-constant of an o. c. circuit (seconds).

$\perp$	$= 1/\tau = \rho/l$, time-constant-reciprocal of an o. c. circuit (seconds $^{-1}$).
$\overleftrightarrow{U}_0$	Initial vector amplitude of the discharging p. d. in an o. c. circuit (volts $\angle$).
U	$= \overleftrightarrow{U}_0/\sqrt{2}$, the r. m. s. value of the initial vector discharging p. d. (volts).
U_0	Initial discharging p. d. in a circuit (volts).
$\bar{u}$, u,	Undamped and damped time-values of condenser p. d. in an o. c. circuit (volts).
$\bar{u}_r$, u_r	Undamped and damped time-values of the component of the condenser p. d. in phase with the current (volts).
V_0, V, v	Initial, r. m. s., and instantaneous values of any oscillating quantity, pertaining to an o. c. circuit.
W_0	Initial energy in a condenser or in a reactance (joules).
W_l	Initial vector amplitude of cyclic energy in reactance, *mn*, Figure 7, *MN*, Figures 12 and 14 (joules).
W_m	Undamped maximum cyclic value of energy in a condenser or reactance (joules).
$\bar{w}$, w	Undamped and damped time-values of energy in condenser or reactance (joules).
w_1	Energy dissipated in a circuit in the first energy cycle (joules).
w_c, w_l	Energy in a condenser, and in a reactance, at a specified time (joules).
w_d	Total expenditure of energy by dissipation from a circuit up to t seconds (joules).
w_0	Energy of charge communicated to a series of condensers (joules).
w_s	Semi-system energy at time t (joules).
XX, YY	Cartesian rectangular coordinates.
X_l, X_c	Reactance of an inductance and of a condenser in an o. c. circuit (ohms).
Y	Admittance of an o. c. circuit (mhos).
Z, z	Impedance of an o. c. circuit (ohms).
$Z_0, z_0 = \sqrt{ls}$	Impedance of an o. c. circuit devoid of resistance (ohms).
ω_0	Angular velocity of an o. c. circuit with its resistance ignored (circular radians per second).
ω	Angular velocity of an o. c. circuit in the presence of its actual resistance (circular radians per second).
Ω	Angular velocity of an ultraperiodic circuit (hyperbolic radians per second).

BIBLIOGRAPHY.

Prof. William Thomson, Phil. Mag., Series 4, **5**, 393 (1853).
——, "Mathematical and Physical Papers," **1**, 540.
H. Feddersen, Pogg. Ann., **103**, 69 (1858).
——, Pogg. Ann., **108**, 497 (1859).
——, " " **113**, 437 (1861).
——, " " **116**, 132 (1862).
Kirchhoff, Pogg. Ann., **121**, 168 (1864).
Helmholtz, Wissensch. Abh., **1**, 531 (1869).
Lorenz, Wied. Ann., **7**, 161 (1879).
Schiller, Pogg. Ann., **152**, 535 (1874).
Clerk Maxwell, "Electricity and Magnetism," **2**, 345 (1881).
Hiecke, Wien. Ber., **96**, 134, (1887).
Trowbridge and Sabine, Am. Acad. Arts and Sciences, 109 (1890).
Boys, Phil. Mag., **30**, 248 (1890).
Miesler, Wien. Ber., **99**, 579 (1890).
Trowbridge and Duane, Phil. Mag., **40**, 211 (1895).
Bjerkness, Wied. Ann., **60**, 121 (1895).
Wulf, Wien. Ber., **105**, 667 (1896).
Helmholtz and Schiller, Wien. Ber., **61**, 30 (1897).
Webster, "Theory of Electricity and Magnetism," 484 (1897).
Alex. Macfarlane, Trans. Am. Inst. El. Engineers, **14**, 163 (1897).
Tallquist, Wien. Ber., **60**, 248 (1897).
Webster, Phys. Rev., **6**, 297 (1898).
Decombe, Comptes Rendus, **126**, 518 (1898).
Lodge and Glazebrook, Camb. Phil. Trans., **18**, 136 (1899).
Battelli and Magri, Phil. Mag., **5**, 1 (1903).
——, Phil. Mag., **5**, 620 (1903).
Sheldon, Jenks and Clarke, "High Frequency Discharges," Trans. Am. El. Therapeutic Assoc. (1903, 1904).
Zenneck, "Electromagnetische Schwingungen" (1905).
Fleming, "The Principles of Wave Telegraphy," 18 (1906).
Steinmetz, "Transient Electric Phenomena and Oscillations," 67 (1909).
——, "Alternating-Current Phenomena," Appendix 2, 409 (1897).

THE GENERAL CIRCULATION OF THE MEAN AND HIGH-LEVEL CALCIUM VAPOR IN THE SOLAR ATMOSPHERE

THE GENERAL CIRCULATION OF THE MEAN AND HIGH-LEVEL CALCIUM VAPOR IN THE SOLAR ATMOSPHERE[1]

By CHARLES E. ST. JOHN

I. INTRODUCTION

Important as is the registering of the solar surface by monochromatic photography through the use of the spectroheliograph, of equal importance are data for the interpretation of spectroheliograms. Such photographs with the α line of hydrogen furnish in some measure the means for their own interpretation, as in the vortical movements shown and described by Hale,[2] and in the motions of the dark hydrogen flocculi such as the writer was fortunate enough to obtain on June 2 and 3, 1908.[3] But since the development of the spectroheliograph by Hale in 1889, and its first successful application, on January 12, 1892, to the photography of the solar surface and the delineation of the forms of those regions where K is reversed, a sufficient amount of definitive work bearing upon the general movement of the calcium vapor has not been done, though the total number of spectroheliograms is now many thousands and daily increasing. This lack of definitive data is especially to be regretted in the case of calcium, because of the remarkable behavior of the H and K lines over the general surface of the sun, over faculae, and over spots, and because these lines are the most favorable for use with the spectroheliograph, and the only ones that can be employed with spectroheliographs of low dispersion.

The history of the H and K lines of calcium, as far as the discovery of their characteristic appearance on the disk of the sun is concerned, is as follows:

In 1872 Young wrote concerning the reversals of H and K visually observed by him: "They were also found to be regularly reversed on the body of the sun itself, in the penumbra and the immediate neighborhood of every important spot." In 1883 Lockyer made the first attempts to photograph the spectra of sun-spots and his plates showed that "in all H and K were seen reversed over the spots, just as Young saw them at Sherman, while the blue calcium line was not reversed."[2] On Rowland's plates used for *The Preliminary Table of Solar Wave-Lengths*, taken as far back as 1886 and 1887, H and K show both single and double reversals,[3] but no notice of this was published at the time. The following observations of the single and double reversals were made independently of each other and of the preceding photographic work. In December 1891 Hale obtained some photographs of the spectrum of a spot in which the bright lines of H and K had such an extent in the surrounding regions that it was suspected that similar reversals might be found on the disk remote from spots. A series of plates was taken which confirmed this suspicion, and in a note from the Kenwood Observatory, under date of January 18, 1892, Hale says "that the H and K lines are reversed not only in the vicinity of spots but in regions irregularly distributed over the entire disk of the sun."[4] M. Deslandres reported the same results from his photographs of the spectra of spots and faculae: "Les raies H et K du calcium apparaissent souvent brillantes," and added, in a footnote: "Ces raies brillantes offrent souvent aussi un reversement au centre."[5]

---

[1] *Contributions from the Mount Wilson Solar Observatory*, No. 48.

[2] *Ibid.*, No. 26; *Astrophysical Journal*, **28**, 1908.

[3] *Ibid.*, 9.

Under date of April 15, 1892, Hale reported from the Kenwood Observatory that on plates taken in December 1891 "most if not all, of these (H and K) reversals were double, i.e., a dark line ran through the center of the bright line."[6] The usual appearance of the H and K lines over the general disk of the sun is that of a broad shading—H_1 or K_1—superposed upon this a bright line—H_2 or K_2—varying greatly in width and intensity and consisting of two components separated by the narrow absorption line—H_3 or K_3—following the notation for the division of these lines introduced by Hale.[7]

---

[1] *American Journal of Science*, November, 1872.

[2] *Proceedings, Royal Society*, **36**, 444, 1884.

[3] Personal letter from Professor Ames.

[4] *Astronomy and Astrophysics*, **11**, 159, 1892.

[5] *Comptes Rendus*, **114**, 277, 1892.

[6] *Astronomy and Astrophysics*, **11**, 414, 1892.

[7] *Publications of the Yerkes Observatory*, Part I, Vol. III, p. 15.

M. Deslandres called attention to the following peculiarities of the H and K lines:

> Le plus souvent, les deux composantes de la raie brillante sont dissymétriques, la composante du côté du rouge étant plus étroite que l'autre, si bien que la raie noire apparaît déplacée vers la rouge par rapport à la raie brillante.[1]

After speaking of the equality, in general, of the bright components over faculae and the occasional inflections of the lines in the neighborhood of spots, he says further:

> L'ensemble des faits précédents peut s'expliquer par un mouvement général de circulation verticale et horizontale des couches hautes et basses de la chromosphère, analogue à celui que présente notre atmosphère. Les couches basses s'élèveraient et seraient attirées vers l'équateur, comme les vents alizés, d'où un rapprochement vers la Terre; les couches élevées auraient un mouvement inverse.[2]

Returning to the subject later, M. Deslandres writes with more definitiveness:

> J'ai déjà indiqué, en 1894, ces particularités qui annoncent un mouvement d'ascension des vapeurs productrices de la raie K_2 et un mouvement de descente des vapeurs K_3. Lorsqu'on se rapproche du bord, la dissymétrie diminue et, près du bord, devient imperceptible, ce qui s'explique parce que les différences des vitesses radiales des vapeurs par rapport à la Terre diminuent elles-mêmes jusqu'à devenir nulles. En même temps, les deux composantes de K_2 s'écartent progressivement, laissant entre elles une raie K_3 qui s'élargit de la même quantité. Ce dernier fait, sur lequel je dois insister, est très net avec une grande image solaire, plus régulier et progressif que ne l'indiquent les dessins déjà publiés. Il tient évidemment à l'épaisseur constamment croissante sous laquelle se présente la chromosphère, pour le rayon Soleil-Terre, lorsque l'on va du centre au bord.[3]

Without actual measurements referred to terrestrial standards the dissymmetry of the bright components of the calcium lines can indicate with certainty only relative motions of the vapors producing K_2 and K_3, respectively, and definite conclusions cannot be drawn as to the actual motions of the vapors producing the lines.

The unsymmetrical character of the central absorption line with respect to the components of the emission line has also been reported by Jewell, who found it more easily observed in the case of K than H.[1] A number of plates were measured by him and as a result it was found,

---

[1] *Comptes Rendus,* **119**, 458, 1894.

[2] *Ibid.*, 459.

[3] *Ibid.* **141**, 381, 1905.

> that the central absorption line varies in position to the extent of 0.025 of an Ångström unit between the plates upon which the central line is symmetrically placed and the plates upon which it is most unsymmetrical. . . . . An attempt was made to measure the position of the emission line in these cases. The measurements were too difficult to make to give any certain results, but there were some indications that the emission line might be slightly displaced toward the violet in the cases of dissymmetry. . . . . The obvious explanation is that in the cases of dissymmetry we have examples of motion in the line of sight, the displacement of the central absorption line being due to falling matter, the extreme difference in velocity, shown by different plates, being about seventy-five miles per minute.[2]

In a later paper he says:

> The narrow central component of the shaded lines . . . . shows a *descending* motion, over the solar surface, of the absorbing matter producing it of . . . . about a mile a second in the case of the H and K lines. . . . . These narrow components of the shaded lines are probably produced by meteoric matter falling into the solar atmosphere. The bright emission components may possibly be caused by the down-rush of this meteoric matter through the denser portions of the chromosphere such that where it meets the up-rush of the matter already referred to, the impact of the collisions or the friction caused produces an intense emission. . . . .[3]

In the paper previously referred to Jewell suggests: "In the case of H and K the central absorption line may possibly be produced by the corona." The plates examined by Jewell were not made with such measurements in view as must be carried out on these difficult lines, but were used incidentally for this purpose. The importance of having plates for this particular purpose was fully recognized and taken into account in the work reported later in this paper.

Some work was done on the H and K lines by Adams in 1905, in which, upon six plates taken on the disk, he measured the position of the absorption lines, and in some cases the position of the bright emission lines. His results for the absorption lines are in apparent disagreement with those of Jewell. Adams says:

[1] *Astrophysical Journal*, **3**, 103, 1896.

[2] *Op. cit.*

[3] *Astrophysical Journal*, **11**, 237, 1900.

> The most striking feature of these results is the general tendency toward a displacement to the violet. . . . . Taking the values already found for the wave-lengths of H and K in the arc spectrum, the average displacement amounts to 0.006 tenth-meters, which would mean a velocity of approach on the part of the calcium vapor producing the absorption lines of 0.41 kilometers a second. . . . . No certain evidence can be found in these observations of any such variation in the motion of the calcium vapor between the center and the limb, as might be expected from a general drift upward in a radial direction. A large amount of material will, however, be necessary before any conclusion can be drawn in regard to this matter. . . . . The results given by the emission lines, H_2 and K_2, also show a displacement toward the violet, although the measurement of these lines is much more difficult than that of the absorption lines. . . . . Upon most of the plates which were measured the violet and the red components are very nearly equal; in several the violet is slightly stronger, and in one distinctly weaker than the red component.[1]

The present state of the case is as follows: M. Deslandres found at the center of the disk dissymmetry with the violet component of K_2 the stronger, the inequality of the components disappearing at the limb. Without measurements he assumed a descending motion of the absorbing vapor and an ascending motion of the emission layer. Jewell found a varying dissymmetry of the components and a measured velocity of descent for the vapor producing the absorption line of about a mile a second. The measurements of the emission line were too difficult to give anything but a slight indication of a displacement toward the violet. Adams found dissymmetry to be the exception, a measured velocity of ascent for the absorbing vapor of 0.41 kilometers a second, and a slight displacement of the emission line toward the violet. The apparent contradiction in the measurements of Jewell and Adams probably depends upon the different standards used for the solar lines and the differences in wave-length assigned to the H and K lines in the arc. As to the conflicting evidence relative to dissymmetry, the explanation suggested by Adams is undoubtedly the correct one: "It seems probable, that while an effect like that found by M. Deslandres is perhaps to be expected, the local conditions of the calcium vapor at different points on the sun's surface vary so much as to mask it completely in many cases."[2]

---

[1] *Contributions from the Mount Wilson Solar Observatory*, No. 6; *Astrophysical Journal*, **23**, 45, 1906.

[2] *Op. cit.*

In reviewing the work already done, three points appear to which particular care should be given in a definitive examination of the question of the general movement of the calcium vapor in the upper and middle levels of the sun's atmosphere: first, an accurate determination should be made of the wave-lengths of K_2 and K_3 at *definite positions* on the sun's surface, referring them to the same standards that were used for determining the wave-lengths of the correponding line in the arc; second, the plates should be taken with reference to the particular ends in view, and exposure times and developments should be such as to bring out as sharply as possible the bright emission line, particularly on plates taken at the center of the sun's disk; third, there should be a large number of observations extending over a sufficiently long period of time to eliminate as far as possible the masking of the general effect by temporary conditions, so that the final mean will reveal the prevailing state of the vapor.

As a preliminary to this investigation the determination of the wave-lengths of the H and K lines of calcium in the arc, the spark, and the electric furnace was made,[1] based on the secondary standards of the International Union for Co-operation in Solar Research, as determined by Fabry and Buisson.[2] It was early decided to confine the investigation to the K line of calcium in the sun because of its greater intensity and the absence of troublesome neighboring lines. The Fabry and Buisson standards being about 40 Ångströms apart in this region, only the standard λ 3935 was conveniently near to K. The wave-length of another iron line, λ 3930, was therefore determined in the arc with the same precision as the H and K lines, in order that there might be an adjacent standard on each side of the K line to which its wave-length could be referred. The results for the wave-lengths of the calcium lines in the arc were λ 3933.667 for K and λ 3968.476 for H, and for the supplementary iron line λ 3930.301.[1]

The points covered in the present paper are: the determination of the wave-lengths of the solar standards employed in terms of arc standards; the measurement of the wave-lengths of the absorption line K_3 and the emission line K_2 at different points on the solar disk as a basis for the study of general radial motion of the calcium vapor; an investigation of the frequently assumed horizontal currents along the solar surface; a study of the absolute and relative widths of the H and K lines at the limb and center; the vertical distribution of the calcium vapor in the chromosphere; the wave-length of the absorption line H_3 at the center and limb; the relative wave-lengths of H and K in the sun; and a general discussion of the data derived in the investigation.

---

[1] *Contributions from the Mount Wilson Solar Observatory*, No. 44; *Astrophysical Journal*, **31**, 143, 1910.

[2] *Astrophysical Journal*, **27**, 169, 1908.

2. DETERMINATION OF THE SOLAR STANDARDS

The spectrographs employed are of the Littrow form and are described as Nos. 2 and 3 in *Contributions from the Mount Wilson Solar Observatory*, No. 44. In the 18-foot spectrograph (No. 2) arranged for the Snow telescope, a 4-inch (10 cm) plane Michelson grating, having 12,500 lines to the inch (492 to the mm), and a 4-inch plane Rowland grating, having 14,438 lines to the inch (568 to the mm), were used, the latter being temporarily free from its regular service in the tower spectrograph, with which also some of the comparison plates were taken. Light from the center of the sun's disk was used for direct comparison with the iron arc, an unmagnified image of which was projected on the slit. The narrow iron spectrum fell on the plate between two narrow strips of the solar spectrum. In the case of the 18-foot spectrograph the occulting bar was free from the instrument. In that of the 30-foot spectrograph the light, easily moving occulting bar is attached to the massive head of the instrument. The plates were measured red right and red left, with at least four settings on the arc line and eight or more on the solar line for each direction. Corrections have been applied for the rotation of the earth on its axis, and the eccentricity of its orbit around the sun, using Campbell's tables.[1] The solar lines λ 3930 and λ 3935 lie in the broad shade of K_1 and therefore present some difficulties for accurate measurement. The results for the solar lines, corrected as noted above and referred to the corresponding arc lines, are given in Table I.

The increase in the wave-lengths of the solar lines over the wave-lengths in the arc is 0.005 Å for both lines.

In measuring the wave-lengths of K near the sun's limb, account must be taken of "pressure-shifts" upon the solar standards. This effect falls off rapidly with increasing distance from the limb, but in this investigation points on the disk were taken at only 1 mm from the limb. Mr. Adams kindly placed at my service his center and limb plates of this region, upon which the shifts of the solar standards were found to be as follows:

---

[1] Scheiner, *Astronomical Spectroscopy* (translated by Frost), Boston, 1898, 338–344.

TABLE I

Solar Standards

Plate	λ 3930	λ 3935	Spectrograph	Grating
396	3930.307	3935.826	18-foot	12,500
398	.306	.821	18-foot	12,500
403	.307	.826	18-foot	14,438
404 (1)	.304	.825	18-foot	14,438
(2)	.308	.825	18-foot	14,438
405 (1)	.316	.824	18-foot	14,438
(2)	.307	.824	18-foot	14,438
406	.306	.826	18-foot	14,438
B 50 (1)	.305	.822	30-foot	14,438
(2)	.306	.820	30-foot	14,438
(3)	.306	.822	30-foot	14,438
B 51 (1)	.305	.823	30-foot	14,438
(2)	.306	.821	30-foot	14,438
Means	3930.306	3935.823		

Plate	λ 3930	λ 3935
112	+0.005	+0.004
120 (1)	+0.004	+0.002
(2)	+0.004	+0.002
134	+0.003	+0.003
Means	+0.004	+0.003

The calcium vapor producing the K_3 absorption line is known to be a high-level vapor and therefore would be subject to very small pressure, possibly less than one atmosphere. The vapor producing the emission line K_2 lies at an intermediate level and may be under a pressure not much different from that of the earth's atmosphere. The results will show that these assumptions are justified. For these lines, then, the solar standards are, for the general disk, λ_A 3930.306 and λ_A 3935.823, and for the limb λ_A 3930.310 and λ_A 3935.826. Since these have been determined in terms of the arc standards used for measuring the wave-lengths of H and K in the arc, the results for K_2 and K_3 in the sun are directly comparable with the results in the arc.

3. THE WAVE-LENGTH OF THE ABSORPTION LINE K_3

The spectrograph was that used with the Snow telescope and described as spectrograph No. 2. The grating was the 8-inch Michelson, used in the third order, where the scale is approximately 1 mm = 1.02 Å. The spectrograph has a first slit 45 mm long and a second slit of the same length but of variable width, so that short sections of the spectrum may be taken. The slit may be only wide enough to allow the spectrum line to pass through, or it may be increased to 12 mm. Both slits and the plate may be moved automatically or by hand. The arrangement permits one to make easily and rapidly successive exposures of the same point on the sun, for detecting changes with time, or exposures of successive points at any desired intervals. It is in a modified form the spectrograph *des vitesses* suggested by M. Deslandres and employed by him in 1892 for the photography of the spectra of spots and faculae, in which he noted for the first time the double reversal of the H and K lines.[1] From such plates taken at closely adjacent points with a long and narrow slit the forms and distribution of the calcium flocculi can be obtained in the manner M. Deslandres has shown.[2] In connection with the present investigation, the writer has had an opportunity to examine some section plates taken by Hale in 1891, when using a long slit and making the first solar survey to which this method "by sections" especially lends itself, and by which he discovered the bright reversals of the H and K lines of calcium at points on the disk of the sun. In the present case the sections used by the writer were 12 mm wide and the lines 45 mm long. They were wide enough to include the solar standards, and the lines were long enough to show the condition of the calcium vapor over a region on the sun 350,000 km in extent. A preliminary survey was made by taking points 1, 2, 3, 4, 7, 12, 17, 25, 35, and 50 mm from the limb and at the center. These were found to be unnecessarily numerous and measurements were confined to three points, namely, 1 mm and 12 mm from the east and west limbs, and the center. The change in the line-of-sight component of any radial movement of the calcium vapor takes place rapidly near the limb. With an image 172 mm in diameter, which is the mean value here used, 51 per cent of the change from limb to center

---

[1] *Comptes Rendus,* **114**, 277, 1892.

[2] *Transactions of the International Union for Co-operation in Solar Research,* II, Plate XII.

TABLE II

Wave-Length of K_3 at 1 mm from the Limb

East			West		
Plate	Date	K_3	Plate	Date	K_3
	1909			1909	
21	Jan. 19	3933.670	42	Jan. 28	3933.663
26	“ 20	.664	69	Feb. 13	.665
43	“ 28	.662	70	“ 13	.673
64	Feb. 8	.669	80	“ 22	.670
68	“ 13	.665	120	March 9	.673
71	“ 13	.658	148	“ 11	.675
120	March 9	.665	151	“ 11	.678
145	“ 10	.672	199	“ 31	.674
151	“ 11	.665	204	April 1	.670
199	“ 31	.666	209	“ 9	.673
Mean		3933.6656	Mean		3933.6714
204	April 1	.666	229	April 15	.673
209	“ 9	.655	234	“ 16	.664
229	“ 15	.661	255	“ 27	.673
234	“ 16	.674	262	“ 29	.671
248	“ 26	.662	353	July 17	.667
255	“ 27	.666	356	“ 20	.672
262	“ 29	.661	358	“ 21	.672
361	July 22	.660	360	“ 22	.662
365	“ 23	.663	362	“ 23	.669
366	“ 24	.665	364	“ 22	.667
Mean		3933.6633	Mean		3933.6690
368	July 24	.660	369	July 24	.670
371	“ 26	.685	370	“ 26	.659
373	“ 27	.652	372	“ 27	.669
376	“ 28	.662	374	“ 27	.662
378	“ 29	.669	375	“ 28	.677
379	“ 30	.669	377	“ 29	.659
383	“ 30	.666	380	“ 30	.666
387	Aug. 2	.662	383	“ 30	.686
389	“ 3	.664	388	Aug. 3	.678
391	“ 5	.665	392	“ 6	.669
Mean		3933.6654	Mean		3933.6695

occurs within 12 mm of the limb. As the total effect is small, plates taken at the center would not give very different results from those taken over the general disk unless points very near the limb were selected. Tables II, III, and IV contain the results for the three points chosen. The plates were measured red right and red left. The results are arranged in groups of ten each, with the plates in serial order, the better to bring out the regularity of the progressive change

TABLE III

WAVE-LENGTH OF K_3 AT 12 mm FROM THE LIMB

Plate	Date	K_3	Plate	Date	K_3
	1909			1909	
21	Jan. 19	3933.675 E	246	April 26	3933.681 W
22	" 19	.675 W	256	" 27	.678 W
26	" 20	.678 E	262	" 29	.672 E
34	" 24	.676 E	356	July 20	.676 W
38	" 28	.667 E	359	" 21	.677 W
42	" 28	.677 W	360	" 22	.667 W
43	" 28	.674 E	361	" 22	.674 E
48	" 29	.673 E	362	" 23	.676 W
50	" 29	.673 E	364	" 23	.669 W
53	" 29	.678 E	365	" 23	.672 E
Mean		3933.6746	Mean		3933.6742
59	Jan. 30	.676 E	366	July 24	.677 E
62	" 30	.678 E	368	" 24	.672 E
64	Feb. 8	.677 E	369	" 24	.671 W
68	" 13	.680 E	370	" 26	.675 W
69	" 13	.678 W	371	" 26	.676 E
70	" 13	.670 W	372	" 27	.675 W
71	" 13	.671 E	373	" 27	.671 E
77	" 22	.673 E	374	" 27	.674 W
80	" 22	.674 W	375	" 28	.671 W
187	March 30	.680 E	376	" 28	.676 E
Mean		3933.6757	Mean		3933.6738
187	March 30	.671 W	378	July 29	.674 E
210	April 9	.674 E	380	" 30	.672 W
210	" 9	.677 W	383	" 30	.675 W
214	" 12	.672 E	383	" 30	.665 E
231	" 15	.678 E	387	Aug. 2	.677 E
231	" 15	.679 W	388	" 3	.667 W
242	" 24	.680 E	389	" 3	.675 E
242	" 24	.677 W	427	Oct. 31	.680 E
244	" 25	.679 E	430	Nov. 1	.671 W
246	" 26	.677 E	434	" 1	.674 E
Mean		3933.6764	Mean		3933.6730

from the limb to the center. In the means for the groups and tables the fourth decimal has been retained as the residuals shown by the least-squares solution are confined to the fourth place except for two points. The wave-length of K_3 is given in absolute units, and referred to the two standards mentioned above. The letters E and W following the wave-lengths in Table III refer to the east and west limbs of the sun, respectively.

TABLE IV

WAVE-LENGTH OF K_3 AT CENTER OF THE DISK

Plate	Date	K_3	Plate	Date	K_3
	1909			1909	
21	Jan. 19	3933.682	366	July 24	3933.683
22	“ 19	.682	368	“ 24	.675
26	“ 20	.676	369	“ 24	.680
34	“ 24	.678	370	“ 26	.681
38	“ 28	.682	371	“ 26	.681
42	“ 28	.684	372	“ 27	.677
50	“ 29	.689	373	“ 27	.687
53	“ 29	.683	374	“ 27	.678
59	“ 30	.682	375	“ 28	.682
62	“ 30	.679	376	“ 28	.676
Mean		3933.6817	Mean		3933.6800
64	Feb. 8	.675	377	July 29	.681
68	“ 13	.677	378	“ 29	.678
70	“ 13	.679	379	“ 30	.686
123	March 9	.678	380	“ 30	.680
124	“ 9	.676	383	“ 30	.675
130	“ 9	.676	387	Aug. 2	.677
136	“ 10	.680	388	“ 3	.688
146	“ 10	.682	389	“ 3	.683
152	“ 11	.680	436	Nov. 1	.683
173	“ 12	.684	436	“ 1	.680
Mean		3933.6787	Mean		3933.6811
197	March 31	.680	444	Nov. 3	.682
197	“ 31	.682	444	“ 3	.676
206	April 1	.684	445	“ 3	.681
236	“ 16	.684	445	“ 3	.677
239	“ 24	.683	461	“ 23	.679
247	“ 26	.677	461	“ 23	.694
356	July 20	.680	462	“ 23	.681
361	“ 22	.672	462	“ 23	.684
362	“ 23	.681	471	“ 27	.678
364	“ 23	.678	471	“ 27	.676
Mean		3933.6801	Mean		3933.6808

The measurements were confined to those portions of the spectrum lines that appeared to represent the prevailing condition of the chromospheric vapor. Regions near spots and faculae were avoided, especially was this the case on the plates taken at the center and at 12 mm from the limb. On the limb plates the bright emission line K_2 was so broad and intense that it did not reveal clearly the presence of the calcium flocculi. The slits of the spectroscope being 45 mm long, it was possible on the other plates to select those portions of the line for measurement in which the bright components of K_2, bounding K_3, were of uniform width for some distance, and not of such great intensity as over the facular regions and the brilliant flocculi. The period covered by this series of observations extends from January 19 to November 27, 1909, and includes twelve rotations of the sun. The plates being taken at irregular intervals represent what must be the prevailing state of the calcium vapor producing the absorption line K_3. The results for the groups are shown in Table V.

TABLE V

MEAN RESULTS FOR THE WAVE-LENGTH OF K_3

	1 mm from the Limb	12 mm from the Limb	Center
	3933.6656 E	3933.6746	3933.6817
	.6714 W	.6757	.6787
	.6633 E	.6764	.6801
	.6690 W	.6742	6800
	.6654 E	.6738	.6811
	.6695 W	.6730	.6808
Final means	3933.6674	3933.6746	3933.6804

Though large variations occur in the separate measurements for a given position, larger than errors of observation, the means of the groups of ten show an unmistakable tendency toward greater wave-lengths as the center of the disk is approached. The agreement among the groups is so complete that the final means must be considered as representing the prevailing condition of the vapor with a high degree of certainty. The change of the line-of-sight component is very rapid near the limb, 15 per cent of the radial motion on the sun appearing as a line-of-sight motion at 1 mm from the limb on an image 172 mm in diameter. The difference between the wave-length at the center and at 1 mm from the limb is 0.013 Å, which is 85 per cent of the change from limb to center. The total displacement between limb and center is therefore 0.015 Å, corresponding to a velocity of *descent* of 1.14 km per second for the upper level of the calcium vapor in the solar atmosphere. The falling of the high-level calcium vapor is a general phenomenon, and though its velocity of descent seems low, it is in fact far greater than hurricane velocities in the terrestrial atmosphere. The highest recorded South Sea hurricane velocity, according to Köppen,[1] is 40 m per second, so that this downrush of the calcium vapor has a mean velocity thirty times as great as the South Sea windstorms, and occasionally far greater.

The measurement of the calcium absorption line K_3 was referred to the two iron lines λ 3935 and λ 3930, which occur in the reversing layer and presumably lie at a lower level. Adams has shown that the hydrogen vapor producing the $H\alpha$ line has a considerably higher rotational velocity than the reversing layer,[2] and that the calcium vapor producing λ 4227 has a velocity intermediate between that of $H\alpha$ and the reversing layer.[3] Hale has shown a correspondingly high velocity for the hydrogen flocculi, but that the bright calcium flocculi give a somewhat lower equatorial velocity and a smaller polar retardation than the reversing layer.[4] The latter result was also obtained by Fox.[5] The calcium vapor producing the K_3 absorption line is a high-level vapor and therefore may have a relatively higher rotational velocity compared with the reversing layer. If such be the case, then the wave-length of K_3 at the east limb should be less than the mean, and that at the west limb greater than the mean, by an amount corresponding to the difference in the line-of-sight velocities of the calcium vapor and the reversing layer. In Table V there is shown a consistent difference between the results for the two limbs, those for the west limb being greater than those for the east limb. Since the probable errors of the means for the east and west limbs separately are ±0.0006 Å and ±0.0007 Å, respectively, it would appear that the difference of the means, which amounts to 0.0052 Å, is, beyond question, real. It seemed worth while to examine the values more closely from the point of view of the rotational velocity. The observations grouped themselves about two latitudes, namely, 6°6 and 38°4. From the data given in Adams' paper,[1] the radial velocities, periods, and angular velocities were calculated for these two latitudes. The differences between the wave-lengths of K_3 at the east and west limbs for latitudes 6°6 and 38°4 are 0.0042 Å and 0.0062 Å, respectively. The velocity of the calcium vapor relative to the reversing layer is sufficient at 6°6 to produce a Doppler effect of 0.0021 Å, and at 38°4 an effect of 0.0031 Å, corresponding to relative line-of-sight velocities of 0.16 km and 0.24 km, respectively. The calculated radial velocities and the resulting periods and angular velocities are given in Table VI.

---

[1] Hann, *Lehrbuch der Meteorologie* (Leipzig, 1906), 281.

[2] *Contributions from the Mount Wilson Solar Observatory*, No. 24; *Astrophysical Journal*, **27**, 213, 1908.

[3] *Contributions from the Mount Wilson Observatory*, No. 33; *Astrophysical Journal*, **29**, 110, 1909.

[4] *Contributions from the Mount Wilson Observatory*, No. 25; *Astrophysical Journal*, **27**, 219, 1908.

[5] *Science*, N.S., **25**, 606, 1907.

TABLE VI

COMPARISON OF ROTATION VELOCITIES FOR K_3, $H\alpha$, AND REVERSING LAYER

ϕ	K_3			$H\alpha$			REVERSING LAYER		
	v	ξ	Period	v	ξ	Period	v	ξ	Period
	km		days	km		days	km		days
6°6	2.20	15°5	23.1	2.13	15°1	23.9	2.04	14°0	24.9
38°4	1.60	15.4	23.4	1.56	14.3	25.4	1.45	13.2	27.4

From this table it is seen that the radial velocity of the calcium vapor producing the absorption line K_3 is about as much higher than that of the hydrogen producing $H\alpha$ as the radial velocity of the latter is higher than that of the reversing layer. The angular velocity of the calcium vapor is consequently greater and more nearly constant than the angular velocity of the hydrogen, and shows therefore less polar retardation. These results are in entire harmony with other observations in this paper showing the high level of the chromospheric calcium.

4. THE WAVE-LENGTH OF THE EMISSION LINE K_2 AND FURTHER CONSIDERATION OF THE WAVE-LENGTH OF THE LINE K_3

The measurements of the bright components of the K_2 line were made outside of the brilliant facular and floccular regions and are difficult since the line on the general disk is weak and its outer edges are poorly defined, especially on the red-facing border. It is present, however, at all points of the disk; and by careful timing of exposures and strong development covering a region of about 5 Å on each side of the line, that is, covering the broad shading due to K_1, a large number of plates suitable for measurement were obtained. Besides the center, the points chosen for observation were 1, 12, 35, 50, and 68 mm from the limb. As will be seen, the total change in wave-length in passing from the limb to the center is not large, and from the cosine law of the distribution of the line-of-sight components of a radial velocity it follows that to produce a variation of 10 per cent in the value of this component, it would be necessary near the center to go 35 mm toward the limb on an image of the size used. This made it feasible to take a series of exposures for points near the center on a single plate, changing the position of the sun's image on the slit a few millimeters for each exposure. In this way the effects of local disturbances in the solar atmosphere could be distributed and the probability increased that the final mean of the measurements would represent the prevailing condition of the vapor. In a more limited way this could be done with the other points selected for measurement, except for that 12 mm from the limb where the change is compara-

---

[1] *Contributions from the Mount Wilson Solar Observatory*, No. 33; *Astrophysical Journal*, **29**, 110, 1909.

TABLE VII

WIDTH OF V K_2 — WIDTH OF R K_2, AND WAVE-LENGTH OF K_3 1 mm FROM THE LIMB

Plate	Difference	K_3	Plate	Difference	K_3
120 W.......	+0.021	3933.673	262 E......	−0.006	3933.661
120 E.......	+0.044	.665	360 W......	+0.005	.662
199 W.......	−0.009	.674	378 E......	−0.004	.669
199 E.......	+0.003	.666	383 W......	+0.004	.686
204 W.......	−0.003	.670	383 E......	−0.002	.666
204 E	+0.022	.666	387 E......	−0.001	.662
209 W.......	+0.003	.673	389 E......	+0.019	.664
209 E.......	+0.017	.655	510 E......	+0.012	.664
229 W.......	+0.006	.673	510 W......	+0.010	.665
229 E.......	+0.002	.661	510 W......	+0.017	.667
234 W.......	−0.005	.664	510 W......	+0.013	.665
234 E.......	+0.009	.674	510 W......	+0.006	.672
248 W.......	+0.015	.673	510 E......	+0.006	.661
248 E	+0.002	.662	510 E......	+0.000	.667
262 W.......	+0.001	.671	510 E......	+0.014	.664
			Means ...	+0.0074	3933.6672

tively rapid. The result for this point is therefore of less weight since successive exposures at this same point on the sun on a single plate would not eliminate local effects.

TABLE VIII

WAVE-LENGTHS OF K_2 AND K_3 AT 12 mm FROM THE LIMB

Plate	Date	K_2	K_3
	1909		
427 (1) E	October 31	3933.660	3933.678
(2) E	“ 31	.657	.679
(3) E	“ 31	.642	.681
(4) E	“ 31	.648	.683
(5) E	“ 31	.653	.680
430 (1) W	November 1	.652	.671
(2) W	“ 1	.647	.671
(3) W	“ 1	.640	.676
(4) W	“ 1	.646	.665
(5) W	“ 1	.643	.667
(6) W	“ 1	.647	.670
(7) W	“ 1	.653	.670
(8) W	“ 1	.653	.675
434 (1) E	“ 1	.660	.674
(2) E	“ 1	.645	.675
437 (1) E	“ 1	.654	.674
(2) E	“ 1	.641	.672
(3) E	“ 1	.656	.675
(4) E	“ 1	.653	.675
(5) E	“ 1	.657	.674
(6) E	“ 1	.657	.672
(7) E	“ 1	.659	.680
(8) E	“ 1	.656	.671
502 (1) W	December 3	.658	.683
(2) W	“ 3	.654	.674
(3) W	“ 3	.648	.673
(4) W	“ 3	.638	.676
508 (1) W	“ 12	.640	.668
(2) W	“ 13	.648	.671
(3) W	“ 13	.643	.679
Means		3933.6503	3933.6744

The exposures were confined to regions on the disk outside of the faculae and flocculi, as in the case of K_3 in the preceding section, and therefore represent the general chromospheric vapor producing K_2.

In the measurement of the bright components of K_2, the method suggested by Adams[1] was followed. "It is evident," he says, "if a is the wave-length of one of these components, and d the difference of wave-length between the absorption line and the second component, that the center of the whole bright line is given by $a+d$."

---

[1] *Contributions from the Mount Wilson Solar Observatory*, No 6; *Astrophysical Journal*, 23, 45, 1906.

Measurements made in accordance with this method give data for the calculation of the wave-length not only of K_2, but of K_3 as well,

TABLE IX

WAVE-LENGTHS OF K_2 AND K_3 AT 35 mm FROM THE LIMB

Plate	Date	K_2	K_3
	1909		
465 (2) E	November 24	3933.656	3933.673
(3) E	" 24	.645	.676
467 (1) W	" 24	.656	.683
(2) W	" 24	.650	.683
(3) W	" 24	.643	.671
(4) W	" 24	.642	.676
468 (2) E	" 24	.658	.680
(3) E	" 24	.653	.683
(4) E	" 24	.656	.682
(6) E	" 24	.653	.683
(7) E	" 24	.646	.676
(8) E	" 24	.643	.683
472 (1) W	" 27	.630	.670
(2) W	" 27	.642	.669
(4) W	" 27	.633	.668
498 (1) W	December 3	.643	.676
Means		3933.6468	3933.6770

TABLE X

WAVE-LENGTHS OF K_2 AND K_3 AT 50 mm FROM THE LIMB

Plate	Date	K_2	K_3
	1909		
509 (1) W	December 13	3933.640	3933.682
(2) W	" 13	.641	.682
(3) W	" 13	.642	.681
(4) E	" 13	.657	.683
(5) E	" 13	.656	.676
(6) E	" 13	.653	.680
511 (3) W	" 23	.624	.673
(4) W	" 23	.639	.683
(6) E	" 23	.651	.681
(8) E	" 23	.651	.672
Means		3933.6454	3933.6793

and in fact part of the results already given for K_3 in Tables II–IV was derived from this material. For completeness these values are reprinted in Tables VII–XII along with the additional results for K_3 and the values of K_2. The figures in parentheses refer to successive exposures on the same plate. Table VII, however, does not give directly the values of K_2.

On the plates 1 mm from the limb the emission components are very broad and strong, and, as far as the eye can judge, symmetrical. They are too broad, however, for a determination of the wave-length of K_2 by the preceding method. But on 30 of these plates, selected for clearness and sharpness of definition and measured primarily for the purpose of obtaining the widths of K_2 and K_3, it was found that, on the whole, the V K_2 component was wider than R K_2, thus indicating a shift of K_2 relative to K_3. This result permits an indirect determination of the wave-length of K_2 for the point 1 mm from the limb. The differences in width of the components of K_2, expressed in Ångströms, and the corresponding values of the wave-length of K_3 are given in Table VII. The mean difference in width of the components of K_2 is +0.0074 Å, and indicates that here as elsewhere on the solar disk the vapor producing the emission line K_2 is rising relatively to that producing the absorption line K_3. The mean wave-length of K_3 from all of the plates 1 mm from the limb is 3933.6674. Since the shift of K_2 relatively to K_3 is one-half the difference in width of V K_2 and R K_2, it follows that the wave-length of K_2 at 1 mm from the limb is 3933.6637. The corrections to be applied to reduce these values to the limb will be given later.

TABLE XI

WAVE-LENGTHS OF K_2 AND K_3 AT 68 mm FROM THE LIMB

Plate	Date	K_2	K_3
	1909		
513 (1) E	December 23	3933.653	3933.680
(2) E	" 23	.648	.677
(3) E	" 23	.645	.678
(4) E	" 23	.637	.680
(5) W	" 23	.632	.680
(7) W	" 23	.629	.675
(8) W	" 23	.624	.684
520 (2) W	" 24	.661	.680
(3) W	" 24	.648	.678
(8) E	" 24	.639	.687
Means		3933.6416	3933.6799

It will be noticed that there is a progressive shortening of the wave-length of K_2 and a progressive lengthening of that of K_3 as the point of observation recedes from the limb toward the center, so that the difference between the wave-lengths of K_2 and K_3 increases continuously from the limb to the center. This result is clearly shown by Table XIII which contains the weighted means of all of the values for K_2 and K_3 given in Tables II–IV and VII–XII, and the respective differences in wave-lengths, for different distances from the limb.

TABLE XII

WAVE-LENGTHS OF K_2 AND K_3 AT CENTER OF SUN'S DISK

Plate	Date	K_2	K_3
	1909		
436 (3)	November 1	3933.654	3933.685
(5)	" 1	.655	.680
(6)	" 1	.645	.677
(7)	" 1	.662	.690
(8)	" 1	.644	.674
(9)	" 1	.653	.680
(1)	" 1	.648	.687
443 (2)	" 3	.637	.679
(3)	" 3	.654	.680
(4)	" 3	.651	.690
(5)	" 3	.645	.684
(6)	" 3	.645	.679
(7)	" 3	.638	.679
(8)	" 3	.642	.680
(9)	" 3	.645	.668
(11)	" 3	.628	.682
(13)	" 3	.642	.677
455 (4)	" 3	.646	.679
(6)	" 3	.661	.678
(7)	" 3	.645	.685
(8)	" 3	.645	.674
(9)	" 3	.640	.682
(10)	" 3	.647	.675
461 (1)	" 23	.645	.675
(2)	" 23	.645	.676
(3)	" 23	.647	.686
(4)	" 23	.627	.689
(7)	" 23	.635	.697
(8)	" 23	.635	.697
462 (2)	" 23	.631	.683
(3)	" 23	.636	.682
(5)	" 23	.639	.678
(7)	" 23	.638	.677
(9)	" 23	.642	.689
(12)	" 23	.627	.688
471 (3)	" 27	.636	.681
(4)	" 27	.611	.675
(6)	" 27	.621	.671
(7)	" 27	.625	.685
(8)	" 27	.627	.671
Means		3933.6410	3933.6811

The figures in parentheses are the weights of the corresponding mean wave-lengths. In general these are proportional to the number of exposures used, except for the point 12 mm which has been given a smaller weight for reasons already stated.

The falling of the K_3 vapor indicated by the results of the preceding section is even more definitely shown by the data in Table XIII, and at the same time there is an equally positive indication that the K_2 calcium is rising.

TABLE XIII

WAVE-LENGTHS OF K_3 AND K_2 AT DIFFERENT DISTANCES FROM LIMB

	1 mm	12 mm	35 mm	50 mm	68 mm	Center
K_3	3933.6674 (63)	.6746 (34)	.6770 (8)	.6793 (5)	.6799 (5)	.6804 (63)
K_2	3933.6637 (24)	.6503 (12)	.6468 (8)	.6454 (5)	.6416 (5)	.6410 (20)
K_3-K_2....	+0.0037	+0.0243	+0.0302	+0.0339	+0.0383	+0.0394
O−C K_3 .	−0.0004	+0.0014	−0.0007	+0.0001	−0.0004	−0.0002
K_2 .	+0.0008	−0.0033	+0.0008	+0.0020	0.0000	0.0000

The evidence is most clearly presented by exhibiting the close agreement of the observed values of the wave-lengths of K_3 and K_2 with an equation of the form

$$\lambda_L + \Delta\lambda \cos E = \lambda$$

in which λ_L is the wave-length at the limb, $\Delta\lambda$ the change in wave-length in passing from limb to center, and E the angular elongation from the center of a point for which the observed wave-length is λ.

Least-squares reductions based upon the data in Table XIII give the following results for the wave-lengths at the limb and the changes in passing from limb to center:

	λ_L	$\Delta\lambda$
K_3............	3933.6655±0.0004	+0.0151±0.0006
K_2............	3933.6668±0.0010	−0.0258±0.0014

The appended quantities are the probable errors. The corresponding residuals for the observed values are given in the last two lines of Table XIII. The results are shown graphically by Fig. 1. The abscissae are distances from the limb, one division corresponding to 1 mm. The ordinates are wave-lengths with one division equal to 0.001 Å. The curves are drawn by points calculated from the

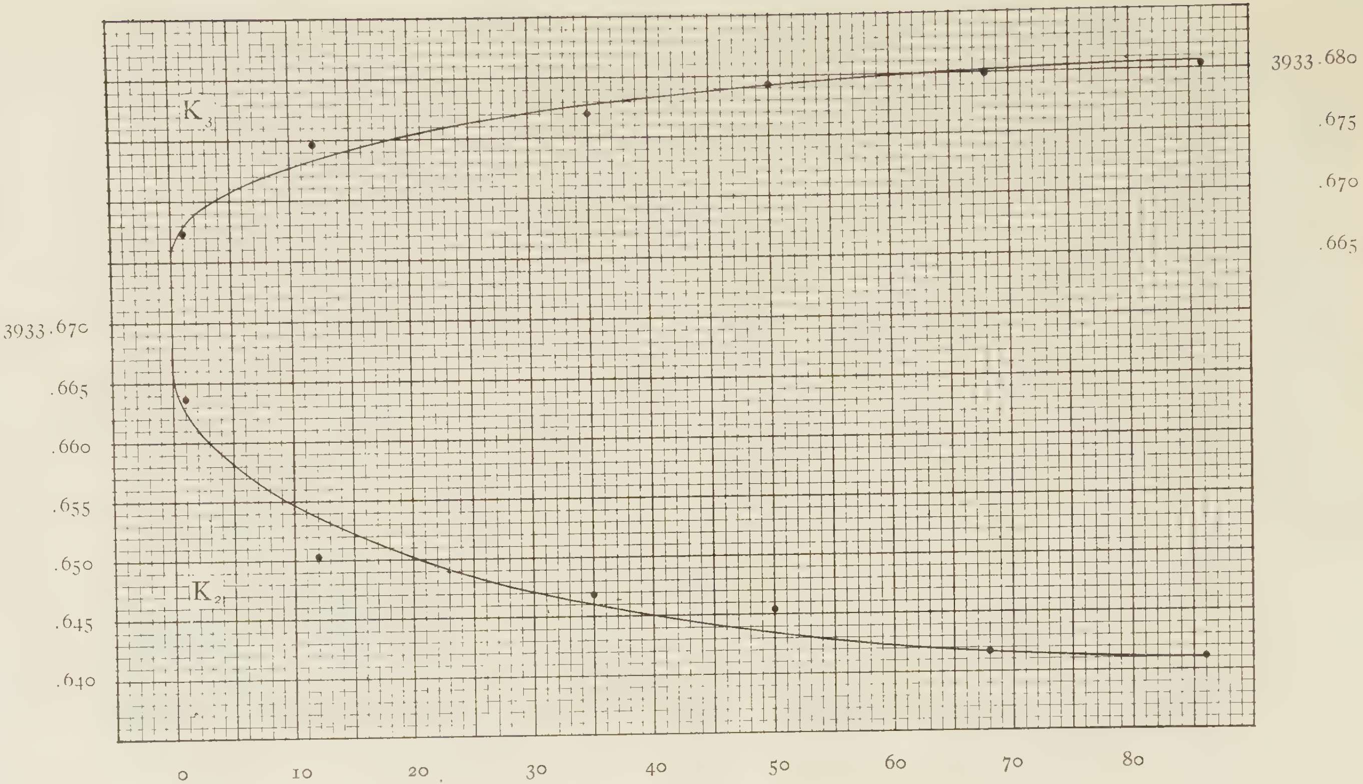

FIG. 1.—Wave-Lengths of K_3 and K_2 for Varying Distances from Limb

cosine law. That for K_3, referred to the ordinate values on the right, has the line λ 3933.6655 (wave-length of K_3 at the limb) as the axis of abscissae and corresponds to an *increase* of 0.0151 Å from limb to center. The curve for K_2, referred to the ordinates at the left, has the line λ 3933.6668 (wave-length of K_2 at the limb) for its axis and corresponds to a *decrease* of 0.0258 Å from limb to center. The dots represent the observed data as collected in Table XIII. Considering the scale of wave-lengths and the difficulties of measurement, especially in the case of K_2, the agreement of the observations with the calculated curves is extremely satisfactory except for the point 12 mm from the limb on the K_2 curve, where, as previously indicated, the effects of temporary conditions are probably not eliminated to the same extent as elsewhere. The curves may be considered as representing the prevailing condition of the vapors to which the respective lines are due, that is, a *downward* velocity for the vapor producing K_3 of 1.14 km per second, and an *upward* velocity for that producing the bright emission line K_2 of 1.97 km per second.

Retaining the fourth decimal, the wave-length of the K line derived from laboratory investigations[1] is 3933.6670 ± 0.0002, which is in close agreement with the limb values given above for K_2 and K_3. It will be noted that the difference between the wave-lengths for K_3 and K in the arc is in the direction agreeing with the relatively low pressure conditions probably associated with the high-level K_3 vapor, and in view of the small pressure shift per atmosphere, viz., 0.002 Å,[2] would tend to strengthen the evidence given later in this paper for the assumption of a low density in the case of the vapor producing the absorption line. This fact cannot be regarded as of positive significance, however, since the difference involved is not greatly in excess of the probable errors; and moreover, the comparison is made between results produced under conditions so vastly different that causes other than difference of pressure might conceivably produce small changes in wave-length.

As far as the writer has been able to ascertain, this is the first direct proof of the agreement of the solar or cosmic wave-length of a substance with its wave-length in a terrestrial source, to the degree of accuracy obtainable in terrestrial comparisons. Only in the case of a substance like hydrogen or calcium, occurring at so high a level in the solar atmosphere that the pressure does not differ greatly from that of the terrestrial atmosphere, and for measurements from which line-of-sight motion may be eliminated, can such an agreement be expected. That an element can exhibit its characteristic properties under such widely differing conditions and in regions so greatly separated in space, thus emphasizing the essential unity of our system, is a fact of profound significance, and an accumulation of exact data establishing such agreement under terrestrial and cosmic conditions is very much to be desired.

---

[1] *Contributions from the Mount Wilson Solar Observatory*, No. 44; *Astrophysical Journal*, **31**, 143, 1910.

[2] Humphreys and Mohler, *Astrophysical Journal*, **3**, 114, 1896.

5. HORIZONTAL MOVEMENTS IN THE SOLAR ATMOSPHERE

The idea of general currents in the sun's atmosphere between the equator and the pole has appeared at various times. Their existence seems in general to have been assumed from analogy to the great movements in the terrestrial atmosphere; but the conditions producing the terrestrial system of circulation, equatorial and polar regions of unequal temperatures, have never been observed in the sun. M. Deslandres, in speaking of vertical and horizontal currents in the solar atmosphere, says:

> Ce mouvement général était prévu par les théories de M. Faye, et les expériences récentes de Mgr. Rougerie. . . . . D'ailleurs, le courant de pôle à l'équateur pourrait avoir lieu dans la photosphère, et le courant inverse de retour au-dessus, mais alors avec des vitesses croissantes pour des hauteurs croissantes.[1]

M. Faye states the following conclusion drawn from his study of the origin of sun-spots and the equal velocity of spots and the photospheric zones in which they lie:

> That these bands move nearly parallel to the equator and never exhibit currents that, as in the upper regions of our atmosphere, would be constantly directed toward the pole.[2]

Oppolzer, when speaking of the upward and downward currents in the solar atmosphere and the interactions of their dynamic and thermal working, says:

---

[1] *Comptes Rendus*, **119**, 459, 1894.

[2] Vogel, *Populäre Astronomie*, Dritte Auflage, 317.

Die Folge davon wird sein, dass die vertikal abwärts gerichtete Bewegung schliesslich aufhört und die oben nachdrängenden Massen gezwungen sind, ihren Weg seitwärts in horizontalen Bahnen zu nehmen. . . . . In den polaren Regionen herrschen aufsteigende Ströme, wie in unserer Erdatmosphäre am Aequator, die in einer gewissen Höhe als horizontale Ströme gegen die niederen Breiten in lang gezogenen Spiralen ziehen. . . . .[1]

To detect, if possible, any differences in the behavior of the calcium vapor between the polar and equatorial regions of the sun, a series of plates was taken at 12 mm from the polar limbs, with the results given in Table XIV. The slit of the spectrograph is fixed in a vertical plane and there is no arrangement for rotating the solar image. For the dates of these plates the polar axis of the sun's image formed an angle of 10° with the vertical.

TABLE XIV

WAVE-LENGTHS OF K_2 AND K_3 AT 12 mm FROM THE POLAR LIMBS

North				South			
Plate	Date	K_2	K_3	Plate	Date	K_2	K_3
	1909				1909		
419 (1)....	Oct. 30	3933.666	.681	420 (1)....	Oct. 30	3933.648	.684
(2)....	" 30	.658	.680	(2)....	" 30	.650	.679
(3)....	" 30	.669	.680	(3)....	" 30	.651	.675
(4)....	" 30	.663	.671	(4)....	" 30	.644	.673
(5)....	" 30	.669	.677	(5)....	" 30	.640	.678
(6)....	" 30	.659	.676	(6)....	" 30	.654	.677
(7)....	" 30	.654	.675	(7)....	" 30	.663	.679
(8)....	" 30	.651	.679	(8)....	" 30	.645	.675
431 (1)....	Nov. 1	.637	.675	426 (1)....	" 30	.633	.669
(2)....	" 1	.631	.666	(4)....	" 30	.635	.679
432 (1)....	" 1	.664	.676	(5)....	" 30	.643	.666
(2)....	" 1	.637	.678	(10)....	" 30	.645	.666
(3)....	" 1	.641	.674	435 (2)....	Nov. 1	.652	.673
(4)....	" 1	.638	.674	(3)....	" 1	.664	.681
(5)....	" 1	.654	.676	(4)....	" 1	.652	.679
(6)....	" 1	.644	.676	(5)....	" 1	.651	.677
(7)....	" 1	.652	.680	(6)....	" 1	.652	.677
(8)....	" 1	.644	.680	(7)....	" 1	.644	.679
(9)....	" 1	.643	.669	(8)....	" 1	.640	.675
(10)....	" 1	.637	.682	(9)....	" 1	.637	.680
Means		3933.6506	.6760	Means		3933.6471	.6761

The final means for Table XIV, and their probable errors, are compared below with those for points 12 mm from the equatorial limbs as given in Table XIII. The figures in parentheses indicate the weights.

---

[1] Vogel, *Populäre Astronomie*, Dritte Auflage, 328.

	Equatorial Limbs	Polar Limbs
K_2	3933.650±0.0008 (12)	3933.649±0.0011 (16)
K_3	3933.675±0.0003 (34)	3933.676±0.0004 (16)

The very high-level calcium vapor producing the absorption line K_3 is particularly well adapted for an examination of the suggestion made by Deslandres that the current from the equator to the pole is high up in the solar atmosphere and has increasing velocities with increasing heights. This vapor ought, therefore, from its extreme altitude, to show the maximum effect. The velocities demanded by the Oppolzer theory are low. The shortest time he suggests for the movement from the pole to the equator is a month. Such a movement taking place in six months would produce a shift in the K line of 0.0012 Å, which is greater than the probable error for the present measurement of the K_3 line. Unless the motion is common to the high-level calcium vapor and the low-level iron vapor of the reversing layer which supplied the secondary standards used, such currents between the equator and the pole cannot greatly exceed the velocity suggested in the preceding sentence. The high-level currents suggested by Deslandres and Oppolzer are in opposite directions. The practical identity of the wave-lengths of K_2 and K_3 in the polar and equatorial regions would, however, negative both hypotheses in the case of the calcium vapor producing the H and K lines. At a point 12 mm from the limb 85 per cent of a horizontal motion would appear as a line-of-sight velocity, and in case of opposite motions in the upper regions and in the reversing layer the relative effect would be greatly increased. The absence of any observable effect for calcium vapor is conclusively shown by comparison of the measurements for the polar and equatorial limbs.

6. WIDTHS OF H AND K AT CENTER AND LIMB

The change in width of the calcium lines H and K in passing from the center to the limb is very marked. There is also a change in the *relative* width of H and K. The absolute measurement of the widths of spectrum lines presents great difficulties, but for similar lines, measured under the same conditions and in immediate sequence, considerable weight can be given to the relative widths when the number of lines is sufficiently large. Measurements were made of H_3 and K_3 on 22 plates taken at 1 mm from the limb, and upon 20 plates taken at the center. In these cases, of course, the second slit was wide enough to admit both H and K, so that the exposure time and development were the same for both lines. H_2 and K_2 were measured on 15 plates taken at 1 mm from the limb, but width measurements were not possible for H_2 and K_2 at points representing the ordinary condition of the vapor, on plates taken at the center. The results are given in Table XV, in which widths are expressed in Ångströms.

TABLE XV

RELATIVE WIDTHS OF H AND K

1 mm FROM LIMB							CENTER			
Plate	H_3	K_3	$K_3 \div H_3$	H_2	K_2	$K_2 \div H_2$	Plate	H_3	K_3	$K_3 \div H_3$
120 (1)..	0.315	0.360	1.14	0.598	0.680	1.14	128 (1)...	0.118	0.138	1.17
(2)..	0.338	0.372	1.10	0.679	0.717	1.06	(2)...	0.119	0.134	1.12
199 (1)..	0.332	0.374	1.13	0.657	0.706	1.07	129 (1)...	0.126	0.154	1.20
(2)...	0.320	0.347	1.09	0.708	0.797	1.12	(2)...	0.124	0.145	1.20
204 (1)...	0.329	0.384	1.17	0.712	0.765	1.07	130 (1)...	0.113	0.141	1.24
(2)..	0.358	0.385	1.08	0.680	0.738	1.08	(2)...	0.104	0.128	1.23
209 (1)..	0.328	0.374	1.14	.....	.....	....	136 (1)...	0.119	0.142	1.20
(2)..	0.276	0.311	1.13	.....	.....	....	(2)...	0.123	0.140	1.14
229 (1)..	0.298	0.350	1.17	0.684	0.760	1.11	146 (1)...	0.137	0.163	1.19
(2)..	0.285	0.327	1.14	.....	.....	....	(2)...	0.128	0.153	1.19
234 (1)...	0.320	0.356	1.11	0.723	0.749	1.03	211 (1)...	0.139	0.163	1.18
(2)..	0.303	0.345	1.14	0.702	0.752	1.07	(2)...	0.127	0.153	1.20
248 (1)...	0.310	0.358	1.16	0.684	0.710	1.04	212 (1)...	0.123	0.149	1.21
(2)...	0.302	0.326	1.08	0.692	0.725	1.05	(2)...	0.149	0.171	1.15
262 (1)...	0.295	0.349	1.18	0.757	0.717	1.03	512 (1)...	0.145	0.165	1.14
(2)...	0.293	0.325	1.11	0.723	0.741	1.02	(2)...	0.138	0.164	1.19
510 (1)..	0.375	0.410	1.09	0.865	0.931	1.08	(3)...	0.127	0.145	1.14
(2)...	0.359	0.424	1.18	0.792	0.840	1.06	(4)...	0.116	0.132	1.14
(3)...	0.352	0.383	1.09	.....	.....	....	(5)...	0.134	0.149	1.11
(4)..	0.201	0.225	1.12	.....	.....	....	(6)...	0.148	0.170	1.15
(5)...	0.222	0.253	1.14	.....	.....	..				
(6)..	0.222	0.255	1.14	.....	.....	..				
Means ...	0.306	0.345	1.13	0.710	0.759	1.07		0.128	0.150	1.17

The writer showed in a previous paper[1] that in the case of the lines produced in the arc the relative width and intensity of K to H increased as the lines became narrower as a result of decrease in the density of the vapor. The condensed data for the arc are given below with the mean results for H and K at the center and limb of the sun. The last line refers to the relative width of H_2 and K_2 at points where the lines are locally strengthened.

---

[1] *Contributions from the Mount Wilson Solar Observatory*, No. 44; *Astrophysical Journal*, **31**, 143, 1910.

Source	Width		Relative Width
	H	K	K ÷ H
Arc, 13 bright lines	0.147	0.177	1.20
Arc, 12 absorption lines	0.064	0.087	1.36
	H_3	K_3	$K_3 \div H_3$
Sun's limb, 22 lines	0.306	0.345	1.13
Sun's center, 20 lines	0.128	0.150	1.17
	H_2	K_2	$K_2 \div H_2$
Sun's limb, 15 lines	0.710	0.759	1.07
Sun's center, 4 lines	.....	.....	1.09

The ratio of K_3 to H_3 increases on passing from the limb to the center, thus showing an increasing preponderance of K_3 over H_3 similar to that shown by K over H when the vapor in the arc decreases in density. An explanation is readily found by assuming that the vapor producing the absorption lines H_3 and K_3 exists in a relatively thin high-level layer in which the effective depth of vapor producing the absorption lines rapidly increases as the limb is approached. The same conditions, of course, explain the absolute increase in width of H_3 and K_3 on passing from the center to the limb, the mean width of K_3 at the limb being 2.3 times its width at the center, and the mean width of H_3 at the limb being 2.4 times its width at the center. The fact that H_3 and K_3 continue to increase in width, however near the limb is approached, would indicate that even at the limb the effective depth is not sufficient to produce black-body absorption. The widths of H_3 and K_3 at the center of the sun's disk are about twice the widths of the corresponding absorption lines for a moderate amount of vapor in the arc, and less than the widths of the corresponding bright lines for a small amount of vapor in the arc. From this low absorptive power in the sun's atmosphere it would appear that the vapor of calcium in the solar envelope producing these absorption lines must be of very moderate thickness and, owing to its high temperature and low pressure, exceedingly rare. The ratio of the width of K_2 to H_2 at the limb is 1.07. From this low ratio it follows by the same line of reasoning that the quantity of vapor producing the emission lines is greater than that producing the absorption lines. The same fact is also shown by the greater absolute width of the emission lines. The measurements of the widths of H_2 and K_2 at the center were not in general possible, but at points of local strengthening the ratio of the width of H_2 to K_2 was found to be 1.09. The increased preponderance of K_2 indicates, as in the case of K_3, a less effective layer at the center than at the limb, but the change in effectiveness between limb and center is much less than in the case of the K_3 absorbing vapor. The absolute widths, however, are greater near the limb, and by their continued increase indicate that even at the limb the vapor is not sufficiently deep and dense to produce black-body radiation. The vapor producing the emission lines is probably at a middle level and in a stratum thicker and under greater pressure than that producing the absorption lines H_3 and K_3, and probably of greater density also, the latter depending, however, upon its temperature. The question of its temperature and consequent increased radiating power will be discussed later in this paper. The intensity of H_2 and K_2 near the limb is also very much greater than over the general disk.

7. DISTRIBUTION OF THE CHROMOSPHERIC CALCIUM VAPOR

To investigate the distribution of the chromospheric calcium vapor, and determine the thickness of the absorbing and emitting layers, a series of plates was taken with a radial slit. The spectroscope was the 30-foot Littrow described as No. 3. It was used in the first order with exposures 12 to 20 times as long as required for the center of the disk. Points were chosen 30° apart around the limb and those spectra selected for measurement which seemed to represent the general chromosphere, that is, outside the vicinity of prominences. The plates were developed strongly until the spectrum of the skylight showed distinctly. The broad shadings in the atmospheric spectrum, due to H_1 and K_1, permitted this treatment of the plates and were favorable to the bringing out of the chromospheric lines. The measurements are extremely difficult to make as it is quite impossible to be sure of the extremity of bright lines which gradually fade out, and equally difficult to determine the point where the lines due to the lower layer of vapor producing the bright disk lines blend into those due to the high-level vapor. As one examines the lines he is quite easily convinced that the lower layer is far the thicker of the two. Near the photosphere the lines are still reversed, consisting of very bright broad lines, with relatively dark centers. The bright components grow narrower and weaker and blend into the more extended central portions. There is an apparent increase in the intensity of the central line just as the two components lose their identity. This was of assistance in forming a judgment as to the upper limit of the originally emitting vapor. The measurements are given in Table XVI, where the heights above the photosphere are given in millimeters with the equivalent of the means in kilometers and in seconds of arc.

TABLE XVI

HEIGHT OF THE CHROMOSPHERIC CALCIUM. MEAN DIAMETER OF SUN'S IMAGE 174 mm

Plate	H_2	K_2	H_3	K_3
	mm	mm	mm	mm
C 2	0.460	0.464	0.171	0.219
C 2	0.400	0.548	0.130	0.169
C 2	0.393	0.461	0.144	0.121
C 3	0.398	0.481	0.190	0.200
C 3	0.474	0.491	0.194	0.212
C 4	0.405	0.407	0.188	0.227
C 4	0.340	0.363	0.126	0.190
C 4	0.419	0.494	0.202	0.217
C 6	0.342	0.345	0.140	0.142
C 6	0.329	0.350	0.194	0.200
C 7	0.403	0.437	0.198	0.209
C 7	0.389	0.473	0.115	0.118
C 7	0.443	0.530	0.117	0.185
Means	0.400	0.450	0.159	0.185
Heights	3200 km 4″.4	3600 km 5″.0	1270 km 1″.8	1480 km 2″.0

A high degree of precision cannot be attributed to the separate measurements but from their general agreement some definite conclusions can be drawn. The height above the photosphere at which the calcium vapor still shows the K line is 600 km greater than that at which the H line disappears; that is, the outer 600 km of calcium vapor is not sufficiently dense to emit the H line to a sensible amount, though still emitting the K line with an appreciable intensity. This is in harmony with the increasing relative intensity of H to K in the arc with decreasing density of the calcium vapor, and with the increasing relative width of K_3 to H_3 in passing from the limb to the center of the sun. The K line, therefore, is the most persistent line due to the vapor of calcium.

The upper limit to which the general chromospheric calcium extends in an appreciable quantity is approximately 5000 km or 7″0 of arc. The outer 1500 km may be assigned with considerable certainty to the vapor producing the absorption line K_3. The upper limit of the layer producing the emission line K_2 is then approximately 3500 km. Its lower limit may be assumed to be that of the upper reversing layer, that is, approximately 700 km. It is of interest to compare the mean height of 53″ found by Belopolsky,[1] who gave attention only to the calcium in prominences and over faculae at the limb, with these results which aim to give what may be called the normal elevations at which the calcium can be detected, in undisturbed regions, by the instrumental equipment employed.

Assuming these thicknesses for the respective layers, it is possible to determine the change in the depth of the layers in the line of sight on approaching the limb, and to compare them with the changes in the width of the line. With a solar image 172 mm in diameter, such as was available for this investigation, and with 697,000 km as the semi-diameter of the photosphere, the following results were obtained for the thickness of the layers:

	At the Center	1 mm from the Limb	At the Limb
Reversing layer......	0–700 km	4,600 km	31,800 km
K_2..................	700 km–3500 km (2800 km)	16,400 km	62,300 km
K_3..................	3500 km–5000 km (1500 km)	7,780 km	45,800 km

The effective depth of the layer assigned to the absorbing vapor is 5.2 times as great at 1 mm from the limb as at the center, while the mean width of K_3 at 1 mm from the limb is 2.3 times its mean width at the center. The measurement of the width of K_2 at the center could not be made on the general disk. Its width at the limb relative to the width of H_2 at the limb is 1.07. The small value of the ratio points to a layer of such great thickness or density that the change in the depth of the layer on passing from the center to the limb would be much less effective than in the case of the absorbing vapor, since the relative width of H to K changes most rapidly when the density of the vapor is very low and the intensity of the lines is weak. As shown on page 63, the ratio of K_2 to H_2 at points at the center of the disk, where the line is greatly strengthened over faculae, is 1.09. The slight increase in the ratio at the center is in accord with the assumption that the lines are so strong that a considerable increase in thickness and density would not alter the ratio greatly, and hence is not in disagreement with the great increase in the thickness of the layer assigned to the emitting vapor, in passing from the center to the limb.

---

[1] *Mitteilungen der Nikolai-Hauptsternwarte zu Pulkowa*, 1, 157, 1906.

The quantitative relation connecting the width of a spectrum line with the thickness of the layer is unknown. The conclusion from the laboratory results is stated by Kayser as follows:[1]

> The width of lines is increased by the thickness of the layer only in those cases in which the curve representing the distribution of intensity within the line falls away slowly on one or both sides, not, on the other hand, when the form of the curve is steep or almost perpendicular on both sides.

The distribution of the intensity within the H and K lines corresponds to the first condition, and it may be assumed for these lines that increased thickness of the radiating or absorbing layer acts in the same direction as increased density. Layers of calcium vapor in the solar atmosphere lying between 700 and 3500 km and between 3500 and 5000 km would be consistent with the observed variations in the widths of K_2 and K_3, respectively, in passing from the center to the limb.

8. THE WAVE-LENGTH OF THE ABSORPTION LINE H_3

For reasons already given, the original plan was to limit the investigation to the K line of calcium; but, on certain plates taken for comparison of the iron arc with the center of the sun and subjected to strong development to bring out the lines in the broad shadings of H_1 and K_1, the H_3 line was particularly well defined, and it was possible to measure it with a good degree of accuracy. The iron lines λ 3966 and λ 3969 were used as solar standards for H_3. The wave-lengths of these lines in the arc have been measured by the writer with reference to the Fabry and Buisson standards and their wave-lengths found to be 3966.068 and 3969.261 respectively.[1] The results for the corresponding solar lines, determined from comparison plates for the iron arc and center of the sun and corrected for the rotation of the earth and the eccentricity of its orbit, are given in Table XVII.

---

[1] *Handbuch der Spectroscopie*, 2, 296.

TABLE XVII

SOLAR STANDARDS FOR H_3

Plate	Date	λ 3966	λ 3969
	1909		
396	October 6	3936.075	3969.269
398	" 6	.071	....
403	" 15	.074	.267
404	" 15	.072	.267
406	" 15	.070	.264
Means		3966.072	3969.267
Arc		3966.068	3969.261

The displacements between center and limb are assumed to be 0.005 Å—the mean of the shifts for λ 3930 and λ 3935 given in this paper and of shifts of other iron lines in this region as found by Adams.[2] The results for the wave-length of H_3 at the center of the disk are given in Table XVIII.

TABLE XVIII

WAVE-LENGTH OF H_3 AT THE CENTER OF THE DISK

Plate	Date	H_3	Plate	Date	H_3
	1909			1909	
404 (1)	October 10	3968.489	412 (4)	October 19	3969.498
405 (2)	" 15	.495	413 (1)	" 19	.487
405 (3)	" 15	.491	413 (2)	" 19	.494
405 (4)	" 15	.487	413 (3)	" 19	.491
406 (1)	" 15	.491	414 (1)	" 19	.489
406 (2)	" 15	.492	414 (2)	" 19	.488
406 (3)	" 16	.492	414 (2)	" 19	.491
412 (1)	" 19	.496	414 (4)	" 19	.495
412 (2)	" 19	.492	416 (1)	" 19	.484
412 (3)	" 19	.469	416 (2)	" 19	.491
Mean		3968.492	Mean		3968.491

---

[1] *Contributions from the Mount Wilson Solar Observatory*, No. 44; *Astrophysical Journal*, **31**, 143, 1910.

[2] *Contributions from the Mount Wilson Solar Observatory*, No. 43; *Astrophysical Journal*, **31**, 30, 1910.

A few plates were taken at 1 mm from the limb for comparing the widths of the H and K lines. Upon these also the wave-length of the H_3 line was measured with the results in Table XIX.

TABLE XIX

WAVE-LENGTH OF H_3 AT 1 mm FROM THE LIMB

East Limb			West Limb		
Plate	Date	H_3	Plate	Date	H_3
	1909			1909	
120	March 9	3968.479	120	March 9	3968.480
145	“ 10	.469	145	“ 10	.478
151	“ 11	.469	151	“ 11	.472
199	“ 31	.475	199	“ 31	.479
204	April 1	.469	204	April 1	.486
209	“ 9	.480	209	“ 9	.487
229	“ 15	.481	229	“ 15	.479
234	“ 16	.489	234	“ 16	.478
248	“ 26	.479	248	“ 26	.483
255	“ 27	.481	255	“ 27	.480
Mean		3968.477	Mean		6938.480

The results deduced from the measurement of H_3 show a satisfactory agreement with those of K_3, especially when it is considered that they depend upon only one-third the number of plates and consequently may be more affected by temporary conditions. The wave-length of H_3 at 1 mm from the west limb exceeds that at 1 mm from the east limb by 0.003 Å, indicating a higher rotational velocity of the calcium vapor than of the reversing layer, in harmony with the results for K_3 (p. 50). The wave-length of H_3 reduced to the limb is 3968.476. The following tabular arrangement exhibits the agreement between the measurements for the two lines.

	H_3	H_3-H_{arc}	K_3	K_3-K_{arc}
Center	3968.491	+0.015	3933.681	+0.014
1 mm from limb	3968.478	+0.002	3933.667	+0.000
At limb	3968.476	0.000	3933.665	−0.002
Arc	3968.476	......	3933.667	......

The weights of the measurements for K_3 are much greater than those for H_3 because of the larger number of the K_3 plates and their consequent wider distribution in time, thus eliminating the effect due to exceptional conditions, and because of the cleaner and better defined character of the K_3 line. The main conclusions in the paper are based therefore on the measurements of the K_3 line, confirmed as they are by the result for the H_3 line.

9. RELATIVE WAVE-LENGTHS OF H AND K IN THE SUN

Adams calls attention to a probable error in the relative wave-lengths of the H and K lines as given in the Rowland tables.[1] Various determinations of the arc value of this quantity are as follows:

H – K IN THE ARC

Rowland*	34.808 Å
Jewell*	34.809
Adams*	34.811
St. John*	34.809
Mean	34.809 Å

* *Contributions from the Mount Wilson Solar Observatory*, No. 44, pp. 1 and 6; *Astrophysical Journal*, **31**, 143 and 148, 1910.

According to these measurements, the difference between the wave-lengths of H and K in terrestrial sources is 34.809, with a very small probable error. The similar behavior of these lines in terrestrial sources would lead to the expectation of similar behavior under solar conditions. The relative wave-lengths of H_3 and K_3 at the center of the sun, found by practically the same observers, are as follows:

$H_3 - K_3$ IN THE SUN

Rowland's tables	34.800 Å
Adams	34.810
This paper	34.810

There can be little doubt, as Adams points out, that the relative wave-lengths of H and K in Rowland's tables are in error by 0.010 Å. It remains to be determined where the error is and how it is distributed between H and K. Using the wave-lengths given in Rowland's tables for the iron lines λ 3930, λ 3935, λ 3966, and λ 3969 as standards, the following results are obtained for H_3 and K_3, based upon the measurements used in calculating the wave-lengths given in this paper from the secondary standards of Fabry and Buisson. For comparison the wave-lengths of H and K given in Rowland's tables of solar wave-lengths are also shown.

---

[1] *Contributions from the Mount Wilson Solar Observatory*, No. 6, p. 8; *Astrophysical Journal*, **23**, 52, 1906.

	H	K	H−K
Rowland's tables...........	3968.625	3933.825	34.800 Å
This paper................	3968.634	3933.824	34.810
Mean of arc results.........	....	....	34.809

There can be little doubt from the above comparison that the error in the relative wave-lengths of H and K referred to arises from an error in the measurement of the H line in the solar spectrum. Such an error, if existing, would on a priori grounds be looked for in the measurement of H rather than in the measurement of K, for reasons, emphasized already in this paper, depending upon the character of the lines and their immediate surroundings.[1]

10. DISCUSSION

The appearance of the broad H and K bands in the solar spectrum has been noted by several observers. The general survey of the solar surface outside of spots and faculae made in this investigation shows the universal presence of the absorption line K_3, with a mean width at the center of the disk of 0.150 Å, and also the practically universal presence of the bright line K_2. This emission line is easily manifest at all points of the surface except near the center of the disk, and even there by properly timed exposures and strong development it can always be obtained. It varies much more in width and intensity than the absorption line K_3. Hundreds of plates have been examined for the breaking up of the broad shading of K_1 into the system of lines

[1] In this connection reference should be made to the wave-lengths of these lines found by Belopolsky, whose paper, "Untersuchung der *Ca*-Linien am Sonnenrande" (*Mitteilungen der Nikolai-Hauptsternwarte zu Pulkowo*, Band I, 164, 1906), has just come to hand. The copy in the Observatory library was lost in the fire on Mount Wilson.

	H	K	H−K
Arc single...........	3968.624	3933.836	34.788 Å
Arc reversed	3968.612	3933.804	34.808
Sun	3968.742	3933.881	34.761

noted by Jewell,[1] but no evidence of such a resolution of the lines has been found. The source of the high radiating power of the vapor producing the emission line K_2 has been attributed by Jewell to the impact of the collision, or the friction, between the falling meteoric matter to which he attributed the production of the absorption line K_3 and the ascending vapor. Hale and Ellerman suggest that it may not be entirely temperature radiation, saying:[2]

> From a strict application of Kirchhoff's law it would appear that the calcium vapor in the lower chromosphere is actually hotter than the calcium vapor which lies above and below it. It seems improbable that the law can be rigorously applied in this case, and hence it may be necessary to attribute the strong radiation of the intermediate layer to causes other than temperature alone. . . . The evidence afforded by photographs taken at successive levels goes to show that in passing from the lower K_1 region up into the K_2 region, the calcium vapor increases greatly in radiating power. For example, eruptive phenomena, which are quite inconspicuous when photographed at the lower K_1 levels, become more and more brilliant as the second slit is moved for successive photographs nearer and nearer to the center of K.

This last is very remarkable inasmuch as material thrown up by eruptions would be expected to have a high temperature and, while passing through the K_1 level, its pressure and density would be such as to broaden the line to the K_1 width.

In this paper it has been shown that the mean upward velocity of the vapor producing K_2 is 1.97 km per second, and the mean downward velocity of the absorbing vapor producing K_3 is 1.14 km per second. It is of interest to consider the loss of mechanical energy suffered by two unit masses of vapor approaching each other with these velocities on the supposition that by collision and internal friction they are reduced to a common velocity. The resulting velocity would be 41.5×10^3 cm per second and the total loss of mechanical energy 2421×10^7 ergs or an equivalent of 578 calories. A small fraction of the liberated energy would suffice to raise the temperature of the calcium vapor sufficiently to account for the increased radiation since, as King has shown, the H and K lines of calcium are high-temperature lines. He says[3] that

---

[1] *Astrophysical Journal*, **3**, 108, 1896.

[2] *Publications of the Yerkes Observatory*, Vol. III, Part I, pp. 16–18.

[3] *Contributions from the Mount Wilson Solar Observatory*, No. 32; *Astrophysical Journal*, **28**, 389, 1908.

> the production of H and K is more complex, but the furnace shows that they may be obtained if the temperature is sufficiently high . . . . without the aid of chemical action. . . . . They are to be rated as high-temperature lines by reason both of the temperature required for their production, and because their increase of strength in the furnace is closely proportional to the temperature—very much more so than in the case of λ 4227.

And again, in a later paper:[1]

> The H and K lines show a very definite behavior when compared with representative arc lines, such as the group near λ 4300. . . . . These arc lines are of fair strength at a temperature just high enough for H and K to become visible. As the temperature rises, H and K increase in intensity (though without decided widening) much faster than do the arc lines, surpassing at the higher furnace temperatures the strongest lines of the λ 4300 group. If this rate of increase is maintained at higher temperatures, the strength of H and K in the arc may easily follow.

If the few hundred degrees between furnace and arc temperatures are sufficient to account for the great change in the intensities of the H and K lines in the two sources, an increase in the temperature of the calcium vapor at the K_2 level of a few hundred degrees would easily account for the higher radiating power of the vapor producing K_2 provided a similar rate of increase in intensity with temperature holds under solar conditions; but here, as in all extra-terrestrial conditions, our only basis for reasoning is the extension of terrestrial laws.

A theoretical value for the specific heat of calcium vapor may be obtained from the following considerations. Calcium is considered to be a monatomic element for which the ratio between the specific heat at constant pressure to the specific heat at constant volume is 1.67. The external work done when a gram-molecule of any gas is raised in temperature one degree centigrade under a constant pressure of one atmosphere is about 2 calories. In the case of a monatomic gas for which the ratio is 1.67 the total heat required to raise the temperature of a gram-molecule one degree is therefore 5 calories. The molecular weight of calcium being the same as its atomic weight, namely 40, its specific heat in a gaseous state would be 0.125. Assuming this value of the specific heat of calcium vapor under solar conditions, the 578 calories of heat resulting from the loss of mechanical energy would raise the temperature of the two unit masses of calcium vapor 2300° C. Other matter, however, is also present, notably hydrogen, to share in the distribution of the energy, and the assumed changes of velocity are probably only partly realized. But with liberal deductions on these grounds, there might still be sufficient heat available to raise the temperature a few hundred degrees. The observed velocity upward may be a resultant velocity, in which case the original upward velocity would be 5.08 km per second, and the loss of mechanical energy fourfold that assumed above.

---

[1] *Contributions from the Mount Wilson Solar Observatory*, No. 38; *Astrophysical Journal*, **29**, 381, 1909.

The fact noted by Hale and Ellerman of the increased radiating power of the calcium vapor in passing from the K_1 to the K_2 level, even in the case of eruptive phenomena, would follow if the temperature of the upper K_2 level were raised and its radiation increased by the meeting of the opposing ascending and descending currents at that relatively high level. The K_2 emission line is too narrow to admit of its being produced by a layer of highly radiating vapor reaching down to the photosphere, where it would be subjected to great pressure. Under such conditions it would have at many points a width equal to that of K_1, a width to which it does not even approximate. Over faculae and around spots, where such conditions must obtain if anywhere, it does not ordinarily reach a width of 0.75 Å, and its edges are well defined, while Hale and Ellerman, in the case of H_1 and K_1, were able to set the second slit of the spectroheliograph 5 and 6 Å from the center of the lines in photographing the low-level calcium and still obtain the characteristic distribution of the low-level vapor showing a practically effective width of 10 to 12 Å for these lines. The radiating power of the calcium vapor appears to increase progressively with increase of height above the K_1 level and to reach its maximum at a considerable elevation, and then to decrease rapidly with further increase in height. The facts point to a cause residing in the region of increased radiation which would be supplied by the transformation of mechanical energy suggested above.

In stating that the vapor producing the K_3 absorption line is descending, it must be understood that the statement refers to the average or more frequently recurring condition. Differences in the measurement of individual lines and of different parts of the same line occur which are greater than the errors of observation and indicate wide variation of the velocities.

If the explanation of the high emissive power of the vapor producing K_2 suggested in this paper represents the true condition of the vapors, there must be a transition layer where the ascending and descending currents meet and intermingle, sometimes one prevailing and sometimes the other, though for the emitting vapor the result is a preponderating upward movement, while for the absorbing vapor the result is a downward movement on the whole. Such must be the condition of the opposing currents, since the upper level is continually reinforced from below, and in general as much vapor reaches the higher levels as descends from them. The generality of the descending motion of the absorbing vapor is at first surprising in view of the constant supply from the lower level. The more intense portion of the absorption lines, however, may be thought of as produced by the cooler vapors descending from the higher level. The upper levels of the intermediate radiating layer expand by decrease of pressure, cool, and continue to rise with a lower and ever-decreasing velocity. As long as their radiating power is comparable with that of the strata to which H_2 and K_2 are mainly due, their decreasing velocities would tend to shift toward the red the center of gravity of the H_2 and K_2 lines due to the more rapidly rising and more highly radiating vapor below. This shift toward the red of the center of the emission lines would be masked by the central absorption line. In the transition state between effectiveness as an emitting and as an absorbing body these layers would not manifest themselves strongly. After their absorption becomes effective and the movement is only slowly upward, the effect would be to strengthen or widen on the violet side and weaken or narrow on the red side the absorption lines due to the cooler and more effective descending vapor, and more or less completely overcome the shift toward the longer wave-length, or at least change the character of the K_3 lines. The average width of K_3 at the center of the sun is 0.150 Å and the average shift is 0.015 Å, so that within the borders of the absorption line resultant effects might be produced which would show as changes of intensity and displacements of the center of gravity, such as are frequently observed.

The slight astigmatism of the grating may have been an advantage in smoothing out irregularities of the lines due to variations of velocity in closely contiguous regions, so causing the preponderating velocities to be more generally manifest. The same result is favored by the fact that a length of 4 mm of the line was in the field of view of the microscope and the setting of the cross-hair was doubtless somewhat influenced by the whole portion of the line in view. It was the practice in obtaining the plates for Tables II–IV to make three exposures on the center, changing the position of the sun's image upon the slit for each exposure. The one most suitable for measurement was selected; and occasionally two were measured, and not infrequently measurements were made at two or three points of the K_3 line on the plates of the limb and center, of which the means only are given in the tables. For these reasons the measurements for K_3 represent less completely the variations in velocity from point to point than the resultant or preponderating velocity. The K_3 absorption line is then the integrated effect due to masses of calcium vapor differing in absorptive power and in velocity, in which the influence of the cooler descending masses is most pronounced. In regions where this absorption is effective, the intermingling of upward and downward moving masses of vapor must result in great turbulence over the general surface; but the data of this investigation show no evidence of the localization of definite regions where upward currents prevail.

In the case of the vapor producing the emission line K_2, the movement is one of ascent over the general disk, though its generality may be more apparent than real. It may rise through the photosphere at definite but closely adjacent points and expand laterally while ascending and so cover the surrounding region. There are indications that this may be the true condition in the wavy outer borders of the emission line and the consequent beaded form of the line, which is sometimes very apparent. Careful comparison of the spectrum of the K line taken with a long slit and a calcium spectroheliogram, made in close proximity of time and with solar images of the same diameter, reveals complete coincidence between slightly widened and intensified portions of the line and the minute calcium flocculi. This is in harmony with the working hypothesis adopted by Hale and Ellerman in which they say:[1] "It is considered that these minute flocculi are columns of calcium vapor, rising above the columns of condensed vapors of which the photospheric 'grains' are the summits."

---

[1] *Publications of the Yerkes Observatory*, Vol. III, Part I, p. 15.

In the measurement and reduction of the plates the bright components of the K line have been considered as part of the same line of which approximately the central portion is cut out by the absorption line K_3. The satisfactory way in which the points fall on the curve shows that this point of view is without doubt the correct one. It is difficult to reconcile it, however, with the observations of Belopolsky, who says:[1]

> Bemerkenswert ist, dass die Componenten der *Ca*-Linien oft ganz von einander unabhängige, verschiedene Geschwindigkeiten (Verschiebungen) zeigen. Ich besitze Spectrogramme vom Jahre 1906, auf welchen die Linien H_1 und H_2 und K_1 und K_2 sich ausserhalb des Sonnenrandes kreuzen, ohne irgendwo zusammenzufliessen.

The writer understands that the subscripts 1 and 2 refer to the red and violet components, respectively, of the H and K lines. Such behavior of the bright components of H and K would be very remarkable and indeed inexplicable upon any current conception. Confirmation of such anomalous effects would be desirable. In the plates taken by the writer with a radial slit across prominences, the appearance has been quite different. The bright components form a broad line projecting a short distance beyond the limb, where in general they narrow rapidly into a less intense, single, fine line extending to the photographic height of the prominence. Less often the line shows a reversal. It is frequently wavy and distorted by the motion of the vapor in the line of sight and sometimes discontinuous, but otherwise entirely normal in appearance.

To determine whether the up-rush of the calcium occurs at all points of the solar surface or whether it is more or less localized, that is, limited to the granulations, a larger solar image is necessary, on which there will be a sufficient separation of the granulations. Such an image 425 mm in diameter will be produced by the new tower telescope of 150 feet (45.7 m) focal length now under construction, and with it the question will be taken up again. On such an image it will be possible, it is hoped, to separate the effects over the photospheric grains from the effects over the interspaces.

Owing to the fact that this investigation has been mainly devoted to the general chromospheric calcium, that is, to the regions outside of faculae and spots, the bearing of the results upon the interpretation of spectroheliograms taken with the second slit inclosing the H_2 or K_2 emission line is important in respect to the less conspicuous and less frequently considered features of the disk. Such a calcium spectroheliogram presents over the general surface a mottled appearance in which the relative dark background is very extensive compared to the small, scattered, and irregularly shaped bright regions. The question arises as to what the background is due. The bright regions have always been attributed to H_2 or K_2. An inspection of hundreds of spectra taken at the center, limb, and intermediate points of the disk, with the H and K lines and with a long slit, shows that the bright emission line is present at every point of the disk, though at times quite inconspicuous over the central regions. It varies greatly in width and intensity, with occasional marked increases of intensity and breadth over short distances. From the universality of its presence the general background of the calcium spectroheliogram may as confidently be assigned to it as are the brilliant flocculi.

---

[1] *Mitteilungen der Nikolai-Hauptsternwarte zu Pulkowo*, 1, 160, 1906.

In the study of such spectroheliograms it should be borne in mind that they are taken with equal exposure times for limb and center. If it were possible to give graduated exposure times, such that the continuous spectrum of the background would be of the same intensity, the spectroheliogram would present a very different appearance. With such exposure times the bright K_2 line for a considerable distance from the limb is as broad and intense as at the center over the faculae, and a spectroheliogram corresponding to such condition would show a border of very brilliant calcium extending some distance inward from the limb, in contrast to the weak and inconspicuous peripheral regions usually shown on such. For equal exposure times the bright K line near the limb is reduced to a lower intensity than at the center, so that notwithstanding the inherent greater intensity of the emission components due to the increasing depth of the radiating layer on approaching the limb, the usual spectroheliogram shows in the peripheral region the same general appearance as over the central portions of the disk. This perhaps is an advantage from some points of view, but for a complete interpretation it is necessary to keep in mind how the actual distribution in the solar atmosphere of the calcium vapor producing the emission lines H_2 and K_2 would manifest

PLATE IX

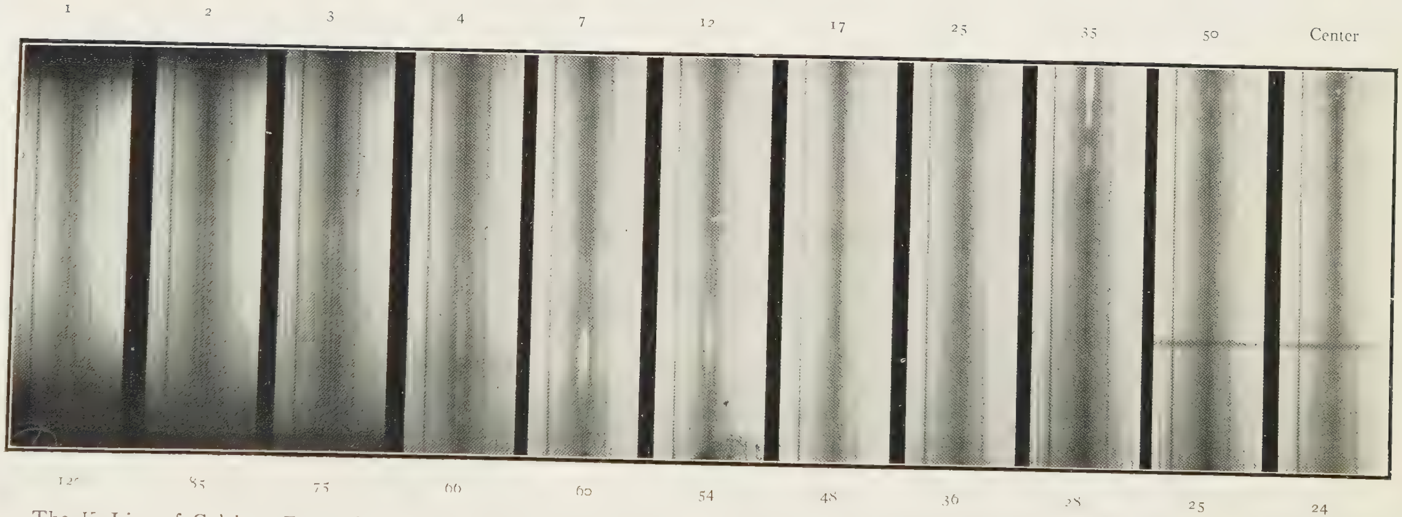

The K Line of Calcium Exposed to Obtain Uniform Intensities. 1909, November 3. Distances from East Limb in Millimeters Above
Exposure Times in Seconds Below. Enlargement 1.4

PLATE X

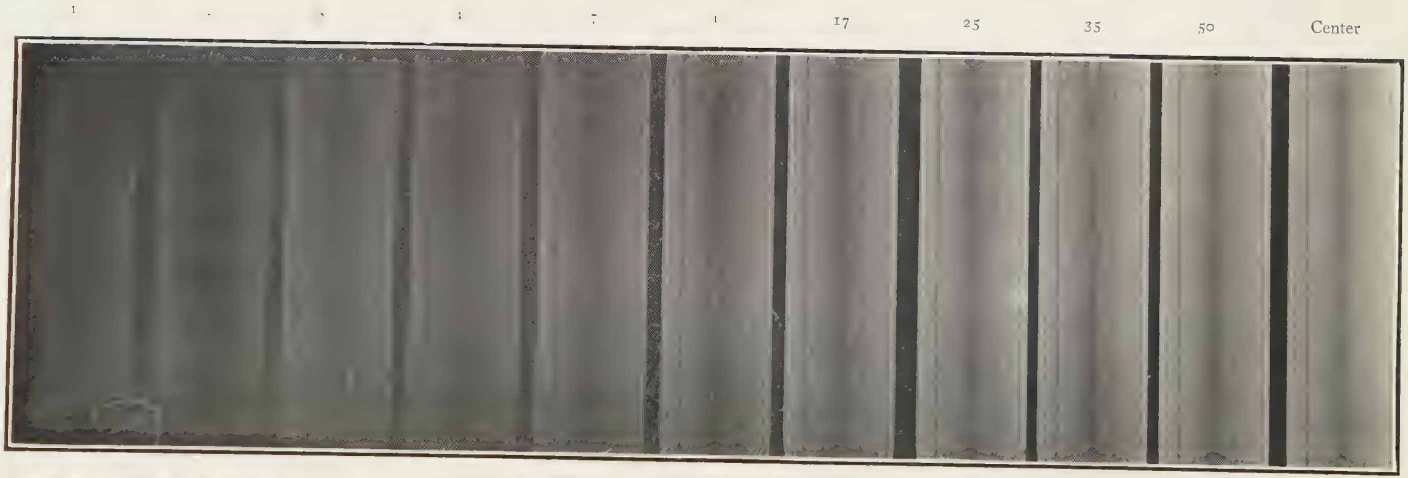

The K Line of Calcium with Constant Exposure Time of 24 Seconds. 1909, November 3. Distance from East Limb in Millimeters Above
Enlargement 1:4

PLATE XI

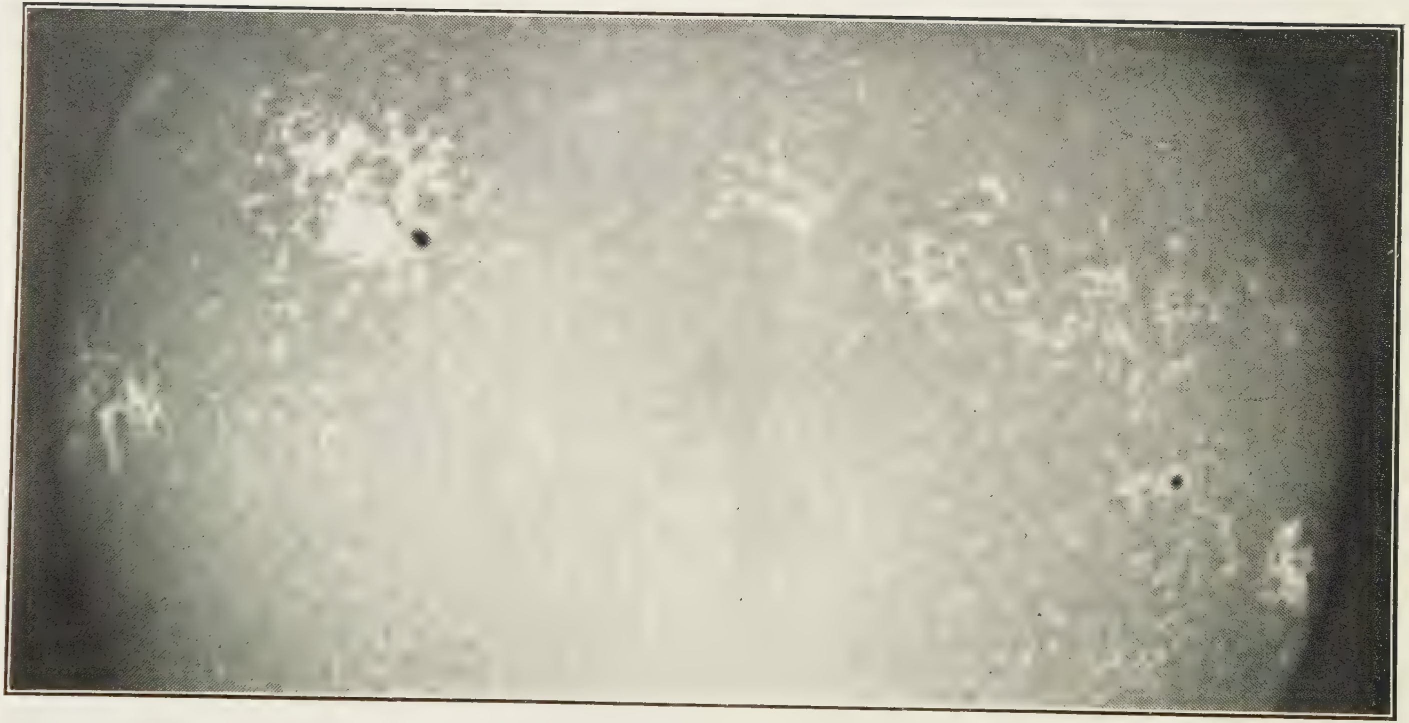

H_2 Spectroheliogram of 1909, November 3. Scale of Original Negative itself under photographic conditions allowing intensities more nearly proportional to the effective thickness of the radiating layer.

Plate IX is a reproduction of a series of exposures from the east limb to the center, timed for nearly uniform intensity. The distances from the limb in millimeters are given above, and the exposure times in seconds below. The progressive widening of the K_2 and K_3 lines in passing from the center to the limb can plainly be seen on the reproduction, and, less distinctly, the increasing dissymmetry of the emission components on passing from the limb to the center. The enlargement is 1.4. Plate X is a reproduction on the same scale of a series of equal exposures at the same points, and Plate XI one, in original size, of the corresponding section from the H_2 spectroheliogram of the same date, so that the positions at which the spectra are taken can be identified and a direct comparison made between corresponding points. The reproduction of the spectroheliogram has been made without any attempt to change the contrast at the limb, and represents more nearly the effects that follow equal exposure times than do the customary reproductions.

GENERAL SUMMARY

1. The calcium vapor producing the absorption line K_3 in the solar spectrum has a descending motion over the general surface of the sun of 1.14 km per second in the mean, as indicated by the progressive increase in the wave-length of the absorption line in passing from the limb to the center of the sun, where the shift toward longer wave-lengths amounts to 0.015 Å. This increase in wave-length corresponds with a high degree of exactness to the calculated line-of-sight component of a radial motion deduced from the observed displacements of 0.015 Å at the center. The agreement is so close that it is not probable that causes other than the downward movement are involved in the mean result. Other causes, if they exist, are occasional and diverse in their action, and their effects are eliminated from the final mean.

2. The calcium vapor to which the bright emission line K_2 is due has an ascending motion over the general surface of the sun of 1.97 km per second in the mean, as indicated by the progressive shortening of the wave-lengths of the emission line on passing from

the limb to the center of the sun, where it reaches a maximum of 0.026 Å. This decrease in the wave-length agrees with the line-of-sight projection of a radial motion of ascent deduced from the displacement of 0.026 Å at the center with such a degree of exactness that, in view of the difficulties involved in the measurements, causes of decrease other than the radial upward movement of the vapor are practically without effect upon the final mean. Such causes, if acting, must be casual.

3. The angular velocity of the high-level calcium vapor producing the absorption line K_3 is nearly constant for the latitudes of observation, being 15°.5 and 15°.4 per day at latitudes 6°.6 and 38°.4, respectively. The corresponding values deduced from Adams' results are 15°.1 and 14°.3 for hydrogen and 14°.4 and 13°.2 for the reversing layer. The high velocity of the calcium vapor producing the K_3 line points to a higher elevation of this layer of calcium vapor than of the hydrogen effective in the production of the *Ha* line.

4. The wave-lengths of K_2 and K_3 reduced to the limb are 3933.667 and 3933.665^5 respectively. The corresponding wave-length in the arc at atmospheric pressure is 3933.667. The mean pressure in the intermediate emitting layer is therefore approximately one atmosphere, but in view of the small pressure-shift as observed by Humphreys and Mohler, the shorter wave-length of the K_3 line may be interpreted as indicating a somewhat lower pressure in the upper absorbing layer, though the smallness of the quantities involved does not permit a positive conclusion.

5. The mean wave-lengths of K_2 and K_3 at points 12 mm from the limb in equatorial regions are 3933.650 and 3933.675, respectively, and at points 12 mm from the limb in polar regions 3933.649 and 3933.676, respectively. The practical agreement for the two positions shows in the case of the intermediate and highest levels of calcium vapor the absence of currents of appreciable velocity parallel to the solar surface.

6. The widths of H_3 and K_3 at the center are 0.128 Å and 0.150 Å, respectively; their widths at 1 mm from the limb are 0.306 Å and 0.345 Å. The widths of these lines at the center compared to the corresponding widths in the arc point to an extremely small quantity of the calcium vapor in the upper levels of the solar atmosphere.

7. The ratio of the widths of K_3 to H_3 at the limb is 1.13; the ratio at the center is 1.17. Experiments with calcium in the arc show that their ratio increases with decrease in the density of the vapor and with weakening of the lines. The assumption of a thin layer of low density with consequent great increase in effective depth on approaching the limb accounts for both the absolute and relative changes in width. The ratio of the width of K_2 to H_2 at the limb is 1.07; the ratio at the center obtained from a small number of intensified lines is 1.09. The low ratio and the small change in the ratio between the limb and center both indicate a relatively dense and thick layer of the emitting vapor as compared with the absorbing layer, since the ratio is the nearer unity the stronger the lines, and the increase of the ratio is marked when lines already weak are still more decreased in intensity.

8. The average appreciable height of the chromospheric calcium shown by a radial slit is about 5000 km above the photosphere. The thickness of the upper absorbing layer is approximately 1500 km. Allowing 700 km for the reversing layer, the emitting layer would have a thickness of approximately 3000 km. The elevation at which the K line is appreciable is about 500 to 600 km above the level at which the H line ceases to show.

9. The wave-length of the H_3 line from 20 plates is 3968.491, 3968.478, and 3968.476, at the center, 1 mm from the limb, and at the limb, respectively. The shift between limb and center is 0.015 Å for the H_3 line, and in agreement with that obtained from the K_3 line.

10. The difference between the wave-lengths of H_3 and K_3 found in this investigation is 34.810 Å. The mean difference between H and K in the arc is 34.809 Å. The difference between H and K in Rowland's tables is 34.800 Å. The indicated error of 0.010 Å in the relative wave-lengths of H and K is in accord with that found by Adams.

11. When the wave-lengths given in Rowland's tables are used for the standards in reducing the measurements upon which the results given in this paper for H_3 and K_3 depend, the wave-lengths of H_3 and K_3 are λ_R 3968.634 and λ_R 3933.824, respectively; the corresponding wave-lengths from Rowland's tables are 3968.625 and 3933.825. The discrepancy occurs in the measurement of the

H line, as would be expected from the poorly defined character of the line in general.

12. A cause for the high radiating power of the emitting layer may be found in its increased temperature resulting from the transformation into heat of the mechanical energy set free by the loss of velocity in the opposing upward and downward currents.

13. The justification for the assumption of a high level, small depth, and extreme tenuity for the absorbing layer is found in the measurements with the radial slit, in the low pressure suggested by the slightly lessened wave-length of the K_3 line, in the narrowness of the absorption lines as compared with their widths in terrestrial sources, in the continued increase in absolute width on passing from the center to the limb, in the increase of the relative width of K_3 to H_3 on passing from the limb to the center, and in the high and nearly constant angular velocity. None of the facts is in disagreement with any part of the assumption and each supports one or more components of the assumption.

MOUNT WILSON SOLAR OBSERVATORY
May 1910

Reprinted from the PHYSICAL REVIEW, Vol. XXXII., No. 1, January, 1911.

VOLUME IONIZATION PRODUCED BY LIGHT OF EXTREMELY SHORT WAVE-LENGTH.

BY FREDERIC PALMER, JR.

INTRODUCTION.

IN 1900 P. Lenard[1] showed that in addition to the well-known Hallwachs effect, or ionization produced at a charged metallic surface when struck by ultra-violet light, there existed also a volume effect which took place in the gas itself, and could be detected at some distance (50 cm.) from the source of illumination. He employed a spark from an induction coil between terminals of aluminum. Since the light from this spark passed through a quartz window and a layer of air more than one centimeter thick it is very unlikely that it contained any effective rays of wave-length less than λ 1800. It seemed worth while, therefore, to investigate the effect of that part of the spectrum discovered by Schumann[2] which lies on the more refrangible side of λ1800. The present research was accordingly begun in February, 1904.

Lenard[1] showed that the ionization observed by him was closely connected with the absorption of ultra-violet light by the gas under investigation. Therefore, since it is known that wave-lengths in the Schumann region are completely absorbed by a thin layer of air at atmospheric pressure, the object of this research was to find out if possible whether this absorption was accompanied by ionization; and if so, whether this result increased as the wave-length of the effective light diminished.

---

[1] Ann Phys., 1, p. 486, 1900; 3, p. 298, 1900.

[2] Smiths. Contrib. No. 1413, 1903; T. Lyman, Astroph. Journ., 23, p. 181, 1906.

E. Bloch[1] has shown that volume ionization produced by the light from an aluminum spark is greatly reduced if the gas under investigation is filtered through a plug of cotton wool; and he therefore has ascribed the effect observed by Lenard to photo-electric particles held in suspension in the gas, and not to ionization of the gas itself. More recently J. Stark[2] from other considerations has stated that the Lenard effect is probably due to photo-electric particles in the gas. He has also shown that volume ionization may be produced by the light from a quartz mercury lamp in certain organic vapors. The effective wave-lengths lay in the region between λ1850 and λ3800. He obtained currents through the vapors as large as 5×10^{-9} amp. under a pressure of about 50 mm.

J. J. Thomson and W. C. McKaye[3] have found that the light from a Wehnelt hot lime-covered cathode produces ionization in air, carbon dioxide, and ammonia; but the currents obtained by them were excessively small.

In this paper it will be shown that comparatively large currents may be obtained in air at atmospheric pressure when the extremely short wave-lengths which lie in the Schumann region are used as a source of illumination.

Before undertaking the main part of the research, Lenard's experiments were repeated both with the steam-jet and with a cylindrical condenser as the detecting apparatus. A Dolezalek electrometer instead of an electroscope was used to measure the leak between the cylinders. The chief sources of error were : (1) irregularities in the illumination produced by the aluminum spark; (2) the Hallwachs effect, which was eliminated by the proper use of soap solution; (3) photo-electric fatigue,[4] which resulted in the falling off of deflections obtained successively in the electrometer under apparently similar conditions.

GENERAL ARRANGEMENT.

Since it is purposed to employ the very short wave-lengths in the Schumann region, the form of the source of light is of the utmost importance. It has been shown[1] that, when the secondary of a transformer is connected without additional capacity to the electrodes of a hydrogen-filled discharge tube containing traces of hydrocarbons, the excitation of the tube gives rise to carbon bands extending from the ultra-violet down to λ1700, and to strong hydrogen lines from λ1650 to λ1250. It was therefore determined to use a tube of this type as the source of illumination. While it is recognized that the carbon bands are capable of producing ionization, this investigation is chiefly concerned with the properties of the shorter waves; and therefore in order to get rid, as much as possible, of the effect produced by the carbon bands the tube was always carefully washed out with pure dry hydrogen several times before use.

---

[1] Comptes Rendus, 146, 17, p. 892.

[2] Phys. Zeitsch., 10, 18, p. 614.

[3] Proc. Comb. Phil. Soc., 14, p. 417, 1908.

[4] Cf. Hallwachs, Phys. Zeitsch., 21, p. 766, 1906.

The apparatus for producing ionization consisted essentially of three parts: (1) the discharge tube, (2) the screen cell, (3) the ionization chamber (see Fig. 1). The discharge tube *A* was a duplicate of the one already described by Lyman.[2] It could be exhausted by a mercury pump and filled with dry hydrogen from a small electrolytic generator. The pressure within could be measured by a McLeod gauge. The tube was excited from the secondary of a small transformer, the primary of which used about 4 amp. from a 110-volt A.-C. lighting circuit. The current through the tube, as measured by Pierce's crystal rectifier,[3] proved to be between .03 and .04 amp.

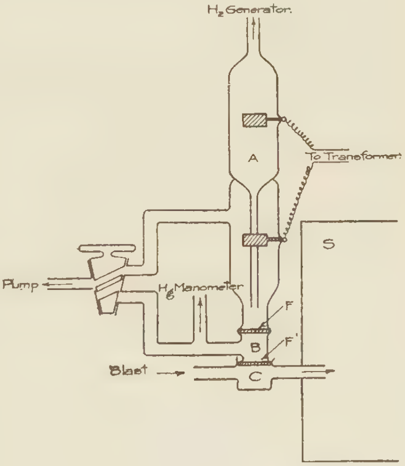

Fig. 1.
Apparatus for producing ionization.

The screen cell *B* was used as a diaphragm to cut off more or less of the effective rays according as the pressure in it was varied.

---

[1] T. Lyman, Astroph. Journ., 23, p. 181, 1906.

[2] *Loc. cit.*

[3] Phys. Rev., 25, p. 31, 1907.

It was 1 cm. in diameter and 1.0 cm. thick, and was separated from the discharge tube by a window of clear white fluorite *F* 1 mm. thick cemented with Khotinski cement. Ordinarily oxygen was used in the cell as an absorbing gas because its behavior was found to be more regular, and its absorption was better known than that of other gases. Dry oxygen could be admitted to the cell from a small electrolytic generator, and the pressure could be read either upon a closed mercury manometer or the McLeod gauge. A three-way stop-cock connected either the cell or the discharge tube to the mercury pump.

Another clear fluorite window *F′* 1 mm. thick separated the screen cell from the ionization chamber *C*, but the latter was arranged to slip over *F′* before being cemented in place so that the under surface of *F′* could be brought to a level with the side tubes of *C*. A blast of the gas under investigation could be maintained through *C* so that the ions, which were formed in this chamber, could be speedily swept away into the testing cylinders. The volume of the chamber was 1.4 c.c., and the distance between its center and the test cylinders 3 cm. Early in the investigation an ionization chamber was used which was open at the bottom so that a vessel containing mercury covered with soap solution could be raised from below to close the opening, and thus prevent surface ionization. However the soap solution was found to be the source of many irregularities in readings obtained, and so the form shown in Fig. 1, made of glass, was finally adopted. A comparison of readings obtained with the two chambers showed almost identical results, which may indicate that the ionization produced by light

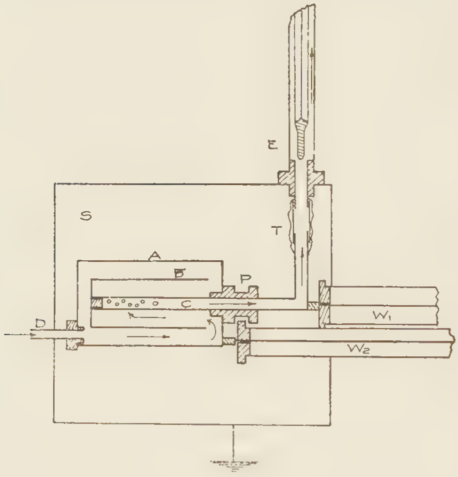

Fig. 2.
Testing apparatus.

of extremely short wave-length is confined to a region very close to the fluorite window F'. The velocity of the gas blast was maintained nearly constant. The value of the velocity was measured by a small open water manometer.

The apparatus for investigating the state of the gas issuing from the ionization chamber consisted of two parts: (1) the test cylinders, (2) the electrometer and its connections (see Fig. 2). The test cylinders of brass consisted of a concentric system of which the outside one A was closed at both ends by brass caps screwed on air-tight. It was 6.0 cm. long and had an inside diameter of 3.5 cm. The inner cylinder B was 5.0 cm. long and 2.0 cm. in diameter outside. The end nearer to the incoming gas was closed with a brass cap. A small brass tube C 0.4 cm. in diameter held B in place. The gas entered the system through the glass tube D which was placed opposite the annular space between A and B. The gas left the cylinders through the holes in the tube C. Thus the gas had to travel down between the cylinders, turn and pass up inside of B, turn again as it entered C, and pass along it for some 15 cm. before finally emerging past a thermometer. It thus seemed probable that even with a small potential gradient between the cylinders and a fairly rapid rate of flow of the gas, it would be possible to catch all of the ions before the gas escaped into the air. This assumption seems to have been justified by the actual performance of the apparatus. The tube C was insulated from A by the vulcanite plug P. A short piece of rubber hose covered with tin foil T connected C to the exit tube E. A stiff wire W_1 connected to C led through a grounded brass tube into the cabinet containing the electrometer and its connections. A similarly screened wire W_2 could be screwed to A, and by means of it A could be charged to any desired potential by a suitable storage battery. The entire cylinder system was enclosed in a large brass cylinder S, 10 cm. in diameter, which could be grounded and thus screen the testing apparatus from all outside influences. The Dolezalek electrometer after being properly adjusted, as described by Rutherford,[1] had a very slight normal leak, and could be made to have a sensitiveness of anything up to 7,500 scale divisions per volt P.D. between the quadrants. The electrometer needle was suspended by a fine quartz fibre, and was charged from a water-battery by contact, usually to a potential of 40–100 volts. The electrometer was placed inside a cabinet lined with tin foil, and all contacts with it were made without opening the cabinet by means of levers operated by strings from the observer's seat. Either pair of quadrants could be connected (1) to the ground, (2) to a source of known E.M.F., (3) to the test cylinders. Deflections of the electrometer needle were read with a telescope and scale at a distance of about 2 meters. A standard cadmium cell of potential $V = 1.0177$ volts was used for calibrating the electrometer. On account of the sensitiveness of this instrument it was necessary to tap off a known fraction of the E.M.F., and suitable resistances were used in a simple potentiometer device to give one-eleventh the E.M.F. of the standard cell.

---

[1] Radioactivity, 2d ed., p. 95.

In using the apparatus it was desirable to know the pressure in the discharge tube which would produce the maximum effect in the ionization chamber. A preliminary experiment in which the pressure of air in the screen cell was kept at a low constant value (about .15 mm.), while the pressure of hydrogen in the tube was varied, showed a sharp increase in the effect up to a pressure of 1 mm. and a more gradual diminution from that point up to 10 mm. In all subsequent work, therefore, the pressure in the discharge tube was kept at an approximately constant pressure of 1 mm. This was also the pressure giving a maximum brilliancy when the tube was excited, though it did not correspond, as might have been expected, to the passage of maximum current through the tube, as was shown by measuring this current by means of Pierce's crystal rectifier. The maximum for the current took place at a pressure of 0.3 to 0.4 mm. To obtain constant results it was necessary that the tube should be excited for a constant short interval of time. A long excitation, by heating the tube, might set free occluded gases and thus change the pressure and therefore the tube's effectiveness. To this end a contact-maker was employed which illuminated the tube for one and one-fourth seconds. This instrument was tested for constancy of operation by connecting it to a chronograph. The greatest deviation from the mean of seven readings proved to be 2.25 per cent.

Another factor which it was necessary to make constant was the velocity with which the gas to be tested was blown through the ionization chamber. This was done by choosing arbitrarily a value on the water manometer which gave a deflection in the electrometer of the desired amount and then regulating the blast so that the manometer indicated this same reading each time an observation was made. The mean error of setting the blast repeatedly upon an arbitrarily chosen manometer reading was found to be about 2 per cent.

During an experiment it has been noticed repeatedly that apparently identical conditions gave rise to electrometer deflections which differed from one another by about five per cent. It seems that practically all of this may be accounted for by variations in the blast and length of exposure.

Manipulation.

Lyman[1] has found that the absorption of light in the Schumann region by oxygen is in the form of a band; and that, as the pressure increases, the absorption spreads much more rapidly toward the less refrangible side than in the other direction. For a column of gas 1 cm. thick at atmospheric pressure the band extends from λ1268 to λ1770, and for a pressure of .02 atmosphere from λ1350 to λ1500.

If oxygen is admitted to the screen cell at pressures varying from .0001 to 1 atmosphere, more and more of the effective rays from the discharge tube will be absorbed in passing through it. Thus the ionization produced in the chamber should be reduced with each increase of pressure in the screen cell. The wave-lengths which are available for the production of ionization in the chamber are those which get through the screen cell at any given pressure, and these may be determined when the width of the oxygen absorption band for the given pressure has been found.

The method of procedure in getting the relation between the two quantities—light entering the ionization chamber, and resultant ionization— is as follows: The pressure in the screen cell is reduced very low and measured on the McLeod gauge. A gas is allowed to blow through the ionization chamber and test cylinders at the desired constant velocity as indicated by the water manometer. Before reaching the chamber the gas has to pass through 30 cm. of glass wool and over 25 cm. of calcium chloride and 25 cm. of phosphorus pentoxide. It is therefore assumed to be dust-free and dry. While one pair of quadrants in the electrometer is kept in connection with the earth, the other pair, connected with the inner of the test cylinders, is now insulated. The contact-maker is set in motion and allowed to excite the discharge tube once. Shortly after the illumination ceases the stream of gas is shut off, and the resulting deflection in the electrometer observed. Both pairs of quadrants, together with the inner test cylinder, are then connected to earth, and oxygen from the electrolytic generator carefully dried over phosphorus pentoxide is admitted to the screen cell changing the pressure therein by a desired amount, as indicated by the closed mercury manometer. The tube is again excited, the resulting deflection made, and so on.

---

[1] Astroph. Journal, 27, p. 87, 1908

Since, as has already been shown, the light of short wave-length entering the ionization chamber depends upon the pressure of oxygen in the screen cell, and since the electrometer deflections are very nearly proportional to the resulting ionization, curves have been obtained showing the relationship existing between these two quantities for different gases. None of the gases used produced measureable deflections when blown unilluminated by the discharge tube through the test cylinders.

Oxygen.

Oxygen, 92 per cent. pure, made by the potassium chlorate black oxide of manganese process and put up in a cylinder under pressure, was passed through distilled water, then through two large U-tubes each arm of which contained 10 cm. of phosphorus pentoxide held in place by plugs of glass wool. These were supported vertically so that the oxygen was forced slowly through the phosphorus pentoxide, not over it. The gas was collected over mercury and finally blown through the ionization chamber. Glass tubing only was used for all connections. After passing the entrance to the water manometer the oxygen was again dried over phosphorus pentoxide before finally entering the chamber. With oxygen thus dried results were obtained which the curve showing pressures of oxygen in the screen cell, in centimeters of mercury, plotted against electrometer deflections is given in Fig. 3, *A*. Since the outer of the test cylinders (*A*, Fig. 2) was charged to a potential $V = -20$ volts, this curve represents the negative leak between the two cylinders. A large proportion of the work has been done with the outer test cylinder at a constant potential $V = \pm 20$ volts. The saturation curves (not here shown) which have been obtained, show that for the gas velocities generally used this value of the potential was sufficient. The gas was at a temperature of 24° C., and its velocity through the ionization chamber was 20 cm./sec. The electrometer had a sensitiveness of 165 cm. per volt P.D. between the quadrants, and its capacity, together with that of the test cylinders and connections was 111 cm., or $111/9 \times 10^{-11}$ farads. Taking the maximum deflection in the above curve, it is easy to see that the insulated pair of quadrants has acquired a potential $V = 55/165$ volts, and, since $Q = VC$, $Q = 55/165 \times 111/9/\times/10^{-11}$, or 4.2×10^{-11} coulombs. If it is assumed that the average current may be obtained by dividing this quantity

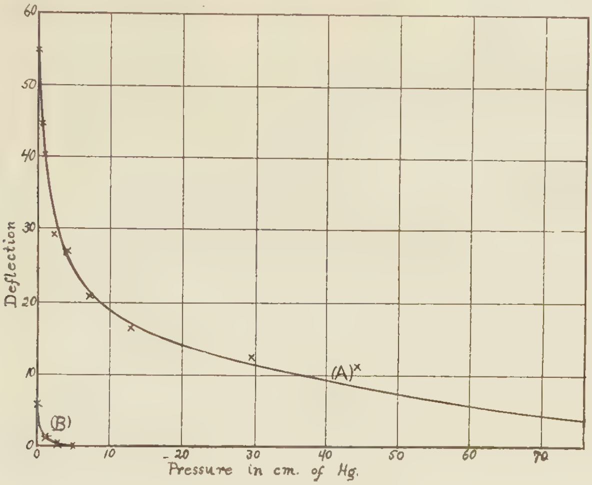

Fig. 3.

(*A*) Negative leak. Oxygen. (*B*) Negative leak. Hydrogen.

by the time during which the gas is exposed to ultra-violet light, then

$$i = \frac{4.2 \times 10^{-11}}{1.25},$$

or the average current is 3.3×10^{-11} amperes. Considerably larger currents have been obtained. The normal rate of leak in the electrometer used in these experiments was 0.4 cm. per *minute*, and the maximum leak in the ionized gas was in this case at the average rate of 44 cm. per *second*.

An examination of curve *A* shows it to be made up of two parts: first, a nearly straight portion, rising slowly as the pressure in the screen cell is changed from 76 to about 19 cm. of mercury; second, a curved part, which rises rapidly as the pressure is reduced from this point down to the lowest value reached. An inspection of Lyman's paper[1] shows that, according to the evidence of the photographic plate, as the pressure in the absorbing cell is reduced from 76 to 19 cm., the width of the absorption band in oxygen becomes only slightly less, *i. e.*, changes from λ1770–1268 at 76 cm. to λ1740–1280 at 19 cm.; while from this point on the band rapidly becomes narrower with decreasing pressure, extending from λ1600 to λ1335 at a pressure of 4 cm., and disappearing entirely below a pressure of 1.5 cm. The absorption band is thus unsymmetrical, the change taking place more rapidly on the less refrangible side of the band. It, therefore, seems justifiable to assume in these experiments that, when the pressure of oxygen in the screen cell is about 19 cm. of mercury, two narrow bands of light pass through into the ionization chamber, in addition to all the light which went through at a pressure of 76 cm. These two bands extend from λ1770 to λ1740, and from λ1280 to λ1268. To them may be due the rise of curve *A*, which takes place slowly between the above pressures. Then, as the pressure in the screen cell is reduced to its lowest value, more and more of the wave-lengths in the Schumann region pass through into the ionization chamber. To these wave-lengths is due the rapid rise of curve *A*, which takes place at the lower pressures. It may be mentioned here that there is no reason to believe that the smallest amount of energy necessary to produce a chemical effect upon a photographic plate is the same as, or even comparable with the smallest amount necessary to produce ionization detectable by the method employed in this research. It is, therefore, quite probable that the sensitiveness of one method differs considerably from that of the other.

---

[1] *Loc. cit.*

In consideration of these facts the author[1] has already stated that volume ionization is produced by light of wave-length less than λ1800, and that this effect increases with decrease in wave-length, at all events in the region between λ1850 and λ1400.

When the outer test cylinder was charged positively the results were, within experimental error, the same as those given above, showing that in the ionization chamber positive and negative ions are formed in equal numbers.

Hydrogen.

The gas was made electrolytically, passed through phosphorus pentoxide and collected over mercury in the same manner as the oxygen. In order to obtain deflections large enough to measure accurately the velocity of the gas stream was increased to 30 cm./sec., and the sensitiveness of the electrometer to 190 cm./volt. However, for the sake of comparison with the oxygen curve, the leak in hydrogen when the outer test cylinder was charged to a potential $V = -20$ volts has been plotted on Fig. 3 as curve B, and is on the same scale as curve A.

Nitrogen.

This gas was prepared by passing the nitrogen from a cylinder obtained from the Lindé Air Products Co. of New York through distilled water, over red hot copper, and through phosphorus pentoxide. It was collected in the same gasometer over mercury and used as were the other gases. The manner in which the gas in the cylinder is made by the company permits the presence of small quantities of argon and helium as impurities, but precludes the possibility of carbon dioxide or monoxide. A specimen of this gas analyzed for traces of oxygen and oxides of nitrogen showed:

---

[1] Nature, 77, p. 582, 1908.

"Oxygen 0.4 per cent., oxides of nitrogen 0.02 per cent. This does not include nitrous oxide or nitrous anhydride. The presence of the latter is, however, almost impossible, and of the former very unlikely." The results obtained with this nitrogen are plotted in Fig. 4. This curve represents the negative leak, since the potential of the outer test cylinder was − 20 volts. Moreover, the gas velocity through the ionization chamber was only 11.5 cm./sec., and the electrometer had a sensitiveness of 75 cm./volt, which corresponds to a capacity of 70 cm.

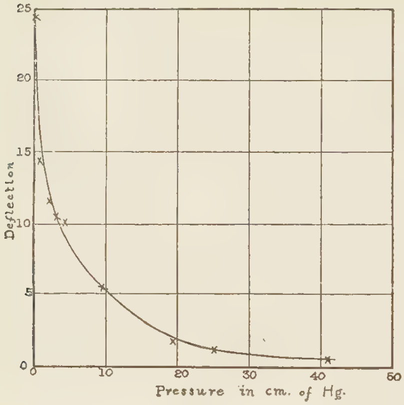

Fig. 4.
Negative leak. Nitrogen.

Nitrogen was also made from potassium nitrite by Gibbs's method. A specimen of this gas which was analyzed gave: "Oxygen none, oxides of nitrogen none." The steep rise of the ionization curve for pressures less than 2 cm. was even greater in this case, which indicates that the sharp rise is not due to the impurity of the gas.

Air.

Air from the laboratory was passed through distilled water, and then through the same tubes of phosphorus pentoxide, being collected as before in the mercury gasometer. The results obtained for the negative leak are shown by the curve in Fig. 5. The conditions of this experiment were similar to those for the other gases, though it is not possible to compare the magnitudes of the curves given thus far, owing to differences in gas velocity and sensitiveness of the electrometer.

Comparison.

It has frequently been shown that absorption and ionization in a gas go hand in hand. Therefore since it is known that air and oxygen absorb light of extremely short wave-length very strongly, while nitrogen is much more transparent and hydrogen hardly absorbs at all, it was to be expected that ionization would be detected in air and in oxygen, but that in nitrogen and in hydrogen, the amount of ionization, if it could be detected at all, would be extremely small. In Fig. 6 are given the ionization curves obtained all in a single day, and under as nearly the same conditions as possible. The gas velocity was less than that of any of the previous curves and was the same for all. The potential of the outer test cylinder was $V = -16$; and the electrometer had a sensitiveness of 170 cm./volt. Under these conditions the ionization in hydrogen, even when the gas velocity was doubled, was so small as to be unmeasurable.

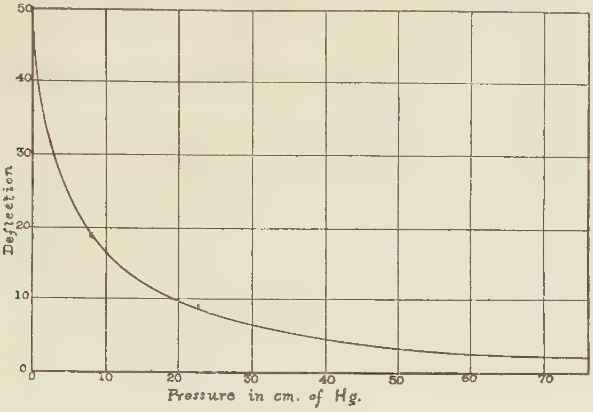

Fig. 5.
Negative leak. Air.

An inspection of the curves indicates that while air and oxygen show marked ionization, and hydrogen practically none, the ionization which takes place in nitrogen is unexpectedly large, and increases greatly for pressures in the screen cell less than 1 cm. Moreover, since a given thickness of air is more transparent than the same thickness of oxygen, it might be expected that the air curve of ionization would be lower than that for oxygen, but the opposite has always been found to be the case. It may be possible that small amounts of ozone, carbon dioxide, and carbon monoxide, present in the air account for a small portion of the ionization detected, but it seems as if much more of it might be due to nitrogen than had previously been supposed possible.

In all four gases there is unmistakable evidence of a sharp rise in the ionization curve when the pressure of oxygen in the screen cell is reduced below 2 cm. Since it was earlier shown that the shortest

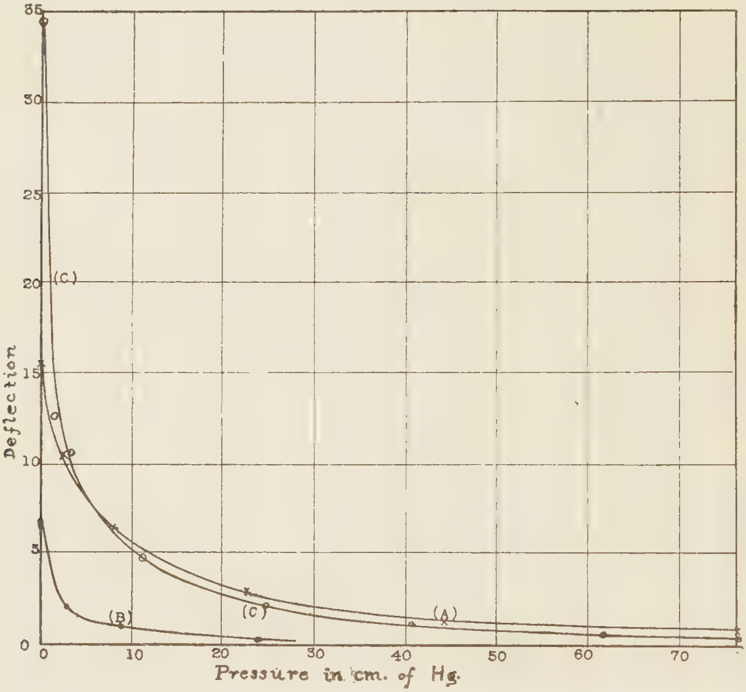

Fig. 6.
Negative leak.

wave-lengths passed through the screen cell only when the pressure in it was as low as 2.5 cm., the above result indicates that ionization increases very greatly as the wave-length decreases, at all events in the region between λ1850 and λ1400.

Although Lyman[1] has found that the absorption of ultra-violet light by nitrogen is small and increases regularly with decreasing wave-length, Schumann[2] states that nitrogen absorbs particular wave-lengths very energetically. It is known that nitrogen absorbs

[1] *Loc. cit.*

[2] *Loc. cit.*

wave-lengths between λ1500 and λ1300, such as pass through the screen cell at the lowest pressures, and if the absorption is particularly energetic in this region it may account for the observed rise in the ionization curve.

DUST.

The work of E. Bloch[1] seems to show that minute particles held in suspension by a gas, when acted upon by ultra-violet light, may produce a photo-electric effect which simulates that of volume ionization. In order to show that the results obtained in these experiments were not due to such a photo-electric effect, a plug of cotton wool 15 cm. long was inserted in the gas blast in addition to the many plugs of glass wool already there. The insertion of the cotton wool produced no detectable effect. It is also to be observed that the ionization in hydrogen is extremely small, yet from the manner of its production, there might be as much dust in hydrogen as in the other gases.

WATER VAPOR.

If water vapor has any effect, it is of great importance in this work, since it might produce absorption in the oxygen of the screen cell, resulting in a *smaller* electrometer deflection than if the oxygen were dry; or it might produce ionization in the gas being tested, resulting in a *larger* deflection. The following experiments will show that water vapor not only has an effect both in the screen cell and in the ionization chamber, but also that this effect is most pronounced.

Curve *A*, Fig. 7, is the same curve previously shown as *A*, Fig. 3, and represents the negative leak in oxygen when both the oxygen in the screen cell and the oxygen in the ionization chamber are dry. If the oxygen in the screen cell is kept dry, while oxygen which is slightly damp is taken from the previously mentioned oxygen cylinder, and passed through the ionization chamber, the result is curve *B* which falls much less rapidly at low pressure than *A* and does not reach it until the pressure in the screen cell has risen to 54 cm. of mercury. If this same undried oxygen from the cylinder is used in the screen cell as well as in the ionization chamber, the result is curve *C*, which is distinctly lower than *B* even up to atmospheric pressure, with the exception of the region below a pressure of 2 cm. of mercury. It was not convenient to saturate the oxygen which was admitted to the screen cell with moisture; so, instead, upon one occasion when the air in the laboratory was exceedingly damp it was admitted directly to the cell, while slightly damp oxygen from the cylinder was passed through the ionization chamber. The resulting state of affairs is shown in curve *D* and is conclusive in regard to the possibility of absorption due to water vapor in the screen cell.

---

[1] *Loc. cit.*

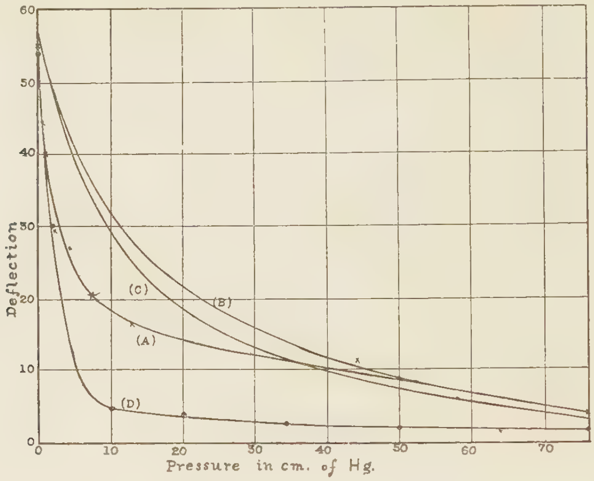

Fig. 7.
Effect of water vapor.

Mercury Vapor.

W. Steubing[1] has found that mercury vapor is ionized by light in the region of λ1800–2400. It is possible that it may be ionized also by light in the region of λ1250–1800. If so, since all of the gases examined were collected over mercury, and since the screen cell was in continuous connection with a mercury manometer, it might be possible for mercury vapor to play a part in the phenomena here under investigation. However, since the vapor pressure of mercury is so small at atmospheric pressure, it is not likely that such minute quantities of this vapor as could mix with the gas under investigation in the gasometer would affect the amount of ionization observed, even if the vapor were capable of producing any effect at all. No effect ascribable to mercury vapor in the ionized gas has been detected in these experiments.

---

[1] J. Stark, Phys. Zeitsch., 10, 18, p. 623.

Since the oxygen admitted to the screen cell is subjected to pressures all the way from atmospheric down to .01 mm. of mercury, it might very well be the case that at the lowest pressures used mercury vapor might constitute nearly one per cent. of the gas in the cell, and might produce a much greater percentage of absorption. Evidence of such an effect has been observed with all the gases examined at very low pressures of oxygen in the screen cell; but this is especially noticeable with nitrogen, since such a large proportion of the observed ionization in this gas is produced with low pressures in the screen cell.

Chemical Changes.

Many investigators have shown that ordinary ultra-violet light changes oxygen into ozone, and Lyman[1] has found that the light of extremely short wave-length used in this work does so to a very marked degree. It is therefore undoubtedly true that some of the oxygen used in the screen cell in these experiments is turned into ozone. However, since it has also been shown[1] that the absorption due to ozone does not differ appreciably from that due to oxygen this fact alone should not be a source of error here; unless, indeed, the method of ionization should prove to be superior to the photographic plate as a detector of absorption. If, on the other hand, the ozone when formed produces or facilitates other chemical changes, it might be possible that the resulting products of such changes would form a very considerable source of error.

Two effects have been observed which might be accounted for on the assumption that the ozone facilitates the formation of a layer of gas very close to the fluorite window, like that described by Hallwachs[2] in his explanation of photo-electric fatigue. One of the observed effects is the falling off of deflections in the electrometer taken successively under apparently the same conditions, when

[1] *Loc. cit.*

[2] Phys. Zeitsch., 21, p. 766, 1906.

the pressure of oxygen in the screen cell is anything from 1 to .0002 atmosphere. This effect is very similar to that ascribed to the presence of mercury vapor, but differs from it in that the deflection can be brought up to its initial maximum value either by waiting for ten minutes between readings, or by admitting fresh oxygen and reëxhausting to the same pressure as before. The first operation might give the ozone time to break up into oxygen, and the gas layer to become dissipated; while the second might be effective through breaking up of the gas layer by the inrush of fresh gas, followed by the loss of some of the ozone by reëxhaustion as well as by the natural process of breaking up into oxygen.

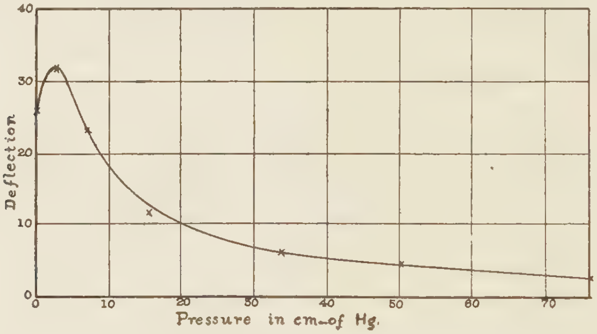

Fig. 8.

Effect of chemical action on fluorite.

The other effect has been observed not infrequently after the apparatus, as shown in Fig. 1, has been in use for some time. It consists of a complete change in the character of both positive and negative ionization curves for pressures less than 2.5 cm. of mercury in the screen cell. Instead of increasing as the pressure in the cell is reduced to its lowest value the curve passes through a maximum at a pressure of about 2 cm., falling off sometimes to only 80 per cent. of its maximum value when the lowest pressures are reached. Fig. 8 represents such a case when $V = -20$ volts and the ionized gas was oxygen. Upon taking apart the apparatus no film was found on the side of the fluorite window F (Fig. 1) next the discharge tube, where one might have been formed from a metallic deposit from the aluminum electrodes; but a film was formed on the side of the window F next the screen cell. No film has ever been found on the window F' (Fig. 1). The film has always been observed whenever the character of the ionization curve has undergone change, as in Fig. 8. Upon one occasion when the film was carefully examined, it was found to consist of two distinct parts; one was composed of fine, white, microscopic dust, which could be brushed off easily by a touch from some cotton wool; the other, when viewed in reflected light, appeared like a very thin film of whitish metal, which could be removed only after soaking in alcohol, and then rubbing briskly with cotton wool. The layer of dust occupied the exact central portion of the window and was in the form of a disc of diameter very little larger than the end of the capillary in the discharge tube, exactly opposite to which it was situated. The other film was also circular in shape, though its outline was not so clearly defined as that of the disc of dust, and its diameter was about three times as great, the two being concentric. On one side a notch in the circumference of the outer film was noted where no deposit existed. In this instance the fluorite window was 2.5 mm. thick, and a close examination showed a flaw on the side next the discharge tube which proved to be in a straight line from the end of the capillary to the notch noted above, thus indicating that the flaw had cast a shadow, in the line of which no chemical action on the fluorite had taken place. This shows that the action must take place extremely close to the window; that the dust layer must be formed by the more intense light which shines down some length of the capillary; and that the larger film must be produced by the weaker illumination which comes from close to the end of the capillary. Furthermore, since no effect has ever been found on the window F', it shows that the effective rays here are the very shortest. When carefully dried oxygen is used in the screen cell the apparatus may run for weeks without the formation of the film; but if oxygen from the storage cylinder is used, or if air is admitted from the room even if partially dried, the film forms quite quickly, sometimes in a day. The formation of the film, then, seems to be due to the action on the fluorite of ozone in the presence of a small amount of water vapor. This suggests that hydrogen peroxide may be the effective agent.

Since the curves shown represent the ionization produced by the sum total of all the light passing through the screen cell at any given pressure, it is not easy to see how a maximum in such a curve could be produced. It is probable that the dust layer described above plays a double role in this process: (1) absorbing much of the light of shortest wave-length, (2) facilitating the formation of a gas layer on the fluorite by presenting a roughened instead of a smooth surface. If it is assumed that this gas layer forms more readily on the roughened surface at low pressures, or that its absorption is abnormally large for such pressures, and that it absorbs the shorter wave-lengths more easily than pure oxygen, it can be seen how starting with a very low pressure in the cell practically all the absorption taking place would be due to the dust film and to the gas layer; but if a little more oxygen were admitted to the cell the gas layer might be disturbed, while the absorption due to the oxygen itself would increase.

If the increase in absorption due to the introduction of the oxygen was not as great as the gain in transparency due to the breaking up of the gas layer, the curve of ionization would rise. As more oxygen was admitted, the increased absorption due to the oxygen would overbalance the decrease due to the change in the gas layer, and therefore the ionization curve would begin to fall again, and would continue to do so up to atmospheric pressure.

It is possible that the effect here described is the same as that noted by C. T. R. Wilson[1] in his experiments on the formation of clouds by ultra-violet light. He has suggested that the formation of hydrogen peroxide by ultra-violet light would explain the phenomena observed by him. Although his source of illumination (zinc spark in air) gave rise to no such extremely short wave-lengths as those effective here, nevertheless it was a much more intense source than the hydrogen tube of these experiments, and might have produced hydrogen peroxide on that account. Lenard[2] has also found that ultra-violet light produces cloud nuclei which are non-electric in character, though he has not suggested what their real nature might be. It is quite possible that these, too, may be minute particles of hydrogen peroxide. It may be also that the roughening of a surface under the action of ultra-violet light noted by many investigators is due to the same cause as that which produced the dust layer described above.

---

[1] Phil. Trans., 192, p. 403, 1899.

[2] Ann. Phys., 3, p. 298, 1900.

Whatever may be the explanation of the phenomenon, it is certain that the maximum in the ionization curve exists only when the film on the fluorite window is present.

Temperature.

The gases examined were all at nearly the same temperature, that is from 15° C. to 25° C. Between these limits there was no detectable temperature effect.

Conclusions.

In conclusion it should be noted that the objection raised by Bloch to Lenard's work (dust) does not apply to the present investigation, since the insertion of a long plug of cotton wool in the gas stream was without effect. Furthermore, since it has been shown that the ionization produced in hydrogen is *extremely* small, this fact proves conclusively that the results obtained were not due to photo-electric action at the inner surface of the ionization chamber. This point meets the objection recently raised by Stark.

Finally, although the hydrogen tube used emitted light of low intensity, it was possible to obtain rather large currents through air, oxygen and nitrogen, owing to the great power of ionization possessed by the very short wave-lengths. Therefore, it seems clear that the reason why J. J. Thomson and McKaye, and others have obtained only extremely small currents in oxygen is because they have not employed a source of illumination emitting light of sufficiently short wave-lengths. The large currents measured by Stark were obtained in vapors having a very complex molecular structure, and not in oxygen. During the course of the present investigation it was found that, if alcohol or ether vapor were mixed with the gas under examination, the electrometer deflection in one second was so large as to be unmeasurable. This shows that for vapors of complex molecular structure the shortest wave-lengths also are capable of producing very large currents.

SUMMARY.

1. Using a discharge tube filled with hydrogen as a source of light and a screen cell filled with oxygen at various pressures, ionization curves have been obtained in air, oxygen, hydrogen and nitrogen.

2. The ionization in air, oxygen and nitrogen is considerable. That in hydrogen is exceedingly small. The currents obtained for all gases are large compared with the values of most other observers.

3. The power of ionization increases greatly with decrease in wave-length of light, at all events in the region below λ1850.

I take this opportunity of thanking Professor G. P. Baxter for valuable suggestions as to the production of pure nitrogen and also for superintending the analysis of the specimens of that gas.

The investigation was carried on in the Jefferson Physical Laboratory at Harvard University.

Haverford College, Haverford, Pa.,
May, 1910.

[Reprinted from the PHYSICAL REVIEW, Vol. XXXII., No. 2, February, 1911.]

THE HALL EFFECT AND SOME ALLIED EFFECTS IN ALLOYS.

BY ALPHEUS W. SMITH.

FROM a study of the data on the electrical conductivity of alloys together with the data from their thermal analysis, Guertler[1] has shown that the curve representing the relation between the electrical conductivity and the concentration of one of the components of a binary alloy will have a singular point, where the components unite to form a compound. It thus becomes possible from the behavior of the electrical conductivity to infer the presence of compounds in the alloy. In a subsequent paper by the same author,[2] it has been pointed out that similar conclusions may be drawn from the curves showing the relation between the temperature coefficient of the electrical resistance of the alloy and the concentration of one of its components. An examination of the thermoelectric properties of certain alloys by Becquerel[3] and others has indicated that the curve connecting the thermoelectric heights and the concentration of one of the components of the alloy shows a singular point, where a compound is formed. While the present investigation has been in progress a paper by Haken[4] has appeared in which a careful study has been made of the relation between the constitution, the thermoelectric heights and the electrical resistance of the following series of alloys: tellurium-antimony, tellurium-bismuth, tellurium-lead, antimony-silver and copper-phosphorus. He finds that wherever compounds appear in these systems, the curves connecting the thermoelectromotive with the concentration of one of the components have well-defined singular points. Similar conclusions are arrived at from the study of the electrical conductivity.

---

[1] Zeitschr. f. anorg. Chem., 51, p. 397, 1906.

[2] Zeitschr. f. anorg. Chem., 54, pp. 58–88, 1907.

[3] Ann. de Chem. et Phys. (4), 8, p. 408, 1866.

[4] Ann. der Phys. (4), 32, p. 291, 1910.

It seemed to the author that where the metals form compounds the Hall effect and the Nernst effect might be expected to behave in a way similar to that in which the thermoelectric height and the electrical conductivity had been found to behave. Such a result seemed the more to be expected from the fact, as Beattie[1] has pointed out, that there seems to be a sort of proportionality between the Hall effect and the thermoelectric heights.

Since in such an investigation so much depends on the purity of the metals from which the alloys are made, on the way in which the alloys have been allowed to cool and on their treatment after solidification, it seemed almost impossible to connect with certainty the data on the Hall effect and on the Nernst effect with the data which other observers had obtained on the thermoelectric heights, the electrical conductivity and the temperature coefficient of the resistance. Furthermore, the data on these quantities is for the most part meager. For the three series of alloys used in this investigation, viz: bismuth-antimony, antimony-cadmium and antimony-zinc, the author has been able only to find data on the thermoelectric heights of the three series and on the electrical conductivity of the bismuth-antimony series. In order, therefore, to make the points aimed at in this investigation, it seemed necessary to study besides the Hall effect and the Nernst effect, the thermoelectric heights, the electrical resistance and the temperature coefficient of the resistance. In the bismuth-antimony alloys the change of resistance in a magnetic field has also been studied.

Although the data obtained in the investigation cannot lay claim to a high degree of accuracy, the conclusions drawn from the data would not be changed by much greater errors than those which are present. Besides the errors of observation it is necessary to remember that there are errors due to slight impurities in the alloys, to small changes in the conditions under which they solidify and to slight differences in treatment after solidification. These sources of error may be of considerable consequence and since it is not possible to eliminate them, a high degree of accuracy is scarcely to be realized. The failure of different observers to obtain consistent values for the Hall effect and the Nernst effect in metals which are the purest to be obtained, shows clearly the importance of the sources of error to which reference has just been made.

---

[1] Roy. Soc. Edinb. Proc. (20), p. 481, and (21), p. 146.

PREPARATION OF ALLOYS.

The bismuth, antimony, cadmium and zinc for the alloys were obtained from C. A. F. Kahlbaum. Ten or fifteen different alloys of each of the following series were prepared: bismuth-antimony, antimony-cadmium and antimony-zinc. The alloys were prepared synthetically and chemical analyses were not made after the preparation. After weighing, the metals were placed in closed hard glass tubes which contained such a small amount of air that the loss of either metal from oxidation would be small. These glass tubes were heated in an electric furnace until both of the metals were fused. When the metals had been sufficiently stirred to insure uniform mixing, they were allowed to cool as quickly as possible to room temperature. The alloys were then fused as quickly as possible and poured into a talc mould which was at room temperature. The mould was made up of two parts which when clamped together formed a rectangular receptacle about 3 cm. long, 1.5 cm. wide and 0.3 cm. deep. Care was taken that the molten alloys should be in contact with the air for as short a time as possible, so that unequal oxidation of the two components might not appreciably change the composition.

After the alloys had been cast in the form of plates the bismuth-antimony plates were ground on a rotating disc with carborundum powder for an abrasive, until they were about 0.1 cm. in thickness. Many of the antimony-cadmium and the antimony-zinc plates were so brittle that they could not be ground and were used nearly as they came from the moulds. They were about 0.3 cm. in thickness. The thickness of the plates was measured in a number of places and the mean of these measurements used in the subsequent calculations.

RESISTANCE.

It was desirable to measure the resistance and the temperature coefficient of the resistance in the specimens in which the Hall effect and the Nernst effect were to be determined. Since these specimens were in the form of rectangular plates of low resistance, their specific resistances could not be determined easily. It was, however, sufficient for the purposes of the present investigation to know approximately the relative specific resistances of the different series of alloys. A simple method of getting the relative specific resistances of the different plates was by comparing the fall of potential over a given distance in one plate with the fall of potential over the same distance in the other plates, when the current density in all of the plates was the same. For this purpose lead wires were soldered to the ends of the plate (Fig. 1). By means of these lead wires the plate was connected through a known resistance R to a battery E of known electromotive force. At A and at B, points on the axis of the plate, was soldered a small copper wire which lead to the d'Arsonval galvanometer G. With the plate immersed in a mixture of ice and water, the deflection corresponding to a given current in the plate was noted. After reversing the current in the plate the deflection was again noted. The mean of four such observations was used in calculating the relative specific resistances of the plates. From the distance between A and B and the thickness and width of each plate, the deflection corresponding to the same current density in each plate was calculated, when the distance between A and B was 1.0 cm. These deflections were proportional to the specific resistances of the plates.

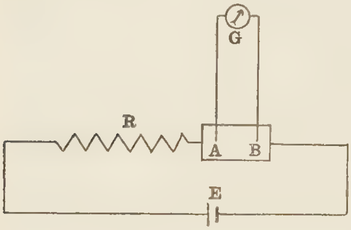

Fig. 1.

In order to obtain the temperature coefficient of the resistance, with a suitable current in the plate, the deflection of the galvanometer was noted, when the plate was immersed in a mixture of ice and water. The plate was then introduced into a steam bath at atmospheric pressure and when temperature equilibrium had been established, the deflection of the galvanometer was again noted. The temperature coefficient of the resistance of the plate is then given by the equation,

$$\alpha = \frac{d_{100} - d_0}{100 d_0},$$

where d_{100} is the deflection when the plate is in the steam-bath and

d_0 the deflection when the plate is in ice and water. In the case of the bismuth-antimony alloys, an oil-bath at room temperature was used instead of the steam bath. The temperature of the oil-bath was determined by a thermometer graduated to 0.1° C. The temperature coefficient of these alloys is, therefore, the average temperature coefficient between 0° and 22° C., while that of the other alloys is the average temperature coefficient between 0° and 100° C. The deflections of the galvanometer were nearly proportional to the applied electromotive forces, so that no serious error was introduced from this source.

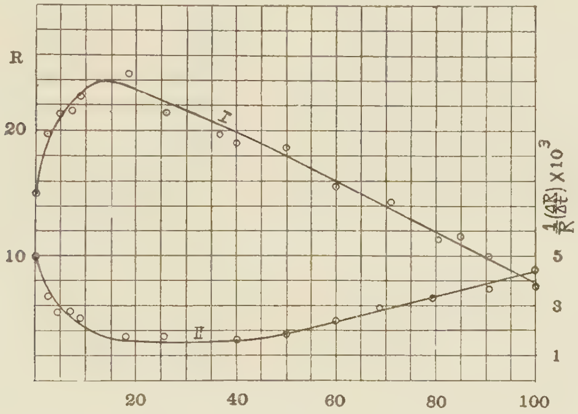

Fig. 2.

Bismuth-antimony alloys. Curve I., electrical resistance. Curve II., temperature coefficient of resistance.

In Fig. 2 the results of the observations on the bismuth-antimony alloys have been plotted. Curve I. shows the relation between the specific resistance at 0° C. and the percentage by weight of antimony. The ordinates are proportional to the specific resistances and the abscissæ give the percentages by weight of antimony. Curve II. shows the dependence of the average temperature coefficient of the resistance between 0° and 22° C. on the composition. The ordinates represent the temperature coefficient of the resistance and the abscissæ have the same meaning as they have in Curve I. It will be observed that whereas the addition of a small amount of antimony causes an increase in the resistance it causes a decrease in the temperature coefficient of the resistance. When about 10 per cent. of antimony is present in the alloy, the resistance reaches a maximum but the temperature coefficient has a minimum. Further increase in the percentage of antimony causes a decrease in the resistance but an increase in the temperature coefficient. The general form of Curve I. is the same as that given by Haken,[1] when resistances instead of electrical conductivities are plotted for ordinates in his curve. The discrepancies may be attributed largely to impurities and to the different conditions under which the alloys solidified.

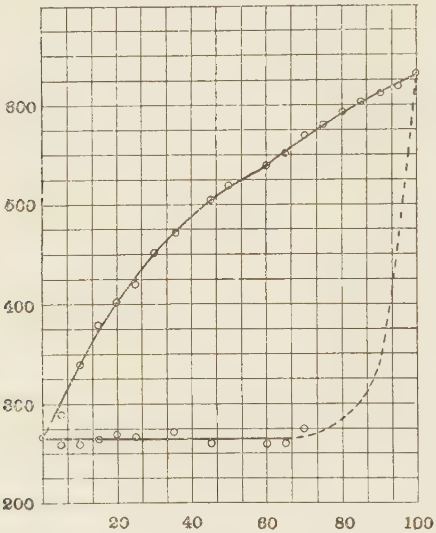

Fig. 3.

Fusion curve for bismuth-antimony alloys.

The fusion curve for bismuth-antimony alloys, as obtained by Hüttner and Tammann[2] is reproduced in Fig. 3. This curve shows that bismuth and antimony form a continuous series of mixed crystals without the formation of any compounds. It appears according to Guertler[3] that it is only where the metals form compounds, that either the curve relating resistance and percentage of one component or the curve relating temperature coefficient of the resistance and percentage of one component shows a singular point. Singular points were not, therefore, to be expected in the curves in Fig. 2. On the other hand, there are in these curves the well defined maximum and minimum which are characteristic of this class of alloys.

Fig. 4 and Fig. 5 give the results for the antimony-cadmium and antimony-zinc alloys, respectively. Curve I. in each figure shows the dependence of the resistance on the composition and Curve II. the dependence of the temperature coefficient of the resistance on the composition. In each of the curves marked I. the ordinates are proportional to the specific resistances at 0° C. and in the curves marked II. the ordinates give the average temperature coefficient between 0° and 100° C. The abscissæ in Fig. 4 are percentages by weight of cadmium and in Fig. 5, percentages by weight of zinc. It will be observed from these curves that with an increasing percentage of cadmium or zinc, the resistance of the alloy increases, at first slowly and then very rapidly, until the metals are present in the ratio of their atomic weights, where the resistance of the alloy is enormously higher than that of either component entering into it. A further increase in the percentage of cadmium or zinc causes the resistance to drop suddenly to a value which is of the order of magnitude of the resistance of the cadmium or zinc.

---

[1] Ibid., p. 327.

[2] Zeitschr. f. anorg. Chem., 44, p. 131, 1905.

[3] Ibid., p. 403.

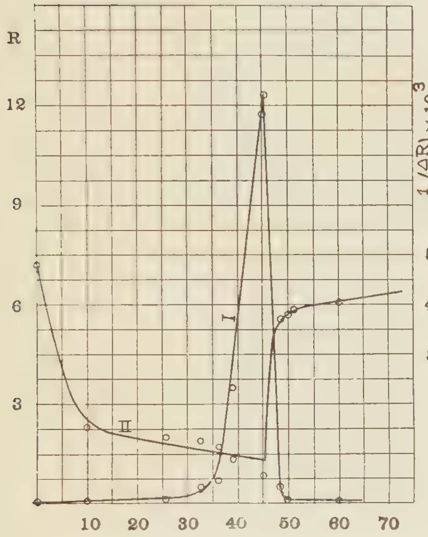

Fig. 4.

Antimony-cadmium alloys. Curve I., electrical resistance. Curve II., temperature coefficient of resistance.

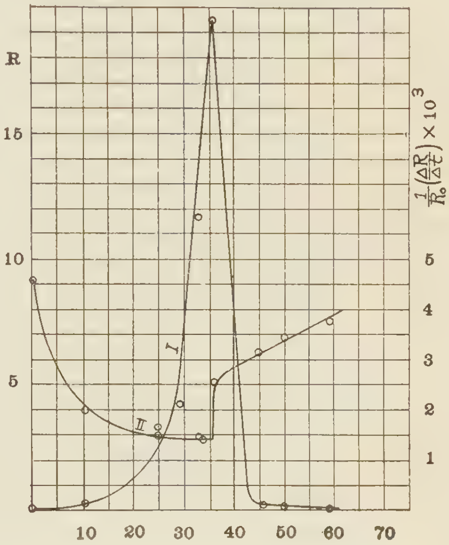

Fig. 5.

Antimony-zinc alloys. Curve I., electrical resistance. Curve II., temperature coefficient of resistance.

The addition of either cadmium or zinc to antimony causes the temperature coefficient of the resistance to decrease. This decrease is at first very rapid, until the alloy contains about 10 per cent. of either cadmium or zinc. With further increase in the concentration of either cadmium or zinc the temperature coefficient of the resistance continues to decrease, more and more slowly, until equal chemical equivalents of the metals are present. When this concentration has been reached for either series of alloys, a further increase of cadmium in one case or of zinc in the other case makes the temperature coefficient jump to a value which is somewhat less than that for a pure metal. Still further increase in the concentration of either cadmium or zinc causes the temperature coefficient of the resistance to increase slowly and it seems to approach the value of that coefficient in the pure metal.

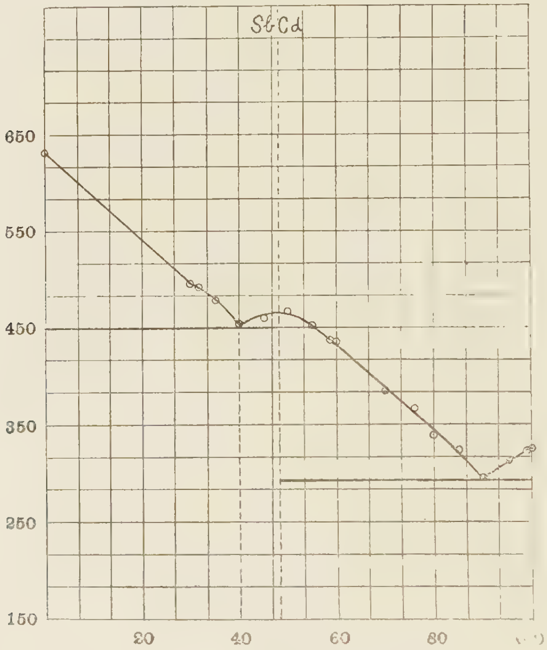

Fig. 6.

Fusion curve for antimony-cadmium alloys.

In Fig. 6 and Fig. 7 are given fusion curves for antimony-cadmium and antimony-zinc alloys respectively, the former by Treitschke,[1] the latter by Monkemeyer.[2] From Fig. 6 it is seen that when the

[1] Zeitschr. f. anorg. Chem., 50, p. 217, 1906.

[2] Zeitschr. f. anorg. Chem., 43, p. 182 ,1905.

antimony and cadmium are present in the ratio of their atomic weights, they form the compound, SbCd. Similarly, the melting curve in Fig. 7 shows that when the antimony and zinc are present in the ratio of their atomic weights, the compound SbZn is formed. An examination of Fig. 4 in connection with Fig. 6 brings out the fact that where the antimony and cadmium form the compound SbCd, the curve relating resistance to composition of the alloy and the curve relating the temperature coefficient of the resistance with the composition each have a singular point. Analogous results are arrived at for the antimony-zinc alloys by an examination of Fig. 5 in connection with Fig. 7. These results confirm the relation pointed out by Guertler[1] between resistance, temperature coefficient of resistance, and composition of the alloy.

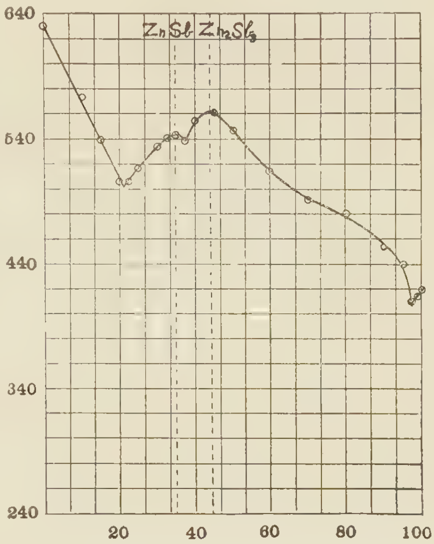

Fig. 7.

Fusion curve for antimony-zinc alloys.

THERMOELECTROMOTIVE FORCES.

For the approximate determination of the thermoelectromotive forces the plates were placed in a rectangular brass box which was separated into two compartments by a partition of hard fiber. The plates were thrust through the partition so that one end of the plate was in one compartment, the other end in the other compartment. One compartment was filled with a mixture of ice and water, the other with water at room temperature. The temperatures of the ends of the plate were determined by means of copper-german-silver thermal couples which were soldered to the ends of the plates. The copper wires of these couples could by means of suitable switches, be connected with a d'Arsonval galvanometer on which the thermoelectromotive force between the ends of the plate could be observed. To prevent error due to drift of temperature, the temperatures of the ends of the plates were determined immediately before and after the observation of the desired electromotive force. The mean of the respective temperatures thus obtained has been used in the calculation of the thermoelectric heights of the plates.

---

[1] Ibid., p. 412.

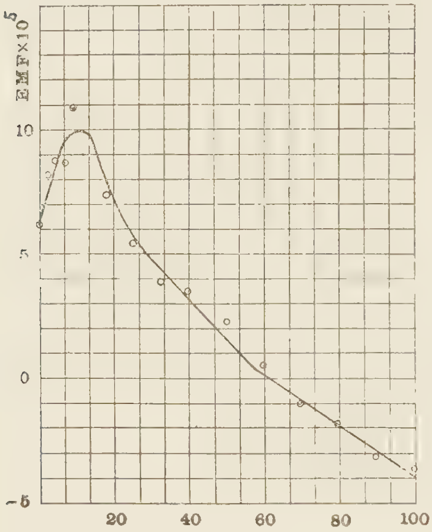

Fig. 8.
Thermoelectric heights of bismuth-antimony alloys.

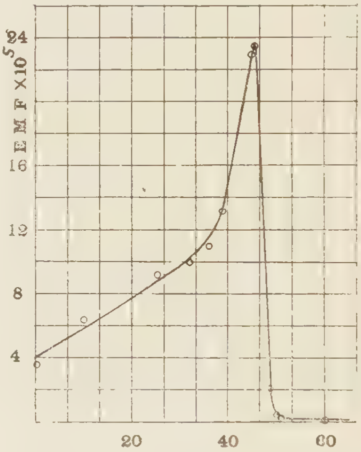

Fig. 9.
Thermoelectric heights of antimony-cadmium alloys.

The results of these observations for the bismuth-antimony alloys are to be found in Fig. 8; those for the antimony-cadmium alloys in Fig. 9; and those for the antimony-zinc alloys in Fig. 10. In each of these curves the ordinates are the average thermoelectric height between 0° and 20° C. The abscissæ in Fig. 8 are weight per cent. antimony; those in Fig. 9 weight per cent. cadmium; and those in Fig. 10 weight per cent. zinc. The character of the curve for the antimony-bismuth alloys is the same as that given recently by Haken[1] and that given earlier by Becquerel.[2] It shows a well defined maxmum when the alloy contains about 10 per cent. of antimony. The curve, however, shows no singular point and a singular point was scarcely to be expected, since there is no compound formed in the bismuth-antimony series. The analogous curves for the antimony-cadmium and for the antimony-zinc alloys agree in form with the curves given by Becquerel for these alloys. There are some discrepancies in the absolute values of the thermoelectric heights. These discrepancies which may be attributed mainly to slight impurities in the alloys, are of no consequence in the present investigation, since the character of the curve was all that was desired. The addition of either cadmium or zinc to antimony causes a decided increase in the thermoelectric heights. This increase becomes more and more rapid with increasing concentration, until equal chemical equivalents of the metals are present. A further increase in the concentration of either cadmium or zinc causes the thermoelectric heights to sink very rapidly to a value which is of the order of magnitude of the thermoelectric height of the antimony. The largest value of the thermoelectric height in the antimony-cadmium series is about seven times that for antimony and the largest value in the antimony-zinc series is about five times that for antimony.

---

[1] Ibid., p. 327.

[2] Ibid., pp. 291–336.

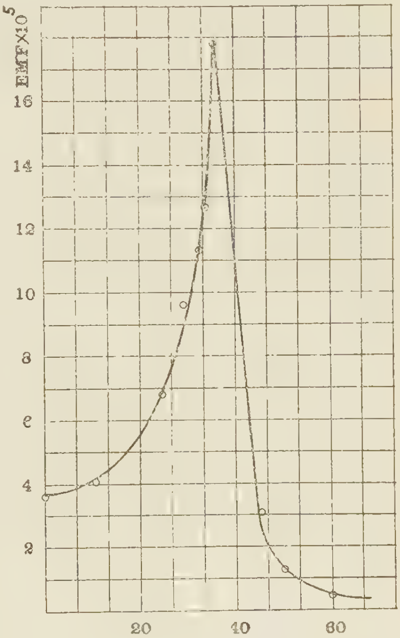

Fig. 10.

Thermoelectric heights of antimony-zinc alloys.

A study of Fig. 9, in connection with Fig. 6 and Fig. 10 in connection with Fig. 7, shows that the singular points in the curves relating the thermoelectric heights with the composition occur where the metals form compounds. It is also seen from these curves that the alloy which has the highest resistance and the least temperature coefficient of the resistance, has the greatest thermoelectric height, and that the singular points in each of the curves appear for the same percentages of metals in the alloys.

THE HALL EFFECT.

The arrangement of the apparatus for the study of the Hall effect and the method of procedure were essentially the same as that used by the author[1] in an earlier paper. The plates, the dimensions of which have already been given, were arranged in the ordinary way for the observation of the Hall electromotive forces. The copper lead wires for connecting the plate to the battery were soldered directly to the plate. On either edge of the plate midway between its ends were soldered the copper lead wires which lead to the galvanometer on which the Hall electromotive forces were to be observed. The plates were mounted on rectangular pieces of hard fiber and held in position by covering the plate and fiber with paraffin. Suitable arrangements were made for holding the plates in position between the poles of the magnet, so that the lines of magnetic force would be perpendicular to the plane of the plate. Observations were made at room temperature.

Experiment has shown that for a given metal or alloy, the Hall electromotive force E is given by the equation,

$$E = R\frac{Hi}{d};$$

where H is the magnetic field in absolute units; i, the current in absolute units; d, the thickness of the plate in centimeters; and R, a constant which is a function of the temperature and the strength of the magnetic field. Since the lead wires which were soldered to the edges of the plate for getting the Hall electromotive forces were not of the same material as the plate itself, there is superimposed on the Hall electromotive force a thermoelectromotive force which is caused by the inequality of temperature between the edges of the plate, when it is in the magnetic field. It has been found that this difference of temperature which was discovered by Ettingshausen, is given by the equation,

---

[1] PHYS. REV., 30, p. 1, 1910.

$$\Delta T = P\frac{Hi}{d};$$

where ΔT is the difference in temperature between the edges of the plate for a given magnetic field; H, the magnetic field in absolute units; i, the current in the plate in absolute units; P, a constant for a particular metal, at a particular temperature and field strength. If E denotes the Hall electromotive force, E' the observed electromotive force, and θ the thermoelectric height of the plate with respect to copper, then $E = E' \pm \theta\Delta T$ and $R' = R \pm P\theta$, where R' is the value of the Hall constant calculated from the observed electromotive force without correction. According to Zahn,[1] $P = 2 \times 10^{-6}$ for antimony and $P = 5 \times 10^{-5}$ for bismuth. Approximate determination of P in the antimony-cadmium and in the antimony-zinc series showed that it would not have a value greater than the value in pure antimony. The error due to this source would not, therefore, exceed about three per cent. for the most unfavorable cases and has been neglected in this work. This source of error has also been neglected in the bismuth-antimony alloys, although it amounted in some cases to about seven per cent. Correction for this error would not have changed the character of the curve and little importance is being attached to the absolute value of the effect.

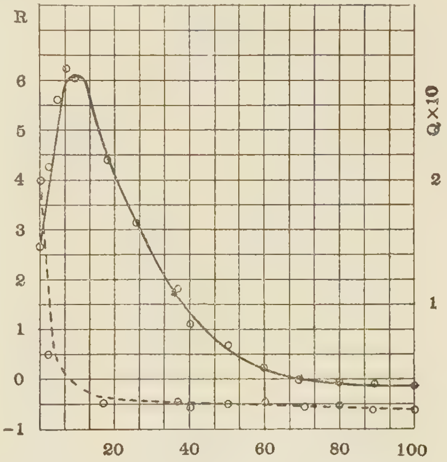

Fig. 11.

Bismuth-antimony alloys. Solid curve shows Hall effect. Dotted curve shows Nernst effect.

The values of R found for the bismuth-antimony alloys have been plotted in Fig. 11. The continuous curve in that figure shows the relation between R and the composition of the alloy. The ordinates are the values of R at room temperature, when the magnetic field is 10,400 absolute units and all of the quantities on which R depends are measured in the units indicated above. The abscissæ are the percentages by weight of antimony. It will be observed that the addition of antimony to bismuth increases the value of R, until the alloy contains about 10 per cent. of antimony when the Hall effect is largest. A further increase in the percentage of antimony causes a rapid decrease in R which becomes nearly zero in an alloy containing about 70 per cent. of antimony. In alloys which contain more than about 70 per cent. of antimony the direction of the effect is the direction of the effect in antimony which is opposite to that in bismuth. It is to be observed that the character of the curve obtained for the Hall effect is very like that obtained for resistance and that for thermoelectric heights. In each case the curve has a maximum when the alloy contains about 10 per cent. of antimony and an increase in the concentration of the antimony above about 10 per cent. causes a continuous decrease in the resistance, in the thermoelectric heights and in the Hall effect.

---

[1] Ann. der Phys., 14, p. 886, 1904.

In the continuous curve in Fig. 12 the Hall constants for the antimony-cadmium alloys have been plotted against the percentages by weight of cadmium, the former as ordinates, the latter as abscissæ. The strength of the magnetic field was 10,400 c.g.s. units. The first addition of cadmium to the antimony causes only a small increase in the Hall effect. With higher concentrations of cadmium the Hall effect increases more and more rapidly, until its value is about one hundred and fifty times the value in pure antimony. This very large value is found where the metals are present in the ratio of their atomic weights. When there is present in the alloy, a small amount of cadmium more than the equivalent of the antimony, the Hall effect drops suddenly to a value which is of the order of magnitude of the value in antimony. With further increase in the concentration of the cadmium the value of R continues to decrease and seems to approach the value of R in cadmium. By referring again to the fusion curves for the antimony-cadmium alloys, it will be seen that the singular point in the curve relating R and the percentage of cadmium, occurs where the antimony and cadmium form the compound SbCd. The behavior of the Hall effect in this respect is analogous to the behavior of the electrical conductivity, the temperature coefficient of the resistance and the thermoelectric heights.

The analogous observations on the antimony-zinc alloys are given in the continuous curve in Fig. 13. Here the abscissæ are the percentages by weight of zinc. The temperature and strength of magnetic field were the same as in the case of the antimony-cadmium series. The first addition of zinc to the antimony seems to have a somewhat greater effect on the magnitude of the Hall effect than does the addition of cadmium. The largest value of the Hall effect in the antimony-zinc alloys is only about one half of the largest value in the antimony-cadmium series. Here again it is noticed that when the antimony and zinc are present in the ratio of their atomic weights the Hall effect has its largest value and the curve shows a singular point. The largest value of the effect in these alloys is about seventy times the value in pure antimony. As soon as there is present in the alloy somewhat more than 35 per cent.

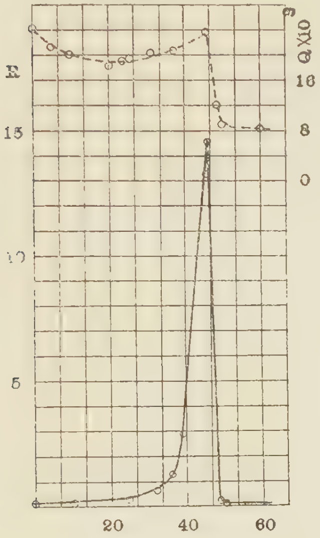

Fig. 12.

Antimony-cadmium alloys. Solid curve shows Hall effect. Dotted curve shows Nernst effect.

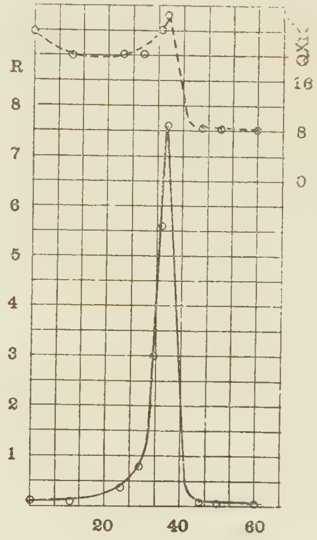

Fig. 13.

Antimony-zinc alloys. Solid curve shows Hall effect. Dotted curve shows Nernst effect.

of zinc, the value of the Hall effect sinks to a small fraction of its largest value, and with further increase in the concentration of the zinc the value of R continues to decrease, apparently approaching the value of R in pure zinc. By reference to Fig. 7 it will be seen that the singular point in this curve which has just been discussed, occurs where the antimony and zinc form the compound SbZn.

Nernst Effect.

v. Ettingshausen and Nernst[1] have shown that when a metal plate through which heat is flowing, is brought into a magnetic field so that the lines of magnetic force are perpendicular to the plane of the plate there is set up a difference of potential between the edges of the plate which are parallel to the direction of the flow of heat. Later experiments by Nernst[2] and others have shown that

$$E = QH\beta\frac{\delta T}{\delta x},$$

where E is the electromotive force between the edges of the plate in c.g.s. units; H, the magnetic field in c.g.s. units; β, the width of the plate in centimeters; $\delta T/\delta x$, the temperature gradient in the plate; Q, a constant which is a function of the temperature of the plate, and of the magnetic field and depends on the material of which the plate is made.

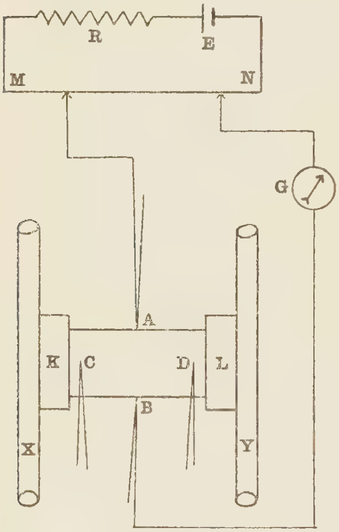

Fig. 14.

To study this effect the plates were soldered to heavy narrow strips of copper K and L (Fig. 14), which had been previously brazed to the copper tubes X and Y, respectively. The tubes and plates were mounted on a suitable frame of hard fiber which afforded the necessary protection from strains and also a means of fastening the plates in the proper position between the poles of the magnet.

---

[1] Wied. Ann., 29, p. 343, 1886.

[2] Wied. Ann., 31, p. 760, 1887.

Steam at atmospheric pressure flowed through one of the tubes and through the other there was a continuous flow of water at room temperature. For the purpose of determining the temperature gradient in the plates, a copper-german-silver thermal couple was soldered to the plate at C and another at D. These points were so chosen that the couples, at a known distance from each other, were on the line midway between top and bottom of the plate. At A and B which lay on the vertical line midway between the edges of the plate was also soldered a copper-german-silver thermal couple. The copper lead wires lead to the d'Arsonval galvanometer on which the Nernst effect was to be observed. In series with the galvanometer was a slide-wire potentiometer MN by means of which any thermoelectromotive force in the circuit due to an inequality of temperature between A and B could be compensated.

The plate was placed between the poles of the magnet with its plane perpendicular to the lines of force and was well packed with cotton wool to prevent loss of heat by radiation. When temperature equilibrium had been realized, the thermoelectromotive forces in the circuit were compensated on the potentiometer and when the magnetic field had been established, the deflection of the galvanometer produced by the difference of potential between A and B was noted. Four such observations were made. The direction of the magnetic field for two of them was opposite to that for the other two.

If the lead wires are not of the same material as the plate which is being examined, the effect discovered by Leduc will always be superposed on the Nernst effect. Leduc[1] found that when a plate traversed by a current of heat is brought into a magnetic field in the way previously described, there occurs a rotation of the isothermal, so that A and B which were originally on the same isothermal are no longer at the same temperature. Since in these experiments the lead wires were of copper, this effect would give an uncompensated thermoelectromotive force in the circuit. It has been found that the value of ΔT, the change of temperature between A and B for a given magnetic field H, is given by the equation,

---

[1] Compt. Rend., 104, p. 1783, 1887.

$$\Delta T = SH\beta\frac{\delta T}{\delta x};$$

where β is the width of the plate and $\frac{\delta T}{\delta X}$, the temperature gradient in the plate. If θ is the thermoelectric height of the plate with respect to copper; E', the observed electromotive force; and E, the electromotive force from the Nernst effect, after correction for the Leduc effect; Q', the constant in the equation for the Nernst effect calculated from the observed electromotive force, and Q the same constant after correction for the Leduc effect, the following equations hold:

$$E = E' \pm \Delta T\theta$$

and

$$Q = Q' \mp S\theta.$$

This source of error for most of the plates is quite large and has been the chief cause of uncertainty in the determination of the Nernst effect. It has been seen that the thermoelectric heights of some of the plates are quite large. In these plates any uncertainty in S introduces large errors in Q. By means of the thermal couples at A and B approximate values of S were obtained for the alloys studied in this paper. The value of S found for antimony was 2.0×10^{-6}, when distances are measured in centimeters; temperatures on the Centigrade scale and magnetic field in absolute units. This value is in fair agreement with that given by Zahn and other observers. With the addition of either cadmium or zinc to the antimony the value of S decreased, so that for an alloy containing 30 per cent. of zinc and 70 per cent. of antimony, or for an alloy containing 40 per cent. of cadmium and 60 per cent. of antimony, the value of S was about one tenth of its value in pure antimony. For alloys containing more than 30 per cent. of zinc and for alloys containing more than 40 per cent. of cadmium the value of S was so small that it was impossible to determine it with any accuracy. For bismuth S was found to be 2.0×10^{-6}. For alloys which contained less than 60 per cent. of antimony S was sometimes less and sometimes greater than in bismuth. The direction of the effect in bismuth and in the alloys which contained less than about 60 per cent. of antimony was opposite to that in antimony. In alloys which contained more than about 60 per cent. of antimony the effect had the same direction as it has in antimony. For an alloy containing about 60 per cent. of antimony the value of *S* was nearly zero. The values of *S* obtained were only approximate and have not been tabulated in this paper, for they were desired only as corrections in the Nernst effect.

In three of the bismuth-antimony alloys, viz., Bi 91 per cent., Sb 9 per cent.; Bi 82 per cent., Sb 18 per cent., Bi 75 per cent., Sb 25 per cent.; it was found that the electromotive force from the Leduc effect was larger than that from the Nernst effect. Since the two electromotive forces have opposite signs, there was an apparent reversal of the Nernst effect for certain magnetic fields. The Leduc effect decreased rather rapidly with increasing magnetic fields, so that for the higher magnetic fields the electromotive force due to the Nernst effect exceeded that due to the Leduc effect and there was no longer an apparent reversal of the effect. The strength of the magnetic field above which there was no apparent reversal of the Nernst effect was considerably less for the plate containing 9 per cent. of antimony than for the plate containing 25 per cent. of antimony.

The results for the bismuth-antimony alloys have been plotted in Fig. 11. The dotted curve shows the relation between *Q* and the percentage by weight of antimony. The ordinates on the right hand side of the figure are for this curve. It will be observed that the direction of the effect is the same in bismuth and in antimony and in any of their alloys. The addition of antimony to bismuth causes a rapid decrease in the magnitude of the effect, so that the effect in an alloy containing 91 per cent. of bismuth and 9 per cent. of antimony is only a little larger than the effect in pure antimony. A further increase in the percentage of antimony causes the Nernst effect to decrease slowly and its value approaches ultimately the value of the effect in antimony.

In Fig. 12 and Fig. 13 the dotted curves give the values of *Q* in the antimony-cadmium and antimony-zinc alloys, respectively. In Fig. 12 the abscissæ are percentages by weight of cadmium and in Fig. 13 they are percentages by weight of zinc. *Q* has been plotted for ordinates in each figure. The addition of either cadmium or zinc to antimony causes a decrease in the magnitude of the Nernst effect. With further increase in the concentration of either cadmium or zinc Q seems to pass through a minimum and then to increase to a value which is about the value of the effect in pure antimony. When the metals are present in the ratio of their atomic weights, where it has been seen that the compounds SbCd and SbZn are formed, each of the curves has a singular point which is very similar to the singular points in the curves which have been previously discussed. The increase in the concentration of the cadmium above that necessary to form the compound SbCd or that of the zinc above that necessary to form the compound SbZn, causes Q to sink rapidly to a value which is of the order of magnitude of its value in either cadmium or zinc. There is considerable uncertainty in the value of Q for the plates which contained equal chemical equivalents of the metals, because the thermoelectric heights of the plates is so large that any uncertainty in S which is small, makes a large error in Q. Concerning the break in the curves at the points indicated there can be no doubt.

Change of Resistance in a Magnetic Field.

To obtain the change of resistance in a magnetic field, the plate with the connections as indicated in Fig. 1 was placed between the poles of a large electromagnet in such a way that the lines of force were perpendicular to the plane of the plate. When temperature equilibrium had been established, with a suitable current in the plate and the magnetic field zero, the deflection of the galvanometer was noted. Everything else remaining unchanged, the magnetic field was established and the deflection of the galvanometer again noted. These observations which were made at room temperature were repeated several times. The direction of the magnetic field was reversed between successive observations. The change of resistance was calculated from the equation,

$$\frac{\Delta R}{R_0} = \frac{d_H - d_0}{d_0},$$

where d_H is the deflection with the plate in a magnetic field of strength H, and d_0 the deflection with the magnetic field zero.

Observations were made on the plates containing less than 50 per cent. of antimony for four different magnetic fields, and on those containing more than 50 per cent. of antimony for three different magnetic fields.

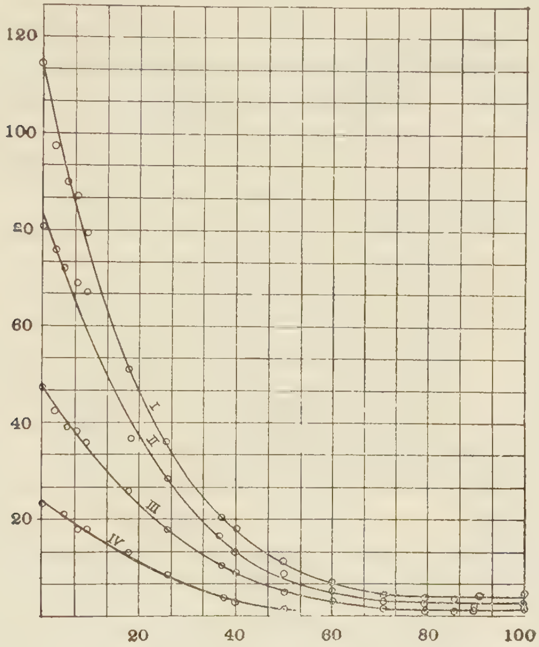

Fig. 15.

Bismuth-antimony alloys. Change of resistance in four different magnetic fields.

The results of these observations have been plotted in Fig. 15, where the ordinates are the percentages of change of resistance and the abscissæ are the percentages by weight of antimony. The curve marked I. is for 21,700 c.g.s. units; II., for 17,700 c.g.s. units; III., for 10,400 c.g.s. units and IV., for 5,500 c.g.s. units. The addition of antimony to bismuth causes the change of resistance in the magnetic field to decrease and this decrease is considerably larger than is to be expected from the additive law, so that an alloy containing about 70 per cent. of antimony shows a change of resistance which is very little larger than the change of resistance in pure antimony. After the alloy contains about 70 per cent. of antimony a further increase in the percentage of antimony seems to have little influence on the change of resistance in the magnetic field.

In Fig. 16 curves are plotted showing the relation between the change of resistance and the strength of the magnetic field, for bismuth and four of these alloys. The ordinates in these curves are percentages of change of resistance and the abscissæ the strength of the magnetic field in kilogausses per square centimeter. Curve I. is for bismuth; II., for Bi 91 per cent., Sb 9 per cent.; III., for Bi 82 per cent., Sb 18 per cent.; IV., for Bi 75 per cent., Sb 25 per cent.; and V., for Bi 50 per cent., Sb 50 per cent. It will be seen that in bismuth the change of resistance increases somewhat more rapidly than the magnetic field. In an alloy containing 91 per cent. of bismuth and 9 per cent. of antimony the resistance still increases somewhat more rapidly than the magnetic field but the deviation from proportionality between change of resistance and strength of magnetic field is less marked than in the case of bismuth. In an alloy containing 18 per cent. or more than 18 per cent. of antimony the change of resistance seems to be nearly proportional to the strength of the magnetic field.

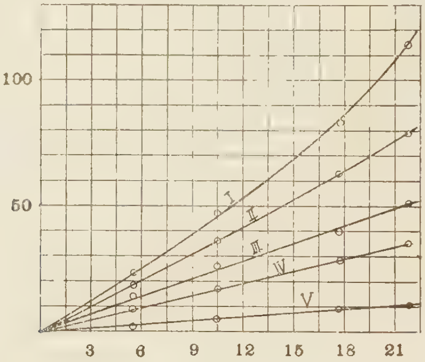

Fig. 16.

Bismuth-antimony alloys. Relation between change of resistance and strength of the magnetic field.

SUMMARY.

The electrical resistance, the temperature coefficient of the resistance, the thermoelectric heights, the Hall effect and the Nernst effect have been studied in three series of alloys, viz., bismuth-antimony, antimony-cadmium, antimony-zinc. For each of these series of alloys curves have been plotted showing the relation, (*a*) between the amount of one component and the electrical resistance, (*b*) between the amount of one component and the temperature coefficient of the resistance, (*c*) between the amount of one component and the thermoelectric heights, (*d*) between the amount of one component and the Hall constant, (*e*) between the amount of one component and the Nernst effect. From these curves the following conclusions may be drawn:

1. In the case of the bismuth-antimony alloys in which no compound of bismuth and antimony is formed, it is found that none of the curves have singular points but that each of them except one shows a well-defined maximum or minimum for an alloy which contains about 90 per cent. of bismuth and 10 per cent. of antimony.

2. In the antimony-cadmium series of alloys in which the compound SbCd is formed, when the metals are present in the ratio of their atomic weights, each of the curves has a well-defined singular point corresponding to the compound SbCd.

3. Similarly, in the antimony-zinc series of alloys in which the compound SbZn is formed when the metals are present in the ratio of their atomic weights, each of the curves has a well-defined singular point corresponding to the compound SbZn.

The change in the resistance of the bismuth-antimony alloys when in a magnetic field has been studied and it has been found that the change of the resistance is not an additive property of these alloys.

Physical Laboratory,
Ohio State University,
Columbus, Ohio.

THE SPECTRA OF SOME GASES IN THE SCHUMANN REGION

By THEODORE LYMAN

This paper contains the results of an investigation on the nature of the radiation from oxygen, hydrogen, nitrogen, helium, and argon in the region of very short wave-lengths. The writer has already published a preliminary report on the subject.[1] Taken in connection with the measurements of the spectra of hydrogen[2] and carbon[3] monoxide, the investigation is intended to complete the study of gas spectra begun by Schumann.[4]

In work on spectra of gases, even more than in most other physical investigations, the value of the results depends on the excellency of the technique. A detailed account of the methods employed, therefore, will be found at the end of this paper. The results themselves are as follows:

The cases of helium and oxygen are easily dismissed. No spectral lines belonging to these substances have been discovered in the region of wave-lengths more refrangible than λ 1900. That is to say, the radiation from these gases, if any exists, is too feeble to be detected by the methods used in this research.

There are two spectra of nitrogen in the region under consideration: the one consists of faint bands with the heads directed toward the more refrangible end of the spectrum, the other is made up of two pairs of sharp lines. The first spectrum is produced when no condenser is included in the discharge-tube circuit. The second is faintly visible under the same conditions but is very much enhanced by the introduction of capacity. No mention was made in the preliminary report of these spectra, for the band spectrum was so feeble that it escaped detection for a long time, while the line spectrum was wrongly attributed to another element.

---

[1] *Jahrbuch der Radioaktivität*, **4**, 246.

[2] *Astrophysical Journal*, **23**, 181, 1906.

[3] *Proc. Am. Acad.*, **45**, 315, 1910.

[4] *Smithsonian Contributions*, No. 1413.

Argon yields no lines corresponding to the red spectrum in this region but a considerable number of lines exist in the blue spectrum. In other words, if the discharge tube contains argon at a pressure of 1 or 2 mm, and if there is no capacity in the circuit, then no lines can be observed on the more refrangible side of λ 1900. On the other hand, if a disruptive discharge is used, a considerable number of lines appear which extend throughout this spectral region. If the pressure in the discharge tube is increased to 1 or 2 cm and if the disruptive discharge is employed, the light given by the gas appears white to the eye. Under these circumstances, most of the lines disappear which were present at a lower pressure.

The spectrum of hydrogen gas has already been thoroughly investigated by Schumann and by the writer, but the existence of a primary spectrum, corresponding to that given by Balmer's formula, still remains in question. The writer has been unable to observe such a spectrum, while Schumann[1] states that, with a spark in hydrogen at atmospheric pressure, he has obtained lines which he believes belong to radiation of this type. The writer has repeated these experiments, using a spark 6 or 7 mm long with terminals of aluminum, copper, and iron in an atmosphere of hydrogen. Under these circumstances, with a disruptive discharge, the four-line spectrum of hydrogen is extremely strong and nearly overpowers the metallic lines, at all events in the visible region. Notwithstanding this, no primary spectrum lines have been obtained even after prolonged exposure.

As the writer has already mentioned in another place,[2] theoretical considerations would not lead one to expect that radiation of the Balmer type would exist in the region between λ 2000, and λ 1250, for the chief series given by Rydberg[3] lies on the less refrangible side of λ 2000, and the chief series, as given by Ritz,[4] lies on the more refrangible side of λ 1250. The first line of the latter series has a wave-length, according to Ritz, of λ 1215.3. This is in the region beyond the transparency of fluorite. It has not been possible to push the investigation of gaseous spectra with a disruptive discharge into this region because of experimental difficulties. The existence of this line, therefore, still remains in doubt.

---

[1] *Astrophysical Journal*, **11**, 312, 1900.

[2] *Report British Association*, 1909, p. 132.

[3] *Astrophysical Journal*, **6**, 233, 1897.

[4] *Annalen der Physik*, **25**, 667, 1908.

Although the writer has been unable to repeat the observations of Schumann on the lines of the Balmer type, a singular spectrum apparently connected with that of hydrogen has recently come under his notice. If argon, containing a trace of hydrogen at a pressure of 2 or 3 mm, is inclosed in a tube with aluminum electrodes, and if no capacity is introduced in the circuit, a characteristic spectrum is obtained. It consists of five groups, each group containing five lines. These groups begin near λ 1650 and extend to λ 1450. They are all similar in appearance but they are not all identical in constitution. The distance between the lines in a group is of the order of from one to four Ångström units. If the last trace of hydrogen is removed from the argon, this spectrum disappears. Nitrogen, oxygen, and helium containing a trace of hydrogen and examined in a tube with aluminum electrodes do not produce these groups. If the argon and hydrogen are examined in a tube with iron electrodes, the intensity of the groups is very much reduced; if electrodes of copper are employed, the lines are extremely feeble. Under any circumstances, they are destroyed by the introduction of capacity. The most important fact in connection with these groups is that they are always found in the spectrum of pure hydrogen, no matter how this gas is prepared nor what electrodes are employed. In this case they are superposed upon a great number of other lines but they may be readily distinguished from the rest of the spectrum. All the groups can be identified in the reproductions of spectra published by Schumann;[1] the group which lies between λ 1590 and λ 1600 is the most striking, for at this point of the spectrum it is not obscured by the presence of strong lines. That these groups are not due to some impurity common to all the electrodes employed has been proved by using terminals of very pure silver furnished through the kindness of Professor T. W. Richards. The spectrum of hydrogen obtained with these electrodes is identical in every respect with the other spectra of this gas. If these groups are due to some impurity in the gas itself, such an impurity must be of a very fundamental character, for it was present in all the hydrogen which the author has employed during the past five years and it was present in the hydrogen used by Schumann.

---

[1] *Smithsonian Contributions*, No. 1413.

It is conceivable that groups of this type may be present in the spectrum of argon, containing a trace of hydrogen, in the visible and ultra-violet regions. At first sight, therefore, a suspicion might exist that the "Groups of Four" observed by Rydberg[1] in argon might in reality be connected with hydrogen, but a comparison of the measurements of the argon and hydrogen spectra shows that such a suspicion is without foundation.

Kayser[2] has observed lines belonging to the spectrum of aluminum in the spectrum of argon when aluminum was used for electrodes, but it is obvious from what has just been stated that the Groups of Five observed in the Schumann region cannot be supposed to have a metallic origin.

Such, in brief, are the results of this investigation. Tables of wave-lengths are to be found at the end of the paper. A detailed description of apparatus and methods follows.

In this investigation, the writer's vacuum spectroscope was employed in a manner which has been already described elsewhere. To insure the purity of the gas under investigation, the type of apparatus shown in Fig. 1 has been finally adopted. The glass discharge tube of the usual form has a ground flange at its lower end. To this flange is attached a fluorite window by means of Khotinski cement, care being taken that the cement is applied only to the outside edge of the flange in order that none of it may come in contact with the gas. This window is indicated in the figure at *A*. The tube thus closed is fastened in a brass cone *B* by means of Khotinski cement. This cone fits air-tight into a cup *C* which in turn screws on to the face-plate of the spectroscope. Thus the gas under examination does not come in contact with the brass of the mounting. This is a considerable improvement over other arrangements. If extreme purity in the gas is not a requisite, it is convenient to attach the fluorite window directly to the bottom of the cup *C*, for with this arrangement the window can be readily cleaned by simply withdrawing the discharge tube.

---

[1] Kayser, *Handbuch der Spectroscopie*, **2**, 577.

[2] *Astrophysical Journal*, **4**, 8, 1896.

The inlet of the discharge tube was connected with a U-tube 40 cm long which was plunged in liquid air. This device served as an effective trap for mercury vapor and for those carbon compounds whose spectrum has proved such an annoyance in former times. The U-tube in turn was connected with a spiral some 20 cm in length, to regulate the flow of gas, and this tube communicated with a suitable reservoir containing the gas under examination and with the mercury pump.

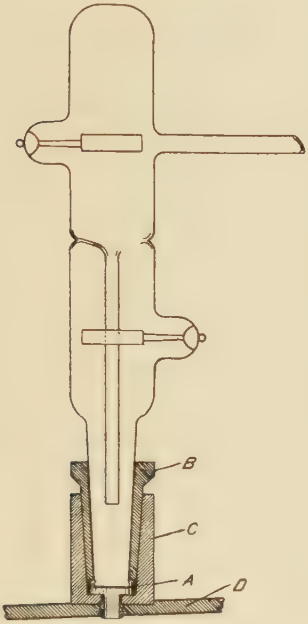

Fig. 1

The tube was excited by a small transformer, made by the Clapp Eastham Company, taking about six amperes in the primary on the 110-volt alternating circuit. The current through the discharge tube was usually between 10 and 15 milliamperes. When a disruptive discharge was desired, a spark-gap was placed in series with the tube and a condenser of 0.026 microfarad capacity was connected in parallel with the coil.

Measurements of wave-lengths were made by comparison with the hydrogen spectrum and the carbon monoxide spectrum, or with known lines of aluminum.

During the course of the experiments the appearance of the light from the discharge tube was frequently examined with a pocket grating spectroscope. The purity of the gas in the tube was estimated by the purity of its spectrum in the visible.

The gases used in this investigation have been prepared for the most part under the direction of Professor Baxter, to whom the writer is greatly indebted.

The oxygen was prepared by heating solid potassium permanganate, the gas was passed through plugs of glass wool, over platinized asbestos, through a wash-bottle and a tower containing potassium hydroxide solution, over solid potassium hydroxide, and finally over phosphorus pentoxide. The apparatus was constructed entirely of glass.

Some trouble was experienced in bringing the discharge tube into a condition which would remain constant from a spectroscopic point of view. A pressure of 5 mm was finally used. In addition to the precautions taken in preparation, the gas was sparked directly before it was admitted to the apparatus. Aluminum electrodes were used. No capacity, beyond that due to the leads, was included in the discharge-tube circuit.

The results were entirely negative, no lines could be attributed to oxygen in the Schumann region. The data collected some years ago in a preliminary investigation confirm this result.

Two specimens of helium were examined; the one was obtained through the kindness of Professor E. P. Adams of Princeton, the other was purchased from Tyrer of London. The latter specimen contained a slight trace of nitrogen which somewhat masked the spectrum of helium in the visible at pressures above 15 mm. At pressures below 5 mm, however, the helium lines appeared without any impurity other than a faint trace of hydrogen. Exposures were made with various pressures from 17 mm to 1 mm; the results of all these experiments were the same, no lines could be attributed to helium in this region; this result is confirmed by all data collected in preliminary investigations on this gas. Aluminum electrodes were used in all cases. Both an uncondensed and a disruptive discharge were employed.

The nitrogen used in the final experiments was made from a mixture of ammonium chloride, sodium nitrite, and potassium bichromate dissolved in water. The gas passed over potassium hydroxide, through concentrated sulphuric acid, and over phosphorus pentoxide, and finally over hot metallic copper.

Owing to the heating of the discharge tube, a gas pressure of 2 mm was selected for the final experiment both in the case of the disruptive discharge and when no capacity was in the circuit.

The feeble character of the band spectrum has been mentioned already. The persistence of the line spectrum consisting of two pairs must be remembered also, for it was this persistence which prevented these lines from being ascribed to their true cause in the early part of the work. All the gases which have been investigated will show these pairs with a disruptive discharge if they contain a trace of nitrogen or even of air. Beside these pairs, there exist faint lines in this spectrum, but their intensity is so feeble that their wave-lengths have not been accurately measured. They are not included in the table.

Three samples of argon have been examined. The first was from Tyrer, the last was prepared as follows: air was drawn through towers containing solid potassium hydroxide. It was then passed over bright copper rolls properly heated, then through a tube containing two parts of magnesium powder, five parts of freshly ignited calcium oxide, and one-fourth part of metallic sodium free from oxide. After leaving this tube the gas passed over a combustion tube of copper oxide and was then collected over a solution of potassium hydroxide. The combustion tubing was heated electrically, which permitted the temperature to be conveniently controlled. The crude argon thus prepared was repeatedly passed over a mixture of lime and metallic magnesium until no further contraction took place. The gas was then mixed with oxygen and sparked in a tube over potassium hydroxide and mercury for several days. From here it was transferred to a new system and was passed repeatedly over phosphorus pentoxide and over a bright copper roll. The resulting gas showed no trace of nitrogen, hydrogen, or oxygen when examined spectroscopically in the visible part of the spectrum.

The final experiments were made with gas prepared as above described, but the results check very well with those obtained when the specimen from Tyrer was employed. The pressure ranged from 1 to 20 mm, depending on the nature of the discharge which it was desired to produce. Electrodes of aluminum, copper, and iron were used.

The wave-lengths of the lines in the "blue" spectrum of argon are to be found in the table on p. 107. Only three lines have been obtained in the white spectrum: of these, two are also found in the blue spectrum; the gas at high pressures, therefore, appears to yield but one new line, λ 1650.0.

It is interesting to contrast the behavior of hydrogen with that of argon. With the former gas, a characteristic line spectrum is produced when no capacity is included in the circuit, while with a disruptive discharge these lines almost completely disappear and no new ones take their place. With the latter gas, just the opposite conditions prevail. Argon gives no lines in the Schumann region when the circuit is without capacity; it is only with a disruptive discharge that its characteristic lines appear.

The origin of the Groups of Five remains undetermined. As has been stated, these groups occur in all hydrogen spectra superposed upon a spectrum composed of fine lines. They have been included in all previous measurements. It is only when a trace of hydrogen is mixed with argon that the groups appear without the accompaniment of the lines. The fact that they do not occur as a separate spectrum when a trace of hydrogen is present in nitrogen, helium, or oxygen, would indicate that they are not due to an impurity contained in the walls of the tube. Moreover, experiments have been made in which the discharge tube was heated by the passage of the current until the capillary showed the sodium lines; such treatment in no way influenced the intensity of the Groups of Five when they were present. The nature of the electrodes affects their intensity, but they are not due to an impurity common to the various metals employed. This has been shown by the fact that they persist in the spectrum of hydrogen when the electrodes are of the purest silver.

The construction of these groups will appear from the following table. The lines of which they are composed are very sharp; they do not differ in character from the rest of the hydrogen spectrum.

GROUPS OF FIVE

Group	1	Diff.	2	Diff.	3	Diff.	4	Diff.	5
I.	1643.0	2.5	1640.5	2.3	1638.2	1.7	1636.5	2.4	1634.1
II.	1599.4	3.2	1596.2	2.6	1593.6	2.1	1591.5	2.5	1589.0
III.	1550.6	3.6	1547.0?	3.1	1543.9	2.3	1541.6	2.4	1539.2
IV.	......	...	1495.5	3.6	1491.9	2.6	1489.3	2.4	1486.9
V.	1445.2	4.2	1441.0	3.0	1438.0	2.8	1435.2	2.2	1433.0

In order of intensity these groups may be listed as follows, beginning with the greatest intensity: II, V, I, III, IV. Of lines in a single group the more refrangible are the stronger. The strongest line in the strongest group, 1589.0, has the intensity 8. Inspection of the columns which give the differences between successive lines in a group show that though the groups are similar they are not identical.

If these groups are compared with the Groups of Four in the ultra-violet, it is clear that the lines in a single group are much closer together than those in Rydberg's arrangement.[1] Even if the first lines in each group are taken as forming one system, the second lines as forming a second system, and so on, the results do not agree with the formula, for the new systems are not identical, and the frequency differences are not those given by Rydberg.

As to the cause of these Groups of Five there are obviously two opinions: either they are due to a very persistent and subtle impurity in the hydrogen, or they form a new spectrum of that gas.

The hydrogen used in the final experiments was produced electrolytically from a barium hydroxide solution; it was passed through distilled water, over solid potassium hydroxide, and was dried over phosphorus pentoxide. As to the spectrum of hydrogen there is little to add. The presence of moisture in the gas tends to enhance the primary spectrum in the visible; in the Schumann region it tends to weaken the many-line spectrum. The spectrum of hydrogen is sensitive to the smothering effect of a heavier gas. Nitrogen mixed with hydrogen weakens the spectrum of the lighter gas without contributing strong lines of its own.

The use of liquid air does away with mercury vapor in the discharge tube. When mercury is present, however, but one line can be attributed to it in this region, that at λ 1850.0.

In the tables which follow, the wave-lengths are in vacuum. Owing to the feebleness of the nitrogen bands, their position may be in error by four-tenths of an Ångström unit; the errors in the line spectra should not exceed two-tenths of a unit.

---

[1] Kayser, *Handbuch der Spectroscopie*, **5**, 69.

NITROGEN

Band Spectrum				Line Spectrum	
λ	I	λ	I	λ	I
1383.7	3	1687.5	2	1492.8	6
1393.5	2	1736.9	2	1494.8	5
1416.1	3	1752.9	3		
1431.6	2	1768.5	3	1742.7	7
1464.8	4	1804.7 ?	2	1745.3	6
1471.1	1	1821.1	4		
1501.1	3	1837.6	5		
1515.4	2	1854.0	3		
1530.6	2	1870.9	2		
1554.4	5				
1611.8 ?	4				
1672.3	3				

ARGON

"Blue" Spectrum

λ	I	λ	I	λ	I	λ	I
1333.7	5	1604.2	4	1827.6	6	1846.9	6
1334.5	7	1607.0	3	1830.6*	10	1850.2	4
1335.8	7	1611.0	4	1831.4*	9	1855.7	9
1460.1	5	1614.8	4	(1834.5)	2	1865.9	8
1463.3	3	1669.7	7	(1835.5)	2	1868.7	8
1465.6	4	1673.5	7	1836.3	9	1873.2	10
1467.9	2	1675.6	7	(1838.1)	2	1877.7	8
1589.5	4	1788.1	5	1839.2	9	1879.7	8
1600.7	5	1807.5	4	(1842.3)	1	1886.1	7
1602.6	2	1820.0	7	1843.1	9		

* Present in the "white" spectrum. ( ) Origin uncertain.

This research has been carried out in great part with the help of a grant from the Bache Fund.

Jefferson Physical Laboratory
Harvard University
December 31, 1910

[Reprinted from the AMERICAN JOURNAL OF SCIENCE, Vol. XXXI, April, 1911.]

ART. XXV.—*On the Heat Generated by Radio-active Substances;* by WILLIAM DUANE.

SINCE the discovery of radio-activity questions relating to the source and the transformations of the energy involved in the processes have been considered of prime importance. Early in the history of the subject Curie and Laborde* discovered that radium generates heat continually, and also that the heat effect increases as the emanation accumulates. A little later Rutherford and Barnes† found that the emanation and the first few products of radium that form its induced activity produce their shares of heat, and more recently still Pegram and Webb‡ have succeeded in detecting a small heat effect in a large mass (about four kilograms) of thorium oxide.

The ordinary methods of measuring heat (an ice calorimeter for instance) are sufficiently sensitive to detect and measure the heat generated by the quantities of radium, its emanation and its induced activity now at our disposal. I have made recently a number of experiments on the heat effects of other radio-active substances, and in these I have had to use special methods. At first I employed a modification of the differential air calorimeter devised by Rutherford and Barnes (l. c.), but this was not sensitive enough and I then constructed a new instrument which is considerably more sensitive than the differential air calorimeter. The method is based on the rapid increase in the vapor tension of a very volatile liquid when the temperature rises. A and A′ (fig. 1) represent two glass vessels, which are joined by the capillary tube B. The vessels are half filled with the volatile liquid, and almost all the air is pumped out by means of a water aspirator through the tube C, which is then sealed off. A small bubble formed out of the residual air left in the vessels is inserted in the tube B, and the displacement of this bubble is observed by means of a reading telescope or by projection with a lamp, lens and scale. I usually employ the latter method, and the displacement of the image on the scale is about eight times that of the bubble in the tube.

It is not difficult to place a bubble of any desired length in the tube B. It is sufficient to turn the apparatus upside down, and let the liquid run out of the tube. Then on replacing the apparatus right side up one finds the tube more or less completely filled with air. The bubble is usually much too long, and to reduce its length all that is necessary is to tilt the apparatus up a little so as to cause a current of the liquid to pass through the tube. This current pushes the bubble down into the portion of tube below and at the side, which is larger than the capillary portion. The bubble remains in this portion of the tube, and the current of the liquid passing it carries along the air little by little, thus reducing the bubble's volume. On repeating this process, causing the current to flow first in one direction and then in the other, one can reduce the bubble to any desired length.

---

* Comptes rendus, cxxxvi, p. 673, 1903.

† Nature, Oct. 29, 1903; Phil. Mag., Feb., 1904.

‡ Science, 1904; Le Radium, 1908.

Fig. 1.

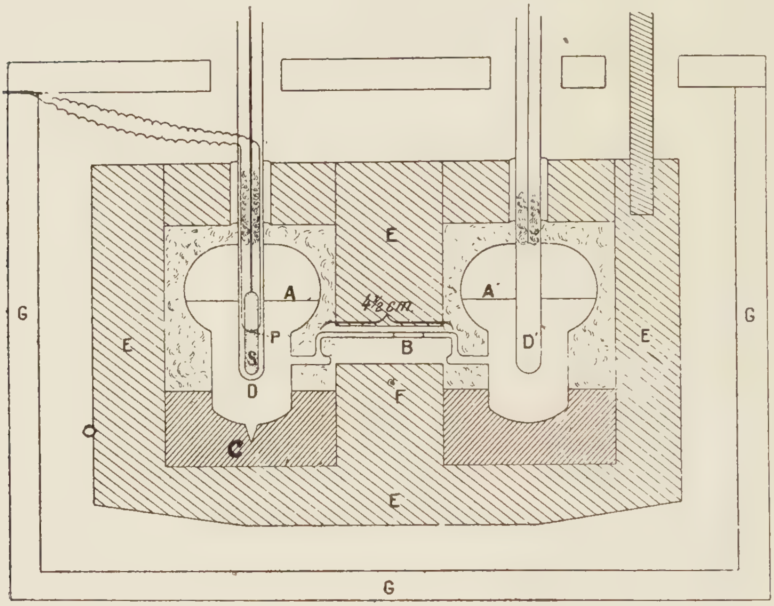

After the bubble has been replaced in the tube, and the apparatus has been prepared for the experiment, the bubble remains in the horizontal part of the tube. It never descends into the large portion, no matter how much the temperature of the room may vary: but it slowly disappears. The air in the bubble dissolves in the liquid more or less rapidly according to the nature of the liquid, the pressure of the air and the dimensions of the apparatus. In my experiments it is necessary to renew the bubble once in two or three weeks: and this is a process requiring about five minutes time.

The form and dimensions of the capillary tube B have been carefully studied. The length of the horizontal part is $4\frac{1}{2}^{\mathrm{cm}}$

and the internal diameter is a little more than $\cdot 5^{mm}$. The internal diameter of the two large parts is about 3^{mm}, and the vertical parts joining the horizontal with the larger parts should not have a larger diameter than the horizontal capillary part. It is easier to control the movement of the bubble, while placing it in the tube and reducing its size, if the capillary tube is not joined to the ends of the larger parts, but to the tops as indicated in the figure.

The volume of each vessel is about 50^{cm^3}.

The interior of the vessels and of the tube must be cleaned most carefully. The least dirt or grease stops the bubble, and in the experiments it is well to choose the part of the tube where the bubble moves most freely.

If a source generating heat is introduced into the tube D, the vapor tension is increased and the liquid pushes the bubble toward the vessel A′. The instrument is very sensitive. In my experiment I found that $1\cdot 5 \times 10^{-4}$ gram-calorie of heat displaced the image of the bubble 1^{mm} on the scale. This sensitiveness is due to the rapid increase of the vapor tension with the temperature. Among the liquids I have tried, ether seems to be the best. Ether cleans and wets the surface of the glass well, it has very little viscosity and its vapor tension increases rapidly with the temperature, about 17^{mm} of mercury per degree centigrade at ordinary temperatures. Ethel chloride works well also but is much less easily manipulated.

The sensitiveness of the instrument varies a great deal with the quantity of air in the vessels. If there is very little air the displacement of the liquid does not change the pressure of the gas much (saturated vapor tensions depending only on the temperature), and an increase of pressure in A due to a slight production of heat is opposed only by a change of lev el of the liquid in A and A′. As ether is a light liquid, this change of level opposes only a slight force to the displacement of the bubble. For great sensitiveness, therefore, one must remove almost all the air from the vessels, leaving only enough to form the bubble. The sensitiveness depends also upon the ratio of the cross-section of the capillary tube to the surface of the liquid in the vessels. A decrease in the cross-section increases the sensitiveness. I have found, however, that (if. the liquid is ether) a tube of less than $\cdot 5^{mm}$ internal diameter does not work well on account of the capillary forces.

Further, the displacement of the image of the bubble is increased by the lens (or reading telescope). It is not desirable, however, to multiply the displacement more than eight or ten times, as the loss in sharpness of image counterbalances the advantage of increased displacement.

In actual practice the protection of the instrument against outside thermal disturbances is just as important as great sensitiveness. In my earlier experiments I imbedded the two vessels in a block, E (fig. 1), of lead (weighing 25 kilograms). The vessels were held in place by a layer of paraffine, which filled the space between them and the lead at the bottom. At the top this space was filled with cotton wool. Two metal rods, F (normal to the plane of the figure), support the block of lead inside a brass box, G. These rods serve as axles about which the lead can be turned, and thus the bubble of air shifted to any desired position in the capillary tube. The box G was completely enveloped in cotton wool contained in a second box of zinc (not represented in the figure). This system of good conducting metal screens separated by spaces filled with non-conducting material furnished excellent protection against thermal disturbances, but was not sufficient where the greatest sensitiveness was required. The whole apparatus, therefore, was placed in an electrical thermostat similar to the one described some years ago in this Journal.*

In my later experiments I have replaced the cotton wool with eider down, and I have added two large blocks of lead on top of the box G. These blocks equalize the variations of temperature coming from above. They are placed one beside the other, leaving just enough space between them for the tubes by which the substances to be examined are lowered into the calorimeter. With these modifications I have found it unnecessary to set the thermostat going, except on those days when the temperature of the room undergoes wide fluctuations.

Very often the heat due to the radio-active processes is produced in relatively large masses of matter. In these cases it is necessary to leave the substance to be examined for a long time in the upper part of the tube by which it enters the calorimeter, in order to be sure that its temperature is as nearly equal to that of the calorimeter as possible. This part of the tube should lie between the two large blocks of lead, and should be of metal to facilitate the equalization of temperatures.

If the generation of heat by the source is relatively large, an appreciable quantity of it may be conducted down the column of air into the calorimeter. In order to avoid this a small quantity of eider down fastened to the end of a very fine glass rod may be inserted into the tube just above the calorimeter. In making an experiment the eider down is removed, the substance to be examined lowered into the calorimeter and the eider down quickly replaced.

Any one of several methods may be used in measuring the heat generated by the source. On lowering the source into the calorimeter one can wait until a sort of thermal equilibrium is reached, when the heat conducted away from the calorimeter equals that given it per second by the source, and observe the maximum displacement of the bubble of air. This method works well provided the instrument is not arranged for very great sensitiveness.

---

* Duane and Lory, this Journal, 1900.

If, however, the apparatus is very sensitive it is better to take the velocity of the bubble as a measure of the heat generated per second. Although the instrument is well protected against thermal disturbances from the outside, yet the bubble does not stay in the same place. The zero of the instrument is not fixed. Nevertheless, if the apparatus has remained undisturbed for a long time, and the temperature throughout has become as nearly equalized as possible, the natural drift of the bubble is slow and regular, and the change in its velocity due to the heat from the source, when it is lowered into the calorimeter, can be measured with considerable precision.

A third method is to compensate the effect of the heat generated in the tube D by generating a known quantity of heat in the corresponding tube D′ (figure 1).

The best method, however, is to compensate the heat effect by absorbing the heat in the tube D itself as fast as it is generated. This can be done by means of a current of electricity flowing across the junction of two metals. Peltier discovered that if the current passes in one direction heat is generated, and if in the opposite direction heat is absorbed at the junction.

In my earlier experiments I inserted a thermo-couple P of iron and nickel wires into the tube D, and I determined the current that absorbed the heat as fast as it was generated, by varying the strength of the current until the velocity of the bubble was the same as its natural drift. In the later experiments I have replaced the simple thermo-couple by a metal tube. The walls of the tube are 1^{mm} thick, and its external diameter is just enough less than the diameter of the tube D to allow of its being inserted easily into the latter. The length of the metal tube is about 4^{cm}, so that the entire tube lies inside the calorimeter. Half of the tube is of iron and the other half of nickel, the two surfaces between the two metals being vertical and parallel to the axis of the tube. An iron wire is soldered to the outer edge of the iron half of the tube and a nickel wire to that of the nickel half, so that a current of electricity descending by the iron wire into the iron half of the tube can pass across the joints into the nickel half and ascend by the nickel wire. With this arrangement, when a source of heat is lowered into the middle of the iron-nickel tube, it is surrounded by a good conductor of heat, and the distribution and compensation of the heat takes place easily and quickly. Thus the thermal equilibrium of the apparatus is not disturbed much by the heat generated by the source.

This method is capable of considerable precision and can be used, without changing the apparatus, to measure heat effects varying from ·001 gram-calorie to 2 gram-calories per hour. Larger heat effects could be measured by increasing the thickness of the iron-nickel tube and iron and nickel wires so as to decrease their electrical resistance and the heat generated in them according to Joule's law.

The iron-nickel tube has been carefully standardized by inserting a small coil of manganine wire of known resistance into the tube, by heating this with a known electric current, and by determining the current in the tube that would exactly absorb the heat produced.

The electric currents were produced by small storage batteries, and their intensities were varied by changing the resistances in plug resistance boxes contained in the circuits. The resistances in these boxes, as well as the other resistances in the circuits, were carefully measured by a standard Wheatstone's bridge. The electric currents were measured by comparing the electromotive forces of the storage cells with that of a standard Weston cell by the potentiometer method, and by dividing these electromotive forces by the total resistance in the circuits.

The following table contains the data obtained in standardizing the iron-nickel tube. The resistance of the small coil inserted into the calorimeter was 9·20 ohms, and that of the lead wires attached to it was negligible. The electromotive force of the standard Weston cell was 1,018 volts, and that of the two cells forming the storage battery 4,153 volts.

TABLE 1.

Total resistance in heating circuit. Ohms	Heat produced in heating circuit calories per hour	Current in iron-nickel tube. Ampere		Heat absorbed per hour per ampere
		Observed	Corrected	
480	·593	·0716	·0716	8·29
550	·450	·0540	·0542	8·30
650	·324	·0392	·0393	8·25
910	·165	·0200	·0197	8·37

The compensations were not always exact, and a small correction was made in the values of the current in the iron-nickel tube. This correction was determined by observing the velocity of the bubble of air.

The heat effect in the iron-nickel tube is due to two causes. Firstly, the heat generated or absorbed at the junctions of the metals according to the direction of the current (Peltier effect), and, secondly, the heat generated according to Joule's law, which is proportional to the square of the current and to the resistance. The fifth column in the table contains the heat absorbed per hour and per ampere by the tube, and it appears that this quantity is independent of the current in the tube. This means that the absorption of heat is proportional to the intensity of the cooling current, i. e., the resistance of the tube is so small that the heat generated according to Joule's law is inappreciable, if the cooling is no larger than ·6 calorie per hour.

The mean value of the heat absorbed (or generated) per hour and per ampere in the iron-nickel tube is 8·3 gram-calories. I found 8·2 calories for the couple used in the earlier experiments.

It is interesting to note that the electromotive force in the surface between the iron and the nickel must be about ·00055 volt to produce this effect.

Fig. 2.

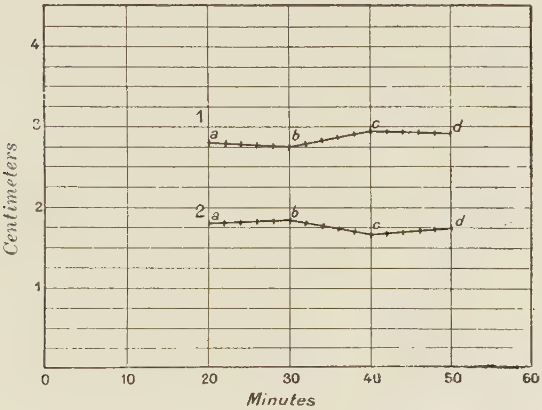

In order to determine the sensitiveness of the instrument I sent a very small current through the iron-nickel tube, and observed the change in the velocity of the bubble due to the heat absorbed or generated. The curves in figure 2 represent the displacements of the image of the bubble. The lines *ab* and *cd* represent the bubble's natural drift. The abscissas of the points *b* are the instants at which the electric current commenced to flow through the tube, and the abscissas of the points *e* are those at which the current was broken. For the first curve the direction of the current was such as to generate heat, and for the second to absorb it. It appears that the displacement of the bubble due to the current was about the same in the two cases but in opposite directions. This confirms Peltier's law, and indicates that the Joule effect is negligible.

The strength of the electric current was ·00019 ampere, and the heat generated or absorbed ·0016 calorie per hour. In ten minutes ·00027 calorie was generated or absorbed and this quantity of heat displaced the image of the bubble about 1·6^{mm}. It follows that one millimeter displacement of the image corresponds with ·00017 calorie of heat absorbed or generated.

In some other experiments I have found that the displacement of the bubble is proportional to the quantity of heat absorbed or generated, *provided that* the absorption or generation is not too rapid.

These results are used in estimating the small correction that must be applied, if the value of the current that exactly absorbs the heat generated by a source has been determined only approximately.

FIG. 3.

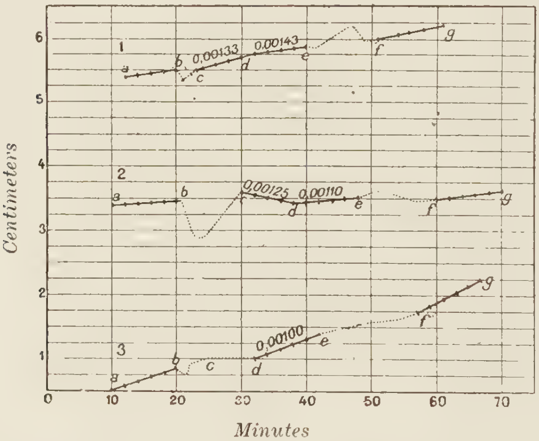

I have measured the heat generated by radiothorium and by polonium. These experiments were described in two notes presented to the Paris Academy of Sciences on June 1 and June 21, 1909.

Since the first experiments I have measured the heat generated by the polonium several times to see if the heat effect decreased with the time according to the law of decay of polonium. Half a given quantity of polonium disappears in about 142 days.

The curves in figure 3 represent the displacement of the bubble in these experiments, the dates being for curve 1 the 4th of May; for curve 2 the 4th of June, and for curve 3 the 25th of June. In each case the lines *ab* and *fg* represent the natural drift of the bubble. The abscissas of the points *b* are the instants at which the polonium was lowered into the calorimeter, and the abscissas of the points *f* are the instants at which the polonium was raised again. The numbers written near the lines *cd* and *de* are the electric currents in amperes which were flowing through the iron-nickel thermo-couple during the corresponding intervals of time.

Between the points *b* and *e* I was searching for the proper value of the current to counterbalance the heat effect, and between the points *e* and *f* I was reducing the current to zero. The last experiment was not as good as the others, because the natural drift of the bubble was large and changed a little during the experiment.

I compared the ionization due to the polonium when spread out in a thin layer on a disk of platinum (*b e*) with that due to a thin layer of radium. The results of the experiments appear in Table 2.

Table 2.

Date of experiment 1909	Current that compensated heat effect. Ampere	Heat produced calorie per hour	Ionization current due to polonium	Weight of $RaBr^{-2}$ that has same activity as polonium g.	Heat effect of this quantity of radium calorie per hour
May 4	·00143	·012	$1{\cdot}3 \times 10^{-7}$	·75	·0110
June 4	·00110	·009	$1{\cdot}19 + 10^{-7}$	·66	·0095
June 25	·00100	·008	$\cdot 99 \times 10^{-7}$	·57	·0084

It is evident that the generation of heat and the ionization current due to the polonium decrease with the time. The ionization current decreases at a rate indicating decay to half value in 136 days, which is very close to the value previously found by other experimenters. The heat effect decays a trifle faster than this, but the differences are not greater than one would expect considering the magnitude of the quantities of heat evolved. It follows from this that the heat effect was certainly due to the polonium.

On account of the difficulty of obtaining saturation in measuring the ionization of the radium and of the polonium, the method of comparing the activities of the two substances must be regarded as approximate only. Remembering this, it appears that the heat generated by the polonium is very close to that generated by the quantity of radium that would produce the same ionization as the polonium.

I have made a number of experiments on phosphorescent salts to see if they generate heat when in the phosphorescent state. Every time I examined such a salt one or two hours after it had been withdrawn from the light of the sun (or of an ultra-violet ray arc lamp), I found a small but measurable generation of heat. Twenty-four hours later not the slightest effect could be detected in the majority of cases, but a few times I observed a small generation of heat and on withdrawing the salt from the calorimeter found that the phosphorescent light had disappeared. It is impossible to affirm, therefore, that the heat effect is directly related to the emission of *visible* phosphorescent light. It may be due to the emission of visible and invisible rays together, or it may be caused by some reaction of a secondary nature.

These researches, however, have suggested to me the following question: if a quantity of radium is mixed with a phosphorescent salt, causing it to phosphoresce brilliantly, does the mixture generate the same quantity of heat as the radium would generate alone? There appear to be three possibilities: (*a*) the energy of the rays is absorbed (at least in part) in producing chemical reactions in the phosphorescent salt. In this case the heat effect of the mixture should be less than that of the radium alone, at least at first. (*b*) the radium rays acting on the atoms and molecules of the salt liberate a part of their chemical or subatomic energy. In this case the heat produced by the mixture should be larger than that produced by the radium alone. (*c*) the energy of the radium rays is rapidly transformed (in part) into the energy of the phosphorescent light without producing other reactions, and in this case, if all the light is absorbed in the vessel containing the mixture, the heat produced should be the same as that due to the radium alone.

In order to investigate this question I made the following experiments. On December 3d, 1909, a certain quantity of a salt containing finely pulverized radium chloride and barium chloride was divided into two parts. One part, A, weighed ·0314 gram and was sealed into a small glass tube. The other part, B, weighing ·0206 gram, was thoroughly mixed with ·267 gram of phosphorescent zinc sulphide, and then sealed in a second glass tube similar to the first.

Several times during the five weeks following the sealing of the tubes I measured the heat effects of each of them, and I also compared the intensity of the γ-radiation emitted by them with that due to a standard tube containing 26·5 grams of radium chloride. The following table (3) contains the results of these experiments:

TABLE 3.

Date of of experiment	Quantity of $RaCl^{-2}$ that produces the same γ-rays		Production of heat calories per hour		Ratio $\frac{A}{B}$
	A	B	A	B	
December 7	1·66	1·07	----	----	1·55
December 7	----	----	·152	·098	1·55
December 21	2·37	1·57	----	----	1·51
December 21	----	----	·199	·129	1·54
January 5	2·39	1·56	----	----	1·53
January 6	----	----	·201	·127	1·58

The γ-radiation and the generation of heat increased between the 7th and the 21st of December, but after that no increase was perceptible. This was due to the accumulation of the emanation and the induced activity, which after three weeks attained approximately their saturation values.

The sixth column contains the ratios between the tubes A and B. It appears that these ratios are the same no matter what the date of the experiment was and no matter whether the γ-rays or the heat effect was measured. It follows that the presence of the phosphorescent salt does not appreciably change the rate of generation of heat by the radium.

The following facts may be noticed in passing: The phosphorescence of the mixture has become less intense than at first but is still brilliant. The light has also changed its color, becoming more orange.

In order to investigate the heat effect in the case where the phosphorescence is produced by the β and γ rays in willemite and in platinum-barium cyanide, I arranged the following experiment: A long, fine tube is inserted into tube B of the calorimeter and around the end of this tube is packed the phosphorescent salt. A very small glass capsule hermetically sealed containing radium can be lowered down the fine tube to the center of the salt. The walls of the tube and capsule are so thin that under these conditions the salt phosphoresces brilliantly.

I compared twice the γ-rays from the capsule with those from the standard and found that the quantity of radium in the capsule corresponded with 1·91 and 1·92 mg. of $RaCl_2$.

The heat effects observed on lowering the radium to the center of the phosphorescent salt were the following:

Table 4.

Salt used	Heat calorie per hour
·67 gr. Platinum-barium cyanide	·170
1·19 gr. Willemite	·172
No phosphorescent salt	·171
No phosphorescent salt	·169

It is evident that the generation of heat is the same whether the phosphorescent salt is present or not. It follows from these two series of experiments that there is no appreciable absorption of energy in producing chemical reactions, and that the rays do not liberate an appreciable amount of chemical subatomic energy.

These results are interesting from the point of view of the amount of energy necessary to effect the organs of sight.

In the first series of experiments the phosphorescence was produced for the most part by the α-rays of the radium. We know that each α-particle that strikes the phosphorescent zinc sulphide produces enough light to affect the eye, and it follows from the experiments described above that the energy of this light is no larger than the energy of the α-particle. The smallest velocity of an α-particle that has been measured and at the same time detected by its scintillation is $5\times10^8 \frac{\text{cm.}}{\text{sec.}}$, and the kinetic energy of the α-particle at this velocity is 8×10^{-7} erg. This energy is about that required to raise $\frac{1}{100}$ of a millegram $\frac{1}{1000}$ of a millimeter. The energy necessary to produce the sensation of sight is less than the above quantity, since only a part of the total light energy enters the eye, and since probably the whole energy of the α-particle is not transformed into luminous energy.

The heat generated by one gram of pure radium can be calculated from the data of Table 3. It is for tube A 110 and for tube B 108 calories per hour. The difference between these two numbers is not greater than the errors of experiment.

The heat effect of one gram of radium calculated from the data of Table 4 is 117 calories per hour, a value considerably larger than the preceding values. This difference cannot be explained by errors of experiment. It is probably due to the fact that the radium employed in the second series of experiments is several years older than that employed in the first series, and contains, therefore, more of the disintegration products of the radium, especially polonium, which generate heat.

I have made a number of attempts to measure the heat produced by the rays from radium at a distance from their source. In the first experiments a thermopile, a bolometer, and a radiometer were tried, but none of these instruments gave satisfactory results. A modified form of differential gas thermometer gave positive indications of a heating effect, but the only instrument that proved satisfactory was the differential calorimeter described in the present paper. I hope shortly to publish some details of these experiments, but will state here simply that the problem is somewhat different from that of measuring the energy of ordinary radiations (at least as far as the penetrating radium rays is concerned), because a relatively large amount of matter is required to stop these penetrating rays, and the heat is generated throughout the mass of this matter.

Proceedings of the American Academy of Arts and Sciences.

Vol. XLVI. No. 19. — April, 1911.

CONTRIBUTIONS FROM THE CHEMICAL LABORATORY
OF HARVARD COLLEGE.

A METHOD FOR DETERMINING HEAT OF EVAPORATION AS APPLIED TO WATER.

By Theodore W. Richards and J. Howard Mathews.

Investigations on Light and Heat published with Aid from the Rumford Fund.

CONTRIBUTIONS FROM THE CHEMICAL LABORATORY OF HARVARD COLLEGE.

A METHOD FOR DETERMINING HEAT OF EVAPORATION AS APPLIED TO WATER.

By Theodore W. Richards and J. Howard Mathews.

Presented by Theodore W. Richards. Received December 24, 1910.

Among usual calorimetric measurements none has been in the past less satisfactory than the measurement of heat of vaporization. The methods employed have been almost as untrustworthy as they have been numerous. The results for water are indeed not very divergent, but in most other cases there is little or no concordance. In the case of ethyl formate, for example, the variation in the values given by different experimenters is over ten per cent; in the case of ethyl acetate, the extreme difference is over thirteen per cent. These cases have been selected because they concern substances carefully investigated by many observers; less carefully studied cases might have been selected which show even greater discrepancies. Evidently most of the results are in error; but which are the correct ones? The newest values are by no means necessarily the best, for wide discrepancies have appeared in the most recent work. Part of the errors were undoubtedly due to impurity in the materials, and some to faults in the methods.

Desiring really to know the heats of evaporation of a few liquids, we felt hopeless concerning our ability to select among these discordant figures. New research was evidently needed, involving great care in purification of material, and careful choice of the best details of experimentation. The present paper contains an account of the evolution of a satisfactory method.

A brief account of previous methods may well precede the description of our own experimental work, as this was based partly on the successes and partly on the failures of others.

The methods used for measurements of heats of evaporation are of two classes. In one the energy used in the process of vaporization is measured; in the other the energy given up by the condensation of vapor is evaluated; each procedure should of course yield the same result. Most of the methods used, particularly the earlier ones, belong to the latter class; because, although those belonging to the first class have the advantage of being independent of the values for the specific heats of the substances used, they are more complicated in manipulation and calculation, and none has proved to be entirely satisfactory.

Joseph Black[1] was the first to make the interesting observation, that in the formation of the vapor phase from the liquid phase heat is absorbed. His first experiments, though extremely crude, were sufficient to show that in the case of water the amount of heat absorbed by this transformation is considerable. Somewhat later Black and Irvine made further experiments in this direction, and found the value 520 calories per gram, which is surprisingly close to the now generally accepted value, considering the crude method with which they worked. In 1781 Watt[2] for a short time attacked the subject at the suggestion of Black, and about fifteen years later returned to it and made a number of measurements, the details and results of which he published He pointed out that heat is lost through radiation, but found no method of measuring this loss. He showed also that the condenser gains heat by conduction when connected directly to the boiler by means of a metallic tube, and sought to overcome this source of error through making the connection by means of a cork, so that metallic contact was avoided. The average of eleven separate determinations gave him the value 525.2 calories, or 625.2 from zero,[3] the values varying from 612.9 to 637.1, a difference of about four per cent; but he expressed his opinion that the true value is not far from 633 calories.

Somewhat later Count Rumford[4] made three experiments concerning the same constant, finding the mean value 667 as the total heat of evaporation from zero, — a result much higher than Watt's. Rumford also determined the heat of evaporation of two or three organic liquids, but these results have no value, since, as he admits, the substances were not pure. In this work he sought to overcome the error due to radiation by starting a determination with the calorimeter water at a temperature as much below the surrounding temperature as it would be above it at the completion of the determination, on the assumption that the gain in heat during the first half of the total time would be exactly counterbalanced by the loss in the second half. This practice has recently been found to be of very doubtful advantage.[5] In 1818 Ure[6] found the value 637.5 calories; and Despretz,[7] in 1823, published the value 631 as the result of one series of measurements, and 640 as the result of a second series, his apparatus having been similar to that used by Rumford. The next work was done by Brix[8] in 1842, who pointed out many of the causes of error and sought to correct them mathematically. His value for water was 640, including the heat given up by the water between 100° and 0°, — a result very close to the most probable figure.

---

[1] See Regnault's Experiences, Part I, p. 635 (1847).

[2] Regnault, Mém. de l'Inst. de France, **21**, 635 (1847); Robinson's Mechanical Philosophy, **2**, 5 (1822).

[3] This latter number includes the heat necessary to raise the gram of water from 0°C to 100°C.

[4] See Biot's Traité de Physique, Vol. 4, p. 710.

In 1847 Regnault[9] published his exhaustive memoir upon this subject, which surpassed in detailed precaution any preceding work. As an average of thirty-eight separate determinations he obtained the value 636.67 calories, the individual values varying between 635.6 and 638.4.

The work of Andrews[10] may be considered somewhat more in detail, because his method was similar to those which have since been usually employed. He distilled the liquid from a screened retort into a spiral condenser placed in a calorimeter, and noted the rise in temperature. The water equivalent of his calorimeter, water, and utensils was only about 280 grams, the amount of water distilled was a little less than two grams, and there was no device to prevent particles of water from being carried over in the vapor, so that the method was still evidently in its infancy. His thermometric precautions and his efforts to apply corrections for heat lost and gained by radiation were very crude, as was also his method for determining specific heats; but nevertheless, for alcohol, he obtained 202.4 at the boiling point, a value which is but three per cent lower than the present accepted value. His two figures for water, 531 and 543 calories (not including the heat required to warm the water), obtained at different rates, were less satisfactory; premature condensation evidently took place in his apparatus.

Favre and Silbermann[11] shortly afterwards measured the heats of vaporization of a number of organic liquids as well as of water, but the amount of material used was very small and the method in general unsatisfactory, so that their results are of but doubtful value.

---

[5] T. W. Richards and L. L. Burgess, J. Am. Chem. Soc., **32**, 449 (1910).

[6] Ure, Phil. Trans., 1818, p. 385.

[7] Despretz, Ann. Chim. Phys., (2) **24**, 323 (1823).

[8] Brix, Pogg. Ann., **55**, 341 (1842).

[9] Regnault, Mém. de l'Inst. de France, **21**, 638.

[10] Andrews, Pogg. Ann., **75**, 501 (1848).

[11] Favre and Silbermann, Ann. Chim. Phys. (3) **37**, 461 (1853).

The next work of importance is that of Berthelot,[12] whose method (a modification of Andrews's) is so well known as to need no description. The vaporizer was placed immediately over the calorimeter and heated by a ring burner, the tube for delivering the vapor passing through the ring. His apparatus, although ingenious, has grave defects, some of which have been pointed out by Schiff[13] and by Kahlenberg.[14] Superheating of the vapor, the most glaring defect, was suspected by the former critic, but the experimental demonstration was first made by the latter. Another source of error is direct radiation from the burner into the calorimeter, for which, however, an approximate although unsatisfactory correction may be applied. There was no device to prevent the vapor which came off from the liquid before it reached the boiling point from gaining access to the condenser.

Passing over the work of Schall,[15] who used the method of Favre and Silbermann, we come to the work of Robert Schiff,[16] who sought to avoid the causes for error in the Berthelot apparatus by removing the source of heat from the neighborhood of the calorimeter, and interposing a small silver trap just before the entrance of the vapor into the condenser. By this ingenious device, particles of unvaporized material that might be carried over by the current of vapor, and most of the liquid resulting from a premature condensation of the vapor, would be caught and prevented from going into the condenser. Some of the earlier experimenters had sought to prevent prematurely condensed liquid from reaching the condenser by making a sharp bend in the vapor delivery tube, so that condensed liquid would run back into the vaporizer, but Schiff's device has the decided advantage that the trap can be placed much closer to the condenser, so that the amount of condensation between this point and the condenser will be smaller. That this was a distinct improvement is apparent in his results; they were among the best that have been made. While the method of Schiff is undoubtedly better than any similar methods previously used, it is objectionable in the case of liquids of higher boiling point, as Kahlenberg has shown. The danger here arises from the fact that a substance of high boiling point condenses in the trap to such an extent that it finally overflows and runs into the condenser.

Another objection, heretofore not mentioned, lies in the fact that the vapor, just before it reaches the calorimeter, passes through a zone, which, though heated, is not quite as high in temperature as the boiling point, and consequently premature condensation is not wholly avoided. By no means all of the heat thus lost finds its way into the calorimeter. The result of this defect is to give a value lower than the true heat of vaporization.

---

[12] Berthelot, C. R., **85**, 646.

[13] Schiff, Liebig's Ann., **234**, 338 (1886).

[14] Kahlenberg, Jour. Phys. Chem., **5**, 215 (1895).

[15] Schall, Ber. Chem. Ges., **17**, 2199 (1884).

[16] Schiff, l. c.

In the hands of Louguinine[17] the apparatus of Schiff has been so perfected as to make it one of the most satisfactory heretofore used. The tube leading to the trap was made large in order to prevent the clogging with condensed liquid. The proximity of the hot trap to the calorimeter necessitated a correction for heat gained therefrom through radiation and conduction. In Schiff's work this correction appears to have been omitted, but Louguinine evaluated this cause of error by keeping the trap hot while he prevented both vapor and liquid from entering the condenser. In this way the heat gained per minute by radiation and conduction can be determined fairly well, and, knowing the time during which vapor enters the condenser and gives up heat, a suitable correction can be made for the heat gained by radiation and conduction during the same period. Louguinine made the distance from the trap to the condenser very short (15 mm.) in order to reduce the premature condensation of the vapor, but our experience indicates that even then he could not have been wholly successful. The fact that his results for the heat of vaporization of water are fairly concordant does not prove the absence of error from this cause. To reduce condensation to zero, the distance between trap and condenser should also be reduced to zero, — an obvious impossibility. Because, as has been said, the effect of the error is to make the heat of vaporization appear less than it really is; Louguinine's three values, 535.61, 537.61, and 538.51 calories per gram are probably too low.

About fourteen years ago J. A. Harker[18] published an elaborate and interesting account of his work. His early rejected experiments demonstrated more conclusively than ever the danger of premature condensation, and he concluded that this cause of error is inevitable, when the vapor is introduced from above. In his later work, fearing that minute drops of water exist in vapor as ordinarily formed in distillation, he passed the vapor through coils in a heated oven, and then through a zone kept at a constant temperature about three degrees above the boiling point. Finally the vapor was admitted into the condensing coil of the calorimeter, through the side of the latter, the temperature being taken at the point of introduction by means of a calibrated thermo-couple. The apparatus was ingenious, but the conduction of heat into the calorimeter from the entering tube must have been considerable, and heat was undoubtedly gained also by direct radiation from the black interior surface of the ebonite chamber at the opening in the side of the calorimeter.

---

[17] Ann. Chim. Phys., (7) **7**, 251 (1896).

[18] Mem. Manchester Lit. and Phil. Soc., (4) **10**, 38 (1896).

He concluded from his experiments, which he wished to be considered as merely preliminary, that the true value for the heat of vaporization of water (not including the heat given out in cooling the water) is about 540 calories. Unfortunately, his data, corrections, and calculations, are not given.

Kahlenberg,[19] in an almost simultaneous investigation, sought to retain all the good qualities of the method of Berthelot, and at the same time endeavored to eliminate its sources of error by an ingenious modification, using the heat generated from an electric current conveyed by a resistance wire immersed under the liquid to be vaporized, in order to produce the vaporization. Thus superheating is avoided, as well as the presence of any flame near the calorimeter. This method, undoubtedly one of the best heretofore used, has yielded fairly good results, which are nevertheless undoubtedly somewhat vitiated by premature condensation.

Other methods which should be considered are the electrical methods of Marshall and Griffiths,[20] of Marshall and Ramsay,[21] of Brown,[22] and of Henning.[23]

The method of Marshall and Griffiths is exceedingly complicated, and the heat of vaporization of but one substance, benzene, has been obtained. The values were determined for the temperature of 50°C., 40°C., 30°C., and 20°C., and the value at the boiling point obtained by extrapolation. Upon this value for benzene, thus obtained, was based all the work done by Marshall and Ramsay. This latter method was merely a comparative method. The electric current was sent through two similar vaporizers in series, and the amount of liquid distilled from each was weighed. The results obtained all depended, therefore, upon the value of the heat of vaporization of one substance, and for this one substance different experimenters had found values differing by over sixteen per cent. The investigators state that they were unable to obtain any satisfactory results for water, perhaps because of electrolysis and its consequent consumption of electrical energy.

---

[19] Kahlenberg, Journal Phys. Chem., **5**, 215 (1895).

[20] Marshall and Griffiths, Phil. Mag. (5) **41**, 1 (1896).

[21] Marshall and Ramsay, Phil. Mag. (5) **41**, 38 (1896).

[22] Brown, Jr. Chem. Soc., **83**, 987 (1903).

[23] Henning, Ann. d. Phys. (4) **21**, 849 (1906).

Brown, working with a single apparatus, passed a current of measured value for a measured time through a wire of known resistance, immersed under the liquid. The portion evaporated was weighed; thus all the data for calculating the heat of evaporation were obtained. As in Ramsay's and Marshall's method the liquid must be at the boiling point before the measured current is passed through, but no knowledge of the specific heat of the liquid is necessary. The results obtained by Brown agree well among themselves, but are even higher in value than those obtained by Marshall and Ramsay.

F. Henning[24] used a method similar in principle to that used by Brown, but superior in detail, because greater precautions were taken to provide against possible errors. The original paper must be consulted for particulars, most of which do not immediately concern the present investigation. The greatest difficulty in this interesting and painstaking work seems to have been that considerable heat was necessarily carried away by the conducting wires, and there seems to have been no entirely satisfactory method for measuring or calculating this uncertain quantity. As the mean of his determinations made at an average temperature of 100.59°, Henning found the heat of vaporization of a gram (weighed in vacuum) of water to be 538.25 calories at 15°. A number of determinations were made also at reduced pressures, but they do not concern us here.

A modification of this electrical method has been proposed by A. Cameron Smith,[25] who suggested that the electrically heated vaporizer be suspended from one arm of an analytical balance. This apparatus is suitable only for lecture demonstrations; many possible sources of error tend to diminish its accuracy.

Among these many methods, Kahlenberg's modification of Berthelot's seemed to be preferable, partly because of its simplicity, and partly because it retains the advantage of the electrical method of heating while avoiding the disadvantages. Hence we used this method as the basis of our own, seeking to discover and correct any sources of error which might still remain in it.

THE EVOLUTION OF THE PRESENT APPARATUS.

One of the most serious causes of error in all calorimetric work is the more or less uncertain correction for cooling. Hence one of the first steps of the present research was the application of the new method of adiabatic calorimetry to the problem.[26] This method, first put into practice about six years ago at Harvard, has since been used successfully in several calorimetric processes, such as the determination of specific heats, heats of neutralization, combustion, and solution. The method consists in warming the surroundings of the calorimeter at the same rate and to the same extent as the calorimeter itself during its operation. This is accomplished by surrounding the calorimeter proper by a watertight jacket, which is immersed in a larger vessel containing dilute alkali. Into the latter can be delivered the requisite amount of acid, the bath being stirred rapidly so as to insure uniformity of temperature. By such a system it is possible to prevent heat-exchange to or from the calorimeter proper, and the thermometer is stationary during both the initial and the final readings.

---

[24] Loc. cit.

[25] Proc. Roy. Soc., Edinburgh, **24**, 450 (1903).

[26] Richards, Forbes, and Henderson, Proc. Am. Acad., **41**, 1 (1905). See also Richards and Jesse, as well as Richards and Burgess, Jour. Am. Chem. Soc., **32**, 268 (1910) and **32**, 431 (1910).

For the measurements of the heat of vaporization a modified form of Kahlenberg's apparatus was combined with the adiabatic method of calorimetry. The exact form of apparatus finally used was reached only by degrees, several successive improvements having been introduced. The first modification of Kahlenberg's vaporizer consisted in the interposition of a trap or hood (C in Figures 1, 3, 4 and 5) between the boiling liquid and the condenser, to prevent drops of unvaporized material from being carried into the latter by the lively current of vapor. The objection to such a trap as that used by Schiff (namely, premature condensation of vapor) was avoided by keeping the trap entirely enclosed by the vapor of the boiling liquid, and therefore at the same temperature. Furthermore it was made in such a form as to prevent any danger of its filling and running over.

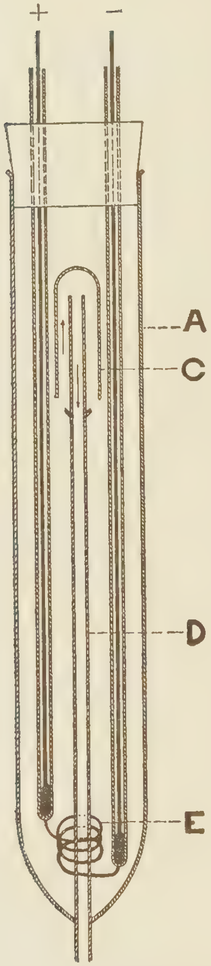

FIGURE 1. First Modification of Kahlenberg's Vaporizer.

The hood or trap (C) over the delivery tube helps to eliminate mechanically carried drops.

With this apparatus a number of preliminary determinations were made, with a condenser and calorimeter to be described presently, and a striking systematic irregularity was observed in the results. The heat of vaporization of benzene, for example, appeared to be about 89 calories when 25 grams took 14 minutes to evaporate, but as much as 93 calories when the time was shortened to 2.5 minutes, with corresponding results for intervening rates. The results are plotted in the accompanying diagram.

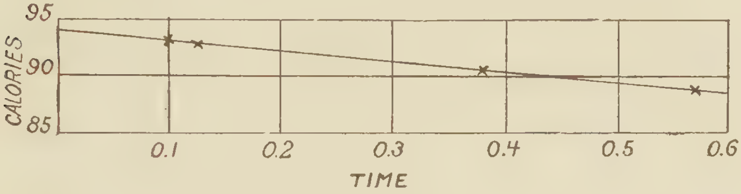

Figure 2. The Effect of Speed of Vaporization on the Results. (Benzene in the Vaporizer shown in Figure 1.)

In the direction of ordinates are plotted the observed values for the heat of vaporization of a gram of benzol in small calories; in the direction of abscissæ are plotted the times (in fractions of a minute) needed for the vaporization of that quantity.

The ordinates represent heats of vaporization in calories, and the abscissæ, the time in minutes required to vaporize one gram. By a comparatively short linear extrapolation we obtain the value 94.1 cal. as the heat of vaporization of benzene. It will be shown in a subsequent paper that this value is very near the most probable value obtained afterwards with better apparatus. Water was found to exhibit precisely the same phenomenon. Previous investigators have not taken into consideration this variation of result produced by varying the rate of distillation, and the oversight undoubtedly accounts for much of the wide variation in the published results.

Consideration of the various possible complications which might bring about this time-effect led to the conclusion that it was probably due to premature condensation between the vaporizer and the condensing coil, and the consequent loss of heat from the vapor thus condensed. Evidently such a loss must be directly proportional to the time required for the vapor to pass through the zone of premature condensation. Further, in accordance with Newton's Law of Cooling, the loss of heat should be proportional to the difference in temperature between the boiling point of the substance and the environment of this zone, — a conclusion later verified by the facts.

Attempts were next made to eliminate as far as possible the zone of premature condensation. The vaporizer was set into an asbestos shield made in the form of a frustum of a cone, the space between the asbestos and the glass being closely packed with cotton, and the outside of the cone covered with bright tin foil to cut down the radiation. In order to place the vaporizer as low as possible and at the same time to prevent its becoming wetted, a shallow glass cup was placed immediately below the asbestos shield. The cup also served to prevent loss of heat by evaporation of the calorimeter water at its surface, or by evaporation of water rising on the vaporizer stem by capillary action or other cause, such evaporation being caused by the presence of the hot tube carrying the vapor. In this manner the distance between the boiling liquid within the vaporizer and the calorimeter water was reduced to a little less than one centimeter.

In spite of the precautions to prevent radiation, the correction for heat gained by the calorimeter due to this cause was increased from about 0.002° to 0.008° per minute, a quantity which was very carefully determined and applied to the results.

This vaporizer yielded results which gave when plotted a line less steep than the previous one. The modification had evidently improved the results, but had not wholly eliminated the cause or causes of error.

In the space above a boiling liquid in a flask, a mist can often be observed. This mist is caused by radiation of heat from the walls of the vessel; and the question arose as to whether the difficulty in obtaining uniform results at various speeds might not be due in part to the formation of such a mist within the vaporizer. The mist would not be entirely caught by the trap, and would thus introduce minute drops of water into the condenser, possibly proportional in amount to the time required for distillation.

In order to discover whether any difficulty arose from this cause, the vaporizer, above the asbestos cone, was surrounded by a jacket through which live steam was passed throughout the measurement. This must have prevented the formation of a mist within the vaporizer; but the results were no better.

The ejection of fine drops from the surface of the boiling liquid — drops which might be swept along by the current of vapor — could not have been the cause of the particular trouble in question. Such an action would seem more likely when the boiling is rapid than when it is slow, an outcome exactly the opposite to that actually observed. Doubtless such an ejection occurs to a slight extent, but in our trap its effect had undoubtedly been much reduced. As will be seen, our final result shows that we have been at least as fortunate as others in eliminating this danger.

Harker, in his desperation on account of obvious premature condensation, resorted to superheating the vapor, in order to insure its being perfectly dry; accordingly we, too, tested this doubtful device. A coil of fine platinum wire was introduced into our vapor delivery tube, extending nearly its whole length, and a small current was sent through the wire. Several determinations made at different speeds and with different strengths of current through the coil, gave higher values than before. With a constant strength of current, the slower the speed, the higher was the result; and with a constant rate of evaporation, the greater the current the higher was the result. Evidently superheating occurred. With some modifications of the parts and the construction of special thermometers it would have been possible to take the temperature of the vapor as it entered the calorimeter; but the unsatisfactory nature of these experiments offered no temptation to the further prosecution of this line of attack.

Being still convinced that the principal premature condensation took place in the narrow zone between the vaporizer and the condenser, we next sought to reduce further this distance, and to protect the vapor passing through it from loss of heat. A new vaporizer having a vacuum jacket was constructed as shown in Figure 3, the walls (B) of the jacket being about one centimeter from the walls (A) of the vaporizer, save at the bottom where the distance was about eight millimeters. Both the outer wall of the vaporizer and the inner wall of

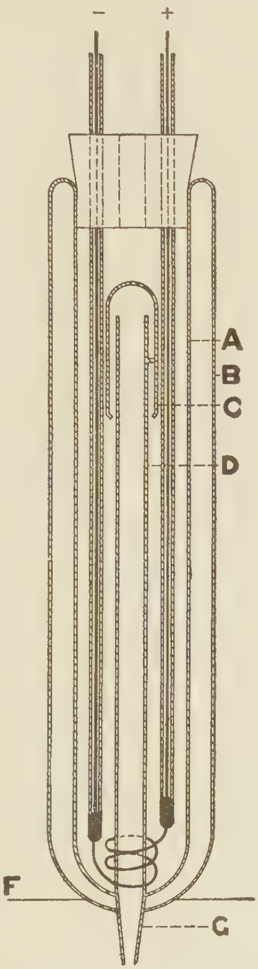

FIGURE 3. A Further Modification of Kahlenberg's Vaporizer.

The compartment containing the liquid and coiled platinum wire for heating is surrounded by a silvered vacuum jacket (AB). The trap (C) is retained. The condenser is attached at G. The vaporizer is immersed in the water of the calorimeter as far as the water-line at F.

the jacket were brightly silvered to a distance of about five centimeters above the vapor exit. The vaporizer was set so low that the level (F) of the calorimeter water came up on its jacket to a height of a few millimeters. This brought the boiling liquid in the vaporizer to within one centimeter of the calorimeter water, largely protected the vapor from condensation in this zone, and prevented most of the evaporation from the surface of the calorimeter water at the line of immersion. The vaporizer projected a short distance through the adiabatic cover, and, since the projecting part was silvered, the amount of radiation was not excessively large. The space around the vaporizer was closely packed with cotton. With this apparatus, values were obtained which were slightly higher than those previously obtained with the earlier forms of apparatus, when made at the same rate; but they were not as consistent as desired, partly because of the fact that the diameter of the exit of the delivery tube was much too large.

Another attempt to reach a better result led to the cutting off of still more of the delivery tube below, the thermal protection being provided only by a rubber cup, cut from a child's ball, placed between the vaporizer and condenser. The rubber cup was packed with cotton, as was also the space around the vaporizer. After a few determinations, however, the apparatus was discarded, because the correction for radiation and conduction was very large (0.040° per minute), and also because of the difficulty in making a tight joint.

The form of apparatus finally adopted combined all the advantages of the preceding forms, and is shown in Figure 4. The boiling liquid was surrounded by a vacuum jacket whose walls were about one centimeter from the walls of the boiling compartment, save at the bottom where the space was but five millimeters across. In addition to the hood covering the upper end of the vapor delivery tube, the tube was also provided with another trap to catch and retain any liquid that might in any way gain access thereto. This trap was placed as low as possible so that the distance between it and the condenser might be reduced to a minimum, yet it was surrounded by the boiling liquid in order to prevent condensation within it. The heating coil was placed so low as to make sure that the liquid surrounding the trap was at the boiling point. If prematurely condensed liquid now gained access to the condenser, it must come entirely from condensation in the short distance between the trap and the calorimeter water, — because all previously condensed liquid was caught in the trap. After an experiment the trap usually contained a few drops of liquid, sufficient to have introduced appreciable error, had it been allowed to reach the condenser.

The interior of the vacuum jacket was brightly silvered to a height of four or five centimeters, the silvering being on both walls, so that any heat passing from the boiling liquid to the calorimeter water by radiation had to pass through two brightly silvered surfaces and a vacuum space. The conduction of heat to the calorimeter through the glass itself cannot be prevented, but was made small by having the glass as light as was consistent with the strength demanded. The proper correction was always applied for heat gained by the calorimeter in these two ways, the necessary observations being always determined before each measurement of latent heat. For several minutes previous to admitting the vapor into the condenser, readings of the temperature were made at intervals of one minute, until the increase became constant and of certain value. The nature of the problem is such as to make this correction absolutely necessary, for the vaporizer must be brought close to the calorimeter water, and radiation and conduction across this small distance cannot be prevented.

After many experiments had been made, not only with water but also with higher boiling substances, the accidental cracking of the vaporizer jacket near the top destroyed its high vacuum; nevertheless the correction for the combined radiation and conduction was then found to be but little greater than before. Apparently the two brightly silvered surfaces effectually prevented radiation.

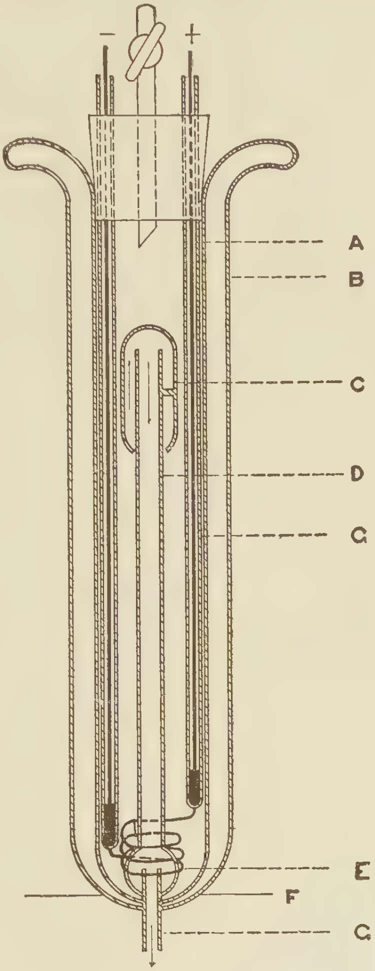

FIGURE 4. Final Form of Vaporizer (½ actual size).

A vacuum jacket (AB), silvered inside, surrounds the hot vessel, which is provided with a stopcock above. The delivery tube has two traps, one over its top (C), and another (E) as near as possible to the water of the calorimeter below. The condenser is attached at the very bottom at G, and F is the waterline, as in Figure 3.

The heating coil had a resistance of about 0.7 ohm, and was supplied with a suitably controlled current of from twelve to eighteen amperes from eight large storage cells. The ends of the coil were sealed into the ends of small glass tubes within which were stout copper wires, contact being made by mercury. It is necessary that the copper wires be heavy so that they may not become heated, and thus superheat the vapor coming into contact with the glass tubes encasing them.

The temperatures at which distillations took place were read from small standardized Anschütz thermometers, whose mercury threads were entirely within the vapor, so that no correction for projecting mercury thread was necessary. The bulb of the thermometer was placed opposite the entrance to the hood, in order to measure the temperature of the vapor actually admitted — a point especially emphasized by Louguinine, who nevertheless merely inferred the temperature from the barometric pressure and the coefficients expressing the dependence of boiling point on pressure.

Another point, usually neglected, is worthy of brief notice. Before the liquid comes to the boiling point, an appreciable quantity of vapor may pass over and be condensed. Obviously this may introduce error, since the assumption is made, in calculating the result, that all the vapor was at the boiling point of the liquid. Moreover, the heat of vaporization is different at different temperatures. In the present experiments this cause of error was eliminated by providing the vaporizer with an outlet and stopcock above, and by passing a very slow current of dried air backwards through the condenser coil and vaporizer until the liquid was boiling at a lively rate, and the temperature of the whole interior was quite at the boiling point of the liquid. This air prevented the vapor from passing into the condenser, so that no premature condensation was possible; its initial temperature was kept close to that of the calorimeter.

Preliminary experiments were made to find whether or not the proximity of the hot coil of platinum wire might superheat the vapor passing in its downward course to the condenser. The wire was first made into a coil about 3 cm. in diameter, and a thermometer suspended therein, the bulb of the thermometer being at the center. The coil and thermometer bulb were then immersed in distilled water in a large open test tube, the current was connected, and the temperature noted at which boiling occurred. The coil was then made about 2 cm. in diameter and the process repeated; finally the wire was coiled as tightly as possible around the thermometer bulb, without actual contact, and the temperature at which boiling took place was noted as before. It was found that there was no danger of superheating from this source, as the temperature recorded by the thermometer was exactly the same in all three cases. As long as the wire is covered with liquid, it matters not whether the resistance wire is coiled loosely or closely around the tube through which the vapor is passing. Hence

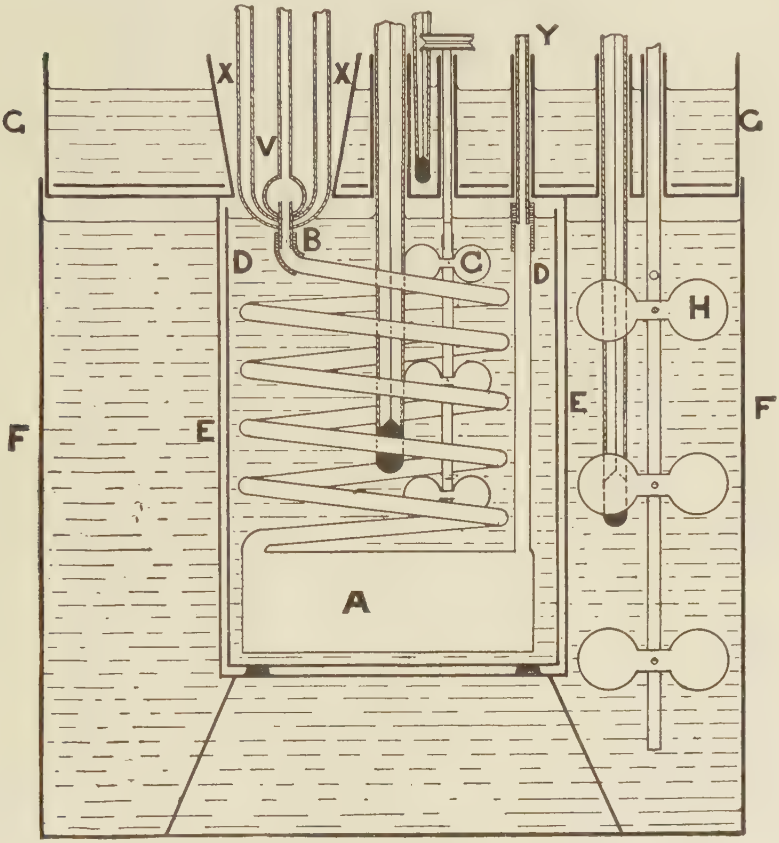

FIGURE 5. The Calorimeter.
The vaporizer (V) is set within a large hole (XX) in the cover. At B is attached the condenser A immersed in water contained in the calorimeter. Between the jacketing vessels E and F is dilute alkali, into which sulphuric acid is dropped in order that the temperature of the surroundings should keep pace with that of the calorimeter proper. C is a stirrer within the calorimeter, H one in the outside vessel.

vapor passing through a tube similarly encircled by hot wire must be free from superheating.

The calorimeter, of about 1.5 liters capacity, was made of thin nickel-plated sheet copper, highly burnished on the outside. It was almost filled with water, and is shown in Figure 5 (D, D). The condenser (A) within the calorimeter was constructed of block tin, the joints being soldered by tin only; it consisted of a spiral tube, 1 meter long and 3 millimeters in internal diameter, coiled in four turns, with a tin cylinder 10 centimeters long and 3 centimeters in diameter at the bottom to serve as a receptacle for the condensed liquid. The tin cylinder had an outlet tube, leading directly up to the air of the room. The tin coil and cylinder together weighed 436.7 grams. The outlet tube or beak of the vaporizer was attached to the worm by a short piece of pure rubber tubing (B). Various preliminary experiments were made as to the position of this joint in relation to the water of the calorimeter, but the details need not be given. Finally, the arrangements shown in the figure was adopted; the silvered jacket of the vaporizer was immersed to the depth of about a centimeter under the water. The water-line was thus protected from heat by the vacuum jacket, and abnormal evaporation and cooling at this point were therefore avoided.

The stirrer (C) within the calorimeter was of the propeller pattern, having six blades, each 1 centimeter long. It was made of copper, and, in order to prevent loss of heat by conduction, extended only to the surface of the water, where it joined a shaft of hard rubber to which was attached the driving mechanism. The scarcely perceptible evolution of heat from the stirrer, being directly proportional to the time of the experiment, was included with the warming due to the proximity of the vaporizer in a single time-correction, and thus eliminated from the result.

The heat capacity of the solid parts of the calorimeter was equivalent to 53.4 grams of water, the separate parts amounting to the following quantities. The finished copper calorimetric vessel weighed 299.95 grams. It was "plated" inside and out with a thin electrolytic film of burnished nickel, which has a specific heat so near that of copper as to cause no appreciable difference in the heat capacity of the whole. The copper vessel was soldered with about 4 grams of solder, the solder consisting half of lead and half of tin, and having therefore a specific heat of about half that of copper. The calorimeter vessel with its nickel and solder was therefore approximately equivalent to the pure copper vessel, weighing 298 grams, and had a heat capacity equivalent to 27.7 grams of water, the specific heat of copper at 21° being about

0.093. It may be noted that the weight of the copper vessel need not be known within two or three grams, for this corresponds to the limit of possible accuracy of the thermometric part of the experimentation. The pure tin condenser weighed 436.7 grams, and therefore had a heat capacity equivalent to 23.6 grams of water, the specific heat of tin at 21° being about 0.054.[27] The thermometer was found by the method of Ostwald-Luther[28] to have a heat capacity equivalent to 1.4 grams of water; and the copper stirrer, weighing 7.7 grams, had a heat capacity of 0.7 on the same basis. These weights have as their sum 53.4 grams.

An important matter of detail lay in the discovery of the time needed for equalization of temperature between the hot liquid accumulating in the condenser and the water of the calorimeter. In order to test this, a glass funnel was substituted for the vaporizer at B, and 17 grams of water were poured little by little through this funnel during 5 minutes. There being no heated object near the calorimeter, the radiation-effect was negligible, and the rise in temperature of the calorimeter water was due only to the hot water introduced.

Immediately after the addition, the reading of the thermometer was a trifle over 1°; in another minute the thermometer read 1.101°; in yet another minute 1.104°. In the 3 minutes following, the thermometer rose 0.001° each minute, and finally remained perfectly constant at 1.107°. Thus in 5 minutes after the last portion of water had been added a constant temperature had been attained, showing that with the rate of stirring usually adopted, this time was sufficient for complete equalization of the temperature within the calorimeter.

The calorimeter was surrounded by a narrow air-space, bounded by a copper can (E) with a burnished nickel-plated lining. This was immersed in a much larger vessel (F) of about ten liters capacity, which contained dilute crude sodium hydroxide. The outer vessel was provided with a basin-shaped cover (G) of about four liters capacity, through which were several openings for thermometers, vaporizer (V), stirrer, etc. The bottom of the cover was coated with bright tin-foil. In this way the calorimeter was entirely surrounded by a uniform temperature, except where the vaporizer protruded through the cover. A powerful stirrer (H), revolving at the rate of 250 revolutions per minute and driven by an electric motor, kept the lower alkaline solution in violent agitation, while the solution in the cover was more gently agitated by means of a perforated ring of heavy sheet copper, lifted by an electric motor and allowed to fall by its own weight. The stirring in the cover need not be so energetic as that below, since the temperature in this part of the bath need not be so accurately adjusted as in the lower compartment.

---

[27] The specific heats of copper and tin usually given (0.094 and 0.055 respectively) correspond to the range between 20° and 100°. The values given above take account of the decrease with decreasing temperature.

[28] Ostwald-Luther, Handbuch, p. 300 (1910).

As the temperature in the calorimeter rose, because of the condensation of the vaporized liquid, concentrated sulphuric acid was run from burettes into both jacketing compartments, so that the environment around the calorimeter was changed in temperature as fast as the calorimeter itself. The details are so similar to those of the other applications of this adiabatic method that they need not be reviewed. The stirring was so effective that the thermometers in different parts of the bath all rose at practically the same rate.

It was found possible to follow the rising temperature of the calorimeter within 0.05° in the lower compartment and within 0.1° in the upper compartment throughout the entire course of the experiment. Suitable tests proved that with so small a difference in temperature there was no danger of appreciable heat-exchange with the surroundings during the brief progress of a determination.

The rise in temperature of the calorimeter was measured by a carefully standardized Beckmann thermometer, having a slender bulb and rather a long scale. Readings to 0.001° were made with certainty by means of a lens. The standardization was effected with very great care by comparison with two Baudin thermometers standardized by the Bureau des Poids et Mesures of Paris. The comparison was conducted by immersing all the thermometers in the water of the adiabatic calorimeter surrounded by its jacket. The calorimeter was covered tightly with a non-conducting cover through which the thermometers and stirrer passed, and the thermometer to be studied was immersed to the depth at which it was subsequently to be used. All the thermometers were placed as closely together as possible in order to insure their having the same temperature. The temperature of the calorimeter water could be held perfectly constant for any desired length of time, so that there was no error due to the lag in any of the thermometers. Readings were made (after gently tapping the thermometers) at every $\frac{1}{10}$° mark, and the corrections were calculated with due account of the corrections for the various standardized thermometers used. The Baudin thermometers had previously been found to agree very closely with an accurate Fuess thermometer, which in its turn had been carefully studied by the Reichsanstalt of Berlin.

The various parts of the apparatus having been described in detail, the actual execution of the experimental work may now be considered.

As may have been inferred, many preliminary determinations were made in order to determine the best conditions, and the various dangers to be avoided. Water, having been the liquid most studied by others, was chosen as the most desirable substance with which to test the apparatus and method.

Over thirty trials were made with the object of finding the best position of the vaporizer and testing various devices to prevent radiation.

Finally the following method of experimentation was adopted : The pan-like copper cover (G, Figure 5) of the calorimeter jacket was placed temporarily upon a raised stand which permitted easy access to its lower surface ; the vaporizer (V) containing the liquid to be investigated was adjusted into its place (packing the space X between its silvered envelope and the copper cover with cotton wool), the empty weighed condenser (A) was then attached to the beak of the vaporizer (B) as it protruded beneath the elevated copper cover, and the thermometer and stirrer were arranged in their orifices. Meanwhile the calorimeter had been almost filled with a weighed amount of water at about 20°, and the jacketing crude alkaline solutions had been adjusted at exactly the same temperature. When all was ready, the copper cover with the suspended condenser was placed into position over the calorimeter, the condenser being immersed very carefully in the calorimeter water. The silvered beak of the vaporizer itself dipped about a centimeter under the surface, as shown in the diagram. The slow backward current of air, which served to prevent the access of vapor to the condenser until all was ready, was then driven through the apparatus, and at the same time the heating electrical current was turned on within the vaporizer. When the liquid was actively boiling, a careful study of the radiation-conduction-effect on the calorimeter was made. This having been accomplished, the actual experiment could begin ; the stopcock (K, Figure 4) above was closed and the backward current of air discontinued. The rapid current of vapor was thus suddenly switched into the condenser, and the temperature of the calorimeter began to rise at a rapid rate. This rate was continuously matched in the environing alkali by admitting acid in suitable quantities, and the experiment proceeded very smoothly until a rise of about 4 degrees had been accomplished. Finally the stopcock (K, Figure 4) above the vaporizer was suddenly opened, the posterior outlet (Y, Figure 5) of the condenser closed, and the electric current cut off. The vapor forming was then free to escape into the air, and when boiling stopped, the condensed liquid was not drawn back into the vaporizer by the sudden vacuum formed upon cessation of boiling. For at least five minutes afterwards, the temperature of the calorimeter was read every minute with as great care as at first. After dismounting the apparatus the condensing coil was dried outside and weighed; and the experiment was thus brought to a close.

The increasing temperature and the increasing heat capacity of the calorimetric system during an experiment cause complications in the calculation which have usually received insufficient attention. At the beginning, the heat capacity of the calorimeter is that of the solid apparatus and the water in which the coil is immersed. As the experiment proceeds, this heat capacity is augmented by the liquid which collects within the condenser. At the end of the distillation the heat capacity of the calorimetric system reaches its maximum. Evidently the value used in the calculation must be taken as the initial heat capacity plus the heat capacity of half the condensed liquid.

Heat is radiated and conducted from the hot vaporizer into the calorimetric system, and correction for this unavoidable complication must be applied. The correction is primarily based upon the measurement of the heat gained during the preliminary minutes before the experiment has been begun, in the usual fashion; but it must be remembered that this value does not apply exactly to the end of the experiment, because the calorimeter has then risen in temperature, and therefore cannot take so much heat from the vaporizer as before. For example, if the temperature of the calorimeter is 20° at first and 24° at the conclusion of the experiment, and if the vaporizer has a temperature of 100°, it is evident that the difference of temperature between the vaporizer and the calorimeter is 80° at first and only 76° at the end. Hence, if the calorimeter gains 0.009° during each preliminary minute, it will be expected to gain only $76/80 \times 0.009° = 0.0085$ during each final minute, and intermediate values during the intervening period. The method of correction for this changing effect is obvious and was easily applied. This practice was justified by the actual results, for the warming effects of the hot vaporizer was always found to be less after the experiment than before. The diminution was manifest even before the vaporizer itself had cooled considerably.

The changing condition of the calorimeter involved a similar detail in the calculation of the heat given out by cooling the condensed liquid from its boiling point to the temperature of the condenser. The heat actually measured in the calorimeter was due of course not only to the heat given out by condensation, but also to that given out by the condensed liquid in falling from the temperature of the vaporizer to that of the calorimeter. The first portion of condensed liquid is cooled to the initial temperature of the calorimeter, the last portion only to the somewhat higher final temperature. Obviously here again the mean temperature must be taken in the calculation. Thus, if the experiment began at 20° and ended at 24° and the barometer indicated 760 mm., the first drop of water was cooled through 80°, the last through only 76°. Obviously here again the average value, 78°, should be taken in the calculation. It is easy to show by means of the calculus that all these compromises in the calculation are legitimate.

The amount of water evaporating into the small air space around the calorimeter during an experiment was negligible both in weight and in thermal effect.

There follows, as a typical example, the complete data and computation of a single case, the second given in the table, selected at random from results.

For five minutes preceding the experiment, the calorimeter gained at a perfectly constant rate of 0.009° per minute. When this was certain the vapor was turned into the condensing coil, and after five minutes more the electric current of 14 amperes was stopped, and the vapor prevented from gaining further access to the coil. In yet five minutes the calorimeter had settled down once more to a rate of increase in temperature corresponding to that observed at first, that is to say, 0.0085° per minute, clearly due only to radiation and condensation from the vaporizer. The heat from the actual condensation had all been imparted to the calorimeter, hence the experiment was considered as concluded. The several data and the simple calculation depending upon them are given below. The barometric pressure was exactly 760.0, hence the steam entered the condenser at 100.0°.

In calculating the heat given out in cooling a gram of water from 100° to the mean temperature of the calorimeter (21.42°) the figures of Barnes[29] were employed, because they probably represent most nearly the present standard of temperature. By graphic integration, the average specific heat of water over this range was found to be 1.0012 times the value at 21.4°; hence is calculated the value 78.67 calories above, corresponding to a fall of 78.58°. The 21° calorie is apparently about 0.9985 times the 15° calorie, hence in terms of the latter the result would be 535.2.

Six determinations were conducted in this way with this vaporizer, two of them being run very slowly and the others with increasing speed. For the slowest about 11 or 12 amperes were usually necessary, and 17 or 18 amperes were required for the fastest. The results are rearranged in the table and renumbered in order of speed, beginning with the fastest, so as to make the dependence of the results upon the

---

[29] Landolt and Börnstein, Tabellen, pp. 393 and 810 (Berlin, 1905).

HEAT OF VAPORIZATION OF WATER.

Determination No. 2.

Time when Reading was taken	Observed Thermom. Reading in Water in Calorimeter (uncorrected).	Increase in Temperature per Minute.
1.21	0.090°	
1.22	0.098°	0.008°
1.23	0.107°	0.009°
1.24	0.116°	0.009°
1.25	0.125°	0.009°
1.26	0.134°	0.009°
1.27	0.143°	0.009°
1.28	0.152°	0.009°
1.29	0.161°	0.009°
	Average,	0.009°
1.29	Vapor turned into coil.	
1.34	Electric current stopped.	
1.35	5.100°	. . .
1.36	5.117°	0.017°
1.37	5.128°	0.009°
1.38	5.138°	0.010°
1.39	5.147° [30]	0.009°
1.40	5.155°	0.008°
1.41	5.164°	0.009°

	Reading of Thermometer.	Correction to reduce Reading to true Temperature.	Corrected Temperature Hydrogen Scale.
Final temperature	5.147°	+18.787	23.934°
Initial temperature	0.161°	+18.760	18.921°
Total rise in temperature			= 5.013°

Rise due to radiation and conduction (2.5 × 0.009° + 7.5 × 0.0085) = 0.086°

Rise in temperature due solely to condensation of vapor and cooling of resulting liquid to temperature of calorimeter = 4.927°

Water equivalent of calorimeter and fittings	53.4 grams
" " water in calorimeter	1252.9
" " ½ the liquid condensed	5.26
Total water equivalent	1311.56 grams

---

[30] Point at which rise of temperature due to condensation of vapor ceased. Further increase of temperature, since the rise did not exceed 0.0085° per minute, was due to radiation from vaporizer.

Weight of condensing coil and condensed liquid	447.219
Weight of condensing coil alone	436.705
Weight of vapor condensed (liquid vaporized)	10.514 grams

Total heat effect per gram $= \frac{1311.6 \times 4.927}{10.514} = 614.63$ cals. at 21°

Heat given out by cooling 1 gram from 100.0° to 21.42° = 78.67 cals. at 21°

Uncorrected heat of vaporization of *one gram* of water = 536.0 cals. at 21°

speed more clearly manifest. The first five experiments made early in December, 1907, were all consecutive; but that numbered 6 was executed long after the others (in January, 1908), after the vacuum jacket had been used for higher boiling liquids, and had unfortunately cracked. Except for its somewhat larger warming correction, no essential difference could be detected between its results and that of the preceding experiment, carried out at the same rate. The last experiment was conducted under a pressure of 757 millimeters of mercury, the others were practically at normal pressure of 760 millimeters.

The table explains itself.

Heat of Evaporation of Water.

Series I, with Vaporizer I.

No. of experiment.	Observed weight condensed water (in air).	Time in minutes.	Time for one gram.	Rise of temperature corrected for radiation from vaporizer.	Water equivalent total.	Difference between temperature of vaporization and mean temperature.	Heat of vaporization + heat of cooling to temperature of calorimeter.	Heat of vaporization of 1 gram (uncorrected) in 21° calories.
1	8.319	3.0	0.36	3.921°	1307.6	78.9	616.3	537.4
2	10.514	5.0	0.48	4.927°	1311.6	78.6	614.6	536.0
3	8.283	4.25	0.51	3.895°	1307.8	78.8	614.9	536.1
4	9.558	8.5	0.89	4.473°	1309.3	78.6	612.6	534.0
5	8.368	9.0	1.07	3.896°	1310.2	78.3	609.9	531.6
6	8.398	9.0	1.07	3.916°	1309.4	78.4	610.5	532.1

It will be noticed that the figure in the last column falls from 537.4 calories per gram, the result of the fastest determination, to 531.8 calories, in the two slowest, — a change of about 1 per cent.

This definite march of the results seems to be referable only to the loss of heat by premature condensation in the part of the tube between the trap and the condenser, — a defect in the method which is inevitable, for the vaporizer could hardly be brought closer to the calorimeter than it was in these experiments.

When the results are plotted, the values for the heat of vaporization being laid out in the direction of ordinates, and the time required for vaporization of 1 gram laid out in the direction of abscissæ, the linear tendency of the results is manifest. The greatest departure of any single result from the straight line representing their average tendency is only 0.6 calorie, or 0.1 per cent of the total thermal quantity being measured. This corresponds to an error of thermometric reading of 0.004°. The agreement therefore is as close as could be expected.

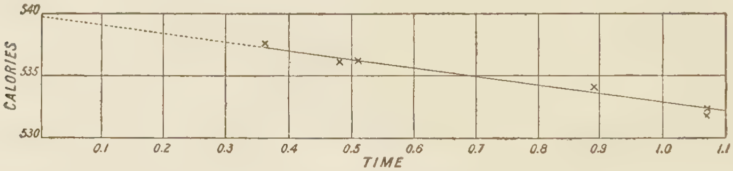

Figure 6. The Heat of Evaporation of Water; First Series.

Time in fractions of a minute is plotted in the direction of abscissæ, and heat of evaporation (in 21° calories) in the direction of ordinates. The dotted line is an extrapolation, giving the value for a hypothetical instantaneous experiment.

By extrapolation to zero time the value 539.6 (cal. 21°) is obtained for the heat of vaporization of a gram of water weighed in air — a value from which the effect of premature condensation must have been eliminated, because there is every reason to believe that this disturbing phenomenon is directly dependent upon the time consumed in the experiment, and that if the experiment could be performed instantaneously the error would wholly disappear. This value becomes 538.8 in terms of the calorie at 15°.

Inspection of the curve shows that the loss of heat in 1 minute must have been 7.0 small calories from this apparatus under these circumstances, and each of the results is evidently to be reduced to a common basis by adding to it this value multiplied by the fraction of a minute required for the vaporization of 1 gram. The results, then, become respectively 539.9, 539.4, 539.7, 540.2, 539.1 and 539.6, in the mean 539.6 (cal. 21°), essentially the same as the value found by the graphic extrapolation, upon which indeed the values are directly dependent.

Feeling that it was desirable to test these conclusions in another apparatus, a new vaporizer was made, — unfortunately, however, with a somewhat wider and heavier exit tube. In this apparatus both the warming effect of the vaporizer upon the calorimeter and the loss of heat from premature condensation were greater than before — the former instead of being about 0.009° per minute became about 0.013, and the correction for premature condensation also increasing from 7 calories per minute to nearly 9.7 calories per minute. The determinations were also somewhat less concordant than before, as was to have been expected on account of the larger correction for radiation and conduction. Nevertheless they add valuable confirmatory evidence to the results given in the previous series, and accordingly are recorded in the following table arranged in the same way as those. Experiments 7, 8, 9, 10 and 11 were consecutive, and were made on the 7th and 8th of April, 1908. Experiment 12 was made at another time, but accords satisfactorily with 11, having about the same rate. During Nos. 7, 9 and 10 the barometer stood at 763 millimeters; during Nos. 8 and 11 at 766 millimeters, and during 12 at 762 millimeters.

HEAT OF EVAPORATION OF WATER.

Series II, with Vaporizer II.

No. of experiment.	Observed weight condensed water (in air).	Time in minutes.	Time for one gram.	Rise of temperature corrected for radiation from vaporizer.	Water equivalent total.	Difference between temperature of vaporization and mean temperature.	Heat of vaporization + heat of cooling to temperature of calorimeter.	Heat of vaporization of 1 gram (uncorrected) in 21° calories.
7	7.435	3.0	0.40	3.484°	1309.0	78.62	613.5	534.9
8	7.170	3.0	0.42	3.376°	1306.9	78.95	615.4	536.4
9	8.740	4.5	0.52	4.091°	1308.6	78.54	612.5	534.0
10	8.625	5.0	0.58	4.034°	1308.6	78.59	612.1	533.5
11	9.040	10.0	1.11	4.190°	1310.1	78.69	607.3	528.6
12	9.150	10.0	1.09	4.250°	1307.8	78.54	607.5	529.0

On extrapolating the steeper but fairly consistent straight line drawn through these determinations, the value 539.3 (cal. 21°) is obtained for the heat of vaporization of a gram of water, a value only about 0.06 per cent lower than that found in the previous series. A part of this difference is due to the slightly higher temperature of boiling in the second series, caused by the greater pressure.

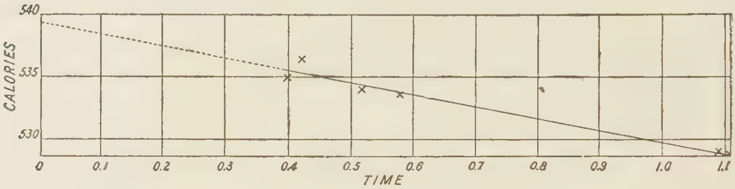

Figure 7. The Heat of Evaporation of Water; Second Series.

Time in fractions of a minute is plotted in the direction of abscissae, and heat of evaporation (in 21° calories) in the direction of ordinates. The dotted line is an extrapolation, giving the value for a hypothetical instantaneous experiment.

The individual determinations may be corrected by adding to them 9.65 multiplied by the time needed for vaporization of 1 gram, because the loss of heat is found through extrapolation to have been 9.65 small calories per minute. Corrected in this way the five determinations become respectively 538.8, 540.5, 539.0, 539.1, 539.3, on the average 539.3 as given before. The average of the results given in this series and those given in the previous series is 539.45. As the second decimal place has no significance, this may be rounded off to 539.5, giving the first series preference, partly because the pressure was more nearly normal, and partly because the apparatus was undoubtedly better and the series more concordant. This value becomes 538.7 in terms of the calorie at 15°. If the weight of the water is reduced to the vacuum standard, both of these figures are diminished by 0.11 per cent. The resulting values may be given in a brief table, together with the same quantity expressed in terms of the c. g. s. units : —

Final Result.

Latent heat of evaporation at 100° of 1.0000
gram (in vacuum) of water equals

538.9 cal.$_{21^\circ}$ or 0.5389 Cal.$_{21^\circ}$
538.1 cal.$_{15^\circ}$ or 0.5381 Cal.$_{15^\circ}$
2251 joules or 2.251 kilojoules

In all the subsequent work the first vaporizer was used, even although its vacuum had been destroyed; and it continued to give excellent results with other substances. The communication of these results must be left for a future publication, partly because the necessary specific heats of the liquids are not yet well enough known. One point, however, in connection with the results may advantageously be mentioned here, because it strengthens highly one's faith in the method of extrapolation employed to eliminate the effect of premature condensation. The loss of heat per gram was 7 calories per minute with steam in the best apparatus (Vaporizer I). With liquids of lower boiling point the loss should be less; with liquids of higher boiling point the loss should be more, if the inference is really justified. As a matter of fact precisely this phenomenon was noticed with different liquids. For example in the case of benzene, where the difference between the temperature of the vaporizer and that of the calorimeter amounted to 60° instead of to about 80°, the loss per minute amounted to about 5.2 calories per minute,[31] a figure strictly proportional to the number 7.0 found in the case of water. Again, with ethyl butyrate, boiling at 122°, the difference between the temperature of the vaporizer and that of the calorimeter was 102° instead of 80°, a fall of temperature which should correspond to a loss of heat of about 9 calories per minute, and the actual loss was found to be about 9.2 calories per minute, an amount as close as could be expected to the computed result. Moreover, in the case of methyl formate, boiling at 32°, the time of the experiment made practically no difference at all in the observed value for the heat of vaporization. Thus it seems perfectly clear that the march in the results is really due to an illicit loss of heat, and that the method employed for correcting the results is the best that can be devised. In conclusion the remark may be made that unfortunate as this inevitable difficulty with the method is, it is no more unfortunate than similar difficulties which come into any other method for determining the latent heat of vaporization. As has been more than once pointed out, the very nature of the problem renders impossible a method wholly free from some sort of correction. Even Henning's far more complicated method had its own difficulties of a somewhat similar kind, as a perusal of his paper will show.

The comparison of our value for the heat of vaporization of a gram of water weighed in vacuum, 538.9 cal._{21° (or 538.1 cal._{15°), with the work of others, speaks strongly in its favor. The value given by Regnault, 536.7, is unquestionably too low. Henning's value, 538.25 cal.$_{15}$ was found at 100.6°. Corrected to 100°, this would be 538.7 cal.$_{15°}$, a value only a trifle above ours. Joly,[32] Harker,[33] and Smith,[34] likewise obtained values near 540.

---

[31] This figure applies only to Vaporizer I, not to the preliminary form used in the benzene series given on p. 13. In the early form the loss per minute was over 9 calories with benzene.

In conclusion we are glad to express our gratitude to the Carnegie Institution of Washington, for generous pecuniary assistance.

Summary.

1. The method of Berthelot and Kahlenberg for determining heats of vaporization has been modified in such a way as to diminish greatly the errors inherent in the experimentation. A Dewar vessel was used as a vaporizer and the calorimetric work was strictly adiabatic.

2. A serious persistent disturbing effect, amounting to about 0.1 per cent of the total per minute, was eliminated by conducting experiments at different speeds and extrapolating the results to a hypothetical instantaneous experiment from which the disturbing effect may be supposed to be eliminated, because this was found to depend essentially upon time. The disturbing effect was probably premature condensation in the very narrow zone between the vaporizer and the condenser.

3. The heat of vaporization of a true gram of water was found by this method to be 538.9 cal.$_{21°}$ or 2.251 kilojoules per gram. A gram molecule therefore requires 9.707 Cal.$_{21°}$ or 40.54 kilojoules, when the vaporization is conducted at 100° ($O = 16.000$, 1 Cal.$_{21°}$ = 4.177 kilojoules).

4. Comparison of this figure with the results of others shows that the method is trustworthy and suitable for general use.

5. Numerous other liquids also have been used in the apparatus, and consistent results with them have been obtained. These will be communicated in a future paper, when the specific heats of the liquids have been determined.

---

[32] Phil. Trans., **186**, 322 (1895). Dependent on Joly's value for the mean calorie between 12° and 100° as determined by the steam calorimeter.

[33] Loc. cit.

[34] Loc. cit.

Proceedings of the American Academy of Arts and Sciences.

Vol. XLVI. No. 20. — April, 1911.

CONTRIBUTIONS FROM THE JEFFERSON PHYSICAL LABORATORY, HARVARD UNIVERSITY.

THE EFFECTS OF SUDDEN CHANGES IN THE INDUCTANCES OF ELECTRIC CIRCUITS AS ILLUSTRATIVE OF THE ABSENCE OF MAGNETIC LAG AND OF THE VON WALTENHOFEN PHENOMENON IN FINELY DIVIDED CORES. CERTAIN MECHANICAL ANALOGIES OF THE ELECTRICAL PROBLEMS.

By B. Osgood Peirce.

With a Plate.

CONTRIBUTIONS FROM THE JEFFERSON PHYSICAL LABORATORY, HARVARD UNIVERSITY.

THE EFFECTS OF SUDDEN CHANGES IN THE INDUCTANCES OF ELECTRIC CIRCUITS AS ILLUSTRATIVE OF THE ABSENCE OF MAGNETIC LAG AND OF THE VON WALTENHOFEN PHENOMENON IN FINELY DIVIDED CORES. CERTAIN MECHANICAL ANALOGIES OF THE ELECTRICAL PROBLEMS.

By B. Osgood Peirce.

Presented May 11, 1910. Received December 31, 1910.

In making some kinds of electrical measurements, one occasionally needs to alter abruptly the inductances of a circuit and to inquire what the effect of the change is upon the march of the currents which the circuit is carrying. If the circuit happens to be a simple one with no magnetic metals and no other circuits near, and if the whole change takes place in a sufficiently short time, it is easy to compute the magnitude and the direction of the corresponding change in the current. If, however, the circuit is complex, or affected by the presence of other inductive circuits in the neighborhood, and if the duration of the change in inductance is long compared with the various time constants which enter, the problem may be much more difficult; though if there be no magnetic metals in the field, the principles laid down more than forty years ago by Maxwell[1] in his dynamical theory of the electromagnetic field, and soon afterwards elaborated and illustrated by Rayleigh and others, point the way to the solution.

In most cases which present themselves in practice, there are masses of magnetizable metal in the form of cores, near the circuits to be studied, and it is often difficult, even if one knows something about the magnetic properties and the history of the cores, to predict exactly what the effects of a given sudden change in the inductances will be.

---

[1] Maxwell, Philosophical Transactions, Dec. 1864; Rayleigh, Philosophical Magazine, **38**, 1869, **39**, 1870, **30**, 1890.

This paper discusses first, with the help of mechanical analogies, a few simple and familiar cases of circuits without cores, with the purpose of emphasizing some facts to be met with also when cores are present, and then gives a number of diagrams obtained from the photographic records of oscillographs in circuits which contained large electromagnets some with solid and some with divided cores. Changes in the inductances of a circuit which contains one or more electromagnets often involve the moving of comparatively large masses of metal, and it is obviously impossible to make such changes instantaneously even though they may be carried out in intervals which are not long relatively to the time constants of the circuit. In solid cores, also, eddy currents tend to mask the effects of sudden changes in the conformation of the circuit, and this, with the fact that the susceptibility of the iron depends not only upon the intensity of the present excitation, but also upon the past experiences of the metal, leads to considerable differences in the magnetic behavior of a circuit according as it does or does not "contain iron." The diagrams show these differences and illustrate some typical conditions which arise in practical work.

It is well known that the final flux of magnetic induction through a solid iron core is not determined by the intensity of the excitation alone even when its magnetic condition at the outset is given, but depends in many cases upon the manner of application of the given excitation, — whether it be made suddenly, by small steps at intervals, or by slow, continuous rise. The diagrams are interesting in this connection because they show that when the core is fairly well divided, the forms of two distinct portions of a current curve, interrupted by a sudden change of inductances, are often almost identical with corresponding portions of two current curves obtained without any such interruption, the one with the original inductances, the other with the final ones.

It may be well to consider briefly at the outset the very simplest case, the familiar one of a single circuit, without iron, of fixed resistance, r ohms, and of inductance originally equal to L_0 henries, which contains a constant electromotive force of E volts and is carrying at the time $t = 0$, a current of C_0 amperes. At this instant ($t = 0$) let the inductance begin to change according to some law, and progressing always in the same direction, let it attain at the time T the given value L_1, after which it shall remain constant.

In order to illustrate graphically the effect of making the given change in inductance in longer or shorter time intervals, it will be convenient to use three rectangular axes for t, C, and T respectively, and to represent the value (L) of the inductance at any time $0 < t < T$, by the expression

$$L_0 + (L_1 - L_0) f\left(\frac{t}{T}\right), \tag{1}$$

where $f(0) = 0$, $f(1) = 1$, and for $0 < x < 1$, $f'(x) > 0$.

The line OK in the tT plane (Figure 1) has the equation $t = T$, and after the value ($T = OF$) has been fixed for T, the course of the current during the change of inductance may be shown by a curve (HQS) in a plane (FRS), the equation of which is $T = T'$. FH, which measures the ordinates of the line AG in the CT plane represents the initial current (C_0) at the time $t = 0$, and the ordinates of the curve MB in the plane COK represent for different values of T the intensities of the current at the end of the change in inductance, when the form of the function f is the same. The vertical distance AB shows the magnitude of the sudden change in the current strength when the change in L is supposed to be instantaneous and is the same whatever form f has.

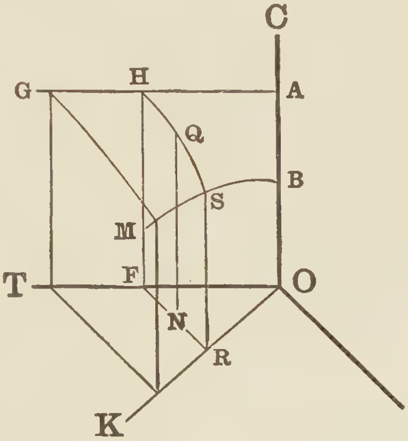

FIGURE 1.

During the interval $0 < t < T$, the current is to be found, of course, by solving the equation

$$E - \frac{d\,(LC)}{dt} = rC, \tag{2}$$

— where L has the variable value given above — and making the constant of integration such that $C = C_0$ when $t = 0$. After the epoch $t = T$, the intensity of the current satisfies the equation

$$E - L_1 \cdot \frac{dC}{dt} = rC, \tag{3}$$

in which the coefficients are constants. Equation (2) may be written in the form

$$\frac{dC}{dt} + \frac{r + L'}{L} \cdot C = \frac{E}{L}, \tag{4}$$

where $L' = dL/dt$, and if we make use of the usual notation,[2] and put $P = (r + L')/L$, $Q = E/L$, we shall have in general

$$C = e^{-p}\left(M + \int_0^t Qe^{r}dt\right), \tag{5}$$

where
$$p = \int_0^t P \cdot dt = \log\left(\frac{L}{L_0}\right) + \int_0^t \frac{rdt}{L}. \tag{6}$$

That is, if $0 \leqq t \leqq T$,

$$C_t = \frac{L_0}{L_t} e^{-\int_0^t \frac{rdt}{L}}\left(C_0 + \frac{E}{L_0}\int_0^t e^{\int_0^t \frac{rdt}{L}} \cdot dt\right), \tag{7}$$

and, in particular,

$$C_T = \frac{L_0}{L_1} e^{-\int_0^T \frac{rdt}{L}}\left(C_0 + \frac{E}{L_0}\int_0^T e^{\int_0^t \frac{rdt}{L}} \cdot dt\right). \tag{8}$$

In this expression L is to progress always in the same direction from L_0 to L_1, and cannot pass through the value zero, so that the limit of C_T as T approaches zero has the familiar value

$$\underset{T \doteq 0}{\text{Limit}}\ C_T = \frac{L_0 C_0}{L_1}, \tag{9}$$

which might have been found directly by integrating (2) with respect to t from 0 to T; the electromagnetic momentum has no sudden change. Equation (9) follows immediately, of course, when one makes use of the usual analogies between the phenomena of ordinary mechanics and those of electromagnetism. Equation (2) is in form like the equation of motion of a system the mass of which changes with the time in a certain given manner and which is under the action of a constant accelerating force and a retarding force proportional to the velocity. Let a moving mass L grow steadily during its motion by the gradual accretion of small particles which, originally at rest, are suddenly made part of the moving system, much as the links of a fine chain which has been lying on a table are successively set in motion when one end of the chain is lifted more and more; or let the mass L decrease steadily by the loss of small particles each of which leaves the system with a parting push which reduces its own velocity to zero and speeds its late companions on their way; then, if C is the velocity of the moving mass, E the accelerating force, and rC the retarding force, the equation of motion will be $d\,(LC)/dt = E - rC$, that is, (2).

---

[2] Forsyth, Treatise on Differential Equations, § 14.

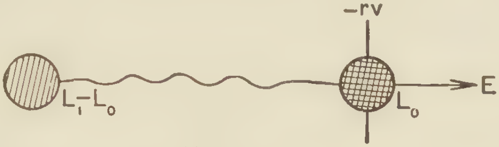

FIGURE 2.

If, when its velocity is C_0, the mass of such a system be instantaneously changed from L_0 to L_1, the principle of the conservation of momentum in impact shows that if C_1 is the velocity immediately after the impulsive change, $L_0 C_0 = L_1 C_1$.

The conventional diagram shown in Figure 2 indicates the nature of this simple mechanical problem. L_0 is a mass furnished with a stiff vane of such a size as to make the air resistance (which is proportional to the velocity) equal to r units when the mass is moving with unit velocity. L_0 is urged to the right by the constant force E and is retarded by a force rv. A slack inextensible string connects L_0 with another mass $L_1 - L_0$, and when the string becomes taut, the impulsive change in the velocity of L_0 corresponds to the change in the current in the inductive circuit when the inductance is impulsively changed from L_0 to L_1.

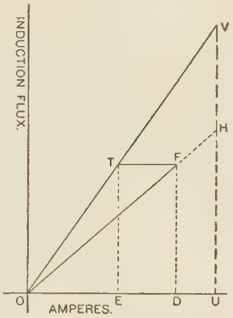

FIGURE 3. The line OFTV represents the change of the induction flux linked with a circuit without iron, when the inductance is suddenly increased.

If the induction flux, N, in a circuit which contains no iron be plotted against the current, the resulting locus is a straight line through the origin, the slope of which is the self-inductance of the circuit. If, then, the lines (OH, OV, Figure 3) corresponding to L_0 and L_1 be drawn, and if when the rising current has attained the value C_0, the inductance be supposed to change suddenly to L_1, the induction flux through the circuit preserves its value unchanged while the current falls from C_0 to C_1, and the point in the diagram which gives the state of the circuit moves from F to T.

If, as is approximately the case with some circuits which have open cores made of very finely divided soft iron, the hysteresis diagram is extremely narrow, so that the inductance may be considered to be a definite function of the current strength, we may represent two different states of the circuit by lines like OFR and OKS of Figure 4. It is then easy to see that in this case also a sudden change from one state to the other when the current had the value OD = C_0 would leave the induction flux through the circuit momentarily unchanged while the current fell to OE = C_1, and the point which represents the state of the circuit would suddenly move from F to K.

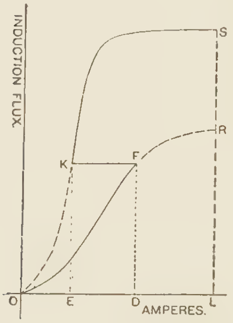

FIGURE 4. The line OFKS represents the growth of the induction flux in a magnet with finely divided core when the inductance of the circuit is suddenly increased.

If, at any instant, the total flux of magnetic induction through any simple circuit, which may or may not contain iron, is N (maxwells), if r is the resistance of the circuit in ohms, C, the current in amperes, and E, the applied electromotive force in volts,

$$E - \frac{1}{10^8} \cdot \frac{dN}{dt} = rC, \tag{10}$$

or

$$\frac{dN}{dt} = 10^8 \cdot r \left(\frac{E}{r} - C \right), \tag{11}$$

and if the final value (E/r) of the current be denoted by C', and the change in N during the time interval t_1 to t_2 by $N_{1,2}$,

$$N_{1,2} = r \cdot 10^8 \int_{t_1}^{t_2} (C' - C)\, dt. \tag{12}$$

If, now, C be plotted against the time (as in an oscillograph diagram) in a curve s (Figure 5) in which l centimeters parallel to the axis of abscissas represent one second, and an ordinate m centimeters long one ampere, the curve will have a horizontal asymptote (CY) at a distance (KC) corresponding to E/r amperes from the time axis, and, if OK represents the time t_1 and OL the time t_2, the area FGDC, or $A_{1,2}$, expressed in square centimeters, is equal to

$$lm \int_{t_1}^{t_2} (C' - C)\, dt, \tag{13}$$

and
$$N_{1,2} = \frac{10^8}{lm}(r \cdot A_{1,2}). \tag{14}$$

The curve ONJ of Figure 6, which has been carefully drawn to scale, represents the growth of the current with the time in a circuit without iron, of resistance r and inductance L. The curve OPT represents the current in the same circuit when the inductance has been increased to $4L$, while the resistance is the same as before. If, when the inductance of the circuit is L, the current rises in the time OU to the value UN, and if then the inductance is instantly increased to $4L$, the current falls to UF and then rises again in the manner indicated by the curve FG, which is the curve OPT moved to the right through a distance OL just great enough to make its ordinate at the time OU equal to one fourth of UN. Since the area between the curve and its asymptote is proportional to the inductance flux through the circuit, it is clear without any of the reasoning of the preceding paragraphs, that

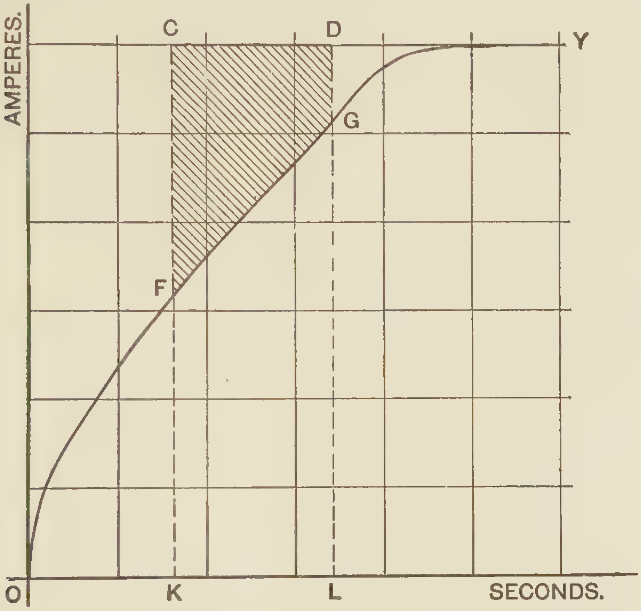

FIGURE 5. If l centimeters parallel to the horizontal axis represent one second, and an ordinate m centimeters long one ampere, $A \cdot 10^8 \cdot r/lm$ (where A is the area, in square centimeters, of CDGF) represents the change in the magnetic flux through the circuit during the interval KL.

there cannot be any impulsive change of the induction flux when the inductance is suddenly increased. A glance at the figure shows, however, that the rate of increase of the induction suddenly becomes much greater than it was just before the change.

Curve ODE of Figure 7 shows the manner of growth of the current in another simple circuit of fixed inductance, 4*L*. If, at the time OW, when the current has attained half its final strength, and the induction flux through the circuit is represented on the scale indicated by equation by OABD, the inductance be suddenly changed to *L*, the current suddenly becomes four times as strong as it was and then falls in a manner shown by the curve ST. The flux through the circuit just after the change is already twice as large as it will be eventually when the current reaches its final value, OA, and it decreases by an amount represented by the area BST, which is half the area AODB. Just before the change the flux was increasing with the time at a rate represented by the length of the line BD; just after the change it decreases at a rate represented by the line BS, which is twice as long as DB.

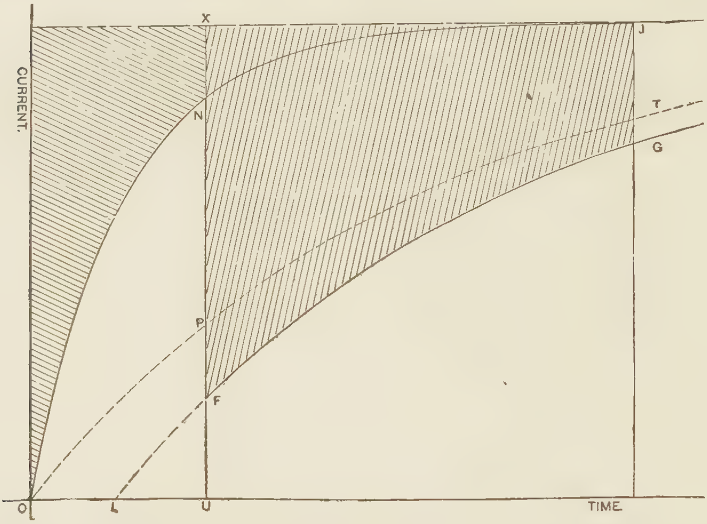

FIGURE 6. The line ONJ represents the current in a circuit of inductance *L* without iron. OPT shows the form of the current in the same circuit when the inductance has been increased to 4*L*. ONFG is the current when the inductance is suddenly changed from *L* to 4*L* at the time OU.

In the case of a circuit which does not contain iron, an increase of inductance without an increase of the resistance usually involves a change of the conformation of the circuit, and this generally requires a considerable fraction of a second, at least, to bring about, so that the formula (9) cannot be used to determine the current strength at the end of the inductance change. To illustrate this fact we may assume that the change from L_0 to L_1 in the time T is brought about at a constant rate so that $L = L_0 + t\,(L_1 - L_0)/T$, and the strength of the current at the time t is given by the equation

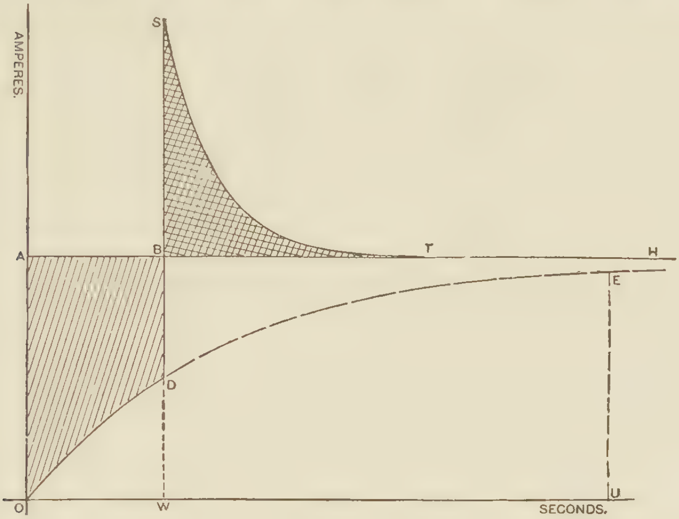

FIGURE 7. ODE shows the current in a simple circuit of fixed inductance, $4L$. If at the time OW, when the current has attained half its final intensity, the inductance is suddenly reduced to L, the course of the current will be ODBST.

$$C = \left(\frac{L_0}{L}\right)^m \cdot \left(C_0 + \frac{ET}{m\,(L_1 - L_0)} \cdot \frac{L^m - L_0{}^m}{L_0{}^m}\right), \tag{15}$$

where

$$m = \frac{rT + L_1 - L_0}{L_1 - L_0}. \tag{16}$$

If, now, $C = E/r$ amperes, $L_0 = 2$ henries, $L_1 = 4$ henries, then, according as T is one second, half a second, one tenth of a second, or one hundredth of a second, the value (C_1) of the current at the end of the interval T is $0.980 \cdot C_0$, $0.962 \cdot C_0$, $0.836 \cdot C_0$, or $0.569 \cdot C_0$, whereas C_1

would be $0.5 \cdot C_0$, if the change in the inductance had been instantaneous.

Figure 8 shows in TW the relative changes in the current in this circuit from $t = 0$ to $t = T$, when T is one tenth of a second, and in TZ the changes when T is one one-hundredth of a second. If the change were instantaneous the course of the current in one tenth of a second would correspond to the line TRU.

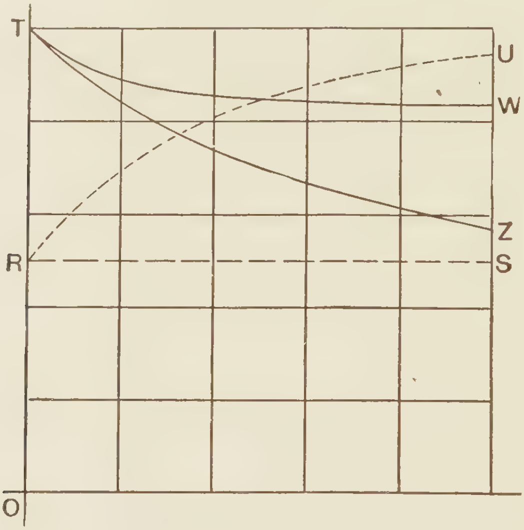

FIGURE 8. If in a certain inductive circuit, without iron, the inductance be instantaneously doubled, the course of the current in the next tenth of a second will be TRU. TW shows the current if the doubling be brought about by a continuous change going on at a constant rate during the whole interval. TZ shows on a different time scale, the course of the current for a hundredth of a second, if during this interval the inductance be changed at a constant rate which results at the end in its being doubled.

We may next consider the somewhat less simple circuit indicated in Figure 9_a, consisting of three parallel branches each of which has self-inductance, but no two of which have mutual inductance. Let r, r_1, r_2 be the resistances of the branches, L, L_1, L_2 their inductances, E, E_1, E_2 the constant electromotive forces of the generators in them, and C, C_1, C_2 the currents. At the time $t = 0$, when the currents and the inductances have given values, let the inductances begin to change according to given laws each of which can be expressed by an equation similar to (1), and let them attain, at the time T, other given values, which they thereafter keep. It is evident that any instant during the interval $0 < t < T$,

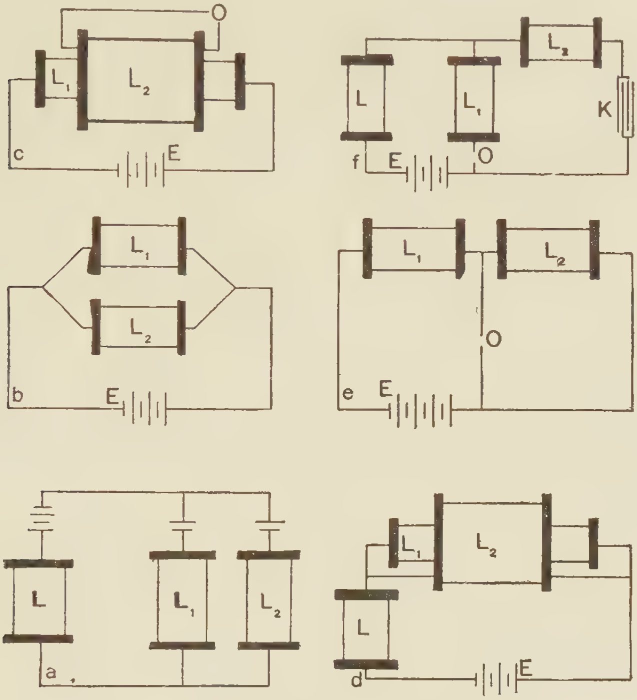

FIGURE 9.

$$
\begin{aligned}
E + E_1 - \frac{d\,(LC)}{dt} - \frac{d\,(L_1C_1)}{dt} &= rC + r_1C_1, \\
E + E_2 - \frac{d\,(LC)}{dt} - \frac{d\,(L_2C_2)}{dt} &= rC + r_2C_2, \qquad (17)\\
C &= C_1 + C_2,
\end{aligned}
$$

or, if we represent differentiation with respect to the time by accents,

$$
\begin{aligned}
(L + L_1)\,C'_1 + LC'_2 + (L' + L'_1 + r + r_1)\,C_1 + (L' + r)\,C_2 &= E + E_1, \qquad (18)\\
LC'_1 + (L + L_2)\,C'_2 + (L' + r)\,C_1 + (L' + L'_2 + r + r_2)\,C_2 &= E + E_2.
\end{aligned}
$$

If, from these equations and others obtained by differentiating them with respect to the time, C_2 and its derivatives be eliminated, we shall get a differential equation of the second order for C_1 in which the inductances and their derivatives are known functions of t, and the initial values of C_1 and C'_1 are also known. This new equation may be found by equating to zero the determinant

$$\begin{vmatrix} L & 2L'+r & L'' & (L+L_1)C''_1+(2L'+2L'_1+r+r_1)C'_1+(L''+L''_1)C_1 \\ L+L_2 & 2L'+2L'_2+r+r_2 & L''+L''_2 & LC''_1+(2L'+r)C'_1+L''C_1 \\ 0 & L & L'+r & (L+L_1)C'_1+(L'+L'_1+r+r_1)C_1-E-E_1 \\ 0 & L+L_2 & L'+L'_2+r+r_2 & LC'_1+(L'+r)C_1-E-E_2 \end{vmatrix} \qquad (19)$$

and, although it may be somewhat simplified, it generally proves rather intractable. If, however, the interval T is so short that the changes in the inductances may be regarded as impulsive, the corresponding changes in the currents may be found immediately, for if the equations be integrated with respect to the time from $t = 0$ to $t = T$, and if T be made to approach zero, while the currents remain finite, it appears that $LC + L_1C_1$ and $LC + L_2C_2$ have the same values just after the impulsive change in the inductances as they had just before the change. The induction flux through each circuit chosen for the equations remains unchanged by the sudden change of inductances.

It is easy to find a number of different problems in mechanics each of which yields equations of motion of the form (17), and is, therefore, analogous in a sense to the electromagnetic problem under consideration. Such an analogy, even though it be difficult to embody it in a working model, sometimes makes clearer to a person already familiar with mechanical principles the nature of the phenomena which he is to look for in interpreting his electrical equations. It will do no harm if, in imagining a mechanical system which is to serve this purpose, we postulate the existence of flexible, inextensible, massless strings, or even, at a pinch, the existence of stiff, nearly massless rods, or of pulley wheels so light that their moments of inertia shall be negligible. It is often desirable to imagine the motions of the masses which in the mechanical system represent the inductances in the electrical problem, to be hindered by retarding forces proportional to the velocities, to represent the electrical resistances. The resistance which the air offers to a body moving through it with a constant velocity not greater than 50 cms. per second is very nearly proportional to that velocity; and since the velocities which in the mechanical case correspond to the currents are usually much smaller than that, the resistance may be sufficiently well indicated by thin wings or vanes of proper size attached to the masses.

In the arrangement shown in Figure 10 the masses L, L_1, L_2, are urged towards the bottom of the diagram by forces of intensity E, E_1, E_2. The lines drawn across the masses indicate wings of such shapes as to make the resistances due to the air r, r_1, r_2 dynes respectively, when the corresponding velocities are one centimeter per second. It is evident from the geometry of the figure that the velocity of L downward is equal to the sum of the velocities of L_1 and L_2 upward. The tension of the string attached to L and passing over the massless pulley A is at every instant half that of the cord which is attached to the massless pulley B, and equal to the tension of the cord which connects L_1 and L_2. The equations of motion of the masses are of the form (17). If, as a consequence of applied forces or impulses, the string should become slack, the analogy between the mechanical and the electromagnetic problems would disappear, and it is sometimes convenient to imagine the masses attached to taut endless strings in some such manner as is shown in Figure 11. It is very easy to construct a model of this kind which will work fairly well if one uses for masses properly loaded roller skates which move about on the level top of a table. The masses may be connected by fine catgut passing around small, cheap pulleys with vertical axes mounted on the table.

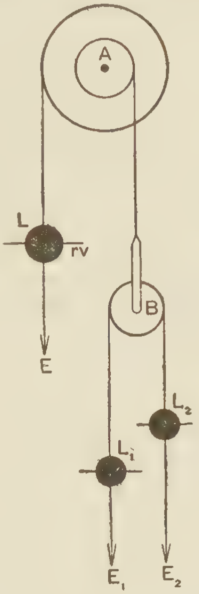

FIGURE 10.

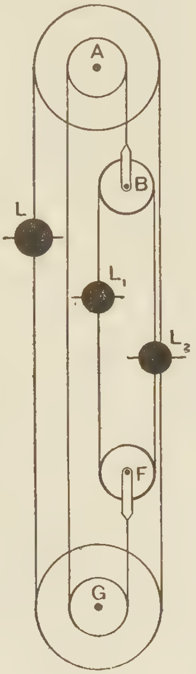

FIGURE 11.

A special case of some practical interest is that indicated in Figure 9_b, where the terminals of a battery without sensible self-inductance are connected by two inductive branches in parallel. The currents are given by the equations

$$L_1 L_2 \frac{d^2 C_1}{dt^2} + [(r + r_1) L_2 + (r + r_2) L_1] \frac{dC_1}{dt} + (r_1 r_2 + r r_1 + r r_2) C_1 = r_2 E \quad (20)$$

$$L_1L_2\frac{d^2C_2}{dt^2} + [(r + r_1)L_2 + (r + r_2)L_1]\frac{dC_2}{dt}$$
$$+ (r_1r_2 + rr_1 + rr_2)C_2 = r_1E,$$

and it is clear that if the inductances are suddenly changed, the products L_1C_1 and L_2C_2 are continuous, and if, in particular, only one of the inductances is altered, the current in the parallel branch is itself continuous.

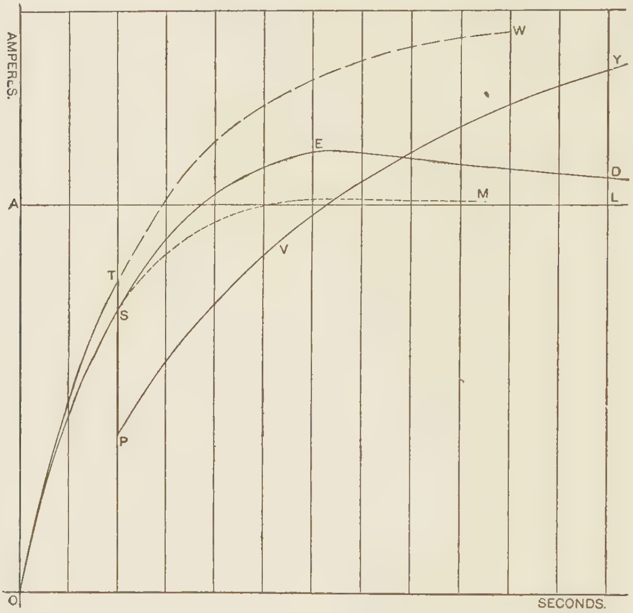

Figure 12. The lines OTW, OSM, show the forms of the currents in two parallel inductive resistances which connect the terminals of a storage battery. When at a given instant, the inductance of one of the parallel branches is suddenly doubled, the current in it changes its value abruptly and takes the course OTPVY, while the current in the other (OSED) suffers no sudden change in strength.

Figures 12 and 13 are drawn to scale for two typical cases which indicate well enough what is usually to be expected. In both diagrams $L_1 = 1$, $L_2 = 1$, $r = 12$, $r_1 = 20$, $r_2 = 30$, $E = 120$ (or these quantities are to be in the proportions here given). The final values of C_1 and C_2 are 3 amperes and 2 amperes.

In the case which corresponds to Figure 12 the battery circuit is closed at a given instant, and 0.02 seconds afterwards, when C_1 has attained the value 1.607 and C_2 the value 1.457, L_1 is suddenly changed from 1 to 2. As a consequence, C_1 falls suddenly to 0.8035, while C_2 remains momentarily unchanged. Before the change, the currents were given by the equations

$$C_1 = 3 - \tfrac{120}{104}\, e^{-24t} - \tfrac{120}{65}\, e^{-50t}, \quad C_2 = 2 + \tfrac{120}{156}\, e^{-24t} - \tfrac{360}{130}\, e^{-50t}, \quad (21)$$

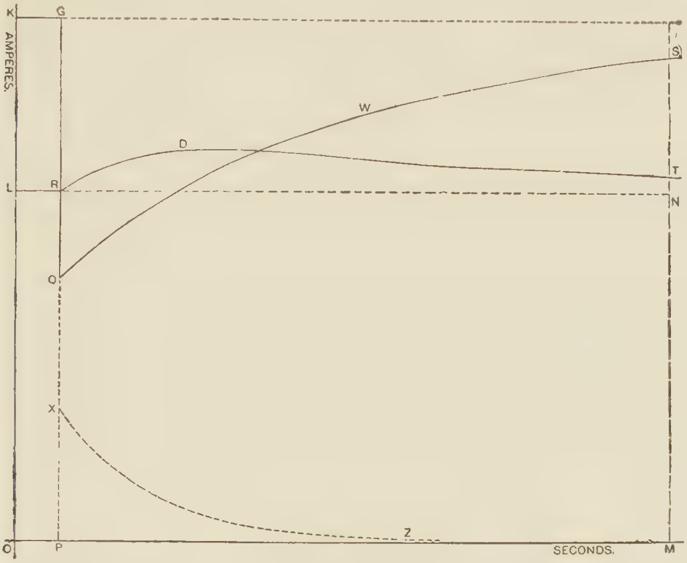

FIGURE 13. After the currents in two parallel inductive resistances which connect the terminals of a storage battery have become steady, at the values OK, OL, the inductance of one of the branches is suddenly doubled so that the current in it takes the course KGQWS. The current in the other branch takes the continuous form LRDT and approaches its final value from above.

and afterwards by the approximate equations

$$C_1 = 3 - 1.912\, e^{-13.48t} - 0.284\, e^{-44.52t},$$
$$C_2 = 2 + 0.803\, e^{-13.48t} - 1.346\, e^{-44.52t}. \quad (22)$$

The line OTPVY shows the course of C_1, and OSED the course of C_2. It will be observed that C_2 approaches its final value from above.

If the change in inductance is made after the currents have attained their final values, the courses of C_1 and C_2 will be those indicated in Figure 13 by the lines KGQS and LRDT. If after the currents have reached their steady values, the main circuit be suddenly broken, C_1

and C_2 instantly acquire equal and opposite values, and the subsequent course of C_1 is given by the equation

$$C_1 = \frac{E(L_1 r_2 - L_2 r_1)}{r_1 r_2 + r r_1 + r r_2} e^{-\frac{r_1 + r_2}{L_1 + L_2} t}. \qquad (23)$$

See in Figure 13 the line GRXZ.

If the terminals of an open battery circuit of inductance L and of resistance r be connected by a number of inductive conductors in parallel, of resistances r_1, r_2, r_3, r_4, etc., and of inductances L_1, L_2, L_3, L_4, etc., and if sudden changes be made in the inductances, the quantities

$$LC + L_1 C_1,\ LC + L_2 C_2,\ LC + L_3 C_3,$$

etc., will be continuous. If L is negligible, and if only some of the other inductances be impulsively changed, the currents in the other branches will be continuous.

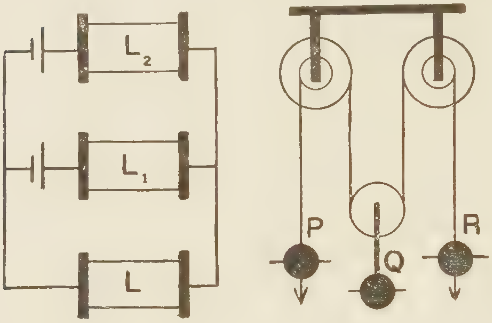

Figure 14.

If, in the arrangement shown in Figure 14, the masses P, Q, R are numerically equal to L_1, L, L_2, respectively, if the velocities of P and R in the direction of the bottom of the page are C_1, C_2, and if the dimensions of the vanes attached to the masses are such that the air offers resistance of r_1, r, r_2 times the velocities to the motion of P, Q, and R, the equations of motion of the masses are identical with the current equations for the electrical circuit shown in the figure.

The currents in two neighboring circuits (Figure 9_c) of self-inductances L_1, L_2, and mutual inductance M, which contain the electromotive forces E_1, E_2, are given by the familiar equations

$$\begin{aligned} E_1 - L_1 \frac{dC_1}{dt} - M\frac{dC_2}{dt} - r_1 C_1 = 0, \\ E_2 - L_2 \frac{dC_2}{dt} - M\frac{dC_1}{dt} - r_2 C_2 = 0, \end{aligned} \qquad (24)$$

and any impulsive changes in the inductances cause such sudden changes in the current as will keep $L_1C_1 + MC_2$ and $L_2C_2 + MC_1$ momentarily unchanged.

Many different working models have been made to illustrate the simple electrical problems which concern two such circuits. Of these some of the best known are due to Maxwell, Rayleigh, J. J. Thomson, Webster, and Boltzmann.

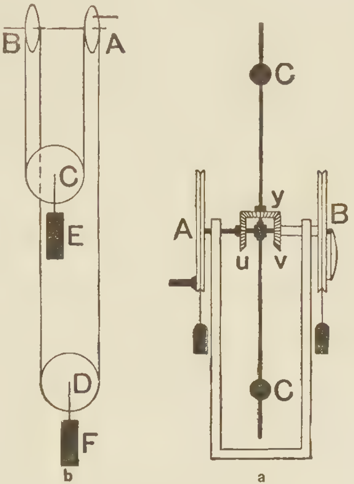

FIGURE 15.

The original model of Maxwell, now in the Cavendish Laboratory, is represented by Figure 15_a, taken from Gray's Absolute Measurements in Electricity and Magnetism, where an excellent account of the apparatus and its theory may be found.

In Lord Rayleigh's model, shown in Figure 15_b, "two similar pulleys A, B, turn upon a piece of round steel fixed horizontally. Over these is hung an endless cord, and the two bights carry similar pendent pulleys, C, D, from which again hang weights, E, F. . . . In the electrical analogy, the rotary velocity of A corresponds to a current in a primary circuit, that of B to a current in the secondary. . . . In the absence of friction there is nothing to correspond to electrical resistance, so that the conductors must be looked on as perfect. If x and y denote the circumferential velocities, in the same direction, of the pulleys A, B, where the cord is in contact with them, $\frac{1}{2}(x + y)$ is the vertical velocity of the pendent pulleys. Also $\frac{1}{2}(x - y)$ is the circumferential velocity of C, D, due to rotation, at the place where the cord engages. If the diameter be here $2a$, the angular velocity is $(x - y)/2a$. Thus, if M be the total mass of each pendent pulley and attachment, Mk^2, the moment of inertia of the revolving parts, the whole kinetic energy corresponding to each is

$$\frac{1}{2}M\left\{\frac{(x+y)^2}{4}+\frac{k}{a^2}\left(\frac{(x-y)^2}{4}\right)\right\}. \tag{25}$$

For the energy of the whole system, we should have the double of this, and, if it were necessary to include them, terms proportional to x^2 and y^2, to represent the energy of the fixed pulleys."

Here $L_1 = L_2 = a^2 + k^2$, $M = a^2 - k^2$, and, if there were no magnetic leakage, k would need to be zero.

Figure 16 represents the model of Professor Sir J. J. Thomson.[3] "It consists of three smooth, parallel, horizontal steel bars on which masses m_1, m_2, m slide, the masses being separated from the bars by friction wheels; the three masses are connected together by a light rigid bar which passes through holes in swivels fixed on the upper part of the masses; the bar can slide backwards and forwards through these holes, so that the only constraint imposed by the bar is to keep the masses in a straight line."

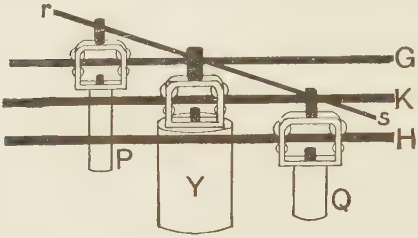

FIGURE 16.

If x'_1, x'_2 are velocities of m_1, m_2, in the same direction, the velocity of M, if it be midway between m_1 and m_2, is $\frac{1}{2}(x'_1 + x'_2)$, and the kinetic energy is of the form

$$\tfrac{1}{2} L_1 x_1'^2 + M x'_1 \cdot x'_2 + \tfrac{1}{2} L_2 x_2'^2, \tag{26}$$

where $L_1 = m_1 + \frac{1}{4} m$, $L_2 = m_2 + \frac{1}{4} m$, $M = \frac{1}{4} m$.

Professor Webster's model is a modification of that of Thomson. "If the middle weight, instead of rolling on a fixed rail, roll on the bar connecting the two other carriages, the coefficients of induction will vary with the position of the middle mass, and moving it along its bar while one of the outer masses is moving will cause the other to move. The centrifugal force tending to make the middle mass roll along its bar will represent the magnetic forces between the currents."

The very elaborate and ingenious model of Boltzmann is described at length in the first fifty pages of his Vorlesungen über Maxwell's Theorie der Elektricität und des Lichtes.

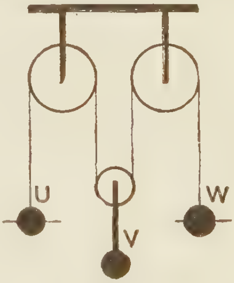

FIGURE 17.

The general features of another simple model illustrative of this electrical problem are shown in Figure 17. The mass of U is $L_1 - M$, that of V is $4\,M$, and that of W, $L_2 - M$. In Figure 18 the strings are represented as stretched over four small pulleys to keep them taut. I have found that this model made of three weighted roller skates, moving over a level table top, and connected in the manner indicated by cords passing around such small cheap pulleys as are obtainable at any ironmonger's shop, may be made to work extremely well. The effects of sudden changes of inductance can be directly observed by dropping suitable masses into the skates as they move. In Figure 14, which illustrates the same problem, the mass of Q is M, and those of P and Q are $L_1 - M$, $L_2 - M$, respectively. Q should have no vane.

---

[3] J. J. Thomson, Elements of the Mathematical Theory of Electricity and Magnetism, Chapter XI.; Webster, Science, Dec. 1895; The Theory of Electricity and Magnetism, § 71.

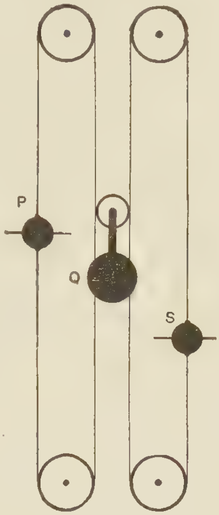

FIGURE 18.

Scores of other models, more or less simple of construction, can easily be devised. It is to be noticed, however, that in some of the models which have been used to illustrate this problem, the masses representative of some of the combinations of the inductances would need to be negative if they were to correspond to cases which occasionally arise in electrical engineering.

If either of the two neighboring circuits contains no battery, the corresponding value of E in equations (24) is to be put equal to zero. Figure 19 is drawn for the case of an induction coil without iron and with no cell in the secondary circuit. The self-inductances of the two circuits are equal. The dotted curve, P, shows the form of the current induced in the secondary circuit when the primary circuit, which has been carrying a steady current, is suddenly broken. If, after a few seconds, the primary circuit containing its battery be closed again, the current in the secondary circuit will have the general form of either Q or S. Q, R, and S are drawn for mutual inductances respectively half as great, nine tenths as great, and equal to, the inductance of either circuit. P is drawn for $M = L/2$, and corresponds, therefore, to Q; the areas V and W are equal. Curves like P corresponding to R and S could be found by exaggerating all of P's ordinates in the ratio 9/5, or the ratio 2.

Figures 20, 21, 22, 23, and 24 illustrate some phenomena which are frequently encountered in the practical use of neighboring inductive circuits. The curves have been drawn to scale for certain numerical values of the resistances, and the inductances so chosen as to make the results typical. There is no iron in either circuit, and only one circuit, the primary, contains a battery.

In Figure 20 the current in the primary circuit is drawn above OX, in the curve OJAZ, and the current in the secondary circuit beneath MN. Each of the circuits has a self-inductance of 2 henries, and the resistances are 30 ohms and 40 ohms. The mutual inductance is at first $\sqrt{2}$, and the currents are given by the equations

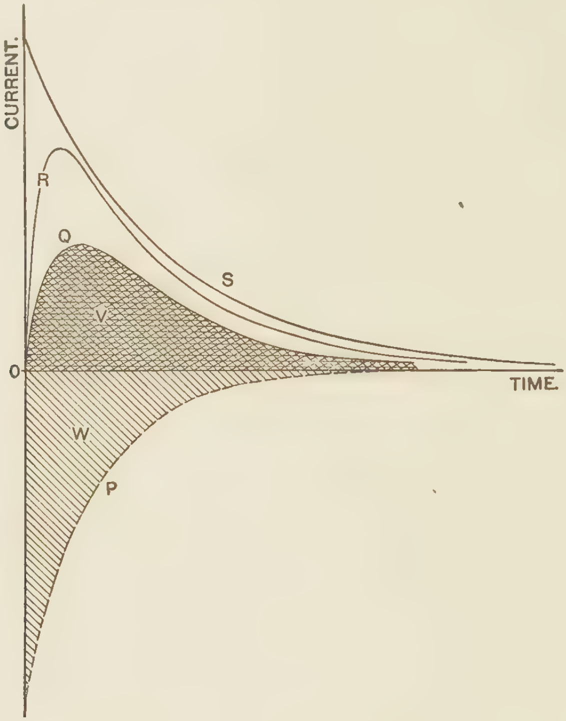

Figure 19. The curves Q, R, S represent for different relative values of the mutual inductance the current induced in the secondary circuit of a certain induction coil without iron, when the primary circuit is suddenly closed.

$$C_1 = 4 - 2.4\,e^{-10t} - 1.6\,e^{-60t}, \quad C_2 = \frac{-2.4}{\sqrt{2}}\left(e^{-10t} - e^{-60t}\right), \quad (27)$$

until the time $OG = 1/20$, when all the inductances are suddenly doubled. The currents are then given by the equations

$$C'_1 = 4 - 1.928\,e^{-5t} - 0.840\,e^{-30t}, \quad C'_2 = 0.891\,e^{-30t} - 1.361\,e^{-5t}. \quad (28)$$

In the case represented by Figure 21, $r_1 = 30$, $r_2 = 40$, $M = \sqrt{2}$, $L_2 = 2$. At the beginning $L_1 = 2$, but at the time OA this is suddenly changed to 4. Before the change in L_1 the currents are given by the equations

$$C_1 = 4 - 2.4\,e^{-10t} - 1.6\,e^{-60t}, \qquad C_2 = \frac{-2.4}{\sqrt{2}}(e^{-10t} - e^{-60t}), \qquad (29)$$

Just before the impulse, $C_1 = 2.465$, and $C_2 = -0.945$; just after, the current in the primary is about 0.822 and the secondary current has the small positive value 0.217. The new currents satisfy the equations

$$C'_1 = 4 - 2.634\,e^{-20t/3} - 0.543\,e^{-30t},\ C'_2 = -0.932\,e^{-20t/3} + 1.149\,e^{-30t}, \quad (30)$$

very nearly. C_2 is plotted below TQ.

Figure 22 shows the manner of growth of two neighboring currents, when $r = 30$, $r = 40$, $L = 2$, $L = 2$, and when M, which is at first $\sqrt{2}$, is suddenly changed to zero at the time OA. When M is changed, the current in the primary circuit suddenly falls from 2.465 to 1.797, and the current in the secondary circuit, which has been negative, rises from -0.945 to $+0.798$. After the change, the currents are given by the simple equations

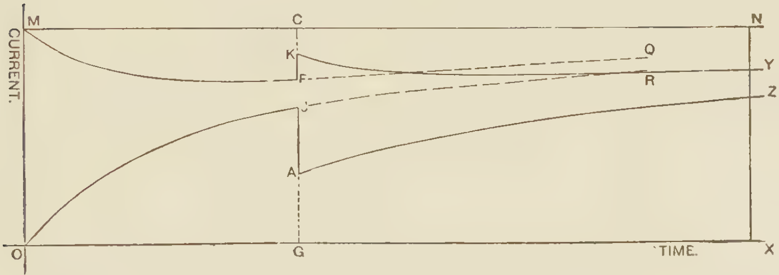

FIGURE 20. OJR and MFQ represent the forms of the primary and secondary currents in a certain induction coil without iron when the primary circuit is closed at the origin of time. If at the time OG, the self-inductances of both circuits and the mutual inductance of the two are suddenly doubled, the currents take the forms OJAZ and MFKY.

$$C'_1 = 4 - 2.203\,e^{-15t}, \qquad C'_2 = 0.798\,e^{-20t}. \qquad (31)$$

Figure 23 exhibits the effects of a sudden change in the value of the mutual inductance between the two circuits already described under Figures 21 and 22, from $\sqrt{2}$ to 1.9, while the other inductances remain unaltered. The primary current is shown by the curve OKRGS, and

OX shows its final value. The second current is represented by the curve ADWU plotted under AN and displaced to the right so that the sudden increase in the absolute strength at the time of the change in *M* may appear. The flux of magnetic induction through the primary circuit is represented on the usual scale by the shaded area. The black area points to a decrease in this flux which goes on from the time XF to the time XG, when the current falls below its final value. The induction flux linked with each of the two circuits is plotted against the time in Figure 24. These quantities are shown to be continuous at the time of change in the inductance, as, of course, they should be.

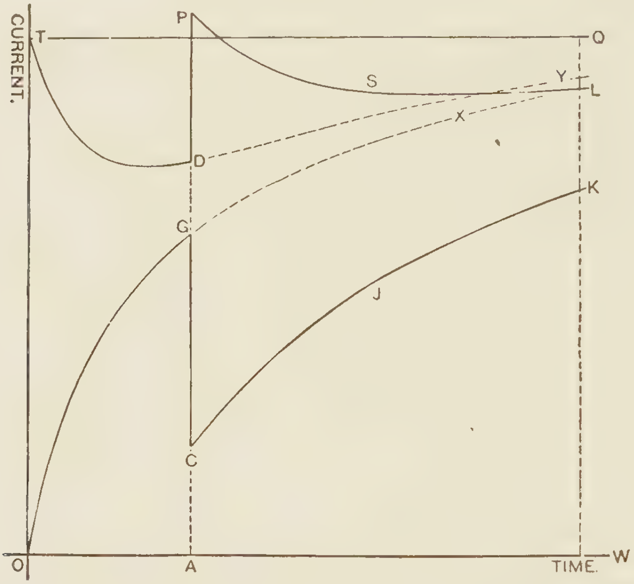

Figure 21. At the time OA, the self-inductance of the primary circuit of a certain induction coil without iron is suddenly doubled, while the self-inductance of the secondary circuit and the mutual inductance of the two remain unchanged. OGCJK shows the course of the primary current and TDPSL that of the secondary current.

Figure 25 shows another arrangement of two neighboring circuits and an analogous mechanical system. The gap O is closed at first, but is suddenly opened when the current has become steady. The mass W moves alone under the action of a force *E* which urges it in the direction of the bottom of the page, and the air resistance. The motion soon becomes steady, but when the string which connects W to X becomes taut the motion is suddenly changed.

Figure 9_d represents a circuit consisting of three parallel branches, each of which has self-inductance and may contain a battery, and two of which have mutual inductance. If L, L_1, L_2 are the self-inductances, r, r_1, r_2 the resistances, C, C_1, C_2 the currents, E, E_1, E_2 the electromotive forces, and M the mutual inductance of the second and third branches, the currents satisfy the equations

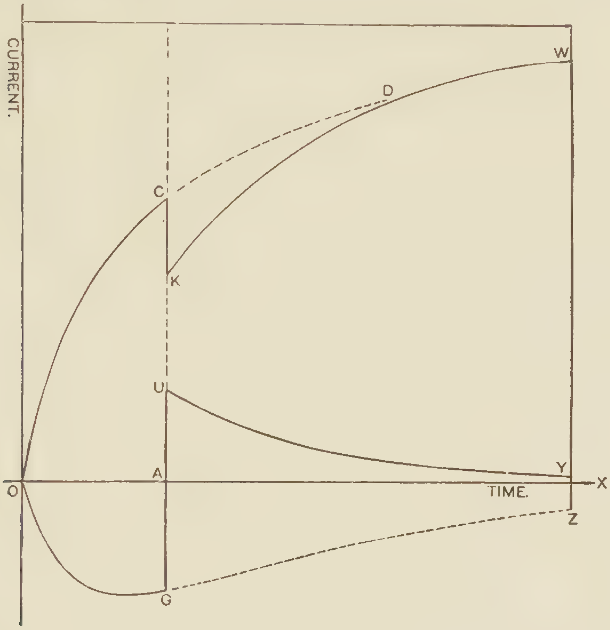

FIGURE 22. At the time OA the mutual inductance of two neighboring circuits, one of which contains a battery, is suddenly reduced to zero. The primary and secondary currents which have been pursuing the courses OCD, OGZ are abruptly changed in value and now follow the lines OCKW and OGAUY.

$$(L + L_1)\frac{dC_1}{dt} + (L + M)\frac{dC_2}{dt} + (r + r_1)\,C_1 + rC_2 = E + E_1, \qquad (32)$$

$$(M + L)\frac{dC_1}{dt} + (L + L_2)\frac{dC_2}{dt} + rC_1 + (r + r_2)\,C_2 = E + E_2,$$

$$C = C_1 + C_2.$$

Any sudden changes in the inductances cause such sudden changes in the currents as shall keep $[(L + L_1) C_1 + (L + M) C_2]$ and $[(L + M) C_1 + (L + L_2) C_2]$ momentarily unchanged. In a case frequently met with in practice, there is no appreciable inductance in the

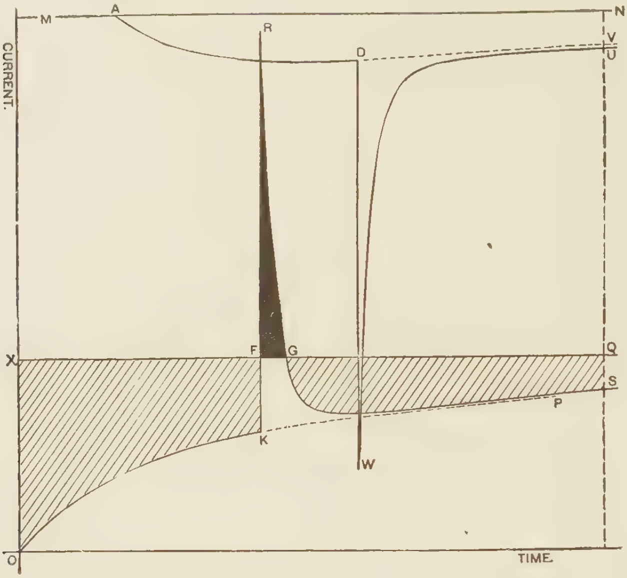

Figure 23. The two circuits of a certain induction coil without iron have equal self-inductances (L, L) and the mutual inductance $L\sqrt{2}$. At the time XF the mutual inductance is suddenly increased to $(1.9)L$, and the currents which have been following the curves OKP, ADV, take the forms KRGS, DWU.

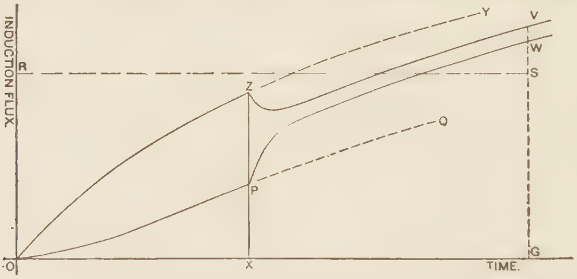

Figure 24. OPW and OZV show, as functions of the time, the fluxes of magnetic induction linked with the two circuits which carry the currents represented in the last figure.

first branch and no electromotive forces in the other branches, so that $L = 0$, $E_1 = 0$, $E_2 = 0$, and any instantaneous change in the inductances will leave

$$(L_1C_1 + MC_2)$$

and $$(MC_1 + L_2C_2)$$

momentarily unchanged.

If in Figure 14

$$P = L_1 - M,$$

$$Q = L + M,$$

$$R = L_2 - M,$$

and if the vanes are of such dimensions as to make the air resistance r_1, r, r_2 when the bodies to which they are attached have unit velocities, the equations of motion of the mechanical system are of the form (32), if E is applied upward to Q.

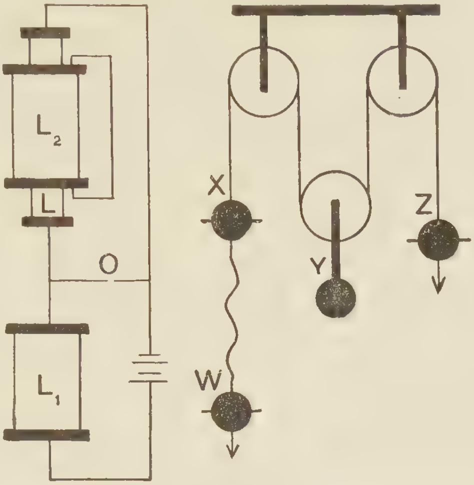

FIGURE 25.

Figure 26 illustrates a special case under this problem where $r = 1$, $r_1 = 20$, $r_2 = 30$, $L_1 = 2$, $L_2 = 3$, $M = 0$, up to the time OC, when by a sudden change in the conformation of the circuit, M is made equal to 2. Before the change $C_1 = 1.986$, $C_2 = 1.324$; the change in M leaves C_1 momentarily unchanged but suddenly reduces C_2 to zero. After the impulse the currents are given by the equations

$$\begin{aligned} C'_1 &= 3 - 1.717\, e^{-5.959t} + 0.703\, e^{-54.541t}, \\ C'_2 &= 2 - 1.428\, e^{-5.959t} - 0.572\, e^{-54.541t}, \end{aligned} \tag{33}$$

very nearly.

If in the arrangement shown in Figure 9_e, the gap O, which has been closed by a stout wire, is suddenly opened, the current falls impulsively to a value which keeps the induction flux through the battery circuit momentarily unchanged.

The mechanical system shown in Figure 27 is analogous to the electrical circuit indicated in Figure 9_f. The gap O, which has been closed, is supposed to be opened at a given signal. The spring S is the analogue of the condenser K.

A circuit which contains an electromagnet has, of course, no definite inductance in the sense of the ratio of the flux of magnetic induction linked with the circuit to the intensity of the current, for this ratio is different for different current strengths, and for a given electromagnet, and a given current depends upon the previous magnetic history of the core.

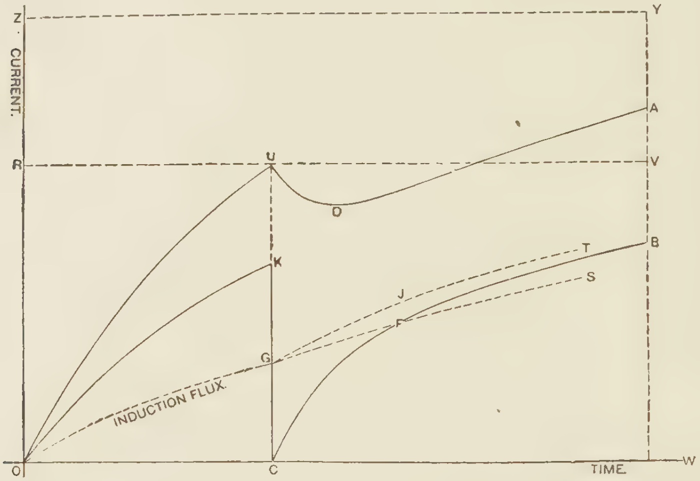

FIGURE 26. Two parallel coils of resistances 20 ohms and 30 ohms and of inductances 2 and 3 respectively, connect, in parallel, the terminals of a storage battery of 1 ohm internal resistance. At the beginning there is no mutual inductance between the branch circuits and the currents follow the curves OU, OK. At the time OC, the conformation of the circuit is suddenly changed so as to introduce a mutual inductance of 2, and as a result, the courses of the two currents are altered: the first follows henceforth the line UDA, the second the line KCFB. The inductions linked with the parallel branches are shown by the dotted curves.

In the case of a single circuit without iron the magnetic flux which accompanies a changing current is at every instant the same as it would be under a steady current of the intensity which the changing current then has. If, however, a second circuit closed on itself is brought into such a position that the two circuits have a mutual inductance, a changing current in the first circuit induces a current in the other which contributes to the flux through the first. If, therefore, an electromagnet has a solid core, the eddy currents induced in it while a current is growing or decreasing in the exciting coil affect the amount of the flux through the core, and it is not possible to obtain a hysteresis

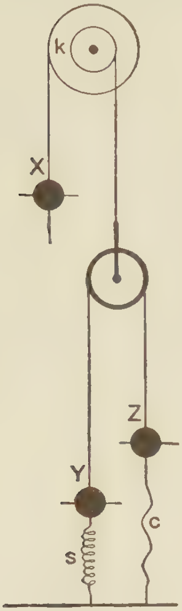

FIGURE 27.

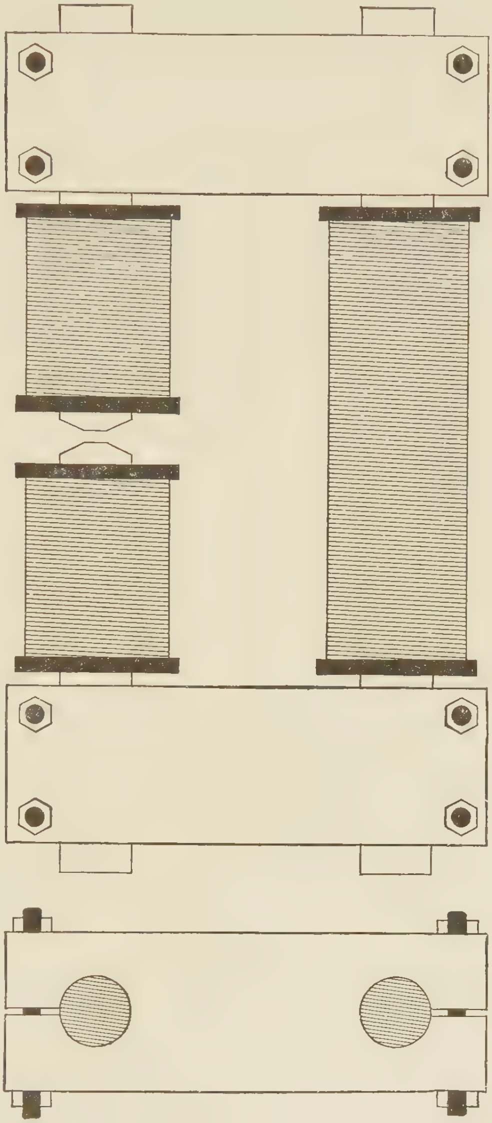

FIGURE 28. The electromagnet TP which has a solid core weighing about 300 kilograms.

diagram for the iron directly from the records of an oscillograph in the coil circuit. It is difficult, indeed, to obtain by any method a satisfactory magnetic curve for such a core, for if the iron starts from a given magnetic state, it is possible to get very different magnetic fluxes from a given exciting current by building up the current more or less slowly. In any useful examination of the magnetic properties of a solid piece of iron which is to be used for any practical purpose, it is essential that the metal be made to go over the same magnetic journeys which it will later be required to make, and at the same speed.

Before we discuss this anomalous magnetization more carefully, we may stop for some moments to study the records of an oscillograph in circuits which contained either the electromagnet TP, Figure 28, which has a solid core, or a certain toroid (DN), about 41 centimeters in mean diameter, the core of which was made of about 25 kilograms of fine, soft, varnished iron wire. It will be seen from Figures 29, 30, 31, 32, 33, 34 that the phenomena are in general what we should expect to find in similar circuits without iron, though eddy currents and the time taken to make the mechanical changes modify somewhat the courses of the currents in the exciting circuits.

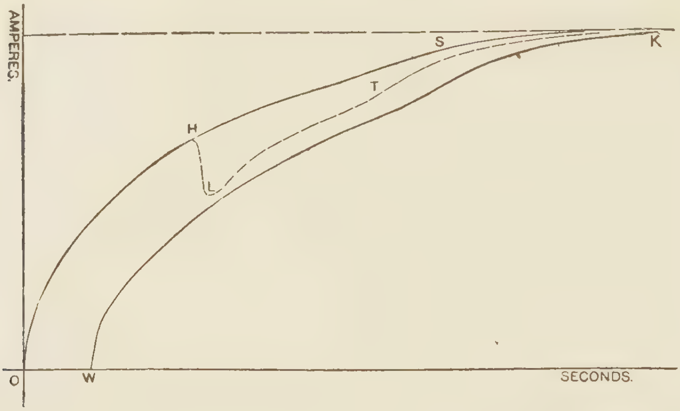

Figure 29. The curve OHS shows the manner of growth of a current in the coil of the magnet TP when the poles are separated by about three inches. WK shows the rise of the same current when the poles are nearly closed by the insertion of a planed block of iron between them. HLT shows the effect of suddenly dropping the block in while the current is growing.

The Anomalous Magnetization of Iron.

In 1863 von Waltenhofen first called attention to the fact that if an increasing current (C) ending in the maximum value (C') be sent through a long solenoid, the final value of the magnetic moment of a bar of soft iron in the solenoid, which was at the outset demagnetized, will depend not only upon the final strength of the current, but also upon the manner of growth of C in attaining this intensity. This moment will be greater if the current be suddenly applied in full strength than if it be made to grow slowly, either continuously or by short steps. If, after the current has remained steady for a short time at the strength C' it be made to decrease to zero, the residual moment of the bar will be less if the circuit be suddenly opened than if the decrease be made slowly by introducing more and more resistance.[4] If the soft iron bar to be magnetized was stout and relatively short, von Waltenhofen was sometimes able to reverse the direction of the remanent magnetism by a sudden break of the circuit. In one instance where the length of the bar was about ten centimeters and the diameter about two centimeters, the magnetic moment while the current was passing was about 45 units, and about —0.20 when the current had been stopped. It seemed to von Waltenhofen that these phenomena could not be due to the induced currents caused by the sudden changes in the exciting current, and he explained them as consequences of the inertia of the molecular magnets turning in a viscous medium. This view seems to have been taken by Fromme, Auerbach, Ewing,

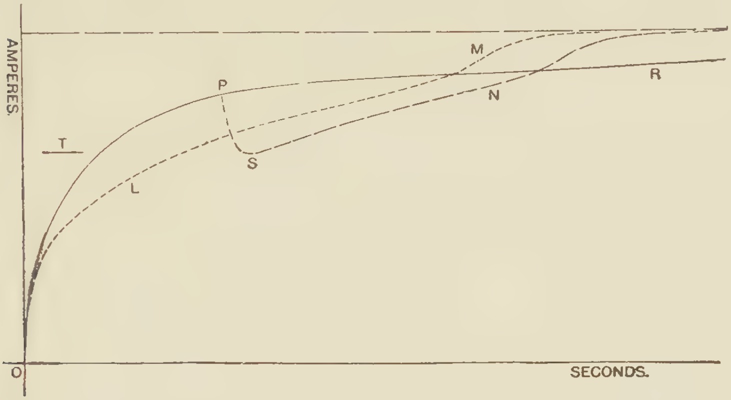

Figure 30. The short coils of the magnet TP are in series with one another and with a battery and an oscillograph. The current follows the line OPR or the line OLM according as the long coil of the magnet is open or closed. When at the point P, the long coil circuit is suddenly closed, the current in the battery follows the line PSN, which despite eddy currents is not very unlike the upper part of OLM.

---

[4] Von Waltenhofen, Poggendorff's Ann. **120**, 1863; Fromme, Poggendorff's Ann., Ergbnd. **7**, 1876; Wied. Ann. **4**, 1878, **5**, 1878, **13**, 1881, **18**, 1883, **44**, 1891; Bartoli and Alessandri, Nuovo Cimento, **8**, 1880; Righi, Mem. di Bologna, **1**, 1880; Peuckert, Wied. Ann. **32**, 1887; Auerbach, Wied. Ann. **14**, 1881, **16**, 1882; Winkelmann's Handbuch der Physik, Band 5; Wiedemann, Lehre von der Elektricität, Band IV; Ewing, Magnetic Induction, § 84; Gumlich und Schmidt, Electrotechnische Zeitschrift, **21**, 1905.

Peuckert, Zielinski and others who have written upon the subject, while G. Wiedemann thought that his researches and those of Righi showed that eddy currents in the iron, and alternating currents induced in the exciting coil accounted best for the observed facts. In describing experiments upon this so-called anomalous magnetization, Wiedemann distinguishes between the permanent moment (P), that is, the remanent moment after the current has ceased, and the total moment (T), which

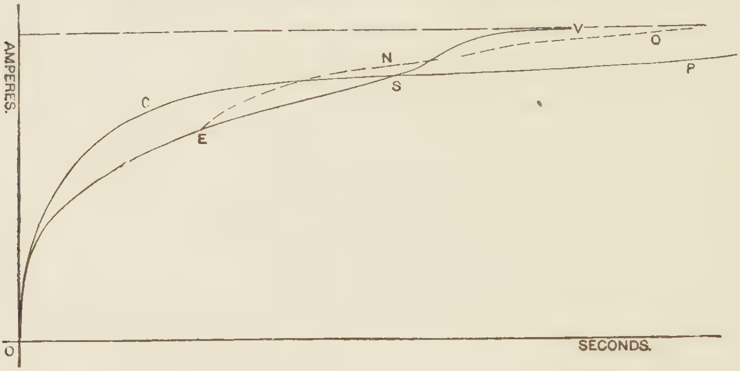

FIGURE 31. The short coils of the magnet TP are in series with one another and with a battery and an oscillograph. The current follows the line OCP or OESV according as the long coil of the magnet is open or closed on itself. When at the point E the long coil which has been closed is suddenly opened, the oscillogram is of the form ENQ which on account of the disturbing effects of eddy currents is not like the upper part of the curve OCSP.

is the moment when the current is steady at its highest value. This last quantity is regarded as the sum of the permanent moment and a moment (V) which vanishes with the current. The suffix a attached to P or T denotes that this moment has been reached after a gradual change in the current, while the suffix f denotes that the current has been suddenly opened or closed. According to Wiedemann, T_a is always smaller than T_f, and P_f than P_a, but these differences are much larger for short stout rods than for relatively long ones, where they become insignificant. $(P_a - P_f)/P_a$ is smaller in the case of a rod made of a bundle of insulated soft iron wires than in the case of a solid rod of the same dimensions. As C' is made larger, $T_f - T_a$ attains a maximum and then sometimes decreases slightly. If the rod to be magnetized is surrounded by a thick metal tube in which eddy currents can be induced, P_f is slightly increased, especially if the current be first slowly raised to C and then suddenly stopped. If shorter and shorter iron rods of a given diameter are tested, P_f gradually decreases to zero under given value of C', and then changes sign; the inversion comes with longer rods when C' is weak than when it is strong. If, with a given rod, C' be gradually increased, the negative moment finally decreases and changes sign. After this there is no inversion and P_f is positive.

It appears from Fromme's experiments that the von Waltenhofen effect is often less marked in straight, finely divided cores than in solid ones, and we may inquire how greatly the division of a straight core may be expected to facilitate the changes in the field (H) within the iron, due to given changes in the exciting circuit. It is clear that if the circuit of an electromagnet be suddenly broken, the decay of the electromagnetic field in the core is much less rapid when the core is solid and eddy currents induced in it shield the inner filaments, than when it is made of wire. Indeed, if eddy currents were non-existent, the field would fall instantaneously to zero, in the absence of magnetic lag, when the current in the coil ceased to flow. If the exciting coil remains closed and some change is suddenly made in its resistance or

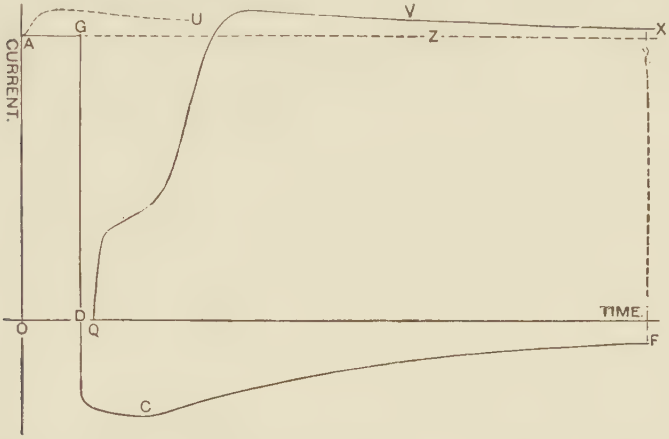

FIGURE 32. The toroid (DN) and the electromagnet (TP) with its poles separated by a gap of about eight centimeters, were placed in parallel across the terminals of a storage battery, with an oscillograph in the toroid branch. QVX shows the course of the current in the toroid which approaches its final value from above (See Figure 12). GCF, with its irregularities of curvature, shows the current in the toroid when the battery circuit was suddenly broken. AU shows the form of the temporary current induced in the toroid when an iron block was suddenly dropped into the gap between the jaws of the electromagnet, after the currents in the circuit had become steady.

in the electromotive force applied to it, the change in the current and therefore the change in the field in the iron caused by the current cannot be made instantaneous, even if eddy currents be wholly shut out, and, though dividing up the core has its effects, we cannot expect them to be so striking as in the case where the exciting circuit is open.

Let us consider a very long, uniformly wound solenoid consisting of N turns of insulated copper wire per centimeter of its length, wound closely upon a long, soft iron prism of square cross-section ($2a \times 2a$)

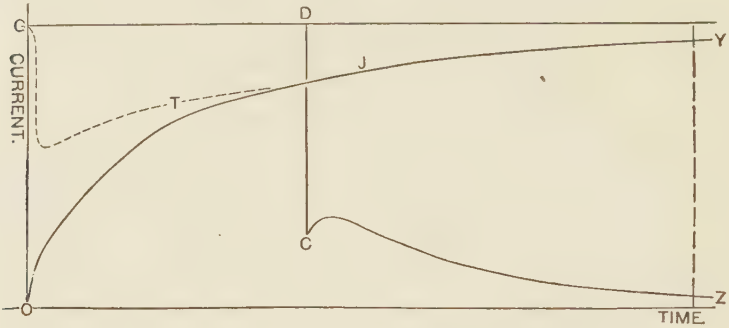

FIGURE 33. The toroid (DN) and the electromagnet (TP), with its jaws separated by a gap of about eight centimeters, were placed in parallel across the poles of a storage battery, with an oscillograph in the electromagnet branch. OJY shows the manner of growth of the current in TP and DCZ the manner of decay of the current when the battery circuit was suddenly broken. If, after the currents in the circuit have become steady, a block of iron was suddenly dropped into the gap in the core of the electromagnet, the induced current took the form GT.

built up compactly of a large number of straight, varnished filaments or "wires" of square cross-section ($c \times c$), with their axes parallel to that of the prism, which shall be used as the z axis. The electric resistance of the solenoid per centimeter of its length parallel to the z axis shall be w, the constant applied electromotive force per centimeter of the axis shall be E, and the intensity of the current in the coil shall be C.[5] Within the core, the magnetic field (H) will have everywhere and always the direction of the axis of the prism, and if q is the current flux at any instant at any point in the iron, ρ the specific resistance of the metal, and μ its magnetic permeability, which for the present purpose shall be regarded as having a fixed uniform value, $q_x = 0$, $q_y = 0$, $H_x = 0$, $H_y = 0$, $H_z = H$, $4\pi q = \text{Curl } H$,

---

[5] Peirce, These Proceedings, **43**, 5, 1907.

$$\frac{\partial H}{\partial t} = \frac{\rho}{4\pi\mu}\left(\frac{\partial^2 H}{\partial x^2} + \frac{\partial^2 H}{\partial y}\right). \tag{34}$$

When there are no eddy currents in the core, the intensity (H) of the magnetic field has at every point of the iron the boundary value $H_S = 4\,\pi NC$, but in general H varies from point to point. The flux of magnetic induction through the turns of the coil per centimeter of its length parallel to the z axis and N times the induction flux through the core are practically equal, and we may write

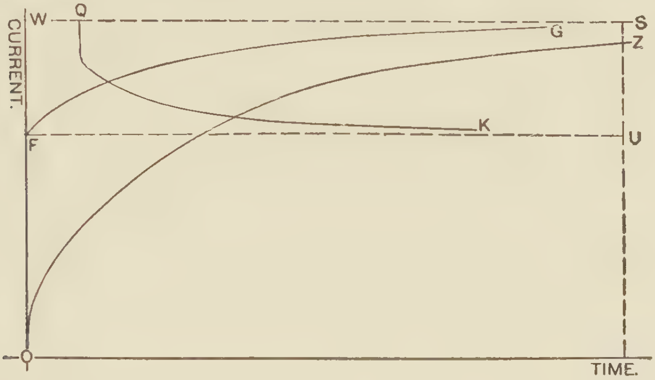

FIGURE 34. Two electromagnets were placed in series with each other and with an oscillograph and a storage battery, and a shunt (S) of small resistance was provided for one of the magnets. OZ shows the form of the battery current when S was closed, QK the fall of this current when S was suddenly opened after the original current had become steady, and FG the rise of the current to its old value when the shunt is again closed.

$$E - \frac{dp}{dt} = E - \mu N \int\int \frac{\partial H}{\partial t} \cdot dx dy = w \cdot C = \frac{w \cdot H_S}{4\,\pi N}, \tag{35}$$

or,

$$E = \frac{w \cdot H_S}{4\,\pi N} + \frac{\mu\rho N}{4\pi\mu} \int\int \left(\frac{\partial^2 H}{\partial x^2} + \frac{\partial^2 H}{\partial y^2}\right) dx dy, \tag{36}$$

where the integration extends over a cross-section of the core.

The vector H is always perpendicular to its curl, and the intensity of the component of the current at any point in the iron, in any direction s, parallel to the xy plane at any instant, is equal to $1/4\,\pi$ times the value at that point, at that instant, of the derivative of H in a direction parallel to the xy plane, and 90° in counter clockwise rotation ahead of s.

Along any curve in the iron parallel to the xy plane, H must be constant if there is no flow of electricity across the curve. At every instant, therefore, the value of H at the boundary common to any two filaments must be everywhere equal to H_S. If the coil circuit is broken, H must be constantly zero at the surface of every filament.

$$E = \frac{w \cdot H_S}{4\pi N} + \frac{\mu\rho n^2 N}{4\pi\mu} \int\int \left(\frac{\partial^2 H}{\partial x^2} + \frac{\partial^2 H}{\partial y^2} \right) dx dy, \tag{37}$$

where the integral is to be taken over the section of one filament.

Eddy currents in any filament which are the same in direction and intensity at all points on any line parallel to the axis do not affect in any way the magnetic field outside the filament.

If, after a steady current E/w has been running in the solenoid, the circuit be instantaneously broken, the value of H falls from $4\pi NE/w$ to 0 at the surface of the prism and at the surface of every filament, and H is given by the equation

$$H = \frac{16 H_0}{\pi^2} \sum_{j=0}^{j=\infty} \sum_{k=0}^{k=\infty} \frac{e^{-\lambda^2 t}}{(2j+1)(2k+1)} \cdot \sin \frac{(2k+1)\pi x}{c} \cdot \sin \frac{(2j+1)\pi y}{c}, \tag{38}$$

$$\lambda^2 = \frac{\pi\rho}{4\mu c^2} [(2k+1)^2 + (2j+1)^2], \tag{39}$$

in every filament. The origin is at one corner of the cross-section of the filament, and the x and y axes are two sides of the section; k and j are integers, and $H_0 = 4\pi NE/w$.

If we differentiate both members of equation (38) with respect to the time, and integrate the result over the cross-section of a filament, we get for the average value for the whole core, at the time t, of the rate of change of the magnetic force in the iron,

$$\frac{1}{c^2} \int\int \frac{\partial H}{\partial t} \cdot dS = \frac{4\rho H_0}{\mu\pi^3 c^2} \sum_{j=0}^{j=\infty} \sum_{k=0}^{k=\infty} \frac{[(2k+1)^2 + (2j+1)^2] e^{-\lambda^2 t}}{(2j+1)^2 (2k+1)^2} = \frac{4\rho H_0}{\mu\pi^3 c^2} \cdot M. \tag{40}$$

At the origin of time, M has the same maximum value for all values of c; and for different values of c (c', c''), M has the same numerical value at times (t', t'') such that $t'/c'^2 = t''/c''^2$, provided μ has the same value in both cases. The smaller the values of μ and c the sooner does M for a given core attain a given value. At $t = 0$, when the change of H in the iron is most rapid at all points, the average value of dH/dt throughout the core is inversely proportional to c^2, that is, the average rate at which H is changing is 100 times as great when the core consists of filaments only one millimeter square as when the filaments are a centimeter square. This analysis illustrates the fact that when the main circuit of an electromagnet is suddenly broken, the changes in excitation to which the iron in a divided core is subject are far more violent than those which the particles of a solid core encounter. It is to be noticed that the average value of dH/dt given above is proportional to the electrical conductivity of the iron and to the intensity of the steady current in the exciting coil before the break.

In a similar manner, it is possible to show that if a given current in the exciting coil of an electromagnet be changed by a sudden increase or decrease in the resistance of the circuit while the applied electromotive force is unaltered, the whole given change of the magnetizing field in the core takes place somewhat more quickly if the core is finely divided than if it is solid. The general fact is, of course, evident without computation.

If the square core of a solenoid, the area of the cross-section of which is A square centimeters, be made of a bundle of infinitely long, straight iron wires placed close together, and if after a steady current of intensity E/w has been running for some time through the circuit so that there is a magnetic field of uniform intensity $H_0 = 4\,\pi NE/w$ in the core, the resistance of the solenoid circuit be suddenly changed to w' ohms per centimeter of length of the core, the current in the coil will gradually change to E/w', and the field in the core finally reaches the uniform value $H_\infty = 4\,\pi NE/w'$. At any instant the field in so much of the space A as is occupied by air is $4\,\pi NC$, for eddy currents in the round wires act like solenoidal current sheets, and do not affect the field outside the wires. Within each wire there are, of course, eddy currents, and at every point in the iron at every instant, the field intensity, H, must satisfy the equation (34).

The induction flux (p) through the solenoid per centimeter of its length is

$$4\,\pi N^2 C\,(A - n^2 B) + \mu N \int\!\!\int H \cdot dx dy, \tag{41}$$

where n^2 is the number of wires in the core and B is the area of the cross-section of each of them. The double integral is to be extended over the cross-sections of all the wires.

Since
$$E - \frac{dp}{dt} = w'C,$$

$$w'C + (A - n^2B)\,4\pi N^2 \cdot \frac{dC}{dt} + \mu N \int\!\!\int \frac{\partial H}{\partial t} \cdot dS = E, \tag{42}$$

and if H_S represents the strength of the magnetic field in the air space within the solenoid, and $A - n^2B$ is written $h \cdot A$,

$$H_S - \frac{4\,\pi NE}{w'} + \frac{4\,\pi N^2hA}{w'} \cdot \frac{dH_S}{dt} + \frac{4\,\pi\mu n^2N^2}{w'} \int\!\!\int \frac{\partial H}{\partial t} \cdot dS = 0, \tag{43}$$

where the double integral is to be taken over the cross-section of a single filament. If we put $H = H' + H_\infty$ and $H_S = H'_S + H_\infty$, the last equation becomes

$$H'_S + \frac{4\,\pi N^2hA}{w'} \cdot \frac{dH'_S}{dt} + \frac{4\,\pi\mu n^2N^2}{w'} \int\!\!\int \frac{\partial H'}{\partial t} \cdot dS, \tag{44}$$

in which H' satisfies at every point the equation

$$\frac{\partial H'}{\partial t} = \frac{\rho}{4\,\pi\mu}\left(\frac{\partial^2 H'}{\partial x^2} + \frac{\partial^2 H'}{\partial y^2}\right) = \frac{\rho}{4\,\mu\pi}\left\{\frac{1}{r} \cdot \frac{\partial}{\partial r}\left(r \cdot \frac{\partial H'}{\partial r}\right)\right\} \tag{45}$$

where r is the distance from the axis of the wire in which the point lies. We are to find a function H' which satisfies equations (44), (45), which, when $t = 0$, is everywhere equal to $H_0 - H_\infty$, and which vanishes everywhere when t is infinite.

If
$$\varpi = \sum Le^{-\beta^2 t} \cdot J_0\,(mr), \tag{46}$$

in which either m or β may be chosen at pleasure and the other computed from the equation

$$m^2\rho = 4\,\pi\mu\beta^2, \tag{47}$$

and if for m in (46) we use the successive roots of the transcendental equation

$$J_0\,(mb)\left(1 - \frac{N^2hA\rho \cdot m^2b^2}{\mu w' b^2}\right) = \frac{2\,\pi n^2N^2\rho}{w'} \cdot mb \cdot J_1\,(mb), \tag{48}$$

where b is the radius of the wire, ϖ satisfies equations (44), (45) and vanishes when t is infinite.

Without any consideration of the question of a possible development of unity in terms of an infinite series of Bessel's Functions of the form $J_0\,(mr)$, where the m's have the values just mentioned, it is clear[6] that, within the comparatively short range from 0 to b, unity may be represented with sufficient accuracy by a few terms (sometimes two) of the form

---

[6] Byerly, Annals of Mathematics for April, 1911.

$$L_1 \cdot J_0(m_1 r) + L_2 \cdot J_0(m_2 r) + L_3 \cdot J_0(m_3 r) + \ldots = \sum L_k \cdot J_0(m_k r), \quad (49)$$

so that

$$H = H_\infty + (H_0 - H_\infty) \sum L_k \cdot e^{-\beta^2 t} \cdot J_0(m_k r) \quad (50)$$

gives the value of the magnetic field at the time t at any desired point in the wire in question, and, therefore, at any desired point in any other wire of the core.

$$\frac{\partial H}{\partial t} = \frac{-(H_0 - H_\infty)\,\rho}{4\,\pi\mu} \sum L_k \cdot m^2 e^{-\beta^2 t} \cdot J_0(mr), \quad (51)$$

and if this be integrated over the cross-section of a wire and divided by πb^2, the result,

$$\Omega = \frac{-(H_0 - H_\infty)\,\rho}{2\,\pi\mu b^2} \sum L_k \cdot e^{-\beta^2 t} \cdot mb \cdot J_1(mb), \quad (52)$$

will represent the average value in the whole core, at the time t, of the time rate of change of the magnetic field. An example will best show the meaning of these rather intractable expressions.

Suppose the core of a long solenoid of square cross-section, ten centimeters on a side, to be built up of straight, round iron rods one millimeter in diameter placed close together; then $h = 0.2146$, $b = 0.05$, $n = 100$. If the resistance of the solenoid coil per centimeter of its length is $\frac{1}{16}$ of an ohm, the specific resistance of the iron 9950 abs-ohms, the number of turns of wire per centimeter of the solenoid 10, and the value of the permeability of the iron 100, then $mb = x$ satisfies the equation

$$J_0(x) \cdot (1 - 1.3666\,x^2) = 1000\,x \cdot J_1(x), \quad (53)$$

and the first root $x = 0.04465$ will suffice, for $m = 0.8930$; and $J_0(0.8930\,r)$ differs from unity by less than one tenth of one per cent over the whole range from $r = 0$ to $r = b$, and from (50)

$$\frac{H - H_\infty}{H_0 - H_\infty} = e^{-6.315t} \cdot J_0(mr), \quad (54)$$

very approximately. In the case of a core of the same cross-sectional area ($0.7854A$), and the same permeability, but wholly without eddy currents, it is easy to show that

$$H = H_\infty + (H_0 - H_\infty) \cdot e^{-kt}, \quad (55)$$

where $k = w't/4\pi N^2 \cdot D$, $D = A[4 + \pi(\mu - 1)]/4$.

For this problem, (55) yields

$$\frac{H - H_\infty}{H_0 - H_\infty} = e^{-6.316t}, \tag{56}$$

and a comparison of (54) and (56) shows that the eddy currents in a core of this wire, one millimeter in diameter, have practically no effect in slowing the changes in magnetism of the iron.

If the core of the given solenoid were made up of rods one centimeter in diameter, mb or x would be given as the roots of the equation

$$J_0(x) \cdot (1 - 0.01366\,x^2) = 10\,x \cdot J_1(x), \tag{57}$$

and it is not very difficult to show by a process of trial and error from Meissel's *Tafel der Bessel'schen Functionen*, that the first three of these roots are approximately equal to 0.4411, 3.8525, 7.0204, and that the corresponding values of $J_0(x)$ and $J_1(x)$ are 0.951946, $-$0.402672, 0.300112, and 0.215229, $-$0.008352, 0.001444.

If, with these roots, we wish to determine such a set of coefficients, (L_1, L_2, L_3) as shall make the mean square of the difference between unity and $\Sigma L \cdot J_0(mr)$ as small as possible, for the range from $r = 0$ to $r = b$, we have to solve the equations

$$A_1 \cdot L_1 + B_{12} \cdot L_2 + B_{13} \cdot L_3 = C_1, \qquad B_{12} \cdot L_1 + A_2 \cdot L_2 + B_{23} \cdot L_3 = C_2$$

$$B_{13} \cdot L_1 + B_{23} L_2 + A_3 L_3 = C_3, \qquad \text{where}$$

$$C_1 = 2\pi b^2 \cdot J_1(x_1)/x_1, \qquad A_1 = \pi b^2 \{[J_0(x_1)]^2 + [J_1(x_1)]^2\},$$

$$B_{12} = b^2 [x_1 \cdot J_0(x_2) \cdot J_1(x_1) - x_2 \cdot J_0(x_1) \cdot J_1(x_2)]/(x_1^2 - x_2^2),$$

as Professor Byerly's theorems show. The computation here indicated shows that $\Omega = 6.096$ or 0.320, approximately, according as $t = 0$ or $t = 0.1$, whereas, if eddy currents were wholly cut out, the corresponding values would be 6.316 and 0.336. These figures illustrate the comparatively slight effect of subdividing the core in the particular case here considered. The results would, of course, be somewhat different numerically, with different assumed values for the constants of the circuit.

It is clear that the inversion of sign in the magnetic moment of a straight iron bar, when the magnetic excitation is suddenly removed, accompanies, at least, a large demagnetizing factor due to the ends of the bar, and no one seems to have observed the phenomenon in the case of closed cores. In rings, however, as in straight bars, the ultimate value of the intensity (I) of magnetization depends very much upon the manner in which the given exciting current is made to attain its final strength.

The experiments of Rücker[7] upon small solid iron toroids seem to show that at moderate excitations there may be a difference of from 6 per cent to as much as 30 per cent in the final flux density due to a given current, according as the current is applied suddenly or by many short steps, and, unlike some other observers, he found a very real difference ($T_f - T_a$), though a smaller one than in the case of the solid metal, for a toroid with core of fine iron wire (Blumendraht). In the case of a large electromagnet with solid, closed core, weighing altogether more than 1500 kilograms, Babbitt found, by a very ingenious method of procedure, a difference of 17.4 per cent between the final flux density in the iron caused by the sudden application of a given current, and the growth from nothing of the same current in 56 steps. The cross-section of this massive core is more than 450 square centimeters in its narrowest part, and eddy currents are so much in evidence that quite two minutes are required for a "suddenly applied" current to attain its steady value.

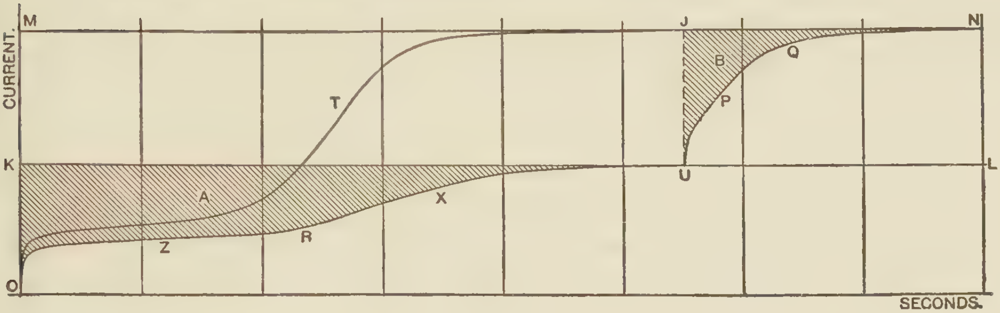

FIGURE 35.

Babbitt also carried out a long series of very accurate measurements extended over several months, upon two small toroids of fine, carefully annealed iron wire, and upon a toroid weighing more than 40 kilograms made of very well softened iron wire about half a millimeter in diameter. His results show conclusively that if one of these softened and demagnetized cores has been first put through the cycle due to a given excitation a considerable number of times to obliterate the effects of the past experiences of the iron, the form of the hysteresis diagram is precisely the same, whether the half cycle be carried out by one reversal of the main switch or in a very large number of steps. In general agreement with these results are some less accurate ones which I obtained three years ago in experimenting upon a transformer which has an exciting coil of 1394 turns and a core of about 120 square centimeters in cross-section, built up of thin strips of varnished sheet iron about ten centimeters wide. This transformer was connected in simple circuit with a storage battery and a rheostat besides a suitable oscillograph. When the circuit was suddenly closed, with such a resistance (x) in the rheostat that the final strength of the current was about 1.10 amperes, the current curve was of the form R as shown in Figure 35, and when after a few seconds x was suddenly removed, so as to bring the final strength of the current up to about 2.30 amperes, the current curve was Q. When the whole journey was made without x the current curve was T. The sum of the flux changes represented by the shaded areas as measured by a Coradi "Grand Planimètre Roulant et à Sphère" was 1126, while the flux change corresponding to the area above the curve T was 1130. The core was not sufficiently well divided to avoid all evidence of eddy currents, for the curve Q does not exactly conform throughout with the upper part of T. This is shown more clearly in Figure 36, taken with the same transformer. Here the area of the shaded portion above K multiplied by the resistance then in the circuit should be equal to so much of the area above C, multiplied by the resistance belonging to it, as lies to the left of the

---

[7] Babbitt, These Proceedings, **46**, 1911; Rücker, Inaugural Dissertation, Halle-Wittenberg, 1905.

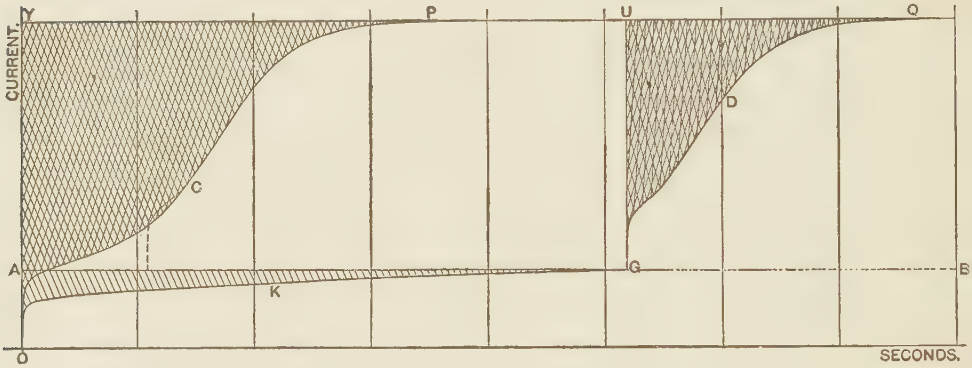

FIGURE 36. Growth from an originally neutral core of a current in a transformer with a laminated core. The effects of eddy currents are here noticeable.

dotted line which rises at about 1.1 seconds after the circuit was closed, and is an exact copy of the curve D moved to the left. This curve coincides with C for a large part of its course, but has a trifle less area above it than that portion of C has which lies to the right of the ordinate at which the lowest part of the dotted curve begins. The shape of D just at the beginning points to the existence of eddy currents.

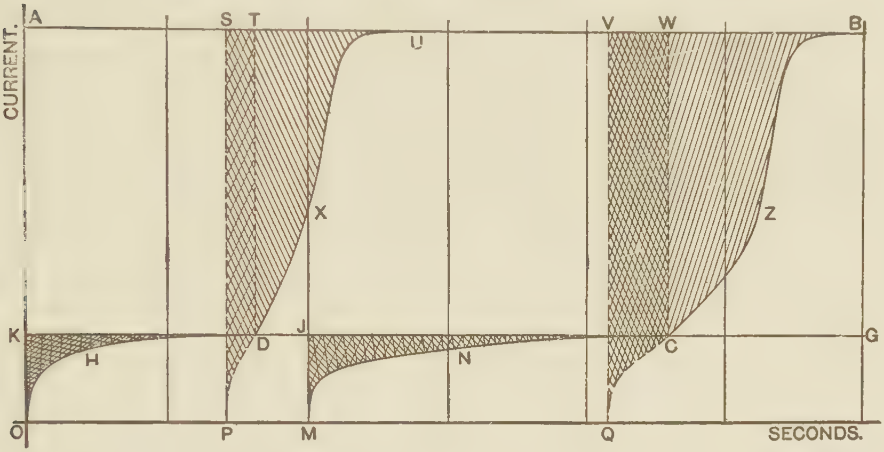

Figure 37. Current curves for a toroid with fine wire core. The second part of a two-stage current is exactly the same as if the current were allowed to grow at once to its final value.

To test more thoroughly the effect upon the flux of magnetic induction through the core of the transformer, of building up the current in different ways, I first measured with great care, by aid of a modified Rubens-du Bois "Panzer Galvanometer," the changes of this flux for a quick reversal of an excitation of 1812 ampere turns. I then measured by means of the planimeter a long series of oscillograph records obtained by reversing the same excitation by a considerable number of steps. All the testing instruments were different in the two cases, and no comparison was possible until the final results were reached and were found to differ from one another by only one part in fourteen hundred. The labor of reducing the oscillograms was so great that this close agreement must be considered accidental, but there can be little doubt, I think, that the flux change due to the single step and the sum of the changes due to the long series of steps which together cover the same change of excitation were practically indistinguishable.

Figure 37 shows copies of oscillograms taken with a number of toroids in series. The core of each toroid was made of perhaps fifteen kilograms of very soft, varnished iron wire, about one tenth of a millimeter in diameter. The curves OHD, PDXU were taken when the cores had been thoroughly demagnetized just before the experiment; the curves MNC, QCZB after the core had been put a number of times through the cycle corresponding to the excitation used. The toroids were in simple circuit with a storage battery, an oscillograph, and a

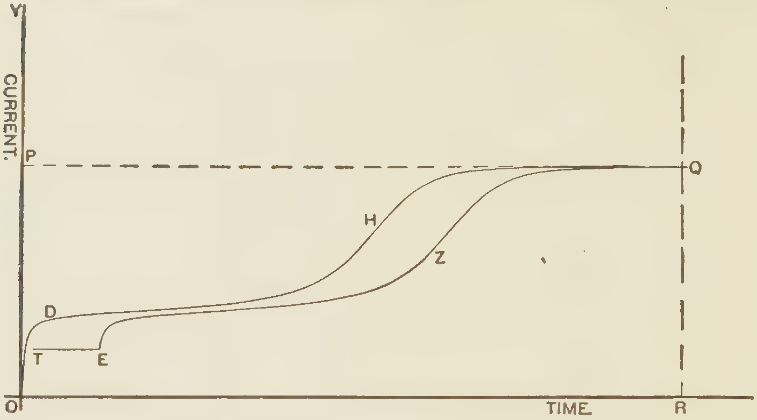

FIGURE 38. ODHQ represents the curve of growth of a current in the exciting coil of the toroid DN, if the circuit was suddenly closed when its resistance was r. If the circuit was first closed with a higher resistance $(r+s)$, which corresponded to a steady current of intensity OT, and if the resistance s was suddenly shunted out, the current rose to the intensity OP in the manner indicated by the curve EZQ, which, as Figure A shows, is of exactly the same form as the upper portion of ODHQ.

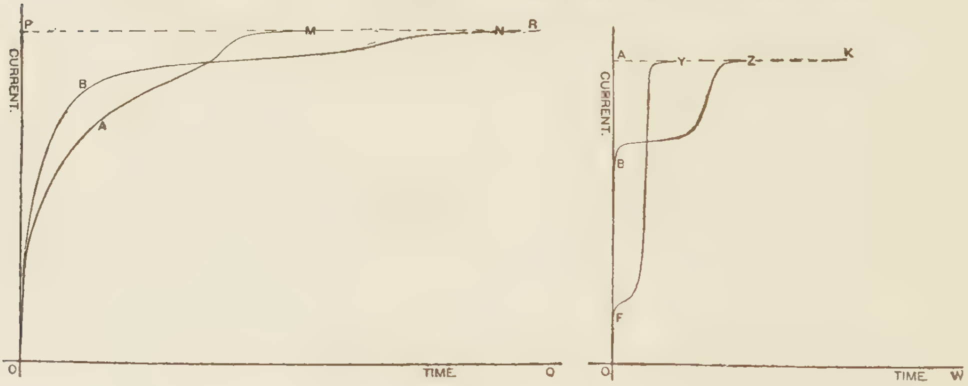

FIGURE 39.

rheostat of resistance x; when the circuit was suddenly closed the current grew to the final value corresponding to this resistance by the curve OHD or MNC, as the case might be. When at the proper time the rheostat resistance was suddenly shunted out of the circuit, the current rose to the value OA by the curve DXU or the curve CZB. If x had been shunted out at the start the current curve had the shape accurately represented, when the starting point had been shifted just far enough to the right, by PDXU or QCZB. It was not possible to detect any difference between the curves DXU and CZB and the upper parts of the curves obtained with x all the time out of circuit. This figure was drawn by superposing several oscillograms, for it is very difficult after one curve has been taken upon the sensitized paper carried by the revolving drum to start another curve some time afterwards at such a point that it shall coincide with the upper part of the first one. This feat has, however, just been accomplished in another case by Mr. John Coulson, who made the records shown in Figures A and B, and has helped me in most of the experimental work of this paper. Figure 38, drawn from another photograph, shows the two curves which coincide in A. The oscillograph was in circuit with the coil of a large toroid of about 41 centimeters in diameter, the core of which is made of soft, varnished iron wire about half a millimeter in diameter. Each record shows a current curve obtained by applying the electromotive force directly to the circuit, and the second part of a current diagram when an extra resistance, at first in the circuit, was suddenly shunted out.

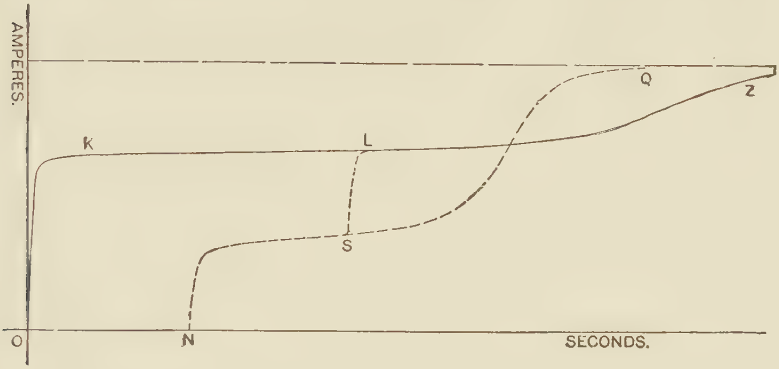

FIGURE 40. The current in one coil of the toroid DN which is in series with a battery follows the line OKLZ or the line NSQ, according as another coil on the same core is open or closed. When this last coil which has been closed is suddenly opened while the battery current is rising, this changes abruptly and follows exactly the upper part of the line OKLZ.

There seems to be in these cases neither a magnetic time lag nor any sensible von Waltenhofen effect.

If an electromagnet has two exciting coils, and if one of them be attached to the terminals of a battery, the form of the battery current will depend upon whether the second coil is open or closed on itself, and the difference is usually noticeable even when the magnet has a large solid core in which eddy currents are being induced. Figure 39 shows curves taken under the two conditions just mentioned for both the electromagnet TP and the toroid DN. To determine whether the closing of the second coil in the case of the electromagnet where strong

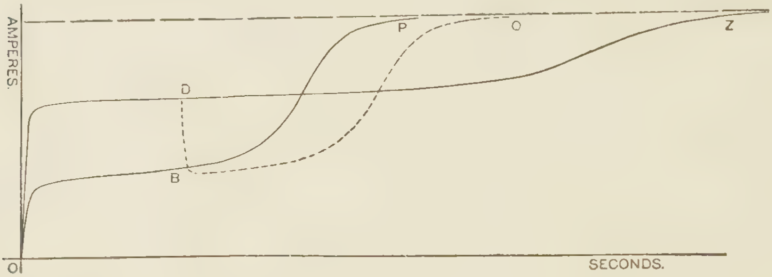

Figure 41. The current in one coil of the toroid DN which is in series with an oscillograph and a battery, follows the curve ODZ or the curve OBP, according as another coil wound on the same core is open or closed in itself. When at the point *D*, the second coil which has been open is suddenly closed, the oscillograph record gives the curve DBQ which except at the very beginning can be exactly superposed upon the upper part of the line OBP.

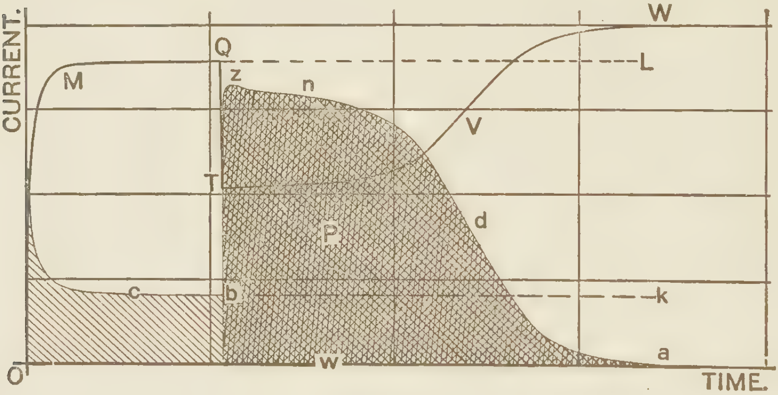

Figure 42.

eddy currents already existed changed the amount of the final flux through the circuit, Mr. Coulson has measured with great care a number of oscillograms taken with this apparatus, and finds the area between the asymptote and the curve OAM to be 6216 on the scale of his planimeter, while the area above the curve OBN is 6214 on the same scale. The areas above the curves agree within a small fraction of one per cent, as they were expected to do.

Figures 40 and 41 exhibit oscillograms taken with the toroid, DN, under sudden opening and closing of the second coil, and these show no signs of von Waltenhofen effects. Figure 42 gives the records of two oscillographs, one in the primary circuit of a toroid which has a core made of soft iron wire only one tenth of a millimeter in diameter, the other in a secondary coil, when a third coil, wound on the same core, was suddenly closed.

In early experiments upon the phenomenon of the reversal of moment in short rods magnetized in a solenoid, when the current was suddenly stopped, it was observed that if the rod had been previously magnetized permanently in the direction in which the current magnetized it, reversal never occurred, but that it always appeared, under favorable circumstances, if the direction of the previous magnetization was the opposite of that which the current gave it. This and like results has led many physicists to think that the molecules of the iron, when the exciting force due to the current is suddenly removed, return to the positions which they had just before the current acted upon them, but that the motion is so much resisted by frictional forces that the kinetic energy is lost when the particles have swung slightly beyond the positions of equilibrium where they are held by the friction. Wiedemann believed, on the other hand, that when the exciting circuit of an electromagnet is suddenly opened, the rise and decay of the Oeffnungsextrastrom induces in the mass of the iron, currents, alternating in direction and decreasing in intensity, and that the magnetization of a rod due to the original current is reversed in sign, under favorable circumstances, by a weaker current in the opposite direction. In the case of closed rings, where demagnetizing factors are absent, anomalous magnetization seems to appear only when eddy currents in the iron so shield the particles inside the mass that they are never exposed to sudden changes in the intensity of the exciting magnetic field.

My thanks are due to the Trustees of the Bache Fund of the National Academy of Sciences, who have lent me some of the apparatus used in measuring the oscillograms mentioned in this paper.

The Jefferson Physical Laboratory,
Cambridge, Mass.

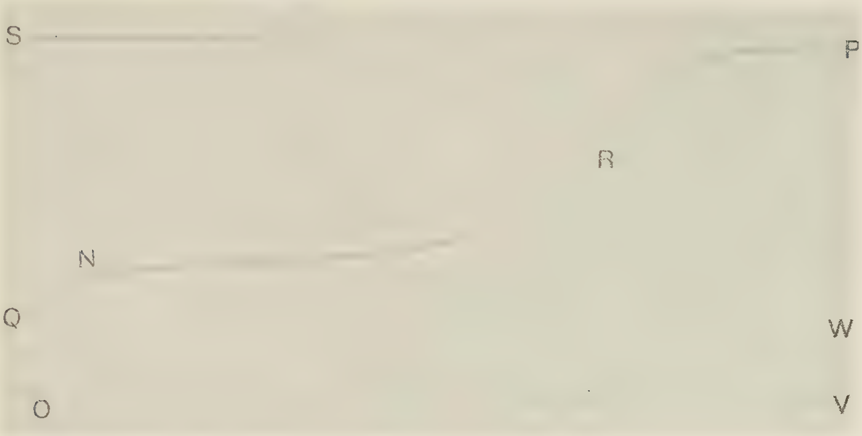

A.

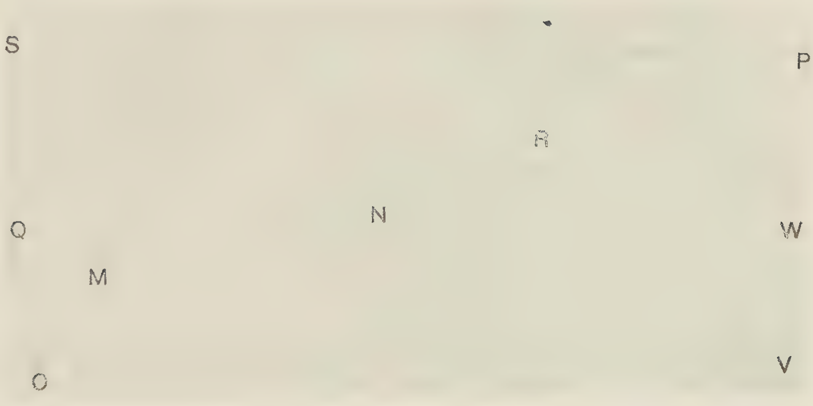

B.

Proceedings of the American Academy of Arts and Sciences.

Vol. XLVI. No. 21. — April, 1911.

CONTRIBUTIONS FROM THE JEFFERSON PHYSICAL LABORATORY, HARVARD UNIVERSITY.

THE INTERNAL RESISTANCE OF THE LEAD ACCUMULATOR.

By Harry W. Morse and Ledyard W. Sargent.

THE INTERNAL RESISTANCE OF THE LEAD ACCUMULATOR.

By Harry W. Morse and Ledyard W. Sargent.

Presented by John Trowbridge, December 14, 1910. Received January 3, 1911.

General Discussion.

1. The internal resistance of a lead accumulator is not a factor of importance in the practical operation of storage batteries. In a small pocket battery it is only a few hundredths of an ohm: in medium sized cells it sinks to a few thousandths, and in large cells, such as are used in regulation and central station work, it is of the order of a few hundred-thousandths of an ohm. In almost every case the cell resistance is so low in comparison with the other resistances in the working circuit that it can be neglected as far as practical calculation is concerned.

But the resistance of a cell and the changes which take place in this factor are of much interest when the behavior of the cell is being studied from a more general point of view. A lead accumulator seems a very simple system indeed at first glance, but it is in fact a very complex one, concealing many problems difficult of solution. While the cell is at rest, fully charged, and therefore containing plates which are good conductors from their center out to the boundary of the electrolyte, its resistance is very nearly that of the acid between these plates, and it can be calculated with fair approximation. But when the cell is working, either on charge or discharge, its condition is most variable. The acid must diffuse through a series of fine channels, and great differences of acid concentration in the different layers of the plates will be set up. Then, too, the particles of lead and lead peroxide, themselves good conductors, will be more or less completely coated with lead sulphate — a bad conductor. The acid concentration will, moreover, be a function of the *rate* at which the cell is working, and the thickness of the lead sulphate coating over a particle of lead or lead peroxide at any given point in the plate will also be a function of the rate.

2. An ideal section of a storage battery of two plates is shown in

Figure 1. *A* is the plate, and its resistance can be assumed to remain fairly constant, except for its temperature coefficient. This factor has a small value within the range of practical operating conditions. *C* is that part of the electrolyte which does not lie very close to the plates. Its total concentration is determined accurately by Faraday's Law and its resistance is a function only of this concentration and of the temperature. *B* is the most active, variable, and interesting part of the cell. It includes the active material, that part of the electrolyte which is in the pores of this material, and that part of the electrolyte which is near the plates. For ordinary rates large concentration changes can be assumed to extend not more than a millimeter or two from the outside surface of the active material before they are equalized by mixture with the main body of the electrolyte.

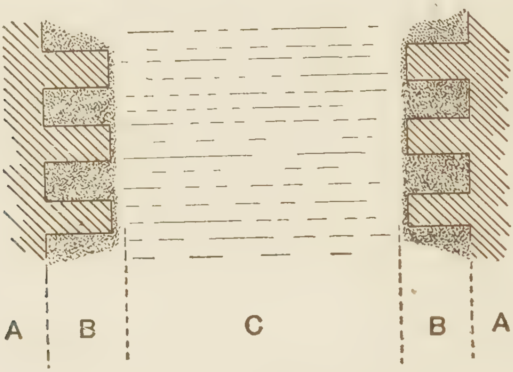

Figure 1. Section through storage cell.

When the cell is at rest, its resistance may be considered as being made up of three parts. *A*, metallic in nature, and therefore with a negative temperature coefficient, but constant at a fixed temperature. *B*, also metallic in its nature, and sufficiently low so that the resistance of the electrolyte in its pores can be neglected in comparison with it. *C*, a purely electrolytic resistance, with positive temperature coefficient, but constant at a fixed temperature.

When the cell is working at a constant rate and fixed temperature, *A* remains constant. *C* is a function only of the total concentration of acid in the cell, and can be made constant by using small plates and a large body of electrolyte. The resistance of *B* now becomes more complex, and may be considered to break up into two parts, one a function of the condition of the active material and the other a function of the concentration of the electrolyte in the pores of the active material and in the layer in immediate contact with its surface.

The change in B during charge will, moreover, be wholly different from the change during discharge, for in both cases the changes in the active material *follow the electrolyte.* During charge the active material first to enter into reaction is that at the surface of the plate, provided the plate has not been allowed to "sulphate" so completely that the conductivity through the active mass has been very greatly reduced. Since the action is taking place at the surface the electrolyte does not have to diffuse far through narrow channels. But as the diffusion path increases and the cell becomes more fully charged, concentrated acid is produced in the pores of the mass. In spite of the decrease in resistance due to this better conducting acid it is still the plate itself which does most of the conducting. It is therefore to be expected that the change of resistance during the charge of a healthy storage cell will not be large.

During discharge a very different state of affairs exists. In this case also action begins at the surface of the plate, where electrolyte is available for the reaction. But as discharge proceeds, and the area of activity recedes into the interior of the active material, acid is used up within the plate and the concentration of the active part of the electrolyte decreases. To this loss is added the loss of conductivity of the plate itself, for the particles of lead and lead peroxide in the outer layers have now been covered with sulphate and more or less completely insulated from each other. The result is as if the distance between the plates had been increased, for the plate surface which is actually carrying current is now well back in the interior of the mass of active material, instead of at the actual outside surface.

It should be kept in mind also that the equalization of concentration differences in a working plate is not cared for wholly by diffusion. While this is a potent factor always, it can be shown to be insufficient to account for the facts. A considerable part of the equalization is probably cared for by local concentration cells at various parts of the plate, and these local actions depend for their efficiency on good conductivity of the plate between the points where the concentration differences exist. Any change in the conducting power will affect the rate of equalization of acid and will displace the area of action within the plate.

Viewed in this way we should hardly expect any very large or very rapid changes in cell resistance, nor any of the peculiar maxima of resistance at various points in charge and discharge which appear in some of the older reports on the subject. It is probable that polarization was not eliminated in these measurements.

On long standing, a storage cell may acquire a very high resistance indeed as the result of complete "sulphation." This term means that the active lead sulphate formed during discharge has gradually changed into the crystalline inactive form and that crystals of this form have completely covered the particles of lead and lead peroxide with an insulating coating. Authentic cases of cells of considerable size, with internal resistance as high as 10 ohms, are known. But under the usual conditions of charge and discharge the sulphate retains its "active" state, and even after standing discharged for a month or more no great change in internal resistance is usually to be observed [see § 15].

3. In its ordinary work, a storage cell is discharged only until the plate potential sinks to about 1.7–1.8 volts. This means usually that only about one quarter of the active material in the plates has entered into reaction and that the increased resistance in the active material is due rather to separation of the particles by sulphate coatings than to complete transformation of the active material at any point into insulating material (sulphate). On charge these sulphate coatings and bridges are rapidly broken down, and the decrease in resistance is therefore much more rapid than that corresponding to change in electrolyte within the plate.

After a period of discharge, with corresponding change in resistance, the cell recovers its original e. m. f. along a curve which is somewhat like a diffusion curve [§ 13]. This curve is made steeper by the equalizing effect of local action as explained in 2. It also recovers its original resistance along a somewhat similar curve. These facts indicate clearly the *dynamic* nature of the whole cell activity, for evidently the change in resistance as well as the change in e. m. f. is fundamentally a function of acid concentration and diffusion. The particles of active material cannot have been completely covered by insulating layers, for on standing the plate returned to its original condition as measured by e. m. f. and resistance.

We must evidently think of the particles of lead and lead peroxide as covered with a spongy or powdery layer of lead sulphate, with interstices so small that diffusion cannot overcome the effect of even a small current and its accompanying exhaustion of acid within the pores. As long as no current is flowing, and when recovery has been allowed to take place completely, the total active surface has not been greatly reduced by the changes in the plate, nor has the "active surface" been far removed from its original plane. But the passage of even a small discharge current causes exhaustion of acid in the pores to such an extent that nearly pure water intervenes between the electrolyte and the conducting material of the plate, and the result is a considerable increase in resistance.

While it is true that the concentration and therefore the resistance of the main body of the electrolyte is completely determined by Faraday's Law, the passage of the same quantity of electricity may result very differently in various types of cells. Change in concentration and resistance will be great in those types which have large weight of plates in proportion to their content of electrolyte. They will be small in the types where weight is not a factor to be considered and where a large excess of acid is maintained.

Other factors which may effect resistance will be discussed in connection with the data of this paper.

4. On page 611 will be found a list of references on the subject of the resistance of galvanic cells and accumulators. Many of these papers were written at a time when the difficulty of such measurements was not understood, and it may be said that the research of Nernst and Haagn (1896) was pioneer work, and that they showed for the first time how to eliminate the disturbing factors of the problem. The measurements of Dolazalek and Gahl (1901) are still more accurate and include data on several types of cell and on various rates of charge and discharge.

Our attention has been turned largely toward the temperature coefficients of resistance under various conditions, for we wished to exhibit as clearly as possible the dynamic nature of the phenomena in the lead accumulator. After investigation of the other methods of measurement, we adopted the form of bridge described by Ayres [**20**]. Ayres himself did not use the bridge for measurements on storage cells, nor indeed for any very low resistances of electrolytic nature. But we have found this type of bridge, with slight alteration, to be most satisfactory for the measurement of electrolytic resistances of the order of 0.01 to 0.10 ohm.

THE BRIDGE AND AUXILIARY APPARATUS.

5. The bridge connections are shown in Figure 2, together with the circuit used in charging and discharging the cell and the secondary bridge on which resistances were measured after balance had been obtained. The bridge itself is symmetric, and contains a meter slide wire of manganin of about 0.40 ohm resistance. At opposite ends of this wire connection is made to the source of alternating current and to the two other arms of the bridge. The cell arm contains the cell under investigation in series with a capacity C_1: the other arm con-

tains a similar and nearly equal capacity C_2 and the variable resistance R. C_1 and C_2 are rolled paraffin paper condensers of about 22 microfarads each, composed of 10 units of 2.2. mf. connected in parallel by No. 11 copper wires soldered at each point and also to the bridge connections. The entire wiring of the bridge was non-inductive.

The cell was maintained at constant temperature in a thermostat and was connected by soldered No. 11 wires terminating in a heavy mercury-metal switch-block so arranged that the cell could be placed in circuit, or cut out, without change in the block resistance and without short-circuiting the cell. The ¼-inch wires of the block switch were kept continually under mercury whichever way the switch was turned, thus keeping contacts bright when the cell was out.

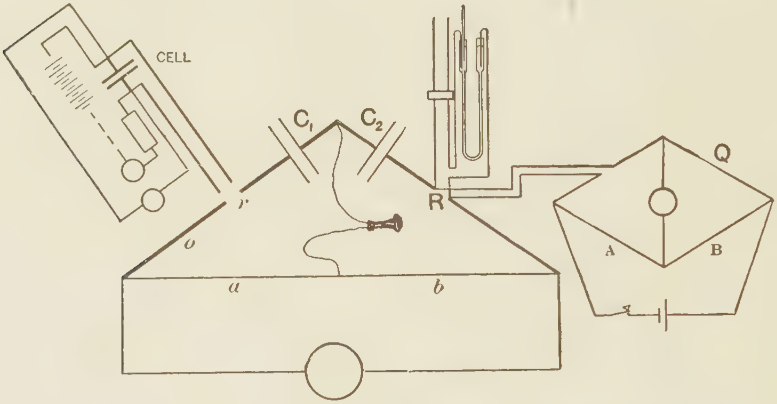

FIGURE 2. Bridge connections for measuring low electrolytic resistances.

The variable resistance R consisted of two parts: One of two parallel wires shunted by a heavy sliding block, and the other, in series with this, was a vertical U-tube of glass containing mercury, as shown in Figure 3. The connecting wires dip into the mercury in the two arms and the cross-section of one arm was decreased or increased by lowering or raising the glass rod. This smoothly variable resistance proved to be of the greatest aid in obtaining the close settings desired.

In parallel with R was a box Wheatstones bridge and galvanometer. R could be thrown over into the X-arm of this bridge by means of a mercury switch, but as the box bridge had a resistance of about 1000 ohms it was found unnecessary to cut it out while making settings on the cell, and during the later measurements the switch was removed, leaving the connections as shown in Figure 2. The ratio of the fixed arm of this auxiliary bridge was 1 : 1000 and resistances could be measured on it to 0.0001 ohm.

During the majority of our measurements a resistance of a few tenths of an ohm ((*O*) in the figure) was kept in the cell arm in series with C_1 and for some measurements of high resistances it was found necessary to introduce a similar resistance in series with the slide-wire and mercury resistances of R.

Measurements were made with "cell in" and "cell out" within as short a time as possible, in order to eliminate any possible changes, and measurements were repeated several times in each case. We were thus measuring the difference between [cell + R_1] and R_1, where R_1 is the resistance of O plus the connections in that arm.

Various sources of alternating current were tried, but none was wholly satisfactory. We had no source of pure sine-waves at our disposal and some trouble from harmonics was experienced. This was removed by using a transformer and various combinations of capacities in the circuit.

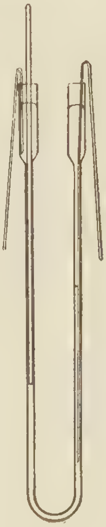

FIGURE 3. Variable mercury resistance.

THEORY OF THIS TYPE OF BRIDGE.

6. The complete theory of this type of bridge may be found in Ayres's paper [20], but our method of operation was necessarily somewhat different from his because of the small magnitudes of the resistances we had to measure.

For the ideal condition of balance we have

$$r/R = a/b = C_2/C \tag{1}$$

where the bridge is non-inductive, the resistances of connections are negligible, a and b are the bridge-wire readings, C_2 is the capacity of the "known" arm, C is the resultant of the capacity of the cell with C_1, r is the resistance of the cell and its leads, and R is that of the opposite arm of the bridge.

Taking into consideration the resistances of the various connections, and that of the coil o inserted in the cell arm, we have, for both bridges, the following equations :

$$\frac{a}{b} = \frac{o + r + u}{R + v}, \tag{2}$$

where u and v are the resistances of the connections on the cell side and the R side respectively;

$$R + w = Q\frac{A}{B} = \text{Q}\,(0.001) = q, \tag{3}$$

where w is the resistance of connection to the auxiliary bridge. Combining (2) and (3) gives

$$o + r = (q - w + v)\frac{a}{b} - u. \tag{4}$$

Upon cutting out the cell and short circuiting that arm of the bridge, we have

$$o = \left(Q'\frac{A}{B} - w + v\right)\frac{a'}{b'} - u = (q' - w + v)\frac{a'}{b'} - u. \tag{5}$$

Subtracting (5) from (4) gives

$$r = \frac{a}{b}\left(q - q'\frac{a'b}{ab'}\right) + \frac{a}{b}\left(\frac{a'b}{ab'} - 1\right)w - \frac{a}{b}\left(\frac{a'b}{ab'} - 1\right)v. \tag{6}$$

During the first part of the investigation a lay between the limits 506 mm. and 507 mm., and during the second part between 481 mm. and 486 mm. In most cases the difference between a and a^1 was less than 0.5 mm., and it was usually about 0.3 mm.

In view of this, the terms containing w and v can at once be neglected. The difference between $q - q'$, the value actually recorded as resistance, and $(q - q')\frac{a'b}{ab'}$, is $(\frac{a'b}{ab'} - 1)\,q'$, which does not exceed 0.0005 ohm, since q' did not exceed 0.25 and the value of the parenthesis was in no case greater than 0.002.

The following observations are deemed interesting in connection with the fact that the bridge reading was not the same with the cell in as when the cell was out.

1. The bridge reading with "cell in" a is smaller than a'.
2. Both with "cell in" and "cell out," the insertion of a condenser (5.2 MF) in parallel with the leads to the cell-switch causes an increase in the value of a or a' as the case may be.
3. Decreasing the frequency by 50% causes no change in a, but a' is thereby decreased.
4. A condenser in parallel with C_1 causes a and a' to decrease.

The last observation is to be expected from the theory of the bridge. It is hard to see how any capacity possessed by the cell could act so as to make a smaller than a'; rather the opposite effect would be expected. The supposition of an inductance in the cell would explain this change in the bridge reading, but a change in the frequency did not affect a, while it did affect a'.

The explanation would seem to be as follows: The configuration of R suggests inductance, and an approximate calculation shows $2\pi n L_2$ to be about 0.01. Now the value of $1/2\pi n C_2$ is about 5. A change of 0.5 mm. from a to a' corresponds to a change of 0.01 in $1/2\pi n C_2$. Calculation gives about 0.01 for $2\pi n L$ for the leads from the cell-switch to the cell, corresponding to $2\pi n L_2$ for the C_2 arm of the bridge. From these considerations it would appear that a rather than a' is more nearly the point where $C_2/C = a/b$, for, with "cell in," the inductive reactance of the C_2 arm is balanced by that of the cell leads.

Since C_1 and C_2 are about the same, and since C_2 has an inductance with it, while C_1 has not, the reactance of the C_2 arm will increase with decrease of frequency faster than the reactance of the C_1 arm; in short, the reactance of the C_2 arm will become greater than that of the C_1 arm, and a' will diminish with decrease in frequency. On the other hand, with "cell in," the two reactances will change equally with change in frequency, that is, a will not change.

7. From the average of all our measurements we have compiled the values for the open circuit resistance of our cell at various temperatures. They are as follows:

TABLE I.

Open Circuit Resistance of Planté Plates at Various Temperatures.

Temperature.	Resistance.	Temperature.	Resistance.
0.0 C°	0.0686	25.0	0.0448
8.5	0.0579	30.0	0.0420
10.0	0.0562	45.0	0.0362
20.0	0.0483	55.0	0.0335

These values are plotted in the full-line curve of Figure 4. In the dotted-line curve on the same figure are given the values for sulphuric acid of the same concentration as that used in our cell. We have chosen the two points indicated by larger circles as the points from which to calculate the remainder of the curve, which is plotted from the empirical formula

$$K_t = K_o \, (1 + ct + c^1t^2)$$

It will be seen that the cell resistance and the acid resistance fall very closely together from zero to 30°. Above this point the cell re-

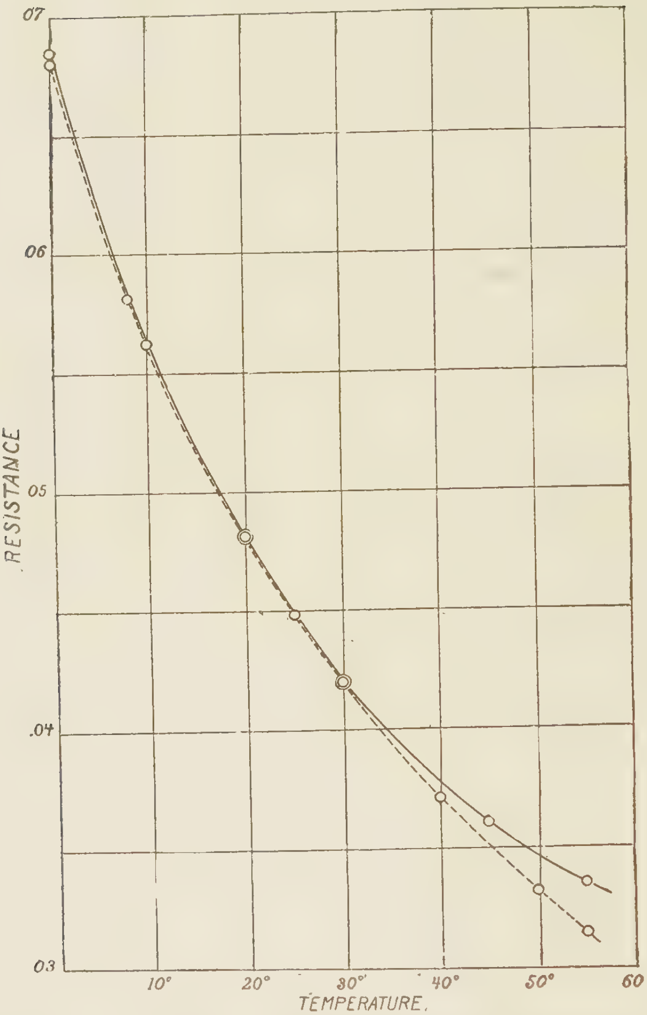

FIGURE 4. Temperature-resistance curves for electrolyte and cell.

sistance does not decrease as rapidly with rise of temperature as does the acid. As a matter of fact the two points at zero do not fall together. So it is evident that both at high and low temperatures the cell resistance is higher than that calculated for the pure acid. This figure indicates merely the shape of the two curves with reference to each other, and by no means indicates that the resistance of the cell is the same as that of sulphuric acid of the same concentration between a pair of platinum electrodes placed in the same geometrical position as the "average plate surfaces." The plate resistance is not negligible and its negative temperature coefficient may account for the higher resistance at the higher temperature in part at least. That the resistance of the plate itself enters is clearly shown by the fact the pasted plates of slightly greater area, placed as nearly as possible the same distance apart, show a decidedly greater resistance on open circuit than that of these Planté plates, which have a solid lead web and lead ribs running their whole length. The cells with pasted plates have nearly .01 ohm more resistance.

TABLE II.

INTERNAL RESISTANCE OF A PLANTÉ CELL DURING DISCHARGE AT 2 AMPERES. TEMPERATURE 8.5° C.

Time.	Cell in.	Cell out.	Cell.	Voltage.
0	.2882	.2304	.0578	2.09 open-circuit 1.85 after closing
10	.2895	.2317	.0578	1.83
22	.2926	.2306	.0620	1.77
37	.2961	.2316	.0645	1.70
52	.3080	.2313	.0767	1.55
62	.3142	.2316	.0836	1.36
71	.3158	.2315	.0843	1.18
77	.3160	.2316	.0844	0.97
81	.3164	.2315	.0849	0.80
86	.3191	.2314	.0877	0.63
96	.3656	.2315	.1341	0.30 [reversed]

8. The values of Table 2 are plotted in the upper curve of Figure 5, and they show the characteristic course of changes in this particular type of plate. The cell changes its internal resistance a little more than 100 percent during complete discharge, and by the time the last value on the list is reached the cell voltage has dropped to zero.

The most interesting thing about the curve is the flat place which occurs after 60–80 minutes of discharge. This is quite characteristic of Planté plates with ribs, but it has never been noticed before by any of the observers who have worked on storage cells. Indication of such a flat place may be seen in some of Haagn's curves, but it would seem that he thought them due to errors of measurement.

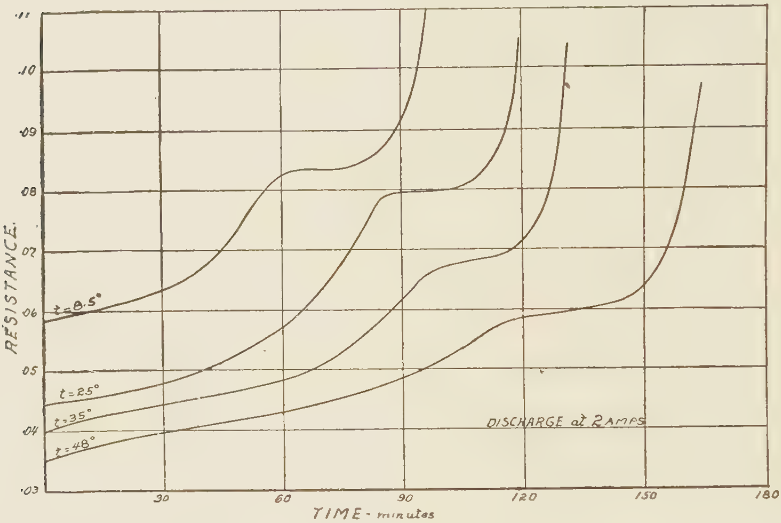

Figure 5. Curves of resistance of Planté cell during discharge at various temperatures.

The reason for the appearance of such a change in curvature seems quite obvious. These plates are of the Gould type, and they have ribs spun from the lead of the originally flat plate. These ribs are changed by formation to form active material, which lies close to the ribs at their tops but which forms a solid mass down toward the center web of the plate. During the first part of the discharge the electrolyte finds active material on the ribs and diffuses largely into the almost open space between them. As this material is used up the action moves further into the plate and presently reaches the mass of material which fills the bottom of the grooves. Here for a time there is material enough at a practically constant distance from the surface of the plate to supply the action, and when this is used up the resistance rises very rapidly and the plate potential shows that the cell is completely discharged.

TABLE III.

Planté Cell. Discharged at 2 Amperes.

Temperature 25° C.					
Time.	Cell.	Voltage.	Time.	Cell.	Voltage.
Open circuit	.0448	..	76	.0690	1.62
0	.0448	..	92	.0796	1.43
8	.0453	1.89	103	.0800	1.28
15	.0472	1.88	110	.0823	1.16
32	.0481	..	120	.1061	0.26
48	.0527	1.78	126	.1365	0.00
62	.0570	1.70			
Temperature 35° C.					
Open circuit	.0400	..	94	.0650	1.57
8	.0399	1.92	105	.0678	1.42
19	.0430	1.91	110	.0682	1.38
33	.0452	1.87	121	.0720	1.25
49	.0465	1.84	127	.0800	0.65
67	.0492	1.77	134	.1300	0.30
82	.0579	1.70	147	.1901	0.00
Temperature 48° C.					
Open circuit	.0351	..	112	.0570	1.65
6	.0358	1.96	120	.0589	1.57
23	.0395	1.95	131	.0598	1.52
37	.0406	1.90	136	.0600	1.47
46	.0420	1.87	144	.0620	1.37
63	.0431	1.84	153	.0653	1.00
79	.0460	1.80	159	.0945	0.52
92	.0488	1.76	173	.1757	0.12
103	.0520	1.70	178	..	0.00

As will be seen later, paste plates show no such flat place in their curves. [§ 11.]

The values for this Planté cell, discharged at 2 amperes at various temperatures [Table III], are all plotted on the curves of Figure 5. The corresponding voltage curves will be found in Figure 6.

The characteristic points appear in each curve, and the flat place moves toward a later point in the discharge curve, as might be expected, when the temperature is raised. This means merely that the material of the plate can be better reached and utilized at the higher temperature, and that therefore more of the active material on the ribs enters the reaction, leaving the mass of material at the bottom of the grooves for a later period of the discharge.

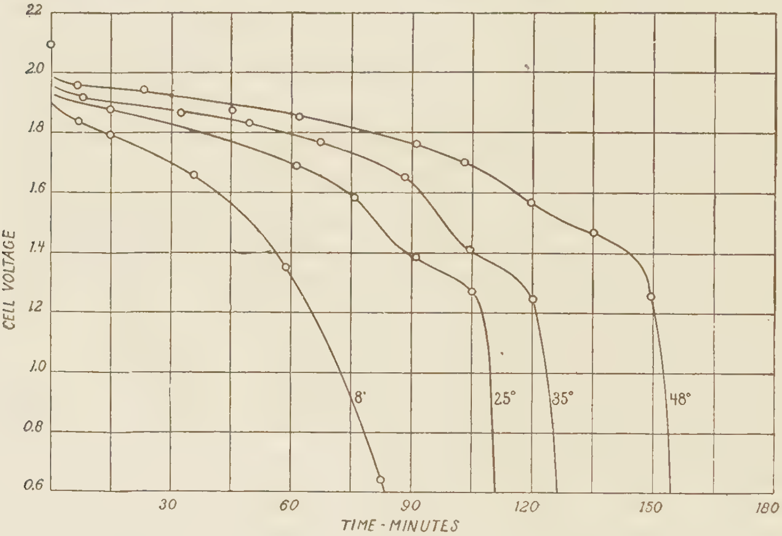

Figure 6. Voltage curves of Planté cell during discharge at various temperatures.

It is by no means easy to be sure that the cell has reached the steady state corresponding to any given temperature, except by maintaining it at the new temperature for several hours. The lag of resistance behind its final value when temperature is quickly changed is very noticeable and caused us much trouble. We finally found it best to keep the cell for at least six hours at the new temperature before trying to take a discharge curve.

It will be noticed that the curve for 25° C. does not fit in very well with the rest of the set. Most of our measurements at this temperature were made at the beginning of the work, and it is quite possible that some lag error has caused this slight variation. The values for resistances at 8.5° were still harder to fix, but the curve given is the average of so many measurements that its correctness is fairly certain. At the higher temperatures the lag becomes much less troublesome. The explanation which suggests itself is that this slow change corresponds to a chemical reaction. Probably lead sulphate is dissolved as the temperature is raised and precipitated as it is lowered. This would be just such a process as would result in the slow adjustment of the cell resistance to a new temperature.

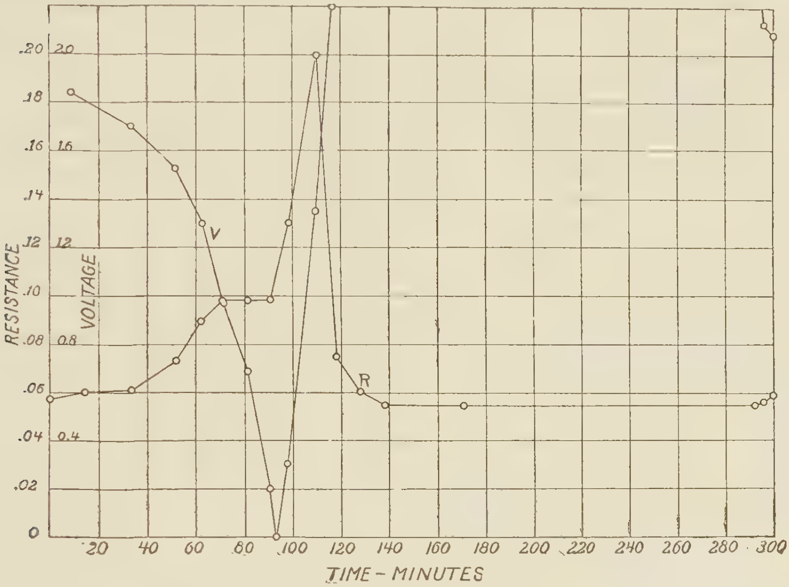

FIGURE 7. Resistance and voltage curves for a Planté cell during complete discharge and reversal.

This explanation is made more probable by some experiments we have made in an ordinary conductivity vessel with platinum electrodes, filled with sulphuric acid from our cell. Some pieces of lead and lead peroxide from a partially discharged cell were placed in the vessel and the conductivity followed after a change in temperature. The lag of resistance behind temperature is just as noticeable in this arrangement as in the more complicated cell under investigation, and there seems to be no doubt that the explanation given is the correct one. A similar lag in the e. m. f. following a change in temperature is to be expected, and this has been noticed by Dolazalek during careful determination of the temperature coefficient of the e. m. f. of a lead storage cell.

The curves of cell voltage during discharge are given in Figure 6, and the flat place in the curve is evident in all except the curve for 8.5°. It is possible that we missed it in this case by not taking points close enough together, as it is quite evident in the curve of Figure 7, which was drawn from another run at the same temperature.

TABLE VI.

Complete Reversal at 2 Amperes. Temperature 8.5° C.

Time.	Cell.	Voltage.	Time.	Cell.	Voltage.
Open circuit	.0577	. . .	110	.2000	−1.36
8	.0585	1.83	118	.0751	−2.30
14	.0600	1.78	128	.0604	−2.33
33	.0610	1.70	138	.0554	−2.35
51	.0739	1.53	147	.0571	−2.37
62	.0904	1.30	171	.0545	−2.44
71	.0980	0.97	293	.0541	−2.56
81	.0980	0.69	Opened	circuit	
91	.0986	0.20	296	.0564	−2.13
93	. . .	0.00	300	.0586	−2.08
98	.1302	−0.31 Reversed			

9. Two criteria have long been considered most pertinent as describing the condition of a storage cell. One of these is the density of the electrolyte, and if care has been taken to keep this density right, it is possible to judge accurately of the condition of the cell by an examination of the electrolyte at a given point in the cell cycle. Usually the density is measured at full charge. It could as well be measured at the end of discharge or at any other known point in the cycle, provided the curves describing the relation between density and voltage

for a given current and at constant temperature were accurately known.

The other criterion of the condition of the cell now in use is the plate potential. In order that this may give useful information it is necessary to have a discharge curve, on which are plotted the cell voltages at various times of discharge at constant current and constant temperature. Once in possession of such a curve, measurement of cell voltage, at a known time after discharge at constant rate has begun, gives accurate information as to the condition of the cell.

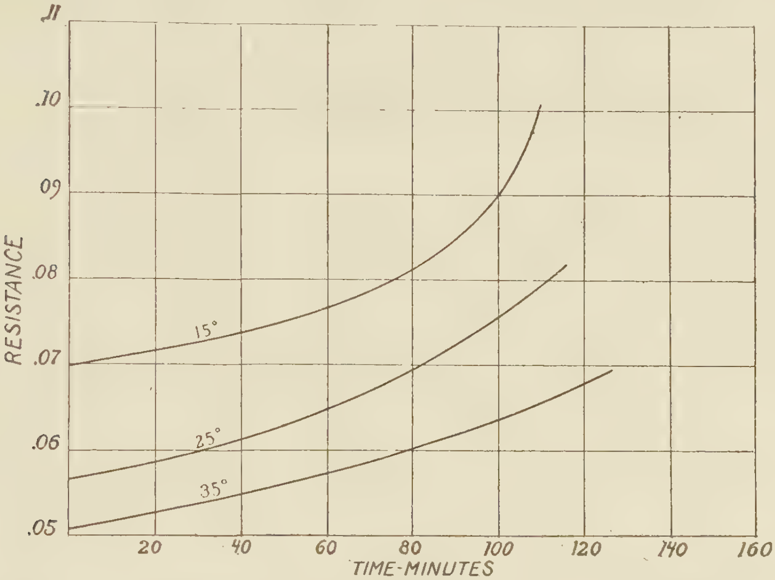

Figure 8. Curves showing resistance of paste plate cell during discharge at various temperatures.

It is evident that a measurement of the cell resistance serves equally well to determine the condition of the cell, for the resistance-time curves of Figure 5 are equally as characteristic as the voltage-time curves of Figure 6. The greater difficulty of measurement of cell resistance will probably prevent any practical application of this fact.

Reversal of a Planté Cell.

10. It was considered a matter of interest to follow a cell at one temperature through complete discharge and then on to more or less complete reversal. If the explanation given on page 591 is correct, it

was to be expected that the resistance would decrease very rapidly after passing through a maximum near the end of complete discharge of the cell, and that the e. m. f. would also reverse rapidly and soon attain nearly its maximum with sign opposite the normal direction in the cell. Table VI. and Figure 7 show how well this is realized:

The data of the above table is plotted in the curves of Figure 7, and they indicate qualitatively but clearly the course of the changes in the cell. It should be mentioned that the sharp point at the maximum of resistance (about .20 ohm) is only a rough approximation, as it was quite impossible to follow the change in this portion of the curve rapidly enough to insure accuracy. It is, however, quite certain that the point given is lower than the true maximum value.

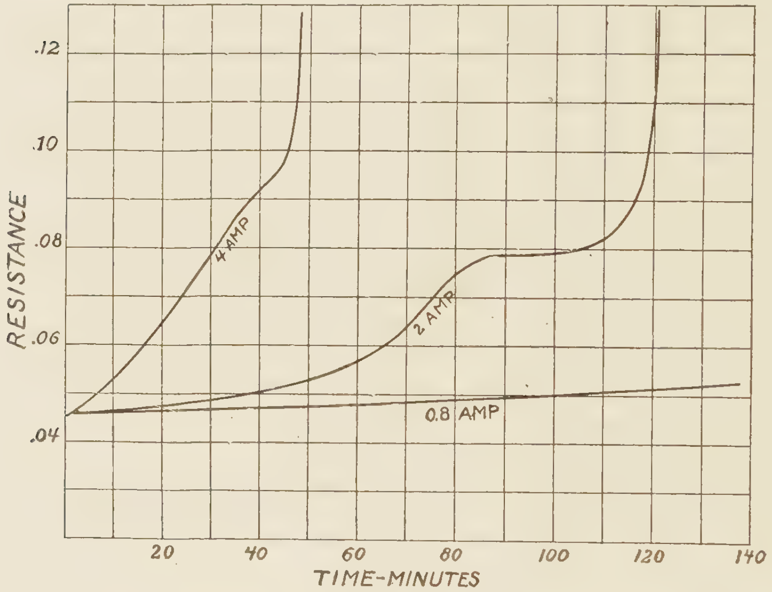

FIGURE 9. Resistance of Planté plate cell at various discharge rates.

PASTED PLATES.

11. New pasted plates were thoroughly charged and put through several cycles until their capacity was approximately constant. They were then set up in a cell with separation of the plates as nearly as possible that of the Planté cells. The curves given in Figure 8 show the course of the resistance during discharge at 2 amperes at various

temperatures. The points of special interest to be noted are the higher resistance of the cell and the smoothness of the curves. These pasted plates were made to have as nearly as possible the same capacity as the Planté cell at the 2-ampere discharge rate.

12. The course of the resistance of our Planté cell at constant temperature, but at various rates of discharge, is clearly shown by the curves of Figure 9. It should be noted that these curves could be used as criteria of cell condition quite as well as voltage curves — and that the cell capacities corresponding to the different rates are clearly given by a statement of the cell resistance, corresponding to the rate in question, at which discharge must be stopped.

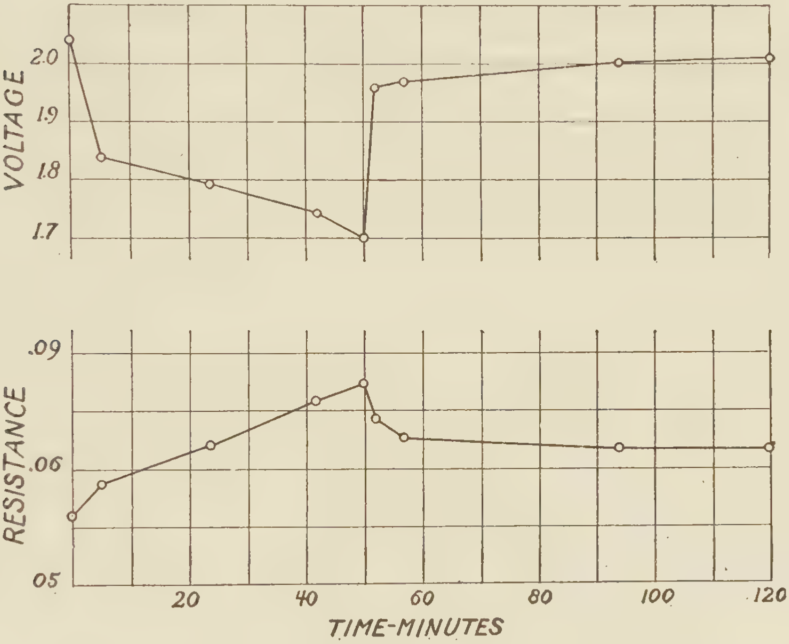

Figure 10. Voltage and resistance during partial discharge followed by recovery.

Recovery.

13. Curves showing resistance and voltage during partial discharge and subsequent recovery on open circuit are given in Figure 10. These curves are characteristic of the general shape of all recovery curves.

Overcharge.

14. The resistance during overcharge seems to be a most variable factor. It rises and falls a thousandth of an ohm or so in one cell but has no regular course.

The disturbing factor must be the escaping gases as there is no other action going on in the cell.

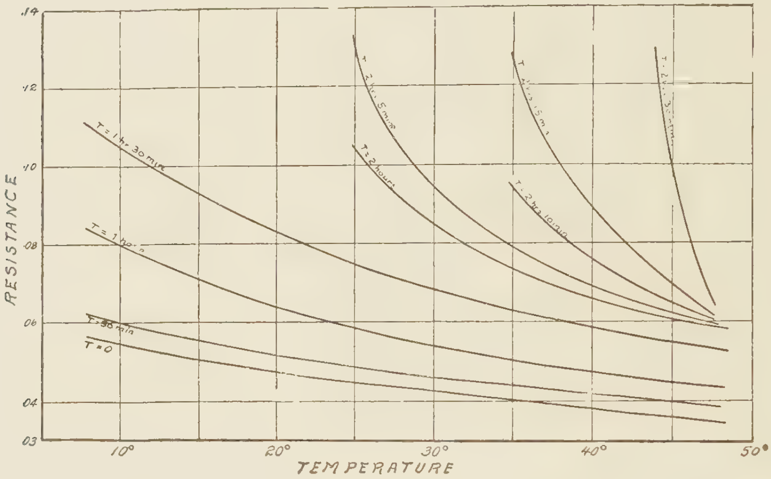

Figure 11. Temperature effect on resistance after various periods of discharge.

Sulphated Plate.

15. Measurements were made over a period of a month or more on a nearly discharged plate. It showed no characteristic course whatever but varied from day to day over a range of several thousandths of an ohm, rising slightly during the first three weeks and then falling again. We evidently did not arrive at a sulphated condition in the usual understanding of the word.

The Temperature-effect on Resistance.

16. The curves of Figure 5 show the course of change of resistance during discharge at constant rate and constant temperature. They are isothermals. From these it is possible to construct *isochronal* curves of resistance *vs.* temperature, the isochronal curve corresponding to the fact that the same total amount of active material has been effected in each case, but at a different temperature. These curves are of special

interest because they show how *dynamic* a thing the momentary equilibrium in such a cell must be. A set of these derived curves is given in Figure 11. The points on the curve T = 0 are for open circuit and they give the temperature-resistance curve of Figure 4. The points on the curve T = 30 are resistances taken from the isothermal curves as they are cut by a vertical line at 30 minutes of discharge, and so on for the other curves.

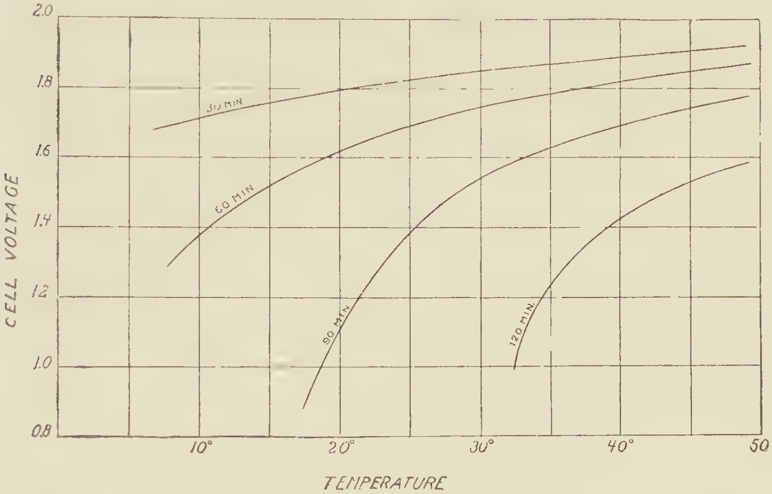

FIGURE 12. Temperature effect on voltage after various periods of discharge.

The slope of the line T = 0 gives the temperature-coefficient of resistance at the temperature corresponding to the point where the slope is determined. The slope at any point on one of the other curves is the temperature coefficient corresponding to the temperature where the slope is taken, but for all the curves except T = 0 the condition of the cell is one of dynamic momentary equilibrium. The slopes are nevertheless temperature coefficients corresponding to this particular state in the cell and they are of great interest in disclosing the condition of the cell. In fact it would be hard to find a more striking expression of the complex system under observation than that given by these curves.

The change in temperature-effect is enormous. At T = 0 the coefficient is about 1.5% per degree C. At T = 150 minutes the coefficient has reached 23% per degree C

The Temperature Effect on Cell Voltage.

17. It must also be true that the isochronal lines of temperature and cell voltage will show a somewhat similar course. For while the resistance is a more complicated function of cell condition than the e. m. f. both factors must be largely determined by diffusion if final analysis were possible. Sections have been made of the isothermal voltage curves of Figure 6 at various times during discharge, and these are plotted in the curves of Figure 12. No attempt has been made to determine the e.m.f. of the fully charged cell at various temperatures.

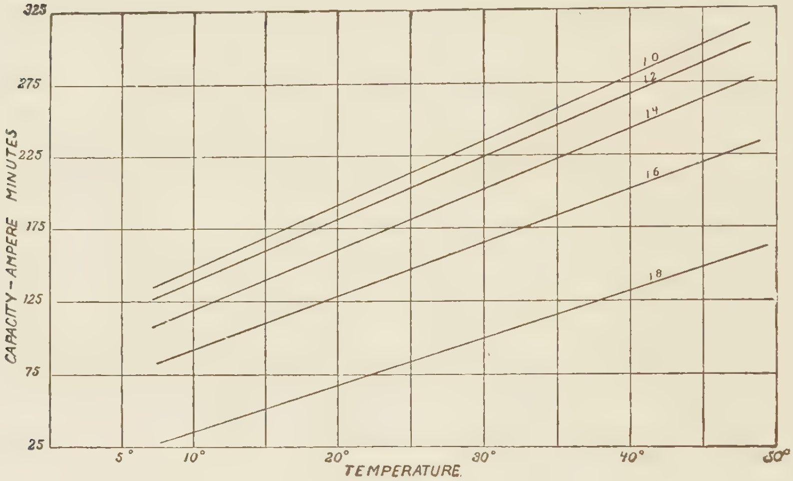

Figure 13. Temperature effect on capacity. Planté plates. One hour rate of discharge.

At 35° C. the coefficient of a cell which has been under discharge for 30 minutes is about 0.006 volts per degree, while that of a cell which has been running at the same rate for two hours is 0.62 volts per degree. [The open circuit temperature coefficient for this acid concentration is about .0003 volts per degree (Dolazalek).]

It should be kept in mind in considering this and the results indicated by the curves of Figure 11, that the cell contains throughout the course of each of the curves, exactly the same amount of each of its constituents. The same quantity of electricity has passed through it, and equal amounts of lead, lead peroxide and lead sulphate are present. The total amount of acid in the whole bulk of the electrolyte is also the same in each case. The only difference is in the distribution of the materials in the cell.

Temperature Coefficient of Capacity.

18. From the data of these measurements it is also possible to calculate the temperature coefficient of the capacity of this type of plate. The values so obtained are plotted in the curves of Figure 13. It will be seen that they are nearly straight lines, and that they remain straight for various end voltages. In practice such plates would hardly ever be discharged below 1.6 volts at this rate, and the temperature coefficient of capacity, for plates discharged to this point, is about 3.5 percent per degree. This coefficient is only applicable to plates of this particular type, and to this discharge rate. For other plate types and various rates the temperature coefficient of capacity has been found to vary from 1.5 to 3.5 percent per degree.

Literature.

1. Hallwachs, Wied. Ann., **22**, 95, 1884.
   Open circuit. Modified Kohlrausch bridge.
2. Preece, Proc. Roy. Soc., **38**, 352, 1885.
   Polarization not excluded.
3. Häberlein, Wied. Ann., **31**, 402, 1887.
   Open circuit only.
4. Boccali, Elektrotech. Ztsch., 1891, p. 51.
   Modified Kohlrausch bridge.
5. Uppenborn, Elektrotech. Ztsch., 1891, p. 157.
6. Froelich, Elektrotech. Ztsch., 1891, p. 370.
7. Streintz, Wied. Ann., **49**, 564, 1893.
   Closed circuit, but polarization not eliminated.
8. Wythe Smith, Physical Soc. London, June 24th, 1892.
9. Nernst, Ztsch. f. Phys. Chem., **14**, 623, 1894.
10. Carhart, Phys. Rev., **2**, 28, 1895.
    Measurements on Daniell cell.
11. Grey, Elektrotech. Ztsch., Aug. 1, 1895.
12. Nernst and Haagn, Ztsch. f. Elektrochem., **2**, 493, 1896.
    Balanced both capacity and resistance.
13. Haagn, Ztsch. f. Elektrochem., **3**, 421, 1897.
14. Haagn, Ztsch. f. Phys. Chem., **23**, 97, 1897.
15. Sieg and Schoop, Elektrotech. Ztsch., 1900, p. 226.

16. Atkins, Phys. Rev., **13**, 102, 1901.
Same method as Carhart (10, above).

17. Bruger, Centrallblatt f. Akk. u. Elemt. etc., **2**, 197, 1901.

18. Dolazalek and Gahl, Ztsch. f. Elektrochem., **7**, 31, 1901.
Most accurate and satisfactory method.

19. Weber and Raberjot, Eclair. Electr., **31**, 201, 1902.

20. Ayres, Phys. Rev. **14**, 17, 1902.
Theory of bridge used by authors.

21. Oates, Electrician, **50**, 1058, 1903.
Modified Kohlrausch method.

Proceedings of the American Academy of Arts and Sciences.

Vol. XLVI. No. 22. — April, 1911.

NOTES ON THE ELECTRICAL CONDUCTIVITY OF ARGENTIC SULPHIDE.

By Hammond Vinton Hayes.

NOTES ON THE ELECTRICAL CONDUCTIVITY OF ARGENTIC SULPHIDE.

By Hammond Vinton Hayes.

Presented February 8, 1911. Received January 18, 1911.

The peculiar action of the sulphide of silver as a conductor of electricity was described by Faraday[1] in 1833. Later Hittorf,[2] in 1851, repeated Faraday's experiments and confirmed the results of the earlier work. In 1902 Streintz,[3] in a study of the conductivity of compressed powders, investigated the behavior of compressed silver sulphide in an electrical circuit and found all of the phenomena described by Faraday and Hittorf. All of these observers attribute to silver sulphide a negative coefficient of resistance for heat, Faraday speaking of it as "an extraordinary case . . . which is in direct contrast with the influence of heat upon metallic bodies."

I have recently conducted a long series of experiments upon the electrical resistance of compressed silver sulphide and, as a result of my observations, am led to the belief that many, if not all, of the phenomena described by earlier experimenters may be explained as due primarily to the condition of the contacts between the specimen of silver sulphide and the electrodes used to connect it into the electrical circuit.

In order to study the behavior of this material I have found it convenient to consider the specimen and its electrodes during three distinct stages or phases of their condition. These will be briefly described.

1st Condition. When the specimen is first placed in circuit it has an extremely high resistance. Upon heating the specimen its conductivity increases with extreme rapidity and, when the source of heat is removed, the conductivity frequently falls to nearly that which originally existed. As an illustration of this action the figures given by Streintz of test upon a sample may be quoted. "At a temperature of 100° the specimen showed a resistance from 3,000 to 1,000 ohms; at 150°, from 400 to 150 ohms; at 220° the resistance measured only from .1 to .2

---

[1] Faraday's Experimental Researches in Electricity, Vol. 1, 432 et seq.

[2] Hittorf, Pogg. Ann., Vol. 84, 1851.

[3] Streintz, Ann. der Physik., Vol. 3, 1900, and Vol. 8, 1902.

of an ohm; and from 230° upward, it appeared to have practically the same resistance." As also noted by Faraday the application of external heat is not necessary, as by the use of a source of current of sufficient voltage the requisite current can be obtained to heat the specimen sufficiently and "break down" its initial resistance.

2nd Condition. After the initial high resistance has been broken down and a current of some strength has passed, I have found no case where the specimen attained its original high resistance. Usually, after cooling, the resistance is but a fraction of that which originally existed but is practically always several times greater than that which exists when the specimen has become heated by a flow of current through it. This stage, where the specimen shows a gradual lowering of apparent resistance with increasing current or an increase in apparent resistance with a diminishing current, but never returns to the abnormally high initial resistance, is termed the second condition of the test.

3rd Condition. After the current has passed through the specimen for some time, — or usually more rapidly if the direction of the current has been reversed,— the characteristics of the sulphide of silver specimen in its second condition are no longer found, and the resistance of the specimen changes little with changes in current strength or with heat. This peculiarity of what is here termed the "third condition" was described by Faraday, who also noted that the properties of the specimen described under the second condition "could not be renewed until a fresh surface of the sulphuret had been applied to the positive pole. This was in consequence of peculiar results of decomposition."

Streintz's tests were made upon small cylinders of compressed silver sulphide approximately two centimeters in length and fifteen hundredths of a square centimeter in cross-section. Electrodes of platinum foil were placed at the two ends of the cylinder and two supplementary electrodes were embedded within the specimen. In my experiments plates of compressed sulphide were used, which were rectangular in shape and roughly three-quarters of an inch in length by five-sixteenths of an inch in width; the average thickness of the plates was about one thirty-second of an inch. Electrodes of platinum, silver and copper were used both in the form of fine wires or of foil. The terminals were pressed into the plates of silver sulphide and the tests conducted both while the specimen and its terminals were in the press and after they had been removed. Many of the specimens studied by me had been prepared by subjecting them to a pressure of 500,000 pounds to the square inch. The pressure used in forcing the terminals into the specimen was approximately 25,000 pounds.

The electrical measurements were made by the use of a Weston milliammeter and voltmeter, included in circuit with the specimen, and a battery having an electro-motive force of 20 volts. The voltmeter was connected about the terminals of the specimen and the current was controlled by the use of resistance coils placed in the direct circuit with specimen, ammeter and battery. A telephone was also so arranged that it could be connected with the terminals of the specimen under test.

An extremely large number of measurements was made on many specimens under varying conditions. The characteristics of this material, as described above, were found throughout the tests and agree with those found and recorded by former experimenters. The use of the telephone in my experiments, however, has, I believe, thrown some new light upon the action which is taking place within the specimen of sulphide of silver during the passage of the electrical current through it.

Consideration of Condition I. I have frequently found that specimens had an initial resistance so high that with 20 volts no measurements of current could be made with the instruments at hand. When connected with a 110-volt lighting circuit there was an immediate fall in resistance and thereafter the 20-volt source sufficed for current measurements. Placing a heated soldering iron in the vicinity of the specimen would frequently be equally effective in lowering the initial resistance of a specimen.

The following table gives characteristic current and voltage readings of specimens when in the first condition.

TABLE I.

Voltage at Terminals.	Current Amperes.	Apparent Resistance.
18.	.06	300. ohms.
17.	.28	61. ohms.
18.	.34	53. ohms.
16.	.38	42. ohms.
4.5	.85	5.3 ohms.

This action appeared to be equally conspicuous with platinum, steel, silver or copper electrodes. During the time that the resistance of this specimen was high, violent "sputtering" or "burning" noises were audible in the telephone, and these noises entirely ceased at the time of making the last measurement recorded above. The noises heard in the telephone were characteristic of those frequently present when a current is passing through an imperfect contact. The subsidence of these noises was indicative of the formation of more perfect contacts.

The existence of these burning noises shows the presence of an imperfect connection between the specimen and one or both of its electrodes and that arcing is taking place at one or both of these places. An examination of all specimens tested has shown that violent action of some kind has taken place at the point of connection between the sulphide pellet and the electrode connected with the positive pole of the battery ; the surface of the specimen has been blackened and some of the fine wires of the electrode have been burned away. On the other hand, the negative ends of the specimens and the electrodes by means of which they have been connected with the negative pole of the battery have been invariably bright and clean.

The probable explanation of the physical action which takes place during the first condition is that despite the close mechanical association of the electrodes and the specimen there is no electrical connection, and an arc must take place between one or both electrodes and the specimen before a current can pass. To produce such an arc requires ionization either by heat or by a sufficient difference of potential at the point or points of discontinuity. It appears from all tests that this action takes place most readily at the negative electrode of the specimen, and that gradually a more or less perfect connection is established at this point. When this action takes place the excessive apparent resistance of the specimen is broken down, and the specimen may be considered as passing from the first into the second condition. In support of this explanation of this phenomenon, the following tests may be described.

The direction of the current through a specimen, the resistance of which had been broken down, was reversed. The noises in the telephone which previously had been present were no longer apparent, and after a short time the changes in resistance characteristic of the second condition ceased to exist and the specimen passed into the third condition. Again, a specimen which was in the third condition had one of its electrodes removed and, after the surface of the specimen had been carefully cleaned where the electrode had previously been, it was clamped under great pressure in the jaws of a steel vise with soft copper surfaces. The figures obtained in this test are given below.

From these figures it will be seen that a perfect connection had been established between the original terminal and the sulphide, but that a good connection had not been made at the terminal which had been clamped in the vise. During the test, while the current was passing from the vise to the sulphide, the noise in the telephone was very great, but when the current was passing through the imperfect connection in the opposite direction no noises could be detected. After the

TABLE II.

Current from Vise to Ag_2S.			Current from Ag_2S to Vise.		
Voltage at Terminals.	Current Amperes.	Apparent Resistance.	Voltage at Terminals.	Current Amperes.	Apparent Resistance.
1.10	.210	5.2	.5	.210	2.4
2. to 3.	.350	..	.48	.390	1.2
1. to 3.	.520	..	.5	.540	.9
2.	.650	3.			
2.5 to	.850 to	..			
3.5	.900	..			

current had passed for a short time a good connection was established at the terminal in the vise and the third condition of the action was established.

What actually takes place at the negative electrode I have not determined. Both Faraday and Hittorf were inclined to the belief that conduction through the sulphide of silver is electrolytic, and Hittorf states that silver was found by him at the junction with the negative electrode. Hittorf also found that, in similar tests made with the oxide of copper, antennae of copper were thrown out from the specimen at the negative pole.

Consideration of Condition II. The second condition exists when a more or less perfect connection has been established at the negative electrode and the contact at the positive terminal is still faulty. All tests of specimens in this condition show the characteristics of measurements of currents and potentials at imperfect contacts in an electrical circuit. The really remarkable peculiarity of the silver sulphide is that contact cannot be established even when the electrodes and the specimen are pressed together under a weight of many tons.

Attention might be called to the fact that there is present a condition of "unilateral" conduction such as has been extensively studied by Professor Pierce,[4] the magnitude of the action being dependent upon the degree to which perfect contact has been obtained at the negative terminal of the specimen. This differential action is shown in Table II., and Table III. given below as a fairly characteristic set of measurements made upon specimens in the second condition. It should be noted that the repeated reversals of current gradually establish perfect connections at the two terminals of the specimen, and thus rapidly obliterate the unilateral conduction and tend to establish the third condition.

---

[4] Pierce, Physical Review, **25** (1907); **28** (1909).

TABLE III.

			Current Reversed.		
Voltage at Terminals.	Current Amperes.	Apparent Resistance.	Voltage at Terminals.	Current Amperes.	Apparent Resistance.
.42	.072	5.8	.27	.072	3.7
.54	.110	4.9	.36	.110	3.2
.82	.200	4.1	.54	.202	2.6
1.08	.310	3.5	.72	.310	2.3
1.04	.350	3.0	.70	.350	2.0
1.04	.405	2.5	.80	.410	1.9
1.16	.480	2.4	.90	.500	1.8
1.38	.640	2.1	1.04	.640	1.6
1.60	.850	1.8	1.30	.830	1.5
1.90	1.350	1.4	1.60	1.300	1.2

It is this second condition which has been specially studied by previous experimenters, and it has been due to the measurements made while the contacts between the electrodes and the specimen were in the condition above described that the negative coefficient of resistance for heat has been attributed to silver sulphide. Increasing temperature of the specimen or increasing difference of potential at its terminals simply promotes the ionization at the imperfect contact or contacts and permits a greater flow of current.

Consideration of Condition III. The condition which I have called the third is that in which fairly good connections have been established between both electrodes and the specimen, and is characterized by an absence of noise in the telephone, with the current passing through the specimen in either direction. The figures given in Table IV. are those obtained from continued tests of the sample, the apparent resistances of which are given in Table III. after it had passed into the third condition.

TABLE IV.

Voltage at Terminals.	Current Amperes.	Apparent Resistance.	Voltage at Terminals.	Current Amperes.	Apparent Resistance.
.08	.072	1.11	.08	.072	1.11
.122	.110	1.11	.122	.110	1.11
.36	.31	1.16	.35	.305	1.15
.58	.500	1.16	.58	.500	1.16
.74	.63	1.17	.74	.63	1.17
1.00	.85	1.17	1.00	.85	1.17

The characteristics of the second condition, it will be seen, have entirely disappeared, and the resistance with increasing current or temperature instead of falling appears to have increased. As stated by Faraday, the removal of the positive electrode from the specimen, and the scraping of the surface so as to present a new layer of the sulphide restores in every case the specimen to the properties previously possessed by it under the second condition.

The conclusions which may be drawn from the above are :

(a) That electrical connection cannot be made between compressed silver sulphide and electrodes of platinum, steel, silver or copper simply by pressure.

(b) That conduction through compressed silver sulphide cannot be obtained until sufficient ionization has occurred at the contacts to allow the passage of an arc.

(c) That connection, when a current has passed, is most readily and completely obtained at the negative terminal of the specimen.

(d) That it is probable that, when perfect connections have been established between the sulphide of silver and its electrodes, the sulphide has a positive rather than a negative coefficient of resistance for increasing temperatures.

Boston, January 25, 1910.

Proceedings of the American Academy of Arts and Sciences.

Vol. XLVI. No. 23. — April, 1911.

CONTRIBUTIONS FROM THE JEFFERSON PHYSICAL LABORATORY, HARVARD UNIVERSITY.

ON THE ELECTROMAGNETIC AND THE THERMOMAGNETIC TRANSVERSE AND LONGITUDINAL EFFECTS IN SOFT IRON.

By Edwin H. Hall and L. L. Campbell.

Investigations on Light and Heat published with Aid from the Rumford Fund.

CONTRIBUTIONS FROM THE JEFFERSON PHYSICAL LABORATORY, HARVARD UNIVERSITY.

ON THE ELECTROMAGNETIC AND THE THERMOMAGNETIC TRANSVERSE AND LONGITUDINAL EFFECTS IN SOFT IRON.

By Edwin H. Hall and L. L. Campbell.

Presented February 8, 1911. Received February 8, 1911.

For many years past the electrical and thermal properties of a certain kind of wrought iron have been, from time to time, under investigation in this laboratory, and a number of papers[1] giving the methods and results of this study have already been published. The present paper has to do with the so-called Hall effect and the allied effects in the same kind of iron. These are so numerous and so unfamiliar to ordinary observation that it seems well to give an enumeration and brief description of them, somewhat like that given by H. Zahn[2] in his comprehensive paper on such phenomena.

In each of Figures 1–4 the rectangle, with very short side projections, or arms, represents pretty accurately, halfscale, the broadside of one of our "plates" of iron, which were each about 5 cm. long between heavy terminal blocks of copper (see Figure 7), and about 2 cm. wide. The circle indicates the size of the flat face of each pole of the electromagnet, the arrow showing the direction of the magnetizing current.

Description of the Transverse Effects.

Hall Effect. — Figure 1, in which EE is the longitudinal electrical current, and $E'E'$ is the transverse electrical current due to the action of the magnet, shows the Hall effect, positive, according to the ordinary convention as to the sign, in this case, the equipotential line which would naturally extend straight across between the arms being rotated by the magnetic action through a small angle in the direction of flow of the Amperian magnetizing current.

---

[1] These Proceedings, **41**, May, 1905; **42**, March, 1907.

[2] Über galvanometrische und thermomagnetische Effekte, Jahr. d. Rad. u. Elek., **5**, 166–218 (1908).

The letter commonly used for the Hall effect coefficient is R; we shall use also ${}_eT_e$ in the same sense, T indicating *transverse*, the initial e indicating that the *longitudinal* flow is *electrical*, the final e indicating that the *transverse* flow is *electrical*. If we let

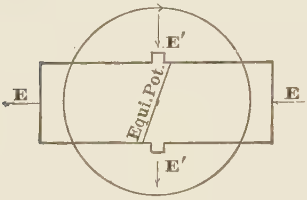

FIGURE 1.

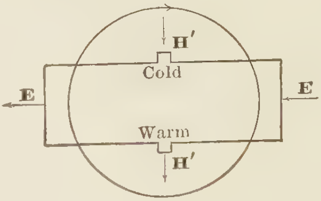

FIGURE 2.

$C =$ the longitudinal current, in absolute units,
$H =$ " intensity of the field " " "
$\Delta P' =$ " diff. of pot. set up between the arms,
$w =$ " width of the plate in cm.,
$t =$ " thickness of the plate in cm.,

we have by definition

$$ {}_eT_e \text{ (or } R) = \frac{\Delta P'}{w} \div \frac{C}{wt} H = \frac{t \Delta P'}{CH}. \qquad (1) $$

Ettingshausen Effect. — In Figure 2, with the longitudinal electrical current EE and the magnetic field just as in Figure 1, we take note of a transverse difference of temperature, $\Delta\theta'$, established by magnetic action. This is the Ettingshausen effect. $\Delta\theta'$, as here represented, is in such a direction that a transverse current of heat would flow in the same direction as the transverse electrical current of Figure 1. In this case the Ettingshausen effect, like the Hall effect of Figure 1, is said to be positive.

Zahn uses P for the Ettingshausen coefficient. We shall use also, in the same sense, ${}_eT_h$, the T, as before, standing for *transverse*, the e for *electrical*, longitudinal, the h for *thermal*, transverse. We have by definition

$$ {}_eT_h \text{ (or } P) = \frac{\Delta\theta'}{w} \div \frac{C}{wt} H = \frac{t \Delta\theta'}{CH} \qquad (2) $$

Nernst Effect. — In Figure 3, with the magnetic field as in Figures 1–2, we have a longitudinal heat-current, HH, and we take note of a transverse difference of potential, $\Delta P'$, established by magnetic action. This is the Nernst effect. This $\Delta P'$, as here represented, is in the same direction as the $\Delta P'$ of Figure 1, in which the longitudinal current was electrical. In this case, we shall call the Nernst effect positive; Zahn would call it negative. Zahn uses Q for the Nernst coefficient with his convention as to the sign. We shall use ${}_hT_e$ as equivalent to his $-Q$, the prefix h indicating a *thermal* longitudinal flow, the T_e indicating a transverse electrical action. We have by definition

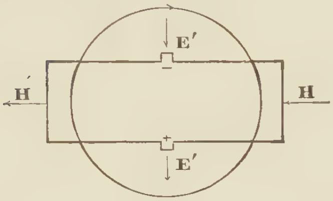

FIGURE 3.

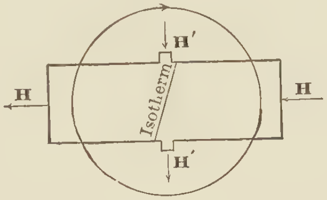

FIGURE 4.

$${}_hT_e \text{ (or } -Q) = \frac{\Delta P'}{w} \div \frac{d\theta}{dl} H, \tag{3}$$

where $\dfrac{d\theta}{dl}$ = the temperature-gradient along the plate.

Leduc Effect. — In Figure 4, with the magnetic field and the longitudinal heat-current as in Figure 3, we take note of the transverse difference of temperature, $\Delta\theta'$, established by magnetic action. This is the Leduc effect. This $\Delta\theta'$, as here represented, is in the same direction as the $\Delta\theta'$ of Figure 2, in which the longitudinal current was electrical. In this case, the Leduc effect is called positive. Zahn uses S for the Leduc coefficient. We shall use also, in the same sense, ${}_hT_h$. We have by definition

$${}_hT_h \text{ (or } S) = \frac{\Delta\theta'}{w} \div \frac{d\theta}{dl} H, \tag{4}$$

The longitudinal effects are defined later, in connection with an account of our work on them.

DESCRIPTION OF APPARATUS.

Each of the iron plates mentioned above was brazed at each end into a thick copper block, as in Figures 7 and 8. After being so fixed each plate was measured in thickness at nine points, the distribution of which is well shown by Figure 5, the distance between (1) and (2), (2) and (3), (4) and (5), etc., being appoximately 1.5 cm.

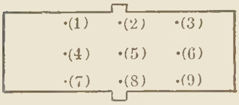

FIGURE 5.

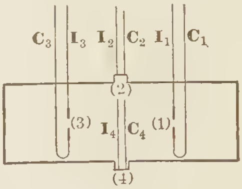

FIGURE 6.

Plate 1.— The measurements of Plate 1 were

Length between coppers . . . . 5.1 cm.,
Width " " . . . . . 1.98 cm.,
Arms about 0.12 cm. long and about 0.10 cm. wide,

	cm.	Pt.	cm.	Pt.	cm.	Pt.
Thickness	0.1490	at 1	0.1460	at 2	0.1505	at 3
	0.1490	" 4	0.1480	" 5	0.1495	" 6
	0.1475	" 7	0.1450	" 8	0.1500	" 9
Means	0.1485		0.1463		0.1500	

As the part of the plate which is particularly important in the transverse effects, the effects that interest us most, is the narrow transverse strip including the arms, the thickness of this part is to be especially considered. This, according to our measurements, is about 0.1463 cm.; but as the method of measurement, by means of vernier calipers with faces of considerable width, must tend to give a maximum value, we take off about 1 per cent from the quantity just given and call the mean thickness of the median transverse strip 0.145 cm.

To Plate 1, eight wires were attached (Figure 6) by means of copper electrolytically deposited. Four of these, C_1, C_2, C_3, C_4, were of copper about 0.017 cm. in diameter, the others, I_1, I_2, I_3, I_4, were of annealed iron wire about 0.020 cm. in diameter. This iron wire was drawn from a portion of the same bar that furnished the plates 1 and 2. These fine iron wires were joined to somewhat heavier iron wires of the same source 15 cm. or more above the iron plate, and the heavier wires, perhaps a meter long, were soldered to copper wires, the junctions being kept in a water bath. The distance between junctions (1) and (3) could not be very accurately determined. It was measured and taken as 2.78 cm. The wires C_1 and C_3 ran down from the points of attachment, passed under the lower edge of the plate, and came up across it on the other face. The distance between C_2 and I_2 and between C_4 and I_4 was perhaps 0.05 cm., each wire being attached to the outer end of the arm. On the face shown in Figure 6, a flat sheet of asbestos about 0.15 cm. thick, arranged so as not to disturb the wires, was cemented by means of asphaltum or melted shellac (the latter was used with Plate 2), the whole being subjected to a temperature high enough to soften the cement and allowed to cool with sufficient pressure on the asbestos sheet to fix it flat in place.

The width of Plate 1 is the direction of the fibre, or grain, of the original iron bar.

Plate 2. — The measurements of Plate 2 were

Length between coppers	5.15 cm.,
Width	2.01 " ,

Arms about 0.10 cm. wide and 0.10 cm. long,

	cm.	Pt.	cm.	Pt.	cm.	Pt.
Thickness (Figure 5)	0.134	at 1	0.135	at 2	0.138	at 3
	0.138	" 4	0.142	" 5	0.145	" 6
	0.140	" 7	0.143	" 8	0.146	" 9
Means	0.137		0.140		0.143	

The face of Plate 2 was smoother at the last than the face of Plate 1, and we have taken as the mean thickness of the arm strip of (2) the mean of the measurements as here recorded, 0.140 cm. The thickness is several per cent greater on one edge of the plate than on the other, but it does not appear that any serious harm can come from this inequality.

The iron wires of Plate 1 (see Figure 6) were with Plate 2 replaced by constantan ("advance") wires, K_1, K_2, etc., about 0.020 cm. in diameter, which had been annealed by heating to bright incandescence by means of an electric current. The distance from junction (1) to junction (3) was now made about 2.62 cm., in order to have them a little nearer the centre of the magnetic field than the corresponding junctions of Plate 1 had been. Wires C_1 and C_2 did not here pass under the lower edge of the plate, but followed the course shown in Figure 6, strips of mica fastened by shellac, melted on, being used for insulation. The wires themselves were bedded in shellac in their course across the plate. The plate was finally backed, on the side shown, with a flat sheet of asbestos about 0.15 cm. thick, according to the description already given.

The length of Plate 2 is the direction of the fibre of the original bar.

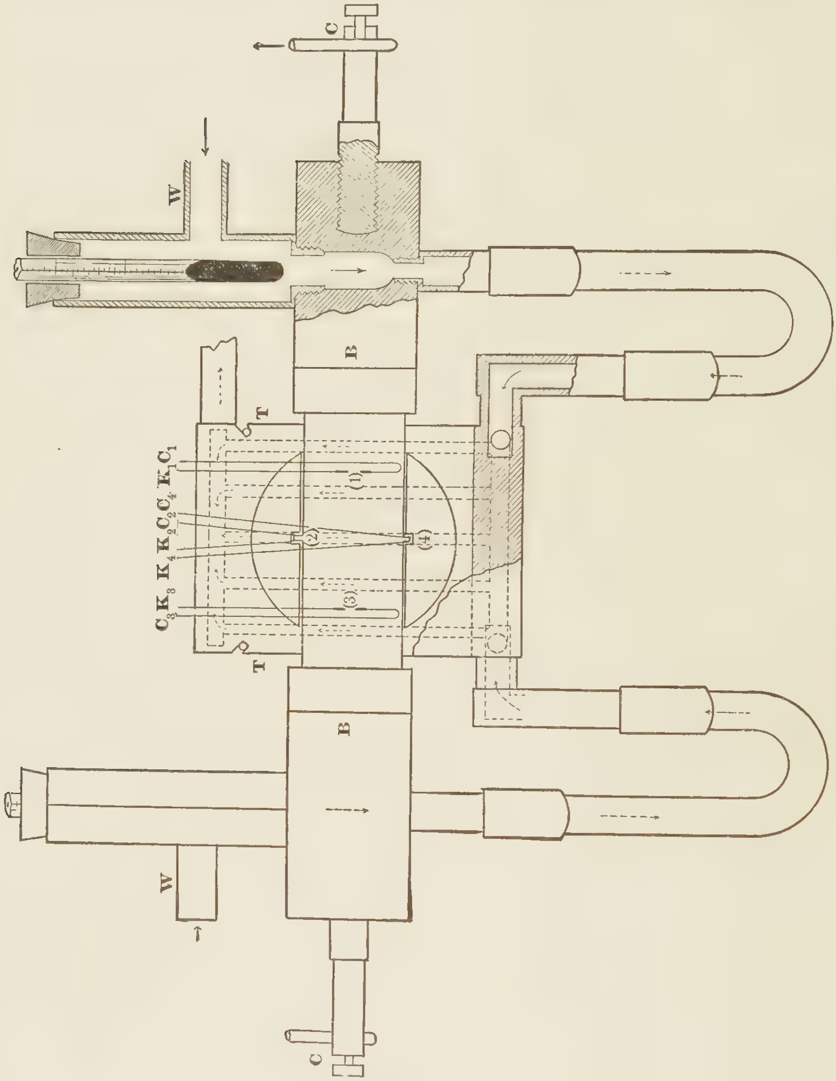

Figure 7.

Mounting the Plates in the Field.

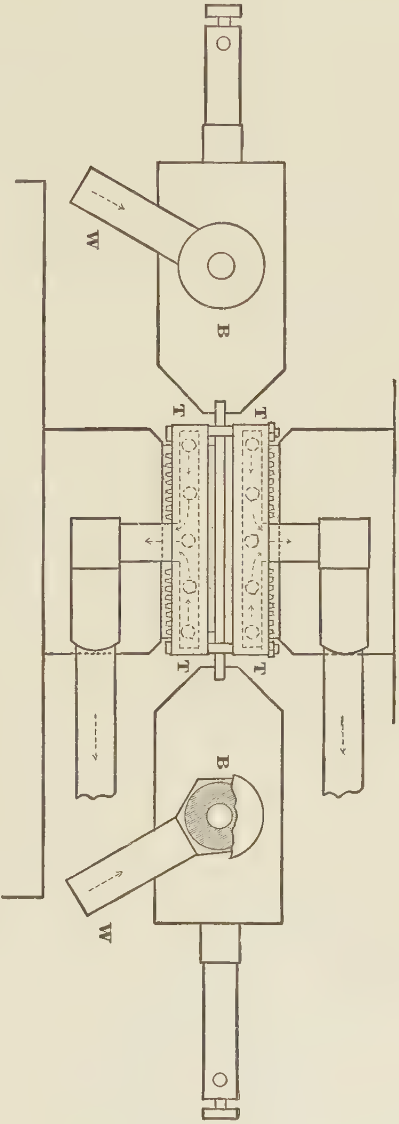

Figure 8.

Figures 7 and 8 show the method of mounting the plates in the magnetic field for the electromagnetic experiments. *T T* is a trough of soft iron consisting of a rectangular one-piece[3] block about 4.5 cm. long, 6.5 cm. tall and 2.0 cm. wide, with a channel 0.5 cm. wide and 5.5 cm. deep cut through it from end to end, leaving an uncut part 1 cm. thick below. Through holes drilled in this uncut portion two streams of water, entering at the ends and meeting at the middle, reach ten vertical passages, five in each wall of the trough. The passages in each wall lead into a horizontal passage at the top, and the two streams of water issuing from the apparatus are reunited into one beyond the range of our figures.

The object of this water circulation is to control the temperature of the trough, and so that of our iron plate, which lies in the channel of the trough, during the electromagnetic observations; for in these it is desirable to have all parts at the same temperature, except as differences may be set up by the magnetic action that we are studying.

---

[3] The trough first used was not from one piece, but was a composite affair soldered together. It leaked more or less, and after much trial the new trough was substituted for it March 26, 1910. Nearly all our observations on the transverse and longitudinal effects made before that date we regard as tentative only and reject from our final results.

The asbestos pad, indicated by a dotted strip in Figure 8, at the back of the plate bears against one face of the channel in the trough. Between the plate and the other face of this channel is a space about 0.2 cm. wide, into which passes the single-turn "test-coil," of 1 cm. radius, by means of which the strength of the magnetic field is measured. The test-coil is in circuit with a ballistic galvanometer and the throw produced when it is suddenly withdrawn from the field is easily and accurately measured. The semicircular pieces above and below the plate are of soft iron of nearly the same thickness as the plate, their object being to insure uniformity of magnetic field over the whole width of the iron under observation. Care is taken to have the plate a little nearer to one face of the channel than to the other, so that it may not be pulled forward on the test-coil side by magnetic action. At each end of the trough near the top is a slot which holds a small brass bar, having a head at one end and a nut at the other and carrying a stud 0.5 cm. long on its middle. This device prevents the walls of the trough from bending toward or from each other during the magnetic action.

During thermomagnetic observations also, with a longitudinal gradient of temperature, the plate was at first kept in the iron trough, without, of course, circulation of the water therein. It appeared, however, after a time, that the nearness of the walls of the trough affected the longitudinal temperature-gradient, and after May 21, 1910, the trough was discarded during thermomagnetic measurements. At this time disks of cork (see Figure 8) about 0.2 cm. thick were cemented to the flat faces of the pole pieces of the magnet, which faces are 4.0 cm. in diameter, and the exposed surface of each disk was cross-cut with a file or saw, in order to reduce the naturally low heat-carrying power of the cork. The asbestos pad at the back of the iron plate was then placed against the cork disk on one pole of the magnet, and the other pole was brought somewhat toward the plate, but not near enough to pull the plate away from the other pole. Most of the thermomagnetic data which we use were obtained after this arrangement had been adopted.

The cork disks remained in use during all the subsequent measurements, even when the iron trough was put back for repetition of electromagnetic observations. Previous to their introduction a facing of asbestos had been used between the pole pieces and the sides of the trough.

The tubes *W* and *W* show where the two streams of water enter the apparatus. The course of these streams is first downward past the thermometer-bulbs, which give the temperature readings called T_n and T_s, through the massive copper blocks *B* and *B*. Then, if electromagnetic experiments are in order, the course followed is that shown by the arrows in Figure 7; but if a temperature-gradient for thermomagnetic work is to be established and maintained, the two streams, one warm and the other cold, pass off at once from *B* and *B* to the sink.

The longitudinal electric current, when one is used, enters by one of the heavy wires *C*, *C*, and passes out by the other.

Plate 1 was studied at intervals from June 5, 1909, to June 29, 1910. All the observations we have to publish on Plate 2 were made during December, 1910.

CALIBRATION OF THE THERMO-ELECTRIC COUPLES.

The "thermo-electric height" between copper and our iron was determined some years ago for various temperatures ranging from 27° to 71°, and from this set of data a curve was plotted which gives the thermo-electric force of a copper-iron couple within these limits. As our iron wires were drawn from a piece of the same iron bar that furnished the iron used in determining these thermo-electric heights, and as they were annealed after drawing, it was assumed that the curve just described would serve for couples made by joining these wires with copper; that is, we assumed the iron wires to be thermo-electrically so like the plate to which we attached them, that we should be justified in ignoring any thermo-electric forces which might arise from differences between the plate and this wire.

But to our surprise and disappointment we found that the thermo-electric force of the couple I_1–*plate*–I_3 was about one tenth-part as that of the couple C_1–*plate*–C_3. This discovery, which was not made at the beginning of our work, taken with the fact that the thermo-electric quality of iron is considerably affected by magnetization, led to the rejection of iron wires and the use of constantan wires in their place, when we came to the preparation of Plate 2.

Experiments to determine whether constantan wire would be appreciably effected in its thermo-electric quality by magnetism were conducted as follows: A piece of annealed constantan wire was fastened by means of shellac, applied melted, within a narrow glass tube across, or through, which ran side-tubes carrying streams of water, one at a temperature near 16° degrees, the other near 76°.

The distance between the streams was about 6 cm., so that the gradient of temperature in the wire between must have been about 10° per cm. The ends of the wire, which was about 130 cm. long, were soldered to copper wires, and the junctions were placed in a suitable water bath, the copper wires leading to the galvanometer. The part of the iron wire lying between the streams of hot and cold water was placed across the space between the magnetic poles in a field the strength of which, for a distance of perhaps 4 cm., was not far from 8000.

Galvanometer readings taken with "field off" and "field on" showed that the change of thermo-electric quality produced in the unequally heated constantan wire by magnetic action, if any such change occurred, was probably too small to yield a change of 3×10^{-8} volt in the thermo-electric force of the circuit.

Four couples of copper and annealed constantan wires were tested for calibration purposes. The temperatures used were those of the tap-water (about 12.5°), boiling ether (about 35.5°), boiling alcohol (about 80°), and boiling water. The method used was substantially that which has been described in previous papers.[4] None of the junctions came into direct contact with any one of the liquids or its vapor, each being protected by an arrangement like that shown in Figure 10. The thermometers used had been studied with considerable care in previous work.

The four couples agreed so closely that for no one of the temperature intervals used in the calibration did the result from any one couple differ so much as one per cent from the mean result given by all. This mean follows:

Temperature interval.	Mean e. m. f. per degree.
11.6°–34.5°	3911 absolute
34.6°–79.1°	4145 "
79.3°–99.9°	4527 "

The thermo-electric current runs from constantan to copper at the hot junction; that is, at ordinary temperatures the copper line on the thermo-electric diagram lies between the iron line and the constantan line.

Plotting a curve through the three points given by the data shown above, we get from it the following table for copper-constantan: —

---

[4] These Proceedings, **41**, p. 42.

Temperature.	Thermo-electric height (microvolts per degree).	Temperature.	Thermo-electric height (microvolts per degree).
0° C.	38.04	60° C.	41.72
10°	38.46	70°	42.71
20°	38.94	80°	43.91
30°	39.50	90°	45.33
40°	40.14	100°	47.10
50°	40.88		

MEASUREMENT OF THE TRANSVERSE EFFECTS.

In giving the results of our observations we shall report on the various transverse effects in the order in which we have defined them. Relations, theoretical or empirical, between some of them will be discussed later, with especial reference to the formulas of Moreau and of Voigt.

Hall Effect. — With Plate 1 we found

1910.	$_eT_e$.	θ.	C_p.	H.
Mar. 29	$+ 714 \times 10^{-5}$	12.7°	2.9	6500
" 30	1024 "	53.0°	"	"

θ here is the temperature of the water flowing through the copper blocks at the end of the plate and the iron trough in which the plate lay. C_p is approximately the strength of the current through the plate, expressed in absolute units; H is approximately the strength of the magnetic field at the middle part of the plate, expressed in absolute units.

The temperature-coefficient of $_eT_e$, as derived from the data here given, is

$$(1024 - 714) \div 714 \, (53 - 12.7) = 0.0108.$$

Thermo-electric action, due to the Ettingshausen transverse temperature-difference acting in the all-iron thermo-electric couple I_2–*plate*–I_4 of Figure 6, is negligible in its influence on the Hall effect as here observed.

With Plate 2, using the circuit C_2–*plate*–C_4, we found

1910.	$_eT_e$.	θ.	C_P.	H.
Dec. 3	$+ 807 \times 10^{-5}$	13.1°	2.94	5150
" 22	781 "	12.7°	2.97	5460
	794 "	12.9°	2.96	5300
" 10	1486×10^{-5} (1464) "	84.5°	2.99	5040

After the observations of December 10, on the Hall effect, it was found that the plate had been several millimeters too high in the magnetic field during the observations of December 3 and 10, so that the strength of the field to which it had been exposed was somewhat uncertain. Proper adjustment was made December 22, and later in the same day the Hall effect was measured again at low temperature. The coefficient found December 22 was about 3.3 per cent lower than that of December 3, though the temperature on the later date was only 0.4° lower, which would account for scarcely 0.5 per cent difference. For the value of ${}_eT_e$ at the mean low temperature, 12.9°, we have taken the mean, 794×10^{-5} of the values found on December 3 and December 22. For the value of ${}_eT_e$ at the high temperature, 84.5°, we have taken the value found December 10 reduced by 1.5 per cent, thus getting 1464×10^{-5}.

For the temperature-coefficient of ${}_eT_e$ in Plate 2, we get

$$(1464 - 794) \div 794\,(84.5 - 12.9) = 0.0118.$$[5]

Ettingshausen Effect. — With Plate 1 we undertook to measure this effect by using the east and the west coils of our galvanometer differentially, connecting the I_2I_4 circuit with the west coil and the C_2C_4 circuit with the east coil and taking care to have the total resistance of one circuit equal to that of the other. This arrangement we called $(I_2–I_4)$ *versus* $(C_2–C_4)$. Lest there might be error from a possible accidental advantage of one coil of the galvanometer over the other in action upon the needle, a series of observations made with this arrangement was always coupled with a $(C_2–C_4)$ *vs.* $(I_2–I_4)$ series, in which the $C_2\ C_4$ circuit was connected with the west coil and the I_2I_4 circuit with the east coil.

The theory of this test was that the Hall effects in the two circuits would just neutralize each other, leaving the Ettingshausen effect in the $C_2\ C_4$ circuit to give an account of itself in the net result. This experimental method was not so good as that used in the study of the

---

[5] Dr. Alpheus W. Smith gave in the Physical Review for Jan., 1910, the results of his study of the Hall effect in various metals through a large range of temperature. Taking data from the diagrams of his paper, we find as the temperature-coefficient of the Hall effect

0.0088	between 22° and 100° in " Kahlbaum iron,"
0.0140	" 23° " " " electrolytic iron.

The mean of these values, 0.0114, agrees very well with the values found by us in Plates 1 and 2.

Ettingshausen effect in Plate 2, and the results here attained are not entitled to any great confidence. They are

1910.	$_eT_h$.	θ.	C_p.	H.
Mar. 29	-375×10^{-10}	12.7	2.86	6500
" 30	-1120 "	53.1	2.85	"

It seems inadvisable to calculate a temperature-coefficient of $_eT_h$ from these data.

With Plate 2 we put the circuit C_4K_4 into connection with the west coil of the galvanometer and the circuit C_2K_2 into connection with the east coil, as in Figure 9.[6] We shall call this arrangement C_4K_4 *vs.* C_2K_2, or (4) *vs.* (2). Series with this arrangement were coupled with series having a (2) *vs.* (4) arrangement, the galvanometer connections being exchanged in the shift from one arrangement to the other. The results are

1910.	$_eT_h$.	θ.	C_p.	H.
Dec. 9	-500×10^{-10} [492]	12.2°	2.94	5000
" 10	621 " [612]	83.9°	30.0	"

The numbers given in brackets, which are the ones to be finally taken, are reached by deducting 1.5 per cent from the numbers immediately above, the deduction being made for reasons given in connection with $_eT_e$.

From these data we get the following temperature-coefficient of $_eT_h$ in Plate 2:

$$(612 - 492) \div 492\ (83.9 - 12.2) = 0.0034.$$

The transverse differences of temperature (between the arms) actually produced by electromagnetic action in the cases here described in Plate 2 were about 0.0053° at the low temperature and 0.0067° at the high temperature. Whether these temperature-differences are set up instantaneously by the magnetic action or whether they grow for a time after the full magnetic field-strength is on, is a question we cannot at present answer with full confidence. The galvanometer was usually read about 45 to 60 seconds after the magnet-current, C_m, was put on. We have not observed any tendency toward galvanometer drift of such a character as to indicate that we should have got larger Ettingshausen effects by waiting longer for these effects to be established.

---

[6] Proportions are not observed in this figure, nor is the device for keeping the two wires separate, except at their soldered junction, within the glass tubes in V shown. For this detail see Figure 10.

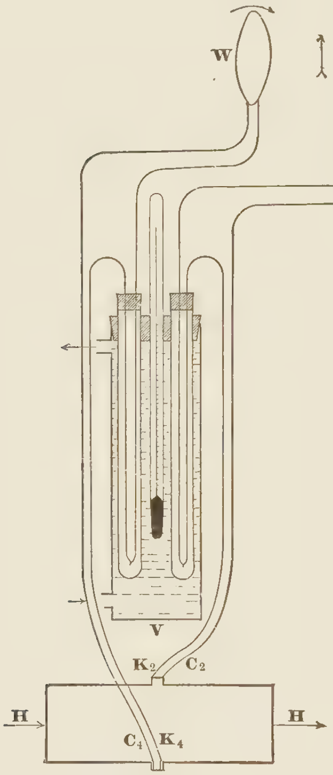

Figure 9.

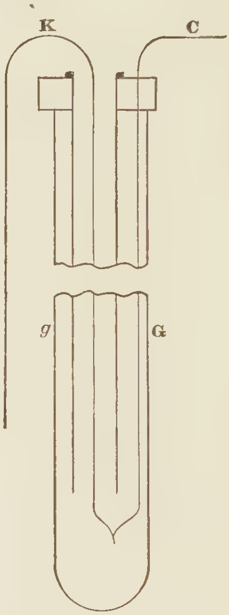

Figure 10.

The Nernst Effect. — With Plate 1 we at first used the iron trough already described, during the thermomagnetic tests. We now reject all the Nernst-effect observations made with this trough between the poles. The remaining results are

1910.	$_hT_e$.	Arm θ.	$\frac{d\theta}{dl}$.	H.
June 4	-944×10^{-6}	45.7°	11.3°	8400
" 10	928 "	44.8°	11.3°	8700
Means	−936 "	45.3°	11.3°	8550

The "arm θ," that is, the temperature of the median cross-line of the plate, was found by connecting either the C_2I_2 circuit or the C_2I_4 circuit with the galvanometer and then bringing the outer junction of the thermo-electric couple to such a temperature as to make the current in the circuit zero.

The temperature gradient $\frac{d\theta}{dl}$ along the plate was found by connecting the thermo-electric circuit $C_1-plate-C_3$ with the galvanometer.

The transverse potential difference, the Nernst effect, was found by means of the circuit $I_2-plate-I_4$, the assumption being made that the thermo-electric difference between the iron plate and the iron wires could safely be neglected, so that no account need be taken here of the fact that a transverse temperature-difference, the Leduc effect, is set up simultaneously with the Nernst effect. It now seems very doubtful whether this assumption was justified; but as we have good reason for supposing that the error thus introduced into the value of $_hT_e$ was not more than 10 per cent, and as we are not sure of the sign of this error, we leave $_hT_e$ for Plate 1 as we have found it.

With Plate 2 the conditions were better. We found arm θ and $d\theta/dl$ in essentially the same way as before. We found the transverse e. m. f., $\Delta E'$ let us say, produced in the circuit $C_2-plate-C_4$ by magnetic action and deducted from this the amount, a large part of the whole, which from a study of the Leduc effect we found to be attributable to a thermo-electric force set up in the circuit $C_2-plate-C_4$ by magnetic action. If we call this e. m. f. Δ_lE' and call the true Nernst transverse difference of potential $\Delta P'$, we have

$$\Delta P' = \Delta E' - \Delta_l E.$$

Thus at 31° we found $\Delta P' = 132.3 - 54.5 = 77.8$ absolute,
and at 60° " " $\Delta P' = 137.0 - 50.3 = 86.7$ "

The results are

1910.	$_hT_e$.	Arm ϑ.	$\frac{d\theta}{dl}$.	H.
Dec. 28	$-$ 880 × 10^{-6}	30.1°	8.4 (N–S)	5550
" 29	840 "	31.7°	8.3 (S–N)	"
Means	860 "	31.0°	8.4	5550
Dec. 30	940 × 10^{-6}	59.3°	7.7 (S–N)	5560
" 30	1020 "	60.3°	7.7 (N–S)	5470
Means	$-$ 980 "	60.0°	7.7	5500

Reference to formula (3) defining $_hT_e$ will show that it contains the factor $1 \div \left(w \times \frac{d\theta}{dl}\right)$, where w is the width. Now as the Nernst $\Delta P'$ is found between two points separated by the width of the main plate plus the length of both arms, it might seem as if w must be taken as this whole distance. On the other hand, as the flow of heat in the arms follows a somewhat dubious course, one may well doubt whether the whole length of the arms should be included. Fortunately, the fact that the width w occurs in combination with the gradient $\frac{d\theta}{dl}$ relieves us from this difficulty. The longitudinal gradient which counts is the gradient on the narrow strip running across from arm to arm and out into the arms, and this gradient will bear the same ratio to the measured gradient $\frac{d\theta}{dl}$ that the width of the main part of the plate bears to the effective width at the arms. Accordingly, we can take w as the width of the plate without the arms and $\frac{d\theta}{dl}$ as the gradient which would exist if the arms were absent, that is, practically, the gradient as measured by means of the circuit C_1–*plate*–C_3. This we have done, here and in dealing with the Leduc effect.

The temperature-coefficient of ${}_hT_e$ we find to be

$$(980 - 860) \div 860\,(60 - 31) = 0.0048.$$

The Leduc Effect. — All of the Leduc observations on Plate 1 were made with the iron trough in use. For this reason, and the further reason that the dubious thermo-electric quality of our iron wire was involved in them, these observations are entitled to far less weight than those made with Plate 2.

The method used with both plates was essentially that indicated in Figure 9, the (2) circuit and the (4) circuit being used differentially, one connected with the west coil of the galvanometer, the other connected with the east coil.

With Plate 1 we found

1910.	${}_hT_h$.	Arm θ.	$\frac{d\theta}{dl}$.	H.
Mar. 31	$+453 \times 10^{-9}$	43 (?)	11.0 (N–S)	6500
Apr. 2	410 "	44 (?)	11.3 "	"
Means	432 "	43.5(?)	11.2	6500
Apr. 1	421×10^{-9}	43 (?)	11.3 (S–N)	6500
" 2	438 "	44 (?)	11.3 "	"
" 9	420 "	45 (?)	11.3 "	"
Means	426 "	44 (?)	11.3	6500
Final means	+429 "	44 (?)	11.3	6500

With Plate 2 we found

1910.	$_hT_h$.	Arm θ.	$\frac{d\theta}{dl}$.	
Dec. 28	$+ 549 \times 10^{-9}$	29.8°	8.3 (N–S)	5600
" 29	586 "	31.3°	8.6 (S–N)	5550
Means	+ 568 "	30.6°	8.5	5600
Dec. 30	$+ 614 \times 10^{-9}$	59.2°	7.9 (S–N)	5470
" "	649 "	61.1°	7.7 (N–S)	5550
Means	+ 632 "	60.2°	7.8	5500

The temperature-coefficient of $_hT_h$ in Plate 2 is, according to these figures,

$$(632–568) \div 568\ (60.2–30.6) = 0.0038.$$

The + sign of $_hT_h$ means, according to our definition, that the isothermal lines are by the magnetic field rotated in the same direction in which the magnetizing current flows.

The difference of temperature actually produced between the arms by this action was about 0.0054°.

The magnet current was usually put on about 45 seconds before the final galvanometer reading showing the Leduc effect was taken. Professor Campbell, who did most of the experimental work in this research, is under the impression that the Leduc effect did not attain its maximum value as soon as the full field-strength was reached, but that it continued, according to the testimony of the galvanometer, to grow for a time after that moment. We cannot speak positively, as yet, on this interesting particular.

RELATIONS OF $_eT_e$, $_eT_h$, ETC.: THE MOREAU FORMULA AND ITS SUGGESTIONS; THE VOIGT FORMULA.

Attempts have been made by various writers to correlate some or all of the various effects which are dealt with in this paper and to connect them with some of the more generally familiar electrical and thermal properties of metals. Naturally the electron theory has been used of late in such efforts; but we shall consider first a suggestion or proposition made by Moreau,[7] about ten years since, in which no mention of the electron theory was made or intended. Indeed, Moreau says, "As, moreover, the variations of $K\,[_eT_h]$ are explained by those of $c\,[_eT_e]$, since the Hall effect is the primordial phenomenon, one is justified in supposing that the molecular state of the plate has a considerable influence on the value of c. This seems to me a new proof that the Hall phenomenon is due to a deformation of the plate under the influence of the magnetic field, and it is enough to explain the differences, often very great, observed between the values of c, for the same body, by different experimenters."

---

[7] C. R., **130** (1900), pp. 122–124, 412–414, 562–565.

It is difficult to see how anyone who has tried the Hall effect with a variety of conditions as to the manner of supporting the metal under examination can attribute this effect to any ordinary distortion of the material. If distortion, or deformation, is the cause of the phenomenon in question, this distortion must be something as remote from ordinary bending and twisting as are the changes of molecular orientation which we imagine to accompany or constitute magnetization.

We might, therefore, pay little attention to the suggestion of Moreau, if he had not given and supported with some experimental evidence an exceedingly simple formula,

$$ {}_eT_e \div \rho = {}_hT_e \div s, \tag{5} $$

in which ${}_eT_e =$ the Hall coefficient,
${}_hT_e =$ " Nernst "
$\rho =$ " specific electrical resistance,
$s =$ " mechanical equivalent of the Thomson-effect coefficient, that is, the amount of heat energy (ergs) absorbed by the unit current (absolute) of electricity per second in going, according to the ordinary convention of current direction, through the metal from a point where the temperature is T degrees C. to a point where it is $(T + 1)$ degrees C.

This formula of Moreau, if it could be substantiated by further experimental evidence, would prove disturbing to the point of view from which the present definition of the Hall coefficient was framed, even if it did not lead to the conclusion that the Hall effect and its various allied effects are due to a deformation of some kind in the material showing these phenomena. For it is to be noted that in the definition of ${}_eT_e$ the relation of the transverse potential-gradient to longitudinal *current-strength*, not to the longitudinal potential-gradient, is expressed. The reasons for this are two: 1st, a notion held by the discoverer at the time of the discovery that the new effect was due to the action of magnetic force on a *current* of electricity, as such, not to the action of such force on a medium containing lines of electrical force,[8] as such; 2d, the fact that it was much easier to measure current-strength than potential-gradient, in the longitudinal direction, in metal sheets of uneven thickness and uncertain quality such as were often used in the early days of the Hall effect.

---

[8] At the suggestion of Professor Rowland an attempt was made to rotate by magnetic force the equipotential lines of a piece of glass under electrical stress. The result was negative. — E. H. H.

It is true that before long it began to be seen that metals of high resistance had, as a rule, high values of ${}_eT_e$, and this fact raised the question whether high transverse potential-gradient might not go naturally with high longitudinal potential-gradient as such. But it was found that, in non-magnetic metals at least, rise of temperature, increasing the resistance and the longitudinal potential-gradient, did not as a rule, if ever, increase[9] the Hall effect proportionally. Accordingly, there has seemed to be no sufficient reason for recasting the definition of ${}_eT_e$ by introducing the potential-gradient instead of the longitudinal current-strength.

But the formula of Moreau suggests, or perhaps is suggested, by such a change of view as this recasting of ${}_eT_e$ would imply. To prove this statement an argument leading to this formula will now be given.

We will treat the matter first in its qualitative aspect; and we will take the case of our soft iron, in order to be the more definite. Figure 1, which is correct for this iron, shows a +Hall effect, the equipotential lines being rotated in the direction of the Amperian current of the field. Such a rotation establishes a transverse potential-gradient, the lower edge of the plate attaining thus the higher potential.

Turning now to Figure 3 and remembering that in iron the Thomson-effect coefficient, s, is negative, so that heat is absorbed by an electrical current when it flows (in the ordinary conventional sense) from high temperature to low temperature in iron, we see that in the present case we must, in order that an electrical current may *not* flow along the plate, have the cold end of the plate at a higher potential than the hot end; that is, we have, under the conditions of Figure 3, a potential-gradient opposite in direction to the temperature-gradient and opposite to the potential-gradient along the plate in Figure 1. Accordingly, our magnetic field, rotating the equipotential lines of this *static* Thomson-effect potential-gradient, would make in our iron the upper edge of the plate electrically positive as compared with the lower edge, thus giving what we call a negative Nernst effect. The Nernst effect in our iron is negative, according to our convention as to signs, and the signs at least of the Moreau formula are correct in this case, ${}_eT_e$ and ρ being both $+$ and ${}_hT_e$ and s both $-$.

---

[9] "The temperature-coefficient of the Hall effect in gold, zinc, platinum, silver and aluminum has . . . been determined and it has been found that with the exception of aluminum there is in each of these cases a decrease in the effect as the temperature is raised from −190° to about 22°." Dr. Alpheus W. Smith, Physical Review, Jàn., 1910.

The quantitative argument is very simple. Writing $\frac{dP}{dl}$ for the potential-gradient which maintains the current C through a plate of width w, thickness t, and specific resistance ρ, we have, using absolute units, $C = \frac{dP}{dl} \times \frac{\omega t}{\rho}$, and accordingly

$$ {}_eT_e = \frac{\Delta P'}{w} \div \frac{C}{wt} H = \left(\frac{\Delta P'}{w} \div \frac{dP}{dl} \right) \frac{\rho}{H}. \tag{6} $$

Taking, as before (equation (3)),

$$ {}_hT_e = \frac{\Delta P'}{w} \div \frac{d\theta}{dl} H, $$

and observing that the *static* Thomson-effect potential-gradient is

$$ s \frac{d\theta}{dl} = \frac{dP}{dl}, $$

we have

$$ {}_hT_e = \left(\frac{\Delta P'}{w} \div \frac{dP}{dl} \right) \frac{s}{H}. \tag{7} $$

If, now, we can assume that the equipotential lines of the electric current in the Hall effect are by magnetic action rotated just as far as the static thermo-electric equipotential lines of the heat current in the Nernst effect, we shall have the parenthesis in equation (6) equal to the parenthesis in (7), and then, dividing (6) by (7), we shall get

$$ {}_eT_e \div {}_hT_e = \rho \div s, \quad \text{or} \quad {}_eT_e \div \rho = {}_hT_e \div s, \tag{8} $$

which is the equation of Moreau.

Before proceeding further it will be well to assemble in one table the various coefficients under discussion, each evaluated, as accurately as our knowledge of the rates of change with temperature will enable us to evaluate it, for various temperatures. We have, the last line relating to Plate 1 and the other lines to Plate 2,

Temp.	${}_eT_e$	${}_eT_h$	${}_hT_h$	${}_hT_e$	ρ	s	S
20°	861×10^{-5}	-505×10^{-10}	545×10^{-9}	-815×10^{-6}	12550	−851	1429
40°	1048 "	538 "	588 "	897 "	13730	961	1370
60°	1235 "	572 "	630 "	980 "	14910	1079	1307
80°	1422 "	604 "	672 "	1062 "	16090	1203	1240
100°	1609 "	638 "	714 "	1144 "	17270	1333	1171
45°	963 "	−971(?) "	430(?) "	−935 "			

(I.)

Previous work[10] has given us 11365 as the value of ρ at 0°C., with a temperature-coefficient 0.00519, and a Thomson-effect formula, running from 32° C. to 182° C., from which we get

$$s = -(107\,T + 2\,T^2)\,419 \times 10^{-5}, \tag{9}$$

T being the absolute temperature.

S of the last column is the estimated "thermo-electric height" of our iron relative to lead. It will be discussed at considerable length in connection with the formula of Voigt.

Testing the Moreau formula with the data given, we find

	Temp.	$({}_eT_e \div \rho) = A.$	${}_hT_e \div s = B.$	$(A - B) \div A.$	
Plate 2	20° C.	$+ 686 \times 10^{-9}$	$+ 958 \times 10^{-9}$	$- 0.40 -$	(II.)
	40°	763 "	934 "	$- 0.22 +$	
	60°	828 "	908 "	$- 0.10 -$	
	80°	884 "	883 "	$- 0.00$	
	100°	932 "	858 "	$+ 0.08 -$	
Plate 1	45°	$+ 686$ "	$+ 944$ "	$- 0.38 -$	

Not all of the temperature-coefficients are sufficiently well known to justify us in pushing the comparison through a greater range of temperature, and in fact the values here set down for A and B are subject to an error of several per cent, probably. But when all reasonable allowance for error has been made, it seems unlikely that the Moreau formula can hold in this iron through any considerable range of temperature. The difference between the result from Plate 1 at 45° and that for Plate 2 at or near the same temperature is less significant as throwing a doubt upon the accuracy of our work than it would be if the two plates had been cut in the same direction from the original iron bar. Plate 2 is far more important, not merely because it has been studied under better conditions, but because the main current in it was in the direction of the fibres of the iron, the direction along which the measurements for ρ and for s have been made.

It appears that the Moreau formula holds in our iron for one temperature, which in Plate 2 is near 80° C. Below this temperature the static Thomson equipotential lines appear to be rotated through a somewhat greater angle, by a given strength of field, than the equipotential lines of an ordinary electric current; but above this temperature the opposite appears to hold.

Comparison of ${}_eT_e \div \rho$ in Table II with ${}_hT_h$ in Table I shows an approach to equality, which may be interpreted as meaning that the equipotential lines of the longitudinal electric current in the Hall effect and the isothermal lines of the longitudinal heat-current in the Leduc effect are rotated in the same direction and to nearly the same extent, at certain temperatures. Detailed comparison gives

---

[10] These Proceedings, **42**, March, 1907.

Temp.	$({}_eT_e \div \rho) = A$	${}_hT_h = B$	$(A - B) \div A$
20°	$+ 686 \times 10^{-9}$	$+ 545 \times 10^{-9}$	+ 0.21 −
40°	763 "	588 "	0 23 −
60°	828 "	630 "	0.24 −
80°	884 "	672 "	0.24 −
100°	932 "	714 "	0.23 +

(III.)

It would seem from this showing that, within the range of temperature here considered, the isothermal lines are rotated in the Leduc effect about three-fourths as far as the equipotential lines are rotated in the Hall effect, the strength of magnetic field being the same on both cases.

Comparison of Tables II and III indicates that, within the range of temperature shown, the static Thomson equipotential lines are rotated farther in the Nernst effect than the isothermal lines are simultaneously turned in the Leduc effect, but that the excess noted diminishes rapidly with rise of temperature and seems likely to become zero or negative with further rise.

As we have in the Moreau formula a suggestion at least of some relation between ${}_eT_e$ and ${}_hT_e$, we might expect to find evidence of a reciprocal relation between ${}_hT_h$ and ${}_eT_h$; that is, between the Leduc effect and the Ettingshausen effect. Reflection shows, however, that one link in the chain of reasoning, if it deserves such a name, is here missing. We go from the Hall effect to the Nernst effect by way of the Thomson effect, the known difference of electric potential which accompanies flow of heat or difference of temperature in iron under normal conditions. But no corresponding difference of temperature necessarily accompanying flow of electricity or difference of electric potential is known to us. On the other hand, if we could find by inspection of the various coefficients before us evidence of a relation between ${}_hT_h$ and ${}_eT_h$, we might perhaps take this as a clue to what could be called the reciprocal of the Thomson effect, and could be described as a temperature-gradient due to potential-gradient. The possibility of such a discovery makes it desirable to examine closely all the relations which a study of our various tables of data suggest.

A look at the uppermost line of Table I shows that, for the temperature 20° C. at least, we have, very nearly,

$$ {}_eT_e \times {}_eT_h = {}_hT_h \times {}_hT_e, \text{ or } {}_eT_e \div {}_hT_e = {}_hT_h \div {}_eT_h. \qquad (10)$$

If we test this formula through the various temperatures we find

Temp.	$({}_eT_e \div {}_hT_e) = A$	$({}_hT_h \div {}_eT_h) = B$	$(A - B) \div A$
20°	− 10.56	− 10.79	− 0.02 +
40°	11.68	10.93	+ 0.06 +
60°	12.60	11.01	+ 0.13 −
80°	13.39	11.11	+ 0.17 +
100°	14.07	11.19	+ 0.20 +

(IV.)

The approximate equality here indicated appears to be closer than that of the Moreau formula. But is it anything more than accident? Going back to the definitions of ${}_eT_e$, etc., we find, putting $\Delta P_1'$ for the transverse potential-difference of the Hall effect and $\Delta P_2'$ for the transverse potential-difference of the Nernst effect,

$$ {}_eT_e \div {}_hT_e = \left(\frac{\Delta P_1'}{w} \div \frac{C}{wt}\right) \div \left(\frac{\Delta P_2'}{w} \div \frac{d\theta}{dl}\right) = \frac{\Delta P_1'}{\Delta P_2'} \times \left(\frac{d\theta}{dl} \div \frac{C}{wt}\right). \qquad (11)$$

The dimensions of this quotient A are those of a temperature-gradient divided by a current density.

We find also

$$ {}_hT_h \div {}_eT_h = \left(\frac{\Delta\theta'_2}{w} \div \frac{d\theta}{dl}\right) \div \left(\frac{\Delta\theta'_1}{w} \div \frac{C}{wt}\right) = \frac{\Delta\theta'_2}{\Delta\theta'_1} \times \left(\frac{C}{wt} \div \frac{d\theta}{dl}\right). \qquad (12)$$

The dimensions of this quotient B are the reciprocal of those of the quotient A, and accordingly it appears probable that we have only an accidental coincidence in the approach to equality shown by A and B.

If we undertake to explain the Ettingshausen effect as due to the magnetic rotation of the isothermal lines of a longitudinal temperature-gradient set up by the electric current along the plate, we see that, as the coefficient ${}_eT_h$ is about 0.09 as large as ${}_hT_h$, we must assume our temperature-gradient in question to be about 0.09 of a degree per centimeter in our plate when the electric current density therein is 1. Such a condition, as a normal attendant of a current in iron, could not have escaped the attention of ordinary experience. If it were set up by the act of magnetization, it would be detected in the longitudinal tests presently to be described.

Is it, then, possible that the Ettingshausen transverse effect is due to an actual displacement of the electric current in our plate, the flow, under the action of the magnet, being stronger along one edge than along the other edge of the plate ? This seems very unlikely, especially in view of the fact that, in Plate 2 at least, the resistance appears to be slightly, very slightly, decreased by magnetization. Indeed, the whole amount of heat generated per minute per unit length of the plate by our current C_p was about 0.6 calorie, and the change in this amount due to the magnetization was probably not so much as 0.00002 calorie.

There is at least one other point of view which is worth trying. The transverse potential-gradient set up in the Hall effect is, apparently, like the Thomson potential-gradient, *static*, maintained without flow of electricity down the gradient, though there may be, if the circuit is properly closed, flow of electricity up this gradient. In the Thomson effect this static condition is attended by, and is apparently due to, a temperature-gradient of the opposite slope. Is it perhaps true that wherever such a static potential-gradient exists in a metal there is an accompanying temperature-gradient, and are the two gradients in iron always of opposite slope ? The Ettingshausen temperature-slope is opposite in our iron to the potential slope of the Hall effect, and to this extent encourages our question ; but when we come to the ratio of the two slopes and compare this with the ratio of the two slopes in the Thomson effect, we find a great difference. In the latter case the ratio is our *s*. The exhibit follows :

Temp.	(${}_eT_e \div {}_eT_h$.)	s.	(${}_eT_e \div {}_eT_h$) ÷ s.	
20°	− 170500	− 851	200.4	(V.)
40°	194800	961	202.7	
60°	216000	1079	200.1	
80°	235000	1203	193.3	
100°	252200	1333	189.2	

We have at least the satisfaction of finding that the ratio of the two ratios, although each changes a good deal, nearly 50 per cent, remains pretty nearly constant,[11] especially at the lower temperatures, where the values of ${}_eT_h$ are probably more accurate than for the higher ones. Indeed, the whole change from 20° to 100° is less than 6 per cent. But the transverse temperature-gradient is only one two-hundredth part of what it should be to make the transverse ratio equal to *s*.

It would be difficult to go farther in this line of inquiry without introducing the electron theory, which we do not propose to discuss in this paper.

---

[11] It should be remembered, however, that the temperature-coefficient of ${}_eT_h$ cannot be regarded as accurately determined.

The Voigt Formula. — Before the appearance of Moreau's equation Voigt[12] had been led by theoretical considerations, not involving consideration of electrons, to propose a formula very like that of Moreau, which, using our own symbols in part, we shall write thus:[13]

$$ {}_{e}T_{e} \div \rho = {}_{h}T_{e} \div \Theta'. \tag{13}$$

Θ', replacing the s of the Moreau formula, is a quantity the definition of which we shall discuss at considerable length, as a number of references to it which we have seen do not make its meaning clear.[14] We cannot well show the significance of Θ' without the use of a diagram.

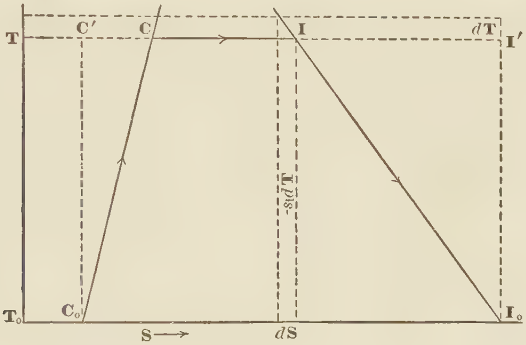

FIGURE 11.

The ordinary thermo-electric diagram has two rectangular axes, the horizontal one representing temperature, the vertical one a variable not usually named here, but which, as one of us pointed out several years ago,[15] is really entropy. Accordingly we make our diagram (Figure 11) as an ordinary temperature-entropy diagram is made, with temperature, absolute C., vertical and entropy (ergs ÷ T) horizontal. In accordance with common practice the T axis is assumed to be identical with the line for lead. The representative lines for copper and iron are here made straight, though in a later figure they are shown as curves. In accordance with the ordinary interpretation of a temperature-entropy diagram, unit quantity of electricity, ten coulombs, flowing (in the ordinary sense) from C_0 to C in copper or from I to I_0 in iron absorbs heat, and *vice versa*, the Thomson effect; flowing from C in copper to I in iron, it absorbs heat, and *vice versa*, the Peltier or Seebeck effect.

---

[12] Wied. Annalen, **67** (1899).

[13] Voigt has a — sign in his equation, which we avoid by making our ${}_{h}T_{e}$ equal his $-Q$.

[14] For example, Zahn appears to confuse Θ', which $= \partial\Theta/\partial T$, with Θ itself.

[15] Proceedings, A. A. A. S., **54** (1904). The paper contains much that I regret publishing, but in its early pages there is this one suggestion which still seems to me valuable. — E. H. H.

If now we denote by $-\Theta_c$[16] the area $T_0TCC_0T_0$ and by $-\Theta_i$ the area $T_0TII_0T_0$, the total, or net, thermo-electric force, in a copper-iron couple having one junction at T_0 (absolute zero) and the other junction at T, is represented by the area

$$C_0CII_0C_0 = -\Theta_i + \Theta_c. \tag{14}$$

If we let $\alpha_c =$ the line T_0C_0 and $\alpha_i = T_0I_0$, we can write

$$-\Theta_c = \alpha_c T + \tfrac{1}{2}\beta_c T^2, \tag{15}$$

and

$$-\Theta_i = \alpha_i T + \tfrac{1}{2}\beta_i T^2, \tag{16}$$

where $\beta_c = (C'C \div T)$ and $\beta_i = -(II' \div T)$.

These equations (15) and (16) correspond to equation (55) of Voigt's paper.

It is evident from our diagram that, if we allow a very small increase of temperature, from T to $T + dT$, and if we let S_i represent the entropy of ten coulombs at I, *the conventional zero of entropy being so taken that* $S_i = TI$, we have

$$-\frac{d\Theta_i}{dT}dT = S_i dT, \quad \text{or} \quad -\frac{d\Theta_i}{dT} = S_i. \tag{17}$$

Now the Θ' of the Voigt formula (13) is $\frac{d\Theta_i}{dT}$, and is therefore equal to our $-S_i$. It is numerically equal to the "thermo-electric height" of iron relative to lead.[17]

The relation of Θ'_i to s_i, the mechanical equivalent of the Thomson-effect coefficient, is readily found. The mechanical equivalent of the Thomson-effect heat absorbed by ten coulombs in rising in iron from

---

[16] We use the — sign here in order to conform to the use of Voigt.

[17] At least is has been so taken by Moreau in his empirical test of the Voigt formula, without protest, so far as we know, from Voigt, though the latter does not, perhaps, say explicitly that his Θ'_m for any metal m has reference to lead.

T to $T + dT$ is $s_t dT$, or rather, since s_t is essentially —, the mechanical equivalent of the heat *given out* in this change is $- s_t dT$, and this is represented by the area between the two adjacent vertical lines of our diagram. Evidently this area is equal to the area between the two adjacent horizontal lines from I' to I, that is, to $(a_t + \Theta'_t)\, dT$, and so we get

$$- s_t = \Theta'_t + a_t, \quad \text{or} \quad \Theta'_t + s_t = -a_t. \tag{18}$$

That is, the sum of Voigt's Θ'_t and the s_t, which Moreau uses in place of Θ'_t, is a constant, represented in Figure 11 by the line $T_0 I_0$ taken as a negative quantity. As we have already identified Θ'_t numerically with the line TI, taken as a negative quantity, we see that s_t is represented by the line II' taken as a negative quantity.

It must be remembered that this simple relation between s_t and Θ'_t results from the assumption made, for the time, in drawing Figure 11, and made also by Voigt, that the iron line is straight. The actual relation between s_t and Θ'_t is, according to our experiments, more complex.

The argument for Voigt's proposition, as expressed in equation (13), we shall not undertake to give; and even when we try to put it to an empirical test by means of our data, we do so with a serious *a priori* doubt as to its value. What real significance can we attach to the formula of Voigt? His $-\Theta'$, the "thermo-electric height" of iron with respect to lead, cannot be taken as a *fundamental* datum for iron. We have, to be sure, identified $-\Theta'$ with our S; but this S does not profess to be the absolute value of the thermo-electric entropy for iron. It is merely what we get for iron when we arbitrarily take the thermo-electric entropy of lead to be zero.

We have proceeded as follows: Assuming the "thermo-electric height" of "galvanoplastic" copper relative to lead to be 380×10^{-8} microvolts, or 380 absolute, at 20° C., from the observations of Matthiessen, and taking the thermo-electric height of our iron with respect to modern commercial copper wire (assumed to be thermo-electrically like Matthiessen's copper) to be 1049 absolute at 20° C., according to our own observations, we get 1429 absolute as the thermo-electric height of our iron with respect to lead at 20° C. But "thermo-electric heights" are merely isothermal entropy-differences, if we reckon entropy, as we do, in ergs $\div$ T. Accordingly in Figure 12 we take the T-axis as the lead line and at 20° C. lay off from this axis a distance 380 to give us the 20°-point on our copper line, and a distance of 1429 to give us the 20°-point on the iron line. The other points of the iron line must be found by means of our formula (9) for the Thomson effect in iron.

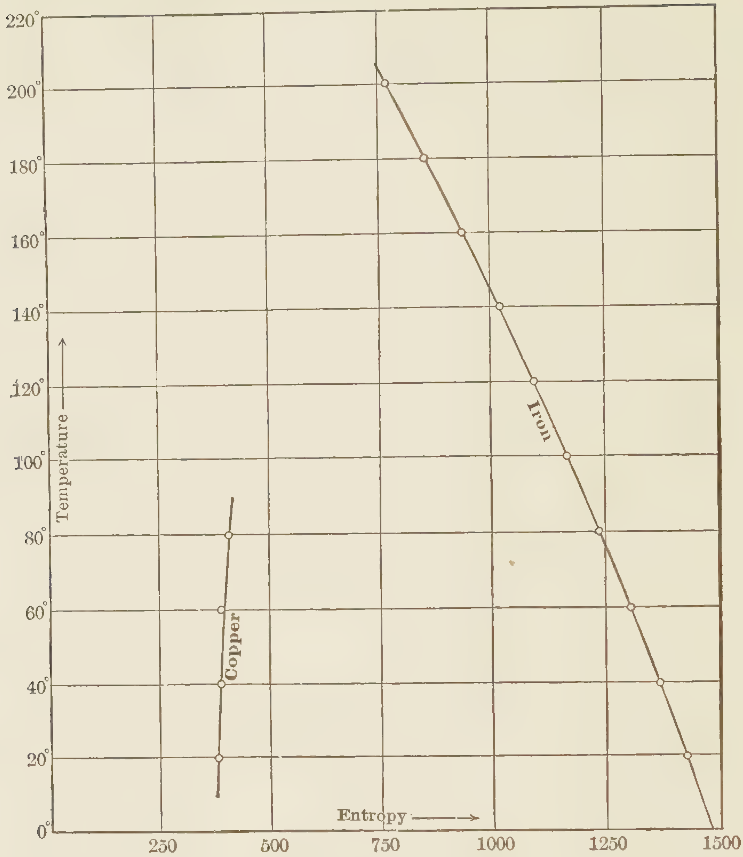

FIGURE 12.

Taking from Figure 11 the relation $TdS = sdT$, we get from (9)

$$dS = -419 \times 10^{-5}\,(107 + 2T)\,dT \;\ldots \qquad (19)$$

Integrated this gives

$$S = K - (107T + T^2) \times 419 \times 10^{-5} \;\ldots \qquad (20)$$

The value of S being taken, on grounds already shown, as 1429 at 20° C., we find the value of K to be 1921. Accordingly the values of S have been calculated which are given in the following table :

Temp.	S (entropy).	Temp.	S.
0° C.	1486	120° C.	1098
20°	1429	140°	1021
40°	1370	160°	941
60°	1307	180°	858
100°	1171	200°	771

(VI.)

With these values of S the iron line of Figure 12 has been plotted. Various points of the copper line have been found by measuring to the left from the corresponding points of the iron line distances representing the thermo-electric heights of iron with respect to copper at the various temperatures. The iron line is decidedly concave toward the left, the copper line, according to our data, has a much smaller inclination from the vertical than the iron line, indicating a much smaller Thomson effect in copper than in iron, and is slightly concave toward the right.

If we now, taking our values of S for certain temperatures, e. g. 20°, 40°, 60°, 80°, 100°, test the Voigt formula for these temperatures, we find,

Temp.	$(-{}_eT_e S \div \rho) = A.$	${}_hT_e = B.$	$(A - B) \div A.$
20°	$-\ 980 \times 10^{-6}$	$-\ 815 \times 10^{-6}$	0.17 —
40°	1046 "	897 "	0.14 —
60°	1083 "	980 "	0.10 —
80°	1096 "	1062 "	0.03 +
100°	1091 "	1144 "	— 0.05 —

(VII.)

Comparison of this table with Table II. will show that the Voigt formula, with the value of $-S$ (or Θ') found as we have found it, agrees with our data considerably better than the Moreau formula does. Each formula is right in our case as to signs[18] and each is satisfied by our data at some one temperature, which is near 80° C. for the Moreau formula and not very many degrees higher for the Voigt formula. Above the temperature of agreement ${}_hT_e$ is too small for the Moreau formula and too large for the Voigt formula. It is to be remembered that neither ${}_eT_e$ nor ${}_hT_e$ has been determined very accurately, nor is the temperature-coefficient of either precisely known. It seems to us, however, very unlikely that our errors of measurement are great enough to account for the disagreement between either formula and our data. It is probable that neither formula is correct.

---

[18] There may be some doubt as to the signs. See the Postscript to this paper.

Of the two, the Moreau formula seems to us the more likely to be useful, as suggestive of true relations which it does not perfectly express. The value of s_i, which we need to know in order to use this formula, we do know or can find. It is a definite property of iron and of iron alone. But the value of Voigt's Θ_i', as we have shown, is merely a property of iron with relation to lead. Now we know that the lead line cannot be regarded as the real boundary of the thermo-electric diagram. The lines for certain metals lie beyond it, below it in the ordinary diagram, to the left of it in such a diagram as that of Figure 11. These metals have a negative thermo-electric height, a negative thermo-electric entropy, as regards lead. Reckoning thermo-electric heights from lead, taking lead as having zero thermo-electric entropy, is quite as arbitrary as taking the freezing point of water for the zero of temperature. We may do injustice here; it is possible that we have not seen the exact meaning of Voigt's Θ'.

However useful the formula of Moreau may be, his thesis that the Hall effect and all the transverse effects associated with it are due to some deformation of the metal plate in the magnetic field appears to be incompetent to explain the observed facts, especially the Ettingshausen effect, and, if taken alone, misleading rather than helpful. It is altogether probable that the electron theory must be used, if all the phenomena observed are to be accounted for.

The Longitudinal Effects.

All of the transverse effects just considered change direction with change of direction of the magnetic field, the sign of the coefficient in each case remaining unchanged. The associated longitudinal effects, which are now to be described, remain, as the argument from symmetry would predict, unchanged in direction with change of direction of the field. One might, from this absence of dependence on the sign of the field magnetism, expect the longitudinal effects to be proportional to the square of the field-strength, and this may be true of some of these effects in some metals, but in general it appears not to be true. The fact seems to be, however, that the longitudinal effects are much less simple functions of field-strength than the transverse effects are and sometimes change direction with change of intensity of the field. Whether they are strictly or very nearly proportional to the longitudinal gradients of potential and temperature respectively, our own experiments do not enable us to say. We shall, however, assume this proportionality and shall accordingly define a certain coefficient for each of the two longitudinal effects which we have found in iron. For the sake of completeness we shall describe two other longitudinal effects which have been observed, though we have not yet made sure of them in iron.[19]

No one of the four longitudinal effects has any assigned name. Each must be designated by a rather long descriptive title.

Longitudinal Electromagnetic Potential-Difference. — With the magnetic field and the EE current as in Figure 1, we may take note of a change of longitudinal potential-gradient, due to transverse magnetic action, without change of strength of the longitudinal current. Of this effect Zahn says, "As its magnitude is found to be proportional to the strength of the primary [longitudinal] current-strength, it may be taken as a change of resistance."

We shall call this effect positive when it produces an increase of resistance. We take as the coefficient

$$ {}_eL_e = \Delta R \div RH, \tag{21}$$

where $R =$ the normal resistance of a certain length of the plate and $\Delta R =$ the increase of resistance of the same length of the plate.

In studying this effect in Plate 1 we connected points (1) and (3) of the plate (see Figure 6), by means of the iron wires, with our galvanometer, introducing into the galvanometer circuit e. m. f. from another circuit, so as to get an approximate balance of forces at the start, thus keeping the scale of the galvanometer within the field of view. Then we applied the magnetic field and observed the deflection produced, which was due to an increase or decrease in one of our counter-balancing e. m. f.'s, the other being not affected by the magnet. This method is troublesome, because it is difficult to keep the requisite degree of equilibrium through an extended series of observations.

This operation gave us for Plate 1 values of ${}_eL_e$ which are exhibited in the following table. The numbers given in the last three columns are approximate only.

1909.	${}_eL_e$.	Arm θ.	C_p.	H.
July 8	$+164 \times 10^{-10}$	22°5	2.96	10500
" 9	148 "	22.0	"	10900
Means	$+156 \times 10^{-10}$	22°	2.96	10700

With Plate 2 a different method was used. Copper wires connected with points (1) and (3) of the plate led to one coil of the galvanometer, while wires from two other points, A and B (see Figure 13), of the plate-circuit led to the other coil. By means of the shunts S_1 and S_2

---

[19] But see p. 664, footnote.

an approximate balance of the galvanometer forces was obtained which remained fairly constant when the span of copper wire AB was kept in a bath of oil to prevent sudden changes of temperature. With this arrangement the following result was obtained with Plate 2:

	$_eL_e$.	Arm θ.	C_p.	H.
Dec. 24, 1910	-59×10^{-10}	13°0	3.0	5400

The value of R was about 113,000, absolute, or 0.000113 ohm, and that of ΔR about -3, absolute. This is a small quantity, and it may therefore be well to give a few details as to the observations. Five series, or "runs" were made, three with the current C_p flowing south through the plate, and two with this current flowing north. It is not safe to depend on observations made without such reversal of the main current; for there is always a possibility of some illegitimate action of the electromagnet circuit on the galvanometer which can be eliminated by combining two series of data, one obtained with the current in the plate running north, the other with this current running south. The five series mentioned gave the following mean galvanometer deflections:

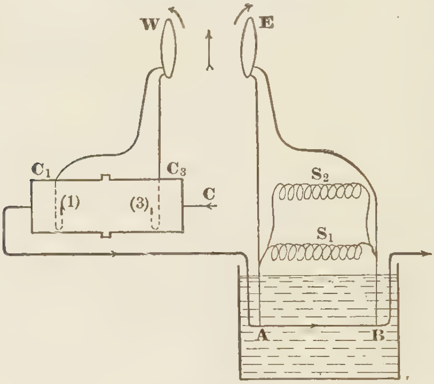

FIGURE 13.

	With C_p north.	With C_p south.
	+ 0.33 cm.	+ 0.11 cm.
	+ 0.24 "	− 0.21 "
		− 0.22 "
Means	+ 0.29 "	− 0.11 "

Final mean $= \frac{1}{2}(0.29 + 0.11) = 0.20$ cm.

The first series with C_p south, which gives a mean deflection discordant in sign with the others, was the shortest series and internally the worst of the five.

One other possibility of error must be considered here. The copper wires C_1 and C_3, being connected with the iron plate, form a thermo-electric couple, and if the action of the magnet should make a difference of temperature amounting to 0.01 degree between the junctions (1) and (3), the thermo-electric action of this copper-iron couple would produce as great a deflection of the galvanometer as that given above, which was taken to indicate a change of resistance. Accordingly, it was necessary to consider the possible magnitude of this second longitudinal effect, which will presently be considered.

It is to be noted that Plate 1 shows in a field of 10,700 an *increase* of resistance which we may represent, on an arbitrary scale, by 16, while Plate 2 shows in a field of 5400 a *decrease* of resistance which we may represent on the same scale by 3. Zahn says, "In ferromagnetic metals there is in weak fields an increase of resistance, in stronger fields a decrease. According to the results of Grunmach for iron and cobalt and a preliminary publication of Blake on measurements in nickel, the initial increase is perhaps due to longitudinal components [of magnetism]." When it is remembered that in one of our plates, (1), the resistance is measured at right angles with the fibres or grain of the iron, while in (2) it is measured in the direction of the fibres, it need not, perhaps, be considered strange that the change of resistance caused by magnetic action is opposite in direction in the two cases. In both cases the change is very small.

We now proceed to the other longitudinal effect which is so intimately connected with the one just discussed.

Longitudinal Electromagnetic Temperature-Difference. — With the magnetic field and the *EE* current as in Figure 1, we may look for a difference of temperature, $\Delta\theta'$, established by magnetic action between two points d cm. apart along the plate. We have spent much time in looking for this effect, especially in Plate 1, being led on by accidental phenomena which simulated it rather persistently, though with discrepancies that were suspicious, until a slight change in the disposition of the plate between the poles of the magnet wiped out the apparent temperature change which we had been studying and possibly gave a slight apparent change in the opposite direction.

With Plate 2 we gave only one day, a whole day, to this particular question. The method used was the following: Copper-constantan couple (1), having one junction at point (1) on the plate and the other in a glass tube placed in a water-bath, was put in circuit with one coil of our galvanometer. Couple (3), with one junction at point (3) on the plate and the other in the water-bath, was put in circuit with the other coil of the galvanometer, opposing the action of couple (1) and nearly balancing it. Then the magnetic field was brought into action and the consequent deflections of the galvanometer were observed.

The day's work gave a net deflection of 0.03 cm. as the result of magnetic action, — a quantity smaller than its own probable error. This deflection, if considered reliable, would indicate a temperature-difference of 0.0008° C., — about a tenth of the temperature-difference that would be needed to account for the apparent change of resistance which has been described above.

The coefficient of the longitudinal effect here looked for but not found may be defined as follows:

$$ {}_eL_h = \frac{\Delta\theta'}{d} \div \frac{C_v}{wt} H. \qquad (22) $$

Longitudinal Thermomagnetic Potential-Difference. — With the magnetic field and the HH current as in Figure 3, we may take note of the difference of potential, $\Delta P'$, set up by magnetic action between two points d cm. apart along the plate. We shall call this effect positive when the potential-gradient thus established is in the same direction as the temperature-gradient along the plate. As the coefficient of this effect we have

$$ {}_hL_e = \frac{\Delta P'}{d} \div \frac{d\theta}{dl} H, \qquad (23) $$

where $\frac{d\theta}{dl}$ means the temperature-gradient along the plate.

We have not looked for this effect in Plate 2. In Plate 1 we studied it at considerable length, because of a disagreement between our observations and those reported by Zahn on the authority of Houllevigue and of Moreau. He says, "The phenomenon is complicated here [in ferromagnetic metals], for the sign is dependent on the field-strength. With small H the potential-gradient established is in the same direction as the temperature-gradient; it reaches a maximum at ordinary temperature [*bei mittlerer Temperatur*] for a field-strength of about 3000 gausses, then vanishes, in nickel for H about 4500, in iron and steel at about double this field-strength, and takes, for higher fields, the opposite direction. The reversal of sign occurs at a lower field-strength the higher the mean temperature of the plate is."

We used at first the iron wires I_1 and I_3, connected with points (1) and (3) on the plate. The outer ends of these wires were permanently joined to copper wires, in junctions like the one shown in Figure 10, and from these junctions the copper wires led to the galvanometer. After such a balance of thermo-electric forces in this circuit as to keep the scale of the galvanometer in the field of vision had been effected, the magnetic force was brought into action. An effect was observed;

but we soon found that the thermo-electric behavior of the iron wires, as well as that of the plate, was affected in such a way by the magnetization that it was impossible to get satisfactory results with this arrangement.

Accordingly we attached two other iron wires, one to each of the copper blocks *B* and *B* of Figure 7, near the ends of the iron plate but well outside the powerful intrapolar region of the magnetic field, within which the iron wires previously used lay. Working with this arrangement we got very considerable effects which showed that transverse magnetization produced in the plate a change of quality or condition such as to make the copper block at the hotter end of the plate electrically positive compared with the copper block at the colder end. This difference of potential, $\Delta P'$, we could and did measure, but there was, and still is, some uncertainty as to the value which should be assigned to *d* in this case. It should not be the whole length of the plate, for the whole length was not subjected to the full strength, *H*, of the magnetic field. We have taken *d* as 80 per cent of the whole length of the plate between the blocks, and have reckoned ${}_hL_e$ accordingly. Each value of this coefficient, as given below, was found from two sets of observations, one made with the heat-current flowing south, the other with it flowing north. As usual, the numbers given in the last three columns are approximate only.

1910.	${}_hL_e$.	Arm θ.	$\frac{d\theta}{dl}$.	H.
June 14–17	80×10^{-5}	47°	13.7	12000
	83 “	47°	13.7	8200
	211 “	47°	13.7	2000
28–29	69 “	48°	13	12000
	73 “	48°	13	7900
	187 “	48°	13	1900

The relation of ${}_hL_e$ to H in these two groups of data is shown by means of the two curves of Figure 14. The × points are for the earlier observations, the ○ points for the later ones. The two curves are very like, and neither suggests a reversal of sign of the effect in question at any stage of magnetization. Why one curve runs notably lower than the other through its whole course we cannot say with full confidence. It is, however, a fact that in the period of the June 14–17 observations the arrangement for getting the sensitiveness of the galvanometer was under suspicion. In the warm, moist atmosphere of a Cambridge summer the problem of insulation in delicate electrical measurements becomes considerable. Leakages occur to a disturbing extent where during the months of artificial heating of the laboratory they need not be regarded. There was perceptible leakage from the magnet-circuit into the galvanometer-circuit during June. Efforts were made to eliminate errors from such disturbances by combining series of observations taken under a variety of conditions, but we cannot be sure that these efforts were entirely successful. It is unlikely, however, that they affected vitally the results at which we arrived.

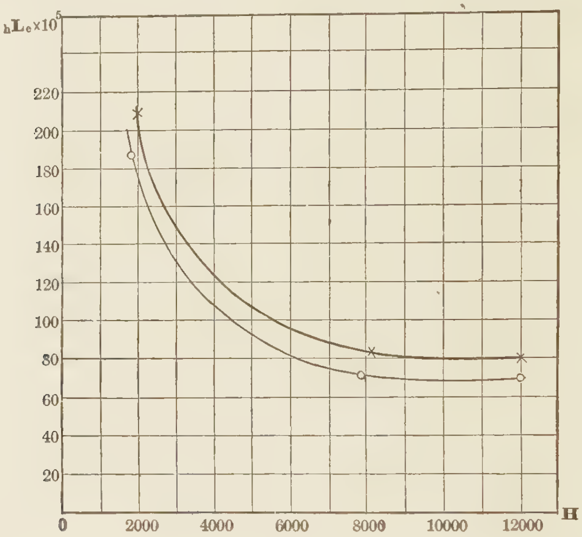

FIGURE 14.

Longitudinal Thermomagnetic Temperature-Difference. — With the magnetic field and the *HH* current as in Figure 3, we may look for an increase or decrease of the temperature-gradient along the plate as the result of magnetic action. This effect was looked for in Plate 1, but its existence was not proved. The method used was substantially the same as that illustrated in Figure 9 for determining a transverse temperature-difference. That is, circuits (1) and (3), acting thermo-electrically only, were set against each other, each having one coil of the galvanometer. The great initial difference of temperature between the junction (1) and the junction (3) made it necessary to place the outer junctions of the (1) circuit and of the (3) circuit in baths at different temperatures.

We thought at one time, in April, 1910, that we had found a rather large positive value for the coefficient in question, which may be defined as follows :

$$ {}_hL_h = \frac{\Delta\theta'}{d} \div \frac{d\theta}{dl}H, \tag{24} $$

$\Delta\theta'$ being the increase of temperature-difference between two points d cm. apart along the plate.

Critical examination of the case, however, showed that in using, as we must with Plate 1, iron wires connected with points (1) and (3), we had brought in a source of error so great as to make the result entirely uncertain.

We hope to try the experiment with Plate 2, using now the constantan-copper junctions (1) and (3).[20]

SUMMARY.

1. A new and descriptive nomenclature is proposed and used for the various transverse and longitudinal coefficients. (See equations (1), (2), (3), (4), (23), (24), (25), (26).) For example, the Hall-effect coefficient is called ${}_eT_e$, the initial subscript e indicating that the longitudinal current is electrical, the T indicating that the effect observed is transverse, the final subscript e indicating that this transverse effect is electrical. The Ettingshausen coefficient is called ${}_eT_h$, the Nernst coefficient ${}_hT_e$, the Leduc coefficient ${}_hT_h$. Each of the four transverse effects is called + when the current to which it gives rise in the exterior part of a transverse circuit leaves the metal plate in the direction of the "ponderomotive" force acting on this plate or in what would be the direction of this force if longitudinal heat-flow were replaced by longitudinal electric flow. This accords with the usual convention regarding the sign of the Hall effect, but is opposite to the usual convention regarding the sign of the Nernst effect.

2. Measurements of ${}_eT_e$, ${}_eT_h$, ${}_hT_e$, ${}_hT_h$, and of their temperature-coefficients through a small range, have been made in a single plate of soft iron, for which the electrical conductivity, the Thomson-effect coefficient, and the thermo-electric height relative to copper, were already well known through previous study of pieces from the same bar that furnished the plate. (See Table I.)

3. The Moreau formula ${}_eT_e \div \rho = {}_hT_e \div s$, in which ρ is the specific resistance, absolute, of the iron, and s is the number of ergs of heat-energy absorbed by ten coulombs in rising through one centigrade degree in iron (the Thomson effect), is discussed theoretically and is

---

[20] See footnote, p. 664.

tested by means of the data for iron. (See Table II.) The formula is true for one temperature, near 80° C., according to our data, but departs progressively from the truth with descent from this temperature and probably with ascent above it. Below the temperature mentioned the first member of the Moreau equation, as here given, is too small; above this temperature it is, probably, too large. Hence Moreau's theory, which would account for the Hall effect by a deformation of the plate under magnetic action (this deformation producing a real rotation of the equipotential lines of the longitudinal electric current), and would account for the Nernst effect as a like and equal rotation of the Thomson-effect equipotential lines of a longitudinal temperature-flow, appears to be ill-founded and, if taken literally, unsafe, though it is likely to be useful in a suggestive way.

4. Following the suggestion of the Moreau formula, we tested the equation ${}_eT_e \div \rho = {}_hT_h$ for various temperatures, to see whether the isothermal lines of the longitudinal temperature-flow are, in a field of given strength, rotated in the same direction and to the same extent as the equipotential lines of a longitudinal electric flow. (See Table III.) The direction is the same in the two cases, but the equipotential lines are, according to this test, rotated about one and a quarter times as far as the isothermal lines, this ratio remaining nearly constant through the whole range of temperature considered, 20° to 100°. (See Table IV.)

5. "Rotation" cannot account for the Ettingshausen effect, since there is no corresponding longitudinal condition to be rotated, none, that is, which can be regarded as adequate to produce the observed transverse effect. On the other hand, the ratio of the Hall transverse potential-gradient to the Ettingshausen transverse temperature-gradient appears to be almost strictly proportional, through a considerable range of temperature, to the Thomson effect s. Thus we have, approximately, ${}_eT_e \div {}_eT_h = 200\, s$, from 20° to 80° or higher. (See Table V.) It should be said, however, that the temperature-coefficient of ${}_eT_h$ cannot be regarded as accurately known. The suggestion is made that the transverse potential-gradient, which is like the Thomson-effect potential-gradient in being *static* (not attended by flow down the gradient), may be the cause of the transverse temperature-gradient, whereas in the Thomson effect the temperature-gradient causes the potential-gradient. It seems likely that the electron theory must here be used, but the attempt is not made in this paper.

6. The Voigt formula ${}_eT_e \div \rho = {}_hT_e \div \Theta'$, in which Θ', the "thermo-electric height" of lead relative to the metal, takes the place of the Thomson effect s of the Moreau formula, is considered. The iron here

studied has never been tested against lead directly, but from Matthiessen's value of the thermo-electric height of "galvanoplastic" copper relative to lead, and from the known thermo-electric height of this iron relative to copper wire of the present day, values of Θ' have been estimated for various temperatures, from 20° to 100°. With these values of Θ', and with values of the other factors taken from or reckoned from direct observations on the iron here studied, the Voigt formula has been tested. (See Table VII.) Like the Moreau formula, it seems to be correct at one temperature, between 80° and 90°, and to be untrue at other temperatures. Unlike the Moreau formula, it fails because the left-hand member is too large below this particular temperature. No constant added to the value of Θ' would make the formula hold true with varying temperature. In this connection it is pointed out that, the ordinary thermo-electric diagram being merely a temperature-entropy diagram (with the temperature-axis horizontal and the entropy-axis vertical, unfortunately contrary to the familiar custom of ordinary thermodynamics), thermo-electric heights are merely entropy-differences. Accordingly, Voigt's Θ', the thermo-electric height of lead relative to any metal, cannot be regarded as a fundamental datum for the metal; for certainly we cannot suppose the entropy of electricity to be zero in lead, as we know there are metals which have a negative thermo-electric height, a negative electric entropy, relative to lead.

7. A thermo-electric diagram is given for copper and iron in which the temperature-axis is made vertical and the entropy-axis horizontal. This diagram shows graphically, by curvature of the iron-line, the law of change of the Thomson-effect coefficient with change of temperature, which law was in an earlier paper expressed algebraically. (See Figure 12.)

8. The longitudinal effect which is shown as a change of resistance of the iron plate by magnetization in the direction of its thickness, the coefficient of which effect is called ${}_{e}L_{e}$, was observed in two iron plates, one cut with its width parallel to the fibres, or grain, of the iron, the other with its length parallel to these fibres. In the former plate there was a very slight *increase* of resistance in a field of 10,700 absolute units, in the latter a still slighter *decrease* of resistance in a field of 5400.

9. The longitudinal effect which is shown as a change of longitudinal potential-gradient, due to magnetization in the direction of the thickness of the plate, in a plate along which a heat-current is flowing, was observed in one of the plates mentioned in (8), the one first described there. It was not looked for in the other plate. The coefficient of this effect is called ${}_{h}L_{e}$. (See equation (25).) According to Zahn, who quotes Houllevigue and Moreau as authorities, the potential-

gradient established in iron by magnetic action is in the same direction as the temperature-gradient in comparatively weak fields, up to perhaps 9000, but is in the opposite direction in stronger fields. In the iron here studied the potential-gradient produced by the magnetization is in the same direction as the temperature-gradient all the way from a field-strength of 1900, the lowest tried, to 12000, the highest tried, though the coefficient ${}_hL_e$ is much larger for weak fields than for strong fields (see Figure 14).

10. The other two longitudinal effects, the coefficients of which may be called ${}_eL_h$ and ${}_hL_h$, were looked for diligently in one plate, but their existence there was not proven.[21]

THE JEFFERSON PHYSICAL LABORATORY,
CAMBRIDGE, MASS.

Postscript added March 11, 1911. — The objection which we have made to the use of Θ'_m, the "thermo-electric height" of lead with respect to any metal m, as a fundamental property of the metal m, seems to me so plain that I have been at great pains to make sure that we have not fallen into some gross blunder of interpretation of Voigt's theory. There can be no question, however, that Moreau takes Voigt's Θ'_m in this way, and I have seen no protest against his doing so. There is possibly room for doubt as to whether Voigt had *lead* in mind or some other, unnamed, material of zero Thomson effect, with reference to which his Θ'_m is to be reckoned, but this question is of little importance.

Apparently Moreau does not criticise Voigt's theoretical discussion. He seems merely to point out that it is different from his own, and to test each empirically by means of data which he has taken from various sources. He says, "I consider a circuit [*chaine*] formed by a metal M and lead, the junctions being at different temperatures. At a point (x, y, z) of M, if X, Y, Z are the components of the thermo-electric electromotive force per unit of length, one has, according to M. Voigt,

$$X = \Theta' \frac{\partial T}{\partial x}, \quad Y = \Theta' \frac{\partial T}{\partial y}, \quad Z = \Theta' \frac{\partial T}{\partial z}, \quad \text{where } \Theta' = \frac{\partial \Theta}{\partial T}. \qquad (1)$$

Θ is a function of the absolute temperature T, and is characteristic of the metal M."

"Let us suppose that a thin slice of the metal M is placed in a magnetic field H, perpendicular to the lines of force, the plane XY coinciding with the plane of the slice, which will be traversed by a current of heat going in the direction OY. Equations (1) give

---

[21] It now appears that magnetization parallel to the thickness decreases notably the longitudinal temperature-gradient in Plate 2. March 11, 1911.

$$X-0, \qquad Y=\Theta'_m\frac{\partial T}{\partial Y}, \qquad Z=0.$$

"M. Voigt supposes that the force Y turns under the action of the field as the electromotive force of the primary current in the Hall phenomenon turns. One obtains, then, along the axis OX, a transverse electromotive force X, which, referred to the unit of length, is

$$X_1=-\frac{C}{\rho}\Theta'_m\frac{\partial T}{\partial y}H$$

(where C is the Hall coefficient, ρ the resistivity of the metal), or, according to equation (3) $[\Phi=\Theta'_m]$,

$$X_1=-\frac{C}{\rho}\Phi\frac{\partial T}{\partial y}H. \tag{4}$$

"This formula (4) gives the thermo-electric effect according to M. Voigt."

We thus get as the expression, according to Voigt, for K, the Nernst coefficient,

$$K^{22}=X_1\div\frac{\partial T}{\partial y}H=-\frac{C}{\rho}\Phi,$$

and this is the expression which Moreau tests by means of data which he gives. For example, he gives the value of Φ as -1619 for iron and -152 for copper, evidently taking Φ as the thermo-electric height of *lead with respect to* the other metals.

As to his own formula for K, Moreau says, contrasting his point of view with that of Voigt, "By assuming that, *only*, the thermo-electric electromotive forces relative to the Thomson effect turn under the action of the field, I have obtained the formula

---

[22] Moreau does not expressly say that $K=-\frac{C}{\rho}\Phi$ according to Voigt. He does, however, put the values of $-\frac{C}{\rho}\Phi$ alongside his own values of K for comparison. Moreau may have been in doubt as to the sign of the Voigt formula.

$$X_2 = KH\frac{\partial T}{\partial y}, \qquad \text{or} \qquad K = \frac{\sigma C}{\rho},$$

σ being the specific heat of electricity."

Moreau, then, seems to admit that Voigt's Y is a real thermo-electric force,

$$\frac{\partial \Theta_m}{\partial T}\frac{\partial T}{\partial y}, \qquad \text{or} \qquad \frac{\partial \Theta}{\partial y},$$

directed along the Y-axis at any point in the metal M, though not the force which he considers significant in the Nernst effect. But it seems to me that this supposed total electromotive force at any point in the metal M is a fiction. The only electromotive forces which we have reason to suppose existing in an unequally heated piece of metal *in open circuit*, as a metal is when tested for the Nernst effect, are those found in the Thomson effect. When we have two unequally heated metals united in a thermo-electric circuit, the total electromotive force at any point in either metal is likely to be something different from that which the Thomson effect alone at that point would account for, but we have no sufficient reason for supposing it to be actually the $\frac{\partial \Theta_m}{\partial T}\frac{\partial T}{\partial y}$ mentioned above. If, for example, we are considering iron and if, for simplicity, we assume that $\partial T/\partial y = 1$, the thermo-electric e. m. f. in the iron at temperature T is, according to Voigt, represented by the length of the line TI, taken as a negative quantity, in Figure 11 of our paper. Now it is true that, if we make this assumption and then integrate around the whole circuit, which we will suppose to be of copper and iron, we shall get the area $C_0CII_0C_0$ as the total e. m. f. of the circuit, which result will be correct. But we should arrive at precisely the same correct integral result if we placed the T_0T line of Figure 11 indefinitely far to the left or to the right of its present position, which would have the effect of increasing or decreasing indefinitely the value of the expression $\partial\Theta_m/\partial T$, the supposed force at any individual point in either metal. I can see, then, no objective reality in Voigt's supposed force Y.

Moreau was, I think, the first to put Voigt's formula for the value of the Nernst coefficient to the numerical test. He gives,[23] the three bottom lines being from his own observations,

---

[23] C. R., **130**, 564 (1900).

	C_{20}. (Nernst.)	Φ_{20}.	$-\frac{C}{\rho}\Phi_{20}$.	$K = \frac{\sigma C}{\rho}$.	K (obs.). (Nernst.)	[σ_{20}.[24]]
Bismuth	−10.1	+8800 or +6400	+0.337 or +0.246	+0.149	+0.196	−1875
Antimony	+0.192	−2240	+0.0097	+0.0090	+0.0094	+2074
Nickel	−0.024	+2280	+0.0039	+0.0026	+0.0073	−1482
Cobalt	+0.0046	+2200	−0.00094	−0.00175	+0.00154	−4073
Iron	+0.0113	−1619	+0.0018	−0.00156	−0.00156	−1412
Steel	+0.0175	−1731	+0.00114	−0.00062	−0.00060	− 952
Copper	−0.00052	−152	−0.000047	−0.000084	−0.000073	+ 275
Zinc	−0.00041	−279	−0.000018	−0.000046	−0.000054	+ 697
	C_0.	Φ_0.	$-\frac{C_0}{\rho_0}\Phi_0$.		K_0 (obs.).	
Soft iron	+0.00837	−1062	+0.000636		−0.000646	
Soft steel	+0.00662	−1351	+0.000814		−0.000596	
Cobalt	+0.00399	+1318	−0.000512		−0.00146	

It will be seen that K, which = our ${}_hT_e$ and Zahn's $-Q$, as calculated from the formula of Moreau and given in the fourth column agrees in sign with K as observed by Nernst in every case except that of cobalt, and that in this case direct observation by Moreau himself gives the same sign which his formula gives. In other words, according to Moreau his own formula gives the right sign for K in every case. Zahn, however, agrees with Nernst in his observation of the sign of the Nernst effect in cobalt.

Moreau finds the Voigt formula, or at least the expression $-\frac{C\Phi}{\rho}$, to give the same signs as his own formula in all the cases examined except those of iron and steel, but I am inclined to the opinion that he has made a mistake of sign in the use of the Voigt formula. It seems to me that the Voigt formula gives the right sign for K in iron and steel and the wrong sign in the other cases. I have not found any perfectly explicit statement by Voigt himself of the relation between the Nernst coefficient and the Hall coefficient, but I reason as follows: If we consider iron and take a case in which $\partial T/\partial y$ is positive, we have, as we saw a little distance back, Y as a negative quantity; that is, according to Voigt, there is a thermo-electric e. m. f. acting in the direction of decreasing y. But with our iron in open circuit, as it would be for the Nernst-effect observations, we have no flow of electricity along the iron, the natural thermo-electric e. m. f. being balanced, or, as Voigt says, *compensated*, by a static charge having a negative potential-gradient in the positive direction of y. If, now, we think of the magnetic field as rotating the equipotential lines of this potential-gradient in the direction of the Amperian current, as the equipotential lines of the primary electric current are rotated in the Hall effect in iron, we get what in our paper has been called, and what Moreau would call, a *negative* Nernst effect.

---

[24] C. R., **130**, 124 (1900).

According to this argument, which deals with a puzzling question and may be incorrect in its conclusion, all the signs in the third column of Moreau's table, as given above, should be changed, and in every case for which the specific heat of electricity within a metal and the thermo-electric height of the metal with respect to lead have the same sign the Moreau formula and the Voigt formula will predict opposite signs for the Nernst effect.

The Moreau formula seems to me profoundly suggestive, though not strictly correct. But the fact that the Voigt formula, which I believe to be fundamentally wrong in one of its factors, gives results numerically so like those of Moreau, and so like the values given by direct observation, is enough to warn us to be cautious in examining every theory and testing every formula relating to the matters here dealt with.

E. H. H.

Proceedings of the American Academy of Arts and Sciences.

Vol. XLVII. No. 1. — May, 1911.

CONTRIBUTIONS FROM THE JEFFERSON PHYSICAL LABORATORY, HARVARD UNIVERSITY.

AN INVESTIGATION OF THE ERRORS IN COOLING CURVES AND METHODS FOR AVOIDING THESE ERRORS; ALSO A NEW FORM OF CRUCIBLE.

By Harvey C. Hayes.

With Six Plates.

Investigations on Light and Heat published with Aid from the Rumford Fund.

CONTRIBUTIONS FROM THE JEFFERSON PHYSICAL
LABORATORY, HARVARD UNIVERSITY.

AN INVESTIGATION OF THE ERRORS IN COOLING CURVES AND METHODS FOR AVOIDING THESE ERRORS; ALSO A NEW FORM OF CRUCIBLE.

By Harvey C. Hayes.

Presented by John Trowbridge, February 8, 1911. Received December 29, 1910.

Two main difficulties are encountered by one who attempts to make an accurate study of the physical properties of alloys. The first difficulty is the preparation of an alloy which shall contain only the desired elements in its make-up. Foreign elements may enter the alloy through lack of purity in the component metals (and the difficulty of getting chemically pure metals is never appreciated until one has attempted it), also impurities are almost sure to get into the alloy from the crucible. The chemist can, with sufficient pains, prepare pure samples of nearly all the metals; but thus far science has not produced a crucible that will keep them pure while melting them into an alloy. Impurities from this source have been a hindrance to the study of alloys, especially a study of their magnetic properties, and have been a cause for more or less error in the work that has thus far been done.

Roberts-Austen, in his classic experiment, showed that solids diffuse, even at comparatively low temperatures. This makes doubtful the possibility of finding a crucible that will not diffuse somewhat into the alloy at such a temperature as the melting point of most metals. One solid that does not seem to diffuse into metals, and apparently the only one that does not, is quicklime. A block of lime with a hollow scooped out ofttimes serves the chemist for a crucible, for all that he requires of a crucible is that it shall hold together long enough to melt a small portion of metal and then slowly cool. But for the study of alloys such a crucible will not suffice, as it is often necessary to chill the melt. A block of lime will not stand such treatment; and even if it would, the lime is so poor a conductor of heat that it would be impossible to chill an alloy through the comparatively thick walls of such a crucible.

The crucible. — The ideal crucible for work on alloys would be one made from thin metal, if we could find some metal that would not diffuse, for we could then readily study the effects of chilling, as the crucible would be a good heat conductor. But since all metals diffuse, even in the solid state, we cannot hope for such a crucible. The best substitute would be one made from thin metal and lined with a thin coating of lime.

The need for such a crucible has been felt by all who have attempted to make anything like an accurate study of alloys, and attempts have been made to perfect one, but until now without success. The author has finally succeeded in lining a steel crucible with a thin coating of lime. These linings are fairly durable so long as they are kept free from moisture, but if left in a damp place the lime slacks and cracks off. With a lining two tenths of a millimeter in thickness I have made seventeen melts, each time chilling in an ice-bath, and at the end of this time the lining was almost intact.

These linings are made from a mixture of finely powdered quicklime and calcium nitrate, about four parts by weight of the lime to one by weight of the nitrate. Care must be taken that the powders are thoroughly mixed. Such a mixture fuses to solid lime when sufficient heat is applied to drive off all the nitric acid.

This last fact is not new. It is often made use of in the chemical department of Harvard University for preparing small boat-shaped crucibles suitable for melting small portions of metal. But one meets with considerable difficulty in keeping the powder in place on the steep sides of the crucible while it is being fused.

The method finally employed is to use a cylindrical-shaped crucible. This is clamped, open end outward, in the chuck of a high-speed lathe and then set spinning. The mixed powder is then carefully blown inside the crucible where the centrifugal force holds it firmly on the sides in the form of an even coating. The spinning crucible is then heated with a blast lamp until all the acid is driven off. It is then removed from the lathe, set in an upright position, and the bottom sprinkled with a coating of the powder. This is finally fused on, the force of gravity keeping the powder in place.

By this method it is possible to give the crucible a very even coating of almost any desired thickness, though the first attempts are usually discouraging. I have found it possible to chill an alloy very satisfactorily through these thin linings.

For work on weakly magnetic alloys, especially for such as fuse above eight hundred degrees centigrade, a factor of safety is added by using for the crucible some weakly magnetic metal such as platinum, as traces of the crucible might diffuse through the thin porous linings: but with linings two millimeters or more in thickness there can be little or no danger from this source.

The perfection of this crucible now makes it possible to prepare an alloy of definite constitution, and this removes one of the main difficulties in the study of alloys.

Investigation of the Errors in Cooling Curves.

More information concerning an alloy can be had from its cooling curve than from any other one source, providing the cooling curve is accurate; and more information can be had from the temperature-time curve than from any other of the various forms. The difficulty of getting such curves is not great providing the cooling is slow; but when one attempts to take a curve for rapid cooling or chilling numerous difficulties arise. The remainder of this paper is devoted to a consideration of these difficulties, the errors that as a result have crept into some of the work on metals, and methods for overcoming these difficulties.

The errors. — The difficulties that arise when one attempts to take a cooling curve where the cooling is rapid, and the errors that arise therefrom, are due to temperature lag and lag in the galvanometer. Temperature lag takes place through the protection tube, through imperfect contact between the tube and the enclosed thermo-couple, and finally through the couple itself. Lag in the galvanometer is a function of the period of this instrument, probably nearly proportional to the period. This lag, which for simplicity will be called the electrical lag, can be almost entirely eliminated by using an Einthoven form of galvanometer (a fine conducting filament suspended in a strong magnetic field), for here the inertia of the moving parts is reduced to a minimum, and the period can be made very short without great loss of sensitiveness. By thus eliminating the electrical lag, I have been able to study the temperature lag in its various phases. The work has been carried out in much the following order:

a. Lag due to all three causes, — tube lag, contact lag, and lag in the junction.

b. Contact lag and lag in the junction.

c. Lag in the junction itself.

Method. — The apparatus used in this work, which is described in detail farther on, consisted essentially of an Einthoven galvanometer with a commutator arrangement, such that this instrument could be thrown in series with either of two thermo-couples. These couples were made of copper against constantan, and were so arranged that one gave the temperature just outside the protection tube, while the other gave the temperature from the inside after the usual manner.

Arrangement of thermo-couples. — The arrangement of these junctions was as follows: A cylindrical copper block five inches long and three inches in diameter had two holes, each three inches deep, drilled symmetrically in one end. A constantan wire was fused to the bottom of one hole, thus forming a junction with the copper block as one element. This couple gave at all times the temperature of that portion of the block which formed the bottom of the hole. Moreover, since the two holes were symmetrically placed and the cooling was made symmetrical, this junction gave the temperature at the bottom of the other hole.

In this second hole an ordinary protection tube was placed with a copper-constantan junction inside. The protection tube was surrounded with a thin film of lead, so that the tube experienced the same external conditions that are met with in taking the cooling curve of a molten metal or alloy. A protection tube open at the end was placed in the hole first mentioned, so that the heat capacity of the two holes should be the same.

Because of its short period — less than one fiftieth of a second — it was possible to alternate the galvanometer rapidly between the two thermo-couples. For most work, however, an alternation of about once a second was found satisfactory.

The cold junction of each couple was kept at the temperature of melting ice, so the deflection of the fiber in the galvanometer was always proportional to the temperature of the hot junction of the couple with which it was in series. This deflection was photographed on a sensitive film which was rotated on the drum of a chronograph. In this way it was possible to photograph on the same film the two curves, one giving the temperature just outside the protection tube, and the other giving the temperature inside the tube, according to the usual manner. These curves were traced by a succession of fine dots, but the alternations were so rapid that in the case of slow cooling the curves appear as an unbroken line. These curves had millivolts for ordinates and time for abscissae, and the apparatus was so arranged that these coördinates were photographed on the film. The difference in height between the two curves at any instant was evidently a measure of the temperature lag due to all three causes, — tube lag, contact lag, and lag in the junction; but thus far there was nothing to indicate what part of this lag was due to each of the three causes.

The curves of the annexed plates, reproduced from the actual photographs, show this lag for both quartz and porcelain protection tubes for different rates of cooling. These curves are reduced to one fifth the original size. The highest temperature in each case was about 550 degrees centigrade.

Similarity of the thermo-couples and calibration. — Curve 1, Plate **1**, which traverses the sheet four times, due to four revolutions of the drum, was taken at a very slow rate of cooling, the time of exposure being about four hours. In place of the ordinary protection tube closed at the end, the tube used in this case was open at the lower end except for a thin film of mica. Here the temperature lag between the two junctions must have been practically zero, because of the slow rate of cooling and because of the thinness of the film separating them. The curve, which is in reality double, shows that the two couples were practically identical throughout the temperature range covered.

A calibration curve for one of these couples was obtained by taking the melting points of pure tin, lead, zinc, and aluminum, also the boiling point of water. These results are given in Table I.

TABLE I.

	Temperature. Deg. Centigrade.	Millivolts (obs.).	Millivolts (calc.).
Boiling water	100	3.85	3.85
Melting tin	232	9.70	9.65
Melting lead	327	14.15	14.19
Melting zinc	419	19.40	19.34
Melting aluminum	657	33.70	33.70

The third column, marked Millivolts (calc.), was obtained by applying the well-known formula connecting temperature and electromotive force,

$$E = a\Theta + b\Theta^2.$$

Here E is the e. m. f. in millivolts and Θ is in degrees centigrade. Substituting in this equation the values of E and Θ, as found for boiling water and melting Al, the values of a and b were found to be 0.0362 and 0.0000229 respectively; and since the variation between the observed and calculated results lies within the limit of error, the curve

$$E = 0.0362\,\Theta + 0.0000229\,\Theta^2$$

has been taken as the calibration curve for the two junctions.

Referring to this formula, it is comparatively easy to find the difference in temperature between the two junctions at any instant during the cooling. Let E_1 be the e. m. f. of the junction within the protection tube, and Θ_1 be the temperature of that junction. Let E_2 and Θ_2 be the e. m. f. and temperature respectively of the other junction at the same instant. Then

$$(\Theta_1 - \Theta_2) = (\sqrt{4bE_1 + a^2} - \sqrt{4bE_2 + a^2})/2b,$$

the maximum temperature lag through quartz and porcelain protection tubes for different rates of cooling, is given in Table II. This is computed from the curves of the accompanying plate (Plates **1** to **6**).

TABLE II.

Quartz.		Porcelain.		
Data of Curve No.	Lag.	Data of Curve No.	Lag.	Time Coördinates. One Division equals
2 Plate **1**	13 deg.	2a Plate **2**	49 deg.	30 sec.
3 Plate **2**	45 "	3a Plate **2**	118 "	15 "
4 Plate **3**	80 "	4a Plate **3**	190 "	10 "
5 Plate **3**	179 "	5a Plate **4**	355 "	5 "
6 Plate **4**	270 "	6a Plate **4**	480 "	3 "

No simple relation between the two curves. — These results show that the error in the cooling curve as usually taken (i. e. by means of a thermo-couple placed inside a protection tube) is large, especially if the rate of cooling is at all large. The question then arises : Is it possible to find a relation between the correct curve and the incorrect curve such that the correct curve can be obtained from the incorrect one, i. e. from the curve taken. Curve 8 (Plate **5**) enables us to answer this question.

In taking this curve, time coördinates of which were three seconds for one space, the copper block was first dipped for an instant to a depth of two inches in ice-water, then removed, then redipped, then removed, etc. The lower line, which is very irregular, as we should expect, is the correct cooling curve. The upper one is the curve obtained by the ordinary method, a junction inside a protection tube. The relation between the two curves is far from simple, and any formula giving this relation must needs be complicated. Thus far no formula has been found.

Incorrect curve may give correct temperature of transformation. — Much of the information, however, that comes from a cooling curve can be had from a curve that is not absolutely correct ; for this information comes from the irregularities of the curve, not from the regular parts. In general, any change in the constitution of a metal is accompanied by a liberation or absorption of heat, thereby causing a kink in the cooling curve. How erroneous can the cooling curve be and still give the temperature of transformation with considerable accuracy?

For simplicity, let us take the case of finding the melting point of a pure metal. In this case the cooling curve for that portion of time in which transformation takes place is a straight line parallel to the time axis. In Figure 1 let the line *abc′d* represent the true cooling curve, while line *abc* represents the cooling curve if no transformation takes place. Let the line *ab′c′d′* represent the cooling curve given by the couple inside the protection tube, and the line *ab′e′* the corresponding curve if no transformation takes place. Then the temperature lag at the beginning of transformation is $\Theta_2 - \Theta_1$, and the corresponding time lag is $t_2 - t_1$. The time through which transformation takes place is $t_0 - t_1$, while $\Theta_1 - \Theta_0$ is the number of degrees through which the melt would cool if no transformation takes place.

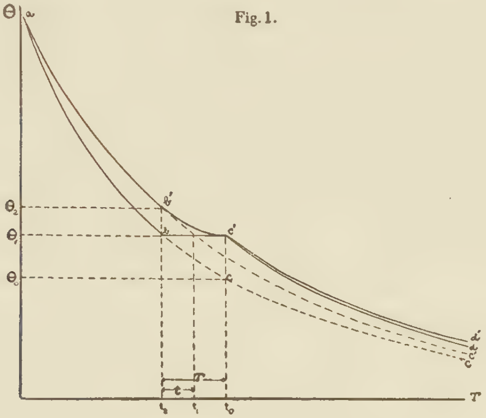
Fig. 1.

It will be seen that

$$\Theta_2 - \Theta_1 = \frac{d\Theta_2}{dT} \cdot \tfrac{1}{2}(t_2 - t_1),$$

if we assume that $\frac{1 d\Theta_2}{2 dT}$ is the averate rate of cooling during the period required for Θ to drop to the temperature of transformation, and that $\frac{d\Theta_2}{dT}$ is the rate of cooling at the beginning of transformation. Also,

$$M(\Theta_1 - \Theta_0) \cdot \bar{S} = ML,$$

where M is the mass in grams of the melt, $\bar{S}$ is the average specific heat, and L is the latent heat of melting. But

$$\Theta_1 - \Theta_0 = \frac{d\Theta_1}{dT} \cdot T$$

approximately, where $\frac{d\Theta_1}{dT}$ is the actual rate of cooling at the beginning of transformation. Therefore

$$\bar{S}\frac{d\Theta_1}{dT} \cdot T = L.$$

For safety,

$$2\,(t_1 - t_2) \leqq T,$$

otherwise the irregularity in Θ_2 will lie wholly above the temperature of transformation.

Therefore, for safety,

$$\bar{S}\frac{d\Theta_1}{dT} \cdot \frac{\Theta_2 - \Theta_1}{\frac{d\Theta_2}{dT}} \leqq L, \qquad \text{or} \qquad \Theta_2 - \Theta_1 \overset{=}{<} \frac{L}{\bar{S}} \cdot \frac{\frac{d\Theta_2}{dT}}{\frac{d\Theta_1}{dT}}.$$

For slow cooling $\frac{d\Theta_1}{dT} = \frac{d\Theta_2}{dT}$ approximately. Then

$$\Theta_2 - \Theta_1 \overset{=}{<} \frac{L}{\bar{S}}.$$

For rapid cooling $\frac{d\Theta_2}{dT} > \frac{d\Theta_1}{dT}$ throughout most of the temperature range covered, and our formula becomes

$$\Theta_2 - \Theta_1 << \frac{L}{\bar{S}},$$

which is meaningless.

For slow cooling, then, the cooling curve will give us the correct temperature of the melting point, providing the temperature lag is less than the ratio between the latent heat of melting and the average specific heat of the metal during the transformation. This value for the specific heat is about equal to the average between the specific heats corresponding to the liquid and solid states, and therefore in general more than the specific heat of the solid. This ratio always gives a fairly large value for $\Theta_2 - \Theta_1$, so we may be fairly sure of obtaining the correct temperature of melting, even though the temperature lag is considerable.

In general an incorrect curve gives incorrect data. — However, in the case of many transformations, such as a change of allotropy, the latent heat of transformation is small, so the ratio $L/\bar{S}$ is small, and the value of $\theta_2 - \theta_1$ must be small if the transformation temperature is to be given with accuracy. This requires that the cooling curve must be nearly correct. Yet Curve 3 shows that for comparatively slow cooling the temperature lag is 45 degrees for quartz protection tubes, and much more for porcelain tubes. The conclusion follows that the ordinary method for taking cooling curves fails to give with accuracy the temperature of such transformations as involve slight absorption or evolution of heat.

Ordinary method of correcting for temperature lag. — This error due to temperature lag has been long recognized, and the following method employed to correct it. Both a cooling and a heating curve is taken. The cooling curve gives a temperature above, while the heating curve gives a temperature below the temperature of transformation. Assuming that the rate of change of temperature is constant, and that the lag is proportional to the rate of change of temperature, then the correct temperature can be obtained as follows:

Let θ_c be the transformation temperature given by the cooling curve,
" θ_h " " " " " " heating "
" a " rate of cooling, assumed uniform,
" b " " heating, " "
" k " temperature lag for unit rate of cooling,
" θ " correct temperature of transformation.

Then

$$\theta_c = \theta + ka$$

$$\theta_h = \theta - kb$$

$$\frac{\theta - \theta_c}{\theta - \theta_h} = -\frac{a}{b}.$$

Therefore

$$\theta = \frac{b}{a+b}\theta_c + \frac{a}{a+b}\theta_h.$$

This method erroneous. — The value of this formula depends upon the correctness of the two assumptions upon which it is based. The rate of change of temperature can be regarded as fairly constant over a considerable period of time when the cooling is slow. The accuracy of the second assumption — that the temperature lag is proportional to the rate of change of temperature — can be tested by the aid of Curves 1′ and 2 (Plate 1), for we can readily find the temperature lag at any time, and also the rate of cooling, and hence the value for k.

On each of these two curves three points were chosen, and the value of $\Theta_2 - \Theta_1$, $\frac{d\Theta}{dT}$, and k computed with the following results (Table III):

TABLE III.

Curve 1′, *Plate* **1.**

Point.	$\Theta_2 - \Theta_1$.	$\frac{d\Theta}{dT}$.	k.	Difference.
1	5.25 degrees	0.373	13.9	1.3
2	3.06 "	0.201	15.2	1.6
3	2.12 "	0.128	16.8	

Curve 2, *Plate* **1.**

Point.	$\Theta_2 - \Theta_1$.	$\frac{d\Theta}{dT}$.	k.	Difference.
1	11.2 degrees	0.622	18.0	1.7
2	8.34 "	0.422	19.7	1.9
3	5.88 "	0.268	21.6	

These results show that the lag is not proportional to the rate of cooling, but that the value of k increases as the value of $d\Theta/dT$ decreases, and that this change in k is nearly linear. This increase in the value of k cannot be accounted for by the fact that the rate of cooling to the point at which the value of k was computed had not been constant but had been decreasing, so that in each case the lag was more than it would have been had the rate of cooling been constant and of the value at the point in question. The lag would be greater in proportion for the higher points as the decrease in the rate of cooling is greater for the portion of the curves before those points.

The true cause for this variation in the value for k does not concern us here. The fact is that the second assumption is not correct, and, unless the heating and cooling curves have the same slope, the formula does not give the correct value for Θ. Moreover, a comparison of the results obtained from Curves 1′ and 2 shows that even under these last named conditions the formula is not trustworthy. Curve 1′ gives a lag of 5.25 degrees centigrade for a rate of cooling of 0.373 degrees per second, while Curve 2 gives a lag of 5.88 degrees centigrade for a rate of cooling of only 0.268 degrees per second.

Contact lag is variable. — These curves were taken with the same quartz protection tube and the same thermo-couples, and the discrepancy is not due to variation in the thermo-couples, as they were tested after each curve and found to have remained constant. The variation was apparently due to change in the contact lag, and this variation is liable to occur between any two curves, as, for instance, between the heating and cooling curves used in determining Θ.

If so much variation can be due to change in the contact lag, it would seem that this lag must be great, perhaps furnishing a large part of the entire lag. A consideration of the ordinary form of thermo-junction should lead one to suspect this, even though the results obtained from Curves 1′ and 2 had not disclosed the fact.

The two elements forming the couple are usually fused together in the form of a bead nearly spherical in shape. Under the most favorable conditions this bead rests on the bottom of the protection tube, though ofttimes it takes a position as shown in Figure 2. In either case the contact between the tube and bead is imperfect. In the first case we have a point, or, at most, a very small surface of contact, and in the second case no contact at all. In the first case the junction can lose its heat by conduction and radiation, though mostly by radiation; and in the second case its heat must leave wholly by radiation. In either case it would seem that the contact lag must be large, and that it would vary with the position of the junction in the tube.

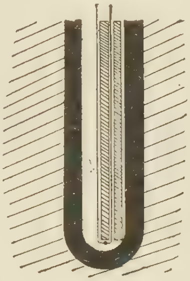
Fig. 2.

Contact lag is great. — To test out the lag due to imperfect contact between tube and junction, a protection tube open at the bottom was used. This allowed the bead of the junction to rest directly on the copper. Here the lag was due to imperfect contact and lag in the couple itself. The lag in the couple was very small, as the material of the couple was a good heat conductor, and because the heat capacity of the couple was small. Several curves were taken with this arrangement of the couples, and in each case the lag was nearly as great as that given by the ordinary arrangement with the same rate of cooling. Curve 10, Plate 5, is a typical example. Here the rate of cooling was the same as that employed in Curves 4 and 4_a.

It is to be noticed that the lag is nearly as great as that registered in Curve 4. This lag is not all due to imperfect contact and lag in the junction, for a thin film of oxide always formed on the surface of the copper, even when the surface was polished before the experiment; and this oxide is a poor heat conductor. However, the experiment gives conclusive proof that the contact lag is great.

Means for reducing this lag. — The only way to reduce this lag is to use a different form of junction. The lag can be materially reduced by pounding the bead down to a thin sheet and fitting it to the bottom of the tube; but even then the contact lag forms a large part of the total lag. A much better form of couple is one in which the tube forms one element, with the other element fused to the inside bottom of this tube.

Such a couple has been patented by C. B. Thwing, and is made by James G. Biddle, Philadelphia. This form of junction, as marketed, has the outer element and tube made thick and heavy, in order to prolong the life of the junction which comes in direct contact with the molten metal. The junction is useless for accurate work on alloys, as it contaminates the melt; but the form of the junction is correct since the tube lag is made small, the tube being a good heat conductor, and the contact lag is entirely eliminated.

Improved form of thermo-couple. — The author makes use of a couple of this form, but places a thin coating of lime on the outside of the tube to avoid contamination. The metal tube which forms one element of the junction is made very thin, thus reducing the lag in the couple itself. The tubes are deposited electrolytically on a wax form; the wire leading from the tube, and the second element leading from the bottom of the tube, having been placed in position on the wax form. These wires are thus sealed to the tube by the process of deposition. In this manner the couples can be made nearly any desired size.

The temperature lag in these junctions is reduced to a minimum. The lime coating can be made very thin, thus causing little lag through the protection tube. The contact lag is small and constant, since the whole surface of the couple is in close contact with the lime coating. Finally the lag in the junction itself is nearly zero, as the heat capacity of the junction is nearly zero.

Comparison of old and improved form. — Curve 11, Plate 5, really two separate curves on the same sheet, gives a comparison of the lag due to the two junctions. The curve on the left was taken under the most favorable conditions applicable to the ordinary method. The protection tube was made of thin quartz, and the junction rested on the bottom of the tube. The curve on the right shows the corresponding lag when the tube-form of couple is used. Here the apparent lag is more than the actual lag, as the tube couple gave a higher e. m. f. than the couple of which the copper block formed one element. The rate of cooling was the same for both curves, and was obtained by immersing the copper block in oil.

In all the curves taken, the protection tube was surrounded with a thin film of lead; yet the cooling curves, except faintly in Curve 1′, give no indication of the freezing point of the lead. This point, however, is plainly shown in the cooling curve taken with the tube-form of couple, even though the rate of cooling was high.

The fact that the heat liberated by the freezing lead causes no irregularity in the cooling curves taken by the ordinary method, leads one to believe that not only does that method fail to give the temperature of transformation with accuracy, but it may fail to give any indication of the existence of a transformation. On the other hand the possibilities of the tube-form of couple are great. These possibilities are not fully shown by Curve 11, as the junction was fairly heavy and the lime coating much thicker than necessary. With a refined couple this lag can be greatly reduced.

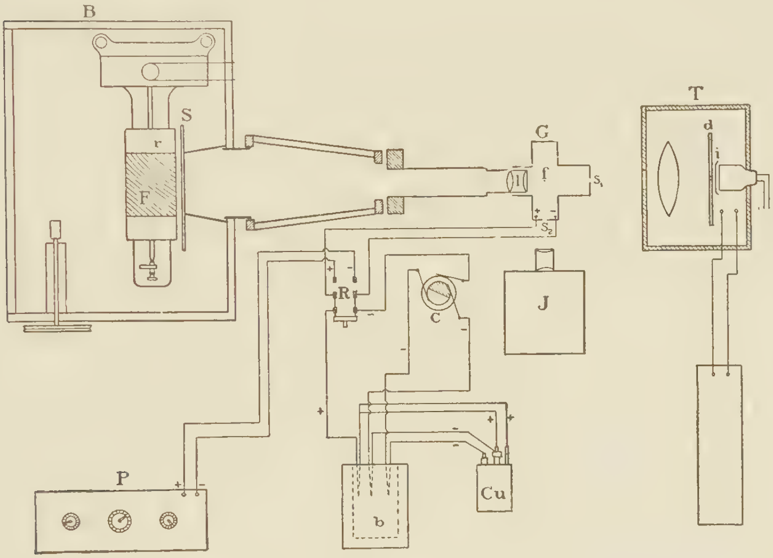

Fig. 3.

The cooling employed in taking Curve 11 was about the same that is employed in the oil-tempering of steel. At this rate of cooling a refined couple would give very little lag, and should give curves sufficiently accurate to throw considerable light on the processes of chilling and tempering.

Against the correcting for temperature lag by means of heating curve. — A study of alloys in the light of Gibb's "Phase Rule" leads one to believe that their characteristics depend greatly on their past history. Having prepared an alloy, it is doubtful if its properties will be the same after it has been remelted. It is then highly desirable that the cooling curve be correct as first taken. The usual method requires the taking of the heating curve, i. e. the remelting of the alloy, in order that we may apply an incorrect formula to give us the temperature of such transformations as are registered on these insensitive curves. This method is cumbersome and, unless the rate of cooling is very slow, is inaccurate. And when we have taken the heating and cooling curves and found the so-called temperature of transformation, it is a question as to what alloy the data belongs.

The tube-form of couple makes it possible to take an accurate cooling curve for slow rates of cooling, and even such rates as are employed in tempering can be taken with a fair degree of accuracy. Thus the second main difficulty in the study of alloys is largely removed.

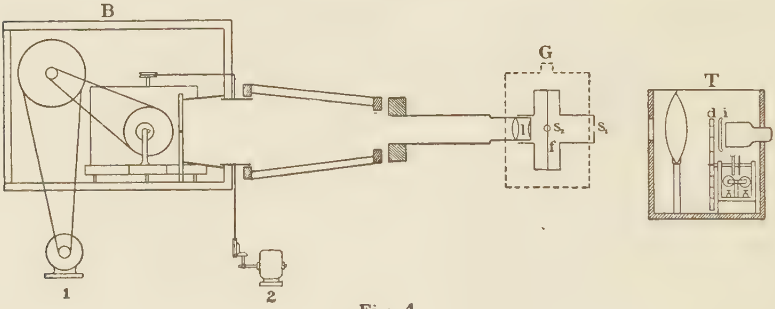

Fig. 4.

Description of the Apparatus.

The recording device. — Figures 3 and 4 represent a top and side view, respectively, of the recording part of the apparatus. A simplified form of Einthoven galvanometer G, in circuit with a thermo-couple, gives the difference in temperature between the hot and cold junction. An ordinary projecting lantern J throws a beam of light through S_2 and illuminates the filament *f* of the galvanometer. By means of the lenses *l*, the light from the filament is focussed on the drum *r* of a chronograph. The screen S carries a narrow slit parallel to the axis of the drum, and thus allows only a spot of light to reach the sensitive film F which is fastened about the drum. A variation in the temperature of the hot junction causes the spot of light to move along the drum in a direction parallel to its axis. If such a movement takes place while the drum rotates, a curve is photographed on the film, the coördinates of which are temperature and time.

Placing the time coördinates. — The chronograph is so arranged that it can be run with either of two motors 1 or 2 (Figure 4). One-tenth horse power A. C. motors are used for this work, as they give to the drum a more uniform rotation than the ordinary clockwork arrangement. Motor 2 is connected to a variable gear, such that the time of rotation for the drum can be varied from forty seconds to two hours. This motor is used to turn the drum whenever a cooling curve is being photographed, the gearing always being so adjusted that the drum rotates about once while the cooling takes place. Box T contains an arrangement for throwing a periodic flash through S_1 of the galvanometer. This light finally passes through the slit in the screen and gives a fine white line on the film. If the drum rotates uniformly and the flashes occur at the end of equal periods of time, and if at the same time a curve is traced by the spot of light coming from the filament, we should have, upon developing the film, a temperature vs. time curve with the time coördinates drawn.

Placing the e. m. f. coördinates. — By means of the double switch R a potentiometer P can be thrown into circuit with the galvanometer, and this instrument can then be made to register millivolts. This arrangement makes it possible to place electromotive force coördinates, on the film. First rotate the drum with no e. m. f. through the galvanometer. The spot of light then traces the zero line on the film. Then repeat this operation for each millivolt, or whatever increment of e. m. f. is desired, until the range of e. m. f. covered by the thermocouple is passed. For this work motor 2 is used, as the gearing here is such that the drum rotates about once in ten seconds.

In order that these coördinates should have the same intensity as the curve, the time of exposure should be the same. This causes a great loss of time, as the period of rotation for the drum is more than one hour when the cooling is slow. This waste of time is avoided by widening the slit S while these coördinates are being made. By making the slit one millimeter wide, the time required for recording one coördinate line is about ten seconds. Thus the total time required for adding the e. m. f. coördinates to one of the curves of this paper is about ten minutes. This method for adding the e. m. f. coördinates amounts to calibrating the galvanometer for each curve, so that the results are largely insured against variation in the galvanometer.

This recording apparatus is essentially the same as that devised by Einthoven and described at length in Annalen der Physik, 1903, Vierte Folge, Band 12. It is without doubt the best form thus far devised for recording rapid cooling, but the expense of the apparatus has tended to prohibit its general use. It therefore seems desirable to describe briefly the simplified form used in this work. Only ordinary ingenuity is required for its construction, and the cost is comparatively small.

The galvanometer. — Figure 5 shows the construction of the galvanometer. The magnetic field is furnished by eight cast-iron ring magnets, arranged in two sections of four. One section is placed above the focussing lenses l, and the other section directly beneath this. A thin brass chamber fitted between the jaws of the compound magnet carries the filament, a platinum fiber about one ten-thousandths of an inch in diameter. These three pieces, with some simple device for varying the tension on the fiber, completes the galvanometer.

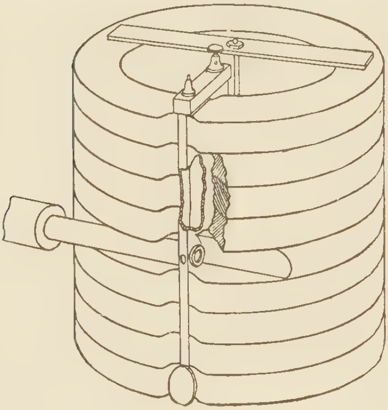

Fig. 5.

Periodic flashes for giving time coördinates. — Figures 6 and 7 show in some detail the mechanism employed for giving periodic flashes. Two rachet wheels, each carrying sixty teeth, are fastened rigidly to an axle (Figure 7). A double electromagnet *m* attracts the armature *a* and causes the clutch *x* to turn the axle. Clutch *y* is so adjusted that the rotation is allowed to proceed only a distance of one tooth. So long as the current continues through *m* the axle is held firmly in position; but whenever this current is broken the armature is pulled back by spring *s* so that clutch *x* falls behind another tooth. Upon making the circuit again, the axle is again rotated a distance of one tooth. A relay operated by a separate circuit is so connected into the circuit which traverses the magnet *m*, that when its armature is back the circuit is made through *m*. The relay is operated by a circuit that is made for an instant once a second, a seconds pendulum being used for accomplishing this. Thus the circuit *m* is broken for an instant once a second, and the axle, therefore, is rotated one division every second.

A thin aluminium disk twenty centimeters in diameter is clamped to the end of the axle by means of a thum-screw. Narrow slits are cut radially into the edge of the disc as shown in Figure 7. This disc is interposed between a Nernst glower and slit S_1 of the galvanometer. Figure 4. An iron screen *i* before the glower allows only a narrow beam of light to fall upon the disc; and whenever a slit in the disc moves across this beam of light a momentary flash passes into S_1. By varying the number of slits in the disc, the period between flashes can be made nearly any length between one second and one minute.

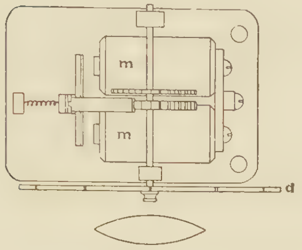

Fig. 6.

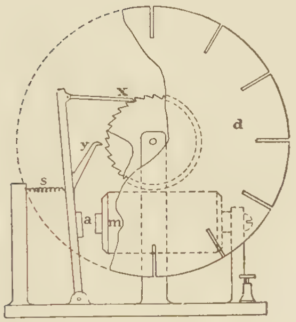

Fig. 7.

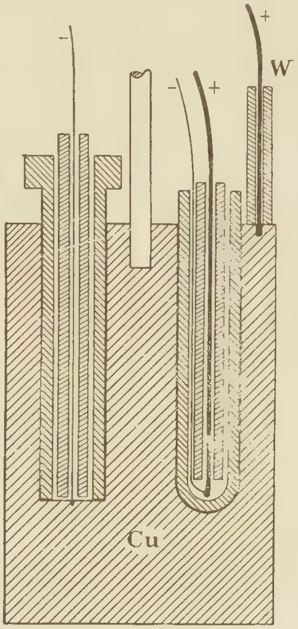

Fig. 8.

THE HEATING PART OF THE APPARATUS.

The copper block and thermo-couples. — The heating part of the apparatus may be briefly described with the aid of Figures 8 and 9. Figure 8 represents the cross-section of a copper cylinder five inches long and three inches in diameter. Two holes, each three inches deep, are symmetrically drilled in the top of the cylinder. These holes have a diameter nearly one millimeter greater than the diameter of the protection tube to be experimented upon. A protection tube is placed in each of the holes in order that the heat capacity may be the same for each. One of these tubes is closed at the lower end and the other one left open. Within the closed tube an ordinary copper-constantan junction is placed, and a constantan wire is passed through the open tube and fused to the copper block. A copper wire *w* is fused to the top of the copper block, and protected from the hot gases of the furnace by means of a short porcelain tube. The space between the closed tube and the copper block is filled with lead. Thus the closed tube experiences the same conditions that are met with in taking an ordinary cooling curve for a molten metal or alloy.

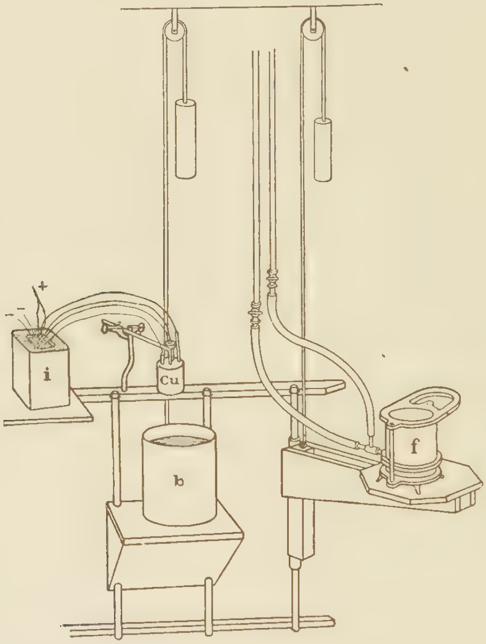

Fig. 9.

The commutator. — The commutator arrangement, by means of which the two thermo-junctions are alternately thrown in series with the galvanometer, is shown in *c*, Figure 3. It might be added that several curves could be photographed on the film by simply changing the form of the commutator. The alternations were about once a second throughout this work, but the period of the galvanometer was only one fiftieth of a second, and the damping very rapid, so that as many as five alternations per second could be made. This means that at least ten such curves could be placed on the same film, and even a greater number when the rate of cooling is slow.

Copper-constantan couples were used throughout this work, principally for the reason that it made possible the use of a copper block. Several reasons made it desirable to use copper. The copper has no transition points in the temperature range covered, so the cooling curves would have no irregularities due to such transitions. Copper being an excellent heat conductor, the temperature at the bottom of the two holes will be nearly the same, even if there are some slight irregularities in the cooling at the surface. Copper and lead is one of the few combinations of metals that do not alloy more or less readily. Lastly, copper against constantan makes a thermo-couple that gives a high thermo-electromotive force.

Validity of the method employed for determining the lag through the protection tube, etc. — Since the validity of this whole paper depends on the condition that the temperature at the bottom of the two holes shall be the same at all times, numerous tests were made to see if this condition were fulfilled. To test this condition, a constantan wire was fused to the bottom of each hole in the block, and the two curves giving the temperature at the bottom of each of the two holes were taken for various rates of cooling. These curves overlapped in nearly all cases, the variation scarcely ever being more than the width of the line. Curve 14, Plate 6, gives such a set of curves for rapid cooling. The curves show the temperature variation between the two junctions at its greatest. On this curve, one space on the time axis represents three seconds.

It might be urged that a large portion of the lag recorded in all cases was due to lag through the lead film which surrounded the tube. Curve 13 (Plate 6), a curve resulting from an accident, offsets this argument. Just after the cooling had started, the tube broke and allowed the lead to come in contact with the junction. This break occurred when the temperature of the block was only a little above the melting-point of the lead. After the experiment was over, the bead of the junction was found about half imbedded in the lead. The cooling here was rapid, having been caused by dipping the copper block in ice-water. The irregularities in the curve, and probably the breaking of the tube, were caused by the water boiling over on the top of the block. Despite this, however, the curves coincide throughout most of their length. This proves conclusively that there was little lag through the lead film.

Furnace and cooling bath arrangement. — Figure 9 shows the arrangement for heating and cooling the copper block. Because of the presence of the thermo-couples it was difficult to move the block from the furnace to the cooling bath. This difficulty was avoided by counterpoising the furnace and bath so that either could be brought to the block. The cooling bath was arranged to slide up and down, being guided in this movement by two vertical rods. The depth to which the block was submerged was regulated by fastening a clamp on one of the guiding rods. The furnace was counterpoised on an arm which could turn about a single guiding rod and thus be brought beneath the block. With this arrangement, the block could be transferred from the furnace to the bath as quickly as it could if the block were movable. The cold junction of both couples were kept at the temperature of melting ice by means of an ice-bath *i*, Figure 9.

Variation in the rate of cooling. — Variation in the rate of cooling was provided as follows: For rapid cooling, the block of copper was surrounded by ice-water to within one centimeter of the top. For the next slower rate the block was dipped in warm water to a depth of one centimeter. The next slower rate was obtained by surrounding the block with oil. A still slower rate was given by setting the copper block on a block of iron that was surrounded by water. The next slower rate was given by allowing the block to cool in air. Finally, the slowest rate was obtained by allowing the block to cool in the furnace. The rate of cooling was thus varied from about half a minute to over two hours.

Need for the research recorded in this paper became apparent to the author upon attempting to study the magnetic properties of some weakly magnetic alloys. The two difficulties which the paper discusses were at once encountered, and had to be overcome before the work could proceed. These difficulties have been largely overcome, and the road now seems to be fairly clear to a large and much neglected field of research.

Jefferson Physical Laboratory
Cambridge, Mass.

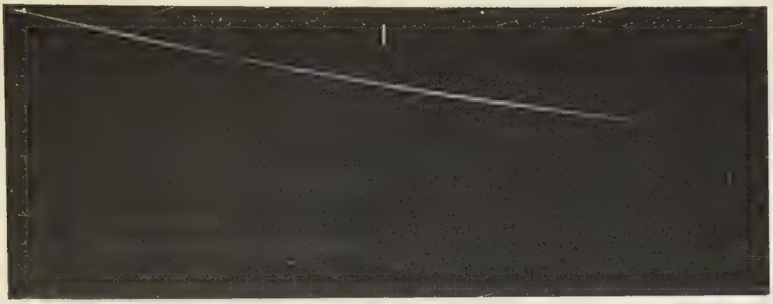
1

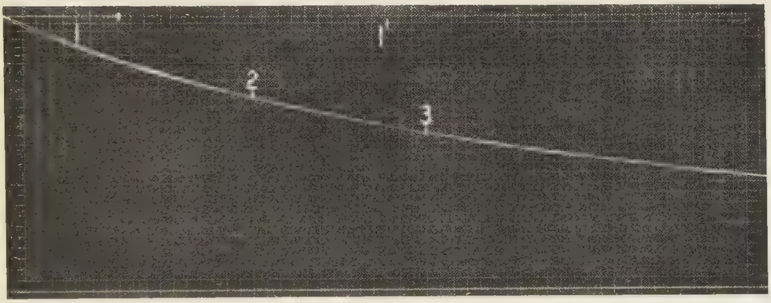
1
1'
2
3

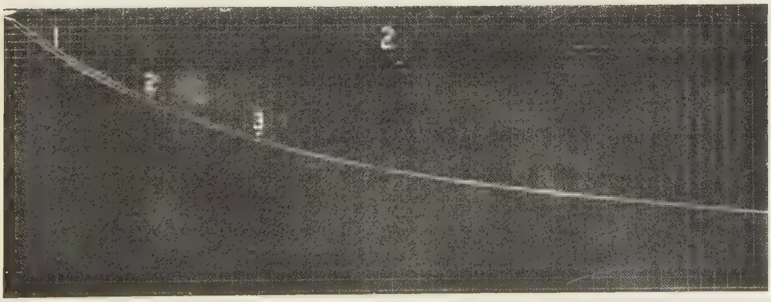
1
2
2
3

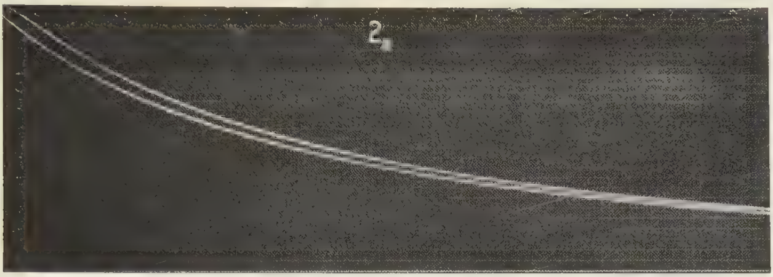
2_1

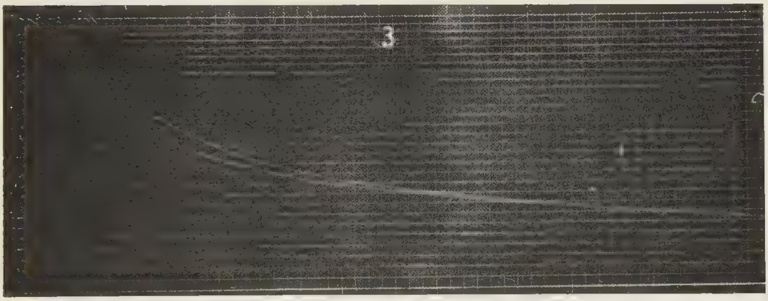
3

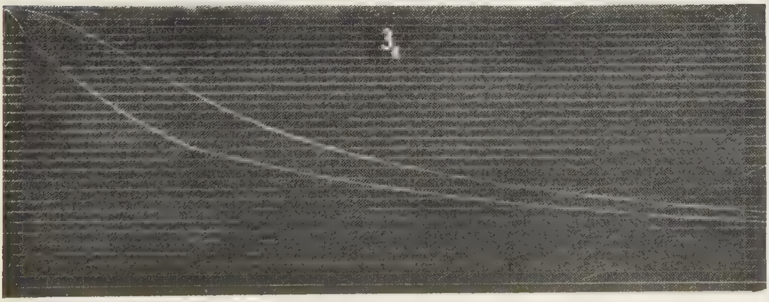
3_1

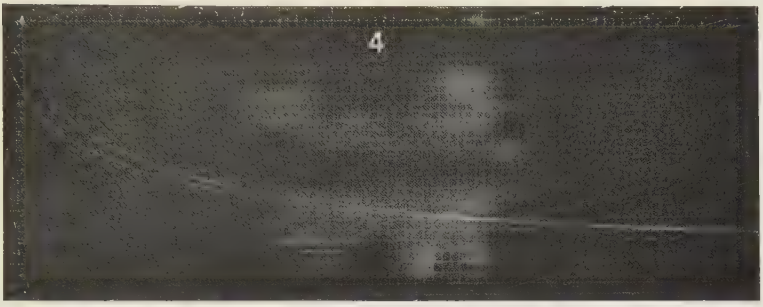
4

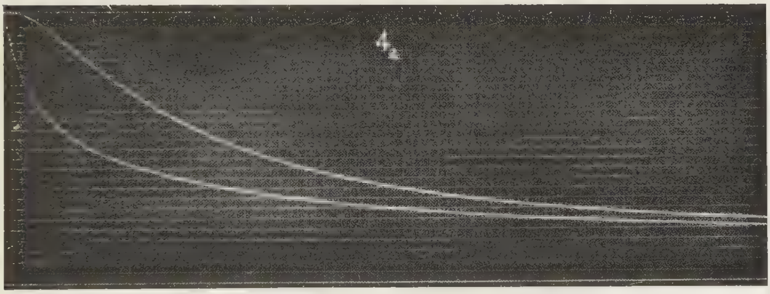
4_2

5

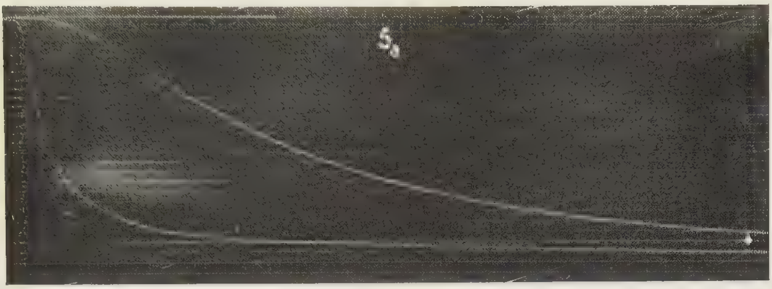

5_a

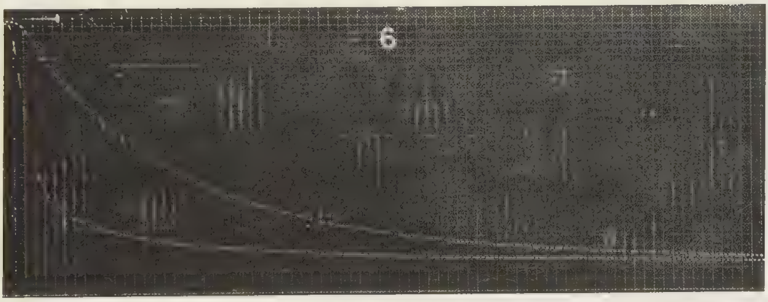

6

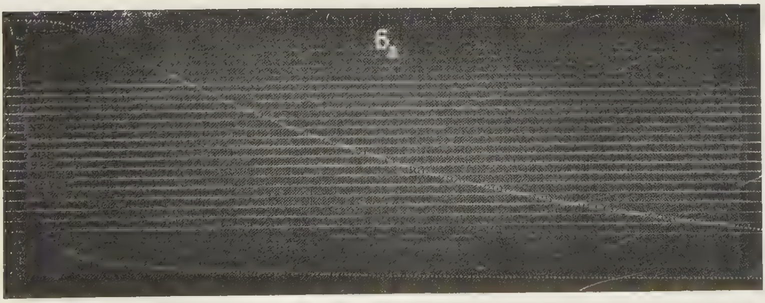

6_a

8

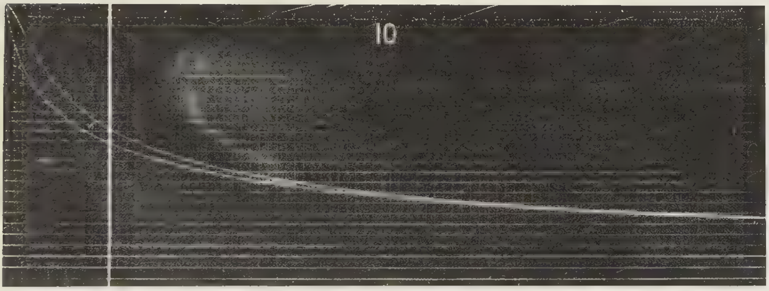
10

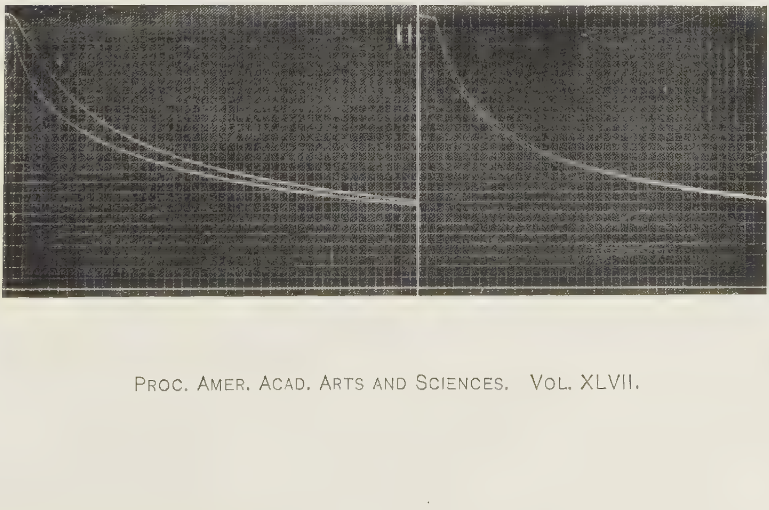
11

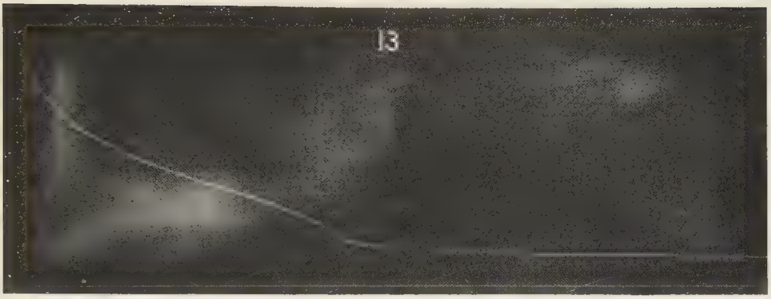
13

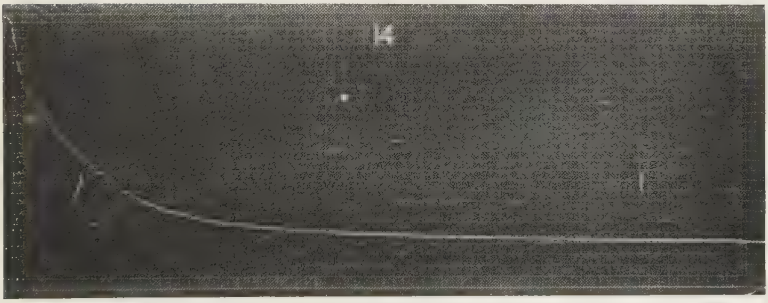
14

A paper presented at the Pacific Coast Meeting of the American Institute of Electrical Engineers, Los Angeles, April 25–28, 1911.

Copyright 1911. By A. I. E. E.

Revised Reprint.
(Subject to final revision for the Transactions.)

CISOIDAL OSCILLATIONS

BY GEORGE A. CAMPBELL

The oscillations here defined as "cisoidal oscillations" are those of the form

$$C \operatorname{cis} pt = C (\cos pt + i \sin pt) = Ce^{ipt} \qquad (1)$$

where t is the time, e the Napierian base, $i = \sqrt{-1}$ the imaginary symbol,[1] and cis an abbreviation for the complete trigonometric expression. The constants C and p may be any scalar quantities, either real or complex. The oscillations are sustained, logarithmically damped or aperiodic, according as the time coefficient p is real, complex, or pure imaginary. The following discussion will, in general, apply indifferently to all three cases.

The use of the term "cisoidal oscillations" emphasizes the distinctive character of the subject, while tending to keep in mind the close connection between these oscillations and sinusoidal oscillations. The fact that one of the algebraic curves is called a "cissoid" can hardly lead to confusion.

The practical importance of cisoidal oscillations rests upon the following properties:

1. In all cases where the principle of superposition holds, any

---

[1] The use of i (or Greek ι) for the imaginary symbol is nearly universal in mathematical work, which is a very strong reason for retaining it in the applications of mathematics in electrical engineering. Aside, however, from the matter of established conventions and facility of reference to mathematical literature, the substitution of the symbol j is objectionable because of the vector terminology with which it has become associated in engineering literature, and also because of the confusion resulting from the divided practice of engineering writers, some using j for $+i$ and others using j for $-i$.

oscillation may be regarded as a compound cisoidal oscillation, *i.e.*, the algebraic summation of simple cisoidal oscillations.

2. Cisoidal oscillations are uniquely simple because the ratio of the instantaneous electromotive force to the instantaneous current is not a function of the time.

3. Cisoidal oscillations involve scalar magnitudes only so that all algebraical relations and operations applying to the real physical phenomena may be extended to them.

4. The solution for cisoidal oscillations in any finite network may be written down directly, without solving differential equations or the use of integration or differentiation.

SCALAR CHARACTER OF CISOIDAL OSCILLATIONS

As complex quantities and exponential functions of complex quantities follow the laws of ordinary algebra, they introduce scalar quantities and not vector quantities. This is a matter of great importance, since ordinary algebra is simpler than vector algebra. The wide-spread use of the term "vector" in connection with complex quantities in alternating current theory is unfortunate for it is logically incorrect, and so has led to confusion, and it also tends to divert attention from the algebraical theory of complex quantities, which is of great practical assistance in the treatment of cisoidal oscillations.

When the direction of a current is confined to one or the other of two opposite directions by the use of a linear conductor, we can vary its scalar magnitude only; it is no more correct to speak of representing this scalar quantity by a vector when it is complex than when it is real. It is only when the electrical phenomena takes place in two or three dimensions in space that vector variables are involved in the mathematical treatment.

With complex quantities the power continues to be the product of electromotive force and current. A steady imaginary current flowing through a resistance, therefore, dissipates negative real power, that is, energy is absorbed by the electrical phenomena taking place, which tends to cool the conductor. Similarly the magnitudes of the kinetic energy of an inductance and the potential energy of a condenser are real negative quantities in case the instantaneous current and potential are pure imaginary. As the power with complex quantities may be either positive or negative, or in general have any argument, the total power in a portion of a network, such as two or more resistances, may vanish because the several powers in the individual elements mutually cancel when added together.

If the current and electromotive force are each cisoidal the associated power is also cisoidal with a time coefficient equal to the algebraical sum of the time coefficients of the electromotive force and current; when these two coefficients are equal and opposite in sign the power is constant with respect to the time.

We might have defined the cisoidal oscillation using throughout $-i$ in place of i, which would change all quantities, including the impedances, to their conjugates. But we follow, of course, the general practice of taking positive quantities as the norm, in consequence of which the sign for inductive reactances is positive, and the sign for capacity reactances is negative.

Correlated Oscillations

The complete formal solution of a sinusoidal alternating current problem by the aid of complex quantities involves the following steps:

1. Resolution of the periodic data into the sum of cisoidal oscillations having the time factors cis $(+pt)$ and cis $(-pt)$.
2. Solution of the problem for the cis $(+pt)$ component taken alone; the solution for the cis $(-pt)$ component is then obtained directly from this by changing all complex quantities to their conjugates.
3. Superposition of these two cisoidal solutions to obtain the real physical oscillation.

It is however not necessary to carry through the formal proof in individual cases, this being replaced by the following correlation between the real and the complex oscillations.

If throughout any invariable network a cisoidal oscillation and a cosinusoidal oscillation (all of one time coefficient p) have electromotive forces and currents of the same effective values (moduli) and angles (arguments), they will be called correlated oscillations.

The alternating powers involved throughout correlated oscillations are equal to each other as regards amplitudes (moduli) and angles (arguments); the cosinusoidal oscillation having also non-alternating power components which are equal, as regards amplitudes (moduli) and phase angles (arguments), to the powers which would be associated with the correlated cisoidal electromotive forces taken with the conjugates of the correlated cisoidal currents.

Or in other words:

The instantaneous cosinusoidal electromotive forces and currents are the real components of the correlated cisoidal electromotive forces and currents multiplied by the factor $\sqrt{2}$.

The instantaneous powers involved in a cosinusoidal oscillation are equal to the real components of the cisoidal powers in the correlated cisoidal oscillation, augmented by the real components of the powers involved in the correlated cisoidal oscillation after changing the currents (or electromotive forces) to their conjugates.

In the typical notation the correlated oscillations thus defined have, if $p=p_1+p_2 i$

Instantaneous	Cisoidal	Cosinusoidal	
e.m.f.	$E e^{ipt}$	$\sqrt{2}\,\lvert E\rvert e^{-p_2 t} \cos\,(p_1 t+arg E)$	
current	$I e^{ipt}$	$\sqrt{2}\,\lvert I\rvert e^{-p_2 t} \cos(p_1 t+arg\ I)$	**(2)**
power	$E I e^{2ipt}$	$\lvert E I\rvert e^{-2p_2 t}\left[\cos(2p_1 t+arg(E I))+\cos arg\,\frac{E}{I}\right]$	
impedance	$\frac{E}{I}$	$\left\lvert\frac{E}{I}\right\rvert \frac{\cos\,(p_1 t+arg\,E)}{\cos\,(p_1 t+arg\ I)}$	

In much of the actual algebraical work connected with cisoidal oscillations, we may drop the time factors e^{ipt} and e^{2ipt} and write only E, I and $E\,I$ (or $P=E\,I$) with considerable resulting simplification and no liability of introducing confusion.

It is to be particularly noted that the magnitudes which are equal to the corresponding cisoidal moduli are the *effective* values of the cosinusoidal electromotive forces or currents and the *amplitudes* of the cosinusoidal power components. On the other hand, the cisoidal arguments are uniformly equal to the corresponding real angles, this angle reducing for the non-oscillatory cosinusoidal power component to the constant angle of lag or lead.

The preceding statements supply the working rules for making the change from the real physical cosinusoidal oscillation to the ideal cisoidal oscillation and vice versa. This connection is, as regards electromotive force and current, one of mutual resolvability as is expressed by the following formulæ:

$$\begin{aligned}
&\sqrt{2}\lvert C\rvert e^{-p_2 t} \cos\,(p_1 t+arg\ C)=\frac{1}{\sqrt{2}}\,Ce^{ipt}+\frac{1}{\sqrt{2}}\,C'\,e^{-ip't}\\
&C\,e^{ipt}=\frac{1}{\sqrt{2}}\left[\sqrt{2}\lvert C\rvert\,e^{-p_2 t}\cos\,(p_1 t+arg\ C)\right]\\
&\qquad+\frac{i}{\sqrt{2}}\left[\sqrt{2}\lvert C\rvert e^{-p_2 t}\cos\,\left(p_1 t+arg\ C-\frac{\pi}{2}\right)\right]
\end{aligned} \tag{3}$$

the first giving the cosinusoid in terms of the correlated cisoid and its conjugate cisoid, the second giving the cisoid in terms of the correlated cosinusoid and the consinusoid with its phase retarded 90 degrees. On account of this mutual resolvability either the cisoidal oscillation or the cosinusoidal oscillation may be regarded as being obtained by summation from the other.

If any particular cisoidal or cosinusoidal oscillation is possible the correlated oscillation is also possible.

It is somewhat arbitrary as to the exact functions which we define as correlated oscillations. The sine might have been taken in place of the cosine and the amplitudes in place of the effective values, but on the whole these alternatives do not seem to afford quite the same convenience, but only because the statements become slightly more involved. We shall however continue to use the term " sinusoid " as the general designation for the sine function having any arbitrary phase angle including thereby the cosine function.

The correlation between the sinusoidal oscillations and cisoidal oscillations is so simple that it is not ordinarily necessary to indicate the step from one to the other in special applications of the method. But this omission has led to the cisoidal solution being in some way regarded as representing the actual sinusoidal oscillation, which is not the case as is very clearly shown by the power relations. It is therefore necessary to lay emphasis upon the fact that the use of complex quantities affords an indirect method, and not a symbolic method of solving real cases of oscillations and that the complete application of the method involves an initial algebraical resolution of the real data and a final algebraical summation of the complex results as an essential and integral part of the method.

General Equations for any Network

In any invariable network the actual distribution of current due to any impressed electromotive forces is such as to make the power dissipated assume the stationary value[2] which is consistent with the conditions imposed by current continuity and the conservation of

---

[2] A function assumes a stationary value when it is not altered by any possible infinitesimal change in the system of variables upon which it depends; the first derivatives of the function, with respect to each of a set of independent variables is zero at a stationary value. Stationary is thus a generalization of maximum, minimum and point of inflection, but without any implication beyond the vanishing gradient.

energy. The theorem assumes that each branch or circuit contains resistance, a condition which corresponds to the physical fact and involves no theoretical limitation as the resistances may be as small as desired, or any number of the resistances may be allowed to vanish completely after playing their part in the formation of the general solution.

This theorem may be established directly from the principles of dynamics, but we will here show that it is the equivalent of the generalized Kirchhoff equations.

The condition imposed by the conservation of energy may be expressed in the form of the equation of activity by equating the total power supplied by the impressed forces to the sum of the powers taken separately by the resistances (including conductances), self-inductances, mutual inductances and capacities. That is

$$\sum e_q\, i_q = \sum R_q\, i_q^2 + \frac{d}{dt}\left(\sum \frac{1}{2} L_q\, i_q^2 + \sum M_{qr}\, i_q\, i_r\right)$$

$$+\frac{d}{dt}\sum \frac{(\int i_q\, dt)^2}{2\, C_q} = \sum R_q\, i_q^2 + \sum L_q\, i_q\, \frac{d\, i_q}{d\, t}$$

$$+\sum M_{qr}\left(i_q \frac{di_r}{dt} + i_r \frac{di_q}{dt}\right) + \sum \frac{i_q \int i_q\, dt}{C_q} \qquad \textbf{(4)}$$

The condition of continuity may be introduced by expressing the currents in terms of any set of independent, circuital currents $c_1, c_2, \ldots c_n$, where n is the number of degrees of freedom of the network. This gives one equation for each of the l branches

$$i_q = a_{q1}\, c_1 + a_{q2}\, c_2 + \ldots a_{qn}\, c_n \qquad (q=1, 2 \ldots l) \qquad \textbf{(5)}$$

where the coefficient $a_{qs} = \pm 1$ or 0, according as branch q is or is not a part of circuit s, the sign in the first case being positive, or negative, according as the positive direction for the branch and for the circuit are or are not concurrent.

The power dissipated $\Sigma R_q\, i_q^2$ is a homogeneous expression of the second order in terms of the n independent circuital currents, while the remainder of equation (**4**) is of the first degree in these currents. The stationary value for the power dissipated under the assumed conditions will therefore be found by first introducing the multiplier $\frac{1}{2}$ as a coefficient for $\Sigma R_q\, i_q^2$ and then differentiating (**4**) with respect to c_s* which gives the following set of n equations:

$$\sum a_{qs}\,e_q = \sum a_{qs}\,R_q\,i_q + \sum a_{qs}\,L_q\frac{di_q}{dt} + \sum M_{qr}\Big(a_{qs}\,\frac{di_r}{dt}$$

$$+a_{rs}\,\frac{di_q}{dt}\Big) + \sum a_{qs}\,\frac{\int i_q\,dt}{C_q}, \quad (s=1,\,2,\,\ldots\,n) \qquad (\mathbf{6})$$

The set of equations (**6**) is identical with the generalized Kirchhoff equations of electromotive force for the n circuits taken in the positive direction for the currents c_s, since the coefficients a_{qs} and a_{rs} provide the proper sign for each effective electromotive force occurring in these circuits and exclude all electromotive forces not occurring in the several circuits. The Kirchhoff laws and the above condition of stationary dissipation are therefore mutually equivalent.

In subsequent work it will be more convenient to merge the conditions of continuity in the equation of activity (**4**) than to use separate equations such as (**5**) to cover these conditions. This may be accomplished either by reducing the currents appearing in the equation of activity to a number equal to and so chosen as to correspond with the degrees of freedom of the network, or by adding fictitious currents which correspond to the significant branch points; *i.e.*, points, in excess of one in each connected part of the system, at which three or more branches meet. Their number being m, the number of branches (including each isolated closed circuit as a branch) being l, and the degrees of freedom being n, the relation holds, $n=l-m$.

---

*To prove this rule let $f=m^{-1}\,F_m+n^{-1}\,F_n$, (where F_m and F_n are homogeneous functions of x, y, z, . . . of order m and n) be given its stationary value, which requires $D_x\,f=D_y\,f=D_z\,f=\;.\;.\;.\;=0$. The sum of the differential coefficients multiplied in order by x, y, z, . . . consequently vanishes, that is,

$$x\,D_x f+y\,D_y f+z\,D_z f+\;.\;.\;.\;=0, \text{ or}$$

$$m^{-1}\,[x\,D_x\,F_m+y\,D_y\,F_m+\;.\;.\;.\,]+n^{-1}\,[x\,D_x\,F_n+y\,D_y\,F_n+\;.\;.\;.\,]=0.$$

By the elementary property of homogeneous functions the bracketed expressions are equal to $m\,F_m$ and $n\,F_n$ so that the relation $F_m+F_n=0$ is satisfied at the stationary value of f. This relation may be considered as a prescribed condition without having any effect on the final stationary result, but we could then eliminate F_m from the original expression for f and write $f=(n^{-1}-m^{-1})\,F_n$, whence the stationary value of F_n, with the condition $F_m+F_n=0$, corresponds to the unconditioned stationary value of f. The application in the paper is for $m=1$, $n=2$ and $f=F_1+\frac{1}{2}\,F_2$

The first transformation is accomplished by replacing the branch currents i_q in (**4**) by circuital currents such as c_s by the aid of such equations as (**5**). Rearranging the terms the form of the equation of activity may still be kept the same as in (**4**), but all quantities, e, i, R, L, M, C now refer to complete circuits and not to individual branches.

The second transformation follows from the identity of the condition of continuity for currents converging on branch point f,

$$\varphi_f = M_{f1}\, i_1 + M_{f2}\, i_2 + \ . \ . \ . \ M_{fr}\, i_r \ . \ . \ . + M_{fl}\, i_l = 0, \qquad (7)$$

$$M_{fr} = \pm 1 \text{ or } 0, \quad f = (l+1, \ . \ . \ . \ l+m),^*$$

with the condition that a fictitious circuit devoid of resistance, inductance, and capacity can experience no resultant electromotive force whatever be the currents flowing in the branches 1, 2, . . . r . . . l with which it has mutual inductances M_{f1}, M_{f2}, . . . M_{fr} . . . M_{fl}. This physical consideration shows that the conditions of continuity will be included in (**4**) by extending the summation to cover fictitious circuits devoid of resistance, etc., and with zero mutual inductances between each other and all real branches excepting only $M_{fr} = \pm 1$ when the real branch r terminates in the branch point f, the sign being positive or negative at the positive or negative end of the branch respectively.

To prove the same analytically we multiply each equation of (**7**) by i_f, take their sum, differentiate with respect to t and add this expression, which we may denote by

$$B = \frac{d}{dt} \sum i_f\, \varphi_f = \frac{d}{dt} \sum\sum M_{fr}\, i_f\, i_r$$

to (**4**), which is permissible since B must be equal to zero. On differentiating (**4**) (with multiplier $\frac{1}{2}$ added to $\Sigma R_q\, i_q^2$) with respect to the real current i_q, B introduces the new terms $\sum \frac{di_f}{dt} \frac{d\varphi_f}{di_q}$ to (**6**), and these are precisely the additional terms required by the conditions of continuity, since $\frac{di_f}{dt}$ plays the part of an undetermined multiplier. Again differentiation

---

*These m fictitious circuits are numbered in sequence with the l real branches so as to make it possible to employ throughout the same notation for circuit constants and currents, *viz.*, R_f, i_f, etc.

with respect to the fictitious current i_f gives $\frac{d}{dt}\varphi_f=0$ or $\varphi_f=0$, the constant of integration being zero, as infinite energy in the fictitious circuits is to be excluded, and these are the equations of continuity (**7**). Thus after the addition of B, equation (**4**) includes all of the conditions of continuity.

It will be assumed in the subsequent work that the network under discussion has been transformed into a set of simple circuits, thus reducing the conditional equations to the equation of activity. The coefficients occurring in this equation and the number of currents entering it will depend upon the particular choice of simple circuits, but the general discussion of the network will be, to a considerable extent, independent of the choice of the simple circuit system. In concrete applications it will be advantageous, in order to have as few variables as possible, to use the first of the above transformations. In general work, however, the second transformation presents the distinct advantage of including all branches symmetrically.

General Equations for Cisoidal Oscillations

For cisoidal oscillations the preceding theorem may be given the following still simpler form:

The activity of the external sources of power which produce a steady cisoidal oscillation in any invariable network assumes the stationary value which is consistent with the conditions imposed by current continuity and the conservation of energy.

With cisoidal oscillations the differentiations and integrations indicated in the equation of activity (**4**) may be carried out and after dividing by the common factor e^{2ipt} and introducing the self and mutual impedances $Z_{qq}\,(=Z_q)$, $Z_{qr}\,(Z_{rq}=Z_{qr})$, the equation becomes

$$\sum_{q=1}^{q=n} E_q\,I_q=\sum_{q=1}^{q=n} Z_q\,I_q^2+2\sum_{r>q=1}^{q<r=n} Z_{qr}\,I_q\,I_r=\sum_{q=1}^{q=n}\sum_{r=1}^{r=n} Z_{qr}\,I_q\,I_r \qquad (\mathbf{8})$$

The left-hand and the right-hand sides of this equation are homogeneous functions of the first and second orders in terms of the currents. Comparison with the first and second order terms in (**4**) shows that the right-hand side of equation (**8**), which is the total power taken by the network, may be substituted in the general theorem for the power dissipated. Or, since the two sides of equation (**8**) are always equal, the left-hand side, which is the power supplied by the sources, may equally well be taken; whence the above theorem follows.

Stationary activity involves stationary driving point impedance and the theorem might be restated in terms of the impedances.

Differentiating equation (**8**) with respect to each of the n currents (after introducing the multiplier $\frac{1}{2}$ for the right-hand side) we have for the general equations determining the distribution of current:

$$\begin{array}{l} Z_{11}I_1+Z_{12}I_2\ldots\ldots\ldots\ldots\ldots\ldots\ldots+Z_{1n}I_n=E_1 \\ Z_{21}I_1+Z_{22}I_2\ldots\ldots\ldots\ldots\ldots\ldots\ldots+Z_{2n}I_n=E_2 \\ \ldots\ldots\ldots\ldots\ldots\ldots\ldots\ldots\ldots\ldots\ldots\ldots\ldots\ldots \\ Z_{n1}I_1+Z_{n2}I_2\ldots\ldots\ldots\ldots\ldots\ldots\ldots+Z_{nn}I_n=E_n \end{array} \qquad (\mathbf{9})$$

The currents are therefore

$$I_q=\sum_{r=1}^{r=n}\frac{A_{qr}}{A}E_r$$

where A is the determinant of the impedances occurring as coefficients of the currents in (**9**) and A_{qr} $(=A_{rq})$ is the co-factor of Z_{qr} in this determinant. Substituting in equation (**8**), we find that the stationary power, that is the power which is actually expended on the network, is

$$P=\sum_{q=1}^{q=n}\sum_{r=1}^{r=n}\frac{A_{qr}}{A}E_qE_r=\frac{A_e-A}{A} \qquad (\mathbf{10})$$

where A_e differs from the determinant A only in having each element Z_{qr} augmented by E_qE_r.

Self- and mutual-admittances may be substituted for the self- and mutual impedances in the right-hand side of equation (8), the form of the expression being kept unchanged by simultaneously substituting potential differences for currents. The solution in terms of the admittances will then be obtained from a determinant in which the admittances enter precisely as do the impedances in "A". For certain problems, as will be readily seen, the admittance determinant is much more convenient than the impedance determinant. While the impedance determinant is made the special object of discussion in the remainder of this paper, it is to be understood that corresponding applications may be made of the admittance determinant.

The Discriminant of a Network

The discriminant A of a network is defined as the determinant having the element Z_{qr} in the qth row and rth column; Z_{qr} being the mutual impedance between circuits q and r or the self-impedance of circuit q when $q=r$; the determinant to include the self- and mutual impedances of the system of simple circuits obtained by eliminating the branch points by closing each branch on itself and replacing each branch point, in excess of one in each connected part of the system, by a fictitious circuit of zero self-impedance connected by mutual impedances $+i$ and $-i$ to the several branches which have their positive or negative ends respectively at this branch point.

This will be taken as the normal form of the discriminant, since it is symmetrical in terms of all of the real branches and real closed circuits of the network. That it is also essentially symmetrical in all of the branch points follows from the fact that the value of the determinant is independent of the choice of the particular branch points to be excluded. The discriminant A is of fundamental importance in the discussion of the network because all effective impedances of the network may be determined directly from its array.

The degree of A in terms of the actual impedances of the network is equal to the number of degrees of freedom of the network, which is the same as the number of branches, reduced by the number of branch points, omitting one in each connected part of the system. The determinant A is of the first degree in each self-impedance, and of the second degree in each mutual impedance when physically considered, that is when the order of the subscripts is ignored ($Z_{rq} \equiv Z_{qr}$).

The co-factor of the product of the elements located at the intersection of rows $j, q, s, \ldots$ with columns $k, r, t \ldots$ respectively of determinant A will be denoted by $A_{jk.qr.st} \ldots = A_\alpha$, where α stands for the paired list $jk.qr.st \ldots$ Thus A has the value $A_\alpha Z_{jk} Z_{qr} Z_{st} \ldots$ in case all other elements in rows $j, q, s, \ldots$ and columns $k, r, t, \ldots$ are replaced by zero; the arithmetical value of the co-factor depends only on the choice of rows $j, q, s, \ldots$ and columns $k, r, t \ldots$ which occur in the subscript; its algebraical sign depends upon the sequence of the rows and columns and is changed by each inversion of rows or columns. It follows that if the same row or column occurs twice in the subscript the value of the co-factor is zero. Where we have occasion to restore one or more rows and an equal number of columns of A to A_α, the elements to be removed from α will be indicated as a divisor of the subscript α. The algebraical value of the expression $A_{\frac{\alpha}{\beta}}$ is uniquely and completely determined by canceling the denominator against a part or the whole of the numerator, making inversions, if necessary, in the numerator or denominator; in case the denominator cannot be entirely eliminated by this process the symbol indicates a determinant with identical rows or columns, and it is therefore equal to zero. For example:

$$A_{\frac{11\cdot22}{12}} = -A_{\frac{12\cdot21}{12}} = -A_{21},\quad A_{12\cdot13}=0,\quad A_{\frac{12\cdot23}{34}} = 0,\quad A_{\frac{11\cdot22}{12\cdot21}} = -A$$

$$\text{and}\quad A_{jk.qr.st\,\ldots} = \frac{D_{Z_{jk}}\,D_{Z_{qr}}\,D_{Z_{st}}\cdots A}{2^{(\delta_{jk}+\delta_{qr}+\delta_{st}\ \ldots\ )}}, \tag{11}$$

$$Z_{rq}\equiv Z_{qr} \not\equiv 0, \qquad \delta_{qr} = \begin{cases} 0 \text{ if } q=r \\ 1 \text{ if } q \neq r \end{cases}$$

where the differentiations correspond to actual physical variations in the impedances and therefore treat mutual impedances with interchanged subscripts as identical.

By applying the following rules the expanded expressions for A and its co-factors may be written down directly from the simple circuit system replacing the network, without reference to the determinant. This method of expansion is often more convenient than the use of the ordinary rules for expanding the determinant.

A is the sum of all possible products in which each circuit is represented either by its self-impedance or by its mutual impedance to another circuit, the mutual impedances occurring, however, in closed cycles of two or more constituents only, so that the subscripts may be written $k\,m$, $m\,q$, $q\,u$, . . . $w\,k$, each cycle introducing the sign-factor + or − according as the cycle contains an odd or an even number of terms; each cycle of three or more circuits also introducing the factor 2 to care for the alternative way of associating the mutual impedances and the circuits of the cycle.

A_{qq} is the coefficient of Z_{qq} in A, *i.e.*, A_{qq} is the value taken by A when circuit q is removed from the network.

A_{qr} is the coefficient of Z_{qr} *after* writing A in symmetrical form with respect to Z_{qr} and Z_{rq}, *i.e.*, A_{qr} is the value taken by $A \div Z_{qr}$ if circuit q is represented in each product by the mutual impedance Z_{qr}.

EFFECTIVE IMPEDANCES OF ANY NETWORK

In the theoretical discussion of networks we are concerned not so much with particular values of the electromotive forces and currents, as with their relative values. For this reason the impedances, which are the ratios of electromotive forces to currents, and the attenuation factors, which are either the ratios of currents to each other, or of electromotive forces to each other, are chosen as the immediate objects of investigation.

Effective impedances may be defined in various ways, for example as:

$$(a)\quad \frac{\text{potential of point } s_j \text{ minus potential of point } s_k}{\text{current at point } s_l},$$

$$(b)\quad \delta\,\frac{\text{power taken by any part } S_p \text{ of network}}{\text{product of currents at points } s_q \text{ and } s_r},$$

($\delta = 1$ or $\frac{1}{2}$ for self and mutual impedances respectively.)

$$(c)\quad \frac{1}{\delta}\,\frac{\text{product of potential differences points } s_t,\ s_u \text{ and } s_v,\ s_w}{\text{power taken by any part } S_x \text{ of network}}$$

($\delta = 1$ or $\frac{1}{2}$ for self- and mutual impedances respectively.)

(*d*) The impedances required to make a normal type of network of the requisite number of parameters equivalent to the given network under specified conditions of operation.

As examples of the above definitions we may instance the following:

The mutual impedance of a transformer is the ratio, with sign reversed, of the electromotive force induced in either winding to the inducing current flowing in the other winding, which falls under definition (*a*) if the secondary is first open-circuited.

In discussing below the power taken by the actual resistances in a network use is made of definition (*b*) in formula (**26**).

The expression, formula (**10**), for the total power taken by a network in terms of the impressed forces, gives, on breaking up the expression into its individual terms, a set of self-impedances and mutual impedances defined in accordance with definition (*c*).

As an example of definition (*d*) we may take the important case where we are concerned only with two accessible circuits in a network and wish to replace the given network by a normal type having only the required three complex parameters. The normal networks which are ordinarily employed are the "T", the "Π," the transformer and the artificial line and for these the effective impedances are given in table I, together with the simple circuit impedances which equal the driving point impedance in either circuit S_q and S_r and the driving-driven point impedance S_{qr} of a single circuit which would give the electromotive force ÷ current ratio actually obtaining when the electromotive force is inserted in q (or r) and the current is measured in r (or q). J_q, J_r, J_{qr} are called the primary, secondary and mutual impedances as they correspond to the primary self-inductance, secondary self-inductance, and mutual inductance following established scientific usage. This terminology is employed throughout this paper, as its extension to three or more circuits is obvious and symmetrical, and it seems to be the only logical system. Many electrical engineers, however, call H_q, H_r, H_{qr}^{-1} (H_{qr} being taken with inductive reactance) the primary impedance, secondary impedance and primary admittance, in case the assumed ratio of turns is 1 to 1.

The table refers to the general case where the two circuits are not symmetrical, but the formulæ are in such form as to facilitate reduction to the special case of symmetrical circuits. In this table different letters are employed for the various effective impedances thus somewhat reducing the multiplication of subscripts.

ELIMINATION OF CONCEALED CIRCUITS

In general we may divide a network into a concealed and an accessible part and it is convenient to eliminate the former from explicit appearance in the impedance determinant A when we are concerned only with the effects which are produced in the accessible part of the network due to causes which are likewise confined to this part of the network.

Elimination of a group of concealed circuits (or of any circuits which contain no impressed forces) from explicit appearance in A is equivalent to the substitution of new effective impedances

$$J_{qr} = \frac{A_{\frac{\alpha}{qr}}}{A_{\alpha}}$$

between accessible circuits q and r where α stands for the product of the original self-impedances of the accessible circuits.

To prove this we notice that the set of Kirchhoff electromotive force equations for the concealed circuits taken alone give

$$I_c = \frac{1}{A_\alpha} \sum_r I_r A_{\frac{\alpha.\,xc}{xr}} \qquad \text{where} \quad \begin{cases} c = \text{any concealed circuit} \\ r = \text{any accessible circuit} \\ x = \text{any circuit} \end{cases}$$

which substituted in the electromotive force equation for any accessible circuit q make the new coefficient of I_r in this equation

$$J_{qr} = Z_{qr} + \frac{1}{A_\alpha} \sum_c Z_{qc} A_{\frac{\alpha.\,qc}{qr}} = \frac{1}{A_\alpha} \left[Z_{qr} A_{\left(\frac{\alpha}{qr}\right)qr} + \sum_c Z_{qc} A_{\left(\frac{\alpha}{qr}\right)qc} \right]$$

after setting $x = q$

$$= \frac{A_{\frac{\alpha}{qr}}}{A_\alpha} = \frac{A_{\frac{\alpha}{rq}}}{A_\alpha} = J_{rq}; \text{ as } A \text{ is symmetrical.} \qquad \textbf{(12)}$$

J_{qr} is thus the new effective mutual impedance (or self-impedance if $q = r$) between accessible circuits q and r.

In the important case where all but two of the circuits are eliminated, we have

$$J_{qq} = \frac{A_{rr}}{A_{qq \cdot rr}}$$

$$J_{rr} = \frac{A_{qq}}{A_{qq \cdot rr}} \qquad \textbf{(13)}$$

$$J_{qr} = \frac{-A_{qr}}{A_{qq \cdot rr}}$$

And if but one circuit q is regarded as accessible, the driving point impedance of the network to an electromotive force inserted in that circuit, is

$$J_{qq} = \frac{A}{A_{qq}} \qquad \textbf{(14)}$$

If we eliminate the circuits corresponding to all of the branch points and to an equal number of the branches which are connected to these branch points but do not form any closed circuit among themselves, it may be shown that: $A_\alpha = 1$; the new effective impedances are equal to sums and differences of the original impedances with coefficients which are 0, ± 1, or ± 2; the circuits which are not eliminated are equal in number to the degrees of freedom of the network. The case falls under that directly derived above by the use of circuital currents.

If $A_\alpha = 0$ the method of elimination fails, which shows that whenever fictitious branch point circuits are eliminated at least one branch connected to each branch point must be included and that the number of closed circuits formed by the branches must not be greater than the excess of eliminated branches over eliminated branch points.

No change is made in the effective self- or mutual impedance of an accessible circuit q by the elimination of circuits which have no mutual impedance with circuit q. That is $A_{\frac{\alpha}{qr}} = Z_{qr} A_\alpha$ since the added q row has but one term Z_{qr} which differs from zero.

A concealed branch of admittance Y which is free from mutual impedances may be eliminated by adding Y to each of the two self-impedances and subtracting Y from the mutual impedance of the two fictitious circuits which replace the terminal branch points of the concealed branch. Any number of concealed branches may be eliminated in this way; the total self-impedance added to any fictitious circuit will equal the total admittance of the eliminated branches terminating at the corresponding branch point; the total mutual impedance subtracted between any two fictitious circuits will equal the total admittance eliminated between the corresponding branch points.

To prove, let the concealed branch impedance be $Z = 1 \div Y = A_\alpha$, then, if the self- and mutual-impedances of the fictitious circuits corresponding to the terminals of this branch are originally Z_1, Z_2 and Z_{12}, they become after the elimination of the concealed branch

$$J_1 = \frac{A_{\frac{\alpha}{11}}}{A_\alpha} = Y \begin{vmatrix} Z_1 & \pm i \\ \pm i & Z \end{vmatrix} = Z_1 + Y$$

$$J_2 = \frac{A_{\frac{\alpha}{22}}}{A_\alpha} = Y \begin{vmatrix} Z_2 & \mp i \\ \mp i & Z \end{vmatrix} = Z_2 + Y$$

$$J_{12} = \frac{A_{\frac{\alpha}{12}}}{A_\alpha} = Y \begin{vmatrix} Z_{12} & \pm i \\ \mp i & Z \end{vmatrix} = Z_{12} - Y$$

Any concealed part of a network connected to the remainder of the network through a group of terminals (*branch points*) $q, r, s, \ldots$ *only* (and having the impedance determinant A_α or A_β according as the concealed part is taken alone or is taken together with the circuits corresponding to the group of accessible terminals) *may be replaced by any one of the following*:

(*a*) Self-impedances $A_{\frac{\alpha}{qq}} \div A_\alpha$ and mutual impedances $A_{\frac{\alpha}{qr}} \div A_\alpha$ added to the fictitious circuits corresponding to the group of terminals.

(*b*) Branches, devoid of mutual impedance, connecting the group of terminals in pairs and having the admittances $-A_{\frac{\alpha}{qr}} \div A_\alpha$. These admittances we will call the equivalent direct admittances of the network.

(*c*) Branches radiating from a common concealed point, one to each of the terminals, with self-impedances $A_{\beta.qq} \div A_\beta$ and mutual impedances $A_{\beta.qr} \div A_\beta$.

(*d*) Branches radiating from a common concealed point, one to each of the group of terminals, these branches being devoid of self-impedance and having mutual impedances $-(A_{\beta.qq} + A_{\beta.rr} - 2\,A_{\beta.qr}) \div 2\,A_\beta$.

(*e*) Branches connecting any one of the terminals q to each of the remaining accessible terminals $r, s, \ldots$, the branch connected to terminal r having the self-impedance $(A_{\beta.qq} + A_{\beta.rr} - 2\,A_{\beta.qr}) \div A_\beta$ and the mutual impedance $(A_{\beta.qq} + A_{\beta.rs} - A_{\beta.qr} - A_{\beta.qs}) \div A_\beta$ to the branch connected to terminal s.

Substitution (*a*) is a restatement of the results previously established for the case of concealed and accessible parts which are not connected the one to the other by mutual impedances.

To show that (*b*) is equivalent to (*a*) apply to (*b*) the theorem for eliminating concealed branches which are devoid of mutual impedances; the fictitious circuits corresponding to the group of terminals will thereby have their mutual impedances increased by $A_{\frac{\alpha}{qr}} \div A_\alpha$ and their self-impedances increased by

$$-\frac{1}{A_\alpha}\sum_{r\,(\neq q)} A_{\frac{\alpha}{qr}} = \frac{1}{A_\alpha}\left(A_{\frac{\alpha}{qq}} - \sum_{r} A_{\frac{\alpha}{qr}}\right) = A_{\frac{\alpha}{qq}} \div A_\alpha$$

since the complete summation with respect to r of the bordered determinants $A_{\frac{\alpha}{qr}}$ equals the determinant A_α bordered by the row q and a column equal to the sum of all of the fictitious circuit columns r, and vanishes since terms $+i$ and $-i$ occur in pairs and cancel, making the column identically equal to zero. Substitution (*b*) having been transformed into substitution (*a*) the two are mutually equivalent.

Substitutions (*c*), (*d*) and (*e*) are readily shown to be mutually equivalent to each other and to the original network by showing that the impedance between any two terminals u and v with all others insulated is $(A_{\beta.uu}+A_{\beta.vv}-2A_{\beta.uv})\div A_{\beta}$.

The direct admittance between two terminals of any network, as defined under (*b*), is equal to one-half of the excess of the grounded admittance of the two terminals taken separately over their grounded admittance when taken together as a single terminal. By the grounded admittance of a terminal is understood the admittance between that terminal and ground with all of the other terminals grounded. As grounded admittance can be readily measured with simple apparatus, this always affords one method of experimentally determining the direct admittance in any network.

COMPLETE ELIMINATION OF EITHER MUTUAL IMPEDANCES OR SELF-IMPEDANCES

It has been shown [(*b*) and (*d*) above] that if we retain a group of terminals as the only accessible part, any network may be replaced either by a set of direct impedances connecting the terminals in pairs, or by a set of mutual impedances between branches radiating from a common point and terminating one at each of the terminals. In the first case all mutual impedances are avoided; in the second case all self-impedances are avoided. Applications to the simple transformer are of interest as showing that in these substitutions an open circuit is taken care of either by parallel self-impedances which are equal but of opposite signs or by infinite mutual impedances differing by finite amounts. The substitutions show that a transformer J_1, J_2, J_{12}, is equivalent to either

(*a*) The six-branch network directly connecting the four terminals, the impedances of which are

$$\frac{J_1 J_2 - J_{12}^2}{J_2},\ \frac{J_1 J_2 - J_{12}^2}{J_1},\ \frac{J_1 J_2 - J_{12}^2}{J_{12}},\ -\frac{J_1 J_2 - J_{12}^2}{J_{12}} \qquad \textbf{(15)}$$

between the primary terminals, the secondary terminals, each of the two pairs of correspondingly poled terminals of primary and secondary and each of the two pairs of non-corresponding terminals of primary and secondary, respectively. (In Figs. 6 and 7 terminals 1-2, 3-4, 1-3, and 2-4, 1-4 and 2-3 respectively.)

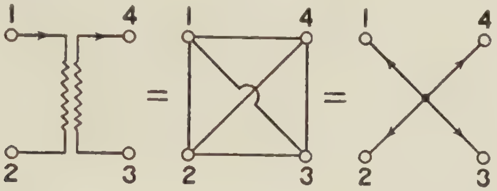

FIG. 6 FIG. 7 FIG. 8

Transformer and equivalent networks having four accessible terminals

Or (*b*) the four-branch network connecting the four terminals to a concealed common point, the mutual impedances being

$$-\frac{J_1}{2}, -\frac{J_2}{2}, \infty+\frac{J_{12}}{4}, \infty-\frac{J_{12}}{4} \qquad (16)$$

between the branches (taken with their positive directions diverging from the common point) which terminate at the same pairs of terminals as for case (*a*), respectively. See Figs. 6 and 8.

In certain cases a mutual impedance may be eliminated by properly augmenting the impedances of not more than four branches, without altering the arrangement of branches in any way or imposing any restriction as to whether they are concealed or accessible. These cases are all included under that of mutual impedance between diagonally opposite branches of a generalized bridge, by which we will understand a network differing from the ordinary bridge only in having the four bridge corners replaced

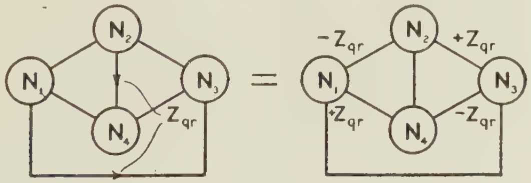

FIG. 9 FIG. 10

Generalized bridge with equivalent mutual and self impedances

by four arbitrary networks; these corner networks may have mutual impedances between one another, but the only branches connecting them are to be the six branches corresponding to the simple bridge. *Mutual impedance between diagonally opposite branches in the generalized bridge is replaceable by an equal amount* *of self-impedance in each of the four bridge-arms, added to or subtracted from the original self-impedance of the arm, according as the arm connects the branches having the mutual impedance with their positive directions concurrent or opposed.* (Figs. 9 and 10.) An important special case is that in which one arm of the bridge is open-circuited and the network reduces to three branches connecting two arbitrary networks otherwise unconnected except possibly by mutual impedances. (Figs. 11 and 12.)

The correctness of the substitution is shown by the fact that

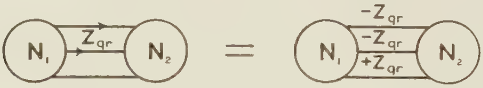

FIG. 11 FIG. 12

Three-branch connection with equivalent mutual and self impedances

the impedance of every closed circuit is the same before and after the substitution, and that this is the most general case is proven by noticing: (1), that the generalized bridge becomes an unrestricted network by admitting any number of branches connecting the four corner networks in pairs; and (2), that with a single branch added to Figs. 9 and 10, it is impossible to keep the self-impedance of every closed circuit the same in the two cases, for the added branch requires different increments according to the circuit through which it is closed.

In the simple bridge circuit there are 15 possible mutual impedances which may be eliminated by taking as the effective branch impedances the six permutations of

$$Z_{12}' = Z_{12} + Z_{12,\,23} + Z_{12,24} + Z_{12,31} + Z_{12,41} + Z_{13,14} + Z_{23,24} + Z_{13,42} + Z_{14,32} \qquad (17)$$

where 1, 2, 3, 4 stand for the bridge corners. The condition for a balance of the bridge arms 12, 23, 34, 41 is therefore always

$$Z_{12}' \, Z_{34}' = Z_{23}' \, Z_{41}' \qquad (18)$$

IMPEDANCE LOCI

It is often of importance to know how the impedances of a network will vary if the self-impedances or mutual impedances of one or more of the branches of the network are varied over lines or areas in any physically possible manner. On account of the magnitude of this subject we shall touch on the simplest case only, namely that of the driving point impedance with a variable impedance added to one branch of the network.

As the discriminant A and its minors are of the first degree in terms of each self-impedance which they contain, it follows that the effective impedances of the network, being equal to the quotient of two of these determinants, are bilinear functions of the individual impedances; thus the driving point impedance of a network at circuit q is connected with a self-impedance Z inserted in any circuit r by a relation of the form

$$S_q = \frac{a\,Z+b}{c\,Z+d} \tag{20}$$

where a, b, c and d are constants.

The property of the bilinear transformation which is of special importance to us is that it transforms circles into circles, that is, if Z be regarded as a variable and be made to traverse any circle whatsoever, the driving point impedance S will also describe a circle. In making this statement the straight line is included as the limit of a circle so that the loci of S and Z may be straight lines as well as circles. This property of the bilinear transformation is discussed at length in the theory of analytic functions and need not be entered into here.

We are especially concerned with the cases where the locus of Z is a straight line such as the axis of reals or the axis of imaginaries, because the first is a variation which it is convenient to make use of in practical measurements and the second forms the extreme boundary realizable with physically possible values of the inserted impedance. We shall find it better to replace the constants a, b, c and d by others, such as the effective transformer impedances or the effective line constants, which have a physical significance.

A network having effective transformer constants J_1, J_2, J_{12} *effects the transformation of the half of the* Z*—plane on the positive side of the reactance axis into the area bounded by a circle with center at* Z_i *and radius* R_i:

$$Z_i = J_1 - \frac{J_{12}^2}{J_2+J_2'}, \qquad R_i = \frac{|J_{12}^2|}{J_2+J_2'} \tag{21}$$

the axis of reals going over into the circumference of a circle having its center at Z_r *and radius* R_r*:*

$$Z_r = J_1 - \frac{J_{12}^2}{J_2 - J_2'}, \qquad R_r = \frac{|J_{12}^2|}{|J_2 - J_2'|} \tag{22}$$

where J_2' *is the conjugate of* J_2 *and* $|J_{12}^2|$ *the modulus of* J_{12}^2*. The two circles cut each other orthogonally at* J_1 *and* $(J_1 - J_{12}^2 \div J_2)$ *which correspond to open and short-circuited secondary. The double points = effective line impedances (far end with sign reversed) are*

$$\left.\begin{matrix} K_1 \\ -K_2 \end{matrix}\right\} = \frac{J_1 - J_2}{2} \pm \tfrac{1}{2}\sqrt{(J_1+J_2)^2 - 4J_{12}^2} \tag{23}$$

Proof: Close the secondary through the added impedance $Z\,x$, where x is a real variable, and the effective driving point impedance at the primary is

$$S_1 = \frac{J_1(J_2+Zx) - J_{12}^2}{J_2+Zx} = J_1 - \frac{J_{12}^2}{J_2+Zx}\;\frac{Z'(J_2+Zx) - Z(J_2'+Z'x)}{J_2Z' - J_2'Z} \tag{24}$$

$$= \left(J_1 - \frac{J_{12}^2\,Z'}{J_2Z' - J_2'Z}\right) + \left(\frac{J_{12}^2\,Z}{J_2Z' - J_2'Z}\right)\left(\frac{J_2' + Z'x}{J_2+Zx}\right) \tag{25}$$

and in this form the expression obviously represents a circle, of which the center is the first term, and the radius the modulus of the last term, since the variable x occurs only in the last factor of the last term and variations in x change the angle but not the modulus of this factor as its numerator is the conjugate of its denominator. If $Z = -Z' = i$, the inserted impedance is pure imaginary and we obtain from (**25**) the constants for the boundary circle as given in (**21**). If $Z = Z' = 1$, the added impedance is real and the effective driving point impedance falls on a circle with the constants as given in (**22**). To determine the double points substitute $Zx = S = K$ in the first part of (**24**) and solve the resulting quadratic in K which gives the values (**23**).

As a practical example of impedance loci, consider Fig. 13, which shows the driving point impedance of a transmission line

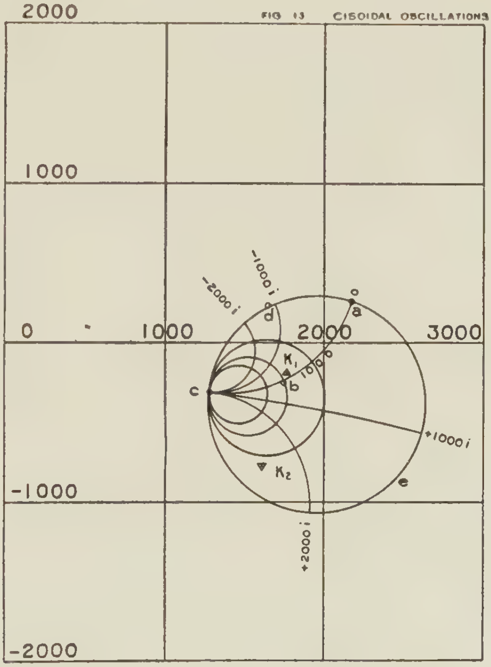

FIG. 13.—Bilinear transformation for a line containing 6.201 wave lengths and having the attenuation constant 0.9123 and the line impedances $K_1 = 1762 - 191\ i$ and $K_2 = 1614 - 781i$ which maps the half plane on the positive side of the imaginary axis into the circle *a d c e* with the rectangular ruling mapping into the orthogonal system of circles.

for a frequency of 1,300 cycles per second, the line containing 6.201 wave lengths, presenting an attenuation constant of 0.9123 and having line impedances $K_1 = 1762 - 191i$ and $K_2 = 1614 - 781i$ for transmission from the driving point to the receiving end and vice versa. The driving point impedances actually measured are the points marked by circles near a, b, c and d for which the far end of the line was closed through a short circuit, through 2,000 ohms, through an open circuit and through a capacity of 0.107 mf. respectively. As but three measurements are necessary in order to completely determine the three bilinear constants, it was necessary to adjust the four observations to the most probable bilinear transformation. It will be seen that the corrections which it was necessary to apply to the observations were small, being in fact well within the errors of observation. The circle *a d c e* corresponds to the entire imaginary axis of Z; the arc *a b c* corresponds to the entire positive axis of Z. Circles are also shown corresponding to values of Z having constant real components of 1,000, 2,000 and 3,000 ohms and constant imaginary components of $\pm 1{,}000$ and $\pm 2{,}000$ ohms. The line impedances K_1 and K_2 are also shown. As the particular line under measurement effects the transformation of the rectangular network shown in Fig. 13 into the orthogonal system of circles, the diagram shows that the driving point impedance has the resistance limits 1,270 to 2,640 ohms and the reactance limits $-1{,}070$ to $+300$ ohms. The diagram as it stands is sufficiently complete to permit of reading off approximately the value of the driving point impedance for any value of the impedance Z bridged at the receiving end of the line.

The following construction will be required below and may be proven here.

The effective joint impedance S of two impedances Z_1, Z_2 in parallel coincides with the intersection of the circles which are tangent to these impedances at the origin and have the individual impedances as chords. This construction follows at once from the circular locus of S for variable modulus of either Z_1 or Z_2 and the fact that if one of the parallel impedances Z_1 vanishes or the other impedance Z_2 becomes infinite the joint impedance is equal to Z_1. This construction is employed in Fig. 15 for obtaining S from Z_1 and Z_2 or vice versa.

Division of Power between the Resistances and Reactances of a Network

The total power taken by a network is the sum of the powers taken by the individual self-impedances and mutual impedances, and to determine the division of this power between parts of the network it is merely necessary to find the summations for each part separately. As the total power and all of its components are directly proportional to the square of the current entering the network at the driving point, it is more convenient to consider, as the immediate object of discussion, the effective impedances which are defined as the ratios of the powers to the driving current squared. Accordingly we shall discuss the effective impedances S, U, $V\,i$ which correspond respectively to the total powers taken by the entire network, by the true resistances alone, and by the reactances alone. From this definition of these impedances it follows that

$$S=U+Vi=\sum_{j=1}^{n}\sum_{k=1}^{n} Z_{jk}\frac{I_j I_k}{I_d^2}=\sum_{j=1}^{n} Z_j\left(\frac{I_j}{I_d}\right)^2+2\sum_{j=1}^{n-1}\sum_{k=j+1}^{n} Z_{jk}\frac{I_j I_k}{I_d^2},$$

$$U=\sum_{j=1}^{n}\sum_{k=1}^{n} R_{jk}\frac{I_j I_k}{I_d^2}, \qquad \text{where } Z_{jk}=R_{jk}+i\,X_{jk} \qquad (26)$$

$$Vi=i\sum_{j=1}^{n}\sum_{k=1}^{n} X_{jk}\frac{I_j I_k}{I_d^2}.$$

The impedance U corresponding to the power taken by the resistances in the general passive network may have any argument, and any modulus which is not greater than the effective resistance of the network. To prove:

Consider an ideal line of zero attenuation containing s wave lengths, closed at the far end through a resistance equal in value to the line impedance K, with an impedance $(R-K)+Bi$ in series at the sending end so as to make the total impedance at the sending end equal to $R+Bi$. A current I flowing at the sending end gives rise to a current I cis $(-2\pi s)$ at the receiving end so that the total power taken by the resistances is

$$P=(R-K)\,I^2+K\,I^2 \text{ cis } (-4\pi s)$$

Therefore

$$U=(R-K)+K \text{ cis } (-4\pi s)$$

an impedance which may obviously assume any argument and any modulus not exceeding R with positive real values of K, $(R-K)$, and s.

The modulus of U can under no circumstances be greater than the effective resistance of the network for if this were the case the correlated sinusoidal oscillation would have, at some part of each oscillation, a negative total consumption of power by the resistances which is obviously impossible when the network contains neither sources of power nor so-called negative resistances, which are excluded throughout this discussion.

In Fig. 14 S and R represent the effective driving point impedance and the effective driving point resistance of the network, while U and Vi show a possible resolution of the impedance S into components corresponding to the powers taken by the true resistances and the reactances respectively. The circle $R\,b\,c\,d$ drawn about the origin with $O\,R$ as a radius is the maximum possible locus of U. If U falls at point b or d the power taken by the reactances has its maximum or its minimum value. If U falls at R the power taken by the reactances is 90 degrees ahead of the power taken by the resistances and this case corresponds to the series arrangement of a resistance and a reactance. (This is for positive reactance; with negative reactance the lead becomes a 90 degree lag.) At point c the relative phases are reversed, the resistances taking power 90 degrees in advance of that taken by the reactances; this case, as follows from the formulæ deduced below for parallel circuits, may be realized theoretically by the association of a pure resistance and a pure positive reactance in parallel. The point of special interest is the origin O; if U vanishes the cisoidal powers taken by the various resistances cancel each other in the summation for the resultant; in the correlated sinusoidal oscillation the power taken by the resistances is constant, that is the total generation of heat in the network does not fluctuate during an oscillation. This would seem to be a property which might have practical application.

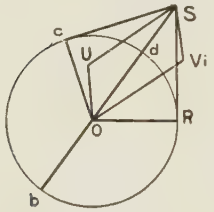

FIG. 14.—Resolution of the driving point impedance S into the impedances corresponding to the power taken by the resistances (U) and by the reactances ($V\,i$); $R\,b\,c$ is the extreme boundary for U.

If λ_1, λ_2, are the maximum and minimum driving point impedance arguments obtainable from the elements employed in a network of driving point impedance $S = R + Xi = |S| \operatorname{cis} \sigma$ the impedance U must lie in the lenticular area common to the two circles which intersect at the effective resistance of the network (R) and are centered at the projections of S on lines drawn through the origin at the angles $(\sigma - \lambda_1)$ and $(\sigma - \lambda_2)$.

Multiply each impedance Z_{jk} in the network by cis $\left(\frac{\pi}{2}-\lambda\right)$. As this leaves the current ratios unchanged the new value of U will be

$$\underline{U}=\sum\sum|Z_{jk}|\cos\left(\frac{\pi}{2}-\lambda+\sigma_{jk}\right)\frac{I_j I_k}{I_d^2}$$

$$=i\cos\lambda\sum\sum|Z_{jk}|\operatorname{cis}\sigma_{jk}\frac{I_j I_k}{I_d^2}$$

$$-\,i\operatorname{cis}\lambda\sum\sum|Z_{jk}|\cos\sigma_{jk}\frac{I_j I_k}{I_d^2}$$

$$=i\,S\cos\lambda-i\,U\operatorname{cis}\lambda$$

Therefore $U=i\,\underline{U}\operatorname{cis}(-\lambda)+S\cos\lambda\operatorname{cis}(-\lambda)$

which expresses the actual value of U in terms of the modified value $\underline{U}$. We may make $\lambda=\lambda_1$ without introducing any resultant negative resistance in the network, for the multiplication of each impedance by cis $\left(\frac{\pi}{2}-\lambda_1\right)$ raises the maximum argument from λ_1 to $\pi\div 2$. The extreme possible boundary limit for U will then be the circle of radius equal to the new effective resistance or

$$\text{Extreme limit for } \underline{U}=|S|\cos\left(\sigma+\frac{\pi}{2}-\lambda_1\right)\operatorname{cis}\mu$$

$$=|S|\sin(\lambda_1-\sigma)\operatorname{cis}\mu$$

where μ is any real angle.

Substituting this in the above equation, we obtain as a necessary condition

$$\text{Limit for } U=|S|\cos\lambda_1\operatorname{cis}(\sigma-\lambda_1)+i|S|\sin(\lambda_1-\sigma)\operatorname{cis}(\mu-\lambda_1)$$

Since the only variable is the unrestricted real quantity μ this locus for U is the circle of which the center is the first term and the radius the modulus of the second term. The first term is the point at the foot of the perpendicular let fall from the extremity of S on the line cis $(\sigma-\lambda_1)$ and the distance from this point to the extremity of R is $||S|\cos\sigma-|S|\cos\lambda_1\operatorname{cis}(\sigma-\lambda_1)|$ $=|S||\operatorname{cis}-\lambda_1||\cos\sigma\operatorname{cis}\lambda_1-\cos\lambda_1\operatorname{cis}\sigma|=|S\sin(\lambda_1-\sigma)|$, the modulus of the second term.

The corresponding proof for the minimum limit is made by substituting $-\left(\frac{\pi}{2}-\lambda_2\right)$ for $\left(\frac{\pi}{2}-\lambda\right)$. That the lenticular area thus defined is a sufficient as well as necessary restriction is proven by the properties of parallel circuits discussed below.

We may note that U cannot vanish unless there is a range of at least 90 degrees in the impedances of the elements entering the network.

All possible distributions of power between the resistances and the reactances, with any given total driving point impedance may be obtained from two reactive resistances in parallel, and it will now be of interest to examine this case in detail. We will assume that the impedances Z_1, Z_2, when connected in parallel are to have a given total effective impedance S and a given impedance U corresponding to the total power taken by the resistances. These conditions give

$$S=\frac{Z_1 Z_2}{Z_1+Z_2}$$

$$U=\frac{Z_1+Z_1'}{2}\left(\frac{Z_2}{Z_1+Z_2}\right)^2+\frac{Z_2+Z_2'}{2}\left(\frac{Z_1}{Z_1+Z_2}\right)^2$$

$$=\frac{(Z_1 S'-Z_1' S)^2}{2 Z_1^2 (Z_1'-S')}+\frac{S+S'}{2} \tag{27}$$

where the first expression for U is in terms of the resistances and current ratios and the second expression is found by substituting for Z_2 its value in terms of Z_1 and S.

$$\left.\begin{aligned} \text{Let }\ F&=|F|\operatorname{cis}\varphi=U-\frac{S+S'}{2} \\ S&=|S|\operatorname{cis}\sigma \\ Z&=|Z|\operatorname{cis}\theta \end{aligned}\right\} \tag{28}$$

and put the last expression for U in the form

$$2\,F Z^2 (Z'-S')=(Z S'-Z' S)^2=-4|Z^2 S^2|\sin^2(\theta-\sigma)$$

where subscripts are omitted as the equation applies equally to Z_1 and Z_2. Taking the imaginary part of this equation before and after multiplying by cis $(-\theta-\varphi)$ we have, after dropping the common factors $2|F\,Z^2|i$ and $2|Z^2\,S|\sin\,(\theta-\sigma)\;i$,

$$|Z|\sin\,(\theta+\varphi)-|S|\sin\,(2\,\theta-\sigma+\varphi)=0$$

$$-|F|=2|S|\sin(\theta-\sigma)\sin(\theta+\varphi)=|S|[(\cos(\sigma+\varphi)-\cos(2\theta-\sigma+\varphi)]$$

$$\text{therefore } Z=|S|\,\frac{\sin\,(2\theta-\sigma+\varphi)}{\sin\,(\theta+\varphi)}\,\text{cis}\,\theta \tag{29}$$

with values of θ given by

$$\cos\,(2\theta-\sigma+\varphi)=\cos\,(\sigma+\varphi)+|F\div S|$$

which is the required solution for Z_1 and Z_2.

The graphical construction for determining S and U when Z_1 and Z_2 are given, or vice versa, are sufficiently simple to be of assistance. The construction rules which are readily deducible from the preceding work are as follows:

Given Z_1 and Z_2 to find S and U, Fig. 15. Find the impedance S of Z_1 and Z_2 in parallel and draw the circle having S as a diameter, on this circle locate points d_1 and d_2 so that arc $S\,d_1=$arc $c_1\,R$, and arc $S\,d_2=$arc $c_2\,R$ where c_1, c_2 and R are the intersections of the circle with Z_1, Z_2, and the resistance axis, using d_1 and d_2 as centers strike circles passing through point R. The other intersection of the circles is the effective impedance U.

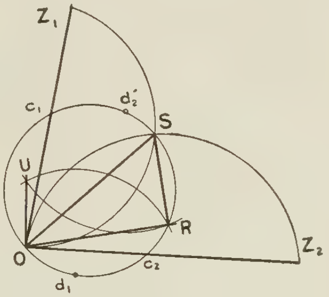

FIG. 15.—Graphical construction for determining the effective driving point impedance (S) and the effective impedance corresponding to the power taken by the resistances (U) for two impedances Z_1 and Z_2 in parallel.

Given S and U to find Z_1 and Z_2. Find the intersections d_1 and d_2 of the circle having S as a diameter and the normal right line bisecting $U\,R$, lay off arc $c_1\,R=$arc $S\,d_1$, and arc $c_2\,R=$arc $S\,d_2$. Then $O\,c_1$ and $O\,c_2$ are the direction lines for Z_1, Z_2 the magnitude of which are found by the intersection therewith of the circles tangent to $O\,c_1$ and $O\,c_2$ which have $O\,S$ as a chord.

The vanishing of U requires a difference of 90 degrees in the two impedances Z_1 and Z_2; if the driving point impedance S is to be pure resistance $(=R)$ we have the important case where the parallel impedances are $(R\pm R\,i)$.

Free Oscillations

The characteristic feature of free oscillations is that, throughout the part of the network over which the oscillation extends, the driving point impedance is equal to zero. This follows from the fact that as the driving point impedance is equal to the impressed electromotive force divided by the current, it vanishes when the electromotive force vanishes, provided the current does not vanish. The criterion for free oscillations is therefore

$$A=O \tag{30}$$

The solution of this equation contains all of the possible values of the time coefficient p. Each possible oscillation is aperiodic or not according as p is pure imaginary or not; p cannot be real for any actual system, since energy must be dissipated in any oscillation which may occur in such a system.

In present day practical applications, complex or imaginary values of p occur, as a rule, only for free vibrations; but there is no inherent reason why such vibrations should not arise as forced vibrations, for that requires only that an alternator be used which gives an electromotive force of constant period and logarithmically decreasing amplitude. This condition is approximately realized by a freely vibrating system which is loosely coupled to the network under consideration.

As an illustration of the application of the method to free oscillations, determine the time coefficients (*i.e.*, the free periods and associated damping constants) for two coupled circuits of impedances Z_1, Z_2, Z_{12}. For this case

$$A=\begin{vmatrix} Z_1 & Z_{12} \\ Z_{12} & Z_2 \end{vmatrix}=Z_1\,Z_2-Z_{12}^2=0$$

$$=[(2\,\delta_1+p\,i)\,(2\,\delta_1'+p\,i)+p_1^2]\,[(2\,\delta_2+p\,i)\,(2\,\delta_2'+p\,i)+p_2^2]$$

$$+k^2\,p^2\,(2\,\delta_1'+p\,i)\,(2\,\delta_2'+p\,i) \tag{31}$$

where $\delta=\frac{R}{2\,L}$, $\delta'=\frac{G}{2\,C}$, $p=\frac{1}{\sqrt{L\,C}}$, $k=\frac{M}{\sqrt{L_1\,L_2}}$,

taken with subscripts 1 and 2 to correspond with the circuits. For small damping constants δ, δ' (**31**) may be developed into a series of which the first terms are

$$p\,i = p_0\,i - \frac{\delta_1(p_0^2-p_2^2)+\delta_1'(p_0^2(1-k^2)-p_2^2)+\delta_2(p_0^2-p_1^2)+\delta_2'(p_0^2(1-k^2)-p_1^2)}{2p_0^2\,(1-k^2)-p_1^2-p_2^2}+\dots \tag{32}$$

$$\text{where } p_0 = \sqrt{\frac{p_1^2+p_2^2 \pm \sqrt{(p_1^2-p_2^2)^2+4\,k^2\,p_1^2\,p_2^2}}{2\,(1-k^2)}} \tag{33}$$

are the time coefficients which would obtain if the circuits were free from all dissipative losses.

In the special case of two identical circuits ($Z_1 = Z_2 = Z$) the determinantal equation becomes $A = (Z+Z_{12})\,(Z-Z_{12}) = 0$

$$\text{or } R+(L \pm M)\,p\,i + \frac{1}{G+C\,p\,i} = 0$$

$$\text{whence } i\,p = -\left(\frac{R}{2\,(L\pm M)}+\frac{G}{2\,C}\right)$$

$$\pm i\sqrt{\frac{1}{(L\pm M)\,C}-\left(\frac{R}{2\,(L\pm M)}-\frac{G}{2\,C}\right)^2} \tag{34}$$

without any restrictions as to the values R, L, M, G and C.

Infinite Number of Circuits—Eddy Currents.

When the number of circuits is increased indefinitely the determinant A becomes of infinite order. The particular application which at once suggests itself is that of eddy currents in a cylindrical core. Consider the core of radius a as being made up of a large number n of concentric hollow tubes of thickness $a \div n$ and radii $q\,a \div n$, ($q = 1, 2, \;.\;.\;.\; n$) and take as the driving winding another tube of radius $(n+1)\;a \div n$ which has infinite conductivity. Then the impedance for tubes q and r per unit of length is

$$Z_{qr} = Z_{rq} = 2\,\pi\,\rho\left(\delta_{qr}\,q + 2\,z\,i\,\frac{q^2}{n^2}\right), \qquad \begin{array}{l} 1 \leqq q \leqq r \leqq n+1 \\ \delta_{qr} = \begin{cases} 1 \text{ if } q = r < n+1 \\ 0 \text{ in other cases.} \end{cases} \end{array} \tag{35}$$

with $z = \dfrac{\pi\,a^2\,\mu\,p}{\rho} = \dfrac{\mu\,p}{R} = \dfrac{Lp}{4\,\pi\,\rho}$, R and L being the longitudinal resistance ($\rho \div \pi\,a^2$) of the core per unit length and inductance $4\,\mu\,\pi^2\,a^2$ of the driving winding per turn per unit length of core.

The driving point impedance of the winding is, if $x = 2zi \div n^2$,

$$S_{n+1} = \frac{A}{A_{n+1,\,n+1}} = 2\pi\rho \frac{\begin{vmatrix} 1+x & x & x & \ldots & x & x \\ x & 2+2^2x & 2^2x & \ldots & 2^2x & 2^2x \\ x & 2^2x & 3+3^2x & \ldots & 3^2x & 3^2x \\ \cdot & \cdot & \cdot & \ldots & \cdot & \cdot \\ \cdot & \cdot & \cdot & \ldots & \cdot & \cdot \\ x & 2^2x & 3^2x & \ldots & n+n^2x & n^2x \\ x & 2^2x & 3^2x & \ldots & n^2x & (n+1)^2x \end{vmatrix}}{\begin{vmatrix} 1+x & x & x & \ldots & x \\ x & 2+2^2x & 2^2x & \ldots & 2^2x \\ x & 2^2x & 3+3^2x & \ldots & 3^2x \\ \cdot & \cdot & \cdot & \ldots & \cdot \\ \cdot & \cdot & \cdot & \ldots & \cdot \\ x & 2^2x & 3^2x & \ldots & n+n^2x \end{vmatrix}},$$

$$= 2\pi\rho \frac{2\,(n+1)!\displaystyle\sum_{k=1}^{n+1}\left(\frac{z\,i}{n^2}\right)^k \frac{(n+k)!}{(k-1)!\,k!\,(n+1-k)!}}{n!\displaystyle\sum_{k=0}^{n}\left(\frac{z\,i}{n^2}\right)^k \frac{(n+k)!}{(k!)^2\,(n-k)!}}$$

the transformation of the determinants into series of powers of $x \div 2 = z\,i \div n^2$ is proven to be correct by its being true for $n = 1$ and 2 and satisfying the difference equations for the numerator (N_n) and the consecutive values of the denominator $(D_{n-2}, D_{n-1}, D_n$ and $D_{n+1})$

$$N_n = D_{n+1} - (n+1)\,D_n$$

$$D_n = (2n-1)\,(1+x)D_{n-1} - (n-1)^2 D_{n-2}$$

which are obtained by adding $(n+1)\,D_n$ to N_n, that is increasing its last element by $(n+1)$, which becomes D_{n+1} and by expanding D_n according to the last row and column after subtracting therefrom the next to the last row and column. For n = infinite,

$$\left.\begin{aligned}
S &= 2\pi\rho\,\frac{2\sum\limits_{k=1}^{\infty}\dfrac{(z\,i)^k}{(k-1)\,!\,k!}}{\sum\limits_{k=0}^{\infty}\dfrac{(z\,i)^k}{(k!\,)^2}} \\
&= 2\pi\rho\,\frac{2\,z\,i+(z\,i)^2+\dfrac{(z\,i)^3}{6}+\;.\;.\;.}{1+z\,i+\dfrac{(z\,i)^2}{4}+\dfrac{(z\,i)^3}{36}\;+\;.\;.\;.} \\
&= 2\,\pi\,\rho\,\frac{-\sqrt{-4\,i\,z}\,J_1\sqrt{-4\,i\,z}}{J_0\sqrt{-4\,i\,z}} \\
&= 4\,\pi\,\rho\,z\,\frac{d}{d\,z}\log J_0\sqrt{-4\,i\,z} \\
&= 4\,\pi\,\rho\,z\,i\left(1+\frac{J_2\sqrt{-4\,i\,z}}{J_0\sqrt{-4\,i\,z}}\right)
\end{aligned}\right\}\qquad(36)$$

which are the well known results expressed in Bessel's functions, To make the formula perfectly general for any driving winding it is necessary only to multiply by the length of the core and the square of the total number of turns in the winding and to add the impedance of the winding which arises externally to the core.

This example shows that certain infinite systems of circuits which are ordinarily solved by partial differential equations may be handled by the general determinantal solution, but of course when transcendental functions are involved, as in the case of eddy currents, the algebraical reduction may introduce some complexity.

Eddy currents in transformer plates give the following results:

For a plate of thickness $2a$, width w and axial length l divided into a large number of $2n$ of sheets of equal thickness and surrounded by a close fitting driving winding of a single turn and zero resistance:

$Z_{qr}=Z_{rq}=\frac{2\,\rho\, w\, n}{a\, l}\left(\delta_{qr}+4\, z\, i\,\frac{q}{n^2}\right)$, $z=\frac{\pi\, a^2\, \mu\, p}{\rho}$, q, r and δ_{qr} as above and the driving point impedance at limit $n=$infinite is

$$S=\frac{2\,\rho\, w}{a\, l}\,\sqrt{4\, z\, i}\,\tanh\sqrt{4\, z\, i} \qquad \textbf{(37)}$$

SKIN EFFECT

For a cylindrical conductor of radius a, length l and steady current resistance R with close fitting return shell of zero resistance, the conductor being divided into n concentric tubes of equal cross section with circuit q comprising adjacent tubes q and $q+1$:

$$Z_{qr}=Z_{rq}=\frac{\mu\, l\, p\, n}{z}\left(\delta_{qr}+\frac{z\, i}{n\, q}\,\delta'_{qr}\right) \qquad \delta_{qr}=\begin{cases} 2, \text{ if } q=r<n \\ 1, \text{ if } q=r=n \\ -1, \text{ if } q=r\pm 1 \\ 0, \text{ in other cases}\end{cases}$$

$$\text{with } z=\frac{\pi\, a^2\, \mu\, p}{\rho}=\frac{\mu\, p\, l}{R} \qquad \delta'_{qr}=\begin{cases} 1, \text{ if } q=r<n \\ 1\div 2, \text{ if } q=r=n \\ 0, \text{ in other cases}\end{cases}$$

and the driving point impedance at limit $n=$infinite is

$$S=-\frac{2\,\mu\, l\, p\, i}{\sqrt{-4\, i\, z}}\;\frac{J_0\sqrt{-4\, i\, z}}{J_1\sqrt{-4\, i\, z}} \qquad \textbf{(38)}$$

Details of Proof. Regard each hollow cylindrical tube as concentrated on its mean diameter, while retaining its actual resistance, $\rho\, n\, l\div\pi\, a^2$. This resistance with sign changed will then be the mutual impedance between any two adjacent circuits, as each tube carries the difference between the currents in the two adjacent circuits of which it forms a common part; no other mutual impedances occur, as no other current products enter the expression for the total energy. The self-impedance of the qth circuit is made up of twice this resistance, together with the inductance $l\div q$; the inductance being found by the single turn solenoid formula 4π cross-section$\div$length, the cross section being $a\, l\div 2\sqrt{q\, n}$ and the length (*i.e.*, mean circumference) being $2\,\pi\, a\sqrt{q\div n}$. For the outermost circuit ($q=n$) this impedance is to be divided by two, since its return circuit is of zero resistance and zero thickness. The impedances Z_{qr} are thus, as stated above. After removing the factor $\mu\, p\, l\, n\div z$ from each element of determinants A and A_{nn} and placing $x = z\,i \div n$, we have

$$S = \frac{A}{A_{nn}} = \lim_{n=\infty} \frac{\mu p l n}{z} \frac{\begin{vmatrix} 2+\frac{x}{1} & -1 & 0 & \cdots & 0 & 0 \\ -1 & 2+\frac{x}{2} & -1 & \cdots & 0 & 0 \\ 0 & -1 & 2+\frac{x}{3} & \cdots & 0 & 0 \\ \cdot & \cdots & \cdots & \cdots & \cdot\;\cdot & \cdot\;\cdot \\ \cdot & \cdots & \cdots & \cdots & \cdot\;\cdot & \cdot\;\cdot \\ 0 & 0 & 0 & \cdots & 2+\frac{x}{n-1} & -1 \\ 0 & 0 & 0 & \cdots & -1 & 1+\frac{x}{2\,n} \end{vmatrix}}{\begin{vmatrix} 2+\frac{x}{1} & -1 & 0 & \cdots & 0 & 0 \\ -1 & 2+\frac{x}{2} & -1 & \cdots & 0 & 0 \\ 0 & -1 & 2+\frac{x}{3} & \cdots & 0 & 0 \\ \cdot & \cdots & \cdots & \cdots & \cdot\;\cdot & \cdot\;\cdot \\ \cdot & \cdots & \cdots & \cdots & \cdot\;\cdot & \cdot\;\cdot \\ 0 & 0 & 0 & \cdots & 2+\frac{x}{n-2} & -1 \\ 0 & 0 & 0 & \cdots & -1 & 2+\frac{x}{n-1} \end{vmatrix}}$$

$$= \frac{\mu p l}{z} \frac{\displaystyle \lim_{x=\infty} \sum_{k=0}^{n} \frac{(2n-k)\ (n-1)!}{2\,(k!)^2\,(n-k)!}\,x^k}{\displaystyle \lim_{x=\infty} \frac{1}{n} \sum_{k=0}^{n-1} \frac{n!}{k!\,(k+1)!\ (n-k-1)!}\,x^k}$$

the correctness of the series expansions for the determinants is readily proven for $n=1$ and 2 directly from the determinants and then extended step by step to any value of n by expanding the determinants according to the terms in the last row and column so as to obtain expressions for the denominator (D_n) and the numerator (N_n) in terms of the denominator with different values of n, *viz*:

$$D_n = \left(2+\frac{x}{n-1}\right) D_{n-1} - D_{n-2}$$

$$N_n = \left(1+\frac{x}{2\,n}\right) D_n - D_{n-1} = D_{n+1} - \left(1+\frac{x}{2\,n}\right) D_n = \tfrac{1}{2}\left(D_{n+1} - D_{n-1}\right)$$

which are readily shown, by substituting the above series expressions, to be identically satisfied for all values of n.

Finally replacing x by its value $z\,i \div n$ and passing to the limit, $n=\infty$

$$S = \frac{\mu p l}{z} \frac{\displaystyle\sum_{k=0}^{\infty} \frac{(z\,i)^k}{(k!)^2}}{\displaystyle\sum_{k=0}^{\infty} \frac{(z\,i)^k}{k!\,(k+1)!}}$$

which is identically formula (**38**), as the numerator is the series for $J_0\sqrt{-4\,i\,z}$ and the denominator is the series for $2\,J_1\sqrt{-4\,i\,z} \div \sqrt{-4\,i\,z}$.

SUMMARY

1. The complex exponential function is shown to be, not a symbolic vector representation of the sinusoidal function, but a scalar function of fundamental importance in its own right, and enjoying algebraical power and energy relations as important as those of real functions. In order to emphasize the basic and distinctive character of the complex exponential function, it is given the name "cisoidal oscillation."

2. The correlation between sinusoidal oscillations and cisoidal oscillations is reduced to a few simple rules which cover power as well as currents and electromotive forces.

3. The general law of distribution of currents in any invariable network is shown to be that of stationary dissipation of power.

4. The law of distribution of cisoidal currents in any invariable network is reduced to that of stationary total power, or to the equivalent condition of stationary driving point impedance or admittance.

5. The cisoidal power is employed as the most convenient means for investigating the division of the instantaneous power between the resistances and reactances of a network.

6. The general solution for cisoidal oscillations in any invariable network is given in determinantal form and it is shown how the various impedances of any particular network may be written down at once and how the elimination of concealed circuits, mutual impedances or self-impedances may be accomplished. Applications to impedance loci, free oscillations and infinite systems of circuits are also given.

[Reprinted from the PHYSICAL REVIEW, Vol. XXXII., No. 6, June, 1911.]

SPARK LENGTH, POTENTIAL AND FREQUENCY OF OSCILLATION: THE "LAG EFFECT" IN ELECTRIC DISCHARGE.

BY J. C. HUBBARD.

INTRODUCTION.

THE spark potential for a given spark length is ordinarily defined as the greatest potential which can be applied to the spark gap for an indefinitely long time without causing the discharge to take place. The usual method of measuring spark potentials has accordingly been that of slowly increasing the potential, keeping the spark length constant, or of slowly diminishing the latter while the potential remains constant, until the discharge occurs. Extensive work has been done on the relation between spark length and potential for steady potentials, an admirable summary of which may be found in Sir J. J. Thomson's Conduction of Electricity through Gases (second edition). The study of short sparks has been especially prominent in recent years owing to the bearing of the phenomena upon the theory of ionization.[1]

It has long been known that a potential greater than the spark potential as defined above may be applied for a short time without producing discharge, especially if the gas be dry and free of dust. This effect has been called the "lag" of the spark, or the lag effect, and on it there has been much experimental work and discussion. Jaumann[2] pointed out some time ago that the time of lag is the interval necessary for some agency to convert the gas from an insulator into a conductor. It has been found that the presence of moisture, or the effect of such agents as ultra-violet light and Roentgen rays, in short, that the introduction by any agency of ions into the field between the electrodes, reduces the time of lag; though the ultimate discharge potential is not much affected.

---

[1] Conduction of Electricity through Gases, pp. 455–460. See also E. H. Williams, PHYS. REV., 31, pp. 216–240, 1910.

[2] Jaumann, Wied. Ann., 55, p. 656.

No very definite attempt seems so far to have been made to study quantitatively the lag effect. A promising method consists in applying electric oscillations of known amplitude and frequency to the spark gap. In a previous communication of mine to this journal[1] very positive indication was found that for sparks produced by an oscillating potential the spark length is a function not only of the maximum potential but also of the frequency of oscillation. The relation found was such that for very slow oscillations the spark potential approached the value for steady potentials, while with increasing frequency and constant spark gap the spark potentials became systematically higher. The work was not undertaken primarily with the object of studying the lag effect, and, as the spark gap in this case was at the break of an inductive circuit where complications due to the motions of parts might arise, in so far as it relates to the lag effect it is not to be considered of final value. There appeared almost simultaneously some interesting experiments by J. Algermissen[2] on the relation of spark length and potential for rapid oscillations of potential leading to similar results. The oscillations were produced in a system containing a spark gap by induction from a neighboring circuit. Sparks up to 2 cm. in length were studied, and complications arising from the length of spark being large in comparison to the radius of spark electrodes were introduced. The result was unmistakable, however, that as the frequency is increased the spark potential is increased for a given spark length.

The present study of alternating spark potentials makes use of a new method designed to give values of the potential and frequency under perfect control, and presents results of observation of a large number of cases together with some general conclusions.

The Source of Potential.

As a source of potential in the present work is used the oscillations set up in a circuit containing inductance and capacity when the initial current is interrupted. The conditions for breaking such a circuit without producing a spark at the break have been given in my paper referred to above. In brief, if the speed of separation of the contacts exceed a certain critical value, called the velocity of break, no spark will be produced on breaking the circuit. This critical velocity was found to be proportional to the frequency and to increase almost linearly with the maximum potential, the effect of damping being negligible. Making use of a circuit breaker operated under the proper conditions it is possible, within the limits set by the attainable velocity of break, to secure oscillations of any desired frequency and initial amplitude.

---

[1] J. C. Hubbard, Phys. Rev., 22, pp. 129–158, March, 1906.

[2] J. Algermissen, Ann. der Phys. (4), 19, p. 1016, April, 1906.

Method and Apparatus.

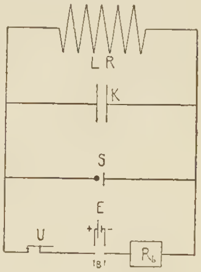

Fig. 1.

The electrical system is shown diagrammatically in Fig. 1. The principal parts consist of the inductance L having the resistance R, a condenser K, battery E, interrupter U, an auxiliary resistance R_b for varying the initial current, and a micrometer spark gap S in parallel with the inductance and capacity. Let the current $i_0 = E/(R + R_b)$ be established, then provided the circuit at U is broken with sufficient suddenness to prevent a spark forming there, we shall have oscillations of potential at the electrodes of the micrometer spark gap, which, in view of the small values of K and R and the large values of L (see measurements below) may be accurately expressed by

$$V = i_0\sqrt{\frac{L}{K}}\, e^{-\frac{R}{2L}t} \sin\left(\frac{t}{\sqrt{KL}}\right)$$

and which have the period $T = 2\pi\sqrt{KL}$.[1]

The method of observation consists in slowly lessening the width of the spark gap while interruptions of the current are being made until a spark takes place. The mean of several spark lengths so found is taken as the spark length corresponding to the initial current in the expression for V given above. The spark observations are made visually.

The condenser and inductance have been very fully described in previous communications from this laboratory and will be only briefly noticed here.

---

[1] Phys. Rev., 22, p. 131, 1906.

The *condenser*[1] consists of two thick steel plates of 25 cm. radius held apart by sets of three small cylinders cut from plane parallel plates of glass. The capacities were calculated from the formula of Kirchhoff. The range used in these experiments was between 200 and 600 cm.

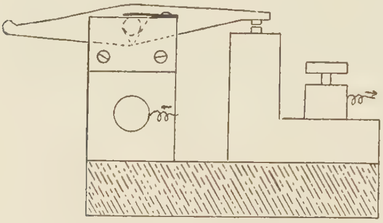

Fig. 2.

The *inductance*[2] consists of a coil of 3,600 turns of no. 18 (B. & S.) double cotton-covered copper wire wound in a large wooden spool. The channel filled with windings has a square cross-section 3 inches on a side, and its internal diameter is 8 in. The coil is divided into six independent sections of ten layers each; with all in series the inductance is 3.01 henries and the resistance 62 ohms. By using various combinations of sections a great range of inductance is possible.

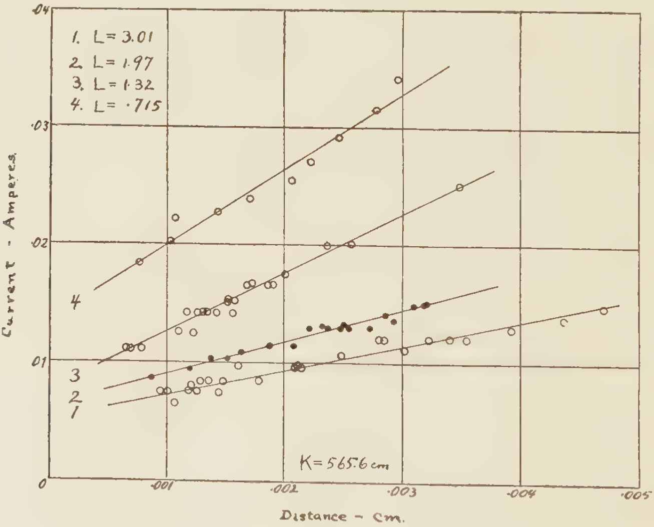

Fig. 3.

Besides this coil there were used two large coils from the Worcester Polytechnic Institute kindly loaned by Professor Duff. These had an inductance when used in series of nearly a henry. It was found, however, that the insulation of these coils was not sufficient for work with any but the smallest sparks.

---

[1] A. G. Webster, PHYS. REV., 6, p. 300, 1898.

[2] J. E. Ives, PHYS. REV., 14, p. 298, 1902.

The *interrupter*, one of several designed by Professor Webster for use with the drop chronograph (*loc. cit.*), may be readily understood by a glance at Fig. 2. The circuit is broken by the falling of a weight on the end of a lever. The requirements are perfect rigidity and freedom from vibration when the lever arm is struck, and a return to negligible resistance of contacts as soon as the circuit is closed. The lever should be of as small moment of inertia as is consistent with these requirements. The lever is of steel, shrunk on a steel axis which turns in V-shaped grooves in the tops of two upright projections of a brass frame. The latter is mounted on a block of ebonite which also carries the mounting for the other contact. A pair of stiff steel springs pressing the upper side of the axis keep it firmly in the grooves, and a stiff band of steel pressing against one end of the axis holds the other end against a metal stop mounted on the outside of the opposite post. Perfect and permanent adjustment is thus secured, the arrangement constituting a Kelvin so-called geometrical slide. The contacts are of silver and rubber bands (not shown), cause the contacts to press together as soon as the weight which operates the lever has done its work. This arrangement has given perfect satisfaction and stands the

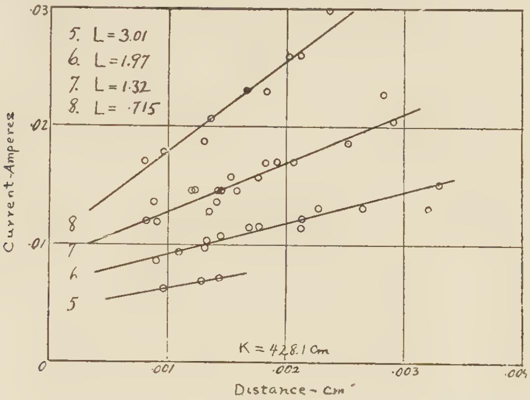

Fig. 4.

roughest usage. The resistance of the interrupter with the circuit closed was invariably found to be a small fraction of an ohm.

The *circuit breaker* first tried was the projectile of the drop chronograph. Several seconds were required to produce a single interruption and many minutes to find a single spark length. In its place was substituted a bicycle wheel operated by an electric motor. The wheel carried a two pound mass of iron on its rim for striking the lever arm of the break, suitable counterpoise being added to the inside of the rim on the opposite side. The wheel was usually rotated so as to produce about two breaks per second.

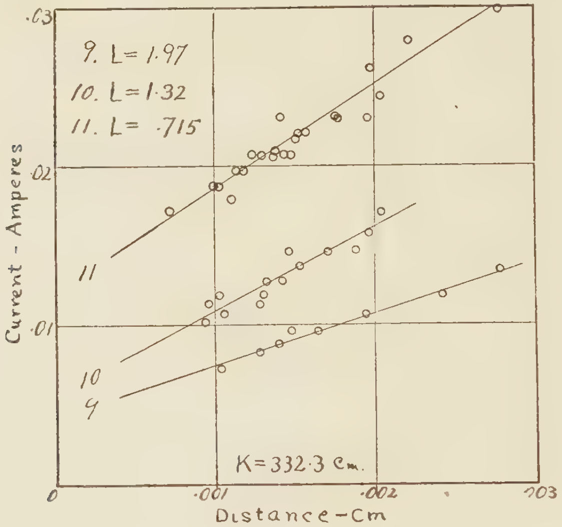

Fig. 5.

The *micrometer spark gap* is very similar in principle to many which have been described before.[1] The spark electrodes were of steel, one of them being a plane 10 × 12 mm., the other a ball 6.25 mm. in diameter mounted on the end of a brass cylinder of nearly the same diameter. These were ground with several pourings of flour of emery then given a high polish with diamantine on soft leather. The amount of labor involved in producing surfaces of high polish, free from scratches, on steel is extraordinary, and I am greatly indebted to Mr. H. F. Stimson, Scholar in Physics in Clark University, who undertook a careful study of the matter. Cleaning of the surfaces was effected by rubbing with soft, clean cloths, then with chamois skin and chalk or jeweller's rouge. Small particles of dust were removed by the use of an air jet. The plane was mounted in parallel ways and the ball with its axis of rotation at an acute angle with the plane. After the passage of a spark the plane was given a small translation and the ball a small rotaton so as to move the near surfaces in opposite directions, thus presenting fresh surfaces for the next spark. During the final measurements a jet of air (see below) was directed into the space between the electrodes. A separate circuit, the leads of which could be attached to the spark electrodes, containing a battery, resistance, and millivoltmeter was used to determine the position of contact of the electrodes. This zero was found immediately after the passage of each spark. It could be determined to one-tenth division of the drumhead of the micrometer screw, corresponding to .00002 cm. The results given here are mostly for sparks from .005 to .0005 cm. in length. The order of accuracy is therefore about one per cent. Difficulties of another sort discussed below render greater accuracy of reading useless for the present purpose.

---

[1] G. M. Hobbs, Phil. Mag. (6), 10, p. 620, December, 1905.

Potentiometer and bridge circuits were arranged for frequently testing respectively the electromotive force E of the battery and the resistance of various parts of the system. For the battery E was used one or two storage cells.

CONTROL EXPERIMENTS.

Frequency of Interruption of the Circuit.—On changing from the drop chronograph to the bicycle-wheel break no change of result was observed, showing that it was immaterial whether the train of oscillations was applied to the spark gap once in many seconds or twice per second.

Surface of the Spark Electrodes.—Different methods of polishing and cleaning gave approximately the same results except for the higher frequencies where the passage of the spark is extremely sensitive to the state of the surfaces. Especial care had to be taken to use only the freshest of materials in cleaning the electrodes.

State of the Gas.—First experiments gave results which varied by 50 per cent. among themselves. After much effort to get more uniform data it was found that a fine jet of air blown from a tapering glass tube into the discharge space reduced the necessary sparking potential to a very much lower value and enabled results to be repeated within a few per cent. of each other (curves 1–11, Figs. 3–5).[1] Such discrepancies as then remained were found to be due to inefficient insulation in the windings of the coil, and before a last series of measurements was made were eliminated almost entirely by placing the coil in kerosene (curves 12–17, Fig. 6). Obviously, as the experiments go, there is no need to consider the effect of changes of atmospheric pressure. It may be remarked, however, that the most consistent results were obtained during rainy weather.

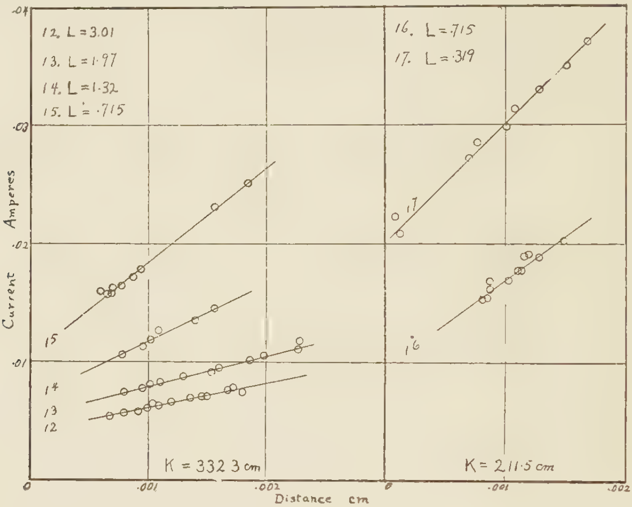

Fig. 6.

POTENTIAL AT THE TIME OF SPARKING.

While the damping in these experiments is small, it is of some interest to know whether the discharge begins during the first maximum of potential. It is conceivable that if the effect of a maximum were just unable to produce a spark it might succeed in forming ions which would enable the spark to pass at some following maximum. The first spark of condenser discharge has long been known to be of different character from the others and has been given the name pilot spark. I have found evidence to show that, given a spark length and the oscillating potential which will just produce a spark, but not greater, the spark will begin during the first maximum of induced potential. A micrometer microscope was focused upon the space between the contacts of the break, and the velocity of break, at first high enough to prevent sparking altogether, was reduced until a very faint spark occurred. The length of the spark together with the known velocity of break and the frequency of oscillation placed the time of occurrence of the spark very near the time of the first maximum of potential, *i. e.*, within one eighth of the period. A small further reduction of the velocity of break caused a complete change in the character of the spark. It was now thick, brilliant and longer and possessed a beaded appearance. This is because the rapidly moving electrode was in

---

[1] The air coming from a filter-pump air-blast, the water in which was usually at about 6° C., passed through a long rubber tube and then through a plug of glass wool to filter out dust, before passing to the spark gap. The air was delivered at approximately the temperature of the room (20°) and was far from being saturated with moisture. The effect of the air was very striking, and seems to show that a part of the lag effect depends upon the number of ions initially present in the air. A tube containing a small quantity of radium placed under the spark gap produced similar results. A systematic study of the effect of various ionizing agents is to be made in later work.

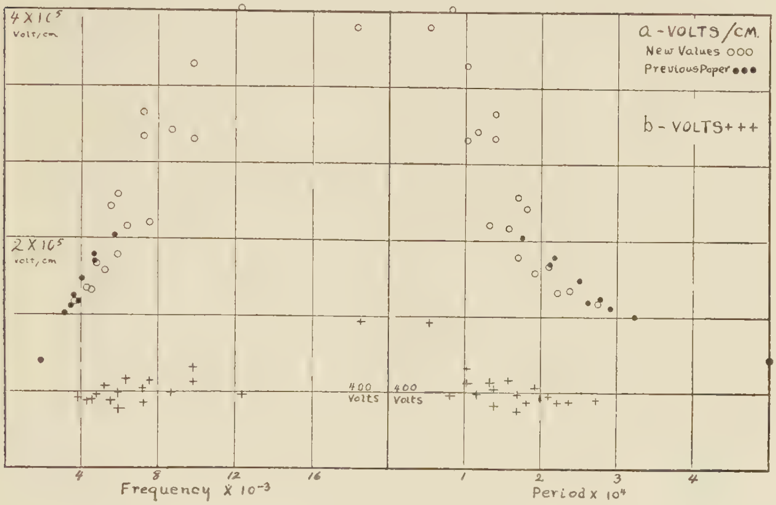

Fig. 7.

different positions at the times of successive oscillations. Measurement showed that the spark length for the first luminous condensation gave a time which invariably came in the second half period, again within one eighth period which was about the reading accuracy of the necessarily low power microscope. The pilot spark which must have preceded it was completely masked. In any event it would seem that the first spark takes place during the first maximum as was directly observed for the limiting case. For *constant* spark lengths at the micrometer spark gap no such changes were observed, which is easily understood as we do not there have the influence of the rapidly widening spark gap in preventing the second and successive discharges from passing. It seems probable, also, that unless the first maximum is great enough to produce a discharge, any ions that might be formed would be swept out of the field, making it less likely that the successive maxima would produce a discharge.

Further evidence on this question will be found in the discussion of results. Assuming that the spark takes place near the end of the first quarter period we have, in the most unfavorable case ($R = 27.1$ ohms, $L = .715$ henry, and $K = 6.28 \times 10^{-10}$ farads), as the value of the damping factor $e^{-\frac{R}{2L}\frac{\pi}{2}\sqrt{KL}} = .9987$, which is unity for our purpose. We therefore take

$$V = i_0 \sqrt{\frac{L}{K}} \sin\left(\frac{t}{\sqrt{KL}}\right)$$

and

$$V_m = i_0 \sqrt{\frac{L}{K}}. \qquad (1)$$

This discussion ignores the fact that the resistance of the coil for rapid oscillations increases somewhat rapidly with the frequency.[1] Since we have a margin of safety of several hundred per cent., it is hardly likely that the effect of the damping need be considered.

RESULTS.

Several series of observations were made to show the relationship between spark length and initial current. The results of these measurements are shown graphically in Figs. 3–6. Abscissæ represent spark lengths in cm., and the ordinates represent the currents in amperes which were flowing at the various times of break and from which the potentials may be calculated from equation (1). Each point shown in the figures is a mean of several, usually five, readings.

---

[1] See, for example, A. Esau, Ann. der Phys. (4), 34, pp. 57 and 81, 1911.

The most important result of the measurements is at once seen from the figures; namely, that with given K and L and within the limits of the experiments the relation between initial current and spark length is a linear one. Lines best representing the results are drawn in the figures and are given numbers which correspond in general to the order in which the experiments were made. Series 1 and 2, however, contain observations weeks apart, some of the other series having been determined in the meantime. All the series obtained with the air jet in use are shown.

During most of the control experiments spark lengths were obtained up to .01 cm. Owing to the gradual deterioration of the insulation of the coils the available region of experiment became more restricted and by the time series 10 was reached it was almost impossible to get results at all, while such as were obtained scattered very badly. The coil was then immersed in kerosene for the remainder of the work, giving much more regular results (series 12–17). Immersion in kerosene did not, however, restore the available working region to its former value. Measurements taken with the two coils furnished by Professor Duff gave consistent readings for only the smallest initial currents which would produce visible sparks. These results indicate very clearly that for satisfactory work with these oscillations coils must be used of which there is no question as to high insulation. A coil is now being designed with which it is hoped to meet such objections in an extension of the work over a wider range of spark lengths and under varied conditions. It must be remarked, however, that no indication has been found of a change of slope of any of these curves due to the progressive deterioration of the insulation.

Treatment of the Observations.—Since the relationship between the initial current and the spark length is a linear one, and the slopes of the lines are affected by change in the inductance or capacity only, it is at once evident that for oscillating potentials under such conditions the period alone and not the amplitude affects the spark constants. We may write

$$i_0 = \alpha x + \beta$$

as expressing the relation between the current i_0 and spark length x. The constants α and β depend only on K and L. Since

$$V_m = i_0\sqrt{L/K}$$

(see equation (1) and discussion above), we may write

$$V_m = \alpha\sqrt{L/K}\cdot x + \beta\sqrt{L/K} = ax + b \qquad (2)$$

where

$$a = \alpha\sqrt{L/K} = f_1(\sqrt{KL}), \text{ etc.}$$

It now remains to examine a and b as functions of the period. In Table I. are given the values of α and β from which the curves in Figs. 3–6 are drawn, together with the corresponding values of a and b, and the periods $T = 2\pi\sqrt{KL}$ and frequencies n. The values of a and b so found are plotted in Fig. 7 as functions both of frequency and of period. The figure at once suggests that, within the errors of experiment, the constant a is a linear function of the frequency. It must be remembered that a few observations more or less in Figs. 3–6 would change the slopes of the lines as well as the intercepts, and at higher frequencies especially the values of a and b are enormously sensitive to errors of original observations. The values of a obtained in my previous paper (*loc. cit.*, p. 154) by an indirect method are given in Table II. and are shown in the figure as filled circles. These agree in a striking manner with the results of the present measurements. This astonished me, inasmuch as the former work was done under entirely different conditions. In the first place, the air jet was not used, though the experiments were carried on in very damp spring weather. Again, in the former case the spark gap was widening at a rapid rate at the instant the spark took place, the rate being such that the electric force was practically uniform between the electrodes from the start. The agreement of the two sets of results raises questions which can only be settled by further experiments. It will be explained if the spark takes place at the time at which the potential gradient has reached its first maximum in both sets of experiments. This is further justification for our use of equation (1) in the present case and of the treatment of the results in the former.

TABLE I.[1]

No.	K, cm.	L, henries.	$T \times 10^4$	$n \times 10^{-3}$	α	β	$a \times 10^{-5}$ $\frac{\text{volts}}{\text{cm.}}$	b, Volts.
1	565.6	3.01	2.73	3.66	2.10	.00523	1.45	362
2	565.6	1.97	2.21	4.52	2.77	628	1.55	352
3	565.6	1.32	1.81	5.52	4.98	764	2.28	350
4	565.6	.715	1.33	7.52	6.34	1360	2.14	458
5	428.1	3.01	2.37	4.22	1.97	440	1.57	350
6	428.1	1.97	1.92	5.21	2.66	662	1.72	426
7	428.1	1.32	1.58	6.35	4.05	878	2.11	462
8	428.1	.715	1.16	8.63	7.63	1026	2.96	397
9	332.3	1.97	1.69	5.90	3.27	415	2.38	303
10	332.3	1.32	1.39	7.21	5.19	565	3.10	338
11	332.3	.715	1.02	9.80	6.53	1202	2.87	529
12	332.3	3.01	2.10	4.76	1.96	422	1.77	382
13	332.3	1.97	1.69	5.90	2.54	540	1.86	394
14	332.3	1.32	1.39	7.21	4.84	696	2.89	416
15	332.3	.715	1.02	9.80	8.02	1024	3.53	451
16	211.5	.715	.814	12.29	7.28	964	4.01	384
17	211.5	.319	.545	18.35	10.46	2092	3.86	771

TABLE II.

From this journal, Vol. 22, p. 154, 1906.

$T \times 10^4$	$n \times 10^{-3}$	$a \times 10^{-5}$ $\frac{\text{volts}}{\text{cm.}}$
1.75	5.72	2.03
2.13	4.69	1.80
2.16	4.63	1.86
2.50	4.00	1.65
2.61	3.83	1.46
2.78	3.60	1.50
2.91	3.44	1.41
3.23	3.10	1.34
5.05	1.98	.93

---

[1] The resistances of the coils $L = 3.01$, 1.97, 1.32, .715, and .319 henries are, respectively, $R = 62.5$, 51.3, 38.8, 27.1, and 17.6 ohms. No other appreciable resistance takes part in the oscillations.

It is interesting to notice the trend of a assuming it to be a linear function of the frequency n. The results in Tables I. and II. give, by least squares, for

$$a = pn + c$$

the values p, = 21.49, and c = 81,800 volts/cm., the constant c is the value for $n = 0$, that is, the value of a for steady potentials. This value is not far from the values of a which have been determined by others with spark lengths of the same order for constant potentials; the results of Earhart,[1] for instance, giving a as about 65,000 volts/cm. A still better agreement will be shown if the observations for the higher frequencies, which are very sensitive to the condition of the electrode surfaces, are left out of account.

It cannot be said whether the constant b depends on the frequency. The values of b are very sensitive to errors in a. The results for b show a trend to larger values with increasing values of n, and indicate a value of about 350 volts for zero frequency, again in agreement with steady potential work. Values of b from the previous paper are not shown for the reason that their absolute values are too largely affected by the residual errors of the method of approximation used in their calculation.

It is unfortunate that means were not available for the measurement of the inductance and resistance of the coils at the various frequencies used. The inductance diminishes slowly, while the resistance rises more rapidly with the frequency.[2] Both these effects, if taken into account, would diminish the calculated values of a and b by several per cent., but not nearly by enough to account for the changes observed in a. For example, for the moderate frequency of 4,000 vib. per sec., our value of a is about three times that for zero frequency. Since a involves the square root of L, the latter, in order to account for the whole change, would have to be diminished by eight ninths or 89 per cent. by the effect of the frequency, an amount which is of entirely different order of magnitude from that indicated by such experiments and theory as are available. These considerations will, however, be taken into account in the new experiments which are being planned.

[1] Earhart, Phil. Mag., VI., 1, p. 147, 1901.

[2] Esau, *loc. cit.;* see also J. G. Coffin, Proc. Amer. Acad., 41, p. 789, 1906, etc.

Summary and Conclusions.

This paper presents a study of the relation between spark length, potential, and frequency for oscillating potentials having frequencies from 4,000 to 18,000 vib. per sec., and for spark lengths ranging from .005 to .0005 cm. The potentials are produced by interrupting a known initial current in a circuit containing inductance and capacity. The interruption is made in such a manner that no spark is produced at the break, thus giving definite values of potential at the electrodes of an auxiliary spark gap.

The effect of different amplitudes and frequencies of potential upon the spark constants a and b in the equation $V = ax + b$, usually employed to relate steady potentials V and spark lengths x, is studied. The experiments relate to air at atmospheric pressure.

1. Evidence is presented showing that the discharge produced by a train of oscillations begins near the time of the first maximum of the potential (control experiments, etc.).

2. It is found that the spark lengths are linearly related to the strengths of initial cu rent (Figs. 3–6), the inductance and capacity in the circuit remaining the same; *i. e.*, the spark constants in the equation $V = ax + b$ are independent of the amplitude alone of the oscillating potential.

3. The spark constants vary with the frequency. The constant a in the equation is, within the limits of the experiments, a rapidly increasing linear function of the frequency. When the frequency is zero, that is, for steady potentials, the value of a reduces to its normal value which for these short sparks is about 6.5×10^4 volts/cm. At a frequency of 4,000 vib./sec., for instance, the value of a is nearly three times normal. This statement means that for an oscillating potential of this frequency the maximum potential of an oscillation necessary to produce a spark must be about three times as great as the sparking value of the steady potential, and so on. The value of b is practically the same as for steady potentials, *i. e.*, about 350 volts, except that there is a slight tendency to increase with the frequency.

4. It may be concluded finally that the lag effect of the electric spark depends upon at least two independent factors: (1) Upon the amount of ionization initially present in the spark gap. This

factor is of an accidental nature and is subject to regulation and control (see control experiments). (2) The lag effect depends also upon some process which takes place in the gas and which takes time for its completion such that the shorter the time the greater is the necessary sparking potential. The latter factor will probably be found to depend upon the nature and condition of the gas (pressure, etc.).

These facts accord in a general way with the theory of the spark discharge as developed by Sir J. J. Thomson.

Apparatus for a further study of this phenomenon is under construction, it being evident (Fig. 6) that it will be possible to obtain results of considerable precision. With such results it may be possible by a study of different gases at different pressures to obtain much greater insight into the problem of ionization by an electric field.

Clark University,
January, 1911.

Proceedings of the American Academy of Arts and Sciences.

Vol. XLVII. No. 2. — May, 1911.

DETERMINATION OF THE ALTITUDE OF AEROPLANES.

By Robert W. Willson.

With Two Plates.

DETERMINATION OF THE ALTITUDE OF AEROPLANES.

By Robert W. Willson.

Presented February 8, 1911. Received December 31, 1910.

The object of this paper is to add something to the discussion of a somewhat novel problem which has arisen as a result of certain developments in the art of aviation during the past year.

Up to the time of the aviation meet at Los Angeles in February, 1910, no greater height had been recorded in the flight of a "heavier than air" machine than about fifteen hundred feet. At that meet Paulhan, in a Blériot machine, reached a height of 4165 feet, the height being determined by triangulation. The reading of his aneroid was 4600 feet.

At the Montreal meeting, in June, Walter E. Brookins attained an altitude of 3523 feet, determined by triangulation, his baroscope reading 200 or 300 feet higher; and at Atlantic City, in July, the same aviator raised the record to 6175 feet, as determined by a triangulation similar to that of the first method described in the following pages. The height by barograph was 6200 feet.

When the project of an aviation meeting at Cambridge was being discussed, the writer agreed to be responsible for the accurate measure of altitudes; and the results obtained and the methods used form the subject of this paper. At that time no official accounts of the experience at other places in making such measurements had been published, but it was agreed that it would be acceptable to the aviators that they should attempt to reach their greatest altitudes when in a vertical plane passing through the starting line of the course, and as nearly as possible at a point over the grandstand. It was also agreed that only one machine should be under observation at any time. Under these conditions the arrangements now to be described were planned. The accompanying map (Plate 1) of the Squantum peninsula and the surrounding country will serve to make the situation clear. The map shows the positions of the two base lines, and gives the ground plan of the flight of Brookins on September 8.

First Method, — The Field Base.

A measured base of 5000 feet was established on the line NS reaching from the extreme northern limit of the course, across the field, passing above the center of the grandstand, and terminating at a point just beyond the boulevard recently built by the Metropolitan Park Commission. The north and south direction was chosen in order that the observations might not be interfered with by the sun at the times of day most favorable for flight. It was expected that the aviators would cross this line near its center on each coil of the ascending spiral, and that the greatest height attained at such a crossing would be taken as the height of record.

At each end of the field base was placed a sextant mounted on a stand (Plate 2), with its plane in the vertical plane of the base line, and the line of sight pointed toward the grandstand, which was nearly midway between the stations. A target placed in the line of sight at a sufficient distance from each sextant served as a substitute for the horizon line, and when the image of the aeroplane was brought to coincide with the target, as it crossed the plane of reference, the altitude was read directly from the vernier of the sextant. The height of the northern station was eighteen feet and of the southern station twenty-six feet above mean low water; it is sufficiently accurate to assume that the sextants were in the same horizontal plane twenty-two feet above mean low water and nine feet above the center of the field.

After some experiments the target was given the form shown in Plate 2. The central lozenge was one foot square and the extreme horizontal length four feet. The wings served to make an approximate setting as the aeroplane approached the plane from either side. The horizon mirror of the sextant was replaced by a larger mirror extending about three inches from the sextant plane, the silvering being removed from a strip one eighth of an inch wide perpendicular to the plane of the sextant. Through this opening the target could be seen by the naked eye placed somewhat to the left of the telescope, and the aeroplane could thus be picked up and followed and an approximate setting made some time before coming to the reference plane. At the critical moment the eye was placed at the telescope and the image of the aeroplane made to cross the center of the lozenge of the target. The use of a light blue shade between the index and horizon glass greatly facilitated the observation by cutting off the glare of the sky. The clamp of the index was replaced by a roller turned by a good-sized milled head, and forming a very convenient "quick slow motion." A "finding plane" of a size corresponding to the new horizon glass was attached to the index glass and carried a level perpendicular to the plane of the sextant, by means of which that plane might be made vertical. These three modifications are all plainly shown in Plate 2.

The observers were connected with each other and with the committee room at the grandstand by a telephone line devoted to this use alone. A chart, shown about one eighth size (Figure 1), was at hand from which the height corresponding to simultaneous observations of the altitude at either end of the base could be read off.

The abscissas and ordinates represent the angles N and S respectively, and the curves give the values of h for each 100 feet, computed from the above formula. The scale was one quarter of an inch for each degree of $N°$ or $S°$, and on this scale it was not difficult to read with an error of less than ten feet up to altitudes of 15,000 feet.

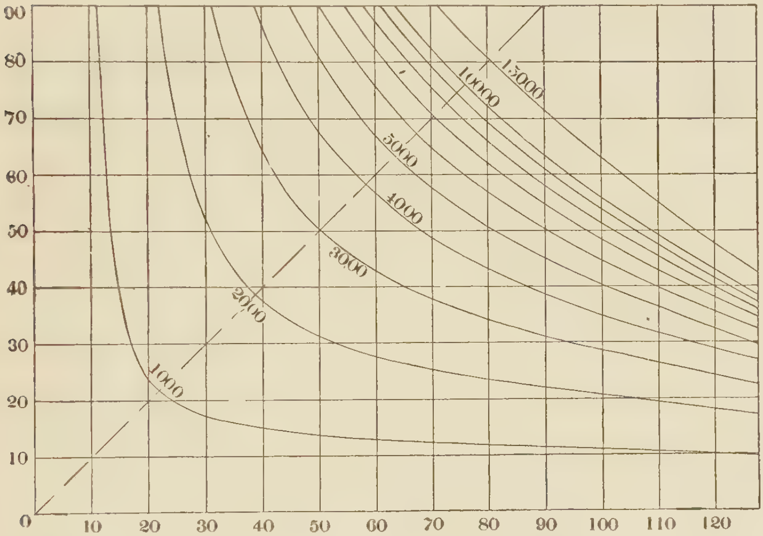

FIGURE 1. Chart for determining approximate altitude from sextant observations.

This chart was not used, as was expected, to give out the altitude a few seconds after each crossing, since the committee deemed it wiser not to make any announcements of altitudes till the end of the day.

THE DISTANT BASE.

As a check on the observation at the field, and in order to give data for a closer investigation of all the circumstances of the flight, a second base was occupied lying nearly east and west, about two and a half miles south of the aviation field. Satisfactory stations were found, one on Forbes Hill in Quincy, at a height of 128 feet above the aviation field (141 feet above mean low water), and the other on the estate of Mrs. E. M. Carey, in Milton, at a height of 71 feet. The length of the base line (QM upon the map, Plate 1) was 6236 feet. The stations were visible to each other, and, although the grandstand was visible from neither, aeroplanes could be observed as soon as they had risen to the height of 50 or 75 feet.

The position of the base was selected so that observations could not at any time be interfered with by the sun, and that the angle of elevation could be measured without an eye prism up to an altitude of more than 15,000 feet above the center of the field.

The distance from the field was not so great that it was necessary to read the angles with great accuracy, while it was sufficiently great to reduce materially the difficulty in following the rapidly moving aeroplanes, so that it was possible to observe quickly and accurately both horizontal and vertical angles without a finding device.

The instruments used were a special theodolite by C. L. Berger reading horizontal angles to 10″ and vertical angles to 20″, and a Buff mining transit reading both horizontal and vertical angles to 20″. Both instruments had full vertical circles, and inverting eyepieces magnifying about thirty diameters.

Through the kindness of Mr. Carl Keller, the New England Telephone Company connected the two end stations and the central station at the field during the entire period of the meet.

It was thus possible to insure simultaneous observations at the two stations in both coördinates. That they were practically simultaneous is clearly shown by the tables which follow, in which the approximate times are given as noted at each station. Where the times differ it is almost always possible to make an exact agreement by altering one or both by a single second, so that the mean of the times would rarely be in error by that amount.

The error of the observers' watches was found by a telephone comparison with the official chronometer on the field immediately before each flight.

By combination of the observations we were able not only to compute the altitudes of the aeroplanes at intervals of forty seconds or less, but also to locate their corresponding positions as projected vertically on the ground plane, and thus to plot so many points of the spiral both in ascent and descent as to form an interesting and useful record of all the details of the flight.

It may here be remarked that the use of this method seems preferable to any that requires the aviator to attain his maximum height at a given point or line. If thus restricted, the Blériot monoplane especially is at a disadvantage, as its construction renders it extremely difficult for the operator to see the ground at points anywhere near directly beneath him. The discussion of his ascending spiral, checked by observations of his descent, fixes his highest point quite accurately without placing any burden upon the aviator himself. (In reference to this point, see the flight of Grahame-White discussed on p. 42.)

The character of the results obtained may best be shown by the records of some of the flights and the methods of discussing them which follow.

To illustrate the whole process, we may take the observations of the flight of Brookins, September 12, the last day when any considerable flight was made, and at a time when the observers had had several days of practice. No great altitude was reached, but the flight was in many respects typical, and exemplifies some of the advantages of the two methods used, as controlling and checking each other.

TABLE I.

Flight of Brookins, Sept. 12, 1910, as Measured by Sextants. Base Line, Distance between Stations, 5000 feet. Sextants 9 feet above Course.

North Station.				South Station.			
No.	Direction.	Time.	Vert. Angle.	Time.	Vert. Angle.	Computed.	Chart.
1	1st, E	$5^h\ 58^m\ 30^s$	17° 7′	$5^h\ 58^m\ 35^s$	13° 57′	697 ft.	694 ft.
2	2nd, W		obtuse[1]	6 0 49	8 56		
3	2nd, E	6 6 55	39 28	7 4	25 50	1533	1529
4	3rd, W	10 45	24 4	10 53	60 26	1791	1799
5	3rd, E	12 35	47 50	39	31 15	1967	1964
6	4th, W	13 10	71 8	17	20 34	1672	1664
7	4th, E	13 35	42 24	45	20 12	1338	1314

[1] Too large to be measured by the sextant.

If the angular altitudes at the two stations are N° and S° respectively, and the length of the field base 5000 feet, the altitude in feet, h, given in column 7, is computed by the expression

$$h = \frac{5000}{\cot N + \cot S}.$$

The values given in column 8 were read directly from the chart referred to above on page 27. A correction of 9 feet has been added to each value, as the sextant base was higher than the middle of the field by that amount.

Only four crossings were well observed in the ascent and two in the descending spiral. The second observation, however, though incomplete, served a purpose, as will appear later. Not only the altitudes, but the projections of the crossing points on the ground line are given by the observations, since the distances of the projection from the north and south stations are $h \cot N$ and $h \cot S$ respectively, and six points in the spiral are thus fixed, making, with the start and finish, eight points in all thus completely determined.

Observations at the Distant Base.

As compared with the eight determinations made by the sextants, twenty-one simultaneous observations were made at the Quincy-Milton base. These are shown in detail in Table II. For purposes of comparison the results of the sextant observations are inserted, unnumbered but in chronological order.

The values of the altitudes in columns 5 and 9 are computed as follows:

Let h be the height of the aeroplane above the center of the field,
C, the length of the base line, 6236 feet,
$q = 128$, and $m = 71$ feet, the heights of Q and M above the center of the field,
α and β, the horizontal angles between the aeroplane and base line at Q and M respectively,
A and B, the angular altitude of the aeroplane at Q and M respectively.

Then

$$\begin{aligned} h &= C \tan A \sin \beta \operatorname{cosec} (\alpha + \beta) + q, \\ &= C \tan B \sin \alpha \operatorname{cosec} (\alpha + \beta) + m. \end{aligned}$$

All effects due to the curvature of the earth and refraction are neglected as being less than the errors of measurement which were expected to occur. The accuracy actually attained would seem, however, to justify the application of such corrections.

TABLE II.

Flight of Brookins, Sept. 12, 1910, as Measured by Transits. Base Line, Distance between Stations, 6236 feet. Course 13 feet above Mean Low Water.

	Quincy Station Height above Course 128 ft.				Milton Station Height above Course 71 ft.			
No.	Time.	Vert. Angle.	Hor. Angle.	Alt.	Time.	Vert. Angle.	Hor. Angle.	Alt.
1	$5^h\ 57^m\ 31^s$	1° 54′	70° 35′	576 ft.	$5^h\ 57^m\ 30^s$	2° 17′	82° 10′	583ft.
2	58 12	2 18	74 30	649	58 13	2 36	77 31	653
	58 32	by sextants		687				
3	58 43	2° 33′	77° 50′	700	58 40	2 47	74 19	705
4	59 24	2 45	83 3	769	59 22	2 51	70 47	770
5	6 0 20	2 39	77 59	861	6 0 20	[2 53]	79 15	865[1]
	0 49	by sextants		940				
6	2 2	3° 24′	67° 53′	1052	2 00	[3 54]	88 29	1054
7	3 8	4 4	65 6	1169	3 10	4 49	89 42	1190
8	3 53	4 44	67 13	1274	3 51	5 23	86 4	1276
9	4 42	5 22	65 31	1358	4 42	6 10	86 7	1362
10	5 13	5 42	63 12	1402	5 13	6 40	87 35	1404
11	5 55	6 13	62 58	1431	5 53	7 16	85 43	1434
12	6 32	6 17	70 48	1482	6 32	6 50	79 19	1488
	7 0	by sextants		1524				
13	7 3	6° 1′	76° 40′	1518	7 2	6 17	76 1	1527
14	7 42	5 45	83 45	1565	7 41	5 44	71 44	1571
15	8 15	5 57	87 53	1597	8 15	5 45	67 55	1602
16	9 16	6 38	86 56	1633	9 15	6 21	66 47	1636
17	10 2	7 24	83 14	1693	10 0	7 10	68 4	1693
18	10 40	8 10	79 59	1759	10 38	8 1	69 10	1758
	10 49	by sextants		1782				
19	11 41	9° 14′	72° 12′	1889	11 40	9 37	74 10	1887
20	12 25	8 7	73 25	1949	12 23	8 34	78 2	1955
	12 37	by sextants		1958				
21	13 11	6° 4′	75° 58′	1674	13 10	6 22	79 8	1674
	13 14	by sextants		1663				
	13 40	by sextants		1311				
	14 40	alighted						

---

[1] In the case of observations 5 and 6 the vertical angles as read off at Milton have each been decreased by 1°. This correction is justified not only by the agreement thus brought about between the two stations, but by the sextant observation at $6^h\ 0^m\ 49^s$ which, as is shown on page 34, indicates an altitude of 940 feet.

To find the horizontal distances D_q and D_m from Q and M, we have, with little extra work and from the same data of computation,

$$D_q = C \sin \beta \operatorname{cosec} (\alpha + \beta) \quad \text{and} \quad D_m = C \sin \alpha \operatorname{cosec} (\alpha + \beta),$$

and by use of these two distances the points are easily plotted with reference to the base line. It is sufficiently accurate, however, and more convenient, to determine the points graphically by drawing lines at the proper angles with the base by means of a protractor and straight edge, and marking their intersection as the position of the aeroplane.

The computations were quickly made on mimeographed forms following the scheme shown on page 33, which gives the original computations for observations 5 and 6 of Table II, using, of course, the uncorrected data. The discrepancy of these results pointed out at once the faulty observations.

The general agreement of the values at the two stations seems to show that the height is fixed by each observation with an error of less than five feet; but observations 5 and 6 at Quincy and Milton, as computed from the recorded data, show differences too large to be ascribed to error of observation. The sextant observation at $6^h\,0^m\,49^s$, although the angle was too great to be measured at the north sextant station (the spiral being far out beyond the course), still shows that the observations at the Quincy station give the correct value, and there seems to be good reason for assuming that the vertical angles were read 1° too large in each case at the Milton station. It appears in the discussion of all the flights that the error most frequently made was in reading the vertical angles. In the whole series of observations but two errors are indicated in the reading of the horizontal angles, one of which will be referred to later.

Time-Altitude Curves.

By plotting the successive values of h, given in Table II as abscissas, with the corresponding times as ordinates, we have the curve given below, Figure 2 (right), the slope of which gives the rate of ascent in feet per minute. The points corresponding to transit observations are indicated by circles, the sextant observations by crosses. The rate of ascent is about 100 feet per minute, and the descent nearly ten times as rapid.

Computation of Altitude from the Fifth, and Sixth Observations of Table II.

Date 1910, Sept. 12
Aviator, Brookins
C = base line
h = height
A, α, q = alt., az. and elevation at Quincy Station.
B, β, m = alt., az. and elevation at Milton Station.

Time	$6^h\ 0^m\ 20^s$	Time	$6^h\ 0^m\ 20^s$	Time	$6^h\ 2^m\ 2^s$	Time	$6^h\ 2^m\ 0^s$
A	2° 39′	B	3° 53′	A	3° 24′	A	4° 54′
β	79 15	α	77 59	β	88 29	α	67 53
$\alpha + \beta$	157 14	$\alpha + \beta$		$\alpha + \beta$	156 22	$\alpha + \beta$	
log C	3.79493	log C	3.79493	log C	3.79493	log C	3.79493
tan A	8.66543	tan B	8.83175	tan A	8.77387	tan B	8.93313
sin β	9.99231	sin α	9.99038	sin β	9.99985	sin α	9.96681
csc $(\alpha + \beta)$	0.41231	csc $(\alpha + \beta)$	0.41231	csc $(\alpha + \beta)$	0.39698	csc $(\alpha + \beta)$	0.39698
log $(h - q)$	2.86498	log $(h - m)$	3.02937	log $(h - q)$	2.96563	log $(h - m)$	3.09185
$h - q$	733	$h - m$	1070	$h - q$	924	$h - m$	1236
q	128	m	71	q	128	m	71
h	861	h	1141	h	1052	h	1307

Representation of the Spiral.

From the observations of Table II we may plot the ground plan of the spiral described in the ascent, and, with somewhat less certainty, that of the much more rapid descent. Each of the sextant observations, too, fixes a point on the spiral, although taken alone they would give little information as to the actual path of the aviator.

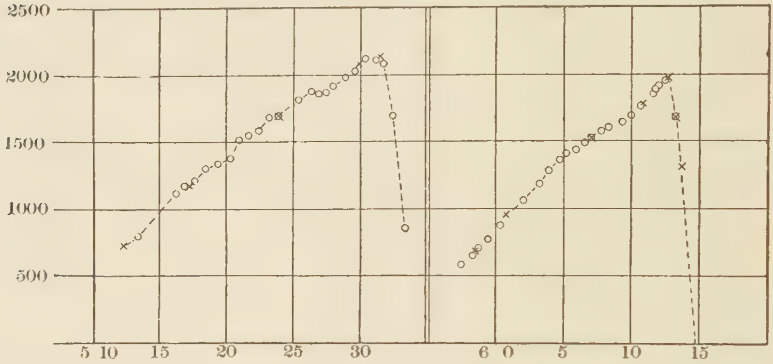

Figure 2. Time-altitude curves of Grahame-White (left) and of Brookins (right), September 12.

In Figure 3 are plotted the points as thus determined, each being numbered to correspond with the observation of Table II on which it depends. The points of crossing the base line are determined by the sextant observations of Table I.

The elevation of the path, as shown in the lower half of the figure, is determined by combining the altitudes from Table I and II with the projections of the observed points of the spiral above.

It is noteworthy that the spiral serves to give with some accuracy the height at the point of the crossing at $6^h\ 0^m\ 49^s$, where the angle was too great to be measured at the north end of the base. The figure shows that the projection of that point, which is marked by the dot between points 5 and 6 of the spiral, is about 900 feet north of that station, or 5900 feet from the south station, at which the vertical angle was measured as 8° 56′. This gives a height of 940 feet (assuming the elevation of the station as 13 feet), and a little further investigation shows that the angle at the north station was about 134°, and confirms the record of the observer that it was not measurable, as the sextant reads only to 128°. The error in position of the projected point is probably less than 150 feet, corresponding to an uncertainty of about 24 feet in the deduced height and 3° in the angular altitude at the north station.

In order that an intelligent judgment may be formed of the general accuracy attained, of the nature and frequency of erroneous observations, which must always occur in such a series, of the possibility of

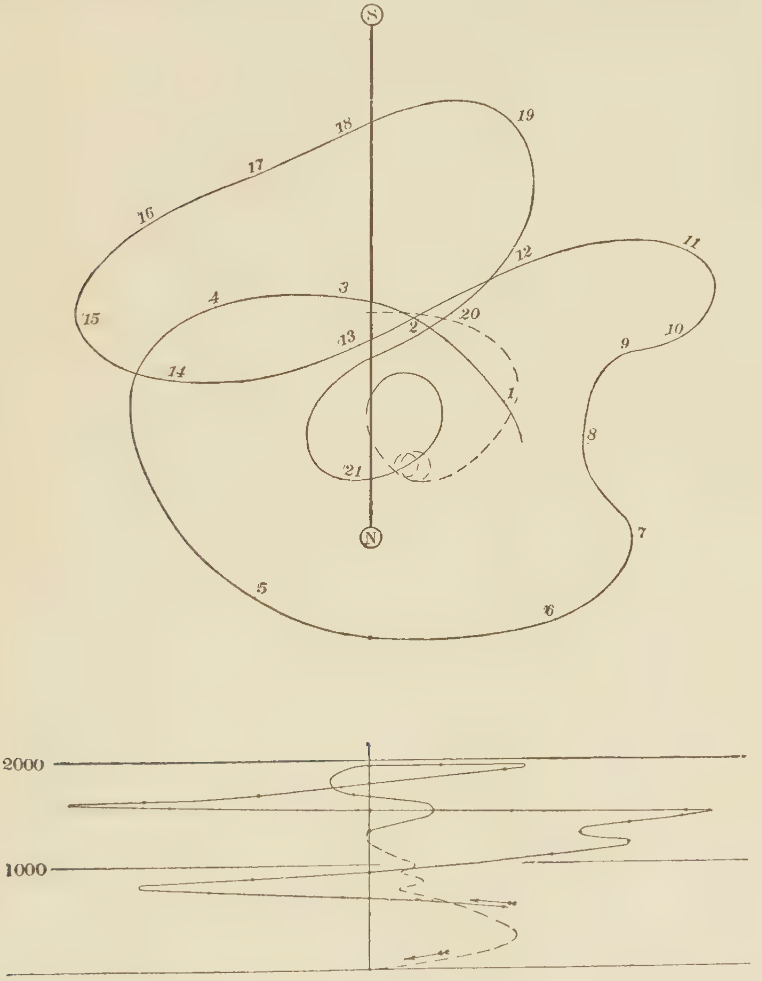

Figure 3. Spiral of Brookins, September 12, plotted from observations of Tables I and II.

correcting such observations, and the effect of rejecting them, three additional sets are given in Tables III, IV, and V. The first is that of Brookins on September 10, in which he reached the greatest altitude of the meet, with three discordant observations, one of which has been corrected, apparently with reason, by altering the vertical angle at the Quincy station by 1°. The others would be brought into line by changes of 10′ and 30′ in the vertical angles at Milton station, but no outside evidence is furnished by the sextants or spiral to justify such a change. In both cases the spiral, Figure 5, indicates that the horizontal angles were probably correctly recorded.

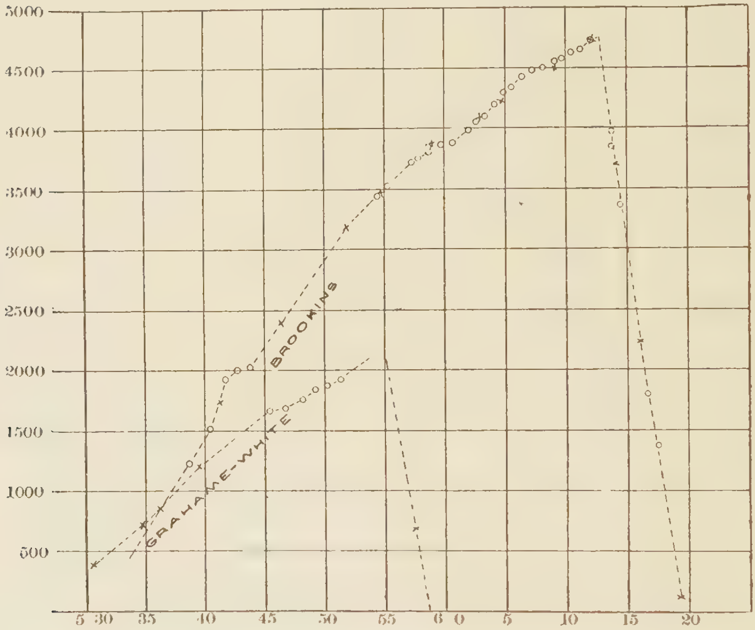

Figure 4. Flights of September 10: Brookins (Wright biplane), Grahame-White (Farman biplane).

The second flight, that of Brookins on September 8, shows two corrections of vertical angle and one change of the time of observation at Quincy, three vertical angles unrecorded at Milton, and one observation marked worthless, the result from which differs 17 feet from that at Quincy. This was on the second occasion of making observations, and naturally contains more errors and uncertainties, but in no case is the height uncertain by so much as five feet.

TABLE III.

FLIGHT OF BROOKINS, SEPT. 10, 1910. WRIGHT BIPLANE. BASE LINE 6236 FEET, COURSE 13 FEET ABOVE MEAN LOW WATER.

	QUINCY STATION. Height above Course 128 ft.				MILTON STATION. Height above Course 71 ft.			
No.	Time.	Vert. Angle.	Hor. Angle.	Altitude.	Time.	Vert. Angle.	Hor. Angle.	Altitude.
1	$5^h\ 38^m\ 37^s$	3° 54′	68° 59′	1220 ft.	$5^h\ 38^m\ 40^s$	4° 24′	88° 7′	1222 ft.
2	40 22	5 47	68 28	1511	40 30	6 28	84 20	1518
3	41 40	[7] 56	80 41	1910[1]	41 44	7 55	71 44	1919
4	42 41	7 44	90 59	2005	42 45	7 8	64 54	1981
5	43 42	7 12	90 20	2019	43 46	6 51	67 6	2023
6	54 13	11 12	69 49	3432	54 19	12 10	88 15	3450
7	55 11	11 53	82 51	3514	55 15	11 49	75 9	3527
8	57 10	15 3	85 36	3713	57 15	14 19	68 35	3715
9	57 52	15 43	82 34	3753	57 55	15 11	70 19	3753
10	58 35	16 16	79 5	3803	58 40	16 16	72 42	3849
11	59 41	16 50	73 42	3858	59 45	17 20	76 48	3865
12	6 0 35	16 36	69 31	3874	0 40	17 43	81 7	3877
13	1 55	15 13	66 1	3986	2 0	10 48	87 55	3986
14	2 37	14 21	71 21	4039	2 36	15 18	84 41	4050
15	3 15	14 29	80 20	4092	3 20	14 29	76 24	4091
16	4 5	16 52	81 48	4201	4 10	16 27	72 0	4199
17	4 50	17 52	74 43	4295	4 55	18 17	77 13	4295
18	5 30	17 58	68 8	4338	5 34	19 23	83 22	4339
19	6 22	17 23	60 27	4419	6 26	20 3	92 31	4427
20	7 14	15 36	58 32	4472	7 19	18 12	98 5	4478
21	8 2	14 33	63 25	4496	8 6	16 21	94 55	4503
22	9 2	14 24	73 2	4530	9 7	15 14	85 42	4549
23	9 39	14 48	78 48	4569	9 42	15 3	79 47	4576
24	10 20	15 29	85 33	4616	10 25	15 5	72 52	4626
25	11 9	17 41	87 2	4646	11 14	16 46	68 45	4645
26	12 2	18 59	76 43	4719	12 6	19 13	76 17	4731
27	13 39	13 45	68 5	3974	13 42	14 30	88 33	3844
28	14 24	11 21	81 10	3356	14 28	11 24	76 40	3364
29	16 34	7 18	67 52	1789	16 38	8 8	83 35	1799
30	17 24	4 41	65 55	1375	17 28	5 23	89 54	1381

[1] Vert. angle at Q has been changed from the recorded value of 6° 56′.

The third flight, Figure 2 (left), is that of Grahame-White on September 12, immediately preceding that of Brookins. The seventh observation shows a corrected vertical angle at Milton, and the twelfth a correction of the horizontal angle at the same station, — one of two instances de-

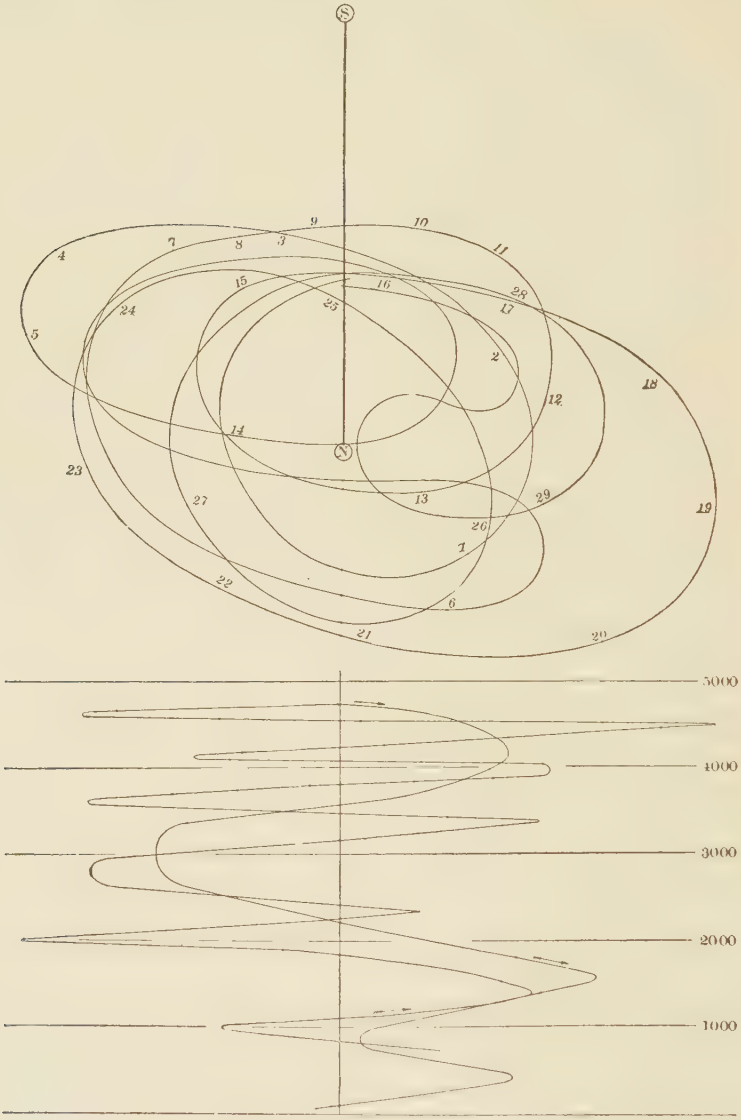

Figure 5. Spiral of Brookins, September 10, plotted from observations of Table III.

TABLE IV.

FLIGHT OF BROOKINS, SEPT. 8, 1910, WRIGHT BIPLANE. BASE LINE, 6236 FEET. COURSE 13 FEET ABOVE MEAN LOW WATER.

	Quincy Station. Height above Course 128 ft.				Milton Station. Height above Course 71 ft.			
No.	Time.	Vert. Angle.	Hor. Angle.	Altitude.	Time.	Vert. Angle.	Hor. Angle.	Altitude.
1	$5^h\ 38^m\ 41^s$	2° 29′	73° 2′	774 ft.	$5^h\ 38^m\ 41^s$	2° 48′	82° 26′	774 ft.
2	39 55	3 42	76 25	973	39 54	[3 55]	76 0	967 [1]
3	41 1	4 21	84 35	1156	41 1	4 19	69 46	1154
4	42 9	4 13	75 17	1319	42 12	4 32	82 14	1322
5	43 37	5 23	77 49	1506	43 36	5 36	77 34	1506
6	48 2	5 26	73 30	1499	48 0	5 54	81 11	1516 [2]
7	49 44	7 11	81 2	1732	49 46	7 8	71 19	1732
8	50 59	8 31	76 4	1888	51 1	8 40	73 22	1885
9	[52] 13	5 48	80 35	1505 [3]	52 7	5 52	73 17	1506
10	54 28	6 10	80 53	1782	54 27	6 16	75 51	1783
11	55 35	7 3	77 3	1880	55 35	7 17	77 30	1879
12	56 28	8 1	78 7	1959	56 26	. . .	74 22	. . . . .
13	57 19	9 22	79 26	2068	57 16	9 15	70 34	2068
14	58 8	10 41	76 10	2148	58 6	10 39	70 32	2145
15	59 35	8 56	76 18	2254	59 35	9 12	77 13	2255
16	6 0 23	9 17	85 3	2363	6 0 24	8 53	68 52	2365
17	1 32	10 36	95 34	2456	1 31	9 22	58 59	2454
18	2 33	12 27	100 24	2528	2 31	10 21	52 31	2532
19	5 11	[17 42]	86 51	2766 [4]	5 6	14 56	54 59	2759
20	6 28	[16 38]	69 35	2886 [4]	6 27	17 4	70 47	2884
21	7 36	14 31	60 20	2992	7 35	16 52	85 28	2994
22	8 51	12 10	55 16	3102	8 51	14 50	98 9	3104
23	9 41	11 12	62 2	3130	9 41	. . . . .	93 44	. . . . .
24	11 56	13 35	87 15	3237	11 54	12 44	[66 23]	3240 [5]
25	12 56	14 46	98 4	3237	12 55	12 42	55 57	3247
26	16 21	22 19	125 42	3419	16 16	14 44	30 49	3413
27	17 33	26 23	111 3	3598	17 33	. . .	36 44	. . . . .
28	18 46	23 32	90 3	3565	18 46	19 5	51 39	3552
29	20 14	18 17	75 54	3647	20 4	18 6	70 35	3651
30	22 36	14 52	86 33	3708	22 36	14 6	68 3	3715
31	23 45	15 21	78 25	3791	23 46	15 23	74 47	3799
32	24 51	15 28	71 28	3831	24 51	16 21	81 7	3837
33	26 23	12 59	91 41	3170	26 26	11 51	63 20	3168

[1] Vert. angle has been increased 1° for Station M.

[2] Marked worthless by observer at M. Clouds between 5 and 6.

[3] Time at Station Q has been decreased by 1^m.

[4] 5° has been added to each of the vertical angles.

[5] 10° has been added to Hor. Angle at Station M (spiral suggested this change and sextant also at $6^h\ 12^m\ 0^s$ confirms it).

tected in the whole series; it was not indicated by comparison with the Quincy values, as there is close agreement with either value of the horizontal angle, but the spiral showed that the horizontal angle must be in error by about 10°, and a sextant observation at almost the same instant corroborates the value of the height given in the table.

TABLE V.

Flight of Grahame-White, Sept. 12, 1910. Farman Biplane, Base Line 6236 feet, Course 13 feet above Mean Low Water.

	Quincy Station. Height above Course 128 ft.				Milton Station. Height above Course 71 ft.			
No.	Time.	Vert. Angle.	Hor. Angle.	Altitude.	Time.	Vert. Angle.	Hor. Angle.	Altitude.
1	5^h 13^m 15^s	2° 25′	79° 51′	792 ft.	5^h 13^m 15^s	2° 37′	77° 23′	796 ft.
2	5 16 12	4 17	64 6	1114	5 16 13	5 2	87 39	1115
3	5 16 52	4 51	70 36	1163	5 16 51	5 21	79 14	1167
4	5 17 44	4 42	83 22	1206	5 17 42	4 42	70 4	1210
5	5 18 30	4 11	86 3	1301	5 18 30	4 12	72 13	1307
6	5 19 24	3 59	78 23	1336	5 19 18	4 13	80 50	1340
7	5 20 19	4 22	70 23	1369	5 20 18	[4][1] 51	87 5	1372
8	5 21 2	4 51	65 34	1501	5 21 2	5 38	91 47	1525
9	5 21 43	5 27	62 51	1538	5 21 44	6 22	92 13	1540
10	5 22 22	6 13	61 14	1582	5 22 21	7 21	90 55	1581
11	5 23 10	7 14	66 6	1673	5 23 9	8 9	81 49	1682
12	5 23 55	8 4	78 33	1687	5 23 54	8 1	[69][2]24	1693
13	5 25 23	6 13	86 14	1813	5 25 21	6 6	71 19	1811
14	5 26 20	6 5	77 20	1873	5 26 19	6 21	80 36	1873
15	5 26 52	5 56	72 6	1854	5 26 50	6 26	85 54	1857
16	5 27 28	6 9	67 14	1851	5 27 25	6 58	89 49	1873
17	5 28 3	6 40	63 29	1910	5 28 2	7 40	92 24	1909
18	5 28 55	8 0	63 51	1981	5 28 55	9 10	87 56	1981
19	5 29 31	8 54	71 59	2020	5 29 30	9 29	77 44	2029
20	5 30 17	8 32	83 49	2111	5 30 18	8 20	69 53	2121
21	5 31 8	7 17	78 35	2104	5 31 8	7 31	78 10	2114
22	5 31 43	7 12	72 23	2093		7 42	84 7	2086
23	5 32 20	6 7	67 47	1687	5 32 20	6 50	86 52	1687
24	5 33 14	3 27	66 5	859	5 33 14	4 0	83 12	851

[1] Vert. angle at Milton recorded 5° 51′.

[2] Hor. angle recorded at Milton was 79° 24′. Spiral proves it to be 69° 24′ and sextant observation at almost same instant corroborates this.

It has been thought worth while to give these observations in detail for those especially interested in the problem. It is evident that there is much information in the tables and curves to which we have not referred; for example, rate of ascent per minute, gradient with and against the wind, etc. The reader who wishes to study them more minutely may therefore wish to plot them on a scale sufficiently large for his purpose. To make use of the sextant as well as the transit observations in plotting the spirals, it is necessary to know the relative position of the two bases. The north end of the field base is distant 15,000 feet and 14,700 feet from Q and M respectively. The south end of the field base is 10,056 feet from Q and 11,005 feet from M.

In regard to these tables we notice that there is apparently a small systematic difference between heights as observed at Q and M. This was at first suspected to be due to error in level of the two stations, but was not the same at all times. It was not due to difference in time of observation at the two stations, for although the setting at Milton was always a fraction of a second later, this could only give rise to a difference of about one foot at most. It may have been partly due to difference in levelling of instruments, and perhaps partly to neglect of refraction and curvature of the earth in the computation.

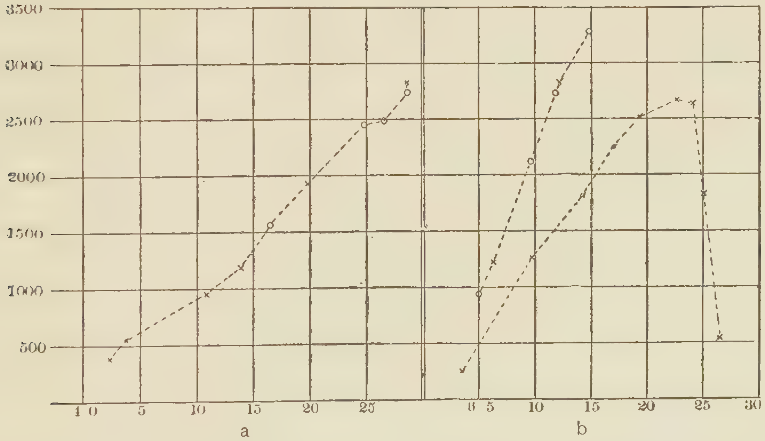

Figure 6. Time-altitude curve. (Left) flight of Johnstone, September 7 (Wright biplane); (right) flight of Grahame-White (Blériot monoplane), and flight of Brookins (Wright biplane).

The time-altitude curves have been plotted for all the flights of the meet which have any special interest. Those of Brookins, Johnstone, and Grahame-White on September 7 are plotted in Figure 6. They show the typical rate of ascent of the Wright biplane, about 100 feet per minute, in direct comparison with the Blériot which was in the air at the same time and rising more than 200 feet per minute.

Figure 4, plotted from Table III, represents the highest flight of the meet, that of Brookins on September 10, at an average rate of about 100 feet per minute. From $5^h\,43^m$ to $5^h\,57^m$ the transits were temporarily assigned to Grahame-White in a Farman biplane, who was far off the course to the southeast and could not be frequently observed by the sextants, while the latter instruments were sufficient for the observations of Brookins, who was describing large but regular circles above the field. At $5^h\,52^m$ Grahame-White was cut off from view at Milton by a large tree which lay farther off the course than it was supposed that any aviator would go in an altitude attempt, and the transits were turned back upon Brookins.

The single sextant observation of Grahame-White's descent, however, combined with the fact that his usual rate on the beginning of the downward spiral was at least 800 feet per minute, enables us to fill out the dotted part of the curve, and conclude that he reached a height of approximately 2200 feet. A comparison of all the curves shows that if the highest point of the ascent is not actually observed by the transits, it may always be closely fixed by the intersection of the upper portions of the curves of ascent and descent.

The spiral of Brookins in this flight is shown in Figure 5. In the long interval between points 5 and 6, when the transits were turned upon Grahame-White, the general curve of the spiral, however, is plainly shown by the sextant observations, although the aviator changed the direction in which he was circling the course, apparently in order to make his crossings against the wind.

Figure 7 shows the time-altitude curve of Brookins on September 8, when he was lost to sight in a light cloud for five minutes at an altitude of 1500 feet, climbed another 500 feet and disappeared a second time, when he stopped his engine, descending to the 1500 foot level again out of the cloud, and then taking a somewhat different line of flight, ascended without further difficulties to a height of nearly 4000 feet. The conditions were such that the early part of the spiral was not well determined, and it does not seem worth while to reproduce it here. The main features are shown on the ground plan which is shown on the map of Plate 1. The very discordant sextant observations at $5^h\,19^m$ and $5^h\,22^m$, shown in Figure 7, are unexplained. The former was made with the machine about 1000 feet south of the southern station, nearly overhead, and moving in a course nearly parallel to the line, so that the vertical angle was changing very rapidly, and the observation difficult.

No such cause can be assigned for the second error, and it is perhaps more probable that both were caused by some accidental disturbance of the vertical plane of the sextant which affected the two observations alike. No other discrepancy approaching this in amount occurred in in the whole course of the observations.

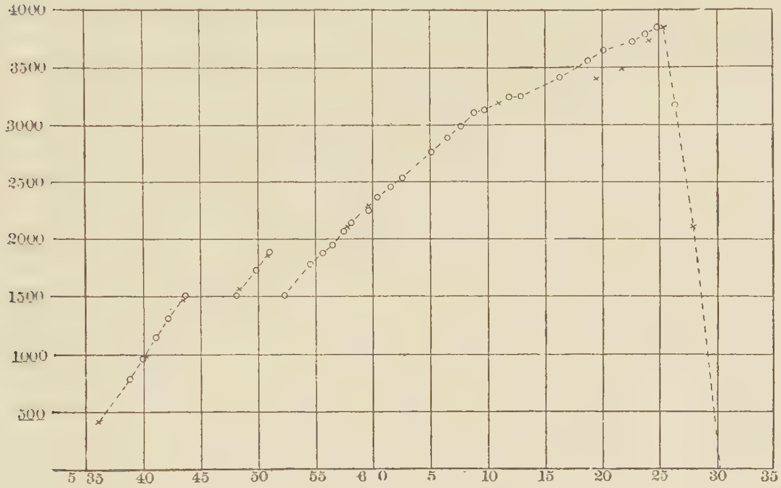

Figure 7. Time-altitude curve: Brookins (Wright biplane), September 8.

It remains to make grateful acknowledgment of the skill of the observers and of the interest of many others, without which this work would have been impossible; especially of the assistance of Mr. William Hunt in the observations and reductions, and in drawing the curves which illustrate this paper.

Students' Astronomical Laboratory,
Harvard University.

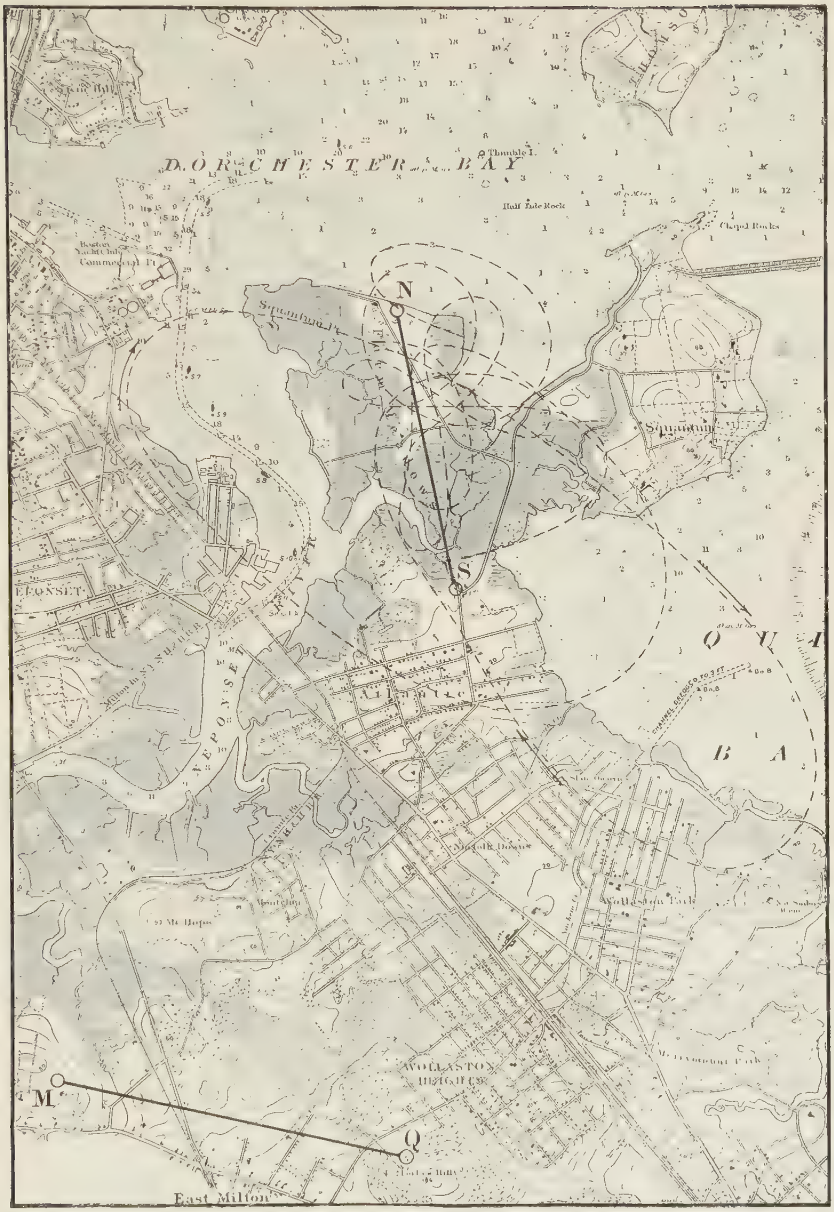
DORCHESTER BAY
Thumble I.
Half Tide Rock
Chapel Rocks
Boston Yacht Club
Commercial Pt.
Squantum Pt.
N
S
Squantum
NEPONSET
NEPONSET RIVER
Atlantic
Q U I
B A
Norfolk Downs
Wollaston Park
Mt. Hope
WOLLASTON HEIGHTS
M
Q
East Milton

WILLSON.—ALTITUDE OF AEROPLANE FLIGHTS.

PLATE 2.

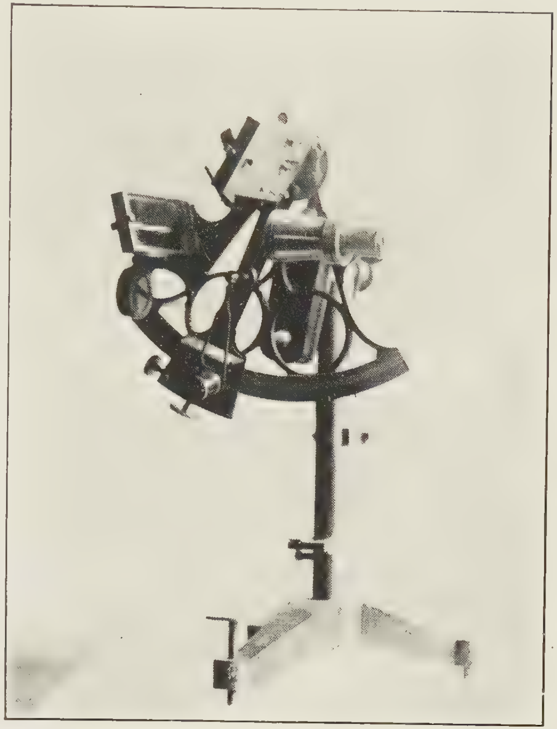

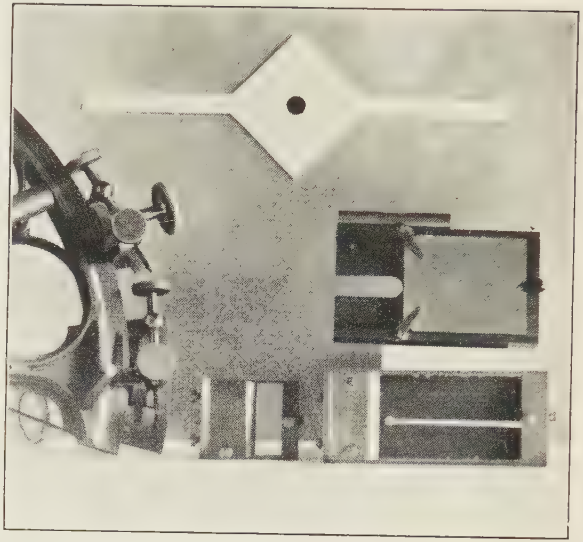

CONTRIBUTIONS FROM THE JEFFERSON PHYSICAL
LABORATORY, HARVARD UNIVERSITY

SENSE OF LOUDNESS

By Wallace C. Sabine

CONTRIBUTIONS FROM THE JEFFERSON PHYSICAL
LABORATORY, HARVARD UNIVERSITY

SENSE OF LOUDNESS

By Wallace C. Sabine

It will be shown here that there is a sense of relative loudness, particularly of equality of loudness, of sounds differing greatly in pitch, that this sense of loudness is accurate, that it is nearly the same for all normal ears, that it is independent of experience, and that therefore it probably has a physical and physiological basis. This investigation has been incidental to a larger investigation on the subject of architectural acoustics. It has bearing, however, on many other problems, such, for example, as the standardization of noises, and on the physiological theory of audition.

The apparatus used consisted of four small organs (Proc. Am. Acad. of Arts and Sciences, 1906) so widely separated from each other as to be beyond the range of each other's influence. Each organ carried seven night-horn organ pipes at octave intervals in pitch, 64, 128, 256, . . . 4096 vibrations per second. The four organs were so connected electrically to a small console of seven keys that on pressing one key, any one, any two, any three or all four organ pipes of the same pitch would sound at once, — the combination of organ pipes sounding being adjusted by an assistant and unknown to the observer.

In other parts of the investigation on architectural acoustics the loudness of the sound emitted by each of the 28 organ pipes in terms of the minimum audible sound for the corresponding pitch had been determined. The experiment was conducted in the large lecture room of the Jefferson Physical Laboratory, and, in the manner explained elsewhere, the computation was made for the loudness of the sound, taking into account the shape of the room and the materials employed in its construction.

The experiment consisted in adjusting the number of pipes which were sounding or in choosing from among the pipes until such an adjustment was accomplished, that, to an observer in a more or less remote part of the room all seven notes, when sounded in succession, seemed to have the same loudness. As the pipes of the same pitch did not all have the same loudness, it was possible by taking various combinations to make this adjustment with considerable accuracy. This statement, however, is subject to an amendment in that all four pipes of the lowest pitch were not sufficiently loud and the faintest of the highest pitch was too loud.

There were ten observers, and each observer carried out four independent experiments. Speaking broadly, in the case of every observer, the four independent experiments agreed among themselves with great accuracy. This was to the great surprise of every observer, each before the trial doubting the possibility of such adjustment. The results of all ten observers were surprisingly concordant.

After the experiment with the first two observers, it seemed possible that their very close agreement arose from their familiarity with the piano, and that it might be that they were adjusting the notes to the "balance" of that particular instrument. The next observer, therefore, was a violinist. Among the observers there was also a 'cellist. Lest the feeling of relative loudness should come from some sub-conscious feeling of vocal effort, although it is difficult to see how this could extend over so great a range as six octaves, singers were tried whose voices were of very different register. Two of the observers, including one of the pianists, were women. Two of the observers were non-musical, one exceedingly so.

The accompanying table gives the results of the observations, the energy of each sound being expressed in terms of minimum audible intensity for that particular pitch, after making all corrections for the reënforcement of the sound by the walls of the room. The observations are recorded in order, the musical characteristic of the observer being indicated.

	Pitch frequency						
Observers	64	128	256	512	1024	2048	4096
1. Piano	$7.0(+)\times10^4$	1.7×10^6	4.4×10^6	8.0×10^6	15.0×10^6	9.6×10^5	$4.5(-)\times10^3$
2. Piano	7.0 +	1.7	4.4	11.2	9.2	12.0	5.2 –
3. Non-musical	7.0 +	1.7	3.6	8.9	6.3	9.6	4.5 –
4. Non-musical	7.0 +	1.7	3.7	7.7	14.5	14.4	5.6 –
5. Violin	7.0 +	1.7	3.5	11.7	13.9	8.0	3.5 –
6. Violin	7.0 +	1.7	4.0	11.4	15.5	15.2	5.2 –
7. 'Cello	7.0 +	1.7	4.2	12.	13.4	9.6	5.1 –
8. Tenor	7.0 +	1.7	3.9	13.3	13.5	10.5	4.0 –
9. Soprano	7.0 +	1.7	4.7	12.9	17.0	9.6	5.4 –
10. Piano	7.0 +	1.7	3.5	13.2	14.5	8.0	4.9 –
	7.0(+)	1.7	4.0	11.0	13.3	10.6	4.8 –

a39001 0069626936

A33 V08
*HARVARD UNIVERSITY CONTRIBUTIONS

INSERT BOOK
MASTER CARD
FACE UP IN
FRONT SLOT
OF S.R. PUNCH

MASTER CARD

GLOBE 901144-0

UNIVERSITY OF ARIZONA
LIBRARY

REMOVE THIS
FROM BOOK
ET. A FEE OF $1.00
L BE CHARGED FOR
SS OR MUTILATION

16365